

SIXTH EDITION

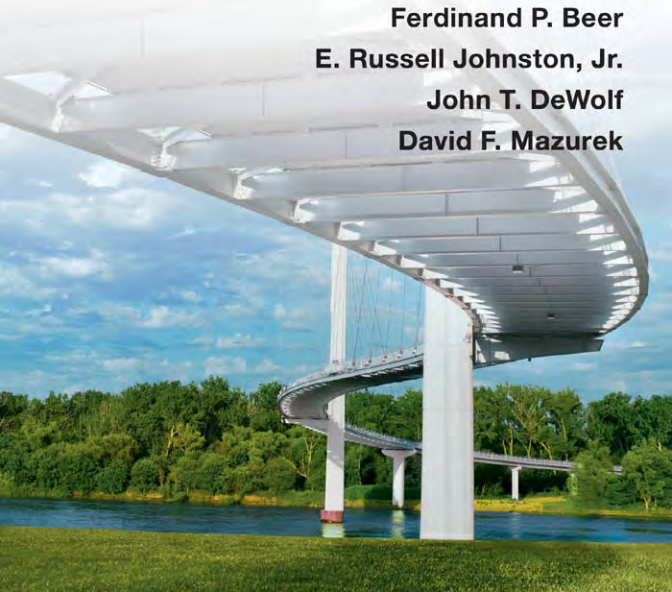
MECHANICS of MATERIALS

Ferdinand P. Beer

E. Russell Johnston, Jr.

John T. DeWolf

David F. Mazurek



This page intentionally left blank

SI Prefixes

Multiplication Factor	Prefix†	Symbol
1 000 000 000 000 = 10 ¹²	tera	T
1 000 000 000 = 10 ⁹	giga	G
1 000 000 = 10 ⁶	mega	M
1 000 = 10 ³	kilo	k
100 = 10 ²	hecto‡	h
10 = 10 ¹	deka‡	da
0.1 = 10 ⁻¹	deci‡	d
0.01 = 10 ⁻²	centi‡	c
0.001 = 10 ⁻³	milli	m
0.000 001 = 10 ⁻⁶	micro	μ
0.000 000 001 = 10 ⁻⁹	nano	n
0.000 000 000 001 = 10 ⁻¹²	pico	p
0.000 000 000 000 001 = 10 ⁻¹⁵	femto	f
0.000 000 000 000 000 001 = 10 ⁻¹⁸	atto	a

† The first syllable of every prefix is accented so that the prefix will retain its identity. Thus, the preferred pronunciation of kilometer places the accent on the first syllable, not the second.

‡ The use of these prefixes should be avoided, except for the measurement of areas and volumes and for the nontechnical use of centimeter, as for body and clothing measurements.

Principal SI Units Used in Mechanics

Quantity	Unit	Symbol	Formula
Acceleration	Meter per second squared	...	m/s ²
Angle	Radian	rad	†
Angular acceleration	Radian per second squared	...	rad/s ²
Angular velocity	Radian per second	...	rad/s
Area	Square meter	...	m ²
Density	Kilogram per cubic meter	...	kg/m ³
Energy	Joule	J	N · m
Force	Newton	N	kg · m/s ²
Frequency	Hertz	Hz	s ⁻¹
Impulse	Newton-second	...	kg · m/s
Length	Meter	m	‡
Mass	Kilogram	kg	‡
Moment of a force	Newton-meter	...	N · m
Power	Watt	W	J/s
Pressure	Pascal	Pa	N/m ²
Stress	Pascal	Pa	N/m ²
Time	Second	s	‡
Velocity	Meter per second	...	m/s
Volume, solids	Cubic meter	...	m ³
Liquids	Liter	L	10 ⁻³ m ³
Work	Joule	J	N · m

† Supplementary unit (1 revolution = 2π rad = 360°).

‡ Base unit.

U.S. Customary Units and Their SI Equivalents

Quantity	U.S. Customary Units	SI Equivalent
Acceleration	ft/s ²	0.3048 m/s ²
	in./s ²	0.0254 m/s ²
Area	ft ²	0.0929 m ²
	in ²	645.2 mm ²
Energy	ft · lb	1.356 J
Force	kip	4.448 kN
	lb	4.448 N
	oz	0.2780 N
Impulse	lb · s	4.448 N · s
Length	ft	0.3048 m
	in.	25.40 mm
	mi	1.609 km
Mass	oz mass	28.35 g
	lb mass	0.4536 kg
	slug	14.59 kg
	ton	907.2 kg
Moment of a force	lb · ft	1.356 N · m
	lb · in.	0.1130 N · m
Moment of inertia		
	Of an area	in ⁴
Of a mass	lb · ft · s ²	0.4162 × 10 ⁶ mm ⁴
		1.356 kg · m ²
Power	ft · lb/s	1.356 W
	hp	745.7 W
Pressure or stress	lb/ft ²	47.88 Pa
	lb/in ² (psi)	6.895 kPa
Velocity	ft/s	0.3048 m/s
	in./s	0.0254 m/s
	mi/h (mph)	0.4470 m/s
	mi/h (mph)	1.609 km/h
Volume, solids	ft ³	0.02832 m ³
	in ³	16.39 cm ³
Liquids	gal	3.785 L
	qt	0.9464 L
Work	ft · lb	1.356 J

MECHANICS OF MATERIALS

This page intentionally left blank

SIXTH EDITION

MECHANICS OF MATERIALS

Ferdinand P. Beer

Late of Lehigh University

E. Russell Johnston, Jr.

Late of University of Connecticut

John T. Dewolf

University of Connecticut

David F. Mazurek

United States Coast Guard Academy





MECHANICS OF MATERIALS, SIXTH EDITION

Published by McGraw-Hill, a business unit of The McGraw-Hill Companies, Inc., 1221 Avenue of the Americas, New York, NY 10020. Copyright © 2012 by The McGraw-Hill Companies, Inc. All rights reserved. Previous editions © 2009, 2006, and 2002. No part of this publication may be reproduced or distributed in any form or by any means, or stored in a database or retrieval system, without the prior written consent of The McGraw-Hill Companies, Inc., including, but not limited to, in any network or other electronic storage or transmission, or broadcast for distance learning.

Some ancillaries, including electronic and print components, may not be available to customers outside the United States.

This book is printed on acid-free paper.

1 2 3 4 5 6 7 8 9 0 QVR/QVR 1 0 9 8 7 6 5 4 3 2 1

ISBN 978-0-07-338028-5

MHID 0-07-338028-8

Vice President, Editor-in-Chief: *Marty Lange*

Vice President, EDP: *Kimberly Meriwether David*

Senior Director of Development: *Kristine Tibbetts*

Global Publisher: *Raghothaman Srinivasan*

Executive Editor: *Bill Stenquist*

Developmental Editor: *Lora Neyens*

Senior Marketing Manager: *Curt Reynolds*

Lead Project Manager: *Sheila M. Frank*

Buyer II: *Sherry L. Kane*

Senior Designer: *Laurie B. Janssen*

Cover Designer: *Ron Bissell*

Cover Image: (front) © *Ervin Photography, Inc.*

Lead Photo Research Coordinator: *Carrie K. Burger*

Photo Research: *Sabina Dowell*

Compositor: *Aptara®, Inc.*

Typeface: *10.5/12 New Caledonia*

Printer: *Quad/Graphics*

All credits appearing on page or at the end of the book are considered to be an extension of the copyright page.

The photos on the front and back cover show the Bob Kerrey Pedestrian Bridge, which spans the Missouri River between Omaha, Nebraska, and Council Bluffs, Iowa. This S-curved structure utilizes a cable-stayed design, and is the longest pedestrian bridge to connect two states.

Library of Congress Cataloging-in-Publication Data

Mechanics of materials / Ferdinand Beer ... [et al.]. — 6th ed.

p. cm.

Includes index.

ISBN 978-0-07-338028-5

ISBN 0-07-338028-8 (alk. paper)

1. Strength of materials—Textbooks. I. Beer, Ferdinand Pierre, 1915–

TA405.B39 2012

620.1'12—dc22

2010037852

About the Authors

As publishers of the books written by Ferd Beer and Russ Johnston, we are often asked how did they happen to write the books together, with one of them at Lehigh and the other at the University of Connecticut.

The answer to this question is simple. Russ Johnston's first teaching appointment was in the Department of Civil Engineering and Mechanics at Lehigh University. There he met Ferd Beer, who had joined that department two years earlier and was in charge of the courses in mechanics. Born in France and educated in France and Switzerland (he held an M.S. degree from the Sorbonne and an Sc.D. degree in the field of theoretical mechanics from the University of Geneva), Ferd had come to the United States after serving in the French army during the early part of World War II and had taught for four years at Williams College in the Williams-MIT joint arts and engineering program. Born in Philadelphia, Russ had obtained a B.S. degree in civil engineering from the University of Delaware and an Sc.D. degree in the field of structural engineering from MIT.

Ferd was delighted to discover that the young man who had been hired chiefly to teach graduate structural engineering courses was not only willing but eager to help him reorganize the mechanics courses. Both believed that these courses should be taught from a few basic principles and that the various concepts involved would be best understood and remembered by the students if they were presented to them in a graphic way. Together they wrote lecture notes in statics and dynamics, to which they later added problems they felt would appeal to future engineers, and soon they produced the manuscript of the first edition of *Mechanics for Engineers*. The second edition of *Mechanics for Engineers* and the first edition of *Vector Mechanics for Engineers* found Russ Johnston at Worcester Polytechnic Institute and the next editions at the University of Connecticut. In the meantime, both Ferd and Russ had assumed administrative responsibilities in their departments, and both were involved in research, consulting, and supervising graduate students—Ferd in the area of stochastic processes and random vibrations, and Russ in the area of elastic stability and structural analysis and design. However, their interest in improving the teaching of the basic mechanics courses had not subsided, and they both taught sections of these courses as they kept revising their texts and began writing together the manuscript of the first edition of *Mechanics of Materials*.

Ferd and Russ's contributions to engineering education earned them a number of honors and awards. They were presented with the Western Electric Fund Award for excellence in the instruction of engineering students by their respective regional sections of the American Society for Engineering Education, and they both received the Distinguished Educator Award from the Mechanics Division of the

same society. In 1991 Russ received the Outstanding Civil Engineer Award from the Connecticut Section of the American Society of Civil Engineers, and in 1995 Ferd was awarded an honorary Doctor of Engineering degree by Lehigh University.

John T. DeWolf, Professor of Civil Engineering at the University of Connecticut, joined the Beer and Johnston team as an author on the second edition of *Mechanics of Materials*. John holds a B.S. degree in civil engineering from the University of Hawaii and M.E. and Ph.D. degrees in structural engineering from Cornell University. His research interests are in the area of elastic stability, bridge monitoring, and structural analysis and design. He is a registered Professional Engineering and a member of the Connecticut Board of Professional Engineers. He was selected as the University of Connecticut Teaching Fellow in 2006.

David F. Mazurek, Professor of Civil Engineering at the United States Coast Guard Academy, joined the team in the fourth edition. David holds a B.S. degree in ocean engineering and an M.S. degree in civil engineering from the Florida Institute of Technology, and a Ph.D. degree in civil engineering from the University of Connecticut. He is a registered Professional Engineer. He has served on the American Railway Engineering & Maintenance of Way Association's Committee 15—Steel Structures for the past seventeen years. Professional interests include bridge engineering, structural forensics, and blast-resistant design.

Contents

Preface xii

List of Symbols xviii

1 Introduction—Concept of Stress 2

- 1.1** Introduction 4
- 1.2** A Short Review of the Methods of Statics 4
- 1.3** Stresses in the Members of a Structure 7
- 1.4** Analysis and Design 8
- 1.5** Axial Loading; Normal Stress 9
- 1.6** Shearing Stress 11
- 1.7** Bearing Stress in Connections 13
- 1.8** Application to the Analysis and Design of Simple Structures 13
- 1.9** Method of Problem Solution 16
- 1.10** Numerical Accuracy 17
- 1.11** Stress on an Oblique Plane under Axial Loading 26
- 1.12** Stress under General Loading Conditions; Components of Stress 27
- 1.13** Design Considerations 30

Review and Summary for Chapter 1 42

2 Stress and Strain—Axial Loading 52

- 2.1** Introduction 54
- 2.2** Normal Strain under Axial Loading 55
- 2.3** Stress-Strain Diagram 57
- *2.4** True Stress and True Strain 61
- 2.5** Hooke's Law; Modulus of Elasticity 62
- 2.6** Elastic versus Plastic Behavior of a Material 64
- 2.7** Repeated Loadings; Fatigue 66
- 2.8** Deformations of Members under Axial Loading 67
- 2.9** Statically Indeterminate Problems 78
- 2.10** Problems Involving Temperature Changes 82
- 2.11** Poisson's Ratio 93
- 2.12** Multiaxial Loading; Generalized Hooke's Law 94
- *2.13** Dilatation; Bulk Modulus 96

- 2.14** Shearing Strain 98
- 2.15** Further Discussion of Deformations under Axial Loading; Relation among E , ν , and G 101
- *2.16** Stress-Strain Relationships for Fiber-Reinforced Composite Materials 103
- 2.17** Stress and Strain Distribution under Axial Loading; Saint-Venant's Principle 113
- 2.18** Stress Concentrations 115
- 2.19** Plastic Deformations 117
- *2.20** Residual Stresses 121

Review and Summary for Chapter 2 129

3 Torsion 140

- 3.1** Introduction 142
- 3.2** Preliminary Discussion of the Stresses in a Shaft 144
- 3.3** Deformations in a Circular Shaft 145
- 3.4** Stresses in the Elastic Range 148
- 3.5** Angle of Twist in the Elastic Range 159
- 3.6** Statically Indeterminate Shafts 163
- 3.7** Design of Transmission Shafts 176
- 3.8** Stress Concentrations in Circular Shafts 179
- *3.9** Plastic Deformations in Circular Shafts 184
- *3.10** Circular Shafts Made of an Elastoplastic Material 186
- *3.11** Residual Stresses in Circular Shafts 189
- *3.12** Torsion of Noncircular Members 197
- *3.13** Thin-Walled Hollow Shafts 200

Review and Summary for Chapter 3 210

4 Pure Bending 220

- 4.1** Introduction 222
- 4.2** Symmetric Member in Pure Bending 224
- 4.3** Deformations in a Symmetric Member in Pure Bending 226
- 4.4** Stresses and Deformations in the Elastic Range 229
- 4.5** Deformations in a Transverse Cross Section 233
- 4.6** Bending of Members Made of Several Materials 242
- 4.7** Stress Concentrations 246
- *4.8** Plastic Deformations 255
- *4.9** Members Made of an Elastoplastic Material 256
- *4.10** Plastic Deformations of Members with a Single Plane of Symmetry 260
- *4.11** Residual Stresses 261
- 4.12** Eccentric Axial Loading in a Plane of Symmetry 270

- 4.13** Unsymmetric Bending 279
- 4.14** General Case of Eccentric Axial Loading 284
- *4.15** Bending of Curved Members 294

Review and Summary for Chapter 4 305

5 Analysis and Design of Beams for Bending 314

- 5.1** Introduction 316
- 5.2** Shear and Bending-Moment Diagrams 319
- 5.3** Relations among Load, Shear, and Bending Moment 329
- 5.4** Design of Prismatic Beams for Bending 339
- *5.5** Using Singularity Functions to Determine Shear and Bending Moment in a Beam 350
- *5.6** Nonprismatic Beams 361

Review and Summary for Chapter 5 370

6 Shearing Stresses in Beams and Thin-Walled Members 380

- 6.1** Introduction 382
- 6.2** Shear on the Horizontal Face of a Beam Element 384
- 6.3** Determination of the Shearing Stresses in a Beam 386
- 6.4** Shearing Stresses τ_{xy} in Common Types of Beams 387
- *6.5** Further Discussion of the Distribution of Stresses in a Narrow Rectangular Beam 390
- 6.6** Longitudinal Shear on a Beam Element of Arbitrary Shape 399
- 6.7** Shearing Stresses in Thin-Walled Members 401
- *6.8** Plastic Deformations 404
- *6.9** Unsymmetric Loading of Thin-Walled Members; Shear Center 414

Review and Summary for Chapter 6 427

7 Transformations of Stress and Strain 436

- 7.1** Introduction 438
- 7.2** Transformation of Plane Stress 440
- 7.3** Principal Stresses: Maximum Shearing Stress 443
- 7.4** Mohr's Circle for Plane Stress 452
- 7.5** General State of Stress 462

- 7.6** Application of Mohr's Circle to the Three-Dimensional Analysis of Stress 464
- *7.7** Yield Criteria for Ductile Materials under Plane Stress 467
- *7.8** Fracture Criteria for Brittle Materials under Plane Stress 469
- 7.9** Stresses in Thin-Walled Pressure Vessels 478
- *7.10** Transformation of Plane Strain 486
- *7.11** Mohr's Circle for Plane Strain 489
- *7.12** Three-Dimensional Analysis of Strain 491
- *7.13** Measurements of Strain; Strain Rosette 494

Review and Summary for Chapter 7 502

8 Principal Stresses under a Given Loading 512

- *8.1** Introduction 514
- *8.2** Principal Stresses in a Beam 515
- *8.3** Design of Transmission Shafts 518
- *8.4** Stresses under Combined Loadings 527

Review and Summary for Chapter 8 540

9 Deflection of Beams 548

- 9.1** Introduction 550
- 9.2** Deformation of a Beam under Transverse Loading 552
- 9.3** Equation of the Elastic Curve 553
- *9.4** Direct Determination of the Elastic Curve from the Load Distribution 559
- 9.5** Statically Indeterminate Beams 561
- *9.6** Using Singularity Functions to Determine the Slope and Deflection of a Beam 571
- 9.7** Method of Superposition 580
- 9.8** Application of Superposition to Statically Indeterminate Beams 582
- *9.9** Moment-Area Theorems 592
- *9.10** Application to Cantilever Beams and Beams with Symmetric Loadings 595
- *9.11** Bending-Moment Diagrams by Parts 597
- *9.12** Application of Moment-Area Theorems to Beams with Unsymmetric Loadings 605
- *9.13** Maximum Deflection 607
- *9.14** Use of Moment-Area Theorems with Statically Indeterminate Beams 609

Review and Summary for Chapter 9 618

10 Columns 630

- 10.1** Introduction 632
- 10.2** Stability of Structures 632
- 10.3** Euler's Formula for Pin-Ended Columns 635
- 10.4** Extension of Euler's Formula to Columns with Other End Conditions 638
- *10.5** Eccentric Loading; the Secant Formula 649
- 10.6** Design of Columns under a Centric Load 660
- 10.7** Design of Columns under an Eccentric Load 675

Review and Summary for Chapter 10 684

11 Energy Methods 692

- 11.1** Introduction 694
- 11.2** Strain Energy 694
- 11.3** Strain-Energy Density 696
- 11.4** Elastic Strain Energy for Normal Stresses 698
- 11.5** Elastic Strain Energy for Shearing Stresses 701
- 11.6** Strain Energy for a General State of Stress 704
- 11.7** Impact Loading 716
- 11.8** Design for Impact Loads 718
- 11.9** Work and Energy under a Single Load 719
- 11.10** Deflection under a Single Load by the Work-Energy Method 722
- *11.11** Work and Energy under Several Loads 732
- *11.12** Castigliano's Theorem 734
- *11.13** Deflections by Castigliano's Theorem 736
- *11.14** Statically Indeterminate Structures 740

Review and Summary for Chapter 11 750

Appendices A1

- A** Moments of Areas A2
- B** Typical Properties of Selected Materials Used in Engineering A12
- C** Properties of Rolled-Steel Shapes A16
- D** Beam Deflections and Slopes A28
- E** Fundamentals of Engineering Examination A29

Photo Credits C1

Index I1

Answers to Problems An1

Preface

OBJECTIVES

The main objective of a basic mechanics course should be to develop in the engineering student the ability to analyze a given problem in a simple and logical manner and to apply to its solution a few fundamental and well-understood principles. This text is designed for the first course in mechanics of materials—or strength of materials—offered to engineering students in the sophomore or junior year. The authors hope that it will help instructors achieve this goal in that particular course in the same way that their other texts may have helped them in statics and dynamics.

GENERAL APPROACH

In this text the study of the mechanics of materials is based on the understanding of a few basic concepts and on the use of simplified models. This approach makes it possible to develop all the necessary formulas in a rational and logical manner, and to clearly indicate the conditions under which they can be safely applied to the analysis and design of actual engineering structures and machine components.

Free-body Diagrams Are Used Extensively. Throughout the text free-body diagrams are used to determine external or internal forces. The use of “picture equations” will also help the students understand the superposition of loadings and the resulting stresses and deformations.

Design Concepts Are Discussed Throughout the Text Whenever Appropriate. A discussion of the application of the factor of safety to design can be found in Chap. 1, where the concepts of both allowable stress design and load and resistance factor design are presented.

A Careful Balance Between SI and U.S. Customary Units Is Consistently Maintained. Because it is essential that students be able to handle effectively both SI metric units and U.S. customary units, half the examples, sample problems, and problems to be assigned have been stated in SI units and half in U.S. customary units. Since a large number of problems are available, instructors can assign problems using each system of units in whatever proportion they find most desirable for their class.

Optional Sections Offer Advanced or Specialty Topics. Topics such as residual stresses, torsion of noncircular and thin-walled members, bending of curved beams, shearing stresses in non-symmetrical

members, and failure criteria, have been included in optional sections for use in courses of varying emphases. To preserve the integrity of the subject, these topics are presented in the proper sequence, wherever they logically belong. Thus, even when not covered in the course, they are highly visible and can be easily referred to by the students if needed in a later course or in engineering practice. For convenience all optional sections have been indicated by asterisks.

CHAPTER ORGANIZATION

It is expected that students using this text will have completed a course in statics. However, Chap. 1 is designed to provide them with an opportunity to review the concepts learned in that course, while shear and bending-moment diagrams are covered in detail in Secs. 5.2 and 5.3. The properties of moments and centroids of areas are described in Appendix A; this material can be used to reinforce the discussion of the determination of normal and shearing stresses in beams (Chaps. 4, 5, and 6).

The first four chapters of the text are devoted to the analysis of the stresses and of the corresponding deformations in various structural members, considering successively axial loading, torsion, and pure bending. Each analysis is based on a few basic concepts, namely, the conditions of equilibrium of the forces exerted on the member, the relations existing between stress and strain in the material, and the conditions imposed by the supports and loading of the member. The study of each type of loading is complemented by a large number of examples, sample problems, and problems to be assigned, all designed to strengthen the students' understanding of the subject.

The concept of stress at a point is introduced in Chap. 1, where it is shown that an axial load can produce shearing stresses as well as normal stresses, depending upon the section considered. The fact that stresses depend upon the orientation of the surface on which they are computed is emphasized again in Chaps. 3 and 4 in the cases of torsion and pure bending. However, the discussion of computational techniques—such as Mohr's circle—used for the transformation of stress at a point is delayed until Chap. 7, after students have had the opportunity to solve problems involving a combination of the basic loadings and have discovered for themselves the need for such techniques.

The discussion in Chap. 2 of the relation between stress and strain in various materials includes fiber-reinforced composite materials. Also, the study of beams under transverse loads is covered in two separate chapters. Chapter 5 is devoted to the determination of the normal stresses in a beam and to the design of beams based on the allowable normal stress in the material used (Sec. 5.4). The chapter begins with a discussion of the shear and bending-moment diagrams (Secs. 5.2 and 5.3) and includes an optional section on the use of singularity functions for the determination of the shear and bending moment in a beam (Sec. 5.5). The chapter ends with an optional section on nonprismatic beams (Sec. 5.6).

Chapter 6 is devoted to the determination of shearing stresses in beams and thin-walled members under transverse loadings. The formula for the shear flow, $q = VQ/I$, is derived in the traditional way. More advanced aspects of the design of beams, such as the determination of the principal stresses at the junction of the flange and web of a W-beam, are in Chap. 8, an optional chapter that may be covered after the transformations of stresses have been discussed in Chap. 7. The design of transmission shafts is in that chapter for the same reason, as well as the determination of stresses under combined loadings that can now include the determination of the principal stresses, principal planes, and maximum shearing stress at a given point.

Statically indeterminate problems are first discussed in Chap. 2 and considered throughout the text for the various loading conditions encountered. Thus, students are presented at an early stage with a method of solution that combines the analysis of deformations with the conventional analysis of forces used in statics. In this way, they will have become thoroughly familiar with this fundamental method by the end of the course. In addition, this approach helps the students realize that stresses themselves are statically indeterminate and can be computed only by considering the corresponding distribution of strains.

The concept of plastic deformation is introduced in Chap. 2, where it is applied to the analysis of members under axial loading. Problems involving the plastic deformation of circular shafts and of prismatic beams are also considered in optional sections of Chaps. 3, 4, and 6. While some of this material can be omitted at the choice of the instructor, its inclusion in the body of the text will help students realize the limitations of the assumption of a linear stress-strain relation and serve to caution them against the inappropriate use of the elastic torsion and flexure formulas.

The determination of the deflection of beams is discussed in Chap. 9. The first part of the chapter is devoted to the integration method and to the method of superposition, with an optional section (Sec. 9.6) based on the use of singularity functions. (This section should be used only if Sec. 5.5 was covered earlier.) The second part of Chap. 9 is optional. It presents the moment-area method in two lessons.

Chapter 10 is devoted to columns and contains material on the design of steel, aluminum, and wood columns. Chapter 11 covers energy methods, including Castigliano's theorem.

PEDAGOGICAL FEATURES

Each chapter begins with an introductory section setting the purpose and goals of the chapter and describing in simple terms the material to be covered and its application to the solution of engineering problems.

Chapter Lessons. The body of the text has been divided into units, each consisting of one or several theory sections followed by sample problems and a large number of problems to be assigned.

Each unit corresponds to a well-defined topic and generally can be covered in one lesson.

Examples and Sample Problems. The theory sections include many examples designed to illustrate the material being presented and facilitate its understanding. The sample problems are intended to show some of the applications of the theory to the solution of engineering problems. Since they have been set up in much the same form that students will use in solving the assigned problems, the sample problems serve the double purpose of amplifying the text and demonstrating the type of neat and orderly work that students should cultivate in their own solutions.

Homework Problem Sets. Most of the problems are of a practical nature and should appeal to engineering students. They are primarily designed, however, to illustrate the material presented in the text and help the students understand the basic principles used in mechanics of materials. The problems have been grouped according to the portions of material they illustrate and have been arranged in order of increasing difficulty. Problems requiring special attention have been indicated by asterisks. Answers to problems are given at the end of the book, except for those with a number set in italics.

Chapter Review and Summary. Each chapter ends with a review and summary of the material covered in the chapter. Notes in the margin have been included to help the students organize their review work, and cross references provided to help them find the portions of material requiring their special attention.

Review Problems. A set of review problems is included at the end of each chapter. These problems provide students further opportunity to apply the most important concepts introduced in the chapter.

Computer Problems. Computers make it possible for engineering students to solve a great number of challenging problems. A group of six or more problems designed to be solved with a computer can be found at the end of each chapter. These problems can be solved using any computer language that provides a basis for analytical calculations. Developing the algorithm required to solve a given problem will benefit the students in two different ways: (1) it will help them gain a better understanding of the mechanics principles involved; (2) it will provide them with an opportunity to apply the skills acquired in their computer programming course to the solution of a meaningful engineering problem. These problems can be solved using any computer language that provide a basis for analytical calculations.

Fundamentals of Engineering Examination. Engineers who seek to be licensed as *Professional Engineers* must take two exams. The first exam, the *Fundamentals of Engineering Examination*, includes subject material from *Mechanics of Materials*. Appendix E lists the topics in *Mechanics of Materials* that are covered in this exam along with problems that can be solved to review this material.

SUPPLEMENTAL RESOURCES

Instructor's Solutions Manual. The Instructor's and Solutions Manual that accompanies the sixth edition continues the tradition of exceptional accuracy and keeping solutions contained to a single page for easier reference. The manual also features tables designed to assist instructors in creating a schedule of assignments for their courses. The various topics covered in the text are listed in Table I, and a suggested number of periods to be spent on each topic is indicated. Table II provides a brief description of all groups of problems and a classification of the problems in each group according to the units used. Sample lesson schedules are also found within the manual.

MCGRAW-HILL CONNECT ENGINEERING

McGraw-Hill Connect Engineering™ is a web-based assignment and assessment platform that gives students the means to better connect with their coursework, with their instructors, and with the important concepts that they will need to know for success now and in the future. With Connect Engineering, instructors can deliver assignments, quizzes, and tests easily online. Students can practice important skills at their own pace and on their own schedule. With Connect Engineering Plus, students also get 24/7 online access to an eBook—an online edition of the text—to aid them in successfully completing their work, wherever and whenever they choose.

Connect Engineering for *Mechanics of Materials* is available at www.mcgrawhillconnect.com

MCGRAW-HILL CREATE™

Craft your teaching resources to match the way you teach! With McGraw-Hill Create™, www.mcgrawhillcreate.com, you can easily rearrange chapters, combine material from other content sources, and quickly upload content you have written like your course syllabus or teaching notes. Arrange your book to fit your teaching style. Create even allows you to personalize your book's appearance by selecting the cover and adding your name, school, and course information. Order a Create book and you'll receive a complimentary print review copy in 3–5 business days or a complimentary electronic review copy (eComp) via email in minutes. Go to www.mcgrawhillcreate.com today and register to experience how McGraw-Hill Create empowers you to teach *your* students *your* way.

McGraw-Hill Higher Education and Blackboard® have teamed up.

Blackboard, the Web-based course-management system, has partnered with McGraw-Hill to better allow students and faculty to use online materials and activities to complement face-to-face teaching. Blackboard features exciting social learning and teaching tools that foster more logical, visually impactful and active learning opportunities for students. You'll transform your closed-door classrooms into communities where students remain connected to their educational experience 24 hours a day.

This partnership allows you and your students access to McGraw-Hill's Connect and Create right from within your Blackboard course—all with one single sign-on.



Not only do you get single sign-on with Connect and Create, you also get deep integration of McGraw-Hill content and content engines right in Blackboard. Whether you're choosing a book for your course or building Connect assignments, all the tools you need are right where you want them—inside of Blackboard.

Gradebooks are now seamless. When a student completes an integrated Connect assignment, the grade for that assignment automatically (and instantly) feeds your Blackboard grade center.

McGraw-Hill and Blackboard can now offer you easy access to industry leading technology and content, whether your campus hosts it, or we do. Be sure to ask your local McGraw-Hill representative for details.

ADDITIONAL ONLINE RESOURCES

Mechanics of Materials 6e also features a companion website (www.mhhe.com/beerjohnston) for instructors. Included on the website are lecture PowerPoints, an image library, and animations. Via the website, instructors can also request access to C.O.S.M.O.S., a complete online solutions manual organization system that allows instructors to create custom homework, quizzes, and tests using end-of-chapter problems from the text. For access to this material, contact your sales representative for a user name and password.

Hands-On Mechanics. Hands-On Mechanics is a website designed for instructors who are interested in incorporating three-dimensional, hands-on teaching aids into their lectures. Developed through a partnership between McGraw-Hill and the Department of Civil and Mechanical Engineering at the United States Military Academy at West Point, this website not only provides detailed instructions for how to build 3-D teaching tools using materials found in any lab or local hardware store but also provides a community where educators can share ideas, trade best practices, and submit their own demonstrations for posting on the site. Visit www.handsonmechanics.com to see how you can put this to use in your classroom.

ACKNOWLEDGMENTS

The authors thank the many companies that provided photographs for this edition. We also wish to recognize the determined efforts and patience of our photo researcher Sabina Dowell.

Our special thanks go to Professor Dean Updike, of the Department of Mechanical Engineering and Mechanics, Lehigh University for his patience and cooperation as he checked the solutions and answers of all the problems in this edition.

We also gratefully acknowledge the help, comments and suggestions offered by the many reviewers and users of previous editions of *Mechanics of Materials*.

John T. DeWolf
David F. Mazurek

List of Symbols

a	Constant; distance
A, B, C, . . .	Forces; reactions
$A, B, C, . . .$	Points
A, \mathcal{A}	Area
b	Distance; width
c	Constant; distance; radius
C	Centroid
$C_1, C_2, . . .$	Constants of integration
C_p	Column stability factor
d	Distance; diameter; depth
D	Diameter
e	Distance; eccentricity; dilatation
E	Modulus of elasticity
f	Frequency; function
F	Force
$F.S.$	Factor of safety
G	Modulus of rigidity; shear modulus
h	Distance; height
H	Force
H, J, K	Points
$I, I_x, . . .$	Moment of inertia
$I_{xy}, . . .$	Product of inertia
J	Polar moment of inertia
k	Spring constant; shape factor; bulk modulus; constant
K	Stress concentration factor; torsional spring constant
l	Length; span
L	Length; span
L_e	Effective length
m	Mass
M	Couple
$M, M_x, . . .$	Bending moment
M_D	Bending moment, dead load (LRFD)
M_L	Bending moment, live load (LRFD)
M_U	Bending moment, ultimate load (LRFD)
n	Number; ratio of moduli of elasticity; normal direction
p	Pressure
P	Force; concentrated load
P_D	Dead load (LRFD)
P_L	Live load (LRFD)
P_U	Ultimate load (LRFD)
q	Shearing force per unit length; shear flow
Q	Force
Q	First moment of area

r	Radius; radius of gyration
\mathbf{R}	Force; reaction
R	Radius; modulus of rupture
s	Length
S	Elastic section modulus
t	Thickness; distance; tangential deviation
\mathbf{T}	Torque
T	Temperature
u, v	Rectangular coordinates
u	Strain-energy density
U	Strain energy; work
\mathbf{v}	Velocity
\mathbf{V}	Shearing force
V	Volume; shear
w	Width; distance; load per unit length
\mathbf{W}, W	Weight, load
x, y, z	Rectangular coordinates; distance; displacements; deflections
$\bar{x}, \bar{y}, \bar{z}$	Coordinates of centroid
Z	Plastic section modulus
α, β, γ	Angles
α	Coefficient of thermal expansion; influence coefficient
γ	Shearing strain; specific weight
γ_D	Load factor, dead load (LRFD)
γ_L	Load factor, live load (LRFD)
δ	Deformation; displacement
ϵ	Normal strain
θ	Angle; slope
λ	Direction cosine
ν	Poisson's ratio
ρ	Radius of curvature; distance; density
σ	Normal stress
τ	Shearing stress
ϕ	Angle; angle of twist; resistance factor
ω	Angular velocity

This page intentionally left blank

MECHANICS OF MATERIALS

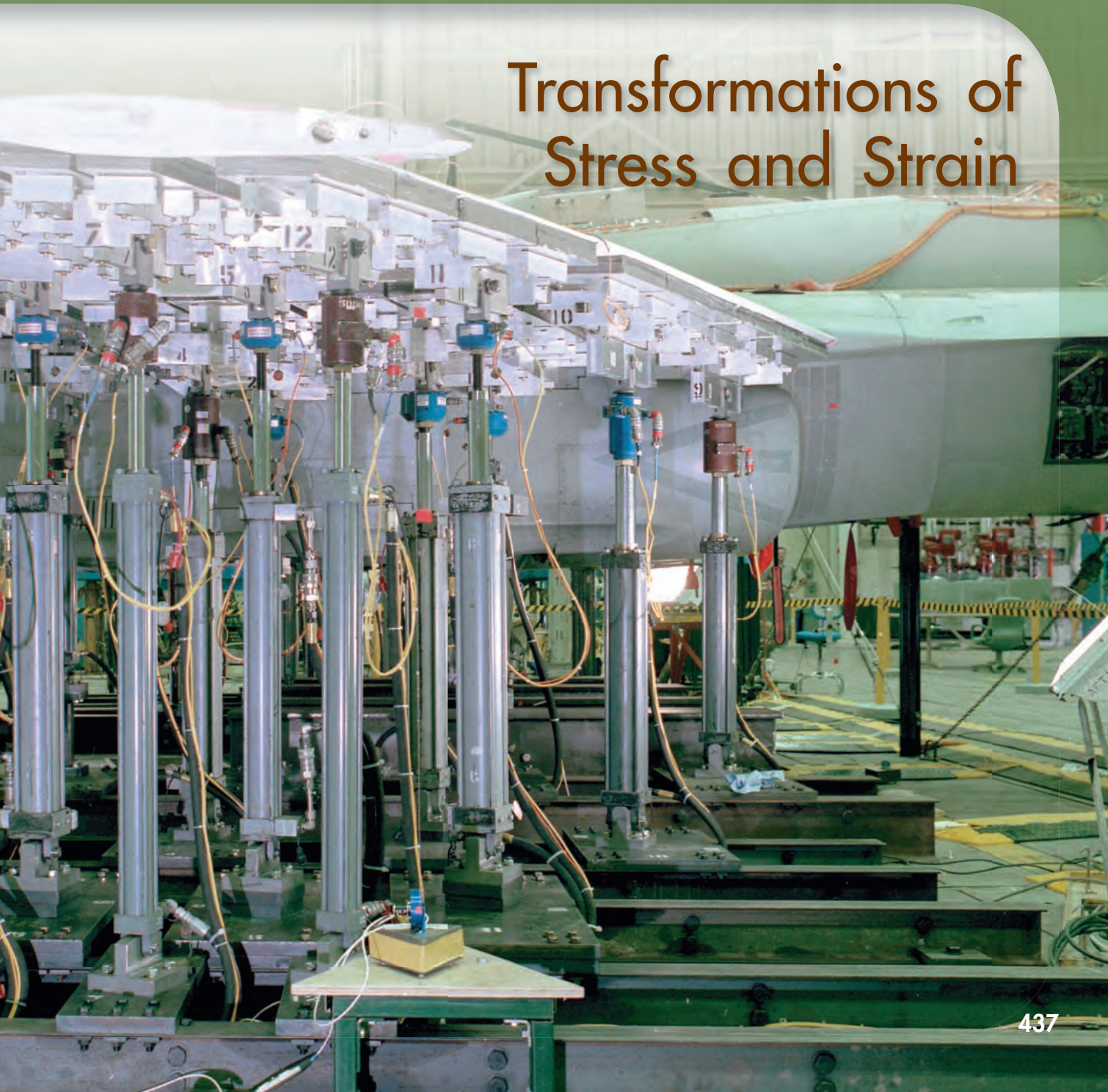
The aircraft shown is being tested to determine how the forces due to lift would be distributed over the wing. This chapter deals with stresses and strains in structures and machine components.



CHAPTER

7

Transformations of Stress and Strain



Chapter 7 Transformations of Stress and Strain

- 7.1 Introduction
- 7.2 Transformation of Plane Stress
- 7.3 Principal Stresses; Maximum Shearing Stress
- 7.4 Mohr's Circle for Plane Stress
- 7.5 General State of Stress
- 7.6 Application of Mohr's Circle to the Three-Dimensional Analysis of Stress
- *7.7 Yield Criteria for Ductile Materials under Plane Stress
- *7.8 Fracture Criteria for Brittle Materials under Plane Stress
- 7.9 Stresses in Thin-Walled Pressure Vessels
- *7.10 Transformation of Plane Strain
- *7.11 Mohr's Circle for Plane Strain
- *7.12 Three-Dimensional Analysis of Strain
- *7.13 Measurements of Strain; Strain Rosette

7.1 INTRODUCTION

We saw in Sec. 1.12 that the most general state of stress at a given point Q may be represented by six components. Three of these components, σ_x , σ_y , and σ_z , define the normal stresses exerted on the faces of a small cubic element centered at Q and of the same orientation as the coordinate axes (Fig. 7.1a), and the other three, τ_{xy} , τ_{yz} , and τ_{zx} ,† the components of the shearing stresses on the same element. As we remarked at the time, the same state of stress will be represented by a different set of components if the coordinate axes are rotated (Fig. 7.1b). We propose in the first part of this chapter to determine how the components of stress are transformed under a rotation of the coordinate axes. The second part of the chapter will be devoted to a similar analysis of the transformation of the components of strain.

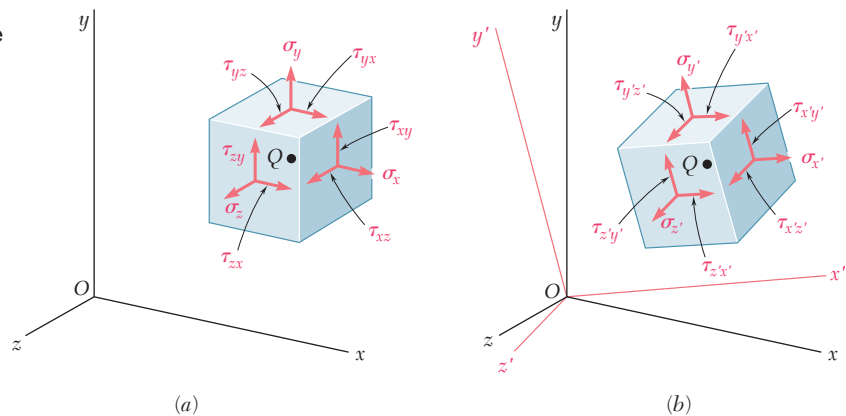


Fig. 7.1 General state of stress at a point.

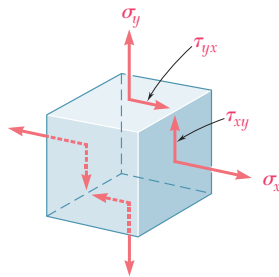


Fig. 7.2 Plane stress.

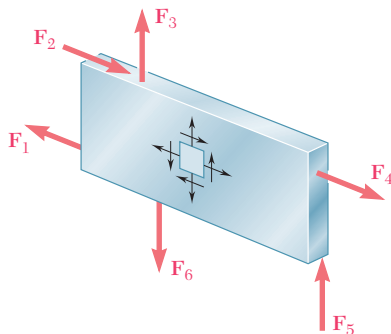


Fig. 7.3 Example of plane stress.

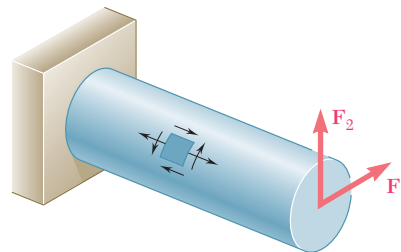


Fig. 7.4 Example of plane stress.

Our discussion of the transformation of stress will deal mainly with *plane stress*, i.e., with a situation in which two of the faces of the cubic element are free of any stress. If the z axis is chosen perpendicular to these faces, we have $\sigma_z = \tau_{zx} = \tau_{zy} = 0$, and the only remaining stress components are σ_x , σ_y , and τ_{xy} (Fig. 7.2). Such a situation occurs in a thin plate subjected to forces acting in the mid-plane of the plate (Fig. 7.3). It also occurs on the free surface of a structural element or machine component, i.e., at any point of the surface of that element or component that is not subjected to an external force (Fig. 7.4).

†We recall that $\tau_{yx} = \tau_{xy}$, $\tau_{zy} = \tau_{yz}$, and $\tau_{zx} = \tau_{xz}$.

Considering in Sec. 7.2 a state of plane stress at a given point Q characterized by the stress components σ_x , σ_y , and τ_{xy} associated with the element shown in Fig. 7.5a, you will learn to determine the components $\sigma_{x'}$, $\sigma_{y'}$, and $\tau_{x'y'}$ associated with that element after it has been rotated through an angle θ about the z axis (Fig. 7.5b). In Sec. 7.3, you will determine the value θ_p of θ for which the stresses $\sigma_{x'}$ and $\sigma_{y'}$ are, respectively, maximum and minimum; these values of the normal stress are the *principal stresses* at point Q , and the faces of the corresponding element define the *principal planes of stress* at that point. You will also determine the value θ_s of the angle of rotation for which the shearing stress is maximum, as well as the value of that stress.

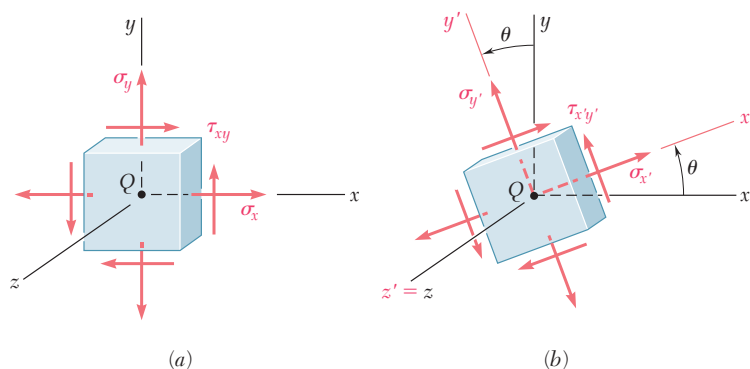


Fig. 7.5 Transformation of stress.

In Sec. 7.4, an alternative method for the solution of problems involving the transformation of plane stress, based on the use of *Mohr's circle*, will be presented.

In Sec. 7.5, the *three-dimensional state of stress* at a given point will be considered and a formula for the determination of the normal stress on a plane of arbitrary orientation at that point will be developed. In Sec. 7.6, you will consider the rotations of a cubic element about each of the principal axes of stress and note that the corresponding transformations of stress can be described by three different Mohr's circles. You will also observe that, in the case of a state of *plane stress* at a given point, the maximum value of the shearing stress obtained earlier by considering rotations in the plane of stress does not necessarily represent the maximum shearing stress at that point. This will bring you to distinguish between *in-plane* and *out-of-plane* maximum shearing stresses.

Yield criteria for ductile materials under plane stress will be developed in Sec. 7.7. To predict whether a material will yield at some critical point under given loading conditions, you will determine the principal stresses σ_a and σ_b at that point and check whether σ_a , σ_b , and the yield strength σ_Y of the material satisfy some criterion. Two criteria in common use are: the *maximum-shearing-strength criterion* and the *maximum-distortion-energy criterion*. In Sec. 7.8, *fracture criteria* for brittle materials under plane stress will be developed in a similar fashion; they will involve the principal stresses σ_a and σ_b at some critical point and the ultimate strength σ_U of the



Photo 7.1
Cylindrical
pressure vessel.



Photo 7.2 Spherical pressure vessel.

material. Two criteria will be discussed: the *maximum-normal-stress* criterion and *Mohr's criterion*.

Thin-walled pressure vessels provide an important application of the analysis of plane stress. In Sec. 7.9, we will discuss stresses in both cylindrical and spherical pressure vessels (Photos 7.1 and 7.2).

Sections 7.10 and 7.11 will be devoted to a discussion of the *transformation of plane strain* and to *Mohr's circle for plane strain*. In Sec. 7.12, we will consider the three-dimensional analysis of strain and see how Mohr's circles can be used to determine the maximum shearing strain at a given point. Two particular cases are of special interest and should not be confused: the case of *plane strain* and the case of *plane stress*.

Finally, in Sec. 7.13, we discuss the use of *strain gages* to measure the normal strain on the surface of a structural element or machine component. You will see how the components ϵ_x , ϵ_y , and γ_{xy} characterizing the state of strain at a given point can be computed from the measurements made with three strain gages forming a *strain rosette*.

7.2 TRANSFORMATION OF PLANE STRESS

Let us assume that a state of plane stress exists at point Q (with $\sigma_z = \tau_{zx} = \tau_{zy} = 0$), and that it is defined by the stress components σ_x , σ_y , and τ_{xy} associated with the element shown in Fig. 7.5a. We propose to determine the stress components $\sigma_{x'}$, $\sigma_{y'}$, and $\tau_{x'y'}$ associated with the element after it has been rotated through an angle θ about

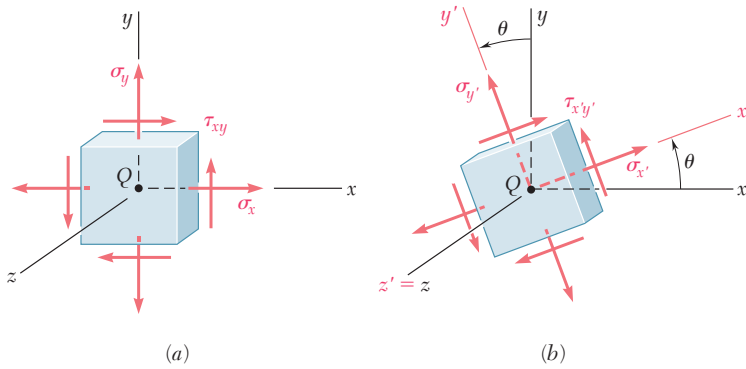


Fig. 7.5 (repeated)

the z axis (Fig. 7.5*b*), and to express these components in terms of σ_x , σ_y , τ_{xy} , and θ .

In order to determine the normal stress $\sigma_{x'}$ and the shearing stress $\tau_{x'y'}$ exerted on the face perpendicular to the x' axis, we consider a prismatic element with faces respectively perpendicular to the x , y , and x' axes (Fig. 7.6*a*). We observe that, if the area of the

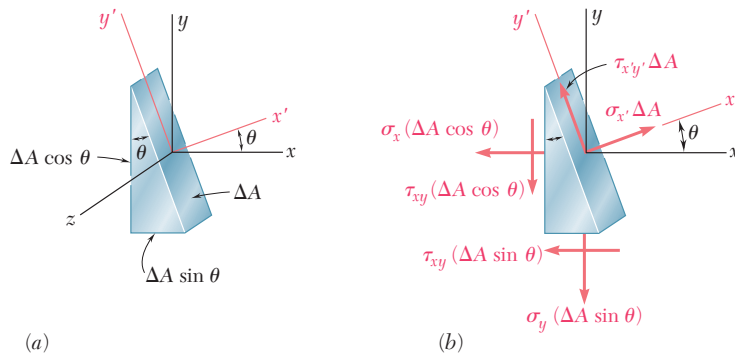


Fig. 7.6

oblique face is denoted by ΔA , the areas of the vertical and horizontal faces are respectively equal to $\Delta A \cos \theta$ and $\Delta A \sin \theta$. It follows that the *forces* exerted on the three faces are as shown in Fig. 7.6*b*. (No forces are exerted on the triangular faces of the element, since the corresponding normal and shearing stresses have all been assumed equal to zero.) Using components along the x' and y' axes, we write the following equilibrium equations:

$$\begin{aligned} \Sigma F_{x'} = 0: \quad & \sigma_{x'} \Delta A - \sigma_x (\Delta A \cos \theta) \cos \theta - \tau_{xy} (\Delta A \cos \theta) \sin \theta \\ & - \sigma_y (\Delta A \sin \theta) \sin \theta - \tau_{xy} (\Delta A \sin \theta) \cos \theta = 0 \end{aligned}$$

$$\begin{aligned} \Sigma F_{y'} = 0: \quad & \tau_{x'y'} \Delta A + \sigma_x (\Delta A \cos \theta) \sin \theta - \tau_{xy} (\Delta A \cos \theta) \cos \theta \\ & - \sigma_y (\Delta A \sin \theta) \cos \theta + \tau_{xy} (\Delta A \sin \theta) \sin \theta = 0 \end{aligned}$$

Solving the first equation for $\sigma_{x'}$ and the second for $\tau_{x'y'}$, we have

$$\sigma_{x'} = \sigma_x \cos^2 \theta + \sigma_y \sin^2 \theta + 2\tau_{xy} \sin \theta \cos \theta \quad (7.1)$$

$$\tau_{x'y'} = -(\sigma_x - \sigma_y) \sin \theta \cos \theta + \tau_{xy}(\cos^2 \theta - \sin^2 \theta) \quad (7.2)$$

Recalling the trigonometric relations

$$\sin 2\theta = 2 \sin \theta \cos \theta \quad \cos 2\theta = \cos^2 \theta - \sin^2 \theta \quad (7.3)$$

and

$$\cos^2 \theta = \frac{1 + \cos 2\theta}{2} \quad \sin^2 \theta = \frac{1 - \cos 2\theta}{2} \quad (7.4)$$

we write Eq. (7.1) as follows:

$$\sigma_{x'} = \sigma_x \frac{1 + \cos 2\theta}{2} + \sigma_y \frac{1 - \cos 2\theta}{2} + \tau_{xy} \sin 2\theta$$

or

$$\sigma_{x'} = \frac{\sigma_x + \sigma_y}{2} + \frac{\sigma_x - \sigma_y}{2} \cos 2\theta + \tau_{xy} \sin 2\theta \quad (7.5)$$

Using the relations (7.3), we write Eq. (7.2) as

$$\tau_{x'y'} = -\frac{\sigma_x - \sigma_y}{2} \sin 2\theta + \tau_{xy} \cos 2\theta \quad (7.6)$$

The expression for the normal stress $\sigma_{y'}$ is obtained by replacing θ in Eq. (7.5) by the angle $\theta + 90^\circ$ that the y' axis forms with the x axis. Since $\cos(2\theta + 180^\circ) = -\cos 2\theta$ and $\sin(2\theta + 180^\circ) = -\sin 2\theta$, we have

$$\sigma_{y'} = \frac{\sigma_x + \sigma_y}{2} - \frac{\sigma_x - \sigma_y}{2} \cos 2\theta - \tau_{xy} \sin 2\theta \quad (7.7)$$

Adding Eqs. (7.5) and (7.7) member to member, we obtain

$$\sigma_{x'} + \sigma_{y'} = \sigma_x + \sigma_y \quad (7.8)$$

Since $\sigma_z = \sigma_{z'} = 0$, we thus verify in the case of plane stress that the sum of the normal stresses exerted on a cubic element of material is independent of the orientation of that element.†

†Cf. first footnote on page 97.

7.3 PRINCIPAL STRESSES; MAXIMUM SHEARING STRESS

The equations (7.5) and (7.6) obtained in the preceding section are the parametric equations of a circle. This means that, if we choose a set of rectangular axes and plot a point M of abscissa $\sigma_{x'}$ and ordinate $\tau_{x'y'}$ for any given value of the parameter θ , all the points thus obtained will lie on a circle. To establish this property we eliminate θ from Eqs. (7.5) and (7.6); this is done by first transposing $(\sigma_x + \sigma_y)/2$ in Eq. (7.5) and squaring both members of the equation, then squaring both members of Eq. (7.6), and finally adding member to member the two equations obtained in this fashion. We have

$$\left(\sigma_{x'} - \frac{\sigma_x + \sigma_y}{2}\right)^2 + \tau_{x'y'}^2 = \left(\frac{\sigma_x - \sigma_y}{2}\right)^2 + \tau_{xy}^2 \quad (7.9)$$

Setting

$$\sigma_{\text{ave}} = \frac{\sigma_x + \sigma_y}{2} \quad \text{and} \quad R = \sqrt{\left(\frac{\sigma_x - \sigma_y}{2}\right)^2 + \tau_{xy}^2} \quad (7.10)$$

we write the identity (7.9) in the form

$$(\sigma_{x'} - \sigma_{\text{ave}})^2 + \tau_{x'y'}^2 = R^2 \quad (7.11)$$

which is the equation of a circle of radius R centered at the point C of abscissa σ_{ave} and ordinate 0 (Fig. 7.7). It can be observed that, due to the symmetry of the circle about the horizontal axis, the same result would have been obtained if, instead of plotting M , we had plotted a point N of abscissa $\sigma_{x'}$ and ordinate $-\tau_{x'y'}$ (Fig. 7.8). This property will be used in Sec. 7.4.

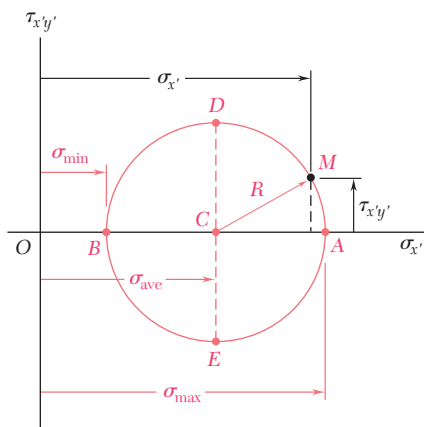


Fig. 7.7 Circular relationship of transformed stresses.

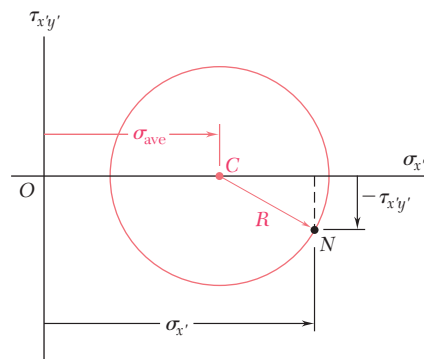


Fig. 7.8 Equivalent formation of stress transformation circle.

The two points A and B where the circle of Fig. 7.7 intersects the horizontal axis are of special interest: Point A corresponds to the maximum value of the normal stress $\sigma_{x'}$, while point B corresponds

to its minimum value. Besides, both points correspond to a zero value of the shearing stress $\tau_{x'y'}$. Thus, the values θ_p of the parameter θ which correspond to points A and B can be obtained by setting $\tau_{x'y'} = 0$ in Eq. (7.6). We write†

$$\tan 2\theta_p = \frac{2\tau_{xy}}{\sigma_x - \sigma_y} \quad (7.12)$$

This equation defines two values $2\theta_p$ that are 180° apart, and thus two values θ_p that are 90° apart. Either of these values can be used to determine the orientation of the corresponding element (Fig. 7.9).

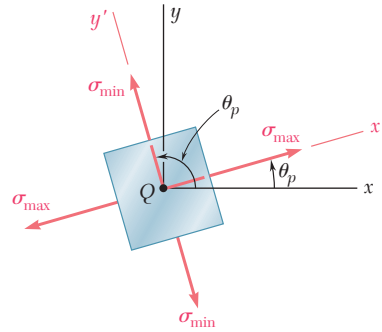


Fig. 7.9 Principal stresses.

The planes containing the faces of the element obtained in this way are called the *principal planes of stress* at point Q , and the corresponding values σ_{\max} and σ_{\min} of the normal stress exerted on these planes are called the *principal stresses* at Q . Since the two values θ_p defined by Eq. (7.12) were obtained by setting $\tau_{x'y'} = 0$ in Eq. (7.6), it is clear that no shearing stress is exerted on the principal planes.

We observe from Fig. 7.7 that

$$\sigma_{\max} = \sigma_{\text{ave}} + R \quad \text{and} \quad \sigma_{\min} = \sigma_{\text{ave}} - R \quad (7.13)$$

Substituting for σ_{ave} and R from Eq. (7.10), we write

$$\sigma_{\max, \min} = \frac{\sigma_x + \sigma_y}{2} \pm \sqrt{\left(\frac{\sigma_x - \sigma_y}{2}\right)^2 + \tau_{xy}^2} \quad (7.14)$$

Unless it is possible to tell by inspection which of the two principal planes is subjected to σ_{\max} and which is subjected to σ_{\min} , it is necessary to substitute one of the values θ_p into Eq. (7.5) in order to determine which of the two corresponds to the maximum value of the normal stress.

Referring again to the circle of Fig. 7.7, we note that the points D and E located on the vertical diameter of the circle correspond to

†This relation can also be obtained by differentiating $\sigma_{x'}$ in Eq. (7.5) and setting the derivative equal to zero: $d\sigma_{x'}/d\theta = 0$.

the largest numerical value of the shearing stress $\tau_{x'y'}$. Since the abscissa of points D and E is $\sigma_{\text{ave}} = (\sigma_x + \sigma_y)/2$, the values θ_s of the parameter θ corresponding to these points are obtained by setting $\sigma_{x'} = (\sigma_x + \sigma_y)/2$ in Eq. (7.5). It follows that the sum of the last two terms in that equation must be zero. Thus, for $\theta = \theta_s$, we write†

$$\frac{\sigma_x - \sigma_y}{2} \cos 2\theta_s + \tau_{xy} \sin 2\theta_s = 0$$

or

$$\tan 2\theta_s = -\frac{\sigma_x - \sigma_y}{2\tau_{xy}} \quad (7.15)$$

This equation defines two values $2\theta_s$ that are 180° apart, and thus two values θ_s that are 90° apart. Either of these values can be used to determine the orientation of the element corresponding to the maximum shearing stress (Fig. 7.10). Observing from Fig. 7.7 that the maximum value of the shearing stress is equal to the radius R of the circle, and recalling the second of Eqs. (7.10), we write

$$\tau_{\text{max}} = \sqrt{\left(\frac{\sigma_x - \sigma_y}{2}\right)^2 + \tau_{xy}^2} \quad (7.16)$$

As observed earlier, the normal stress corresponding to the condition of maximum shearing stress is

$$\sigma' = \sigma_{\text{ave}} = \frac{\sigma_x + \sigma_y}{2} \quad (7.17)$$

Comparing Eqs. (7.12) and (7.15), we note that $\tan 2\theta_s$ is the negative reciprocal of $\tan 2\theta_p$. This means that the angles $2\theta_s$ and $2\theta_p$ are 90° apart and, therefore, that the angles θ_s and θ_p are 45° apart. We thus conclude that *the planes of maximum shearing stress are at 45° to the principal planes*. This confirms the results obtained earlier in Sec. 1.12 in the case of a centric axial loading (Fig. 1.38) and in Sec. 3.4 in the case of a torsional loading (Fig. 3.19.)

We should be aware that our analysis of the transformation of plane stress has been limited to rotations *in the plane of stress*. If the cubic element of Fig. 7.5 is rotated about an axis other than the z axis, its faces may be subjected to shearing stresses larger than the stress defined by Eq. (7.16). As you will see in Sec. 7.5, this occurs when the principal stresses defined by Eq. (7.14) have the same sign, i.e., when they are either both tensile or both compressive. In such cases, the value given by Eq. (7.16) is referred to as the maximum *in-plane* shearing stress.

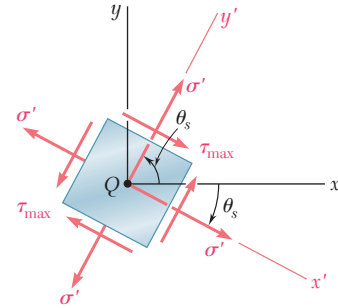


Fig. 7.10 Maximum shearing stress.

†This relation may also be obtained by differentiating $\tau_{x'y'}$ in Eq. (7.6) and setting the derivative equal to zero: $d\tau_{x'y'}/d\theta = 0$.

EXAMPLE 7.01

For the state of plane stress shown in Fig. 7.11, determine (a) the principal planes, (b) the principal stresses, (c) the maximum shearing stress and the corresponding normal stress.

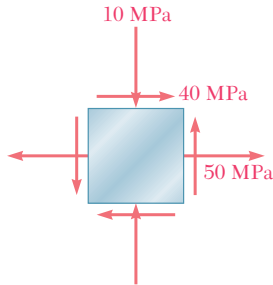


Fig. 7.11

(a) Principal Planes. Following the usual sign convention, we write the stress components as

$$\sigma_x = +50 \text{ MPa} \quad \sigma_y = -10 \text{ MPa} \quad \tau_{xy} = +40 \text{ MPa}$$

Substituting into Eq. (7.12), we have

$$\begin{aligned} \tan 2\theta_p &= \frac{2\tau_{xy}}{\sigma_x - \sigma_y} = \frac{2(+40)}{50 - (-10)} = \frac{80}{60} \\ 2\theta_p &= 53.1^\circ \quad \text{and} \quad 180^\circ + 53.1^\circ = 233.1^\circ \\ \theta_p &= 26.6^\circ \quad \text{and} \quad 116.6^\circ \end{aligned}$$

(b) Principal Stresses. Formula (7.14) yields

$$\begin{aligned} \sigma_{\max, \min} &= \frac{\sigma_x + \sigma_y}{2} \pm \sqrt{\left(\frac{\sigma_x - \sigma_y}{2}\right)^2 + \tau_{xy}^2} \\ &= 20 \pm \sqrt{(30)^2 + (40)^2} \\ \sigma_{\max} &= 20 + 50 = 70 \text{ MPa} \\ \sigma_{\min} &= 20 - 50 = -30 \text{ MPa} \end{aligned}$$

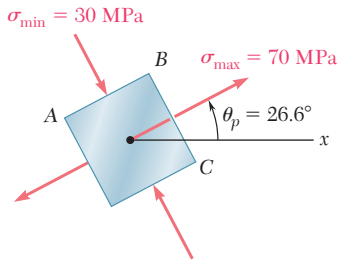


Fig. 7.12

The principal planes and principal stresses are sketched in Fig. 7.12. Making $\theta = 26.6^\circ$ in Eq. (7.5), we check that the normal stress exerted on face BC of the element is the maximum stress:

$$\begin{aligned} \sigma_{x'} &= \frac{50 - 10}{2} + \frac{50 + 10}{2} \cos 53.1^\circ + 40 \sin 53.1^\circ \\ &= 20 + 30 \cos 53.1^\circ + 40 \sin 53.1^\circ = 70 \text{ MPa} = \sigma_{\max} \end{aligned}$$

(c) Maximum Shearing Stress. Formula (7.16) yields

$$\tau_{\max} = \sqrt{\left(\frac{\sigma_x - \sigma_y}{2}\right)^2 + \tau_{xy}^2} = \sqrt{(30)^2 + (40)^2} = 50 \text{ MPa}$$

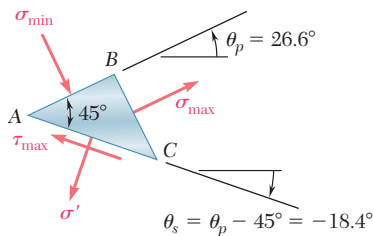


Fig. 7.13

Since σ_{\max} and σ_{\min} have opposite signs, the value obtained for τ_{\max} actually represents the maximum value of the shearing stress at the point considered. The orientation of the planes of maximum shearing stress and the sense of the shearing stresses are best determined by passing a section along the diagonal plane AC of the element of Fig. 7.12. Since the faces AB and BC of the element are contained in the principal planes, the diagonal plane AC must be one of the planes of maximum shearing stress (Fig. 7.13). Furthermore, the equilibrium conditions for the prismatic element ABC require that the shearing stress exerted on AC be directed as shown. The cubic element corresponding to the maximum shearing stress is shown in Fig. 7.14. The normal stress on each of the four faces of the element is given by Eq. (7.17):

$$\sigma' = \sigma_{\text{ave}} = \frac{\sigma_x + \sigma_y}{2} = \frac{50 - 10}{2} = 20 \text{ MPa}$$

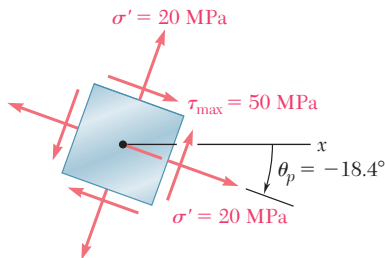
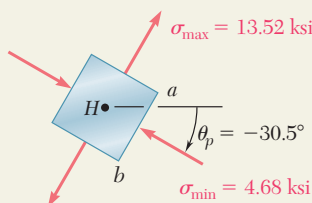
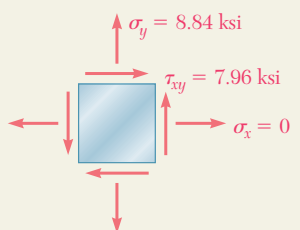
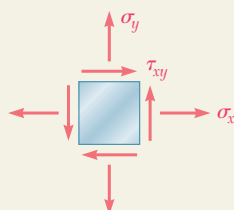
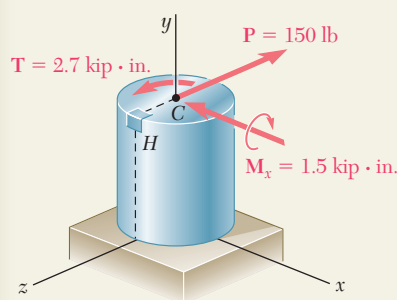
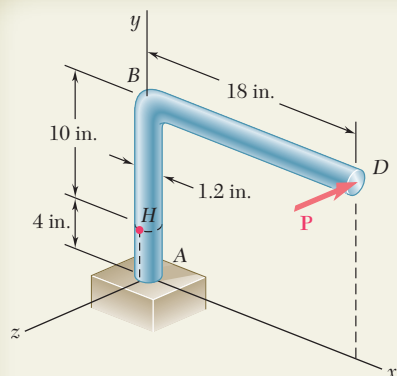


Fig. 7.14



SAMPLE PROBLEM 7.1

A single horizontal force \mathbf{P} of magnitude 150 lb is applied to end D of lever ABD . Knowing that portion AB of the lever has a diameter of 1.2 in., determine (a) the normal and shearing stresses on an element located at point H and having sides parallel to the x and y axes, (b) the principal planes and the principal stresses at point H .

SOLUTION

Force-Couple System. We replace the force \mathbf{P} by an equivalent force-couple system at the center C of the transverse section containing point H :

$$P = 150 \text{ lb} \quad T = (150 \text{ lb})(18 \text{ in.}) = 2.7 \text{ kip} \cdot \text{in.}$$

$$M_x = (150 \text{ lb})(10 \text{ in.}) = 1.5 \text{ kip} \cdot \text{in.}$$

a. Stresses σ_x , σ_y , τ_{xy} at Point H . Using the sign convention shown in Fig. 7.2, we determine the sense and the sign of each stress component by carefully examining the sketch of the force-couple system at point C :

$$\sigma_x = 0 \quad \sigma_y = +\frac{Mc}{I} = +\frac{(1.5 \text{ kip} \cdot \text{in.})(0.6 \text{ in.})}{\frac{1}{4}\pi (0.6 \text{ in.})^4} \quad \sigma_y = +8.84 \text{ ksi} \quad \blacktriangleleft$$

$$\tau_{xy} = +\frac{Tc}{J} = +\frac{(2.7 \text{ kip} \cdot \text{in.})(0.6 \text{ in.})}{\frac{1}{2}\pi (0.6 \text{ in.})^4} \quad \tau_{xy} = +7.96 \text{ ksi} \quad \blacktriangleleft$$

We note that the shearing force \mathbf{P} does not cause any shearing stress at point H .

b. Principal Planes and Principal Stresses. Substituting the values of the stress components into Eq. (7.12), we determine the orientation of the principal planes:

$$\tan 2\theta_p = \frac{2\tau_{xy}}{\sigma_x - \sigma_y} = \frac{2(7.96)}{0 - 8.84} = -1.80$$

$$2\theta_p = -61.0^\circ \quad \text{and} \quad 180^\circ - 61.0^\circ = +119^\circ$$

$$\theta_p = -30.5^\circ \quad \text{and} \quad +59.5^\circ \quad \blacktriangleleft$$

Substituting into Eq. (7.14), we determine the magnitudes of the principal stresses:

$$\sigma_{\max, \min} = \frac{\sigma_x + \sigma_y}{2} \pm \sqrt{\left(\frac{\sigma_x - \sigma_y}{2}\right)^2 + \tau_{xy}^2}$$

$$= \frac{0 + 8.84}{2} \pm \sqrt{\left(\frac{0 - 8.84}{2}\right)^2 + (7.96)^2} = +4.42 \pm 9.10$$

$$\sigma_{\max} = +13.52 \text{ ksi} \quad \blacktriangleleft$$

$$\sigma_{\min} = -4.68 \text{ ksi} \quad \blacktriangleleft$$

Considering face ab of the element shown, we make $\theta_p = -30.5^\circ$ in Eq. (7.5) and find $\sigma_{x'} = -4.68 \text{ ksi}$. We conclude that the principal stresses are as shown.

PROBLEMS

7.1 through 7.4 For the given state of stress, determine the normal and shearing stresses exerted on the oblique face of the shaded triangular element shown. Use a method of analysis based on the equilibrium of that element, as was done in the derivations of Sec. 7.2.

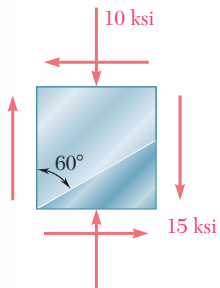


Fig. P7.1

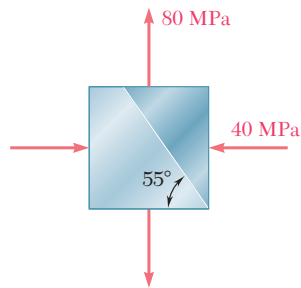


Fig. P7.2

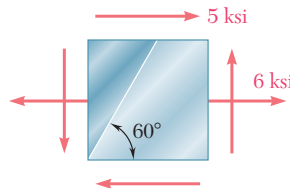


Fig. P7.3

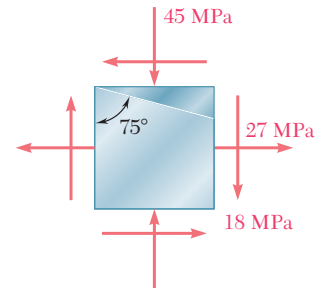


Fig. P7.4

7.5 through 7.8 For the given state of stress, determine (a) the principal planes, (b) the principal stresses.

7.9 through 7.12 For the given state of stress, determine (a) the orientation of the planes of maximum in-plane shearing stress, (b) the maximum in-plane shearing stress, (c) the corresponding normal stress.

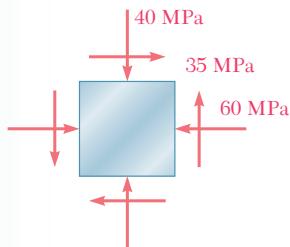


Fig. P7.5 and P7.9

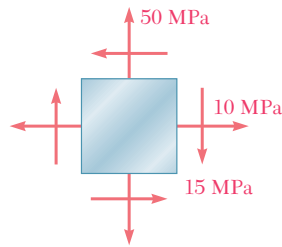


Fig. P7.6 and P7.10

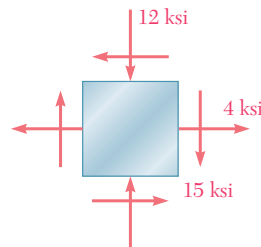


Fig. P7.7 and P7.11

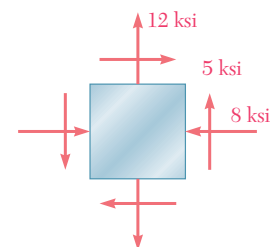


Fig. P7.8 and P7.12

7.13 through 7.16 For the given state of stress, determine the normal and shearing stresses after the element shown has been rotated through (a) 25° clockwise, (b) 10° counterclockwise.

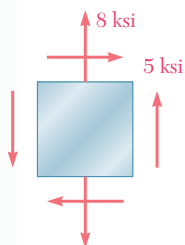


Fig. P7.13

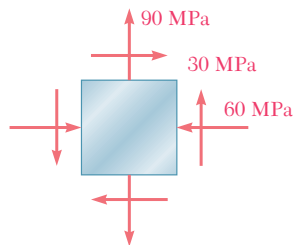


Fig. P7.14

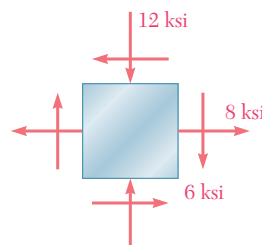


Fig. P7.15

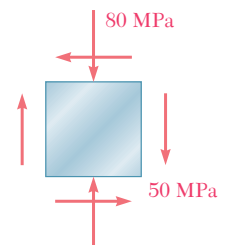


Fig. P7.16

- 7.17 and 7.18** The grain of a wooden member forms an angle of 15° with the vertical. For the state of stress shown, determine (a) the in-plane shearing stress parallel to the grain, (b) the normal stress perpendicular to the grain.

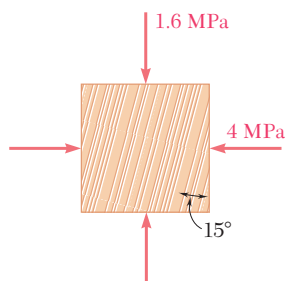


Fig. P7.17

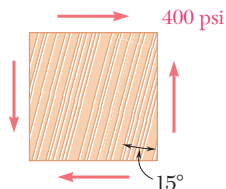


Fig. P7.18

- 7.19** A steel pipe of 12-in. outer diameter is fabricated from $\frac{1}{4}$ -in.-thick plate by welding along a helix that forms an angle of 22.5° with a plane perpendicular to the axis of the pipe. Knowing that a 40-kip axial force \mathbf{P} and an 80-kip \cdot in. torque \mathbf{T} , each directed as shown, are applied to the pipe, determine σ and τ in directions, respectively, normal and tangential to the weld.

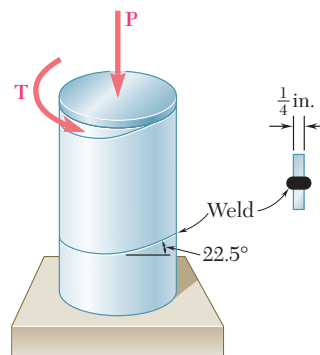


Fig. P7.19

- 7.20** Two members of uniform cross section 50×80 mm are glued together along plane $a-a$ that forms an angle of 25° with the horizontal. Knowing that the allowable stresses for the glued joint are $\sigma = 800$ kPa and $\tau = 600$ kPa, determine the largest centric load \mathbf{P} that can be applied.

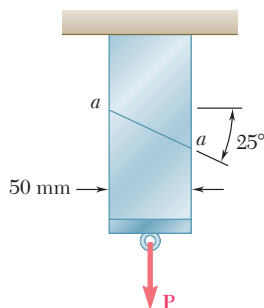


Fig. P7.20

- 7.21** Two steel plates of uniform cross section 10×80 mm are welded together as shown. Knowing that centric 100-kN forces are applied to the welded plates and that $\beta = 25^\circ$, determine (a) the in-plane shearing stress parallel to the weld, (b) the normal stress perpendicular to the weld.

- 7.22** Two steel plates of uniform cross section 10×80 mm are welded together as shown. Knowing that centric 100-kN forces are applied to the welded plates and that the in-plane shearing stress parallel to the weld is 30 MPa, determine (a) the angle β , (b) the corresponding normal stress perpendicular to the weld.

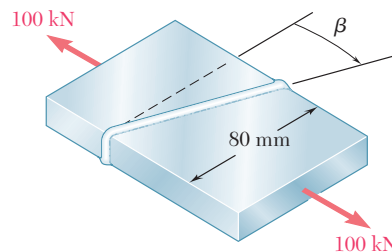


Fig. P7.21 and P7.22

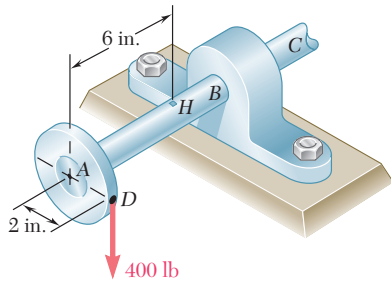


Fig. P7.23

7.23 A 400-lb vertical force is applied at D to a gear attached to the solid 1-in. diameter shaft AB . Determine the principal stresses and the maximum shearing stress at point H located as shown on top of the shaft.

7.24 A mechanic uses a crowfoot wrench to loosen a bolt at E . Knowing that the mechanic applies a vertical 24-lb force at A , determine the principal stresses and the maximum shearing stress at point H located as shown on top of the $\frac{3}{4}$ -in. diameter shaft.

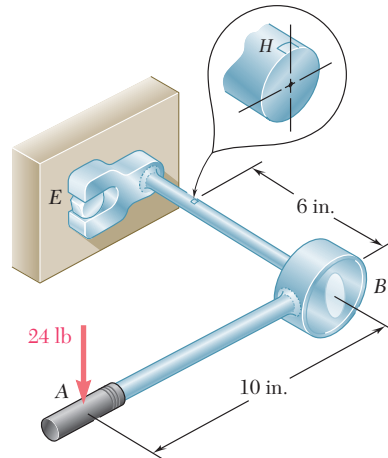


Fig. P7.24

7.25 The steel pipe AB has a 102-mm outer diameter and a 6-mm wall thickness. Knowing that arm CD is rigidly attached to the pipe, determine the principal stresses and the maximum shearing stress at point K .

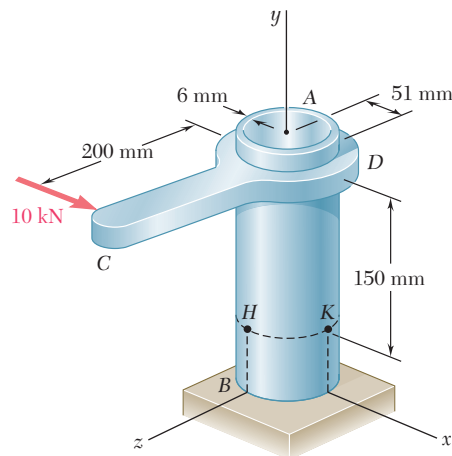


Fig. P7.25

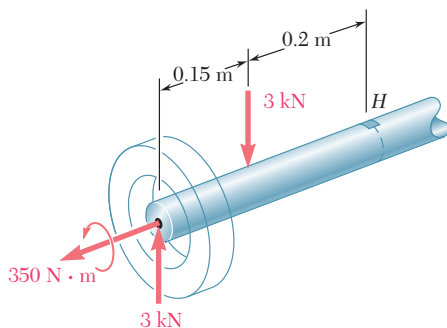


Fig. P7.26

7.26 The axle of an automobile is acted upon by the forces and couple shown. Knowing that the diameter of the solid axle is 32 mm, determine (a) the principal planes and principal stresses at point H located on top of the axle, (b) the maximum shearing stress at the same point.

- 7.27** For the state of plane stress shown, determine (a) the largest value of τ_{xy} for which the maximum in-plane shearing stress is equal to or less than 12 ksi, (b) the corresponding principal stresses.

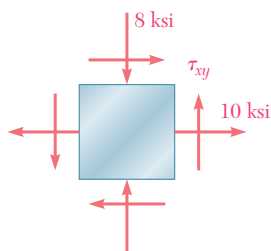


Fig. P7.27

- 7.28** For the state of plane stress shown, determine the largest value of σ_y for which the maximum in-plane shearing stress is equal to or less than 75 MPa.

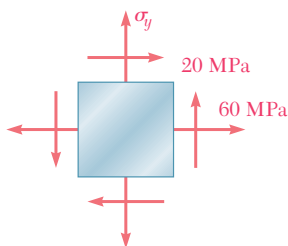


Fig. P7.28

- 7.29** Determine the range of values of σ_x for which the maximum in-plane shearing stress is equal to or less than 10 ksi.

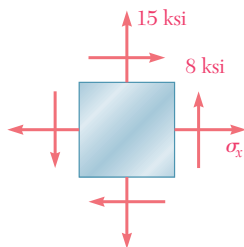


Fig. P7.29

- 7.30** For the state of plane stress shown, determine (a) the value of τ_{xy} for which the in-plane shearing stress parallel to the weld is zero, (b) the corresponding principal stresses.

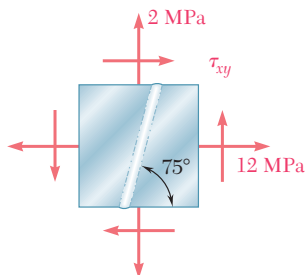


Fig. P7.30

7.4 MOHR'S CIRCLE FOR PLANE STRESS

The circle used in the preceding section to derive some of the basic formulas relating to the transformation of plane stress was first introduced by the German engineer Otto Mohr (1835–1918) and is known as *Mohr's circle* for plane stress. As you will see presently, this circle can be used to obtain an alternative method for the solution of the various problems considered in Secs. 7.2 and 7.3. This method is based on simple geometric considerations and does not require the use of specialized formulas. While originally designed for graphical solutions, it lends itself well to the use of a calculator.

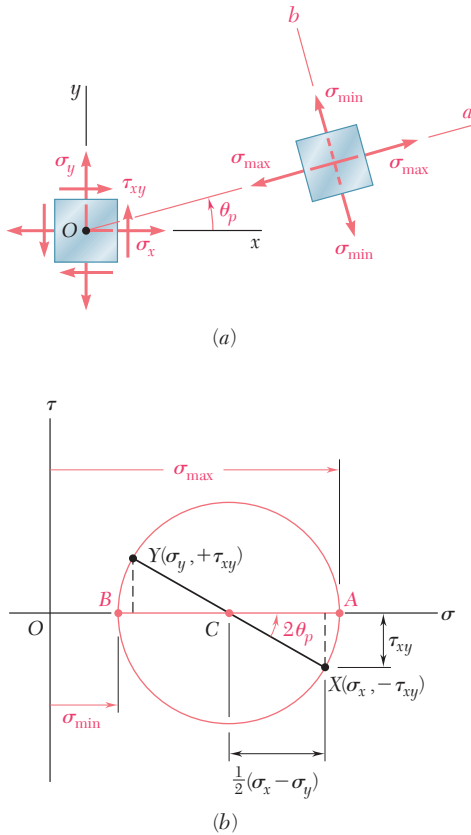


Fig. 7.15 Mohr's circle.

Consider a square element of a material subjected to plane stress (Fig. 7.15a), and let σ_x , σ_y , and τ_{xy} be the components of the stress exerted on the element. We plot a point X of coordinates σ_x and $-\tau_{xy}$, and a point Y of coordinates σ_y and $+\tau_{xy}$ (Fig. 7.15b). If τ_{xy} is positive, as assumed in Fig. 7.15a, point X is located below the σ axis and point Y above, as shown in Fig. 7.15b. If τ_{xy} is negative, X is located above the σ axis and Y below. Joining X and Y by a straight line, we define the point C of intersection of line XY with the σ axis and draw the circle of center C and diameter XY . Noting that the abscissa of C and the radius of the circle are respectively equal to the quantities σ_{ave} and R defined by Eqs. (7.10), we conclude that the circle obtained is Mohr's circle for plane stress. Thus the abscissas of points A and B where the circle intersects the σ axis represent respectively the principal stresses σ_{max} and σ_{min} at the point considered.

We also note that, since $\tan(XCA) = 2\tau_{xy}/(\sigma_x - \sigma_y)$, the angle XCA is equal in magnitude to one of the angles $2\theta_p$ that satisfy Eq. (7.12). Thus, the angle θ_p that defines in Fig. 7.15a the orientation of the principal plane corresponding to point A in Fig. 7.15b can be obtained by dividing in half the angle XCA measured on Mohr's circle. We further observe that if $\sigma_x > \sigma_y$ and $\tau_{xy} > 0$, as in the case considered here, the rotation that brings CX into CA is counterclockwise. But, in that case, the angle θ_p obtained from Eq. (7.12) and defining the direction of the normal Oa to the principal plane is positive; thus, the rotation bringing Ox into Oa is also counterclockwise. We conclude that the senses of rotation in both parts of Fig. 7.15 are the same; if a counterclockwise rotation through $2\theta_p$ is required to bring CX into CA on Mohr's circle, a counterclockwise rotation through θ_p will bring Ox into Oa in Fig. 7.15a.†

Since Mohr's circle is uniquely defined, the same circle can be obtained by considering the stress components $\sigma_{x'}$, $\sigma_{y'}$, and $\tau_{x'y'}$, corresponding to the x' and y' axes shown in Fig. 7.16a. The point X' of coordinates $\sigma_{x'}$ and $-\tau_{x'y'}$, and the point Y' of coordinates $\sigma_{y'}$ and $+\tau_{x'y'}$, are therefore located on Mohr's circle, and the angle $X'CA$ in Fig. 7.16b must be equal to twice the angle $x'Oa$ in Fig. 7.16a. Since, as noted before, the angle XCA is twice the angle xOa , it follows that

†This is due to the fact that we are using the circle of Fig. 7.8 rather than the circle of Fig. 7.7 as Mohr's circle.

the angle XCX' in Fig. 7.16*b* is twice the angle xOx' in Fig. 7.16*a*. Thus the diameter $X'Y'$ defining the normal and shearing stresses $\sigma_{x'}$, $\sigma_{y'}$, and $\tau_{x'y'}$ can be obtained by rotating the diameter XY through an angle equal to twice the angle θ formed by the x' and x axes in Fig. 7.16*a*. We note that the rotation that brings the diameter XY into the diameter $X'Y'$ in Fig. 7.16*b* has the same sense as the rotation that brings the xy axes into the $x'y'$ axes in Fig. 7.16*a*.

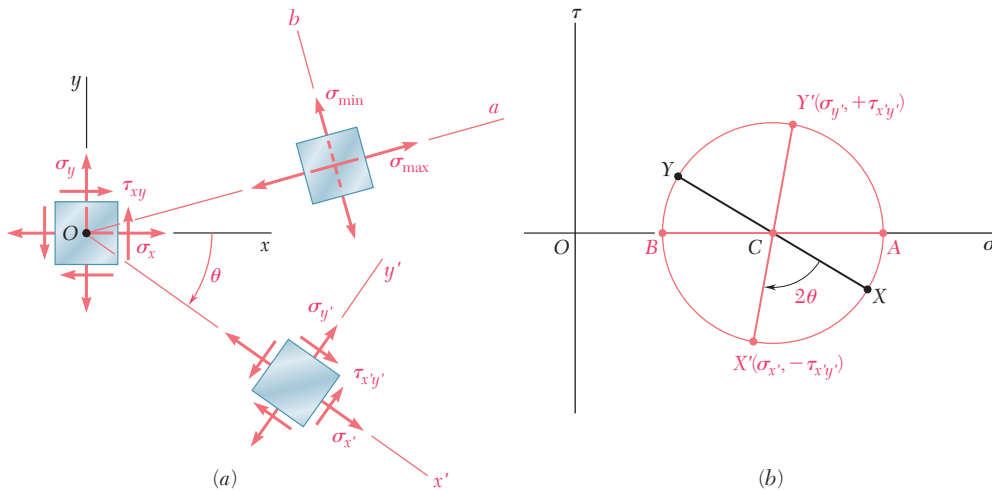


Fig. 7.16

The property we have just indicated can be used to verify the fact that the planes of maximum shearing stress are at 45° to the principal planes. Indeed, we recall that points D and E on Mohr's circle correspond to the planes of maximum shearing stress, while A and B correspond to the principal planes (Fig. 7.17*b*). Since the diameters AB and DE of Mohr's circle are at 90° to each other, it follows that the faces of the corresponding elements are at 45° to each other (Fig. 7.17*a*).

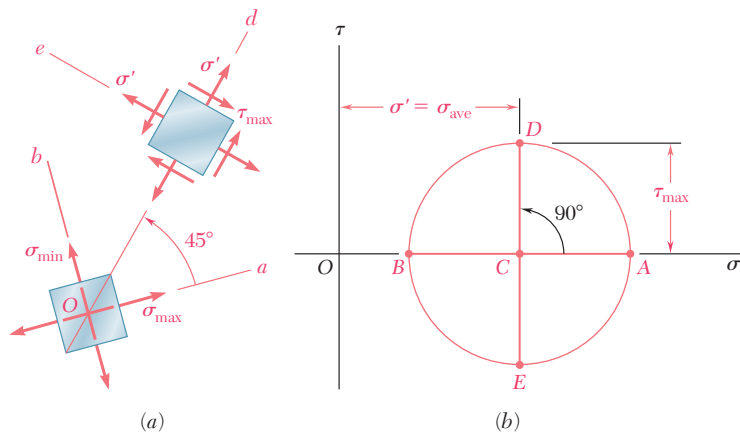


Fig. 7.17

The construction of Mohr's circle for plane stress is greatly simplified if we consider separately each face of the element used to define the stress components. From Figs. 7.15 and 7.16 we observe that, when the shearing stress exerted on a *given face* tends to rotate the element *clockwise*, the point on Mohr's circle corresponding to that face is located *above* the σ axis. When the shearing stress on a given face tends to rotate the element *counterclockwise*, the point corresponding to that face is located *below* the σ axis (Fig. 7.18).† As far as the normal stresses are concerned, the usual convention holds, i.e., a tensile stress is considered as positive and is plotted to the right, while a compressive stress is considered as negative and is plotted to the left.

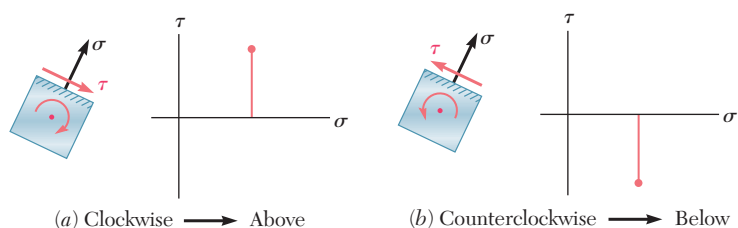


Fig. 7.18 Convention for plotting shearing stress on Mohr's circle.

EXAMPLE 7.02

For the state of plane stress already considered in Example 7.01, (a) construct Mohr's circle, (b) determine the principal stresses, (c) determine the maximum shearing stress and the corresponding normal stress.

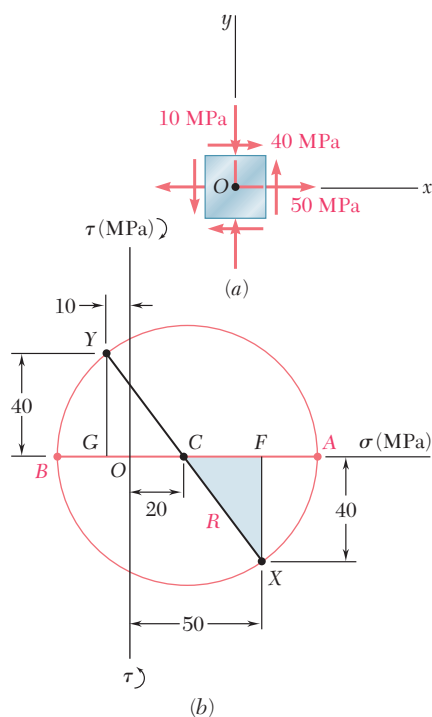


Fig. 7.19

(a) Construction of Mohr's Circle.

We note from Fig. 7.19a that the normal stress exerted on the face oriented toward the x axis is tensile (positive) and that the shearing stress exerted on that face tends to rotate the element counterclockwise. Point X of Mohr's circle, therefore, will be plotted to the right of the vertical axis and below the horizontal axis (Fig. 7.19b). A similar inspection of the normal stress and shearing stress exerted on the upper face of the element shows that point Y should be plotted to the left of the vertical axis and above the horizontal axis. Drawing the line XY, we obtain the center C of Mohr's circle; its abscissa is

$$\sigma_{\text{ave}} = \frac{\sigma_x + \sigma_y}{2} = \frac{50 + (-10)}{2} = 20 \text{ MPa}$$

Since the sides of the shaded triangle are

$$CF = 50 - 20 = 30 \text{ MPa} \quad \text{and} \quad FX = 40 \text{ MPa}$$

the radius of the circle is

$$R = CX = \sqrt{(30)^2 + (40)^2} = 50 \text{ MPa}$$

†The following jingle is helpful in remembering this convention. "In the kitchen, the *clock* is above, and the *counter* is below."

(b) Principal Planes and Principal Stresses. The principal stresses are

$$\sigma_{\max} = OA = OC + CA = 20 + 50 = 70 \text{ MPa}$$

$$\sigma_{\min} = OB = OC - BC = 20 - 50 = -30 \text{ MPa}$$

Recalling that the angle ACX represents $2\theta_p$ (Fig. 7.19b), we write

$$\tan 2\theta_p = \frac{FX}{CF} = \frac{40}{30}$$

$$2\theta_p = 53.1^\circ \quad \theta_p = 26.6^\circ$$

Since the rotation which brings CX into CA in Fig. 7.20b is counterclockwise, the rotation that brings Ox into the axis Oa corresponding to σ_{\max} in Fig. 7.20a is also counterclockwise.

(c) Maximum Shearing Stress. Since a further rotation of 90° counterclockwise brings CA into CD in Fig. 7.20b, a further rotation of 45° counterclockwise will bring the axis Oa into the axis Od corresponding to the maximum shearing stress in Fig. 7.20a. We note from Fig. 7.20b that $\tau_{\max} = R = 50 \text{ MPa}$ and that the corresponding normal stress is $\sigma' = \sigma_{\text{ave}} = 20 \text{ MPa}$. Since point D is located above the σ axis in Fig. 7.20b, the shearing stresses exerted on the faces perpendicular to Od in Fig. 7.20a must be directed so that they will tend to rotate the element clockwise.

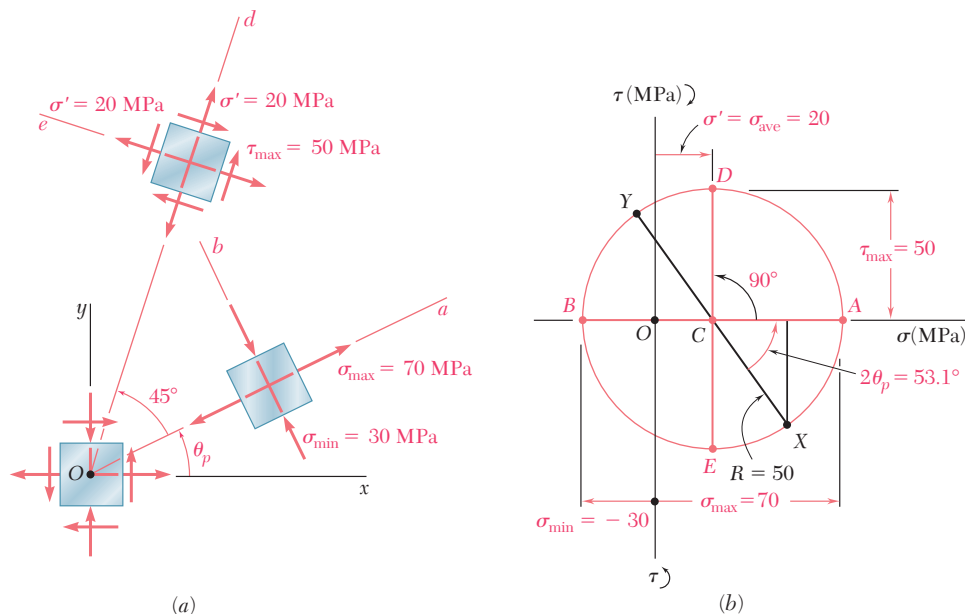


Fig. 7.20

Mohr's circle provides a convenient way of checking the results obtained earlier for stresses under a centric axial loading (Sec. 1.12) and under a torsional loading (Sec. 3.4). In the first case (Fig. 7.21a), we have $\sigma_x = P/A$, $\sigma_y = 0$, and $\tau_{xy} = 0$. The corresponding points X and Y define a circle of radius $R = P/2A$ that passes through the

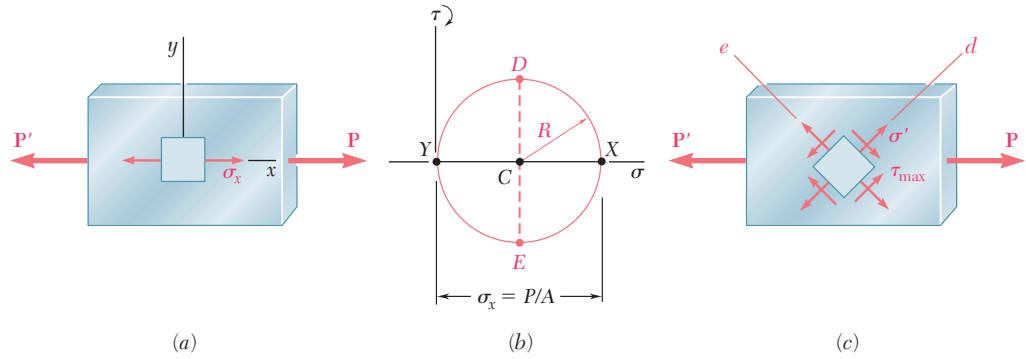


Fig. 7.21 Mohr's circle for centric axial loading.

origin of coordinates (Fig. 7.21b). Points D and E yield the orientation of the planes of maximum shearing stress (Fig. 7.21c), as well as the values of τ_{\max} and of the corresponding normal stresses σ' :

$$\tau_{\max} = \sigma' = R = \frac{P}{2A} \quad (7.18)$$

In the case of torsion (Fig. 7.22a), we have $\sigma_x = \sigma_y = 0$ and $\tau_{xy} = \tau_{\max} = Tc/J$. Points X and Y , therefore, are located on the τ axis,

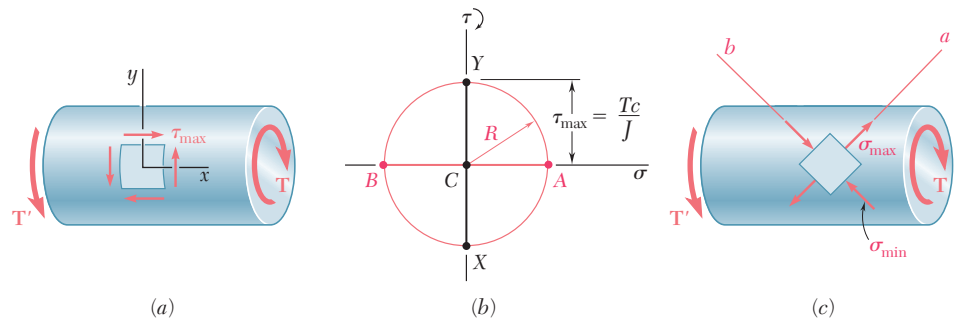
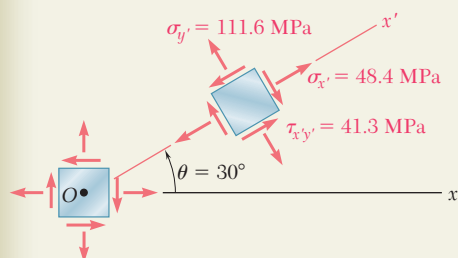
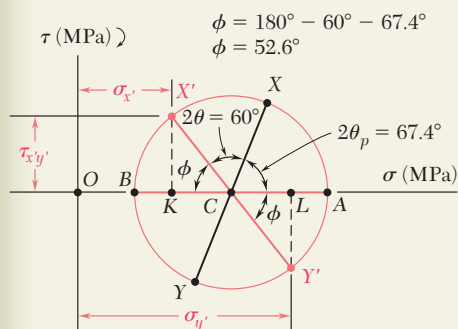
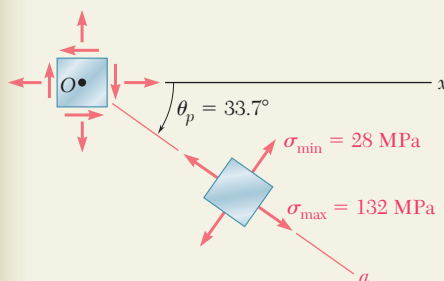
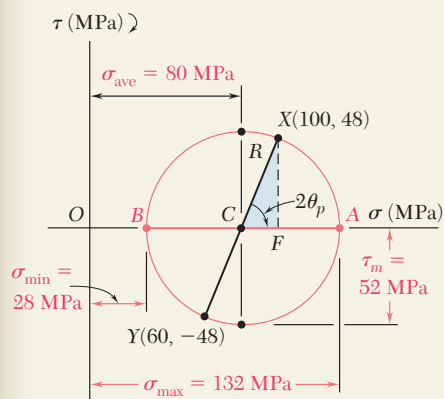
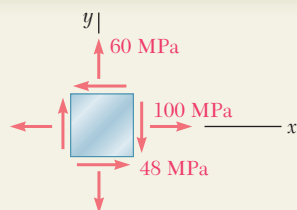


Fig. 7.22 Mohr's circle for torsional loading.

and Mohr's circle is a circle of radius $R = Tc/J$ centered at the origin (Fig. 7.22b). Points A and B define the principal planes (Fig. 7.22c) and the principal stresses:

$$\sigma_{\max, \min} = \pm R = \pm \frac{Tc}{J} \quad (7.19)$$



SAMPLE PROBLEM 7.2

For the state of plane stress shown, determine (a) the principal planes and the principal stresses, (b) the stress components exerted on the element obtained by rotating the given element counterclockwise through 30° .

SOLUTION

Construction of Mohr's Circle. We note that on a face perpendicular to the x axis, the normal stress is tensile and the shearing stress tends to rotate the element clockwise; thus, we plot X at a point 100 units to the right of the vertical axis and 48 units above the horizontal axis. In a similar fashion, we examine the stress components on the upper face and plot point $Y(60, -48)$. Joining points X and Y by a straight line, we define the center C of Mohr's circle. The abscissa of C , which represents σ_{ave} , and the radius R of the circle can be measured directly or calculated as follows:

$$\sigma_{ave} = OC = \frac{1}{2}(\sigma_x + \sigma_y) = \frac{1}{2}(100 + 60) = 80 \text{ MPa}$$

$$R = \sqrt{(CF)^2 + (FX)^2} = \sqrt{(20)^2 + (48)^2} = 52 \text{ MPa}$$

a. Principal Planes and Principal Stresses. We rotate the diameter XY clockwise through $2\theta_p$ until it coincides with the diameter AB . We have

$$\tan 2\theta_p = \frac{XF}{CF} = \frac{48}{20} = 2.4 \quad 2\theta_p = 67.4^\circ \quad \theta_p = 33.7^\circ$$

The principal stresses are represented by the abscissas of points A and B :

$$\sigma_{max} = OA = OC + CA = 80 + 52 \quad \sigma_{max} = +132 \text{ MPa}$$

$$\sigma_{min} = OB = OC - BC = 80 - 52 \quad \sigma_{min} = +28 \text{ MPa}$$

Since the rotation that brings XY into AB is clockwise, the rotation that brings Ox into the axis Oa corresponding to σ_{max} is also clockwise; we obtain the orientation shown for the principal planes.

b. Stress Components on Element Rotated 30° . Points X' and Y' on Mohr's circle that correspond to the stress components on the rotated element are obtained by rotating XY counterclockwise through $2\theta = 60^\circ$. We find

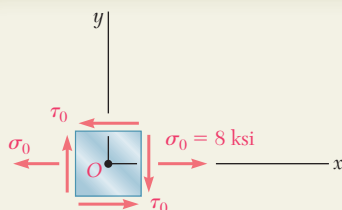
$$\phi = 180^\circ - 60^\circ - 67.4^\circ \quad \phi = 52.6^\circ$$

$$\sigma_{x'} = OK = OC - KC = 80 - 52 \cos 52.6^\circ \quad \sigma_{x'} = +48.4 \text{ MPa}$$

$$\sigma_{y'} = OL = OC + CL = 80 + 52 \cos 52.6^\circ \quad \sigma_{y'} = +111.6 \text{ MPa}$$

$$\tau_{x'y'} = KX' = 52 \sin 52.6^\circ \quad \tau_{x'y'} = 41.3 \text{ MPa}$$

Since X' is located above the horizontal axis, the shearing stress on the face perpendicular to Ox' tends to rotate the element clockwise.



SAMPLE PROBLEM 7.3

A state of plane stress consists of a tensile stress $\sigma_0 = 8$ ksi exerted on vertical surfaces and of unknown shearing stresses. Determine (a) the magnitude of the shearing stress τ_0 for which the largest normal stress is 10 ksi, (b) the corresponding maximum shearing stress.

SOLUTION

Construction of Mohr's Circle. We assume that the shearing stresses act in the senses shown. Thus, the shearing stress τ_0 on a face perpendicular to the x axis tends to rotate the element clockwise and we plot the point X of coordinates 8 ksi and τ_0 above the horizontal axis. Considering a horizontal face of the element, we observe that $\sigma_y = 0$ and that τ_0 tends to rotate the element counterclockwise; thus, we plot point Y at a distance τ_0 below O .

We note that the abscissa of the center C of Mohr's circle is

$$\sigma_{\text{ave}} = \frac{1}{2}(\sigma_x + \sigma_y) = \frac{1}{2}(8 + 0) = 4 \text{ ksi}$$

The radius R of the circle is determined by observing that the maximum normal stress, $\sigma_{\text{max}} = 10$ ksi, is represented by the abscissa of point A and writing

$$\begin{aligned}\sigma_{\text{max}} &= \sigma_{\text{ave}} + R \\ 10 \text{ ksi} &= 4 \text{ ksi} + R \quad R = 6 \text{ ksi}\end{aligned}$$

a. Shearing Stress τ_0 . Considering the right triangle CFX , we find

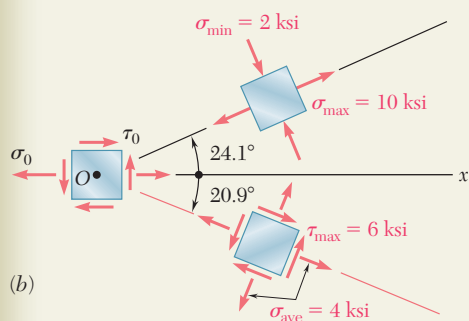
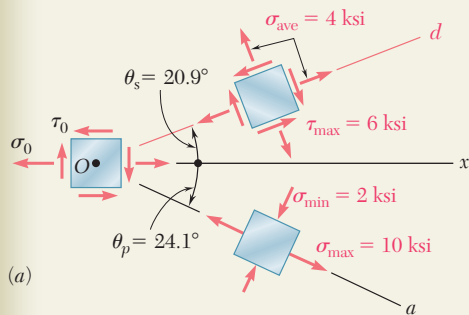
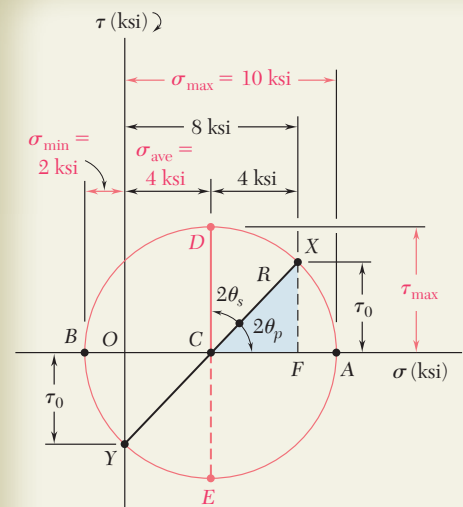
$$\begin{aligned}\cos 2\theta_p &= \frac{CF}{CX} = \frac{CF}{R} = \frac{4 \text{ ksi}}{6 \text{ ksi}} & 2\theta_p &= 48.2^\circ \downarrow & \theta_p &= 24.1^\circ \downarrow \\ \tau_0 &= FX = R \sin 2\theta_p = (6 \text{ ksi}) \sin 48.2^\circ & \tau_0 &= 4.47 \text{ ksi} \quad \blacktriangleleft\end{aligned}$$

b. Maximum Shearing Stress. The coordinates of point D of Mohr's circle represent the maximum shearing stress and the corresponding normal stress.

$$\begin{aligned}\tau_{\text{max}} &= R = 6 \text{ ksi} & \tau_{\text{max}} &= 6 \text{ ksi} \quad \blacktriangleleft \\ 2\theta_s &= 90^\circ - 2\theta_p = 90^\circ - 48.2^\circ = 41.8^\circ \uparrow & \theta_s &= 20.9^\circ \uparrow\end{aligned}$$

The maximum shearing stress is exerted on an element that is oriented as shown in Fig. *a*. (The element upon which the principal stresses are exerted is also shown.)

Note. If our original assumption regarding the sense of τ_0 was reversed, we would obtain the same circle and the same answers, but the orientation of the elements would be as shown in Fig. *b*.



PROBLEMS

- 7.31** Solve Probs. 7.5 and 7.9, using Mohr's circle.
- 7.32** Solve Probs. 7.7 and 7.11, using Mohr's circle.
- 7.33** Solve Prob. 7.10, using Mohr's circle.
- 7.34** Solve Prob. 7.12, using Mohr's circle.
- 7.35** Solve Prob. 7.13, using Mohr's circle.
- 7.36** Solve Prob. 7.14, using Mohr's circle.
- 7.37** Solve Prob. 7.15, using Mohr's circle.
- 7.38** Solve Prob. 7.16, using Mohr's circle.
- 7.39** Solve Prob. 7.17, using Mohr's circle.
- 7.40** Solve Prob. 7.18, using Mohr's circle.
- 7.41** Solve Prob. 7.19, using Mohr's circle.
- 7.42** Solve Prob. 7.20, using Mohr's circle.
- 7.43** Solve Prob. 7.21, using Mohr's circle.
- 7.44** Solve Prob. 7.22, using Mohr's circle.
- 7.45** Solve Prob. 7.23, using Mohr's circle.
- 7.46** Solve Prob. 7.24, using Mohr's circle.
- 7.47** Solve Prob. 7.25, using Mohr's circle.
- 7.48** Solve Prob. 7.26, using Mohr's circle.
- 7.49** Solve Prob. 7.27, using Mohr's circle.
- 7.50** Solve Prob. 7.28, using Mohr's circle.
- 7.51** Solve Prob. 7.29, using Mohr's circle.
- 7.52** Solve Prob. 7.30, using Mohr's circle.
- 7.53** Solve Prob. 7.30, using Mohr's circle and assuming that the weld forms an angle of 60° with the horizontal.

7.54 and 7.55 Determine the principal planes and the principal stresses for the state of plane stress resulting from the superposition of the two states of stress shown.

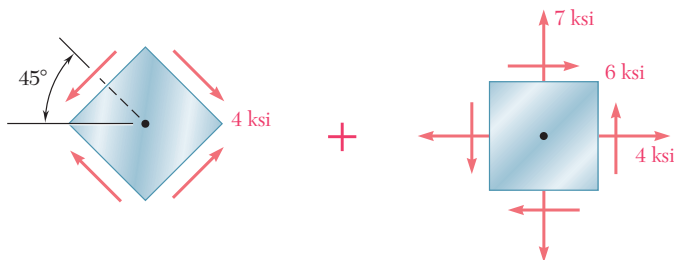


Fig. P7.54

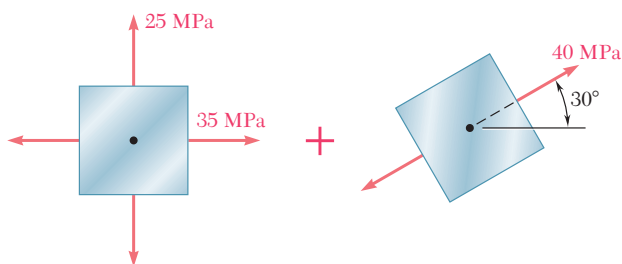


Fig. P7.55

7.56 and 7.57 Determine the principal planes and the principal stresses for the state of plane stress resulting from the superposition of the two states of stress shown.

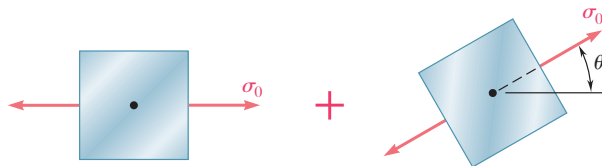


Fig. P7.56

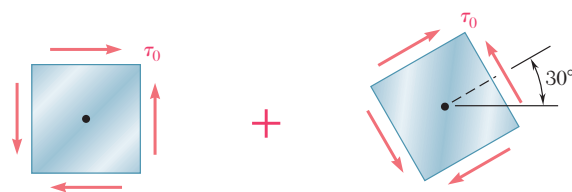


Fig. P7.57

- 7.58** For the state of stress shown, determine the range of values of θ for which the magnitude of the shearing stress $\tau_{x'y'}$ is equal to or less than 8 ksi.

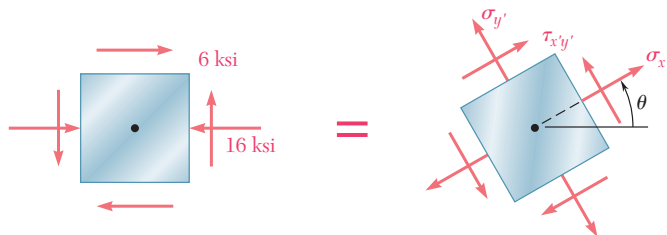


Fig. P7.58

- 7.59** For the state of stress shown, determine the range of values of θ for which the normal stress $\sigma_{x'}$ is equal to or less than 50 MPa.

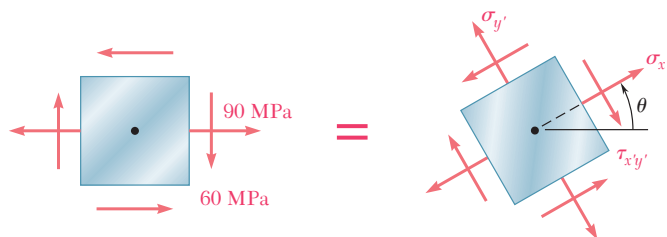


Fig. P7.59 and P7.60

- 7.60** For the state of stress shown, determine the range of values of θ for which the normal stress $\sigma_{x'}$ is equal to or less than 100 MPa.

- 7.61** For the element shown, determine the range of values of τ_{xy} for which the maximum tensile stress is equal to or less than 60 MPa.

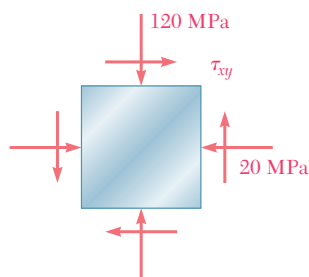


Fig. P7.61 and P7.62

- 7.62** For the element shown, determine the range of values of τ_{xy} for which the maximum in-plane shearing stress is equal to or less than 150 MPa.

- 7.63** For the state of stress shown it is known that the normal and shearing stresses are directed as shown and that $\sigma_x = 14$ ksi, $\sigma_y = 9$ ksi, and $\sigma_{\min} = 5$ ksi. Determine (a) the orientation of the principal planes, (b) the principal stress σ_{\max} , (c) the maximum in-plane shearing stress.

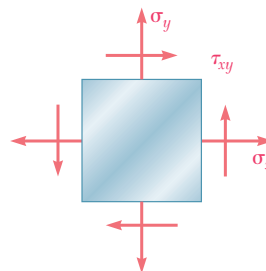


Fig. P7.63

7.64 The Mohr's circle shown corresponds to the state of stress given in Fig. 7.5*a* and *b*. Noting that $\sigma_{x'} = OC + (CX') \cos (2\theta_p - 2\theta)$ and that $\tau_{x'y'} = (CX') \sin (2\theta_p - 2\theta)$, derive the expressions for $\sigma_{x'}$ and $\tau_{x'y'}$ given in Eqs. (7.5) and (7.6), respectively. [Hint: Use $\sin (A + B) = \sin A \cos B + \cos A \sin B$ and $\cos (A + B) = \cos A \cos B - \sin A \sin B$.]

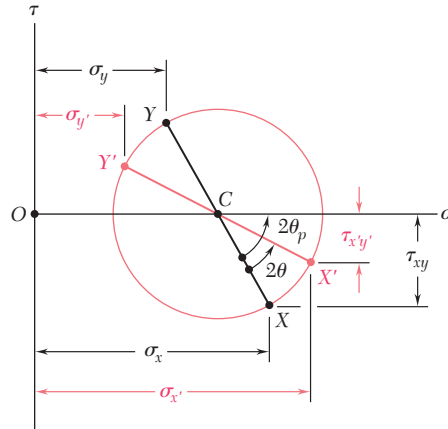


Fig. P7.64

7.65 (a) Prove that the expression $\sigma_x \sigma_y - \tau_{x'y'}^2$, where σ_x , σ_y , and $\tau_{x'y'}$ are components of the stress along the rectangular axes x' and y' , is independent of the orientation of these axes. Also, show that the given expression represents the square of the tangent drawn from the origin of the coordinates to Mohr's circle. (b) Using the invariance property established in part *a*, express the shearing stress τ_{xy} in terms of σ_x , σ_y , and the principal stresses σ_{\max} and σ_{\min} .

7.5 GENERAL STATE OF STRESS

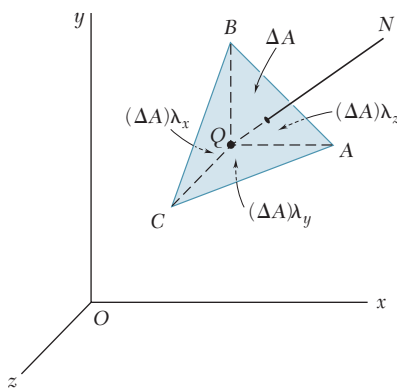


Fig. 7.23

In the preceding sections, we have assumed a state of plane stress with $\sigma_z = \tau_{zx} = \tau_{zy} = 0$, and have considered only transformations of stress associated with a rotation about the z axis. We will now consider the general state of stress represented in Fig. 7.1*a* and the transformation of stress associated with the rotation of axes shown in Fig. 7.1*b*. However, our analysis will be limited to the determination of the *normal stress* σ_n on a plane of arbitrary orientation.

Consider the tetrahedron shown in Fig. 7.23. Three of its faces are parallel to the coordinate planes, while its fourth face, ABC , is perpendicular to the line QN . Denoting by ΔA the area of face ABC , and by λ_x , λ_y , λ_z the direction cosines of line QN , we find that the areas of the faces perpendicular to the x , y , and z axes are, respectively, $(\Delta A)\lambda_x$, $(\Delta A)\lambda_y$, and $(\Delta A)\lambda_z$. If the state of stress at point Q is defined by the stress components σ_x , σ_y , σ_z , τ_{xy} , τ_{yz} , and τ_{zx} , then the *forces* exerted on the faces parallel to the coordinate planes can be obtained by multiplying the appropriate stress components by the area of each face (Fig. 7.24). On the other hand, the forces exerted on face ABC consist of a normal force of magnitude $\sigma_n \Delta A$ directed along QN , and of a shearing force of magnitude $\tau \Delta A$ perpendicular to QN but of otherwise unknown direction. Note that, since QBC ,

QCA , and QAB , respectively, face the negative x , y , and z axes, the forces exerted on them must be shown with negative senses.

We now express that the sum of the components along QN of all the forces acting on the tetrahedron is zero. Observing that the component along QN of a force parallel to the x axis is obtained by multiplying the magnitude of that force by the direction cosine λ_x , and that the components of forces parallel to the y and z axes are obtained in a similar way, we write

$$\begin{aligned}\Sigma F_n = 0: \quad & \sigma_n \Delta A - (\sigma_x \Delta A \lambda_x) \lambda_x - (\tau_{xy} \Delta A \lambda_x) \lambda_y - (\tau_{xz} \Delta A \lambda_x) \lambda_z \\ & - (\tau_{yx} \Delta A \lambda_y) \lambda_x - (\sigma_y \Delta A \lambda_y) \lambda_y - (\tau_{yz} \Delta A \lambda_y) \lambda_z \\ & - (\tau_{zx} \Delta A \lambda_z) \lambda_x - (\tau_{zy} \Delta A \lambda_z) \lambda_y - (\sigma_z \Delta A \lambda_z) \lambda_z = 0\end{aligned}$$

Dividing through by ΔA and solving for σ_n , we have

$$\sigma_n = \sigma_x \lambda_x^2 + \sigma_y \lambda_y^2 + \sigma_z \lambda_z^2 + 2\tau_{xy} \lambda_x \lambda_y + 2\tau_{yz} \lambda_y \lambda_z + 2\tau_{zx} \lambda_z \lambda_x \quad (7.20)$$

We note that the expression obtained for the normal stress σ_n is a *quadratic form* in λ_x , λ_y , and λ_z . It follows that we can select the coordinate axes in such a way that the right-hand member of Eq. (7.20) reduces to the three terms containing the squares of the direction cosines.† Denoting these axes by a , b , and c , the corresponding normal stresses by σ_a , σ_b , and σ_c , and the direction cosines of QN with respect to these axes by λ_a , λ_b , and λ_c , we write

$$\sigma_n = \sigma_a \lambda_a^2 + \sigma_b \lambda_b^2 + \sigma_c \lambda_c^2 \quad (7.21)$$

The coordinate axes a , b , c are referred to as the *principal axes of stress*. Since their orientation depends upon the state of stress at Q , and thus upon the position of Q , they have been represented in Fig. 7.25 as attached to Q . The corresponding coordinate planes are known as the *principal planes of stress*, and the corresponding normal stresses σ_a , σ_b , and σ_c as the *principal stresses* at Q .‡

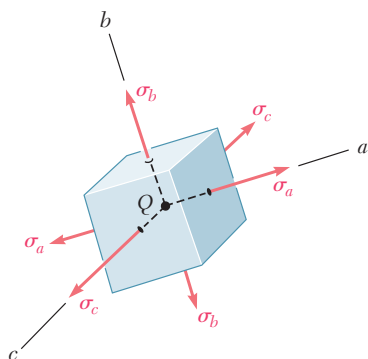


Fig. 7.25 Principal stresses.

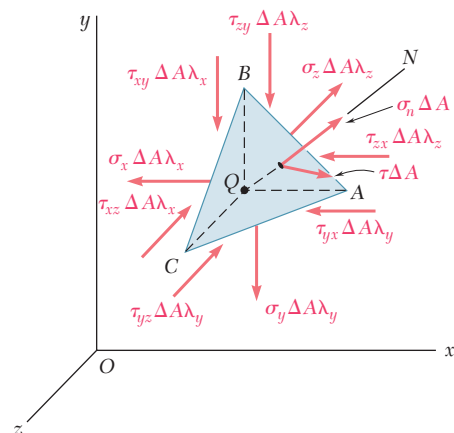


Fig. 7.24

†In Sec. 9.16 of F. P. Beer and E. R. Johnston, *Vector Mechanics for Engineers*, 9th ed., McGraw-Hill Book Company, 2010, a similar quadratic form is found to represent the moment of inertia of a rigid body with respect to an arbitrary axis. It is shown in Sec. 9.17 that this form is associated with a *quadric surface*, and that reducing the quadratic form to terms containing only the squares of the direction cosines is equivalent to determining the principal axes of that surface.

‡For a discussion of the determination of the principal planes of stress and of the principal stresses, see S. P. Timoshenko and J. N. Goodier, *Theory of Elasticity*, 3d ed., McGraw-Hill Book Company, 1970, Sec. 77.

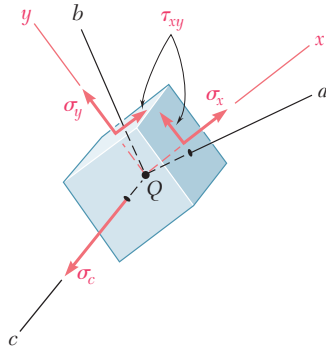


Fig. 7.26

7.6 APPLICATION OF MOHR'S CIRCLE TO THE THREE-DIMENSIONAL ANALYSIS OF STRESS

If the element shown in Fig. 7.25 is rotated about one of the principal axes at Q , say the c axis (Fig. 7.26), the corresponding transformation of stress can be analyzed by means of Mohr's circle as if it were a transformation of plane stress. Indeed, the shearing stresses exerted on the faces perpendicular to the c axis remain equal to zero, and the normal stress σ_c is perpendicular to the plane ab in which the transformation takes place and, thus, does not affect this transformation. We therefore use the circle of diameter AB to determine the normal and shearing stresses exerted on the faces of the element as it is rotated about the c axis (Fig. 7.27). Similarly, circles of diameter BC and CA can be used to determine the stresses on the element as it is rotated about the a and b axes, respectively. While our analysis will be limited to rotations about the principal axes, it could be shown that any other transformation of axes would lead to stresses represented in Fig. 7.27 by a point located within the shaded area. Thus, the radius

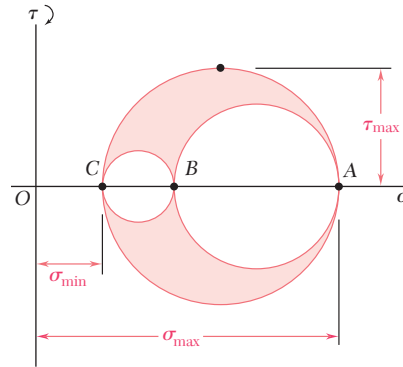


Fig. 7.27 Mohr's circles for general state of stress.

of the largest of the three circles yields the maximum value of the shearing stress at point Q . Noting that the diameter of that circle is equal to the difference between σ_{\max} and σ_{\min} , we write

$$\tau_{\max} = \frac{1}{2} |\sigma_{\max} - \sigma_{\min}| \quad (7.22)$$

where σ_{\max} and σ_{\min} represent the *algebraic* values of the maximum and minimum stresses at point Q .

Let us now return to the particular case of *plane stress*, which was discussed in Secs. 7.2 through 7.4. We recall that, if the x and y axes are selected in the plane of stress, we have $\sigma_z = \tau_{zx} = \tau_{zy} = 0$. This means that the z axis, i.e., the axis perpendicular to the plane of stress, is one of the three principal axes of stress. In a Mohr-circle diagram, this axis corresponds to the origin O , where $\sigma = \tau = 0$. We also recall that the other two principal axes correspond to points A and B where Mohr's circle for the xy plane intersects the σ axis. If A and B are located on opposite sides of the origin O (Fig. 7.28),

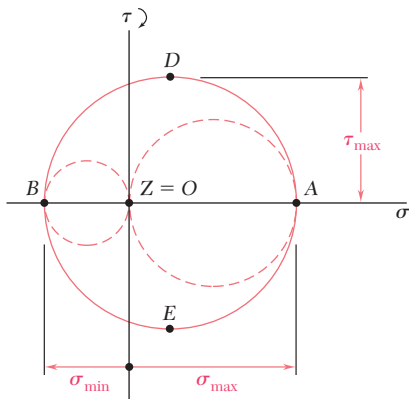


Fig. 7.28

the corresponding principal stresses represent the maximum and minimum normal stresses at point Q , and the maximum shearing stress is equal to the maximum “in-plane” shearing stress. As noted in Sec. 7.3, the planes of maximum shearing stress correspond to points D and E of Mohr's circle and are at 45° to the principal planes corresponding to points A and B . They are, therefore, the shaded diagonal planes shown in Figs. 7.29*a* and *b*.

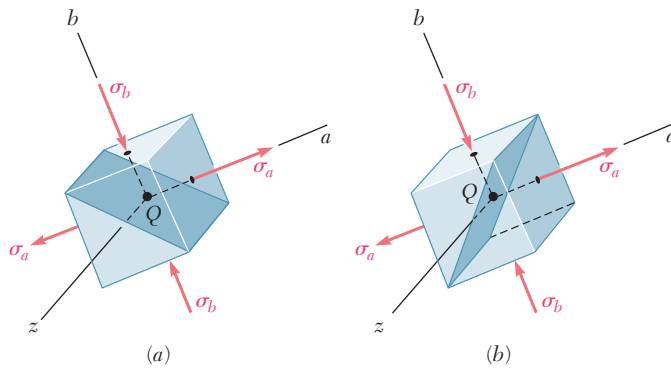


Fig. 7.29

If, on the other hand, A and B are on the same side of O , that is, if σ_a and σ_b have the same sign, then the circle defining σ_{\max} , σ_{\min} , and τ_{\max} is *not* the circle corresponding to a transformation of stress within the xy plane. If $\sigma_a > \sigma_b > 0$, as assumed in Fig. 7.30, we have $\sigma_{\max} = \sigma_a$, $\sigma_{\min} = 0$, and τ_{\max} is equal to the radius of the circle defined by points O and A , that is, $\tau_{\max} = \frac{1}{2} \sigma_{\max}$. We also note that the normals Qd' and Qe' to the planes of maximum shearing stress are obtained by rotating the axis Qa through 45° within the za plane. Thus, the planes of maximum shearing stress are the shaded diagonal planes shown in Figs. 7.31*a* and *b*.

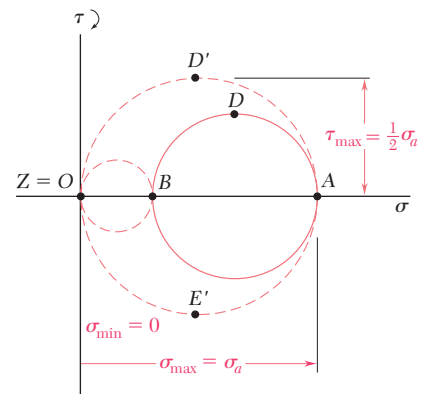


Fig. 7.30

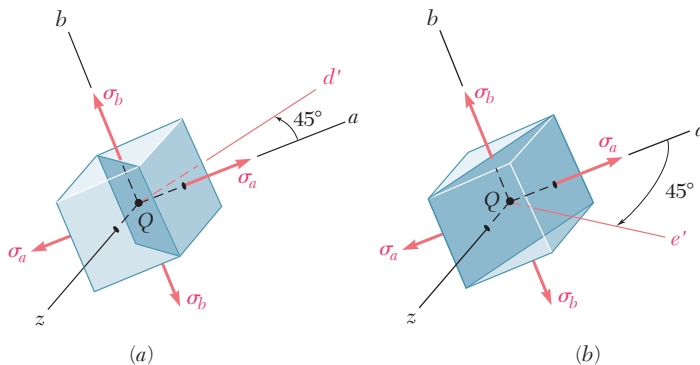


Fig. 7.31

EXAMPLE 7.03

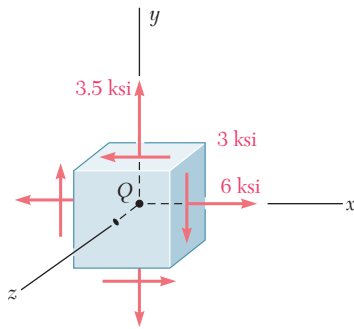


Fig. 7.32

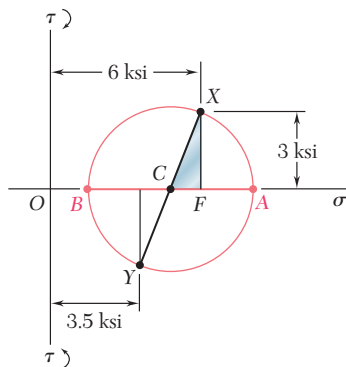


Fig. 7.33

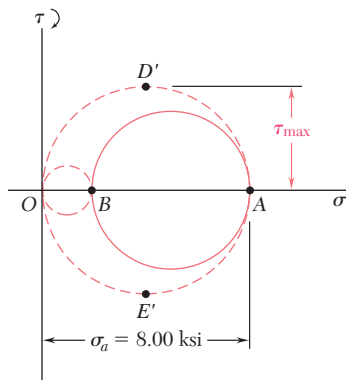


Fig. 7.35

For the state of plane stress shown in Fig. 7.32, determine (a) the three principal planes and principal stresses, (b) the maximum shearing stress.

(a) Principal Planes and Principal Stresses. We construct Mohr's circle for the transformation of stress in the xy plane (Fig. 7.33). Point X is plotted 6 units to the right of the τ axis and 3 units above the σ axis (since the corresponding shearing stress tends to rotate the element clockwise). Point Y is plotted 3.5 units to the right of the τ axis and 3 units below the σ axis. Drawing the line XY , we obtain the center C of Mohr's circle for the xy plane; its abscissa is

$$\sigma_{\text{ave}} = \frac{\sigma_x + \sigma_y}{2} = \frac{6 + 3.5}{2} = 4.75 \text{ ksi}$$

Since the sides of the right triangle CFX are $CF = 6 - 4.75 = 1.25$ ksi and $FX = 3$ ksi, the radius of the circle is

$$R = CX = \sqrt{(1.25)^2 + (3)^2} = 3.25 \text{ ksi}$$

The principal stresses in the plane of stress are

$$\sigma_a = OA = OC + CA = 4.75 + 3.25 = 8.00 \text{ ksi}$$

$$\sigma_b = OB = OC - BC = 4.75 - 3.25 = 1.50 \text{ ksi}$$

Since the faces of the element that are perpendicular to the z axis are free of stress, these faces define one of the principal planes, and the corresponding principal stress is $\sigma_z = 0$. The other two principal planes are defined by points A and B on Mohr's circle. The angle θ_p through which the element should be rotated about the z axis to bring its faces to coincide with these planes (Fig. 7.34) is half the angle ACX . We have

$$\tan 2\theta_p = \frac{FX}{CF} = \frac{3}{1.25}$$

$$2\theta_p = 67.4^\circ \downarrow \quad \theta_p = 33.7^\circ \downarrow$$

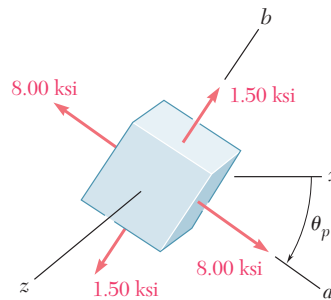


Fig. 7.34

(b) Maximum Shearing Stress. We now draw the circles of diameter OB and OA , which correspond respectively to rotations of the element about the a and b axes (Fig. 7.35). We note that the maximum shearing stress is equal to the radius of the circle of diameter OA . We thus have

$$\tau_{\text{max}} = \frac{1}{2} \sigma_a = \frac{1}{2} (8.00 \text{ ksi}) = 4.00 \text{ ksi}$$

Since points D' and E' , which define the planes of maximum shearing stress, are located at the ends of the vertical diameter of the circle corresponding to a rotation about the b axis, the faces of the element of Fig. 7.34 can be brought to coincide with the planes of maximum shearing stress through a rotation of 45° about the b axis.

*7.7 YIELD CRITERIA FOR DUCTILE MATERIALS UNDER PLANE STRESS

Structural elements and machine components made of a ductile material are usually designed so that the material will not yield under the expected loading conditions. When the element or component is under uniaxial stress (Fig. 7.36), the value of the normal stress σ_x that will cause the material to yield can be obtained readily from a tensile test conducted on a specimen of the same material, since the test specimen and the structural element or machine component are in the same state of stress. Thus, regardless of the actual mechanism that causes the material to yield, we can state that the element or component will be safe as long as $\sigma_x < \sigma_Y$, where σ_Y is the yield strength of the test specimen.

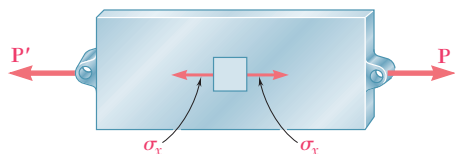


Fig. 7.36 Structural element under uniaxial stress.

On the other hand, when a structural element or machine component is in a state of plane stress (Fig. 7.37a), it is found convenient to use one of the methods developed earlier to determine the principal stresses σ_a and σ_b at any given point (Fig. 7.37b). The material can then be regarded as being in a state of biaxial stress at that point. Since this state is different from the state of uniaxial stress found in a specimen subjected to a tensile test, it is clearly not possible to predict directly from such a test whether or not the structural element or machine component under investigation will fail. Some criterion regarding the actual mechanism of failure of the material must first be established, which will make it possible to compare the effects of both states of stress on the material. The purpose of this section is to present the two yield criteria most frequently used for ductile materials.

Maximum-Shearing-Stress Criterion. This criterion is based on the observation that yield in ductile materials is caused by slippage of the material along oblique surfaces and is due primarily to shearing stresses (cf. Sec. 2.3). According to this criterion, a given structural component is safe as long as the maximum value τ_{\max} of the shearing stress in that component remains smaller than the corresponding value of the shearing stress in a tensile-test specimen of the same material as the specimen starts to yield.

Recalling from Sec. 1.11 that the maximum value of the shearing stress under a centric axial load is equal to half the value of the corresponding normal, axial stress, we conclude that the maximum shearing stress in a tensile-test specimen is $\frac{1}{2}\sigma_Y$ as the specimen starts to yield. On the other hand, we saw in Sec. 7.6 that, for plane stress, the maximum value τ_{\max} of the shearing stress is equal to $\frac{1}{2}|\sigma_{\max}|$ if the principal stresses are either both positive or both negative, and to $\frac{1}{2}|\sigma_{\max} - \sigma_{\min}|$ if the maximum stress is positive and the

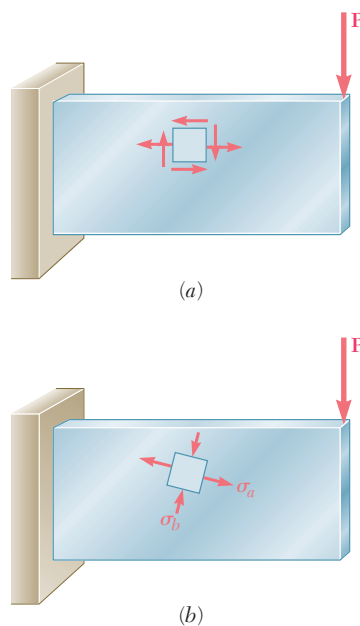


Fig. 7.37 Structural element in state of plane stress.

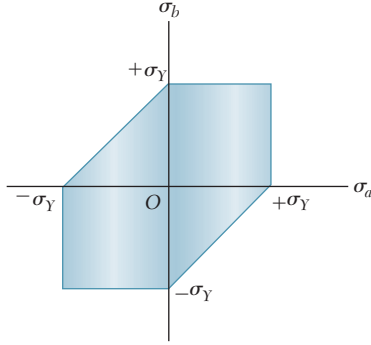


Fig. 7.38 Tresca's hexagon.

minimum stress negative. Thus, if the principal stresses σ_a and σ_b have the same sign, the maximum-shearing-stress criterion gives

$$|\sigma_a| < \sigma_Y \quad |\sigma_b| < \sigma_Y \quad (7.23)$$

If the principal stresses σ_a and σ_b have opposite signs, the maximum-shearing-stress criterion yields

$$|\sigma_a - \sigma_b| < \sigma_Y \quad (7.24)$$

The relations obtained have been represented graphically in Fig. 7.38. Any given state of stress will be represented in that figure by a point of coordinates σ_a and σ_b , where σ_a and σ_b are the two principal stresses. If this point falls within the area shown in the figure, the structural component is safe. If it falls outside this area, the component will fail as a result of yield in the material. The hexagon associated with the initiation of yield in the material is known as *Tresca's hexagon* after the French engineer Henri Edouard Tresca (1814–1885).

Maximum-Distortion-Energy Criterion. This criterion is based on the determination of the distortion energy in a given material, i.e., of the energy associated with changes in shape in that material (as opposed to the energy associated with changes in volume in the same material). According to this criterion, also known as the *von Mises criterion*, after the German-American applied mathematician Richard von Mises (1883–1953), a given structural component is safe as long as the maximum value of the distortion energy per unit volume in that material remains smaller than the distortion energy per unit volume required to cause yield in a tensile-test specimen of the same material. As you will see in Sec. 11.6, the distortion energy per unit volume in an isotropic material under plane stress is

$$u_d = \frac{1}{6G} (\sigma_a^2 - \sigma_a \sigma_b + \sigma_b^2) \quad (7.25)$$

where σ_a and σ_b are the principal stresses and G the modulus of rigidity. In the particular case of a tensile-test specimen that is starting to yield, we have $\sigma_a = \sigma_Y$, $\sigma_b = 0$, and $(u_d)_Y = \sigma_Y^2/6G$. Thus, the maximum-distortion-energy criterion indicates that the structural component is safe as long as $u_d < (u_d)_Y$, or

$$\sigma_a^2 - \sigma_a \sigma_b + \sigma_b^2 < \sigma_Y^2 \quad (7.26)$$

i.e., as long as the point of coordinates σ_a and σ_b falls within the area shown in Fig. 7.39. This area is bounded by the ellipse of equation

$$\sigma_a^2 - \sigma_a \sigma_b + \sigma_b^2 = \sigma_Y^2 \quad (7.27)$$

which intersects the coordinate axes at $\sigma_a = \pm \sigma_Y$ and $\sigma_b = \pm \sigma_Y$. We can verify that the major axis of the ellipse bisects the first and third quadrants and extends from A ($\sigma_a = \sigma_b = \sigma_Y$) to B ($\sigma_a = \sigma_b = -\sigma_Y$), while its minor axis extends from C ($\sigma_a = -\sigma_b = -0.577\sigma_Y$) to D ($\sigma_a = -\sigma_b = 0.577\sigma_Y$).

The maximum-shearing-stress criterion and the maximum-distortion-energy criterion are compared in Fig. 7.40. We note that the ellipse passes through the vertices of the hexagon. Thus, for the states of stress represented by these six points, the two criteria give

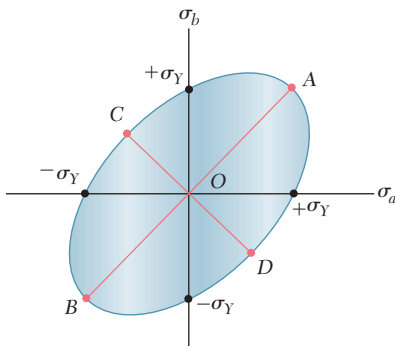


Fig. 7.39 Von Mises criterion.

the same results. For any other state of stress, the maximum-shearing-stress criterion is more conservative than the maximum-distortion-energy criterion, since the hexagon is located within the ellipse.

A state of stress of particular interest is that associated with yield in a torsion test. We recall from Fig. 7.22 of Sec. 7.4 that, for torsion, $\sigma_{\min} = -\sigma_{\max}$; thus, the corresponding points in Fig. 7.40 are located on the bisector of the second and fourth quadrants. It follows that yield occurs in a torsion test when $\sigma_a = -\sigma_b = \pm 0.5\sigma_Y$ according to the maximum-shearing-stress criterion, and when $\sigma_a = -\sigma_b = \pm 0.577\sigma_Y$ according to the maximum-distortion-energy criterion. But, recalling again Fig. 7.22, we note that σ_a and σ_b must be equal in magnitude to τ_{\max} , that is, to the value obtained from a torsion test for the yield strength τ_Y of the material. Since the values of the yield strength σ_Y in tension and of the yield strength τ_Y in shear are given for various ductile materials in Appendix B, we can compute the ratio τ_Y/σ_Y for these materials and verify that the values obtained range from 0.55 to 0.60. Thus, the maximum-distortion-energy criterion appears somewhat more accurate than the maximum-shearing-stress criterion as far as predicting yield in torsion is concerned.

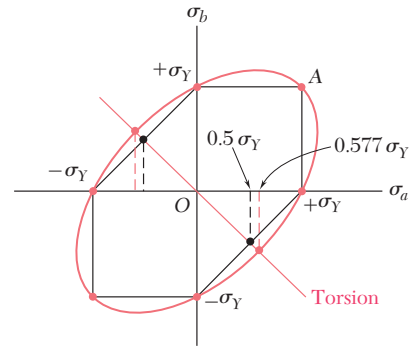


Fig. 7.40

*7.8 FRACTURE CRITERIA FOR BRITTLE MATERIALS UNDER PLANE STRESS

As we saw in Chap. 2, brittle materials are characterized by the fact that, when subjected to a tensile test, they fail suddenly through rupture—or fracture—without any prior yielding. When a structural element or machine component made of a brittle material is under uniaxial tensile stress, the value of the normal stress that causes it to fail is equal to the ultimate strength σ_U of the material as determined from a tensile test, since both the tensile-test specimen and the element or component under investigation are in the same state of stress. However, when a structural element or machine component is in a state of plane stress, it is found convenient to first determine the principal stresses σ_a and σ_b at any given point, and to use one of the criteria indicated in this section to predict whether or not the structural element or machine component will fail.

Maximum-Normal-Stress Criterion. According to this criterion, a given structural component fails when the maximum normal stress in that component reaches the ultimate strength σ_U obtained from the tensile test of a specimen of the same material. Thus, the structural component will be safe as long as the absolute values of the principal stresses σ_a and σ_b are both less than σ_U :

$$|\sigma_a| < \sigma_U \quad |\sigma_b| < \sigma_U \quad (7.28)$$

The maximum-normal-stress criterion can be expressed graphically as shown in Fig. 7.41. If the point obtained by plotting the values σ_a and σ_b of the principal stresses falls within the square area shown in the figure, the structural component is safe. If it falls outside that area, the component will fail.

The maximum-normal-stress criterion, also known as *Coulomb's criterion*, after the French physicist Charles Augustin de Coulomb

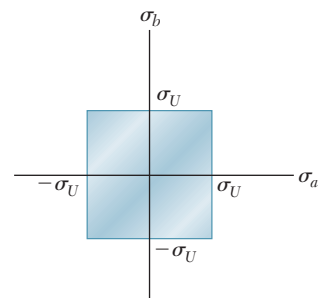


Fig. 7.41 Coulomb's criterion.

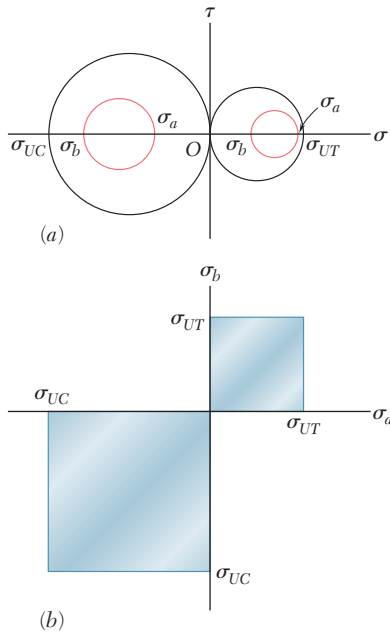


Fig. 7.43

(1736–1806), suffers from an important shortcoming, since it is based on the assumption that the ultimate strength of the material is the same in tension and in compression. As we noted in Sec. 2.3, this is seldom the case, because of the presence of flaws in the material, such as microscopic cracks or cavities, which tend to weaken the material in tension, while not appreciably affecting its resistance to compressive failure. Besides, this criterion makes no allowance for effects other than those of the normal stresses on the failure mechanism of the material.†

Mohr's Criterion. This criterion, suggested by the German engineer Otto Mohr, can be used to predict the effect of a given state of plane stress on a brittle material, when results of various types of tests are available for that material.

Let us first assume that a tensile test and a compressive test have been conducted on a given material, and that the values σ_{UT} and σ_{UC} of the ultimate strength in tension and in compression have been determined for that material. The state of stress corresponding to the rupture of the tensile-test specimen can be represented on a Mohr-circle diagram by the circle intersecting the horizontal axis at O and σ_{UT} (Fig. 7.43a). Similarly, the state of stress corresponding to the failure of the compressive-test specimen can be represented by the circle intersecting the horizontal axis at O and σ_{UC} . Clearly, a state of stress represented by a circle entirely contained in either of these circles will be safe. Thus, if both principal stresses are positive, the state of stress is safe as long as $\sigma_a < \sigma_{UT}$ and $\sigma_b < \sigma_{UT}$; if both principal stresses are negative, the state of stress is safe as long as $|\sigma_a| < |\sigma_{UC}|$ and $|\sigma_b| < |\sigma_{UC}|$. Plotting the point of coordinates σ_a and σ_b (Fig. 7.43b), we verify that the state of stress is safe as long as that point falls within one of the square areas shown in that figure.

In order to analyze the cases when σ_a and σ_b have opposite signs, we now assume that a torsion test has been conducted on the material and that its ultimate strength in shear, τ_U , has been determined. Drawing the circle centered at O representing the state of stress corresponding to the failure of the torsion-test specimen (Fig. 7.44a), we observe that any state of stress represented by a circle entirely contained in that circle is also safe. Mohr's criterion is a logical extension of this observation: According to Mohr's criterion, a state of stress is safe if it is represented by a circle located entirely within the area bounded

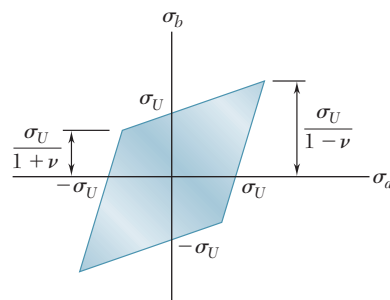


Fig. 7.42 Saint-Venant's criterion.

†Another failure criterion known as the *maximum-normal-strain criterion*, or Saint-Venant's criterion, was widely used during the nineteenth century. According to this criterion, a given structural component is safe as long as the maximum value of the normal strain in that component remains smaller than the value ϵ_U of the strain at which a tensile-test specimen of the same material will fail. But, as will be shown in Sec. 7.12, the strain is maximum along one of the principal axes of stress, if the deformation is elastic and the material homogeneous and isotropic. Thus, denoting by ϵ_a and ϵ_b the values of the normal strain along the principal axes in the plane of stress, we write

$$|\epsilon_a| < \epsilon_U \quad |\epsilon_b| < \epsilon_U \quad (7.29)$$

Making use of the generalized Hooke's law (Sec. 2.12), we could express these relations in terms of the principal stresses σ_a and σ_b and the ultimate strength σ_U of the material. We would find that, according to the maximum-normal-strain criterion, the structural component is safe as long as the point obtained by plotting σ_a and σ_b falls within the area shown in Fig. 7.42 where ν is Poisson's ratio for the given material.

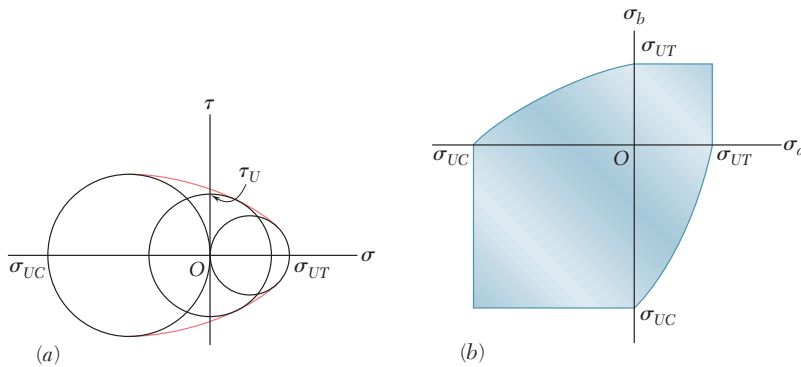


Fig. 7.44 Mohr's criterion.

by the envelope of the circles corresponding to the available data. The remaining portions of the principal-stress diagram can now be obtained by drawing various circles tangent to this envelope, determining the corresponding values of σ_a and σ_b , and plotting the points of coordinates σ_a and σ_b (Fig. 7.44b).

More accurate diagrams can be drawn when additional test results, corresponding to various states of stress, are available. If, on the other hand, the only available data consists of the ultimate strengths σ_{UT} and σ_{UC} , the envelope in Fig. 7.44a is replaced by the tangents AB and $A'B'$ to the circles corresponding respectively to failure in tension and failure in compression (Fig. 7.45a). From the similar triangles drawn in that figure, we note that the abscissa of the center C of a circle tangent to AB and $A'B'$ is linearly related to its radius R . Since $\sigma_a = OC + R$ and $\sigma_b = OC - R$, it follows that σ_a and σ_b are also linearly related. Thus, the shaded area corresponding to this simplified Mohr's criterion is bounded by straight lines in the second and fourth quadrants (Fig. 7.45b).

Note that in order to determine whether a structural component will be safe under a given loading, the state of stress should be calculated at all critical points of the component, i.e., at all points where stress concentrations are likely to occur. This can be done in a number of cases by using the stress-concentration factors given in Figs. 2.60, 3.29, 4.27, and 4.28. There are many instances, however, when the theory of elasticity must be used to determine the state of stress at a critical point.

Special care should be taken when *macroscopic cracks* have been detected in a structural component. While it can be assumed that the test specimen used to determine the ultimate tensile strength of the material contained the same type of flaws (i.e., *microscopic cracks* or cavities) as the structural component under investigation, the specimen was certainly free of any detectable macroscopic cracks. When a crack is detected in a structural component, it is necessary to determine whether that crack will tend to propagate under the expected loading condition and cause the component to fail, or whether it will remain stable. This requires an analysis involving the energy associated with the growth of the crack. Such an analysis is beyond the scope of this text and should be carried out by the methods of fracture mechanics.

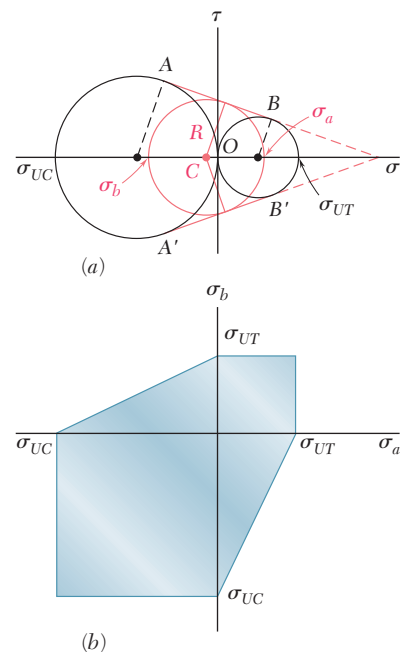
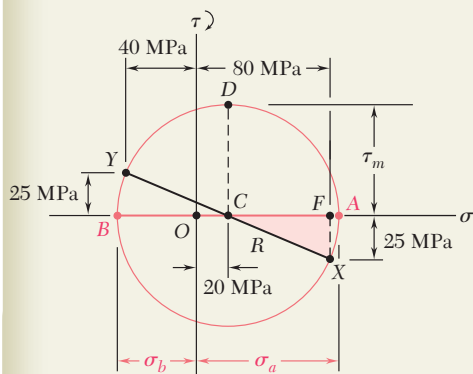
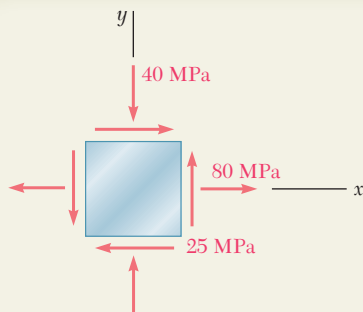


Fig. 7.45 Simplified Mohr's criterion.



SAMPLE PROBLEM 7.4

The state of plane stress shown occurs at a critical point of a steel machine component. As a result of several tensile tests, it has been found that the tensile yield strength is $\sigma_Y = 250$ MPa for the grade of steel used. Determine the factor of safety with respect to yield, using (a) the maximum-shearing-stress criterion, and (b) the maximum-distortion-energy criterion.

SOLUTION

Mohr's Circle. We construct Mohr's circle for the given state of stress and find

$$\sigma_{\text{ave}} = OC = \frac{1}{2}(\sigma_x + \sigma_y) = \frac{1}{2}(80 - 40) = 20 \text{ MPa}$$

$$\tau_m = R = \sqrt{(CF)^2 + (FX)^2} = \sqrt{(60)^2 + (25)^2} = 65 \text{ MPa}$$

Principal Stresses

$$\sigma_a = OC + CA = 20 + 65 = +85 \text{ MPa}$$

$$\sigma_b = OC - BC = 20 - 65 = -45 \text{ MPa}$$

a. Maximum-Shearing-Stress Criterion. Since for the grade of steel used the tensile strength is $\sigma_Y = 250$ MPa, the corresponding shearing stress at yield is

$$\tau_Y = \frac{1}{2} \sigma_Y = \frac{1}{2}(250 \text{ MPa}) = 125 \text{ MPa}$$

$$\text{For } \tau_m = 65 \text{ MPa:} \quad F.S. = \frac{\tau_Y}{\tau_m} = \frac{125 \text{ MPa}}{65 \text{ MPa}} \quad F.S. = 1.92 \quad \blacktriangleleft$$

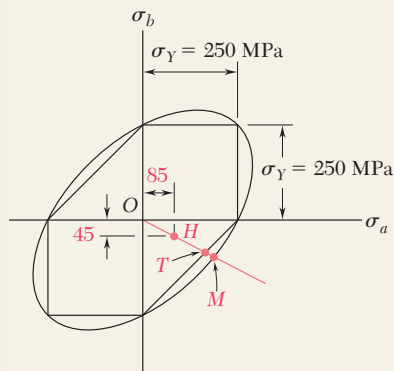
b. Maximum-Distortion-Energy Criterion. Introducing a factor of safety into Eq. (7.26), we write

$$\sigma_a^2 - \sigma_a \sigma_b + \sigma_b^2 = \left(\frac{\sigma_Y}{F.S.} \right)^2$$

For $\sigma_a = +85$ MPa, $\sigma_b = -45$ MPa, and $\sigma_Y = 250$ MPa, we have

$$(85)^2 - (85)(-45) + (45)^2 = \left(\frac{250}{F.S.} \right)^2$$

$$114.3 = \frac{250}{F.S.} \quad F.S. = 2.19 \quad \blacktriangleleft$$



Comment. For a ductile material with $\sigma_Y = 250$ MPa, we have drawn the hexagon associated with the maximum-shearing-stress criterion and the ellipse associated with the maximum-distortion-energy criterion. The given state of plane stress is represented by point H of coordinates $\sigma_a = 85$ MPa and $\sigma_b = -45$ MPa. We note that the straight line drawn through points O and H intersects the hexagon at point T and the ellipse at point M . For each criterion, the value obtained for $F.S.$ can be verified by measuring the line segments indicated and computing their ratios:

$$(a) F.S. = \frac{OT}{OH} = 1.92 \quad (b) F.S. = \frac{OM}{OH} = 2.19$$

PROBLEMS

- 7.66** For the state of plane stress shown, determine the maximum shearing stress when (a) $\sigma_x = 6$ ksi and $\sigma_y = 18$ ksi, (b) $\sigma_x = 14$ ksi and $\sigma_y = 2$ ksi. (Hint: Consider both in-plane and out-of-plane shearing stresses.)

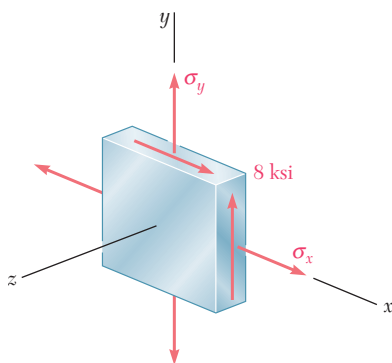


Fig. P7.66 and P7.67

- 7.67** For the state of plane stress shown, determine the maximum shearing stress when (a) $\sigma_x = 0$ and $\sigma_y = 12$ ksi, (b) $\sigma_x = 21$ ksi and $\sigma_y = 9$ ksi. (Hint: Consider both in-plane and out-of-plane shearing stresses.)

- 7.68** For the state of stress shown, determine the maximum shearing stress when (a) $\sigma_y = 40$ MPa, (b) $\sigma_y = 120$ MPa. (Hint: Consider both in-plane and out-of-plane shearing stresses.)

- 7.69** For the state of stress shown, determine the maximum shearing stress when (a) $\sigma_y = 20$ MPa, (b) $\sigma_y = 140$ MPa. (Hint: Consider both in-plane and out-of-plane shearing stresses.)

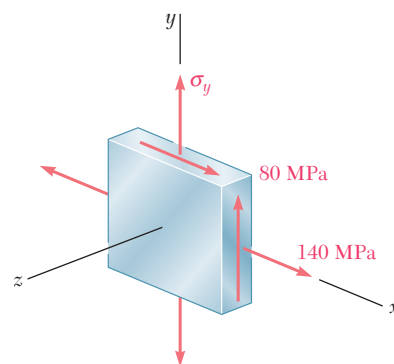


Fig. P7.68 and P7.69

- 7.70 and 7.71** For the state of stress shown, determine the maximum shearing stress when (a) $\sigma_z = +4$ ksi, (b) $\sigma_z = -4$ ksi, (c) $\sigma_z = 0$.

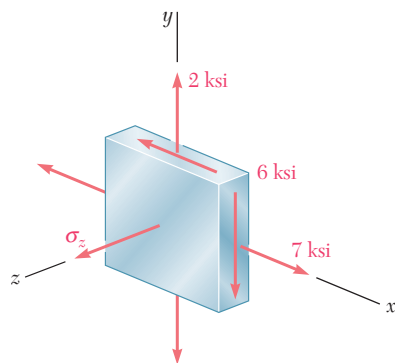


Fig. P7.70

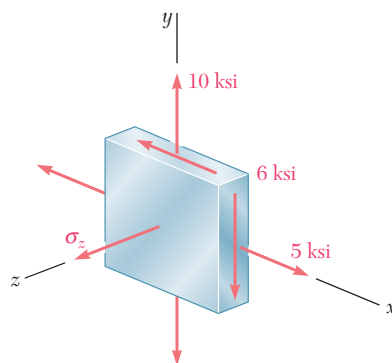


Fig. P7.71

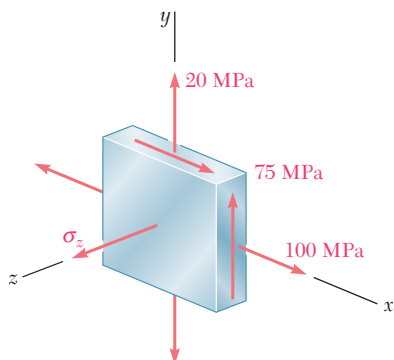


Fig. P7.72

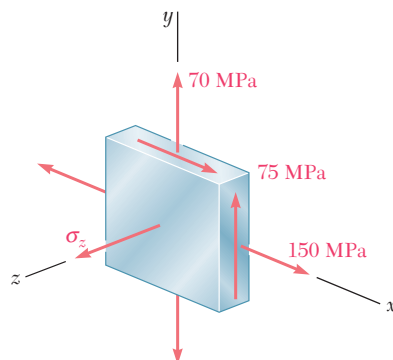


Fig. P7.73

7.72 and 7.73 For the state of stress shown, determine the maximum shearing stress when (a) $\sigma_z = 0$, (b) $\sigma_z = +45$ MPa, (c) $\sigma_z = -45$ MPa.

7.74 For the state of stress shown, determine two values of σ_y for which the maximum shearing stress is 10 ksi.

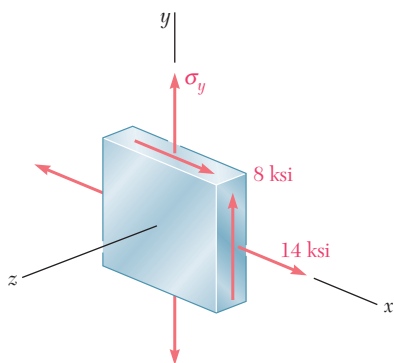


Fig. P7.74

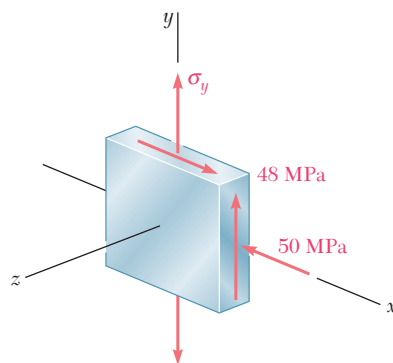


Fig. P7.75

7.75 For the state of stress shown, determine two values of σ_y for which the maximum shearing stress is 73 MPa.

7.76 For the state of stress shown, determine the value of τ_{xy} for which the maximum shearing stress is (a) 10 ksi, (b) 8.25 ksi.

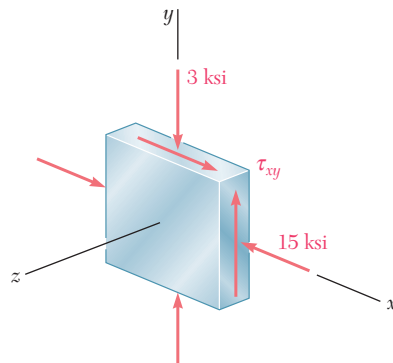


Fig. P7.76

- 7.77** For the state of stress shown, determine the value of τ_{xy} for which the maximum shearing stress is (a) 60 MPa, (b) 78 MPa.

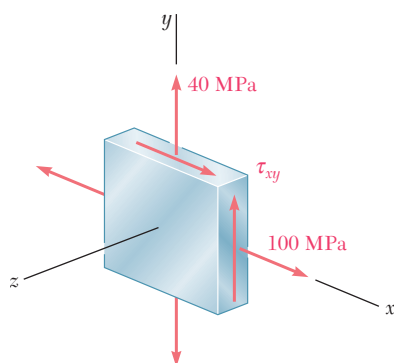


Fig. P7.77

- 7.78** For the state of stress shown, determine two values of σ_y for which the maximum shearing stress is 80 MPa.

- 7.79** For the state of stress shown, determine the range of values of τ_{xz} for which the maximum shearing stress is equal to or less than 60 MPa.

- *7.80** For the state of stress of Prob. 7.69, determine (a) the value of σ_y for which the maximum shearing stress is as small as possible, (b) the corresponding value of the shearing stress.

- 7.81** The state of plane stress shown occurs in a machine component made of a steel with $\sigma_Y = 325$ MPa. Using the maximum-distortion-energy criterion, determine whether yield will occur when (a) $\sigma_0 = 200$ MPa, (b) $\sigma_0 = 240$ MPa, (c) $\sigma_0 = 280$ MPa. If yield does not occur, determine the corresponding factor of safety.

- 7.82** Solve Prob. 7.81, using the maximum-shearing-stress criterion.

- 7.83** The state of plane stress shown occurs in a machine component made of a steel with $\sigma_Y = 45$ ksi. Using the maximum-distortion-energy criterion, determine whether yield will occur when (a) $\tau_{xy} = 9$ ksi, (b) $\tau_{xy} = 18$ ksi, (c) $\tau_{xy} = 20$ ksi. If yield does not occur, determine the corresponding factor of safety.

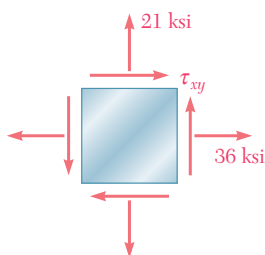


Fig. P7.83

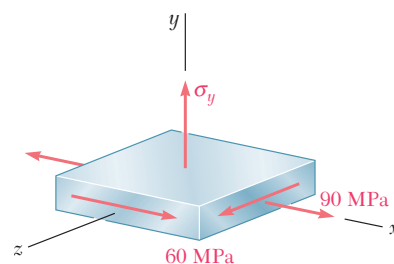


Fig. P7.78

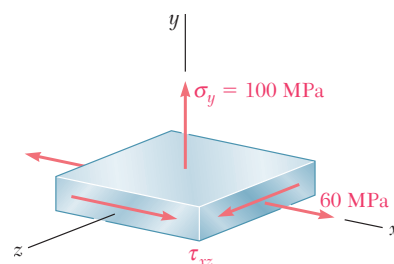


Fig. P7.79

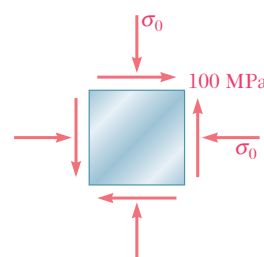


Fig. P7.81

- 7.84** Solve Prob. 7.83, using the maximum-shearing-stress criterion.

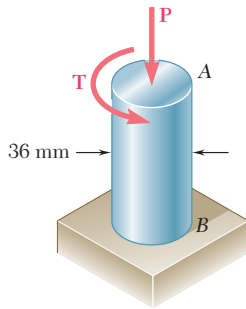


Fig. P7.85

7.85 The 36-mm-diameter shaft is made of a grade of steel with a 250-MPa tensile yield stress. Using the maximum-shearing-stress criterion, determine the magnitude of the torque T for which yield occurs when $P = 200$ kN.

7.86 Solve Prob. 7.85, using the maximum-distortion-energy criterion.

7.87 The 1.75-in.-diameter shaft AB is made of a grade of steel for which the yield strength is $\sigma_Y = 36$ ksi. Using the maximum-shearing-stress criterion, determine the magnitude of the force P for which yield occurs when $T = 15$ kip \cdot in.

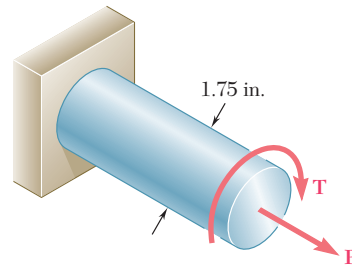


Fig. P7.87

7.88 Solve Prob. 7.87, using the maximum-distortion-energy criterion.

7.89 and 7.90 The state of plane stress shown is expected to occur in an aluminum casting. Knowing that for the aluminum alloy used $\sigma_{UT} = 80$ MPa and $\sigma_{UC} = 200$ MPa and using Mohr's criterion, determine whether rupture of the casting will occur.

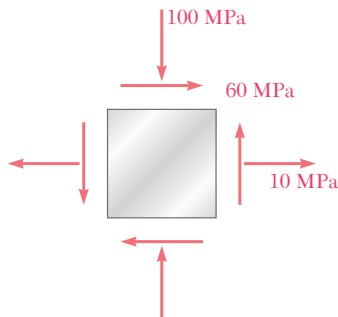


Fig. P7.89

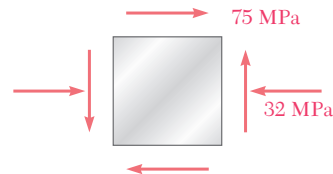


Fig. P7.90

7.91 and 7.92 The state of plane stress shown is expected to occur in an aluminum casting. Knowing that for the aluminum alloy used $\sigma_{UT} = 10$ ksi and $\sigma_{UC} = 30$ ksi and using Mohr's criterion, determine whether rupture of the casting will occur.

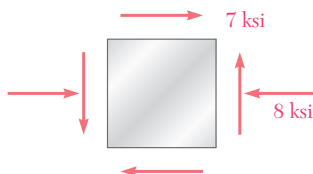


Fig. P7.91

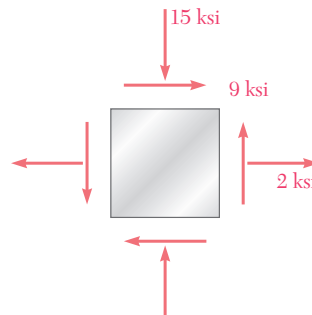


Fig. P7.92

- 7.93** The state of plane stress shown will occur at a critical point in an aluminum casting that is made of an alloy for which $\sigma_{UT} = 10$ ksi and $\sigma_{UC} = 25$ ksi. Using Mohr's criterion, determine the shearing stress τ_0 for which failure should be expected.

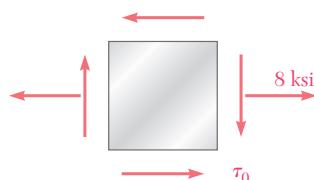


Fig. P7.93

- 7.94** The state of plane stress shown will occur at a critical point in a pipe made of an aluminum alloy for which $\sigma_{UT} = 75$ MPa and $\sigma_{UC} = 150$ MPa. Using Mohr's criterion, determine the shearing stress τ_0 for which failure should be expected.

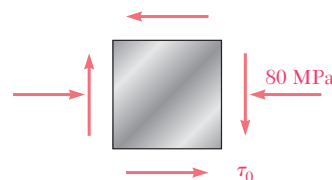


Fig. P7.94

- 7.95** The cast-aluminum rod shown is made of an alloy for which $\sigma_{UT} = 60$ MPa and $\sigma_{UC} = 120$ MPa. Using Mohr's criterion, determine the magnitude of the torque \mathbf{T} for which failure should be expected.

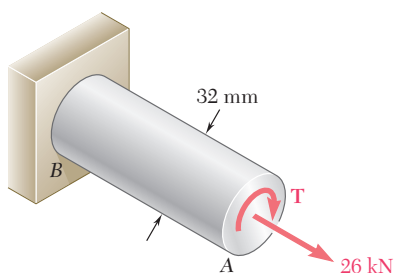


Fig. P7.95

- 7.96** The cast-aluminum rod shown is made of an alloy for which $\sigma_{UT} = 70$ MPa and $\sigma_{UC} = 175$ MPa. Knowing that the magnitude T of the applied torques is slowly increased and using Mohr's criterion, determine the shearing stress τ_0 that should be expected at rupture.

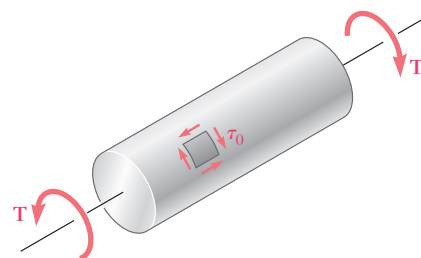


Fig. P7.96

- 7.97** A machine component is made of a grade of cast iron for which $\sigma_{UT} = 8$ ksi and $\sigma_{UC} = 20$ ksi. For each of the states of stress shown, and using Mohr's criterion, determine the normal stress σ_0 at which rupture of the component should be expected.

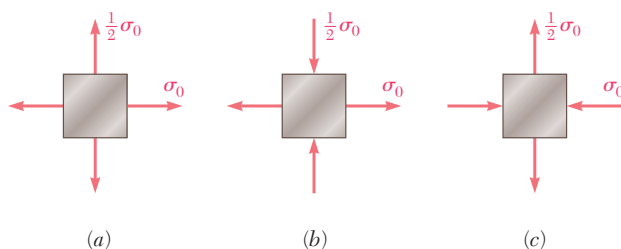


Fig. P7.97

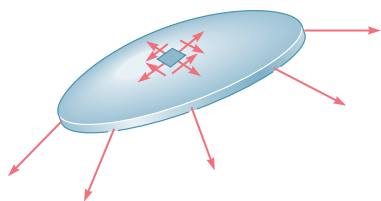


Fig. 7.46 Assumed stress distribution in thin-walled pressure vessels.

7.9 STRESSES IN THIN-WALLED PRESSURE VESSELS

Thin-walled pressure vessels provide an important application of the analysis of plane stress. Since their walls offer little resistance to bending, it can be assumed that the internal forces exerted on a given portion of wall are tangent to the surface of the vessel (Fig. 7.46). The resulting stresses on an element of wall will thus be contained in a plane tangent to the surface of the vessel.

Our analysis of stresses in thin-walled pressure vessels will be limited to the two types of vessels most frequently encountered: cylindrical pressure vessels and spherical pressure vessels (Photos 7.3 and 7.4).



Photo 7.3 Cylindrical pressure vessels.



Photo 7.4 Spherical pressure vessels.

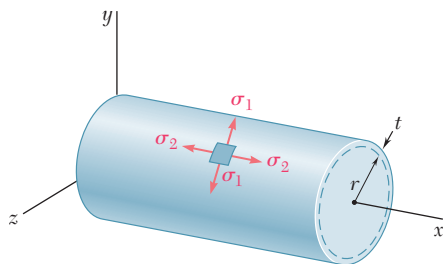


Fig. 7.47 Pressurized cylindrical vessel.

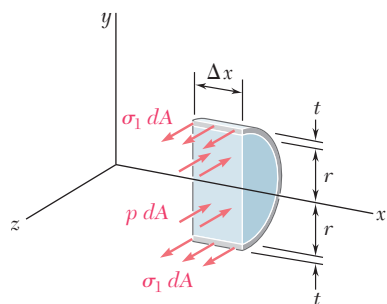


Fig. 7.48 Free body to determine hoop stress.

Consider a cylindrical vessel of inner radius r and wall thickness t containing a fluid under pressure (Fig. 7.47). We propose to determine the stresses exerted on a small element of wall with sides respectively parallel and perpendicular to the axis of the cylinder. Because of the axisymmetry of the vessel and its contents, it is clear that no shearing stress is exerted on the element. The normal stresses σ_1 and σ_2 shown in Fig. 7.47 are therefore principal stresses. The stress σ_1 is known as the *hoop stress*, because it is the type of stress found in hoops used to hold together the various slats of a wooden barrel, and the stress σ_2 is called the *longitudinal stress*.

In order to determine the hoop stress σ_1 , we detach a portion of the vessel and its contents bounded by the xy plane and by two planes parallel to the yz plane at a distance Δx from each other (Fig. 7.48). The forces parallel to the z axis acting on the free body defined in this fashion consist of the elementary internal forces $\sigma_1 dA$ on the wall sections, and of the elementary pressure forces $p dA$ exerted on the portion of fluid included in the free body. Note that p denotes the *gage pressure* of the fluid, i.e., the excess of the inside pressure over the outside atmospheric pressure. The resultant of the internal forces $\sigma_1 dA$ is equal to the product of σ_1 and of the cross-sectional area $2t \Delta x$ of the wall, while the resultant of the pressure forces $p dA$ is equal to the product of p and of the area $2r \Delta x$. Writing the equilibrium equation $\Sigma F_z = 0$, we have

$$\Sigma F_z = 0: \quad \sigma_1(2t \Delta x) - p(2r \Delta x) = 0$$

and, solving for the hoop stress σ_1 ,

$$\sigma_1 = \frac{pr}{t} \quad (7.30)$$

To determine the longitudinal stress σ_2 , we now pass a section perpendicular to the x axis and consider the free body consisting of the portion of the vessel and its contents located to the left of the section

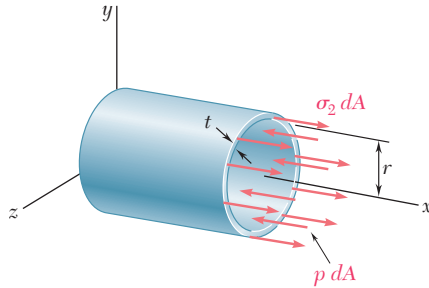


Fig. 7.49 Free body to determine longitudinal stress.

(Fig. 7.49). The forces acting on this free body are the elementary internal forces $\sigma_2 dA$ on the wall section and the elementary pressure forces $p dA$ exerted on the portion of fluid included in the free body. Noting that the area of the fluid section is πr^2 and that the area of the wall section can be obtained by multiplying the circumference $2\pi r$ of the cylinder by its wall thickness t , we write the equilibrium equation:†

$$\Sigma F_x = 0: \quad \sigma_2(2\pi r t) - p(\pi r^2) = 0$$

and, solving for the longitudinal stress σ_2 ,

$$\sigma_2 = \frac{pr}{2t} \quad (7.31)$$

We note from Eqs. (7.30) and (7.31) that the hoop stress σ_1 is twice as large as the longitudinal stress σ_2 :

$$\sigma_1 = 2\sigma_2 \quad (7.32)$$

†Using the mean radius of the wall section, $r_m = r + \frac{1}{2}t$, in computing the resultant of the forces on that section, we would obtain a more accurate value of the longitudinal stress, namely,

$$\sigma_2 = \frac{pr}{2t} \frac{1}{1 + \frac{t}{2r}} \quad (7.31')$$

However, for a thin-walled pressure vessel, the term $t/2r$ is sufficiently small to allow the use of Eq. (7.31) for engineering design and analysis. If a pressure vessel is not thin-walled (i.e., if $t/2r$ is not small), the stresses σ_1 and σ_2 vary across the wall and must be determined by the methods of the theory of elasticity.

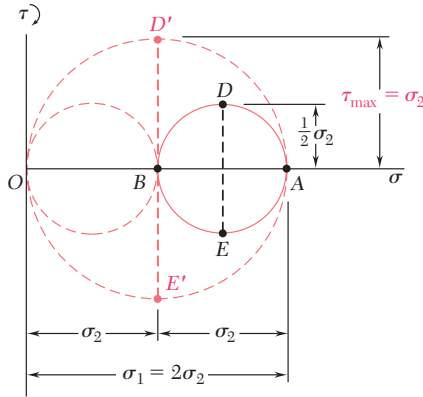


Fig. 7.50 Mohr's circle for element of cylindrical pressure vessel.

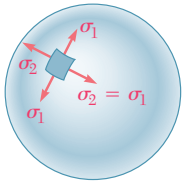


Fig. 7.51 Pressurized spherical vessel.

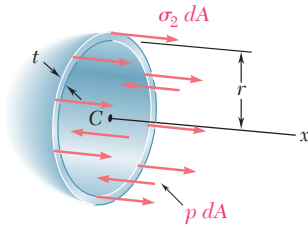


Fig. 7.52 Free body to determine wall stress.

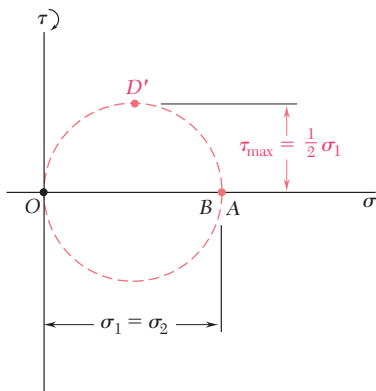


Fig. 7.53 Mohr's circle for element of spherical pressure vessel.

Drawing Mohr's circle through the points A and B that correspond respectively to the principal stresses σ_1 and σ_2 (Fig. 7.50), and recalling that the maximum in-plane shearing stress is equal to the radius of this circle, we have

$$\tau_{\max (\text{in plane})} = \frac{1}{2} \sigma_2 = \frac{pr}{4t} \quad (7.33)$$

This stress corresponds to points D and E and is exerted on an element obtained by rotating the original element of Fig. 7.47 through 45° *within the plane* tangent to the surface of the vessel. The maximum shearing stress in the wall of the vessel, however, is larger. It is equal to the radius of the circle of diameter OA and corresponds to a rotation of 45° about a longitudinal axis and *out of the plane* of stress.† We have

$$\tau_{\max} = \sigma_2 = \frac{pr}{2t} \quad (7.34)$$

We now consider a spherical vessel of inner radius r and wall thickness t , containing a fluid under a gage pressure p . For reasons of symmetry, the stresses exerted on the four faces of a small element of wall must be equal (Fig. 7.51). We have

$$\sigma_1 = \sigma_2 \quad (7.35)$$

To determine the value of the stress, we pass a section through the center C of the vessel and consider the free body consisting of the portion of the vessel and its contents located to the left of the section (Fig. 7.52). The equation of equilibrium for this free body is the same as for the free body of Fig. 7.49. We thus conclude that, for a spherical vessel,

$$\sigma_1 = \sigma_2 = \frac{pr}{2t} \quad (7.36)$$

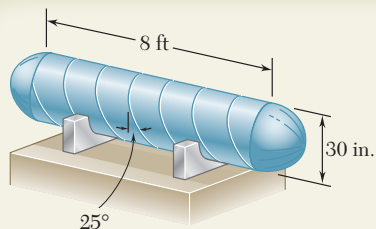
Since the principal stresses σ_1 and σ_2 are equal, Mohr's circle for transformations of stress within the plane tangent to the surface of the vessel reduces to a point (Fig. 7.53); we conclude that the in-plane normal stress is constant and that the in-plane maximum shearing stress is zero. The maximum shearing stress in the wall of the vessel, however, is not zero; it is equal to the radius of the circle of diameter OA and corresponds to a rotation of 45° out of the plane of stress. We have

$$\tau_{\max} = \frac{1}{2} \sigma_1 = \frac{pr}{4t} \quad (7.37)$$

†It should be observed that, while the third principal stress is zero on the outer surface of the vessel, it is equal to $-p$ on the inner surface, and is represented by a point $C(-p, 0)$ on a Mohr-circle diagram. Thus, close to the inside surface of the vessel, the maximum shearing stress is equal to the radius of a circle of diameter CA , and we have

$$\tau_{\max} = \frac{1}{2} (\sigma_1 + p) = \frac{pr}{2t} \left(1 + \frac{t}{r} \right)$$

For a thin-walled vessel, however, the term t/r is small, and we can neglect the variation of τ_{\max} across the wall section. This remark also applies to spherical pressure vessels.



SAMPLE PROBLEM 7.5

A compressed-air tank is supported by two cradles as shown; one of the cradles is designed so that it does not exert any longitudinal force on the tank. The cylindrical body of the tank has a 30-in. outer diameter and is fabricated from a $\frac{3}{8}$ -in. steel plate by butt welding along a helix that forms an angle of 25° with a transverse plane. The end caps are spherical and have a uniform wall thickness of $\frac{5}{16}$ in. For an internal gage pressure of 180 psi, determine (a) the normal stress and the maximum shearing stress in the spherical caps. (b) the stresses in directions perpendicular and parallel to the helical weld.

SOLUTION

a. Spherical Cap. Using Eq. (7.36), we write

$$p = 180 \text{ psi}, t = \frac{5}{16} \text{ in.} = 0.3125 \text{ in.}, r = 15 - 0.3125 = 14.688 \text{ in.}$$

$$\sigma_1 = \sigma_2 = \frac{pr}{2t} = \frac{(180 \text{ psi})(14.688 \text{ in.})}{2(0.3125 \text{ in.})} \quad \sigma = 4230 \text{ psi} \quad \blacktriangleleft$$

We note that for stresses in a plane tangent to the cap, Mohr's circle reduces to a point (A, B) on the horizontal axis and that all in-plane shearing stresses are zero. On the surface of the cap the third principal stress is zero and corresponds to point O. On a Mohr's circle of diameter AO, point D' represents the maximum shearing stress; it occurs on planes at 45° to the plane tangent to the cap.

$$\tau_{\max} = \frac{1}{2} (4230 \text{ psi}) \quad \tau_{\max} = 2115 \text{ psi} \quad \blacktriangleleft$$

b. Cylindrical Body of the Tank. We first determine the hoop stress σ_1 and the longitudinal stress σ_2 . Using Eqs. (7.30) and (7.32), we write

$$p = 180 \text{ psi}, t = \frac{3}{8} \text{ in.} = 0.375 \text{ in.}, r = 15 - 0.375 = 14.625 \text{ in.}$$

$$\sigma_1 = \frac{pr}{t} = \frac{(180 \text{ psi})(14.625 \text{ in.})}{0.375 \text{ in.}} = 7020 \text{ psi} \quad \sigma_2 = \frac{1}{2} \sigma_1 = 3510 \text{ psi}$$

$$\sigma_{\text{ave}} = \frac{1}{2} (\sigma_1 + \sigma_2) = 5265 \text{ psi} \quad R = \frac{1}{2} (\sigma_1 - \sigma_2) = 1755 \text{ psi}$$

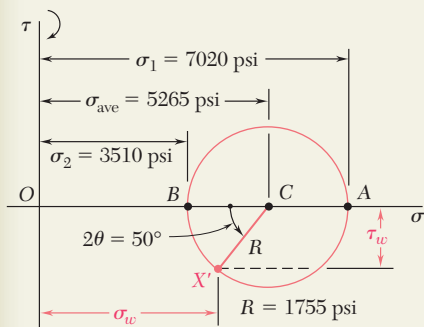
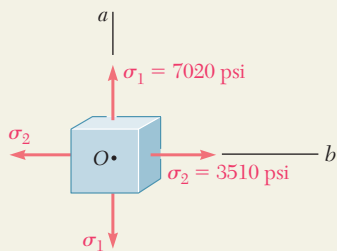
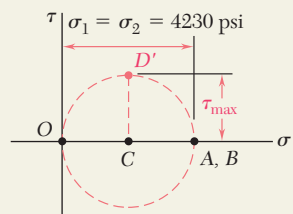
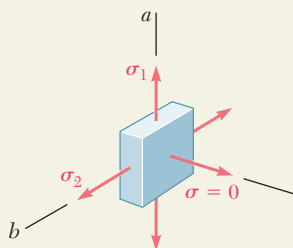
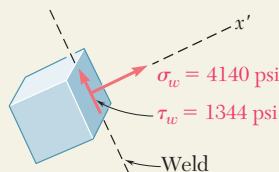
Stresses at the Weld. Noting that both the hoop stress and the longitudinal stress are principal stresses, we draw Mohr's circle as shown.

An element having a face parallel to the weld is obtained by rotating the face perpendicular to the axis Ob counterclockwise through 25° . Therefore, on Mohr's circle we locate the point X' corresponding to the stress components on the weld by rotating radius CB counterclockwise through $2\theta = 50^\circ$.

$$\sigma_w = \sigma_{\text{ave}} - R \cos 50^\circ = 5265 - 1755 \cos 50^\circ \quad \sigma_w = +4140 \text{ psi} \quad \blacktriangleleft$$

$$\tau_w = R \sin 50^\circ = 1755 \sin 50^\circ \quad \tau_w = 1344 \text{ psi} \quad \blacktriangleleft$$

Since X' is below the horizontal axis, τ_w tends to rotate the element counterclockwise.



PROBLEMS

7.98 A spherical gas container made of steel has a 5-m outer diameter and a wall thickness of 6 mm. Knowing that the internal pressure is 350 kPa, determine the maximum normal stress and the maximum shearing stress in the container.

7.99 The maximum gage pressure is known to be 8 MPa in a spherical steel pressure vessel having a 250-mm outer diameter and a 6-mm wall thickness. Knowing that the ultimate stress in the steel used is $\sigma_U = 400$ MPa, determine the factor of safety with respect to tensile failure.

7.100 A basketball has a 9.5-in. outer diameter and a 0.125-in. wall thickness. Determine the normal stress in the wall when the basketball is inflated to a 9-psi gage pressure.

7.101 A spherical pressure vessel of 900-mm outer diameter is to be fabricated from a steel having an ultimate stress $\sigma_U = 400$ MPa. Knowing that a factor of safety of 4.0 is desired and that the gage pressure can reach 3.5 MPa, determine the smallest wall thickness that should be used.

7.102 A spherical pressure vessel has an outer diameter of 10 ft and a wall thickness of 0.5 in. Knowing that for the steel used $\sigma_{all} = 12$ ksi, $E = 29 \times 10^6$ psi, and $\nu = 0.29$, determine (a) the allowable gage pressure, (b) the corresponding increase in the diameter of the vessel.

7.103 A spherical gas container having an outer diameter of 5 m and a wall thickness of 22 mm is made of steel for which $E = 200$ GPa and $\nu = 0.29$. Knowing that the gage pressure in the container is increased from zero to 1.7 MPa, determine (a) the maximum normal stress in the container, (b) the corresponding increase in the diameter of the container.

7.104 A steel penstock has a 750-mm outer diameter, a 12-mm wall thickness, and connects a reservoir at A with a generating station at B. Knowing that the density of water is 1000 kg/m^3 , determine the maximum normal stress and the maximum shearing stress in the penstock under static conditions.

7.105 A steel penstock has a 750-mm outer diameter and connects a reservoir at A with a generating station at B. Knowing that the density of water is 1000 kg/m^3 and that the allowable normal stress in the steel is 85 MPa, determine the smallest thickness that can be used for the penstock.

7.106 The bulk storage tank shown in Photo 7.3 has an outer diameter of 3.3 m and a wall thickness of 18 mm. At a time when the internal pressure of the tank is 1.5 MPa, determine the maximum normal stress and the maximum shearing stress in the tank.

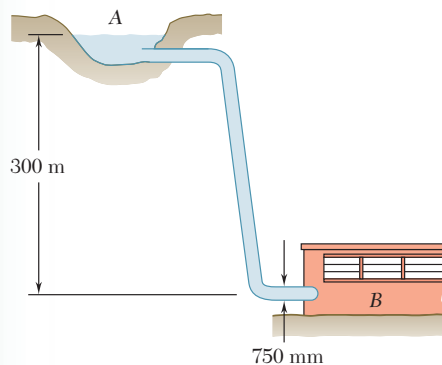


Fig. P7.104 and P7.105

7.107 Determine the largest internal pressure that can be applied to a cylindrical tank of 5.5-ft outer diameter and $\frac{5}{8}$ -in. wall thickness if the ultimate normal stress of the steel used is 65 ksi and a factor of safety of 5.0 is desired.

7.108 A cylindrical storage tank contains liquefied propane under a pressure of 1.5 MPa at a temperature of 38°C. Knowing that the tank has an outer diameter of 320 mm and a wall thickness of 3 mm, determine the maximum normal stress and the maximum shearing stress in the tank.

7.109 The unpressurized cylindrical storage tank shown has a $\frac{3}{16}$ -in. wall thickness and is made of steel having a 60-ksi ultimate strength in tension. Determine the maximum height h to which it can be filled with water if a factor of safety of 4.0 is desired. (Specific weight of water = 62.4 lb/ft³.)

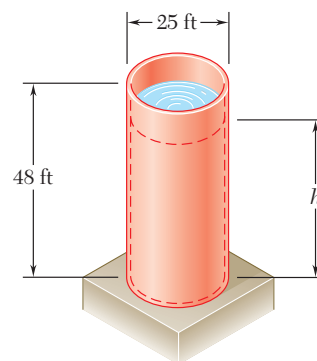


Fig. P7.109

7.110 For the storage tank of Prob. 7.109, determine the maximum normal stress and the maximum shearing stress in the cylindrical wall when the tank is filled to capacity ($h = 48$ ft).

7.111 A standard-weight steel pipe of 12-in. nominal diameter carries water under a pressure of 400 psi. (a) Knowing that the outside diameter is 12.75 in. and the wall thickness is 0.375 in., determine the maximum tensile stress in the pipe. (b) Solve part a, assuming an extra-strong pipe is used, of 12.75-in. outside diameter and 0.5-in. wall thickness.

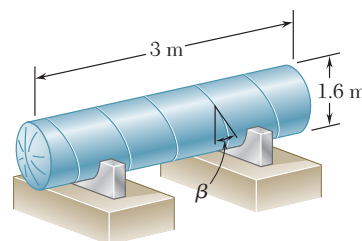


Fig. P7.112

7.112 The pressure tank shown has a 8-mm wall thickness and butt-welded seams forming an angle $\beta = 20^\circ$ with a transverse plane. For a gage pressure of 600 kPa, determine, (a) the normal stress perpendicular to the weld, (b) the shearing stress parallel to the weld.

7.113 For the tank of Prob. 7.112, determine the largest allowable gage pressure, knowing that the allowable normal stress perpendicular to the weld is 120 MPa and the allowable shearing stress parallel to the weld is 80 MPa.

7.114 For the tank of Prob. 7.112, determine the range of values of β that can be used if the shearing stress parallel to the weld is not to exceed 12 MPa when the gage pressure is 600 kPa.

7.115 The steel pressure tank shown has a 750-mm inner diameter and a 9-mm wall thickness. Knowing that the butt-welded seams form an angle $\beta = 50^\circ$ with the longitudinal axis of the tank and that the gage pressure in the tank is 1.5 MPa, determine, (a) the normal stress perpendicular to the weld, (b) the shearing stress parallel to the weld.

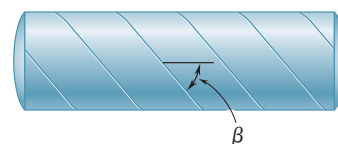


Fig. P7.115 and P7.116

7.116 The pressurized tank shown was fabricated by welding strips of plate along a helix forming an angle β with a transverse plane. Determine the largest value of β that can be used if the normal stress perpendicular to the weld is not to be larger than 85 percent of the maximum stress in the tank.

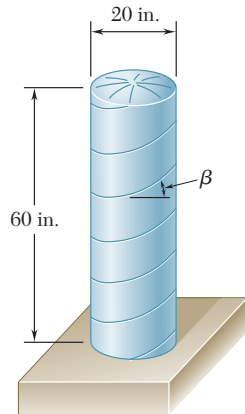


Fig. P7.117

7.117 The cylindrical portion of the compressed-air tank shown is fabricated of 0.25-in.-thick plate welded along a helix forming an angle $\beta = 30^\circ$ with the horizontal. Knowing that the allowable stress normal to the weld is 10.5 ksi, determine the largest gage pressure that can be used in the tank.

7.118 For the compressed-air tank of Prob. 7.117, determine the gage pressure that will cause a shearing stress parallel to the weld of 4 ksi.

7.119 Square plates, each of 0.5-in. thickness, can be bent and welded together in either of the two ways shown to form the cylindrical portion of a compressed-air tank. Knowing that the allowable normal stress perpendicular to the weld is 12 ksi, determine the largest allowable gage pressure in each case.

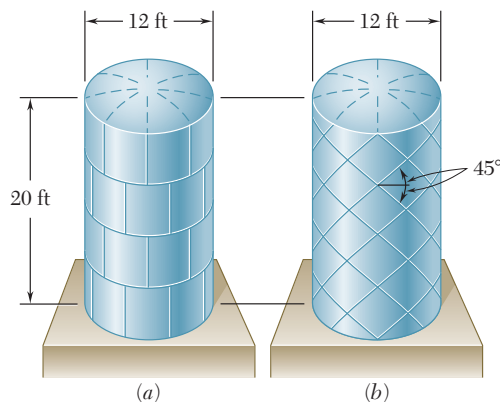


Fig. P7.119

7.120 The compressed-air tank AB has an inner diameter of 450 mm and a uniform wall thickness of 6 mm. Knowing that the gage pressure inside the tank is 1.2 MPa, determine the maximum normal stress and the maximum in-plane shearing stress at point *a* on the top of the tank.

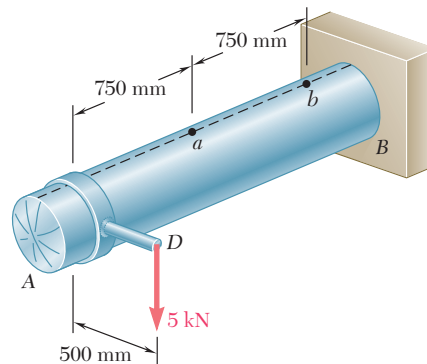


Fig. P7.120

7.121 For the compressed-air tank and loading of Prob. 7.120, determine the maximum normal stress and the maximum in-plane shearing stress at point *b* on the top of the tank.

7.122 The compressed-air tank AB has a 250-mm outside diameter and an 8-mm wall thickness. It is fitted with a collar by which a 40-kN force \mathbf{P} is applied at B in the horizontal direction. Knowing that the gage pressure inside the tank is 5 MPa, determine the maximum normal stress and the maximum shearing stress at point K .

7.123 In Prob. 7.122, determine the maximum normal stress and the maximum shearing stress at point L .

7.124 A pressure vessel of 10-in. inner diameter and 0.25-in. wall thickness is fabricated from a 4-ft section of spirally-welded pipe AB and is equipped with two rigid end plates. The gage pressure inside the vessel is 300 psi and 10-kip centric axial forces \mathbf{P} and \mathbf{P}' are applied to the end plates. Determine (a) the normal stress perpendicular to the weld, (b) the shearing stress parallel to the weld.

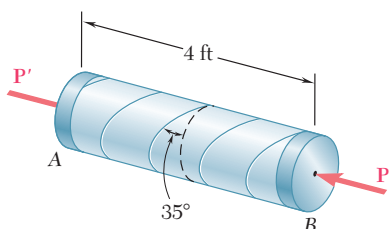


Fig. P7.124

7.125 Solve Prob. 7.124, assuming that the magnitude P of the two forces is increased to 30 kips.

7.126 A brass ring of 5-in. outer diameter and 0.25-in. thickness fits exactly inside a steel ring of 5-in. inner diameter and 0.125-in. thickness when the temperature of both rings is 50°F. Knowing that the temperature of both rings is then raised to 125°F, determine (a) the tensile stress in the steel ring, (b) the corresponding pressure exerted by the brass ring on the steel ring.

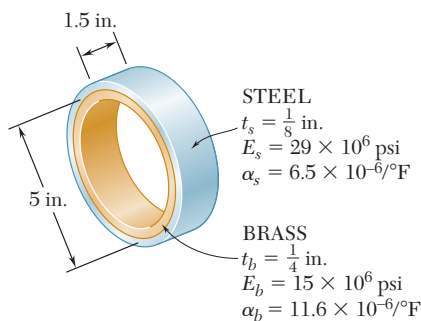


Fig. P7.126

7.127 Solve Prob. 7.126, assuming that the brass ring is 0.125 in. thick and the steel ring is 0.25 in. thick.

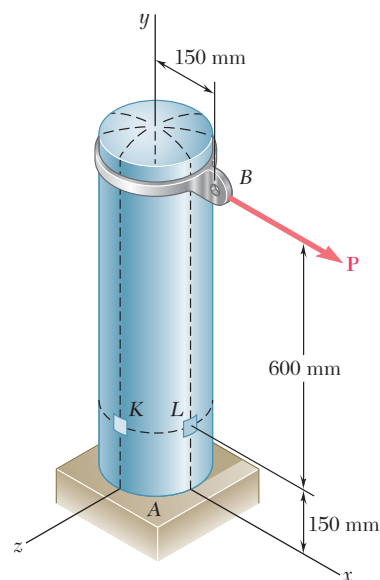


Fig. P7.122

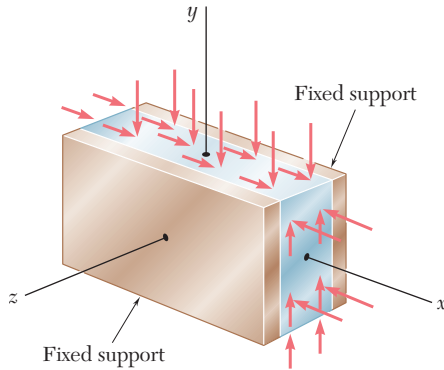


Fig. 7.54 Plane strain example: laterally restrained plate.

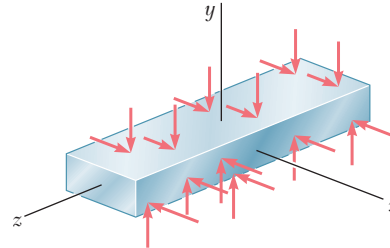


Fig. 7.55 Plane strain example: bar of infinite length.

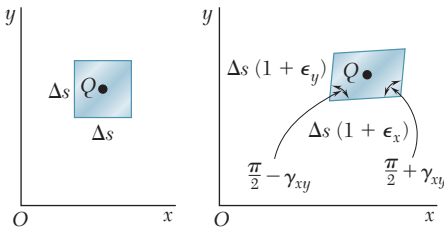


Fig. 7.56 Plane strain element deformation.

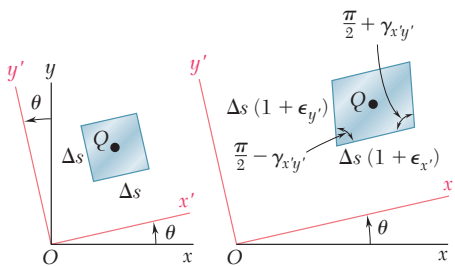


Fig. 7.57 Transformation of plane strain element.

*7.10 TRANSFORMATION OF PLANE STRAIN

Transformations of *strain* under a rotation of the coordinate axes will now be considered. Our analysis will first be limited to states of *plane strain*, i.e., to situations where the deformations of the material take place within parallel planes, and are the same in each of these planes. If the z axis is chosen perpendicular to the planes in which the deformations take place, we have $\epsilon_z = \gamma_{zx} = \gamma_{zy} = 0$, and the only remaining strain components are ϵ_x , ϵ_y , and γ_{xy} . Such a situation occurs in a plate subjected along its edges to uniformly distributed loads and restrained from expanding or contracting laterally by smooth, rigid, and fixed supports (Fig. 7.54). It would also be found in a bar of infinite length subjected on its sides to uniformly distributed loads since, by reason of symmetry, the elements located in a given transverse plane cannot move out of that plane. This idealized model shows that, in the actual case of a long bar subjected to uniformly distributed transverse loads (Fig. 7.55), a state of plane strain exists in any given transverse section that is not located too close to either end of the bar.†

Let us assume that a state of plane strain exists at point Q (with $\epsilon_z = \gamma_{zx} = \gamma_{zy} = 0$), and that it is defined by the strain components ϵ_x , ϵ_y , and γ_{xy} associated with the x and y axes. As we know from Secs. 2.12 and 2.14, this means that a square element of center Q , with sides of length Δs respectively parallel to the x and y axes, is deformed into a parallelogram with sides of length respectively equal to $\Delta s(1 + \epsilon_x)$ and $\Delta s(1 + \epsilon_y)$, forming angles of $\frac{\pi}{2} - \gamma_{xy}$ and $\frac{\pi}{2} + \gamma_{xy}$ with each other (Fig. 7.56). We recall that, as a result of the deformations of the other elements located in the xy plane, the element considered may also undergo a rigid-body motion, but such a motion is irrelevant to the determination of the strains at point Q and will be ignored in this analysis. Our purpose is to determine in terms of ϵ_x , ϵ_y , γ_{xy} , and θ the strain components ϵ'_x , ϵ'_y , and γ'_{xy} associated with the frame of reference $x'y'$ obtained by rotating the x and y axes through the angle θ . As shown in Fig. 7.57, these new strain

†It should be observed that a state of *plane strain* and a state of *plane stress* (cf. Sec. 7.1) do not occur simultaneously, except for ideal materials with a Poisson ratio equal to zero. The constraints placed on the elements of the plate of Fig. 7.54 and of the bar of Fig. 7.55 result in a stress σ_z different from zero. On the other hand, in the case of the plate of Fig. 7.3, the absence of any lateral restraint results in $\sigma_z = 0$ and $\epsilon_z \neq 0$.

components define the parallelogram into which a square with sides respectively parallel to the x' and y' axes is deformed.

We first derive an expression for the normal strain $\epsilon(\theta)$ along a line AB forming an arbitrary angle θ with the x axis. To do so, we consider the right triangle ABC , which has AB for hypotenuse (Fig. 7.58a), and the oblique triangle $A'B'C'$ into which triangle ABC is deformed (Fig. 7.58b). Denoting by Δs the length of AB , we express the length of $A'B'$ as $\Delta s [1 + \epsilon(\theta)]$. Similarly, denoting by Δx and Δy the lengths of sides AC and CB , we express the lengths of $A'C'$ and $C'B'$ as $\Delta x (1 + \epsilon_x)$ and $\Delta y (1 + \epsilon_y)$, respectively. Recalling from Fig. 7.56 that the right angle at C in Fig. 7.58a deforms into an angle equal to $\frac{\pi}{2} + \gamma_{xy}$ in Fig. 7.58b, and applying the law of cosines to triangle $A'B'C'$, we write

$$\begin{aligned} (A'B')^2 &= (A'C')^2 + (C'B')^2 - 2(A'C')(C'B') \cos\left(\frac{\pi}{2} + \gamma_{xy}\right) \\ (\Delta s)^2 [1 + \epsilon(\theta)]^2 &= (\Delta x)^2 (1 + \epsilon_x)^2 + (\Delta y)^2 (1 + \epsilon_y)^2 \\ &\quad - 2(\Delta x)(1 + \epsilon_x)(\Delta y)(1 + \epsilon_y) \cos\left(\frac{\pi}{2} + \gamma_{xy}\right) \end{aligned} \quad (7.38)$$

But from Fig. 7.58a we have

$$\Delta x = (\Delta s) \cos \theta \quad \Delta y = (\Delta s) \sin \theta \quad (7.39)$$

and we note that, since γ_{xy} is very small,

$$\cos\left(\frac{\pi}{2} + \gamma_{xy}\right) = -\sin \gamma_{xy} \approx -\gamma_{xy} \quad (7.40)$$

Substituting from Eqs. (7.39) and (7.40) into Eq. (7.38), recalling that $\cos^2 \theta + \sin^2 \theta = 1$, and neglecting second-order terms in $\epsilon(\theta)$, ϵ_x , ϵ_y , and γ_{xy} , we write

$$\epsilon(\theta) = \epsilon_x \cos^2 \theta + \epsilon_y \sin^2 \theta + \gamma_{xy} \sin \theta \cos \theta \quad (7.41)$$

Equation (7.41) enables us to determine the normal strain $\epsilon(\theta)$ in any direction AB in terms of the strain components ϵ_x , ϵ_y , γ_{xy} , and the angle θ that AB forms with the x axis. We check that, for $\theta = 0$, Eq. (7.41) yields $\epsilon(0) = \epsilon_x$ and that, for $\theta = 90^\circ$, it yields $\epsilon(90^\circ) = \epsilon_y$. On the other hand, making $\theta = 45^\circ$ in Eq. (7.41), we obtain the normal strain in the direction of the bisector OB of the angle formed by the x and y axes (Fig. 7.59). Denoting this strain by ϵ_{OB} , we write

$$\epsilon_{OB} = \epsilon(45^\circ) = \frac{1}{2} (\epsilon_x + \epsilon_y + \gamma_{xy}) \quad (7.42)$$

Solving Eq. (7.42) for γ_{xy} , we have

$$\gamma_{xy} = 2\epsilon_{OB} - (\epsilon_x + \epsilon_y) \quad (7.43)$$

This relation makes it possible to express the *shearing strain* associated with a given pair of rectangular axes in terms of the *normal strains* measured along these axes and their bisector. It will play a fundamental role in our present derivation and will also be used in Sec. 7.13 in connection with the experimental determination of shearing strains.

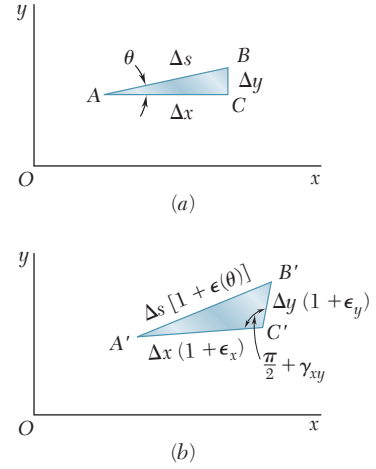


Fig. 7.58

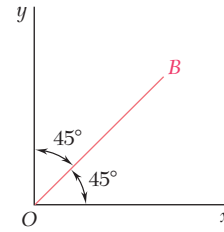


Fig. 7.59

Recalling that the main purpose of this section is to express the strain components associated with the frame of reference $x'y'$ of Fig. 7.57 in terms of the angle θ and the strain components ϵ_x , ϵ_y , and γ_{xy} associated with the x and y axes, we note that the normal strain $\epsilon_{x'}$ along the x' axis is given by Eq. (7.41). Using the trigonometric relations (7.3) and (7.4), we write this equation in the alternative form

$$\epsilon_{x'} = \frac{\epsilon_x + \epsilon_y}{2} + \frac{\epsilon_x - \epsilon_y}{2} \cos 2\theta + \frac{\gamma_{xy}}{2} \sin 2\theta \quad (7.44)$$

Replacing θ by $\theta + 90^\circ$, we obtain the normal strain along the y' axis. Since $\cos(2\theta + 180^\circ) = -\cos 2\theta$ and $\sin(2\theta + 180^\circ) = -\sin 2\theta$, we have

$$\epsilon_{y'} = \frac{\epsilon_x + \epsilon_y}{2} - \frac{\epsilon_x - \epsilon_y}{2} \cos 2\theta - \frac{\gamma_{xy}}{2} \sin 2\theta \quad (7.45)$$

Adding Eqs. (7.44) and (7.45) member to member, we obtain

$$\epsilon_{x'} + \epsilon_{y'} = \epsilon_x + \epsilon_y \quad (7.46)$$

Since $\epsilon_z = \epsilon_{z'} = 0$, we thus verify in the case of plane strain that the sum of the normal strains associated with a cubic element of material is independent of the orientation of that element.[†]

Replacing now θ by $\theta + 45^\circ$ in Eq. (7.44), we obtain an expression for the normal strain along the bisector OB' of the angle formed by the x' and y' axes. Since $\cos(2\theta + 90^\circ) = -\sin 2\theta$ and $\sin(2\theta + 90^\circ) = \cos 2\theta$, we have

$$\epsilon_{OB'} = \frac{\epsilon_x + \epsilon_y}{2} - \frac{\epsilon_x - \epsilon_y}{2} \sin 2\theta + \frac{\gamma_{xy}}{2} \cos 2\theta \quad (7.47)$$

Writing Eq. (7.43) with respect to the x' and y' axes, we express the shearing strain $\gamma_{x'y'}$ in terms of the normal strains measured along the x' and y' axes and the bisector OB' :

$$\gamma_{x'y'} = 2\epsilon_{OB'} - (\epsilon_{x'} + \epsilon_{y'}) \quad (7.48)$$

Substituting from Eqs. (7.46) and (7.47) into (7.48), we obtain

$$\gamma_{x'y'} = -(\epsilon_x - \epsilon_y) \sin 2\theta + \gamma_{xy} \cos 2\theta \quad (7.49)$$

Equations (7.44), (7.45), and (7.49) are the desired equations defining the transformation of plane strain under a rotation of axes in the plane of strain. Dividing all terms in Eq. (7.49) by 2, we write this equation in the alternative form

$$\frac{\gamma_{x'y'}}{2} = -\frac{\epsilon_x - \epsilon_y}{2} \sin 2\theta + \frac{\gamma_{xy}}{2} \cos 2\theta \quad (7.49')$$

and observe that Eqs. (7.44), (7.45), and (7.49') for the transformation of plane strain closely resemble the equations derived in Sec. 7.2 for the transformation of plane stress. While the former may be obtained from the latter by replacing the normal stresses by the corresponding normal strains, it should be noted, however, that the shearing stresses τ_{xy} and $\tau_{x'y'}$ should be replaced by *half* of the corresponding shearing strains, i.e., by $\frac{1}{2}\gamma_{xy}$ and $\frac{1}{2}\gamma_{x'y'}$, respectively.

[†]Cf. first footnote on page 97.

Since the equations for the transformation of plane strain are of the same form as the equations for the transformation of plane stress, the use of Mohr's circle can be extended to the analysis of plane strain. Given the strain components ϵ_x , ϵ_y , and γ_{xy} defining the deformation represented in Fig. 7.56, we plot a point $X(\epsilon_x, -\frac{1}{2}\gamma_{xy})$ of abscissa equal to the normal strain ϵ_x and of ordinate equal to minus half the shearing strain γ_{xy} , and a point $Y(\epsilon_y, +\frac{1}{2}\gamma_{xy})$ (Fig. 7.60). Drawing the diameter XY , we define the center C of Mohr's circle for plane strain. The abscissa of C and the radius R of the circle are respectively equal to

$$\epsilon_{\text{ave}} = \frac{\epsilon_x + \epsilon_y}{2} \quad \text{and} \quad R = \sqrt{\left(\frac{\epsilon_x - \epsilon_y}{2}\right)^2 + \left(\frac{\gamma_{xy}}{2}\right)^2} \quad (7.50)$$

We note that if γ_{xy} is positive, as assumed in Fig. 7.56, points X and Y are plotted, respectively, below and above the horizontal axis in Fig. 7.60. But, in the absence of any overall rigid-body rotation, the side of the element in Fig. 7.56 that is associated with ϵ_x is observed to rotate counterclockwise, while the side associated with ϵ_y is observed to rotate clockwise. Thus, if the shear deformation causes a given side to rotate *clockwise*, the corresponding point on Mohr's circle for plane strain is plotted *above* the horizontal axis, and if the deformation causes the side to rotate *counterclockwise*, the corresponding point is plotted *below* the horizontal axis. We note that this convention matches the convention used to draw Mohr's circle for plane stress.

Points A and B where Mohr's circle intersects the horizontal axis correspond to the *principal strains* ϵ_{max} and ϵ_{min} (Fig. 7.61a). We find

$$\epsilon_{\text{max}} = \epsilon_{\text{ave}} + R \quad \text{and} \quad \epsilon_{\text{min}} = \epsilon_{\text{ave}} - R \quad (7.51)$$

where ϵ_{ave} and R are defined by Eqs. (7.50). The corresponding value θ_p of the angle θ is obtained by observing that the shearing strain is zero for A and B . Setting $\gamma_{x'y'} = 0$ in Eq. (7.49), we have

$$\tan 2\theta_p = \frac{\gamma_{xy}}{\epsilon_x - \epsilon_y} \quad (7.52)$$

The corresponding axes a and b in Fig. 7.61b are the *principal axes of strain*. The angle θ_p , which defines the direction of the principal axis Oa in Fig. 7.61b corresponding to point A in Fig. 7.61a, is equal to half of the angle XCA measured on Mohr's circle, and the rotation that brings Ox into Oa has the same sense as the rotation that brings the diameter XY of Mohr's circle into the diameter AB .

We recall from Sec. 2.14 that, in the case of the elastic deformation of a homogeneous, isotropic material, Hooke's law for shearing stress and strain applies and yields $\tau_{xy} = G\gamma_{xy}$ for any pair of rectangular x and y axes. Thus, $\gamma_{xy} = 0$ when $\tau_{xy} = 0$, which indicates that the principal axes of strain coincide with the principal axes of stress.

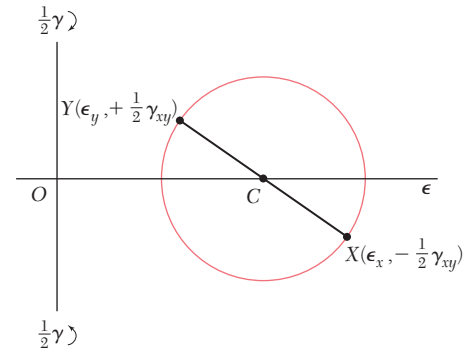


Fig. 7.60 Mohr's circle for plane strain.

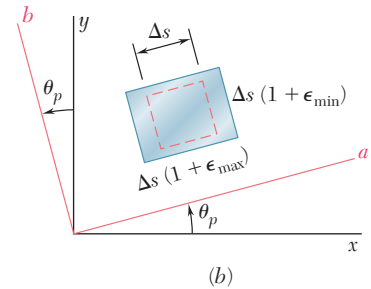
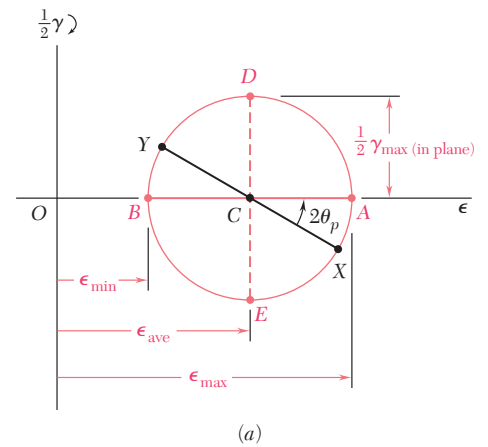


Fig. 7.61 Principal strain determination.

The maximum in-plane shearing strain is defined by points D and E in Fig. 7.61a. It is equal to the diameter of Mohr's circle. Recalling the second of Eqs. (7.50), we write

$$\gamma_{\max}(\text{in plane}) = 2R = \sqrt{(\epsilon_x - \epsilon_y)^2 + \gamma_{xy}^2} \quad (7.53)$$

Finally, we note that the points X' and Y' that define the components of strain corresponding to a rotation of the coordinate axes through an angle θ (Fig. 7.57) are obtained by rotating the diameter XY of Mohr's circle in the same sense through an angle 2θ (Fig. 7.62).

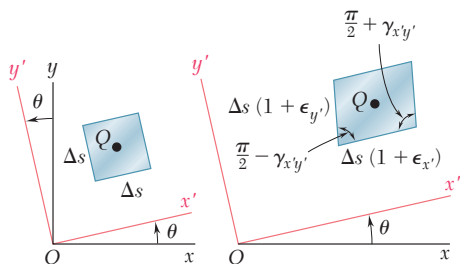


Fig. 7.57 (repeated)

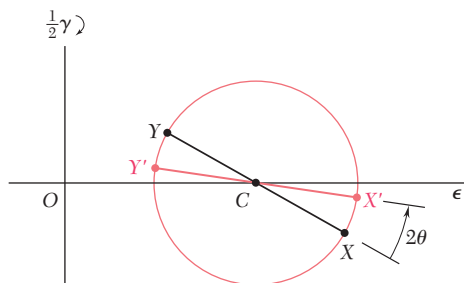


Fig. 7.62

EXAMPLE 7.04

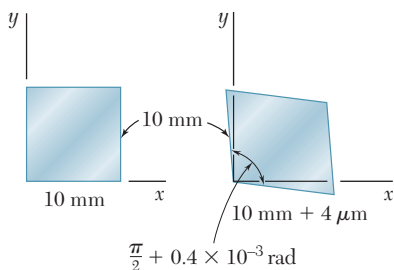


Fig. 7.63

In a material in a state of plane strain, it is known that the horizontal side of a 10×10 -mm square elongates by $4 \mu\text{m}$, while its vertical side remains unchanged, and that the angle at the lower left corner increases by 0.4×10^{-3} rad (Fig. 7.63). Determine (a) the principal axes and principal strains, (b) the maximum shearing strain and the corresponding normal strain.

(a) Principal Axes and Principal Strains. We first determine the coordinates of points X and Y on Mohr's circle for strain. We have

$$\epsilon_x = \frac{+4 \times 10^{-6} \text{ m}}{10 \times 10^{-3} \text{ m}} = +400 \mu \quad \epsilon_y = 0 \quad \left| \frac{\gamma_{xy}}{2} \right| = 200 \mu$$

Since the side of the square associated with ϵ_x rotates *clockwise*, point X of coordinates ϵ_x and $|\gamma_{xy}/2|$ is plotted *above* the horizontal axis. Since $\epsilon_y = 0$ and the corresponding side rotates *counterclockwise*, point Y is plotted directly *below* the origin (Fig. 7.64). Drawing the diameter XY , we determine the center C of Mohr's circle and its radius R . We have

$$OC = \frac{\epsilon_x + \epsilon_y}{2} = 200 \mu \quad OY = 200 \mu$$

$$R = \sqrt{(OC)^2 + (OY)^2} = \sqrt{(200 \mu)^2 + (200 \mu)^2} = 283 \mu$$

The principal strains are defined by the abscissas of points A and B . We write

$$\epsilon_a = OA = OC + R = 200 \mu + 283 \mu = 483 \mu$$

$$\epsilon_b = OB = OC - R = 200 \mu - 283 \mu = -83 \mu$$

The principal axes Oa and Ob are shown in Fig. 7.65. Since $OC = OY$, the angle at C in triangle OCY is 45° . Thus, the angle $2\theta_p$ that brings XY into AB is 45° and the angle θ_p bringing Ox into Oa is 22.5° .

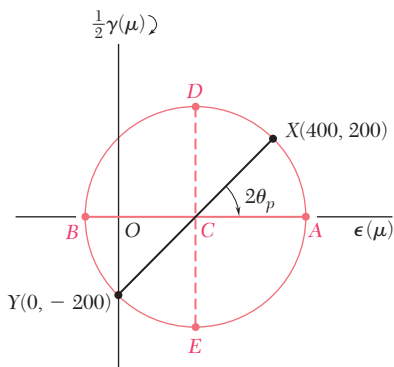


Fig. 7.64

(b) Maximum Shearing Strain. Points D and E define the maximum in-plane shearing strain which, since the principal strains have opposite signs, is also the actual maximum shearing strain (see Sec. 7.12). We have

$$\frac{\gamma_{\max}}{2} = R = 283 \mu \quad \gamma_{\max} = 566 \mu$$

The corresponding normal strains are both equal to

$$\epsilon' = OC = 200 \mu$$

The axes of maximum shearing strain are shown in Fig. 7.66.

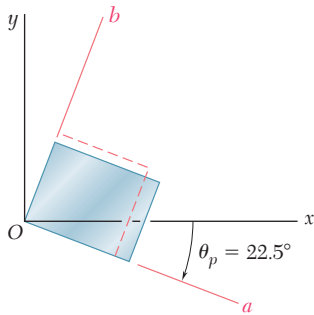


Fig. 7.65

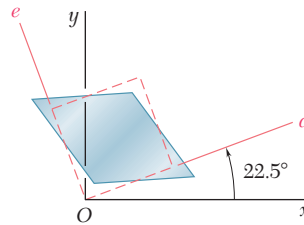


Fig. 7.66

*7.12 THREE-DIMENSIONAL ANALYSIS OF STRAIN

We saw in Sec. 7.5 that, in the most general case of stress, we can determine three coordinate axes a , b , and c , called the principal axes of stress. A small cubic element with faces respectively perpendicular to these axes is free of shearing stresses (Fig. 7.25); i.e., we have $\tau_{ab} = \tau_{bc} = \tau_{ca} = 0$. As recalled in the preceding section, Hooke's law for shearing stress and strain applies when the deformation is elastic and the material homogeneous and isotropic. It follows that, in such a case, $\gamma_{ab} = \gamma_{bc} = \gamma_{ca} = 0$, i.e., the axes a , b , and c are also *principal axes of strain*. A small cube of side equal to unity, centered at Q and with faces respectively perpendicular to the principal axes, is deformed into a rectangular parallelepiped of sides $1 + \epsilon_a$, $1 + \epsilon_b$, and $1 + \epsilon_c$ (Fig. 7.67).

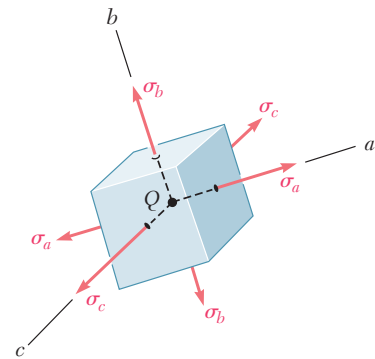


Fig. 7.25 (repeated)

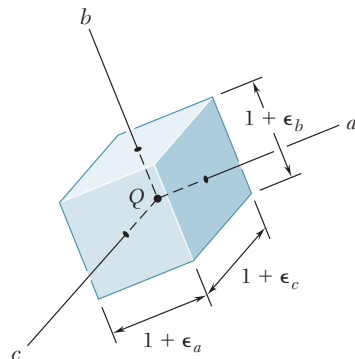


Fig. 7.67 Principal strains.

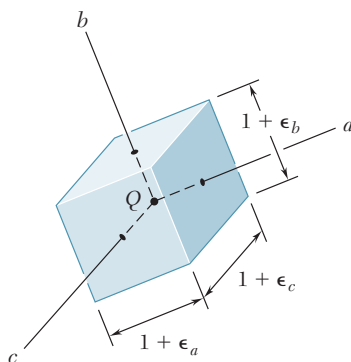


Fig. 7.67 (repeated)

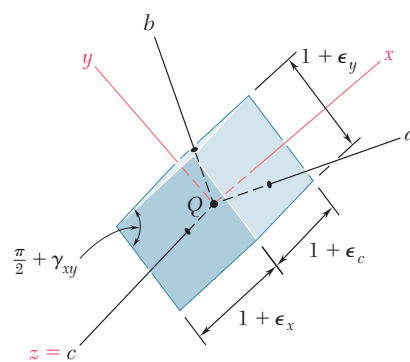


Fig. 7.68

If the element of Fig. 7.67 is rotated about one of the principal axes at Q , say the c axis (Fig. 7.68), the method of analysis developed earlier for the transformation of plane strain can be used to determine the strain components ϵ_x , ϵ_y , and γ_{xy} associated with the faces perpendicular to the c axis, since the derivation of this method did not involve any of the other strain components.† We can, therefore, draw Mohr's circle through the points A and B corresponding to the principal axes a and b (Fig. 7.69). Similarly, circles of diameters BC and CA can be used to analyze the transformation of strain as the element is rotated about the a and b axes, respectively.

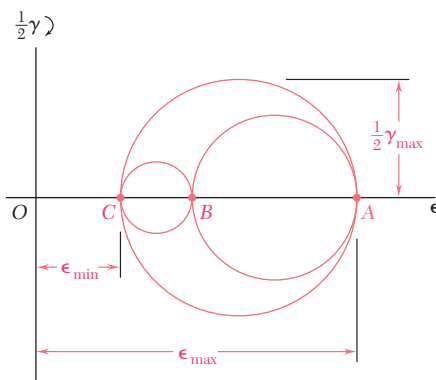


Fig. 7.69 Mohr's circle for three-dimensional analysis of strain.

The three-dimensional analysis of strain by means of Mohr's circle is limited here to rotations about principal axes (as was the case for the analysis of stress) and is used to determine the maximum shearing strain γ_{\max} at point Q . Since γ_{\max} is equal to the diameter of the largest of the three circles shown in Fig. 7.69, we have

$$\gamma_{\max} = |\epsilon_{\max} - \epsilon_{\min}| \quad (7.54)$$

where ϵ_{\max} and ϵ_{\min} represent the *algebraic* values of the maximum and minimum strains at point Q .

†We note that the other four faces of the element remain rectangular and that the edges parallel to the c axis remain unchanged.

Returning to the particular case of *plane strain*, and selecting the x and y axes in the plane of strain, we have $\epsilon_z = \gamma_{zx} = \gamma_{zy} = 0$. Thus, the z axis is one of the three principal axes at Q , and the corresponding point in the Mohr-circle diagram is the origin O , where $\epsilon = \gamma = 0$. If the points A and B that define the principal axes within the plane of strain fall on opposite sides of O (Fig. 7.70a), the corresponding principal strains represent the maximum and minimum normal strains at point Q , and the maximum shearing strain is equal to the maximum in-plane shearing strain corresponding to points D and E . If, on the other hand, A and B are on the same side of O (Fig. 7.70b), that is, if ϵ_a and ϵ_b have the same sign, then the maximum shearing strain is defined by points D' and E' on the circle of diameter OA , and we have $\gamma_{\max} = \epsilon_{\max}$.

We now consider the particular case of *plane stress* encountered in a thin plate or on the free surface of a structural element or machine component (Sec. 7.1). Selecting the x and y axes in the plane of stress, we have $\sigma_z = \tau_{zx} = \tau_{zy} = 0$ and verify that the z axis is a principal axis of stress. As we saw earlier, if the deformation is elastic and if the material is homogeneous and isotropic, it follows from Hooke's law that $\gamma_{zx} = \gamma_{zy} = 0$; thus, the z axis is also a principal axis of strain, and Mohr's circle can be used to analyze the transformation of strain in the xy plane. However, as we shall see presently, it does *not* follow from Hooke's law that $\epsilon_z = 0$; indeed, a state of plane stress does not, in general, result in a state of plane strain.†

Denoting by a and b the principal axes within the plane of stress, and by c the principal axis perpendicular to that plane, we let $\sigma_x = \sigma_a$, $\sigma_y = \sigma_b$, and $\sigma_z = 0$ in Eqs. (2.28) for the generalized Hooke's law (Sec. 2.12) and write

$$\epsilon_a = \frac{\sigma_a}{E} - \frac{\nu\sigma_b}{E} \quad (7.55)$$

$$\epsilon_b = -\frac{\nu\sigma_a}{E} + \frac{\sigma_b}{E} \quad (7.56)$$

$$\epsilon_c = -\frac{\nu}{E}(\sigma_a + \sigma_b) \quad (7.57)$$

Adding Eqs. (7.55) and (7.56) member to member, we have

$$\epsilon_a + \epsilon_b = \frac{1-\nu}{E}(\sigma_a + \sigma_b) \quad (7.58)$$

Solving Eq. (7.58) for $\sigma_a + \sigma_b$ and substituting into Eq. (7.57), we write

$$\epsilon_c = -\frac{\nu}{1-\nu}(\epsilon_a + \epsilon_b) \quad (7.59)$$

The relation obtained defines the third principal strain in terms of the "in-plane" principal strains. We note that, if B is located between A and C on the Mohr-circle diagram (Fig. 7.71), the maximum shearing strain is equal to the diameter CA of the circle corresponding to a rotation about the b axis, out of the plane of stress.

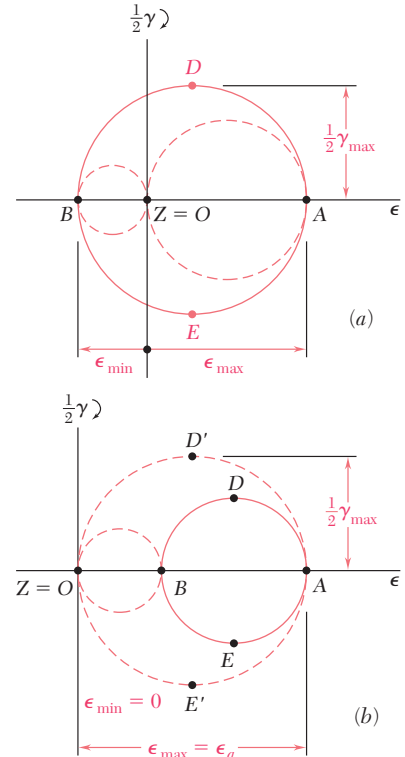


Fig. 7.70 Mohr's circle for plane strain.

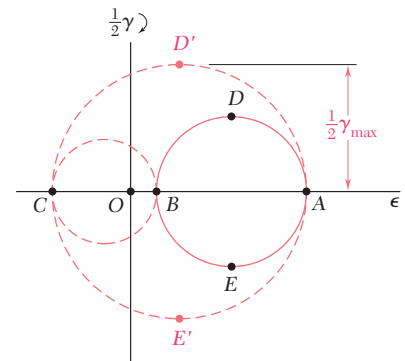


Fig. 7.71 Mohr's circle strain analysis for plane stress.

†See footnote on page 486.

EXAMPLE 7.05

As a result of measurements made on the surface of a machine component with strain gages oriented in various ways, it has been established that the principal strains on the free surface are $\epsilon_a = +400 \times 10^{-6}$ in./in. and $\epsilon_b = -50 \times 10^{-6}$ in./in. Knowing that Poisson's ratio for the given material is $\nu = 0.30$, determine (a) the maximum in-plane shearing strain, (b) the true value of the maximum shearing strain near the surface of the component.

(a) Maximum In-Plane Shearing Strain. We draw Mohr's circle through the points A and B corresponding to the given principal strains (Fig. 7.72). The maximum in-plane shearing strain is defined by points D and E and is equal to the diameter of Mohr's circle:

$$\gamma_{\max (\text{in plane})} = 400 \times 10^{-6} + 50 \times 10^{-6} = 450 \times 10^{-6} \text{ rad}$$

(b) Maximum Shearing Strain. We first determine the third principal strain ϵ_c . Since we have a state of plane stress on the surface of the machine component, we use Eq. (7.59) and write

$$\begin{aligned} \epsilon_c &= -\frac{\nu}{1-\nu}(\epsilon_a + \epsilon_b) \\ &= -\frac{0.30}{0.70}(400 \times 10^{-6} - 50 \times 10^{-6}) = -150 \times 10^{-6} \text{ in./in.} \end{aligned}$$

Drawing Mohr's circles through A and C and through B and C (Fig. 7.73), we find that the maximum shearing strain is equal to the diameter of the circle of diameter CA:

$$\gamma_{\max} = 400 \times 10^{-6} + 150 \times 10^{-6} = 550 \times 10^{-6} \text{ rad}$$

We note that, even though ϵ_a and ϵ_b have opposite signs, the maximum in-plane shearing strain does not represent the true maximum shearing strain.

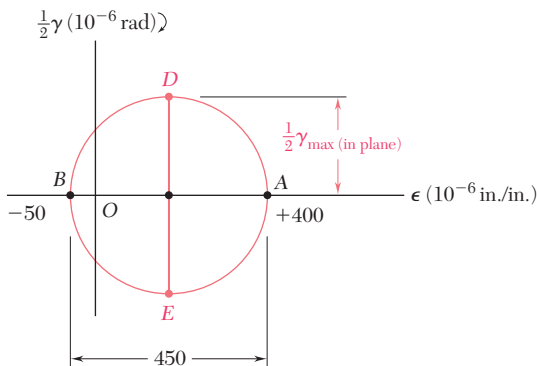


Fig. 7.72

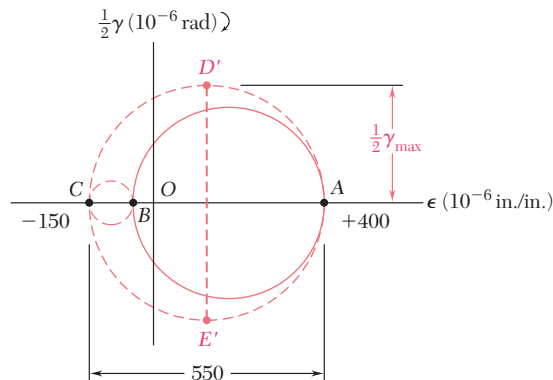


Fig. 7.73

*7.13 MEASUREMENTS OF STRAIN; STRAIN ROSETTE

The normal strain can be determined in any given direction on the surface of a structural element or machine component by scribing two gage marks A and B across a line drawn in the desired direction and measuring the length of the segment AB before and after the

load has been applied. If L is the undeformed length of AB and δ its deformation, the normal strain along AB is $\epsilon_{AB} = \delta/L$.

A more convenient and more accurate method for the measurement of normal strains is provided by electrical strain gages. A typical electrical strain gage consists of a length of thin wire arranged as shown in Fig. 7.74 and cemented to two pieces of paper. In order to measure the strain ϵ_{AB} of a given material in the direction AB , the gage is cemented to the surface of the material, with the wire folds running parallel to AB . As the material elongates, the wire increases in length and decreases in diameter, causing the electrical resistance of the gage to increase. By measuring the current passing through a properly calibrated gage, the strain ϵ_{AB} can be determined accurately and continuously as the load is increased.

The strain components ϵ_x and ϵ_y can be determined at a given point of the free surface of a material by simply measuring the normal strain along x and y axes drawn through that point. Recalling Eq. (7.43) of Sec. 7.10, we note that a third measurement of normal strain, made along the bisector OB of the angle formed by the x and y axes, enables us to determine the shearing strain γ_{xy} as well (Fig. 7.75):

$$\gamma_{xy} = 2\epsilon_{OB} - (\epsilon_x + \epsilon_y) \quad (7.43)$$

It should be noted that the strain components ϵ_x , ϵ_y , and γ_{xy} at a given point could be obtained from normal strain measurements made along *any three* lines drawn through that point (Fig. 7.76). Denoting respectively by θ_1 , θ_2 , and θ_3 the angle each of the three lines forms with the x axis, by ϵ_1 , ϵ_2 , and ϵ_3 the corresponding strain measurements, and substituting into Eq. (7.41), we write the three equations

$$\begin{aligned} \epsilon_1 &= \epsilon_x \cos^2 \theta_1 + \epsilon_y \sin^2 \theta_1 + \gamma_{xy} \sin \theta_1 \cos \theta_1 \\ \epsilon_2 &= \epsilon_x \cos^2 \theta_2 + \epsilon_y \sin^2 \theta_2 + \gamma_{xy} \sin \theta_2 \cos \theta_2 \\ \epsilon_3 &= \epsilon_x \cos^2 \theta_3 + \epsilon_y \sin^2 \theta_3 + \gamma_{xy} \sin \theta_3 \cos \theta_3 \end{aligned} \quad (7.60)$$

which can be solved simultaneously for ϵ_x , ϵ_y , and γ_{xy} .†

The arrangement of strain gages used to measure the three normal strains ϵ_1 , ϵ_2 , and ϵ_3 is known as a *strain rosette*. The rosette used to measure normal strains along the x and y axes and their bisector is referred to as a 45° rosette (Fig. 7.75). Another rosette frequently used is the 60° rosette (see Sample Prob. 7.7).

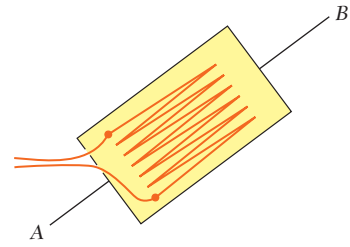


Fig. 7.74 Electrical strain gage.

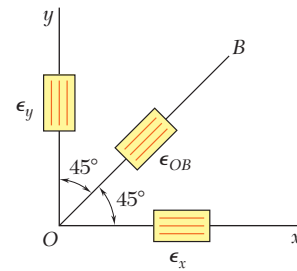


Fig. 7.75

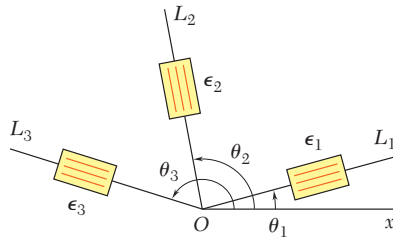
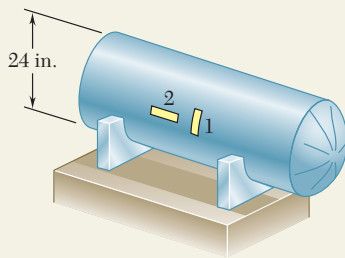


Fig. 7.76 Strain rosette.

†It should be noted that the free surface on which the strain measurements are made is in a state of *plane stress*, while Eqs. (7.41) and (7.43) were derived for a state of *plane strain*. However, as observed earlier, the normal to the free surface is a principal axis of strain and the derivations given in Sec. 7.10 remain valid.

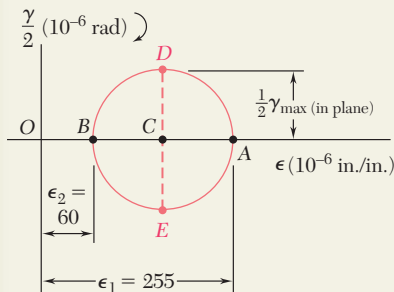


SAMPLE PROBLEM 7.6

A cylindrical storage tank used to transport gas under pressure has an inner diameter of 24 in. and a wall thickness of $\frac{3}{4}$ in. Strain gages attached to the surface of the tank in transverse and longitudinal directions indicate strains of 255×10^{-6} and 60×10^{-6} in./in. respectively. Knowing that a torsion test has shown that the modulus of rigidity of the material used in the tank is $G = 11.2 \times 10^6$ psi, determine (a) the gage pressure inside the tank, (b) the principal stresses and the maximum shearing stress in the wall of the tank.

SOLUTION

a. Gage Pressure Inside Tank. We note that the given strains are the principal strains at the surface of the tank. Plotting the corresponding points A and B , we draw Mohr's circle for strain. The maximum in-plane shearing strain is equal to the diameter of the circle.



$$\gamma_{\max (\text{in plane})} = \epsilon_1 - \epsilon_2 = 255 \times 10^{-6} - 60 \times 10^{-6} = 195 \times 10^{-6} \text{ rad}$$

From Hooke's law for shearing stress and strain, we have

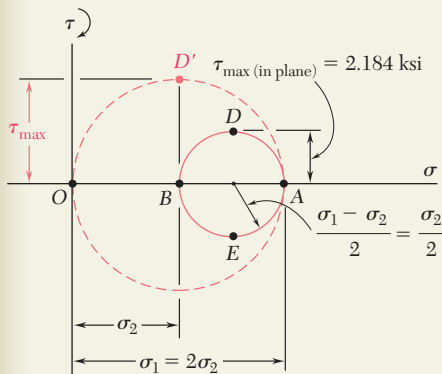
$$\begin{aligned} \tau_{\max (\text{in plane})} &= G \gamma_{\max (\text{in plane})} \\ &= (11.2 \times 10^6 \text{ psi})(195 \times 10^{-6} \text{ rad}) \\ &= 2184 \text{ psi} = 2.184 \text{ ksi} \end{aligned}$$

Substituting this value and the given data in Eq. (7.33), we write

$$\tau_{\max (\text{in plane})} = \frac{pr}{4t} \quad 2184 \text{ psi} = \frac{p(12 \text{ in.})}{4(0.75 \text{ in.})}$$

Solving for the gage pressure p , we have

$$p = 546 \text{ psi} \quad \blacktriangleleft$$

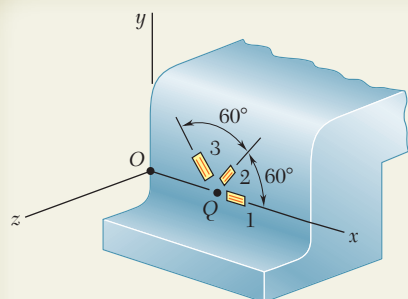


b. Principal Stresses and Maximum Shearing Stress. Recalling that, for a thin-walled cylindrical pressure vessel, $\sigma_1 = 2\sigma_2$, we draw Mohr's circle for stress and obtain

$$\begin{aligned} \sigma_2 &= 2\tau_{\max (\text{in plane})} = 2(2.184 \text{ ksi}) = 4.368 \text{ ksi} & \sigma_2 &= 4.37 \text{ ksi} \quad \blacktriangleleft \\ \sigma_1 &= 2\sigma_2 = 2(4.368 \text{ ksi}) & \sigma_1 &= 8.74 \text{ ksi} \quad \blacktriangleleft \end{aligned}$$

The maximum shearing stress is equal to the radius of the circle of diameter OA and corresponds to a rotation of 45° about a longitudinal axis.

$$\tau_{\max} = \frac{1}{2} \sigma_1 = \sigma_2 = 4.368 \text{ ksi} \quad \tau_{\max} = 4.37 \text{ ksi} \quad \blacktriangleleft$$



SAMPLE PROBLEM 7.7

Using a 60° rosette, the following strains have been determined at point Q on the surface of a steel machine base:

$$\epsilon_1 = 40 \mu \quad \epsilon_2 = 980 \mu \quad \epsilon_3 = 330 \mu$$

Using the coordinate axes shown, determine at point Q , (a) the strain components ϵ_x , ϵ_y , and γ_{xy} , (b) the principal strains, (c) the maximum shearing strain. (Use $\nu = 0.29$.)

SOLUTION

a. Strain Components ϵ_x , ϵ_y , γ_{xy} . For the coordinate axes shown

$$\theta_1 = 0 \quad \theta_2 = 60^\circ \quad \theta_3 = 120^\circ$$

Substituting these values into Eqs. (7.60), we have

$$\begin{aligned} \epsilon_1 &= \epsilon_x(1) + \epsilon_y(0) + \gamma_{xy}(0)(1) \\ \epsilon_2 &= \epsilon_x(0.500)^2 + \epsilon_y(0.866)^2 + \gamma_{xy}(0.866)(0.500) \\ \epsilon_3 &= \epsilon_x(-0.500)^2 + \epsilon_y(0.866)^2 + \gamma_{xy}(0.866)(-0.500) \end{aligned}$$

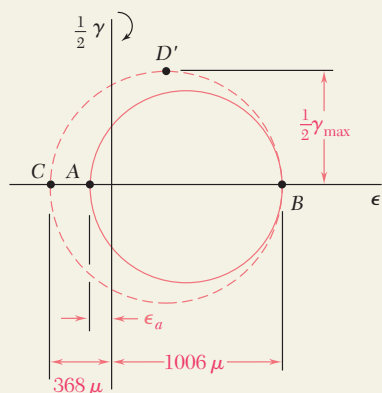
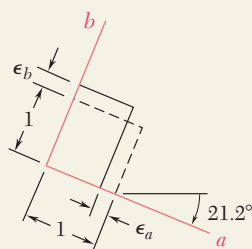
Solving these equations for ϵ_x , ϵ_y , and γ_{xy} , we obtain

$$\epsilon_x = \epsilon_1 \quad \epsilon_y = \frac{1}{3}(2\epsilon_2 + 2\epsilon_3 - \epsilon_1) \quad \gamma_{xy} = \frac{\epsilon_2 - \epsilon_3}{0.866}$$

Substituting the given values for ϵ_1 , ϵ_2 , and ϵ_3 , we have

$$\begin{aligned} \epsilon_x &= 40 \mu & \epsilon_y &= \frac{1}{3}[2(980) + 2(330) - 40] & \epsilon_y &= +860 \mu \\ \gamma_{xy} &= (980 - 330)/0.866 & \gamma_{xy} &= 750 \mu \end{aligned}$$

These strains are indicated on the element shown.



b. Principal Strains. We note that the side of the element associated with ϵ_x rotates counterclockwise; thus, we plot point X below the horizontal axis, i.e., $X(40, -375)$. We then plot $Y(860, +375)$ and draw Mohr's circle.

$$\begin{aligned} \epsilon_{ave} &= \frac{1}{2}(860 \mu + 40 \mu) = 450 \mu \\ R &= \sqrt{(375 \mu)^2 + (410 \mu)^2} = 556 \mu \\ \tan 2\theta_p &= \frac{375 \mu}{410 \mu} \quad 2\theta_p = 42.4^\circ \downarrow \quad \theta_p = 21.2^\circ \downarrow \end{aligned}$$

Points A and B correspond to the principal strains. We have

$$\begin{aligned} \epsilon_a &= \epsilon_{ave} - R = 450 \mu - 556 \mu & \epsilon_a &= -106 \mu \\ \epsilon_b &= \epsilon_{ave} + R = 450 \mu + 556 \mu & \epsilon_b &= +1006 \mu \end{aligned}$$

Since $\sigma_z = 0$ on the surface, we use Eq. (7.59) to find the principal strain ϵ_c :

$$\epsilon_c = -\frac{\nu}{1-\nu}(\epsilon_a + \epsilon_b) = -\frac{0.29}{1-0.29}(-106 \mu + 1006 \mu) \quad \epsilon_c = -368 \mu$$

c. Maximum Shearing Strain. Plotting point C and drawing Mohr's circle through points B and C , we obtain point D' and write

$$\frac{1}{2} \gamma_{max} = \frac{1}{2}(1006 \mu + 368 \mu) \quad \gamma_{max} = 1374 \mu$$

PROBLEMS

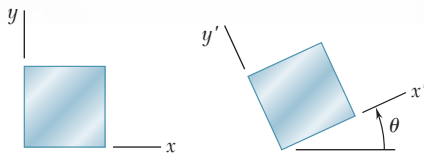


Fig. P7.128 through P7.135

7.128 through 7.131 For the given state of plane strain, use the method of Sec. 7.10 to determine the state of plane strain associated with axes x' and y' rotated through the given angle θ .

	ϵ_x	ϵ_y	γ_{xy}	θ
7.128 and 7.132	-500μ	$+250\mu$	0	$15^\circ \nearrow$
7.129 and 7.133	$+240\mu$	$+160\mu$	$+150\mu$	$60^\circ \searrow$
7.130 and 7.134	-800μ	$+450\mu$	$+200\mu$	$25^\circ \searrow$
7.131 and 7.135	0	$+320\mu$	-100μ	$30^\circ \nearrow$

7.132 through 7.135 For the given state of plane strain, use Mohr's circle to determine the state of plane strain associated with axes x' and y' rotated through the given angle θ .

7.136 through 7.139 The following state of strain has been measured on the surface of a thin plate. Knowing that the surface of the plate is unstressed, determine (a) the direction and magnitude of the principal strains, (b) the maximum in-plane shearing strain, (c) the maximum shearing strain. (Use $\nu = \frac{1}{3}$)

	ϵ_x	ϵ_y	γ_{xy}
7.136	-260μ	-60μ	$+480\mu$
7.137	-600μ	-400μ	$+350\mu$
7.138	$+160\mu$	-480μ	-600μ
7.139	$+30\mu$	$+570\mu$	$+720\mu$

7.140 through 7.143 For the given state of plane strain, use Mohr's circle to determine (a) the orientation and magnitude of the principal strains, (b) the maximum in-plane strain, (c) the maximum shearing strain.

	ϵ_x	ϵ_y	γ_{xy}
7.140	$+60\mu$	$+240\mu$	-50μ
7.141	$+400\mu$	$+200\mu$	$+375\mu$
7.142	$+300\mu$	$+60\mu$	$+100\mu$
7.143	-180μ	-260μ	$+315\mu$

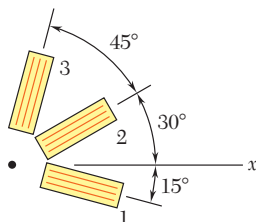


Fig. P7.144

7.144 Determine the strain ϵ_x knowing that the following strains have been determined by use of the rosette shown:

$$\epsilon_1 = +480\mu \quad \epsilon_2 = -120\mu \quad \epsilon_3 = +80\mu$$

- 7.145** The strains determined by the use of the rosette shown during the test of a machine element are

$$\epsilon_1 = +600\mu \quad \epsilon_2 = +450\mu \quad \epsilon_3 = -75\mu$$

Determine (a) the in-plane principal strains, (b) the in-plane maximum shearing strain.

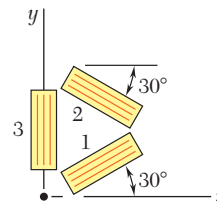


Fig. P7.145

- 7.146** The rosette shown has been used to determine the following strains at a point on the surface of a crane hook:

$$\begin{aligned} \epsilon_1 &= +420 \times 10^{-6} \text{ in./in.} & \epsilon_2 &= -45 \times 10^{-6} \text{ in./in.} \\ \epsilon_4 &= +165 \times 10^{-6} \text{ in./in.} \end{aligned}$$

(a) What should be the reading of gage 3? (b) Determine the principal strains and the maximum in-plane shearing strain.

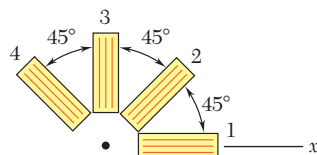


Fig. P7.146

- 7.147** The strains determined by the use of the rosette attached as shown during the test of a machine element are

$$\begin{aligned} \epsilon_1 &= -93.1 \times 10^{-6} \text{ in./in.} & \epsilon_2 &= +385 \times 10^{-6} \text{ in./in.} \\ \epsilon_3 &= +210 \times 10^{-6} \text{ in./in.} \end{aligned}$$

Determine (a) the orientation and magnitude of the principal strains in the plane of the rosette, (b) the maximum in-plane shearing strain.

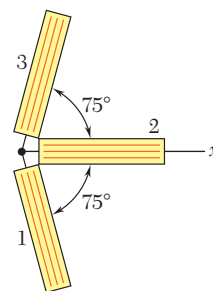


Fig. P7.147

- 7.148** Using a 45° rosette, the strains ϵ_1 , ϵ_2 and ϵ_3 have been determined at a given point. Using Mohr's circle, show that the principal strains are:

$$\epsilon_{\max, \min} = \frac{1}{2}(\epsilon_1 + \epsilon_3) \pm \frac{1}{\sqrt{2}} \left[(\epsilon_1 - \epsilon_2)^2 + (\epsilon_2 - \epsilon_3)^2 \right]^{1/2}$$

(Hint: The shaded triangles are congruent.)

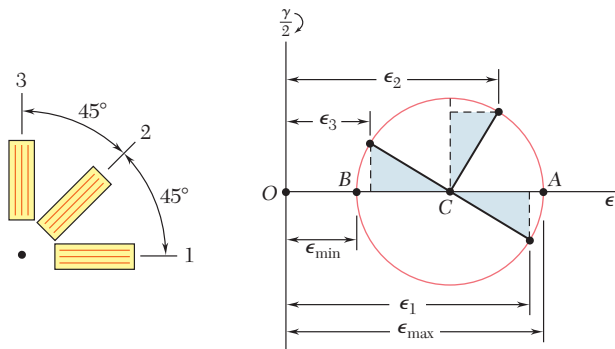


Fig. P7.148

- 7.149** Show that the sum of the three strain measurements made with a 60° rosette is independent of the orientation of the rosette and equal to

$$\epsilon_1 + \epsilon_2 + \epsilon_3 = 3\epsilon_{\text{avg}}$$

where ϵ_{avg} is the abscissa of the center of the corresponding Mohr's circle.

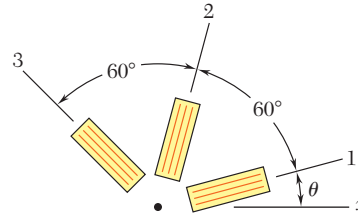


Fig. P7.149

- 7.150** A single strain gage is cemented to a solid 4-in.-diameter steel shaft at an angle $\beta = 25^\circ$ with a line parallel to the axis of the shaft. Knowing that $G = 11.5 \times 10^6$ psi, determine the torque \mathbf{T} indicated by a gage reading of 300×10^{-6} in./in.

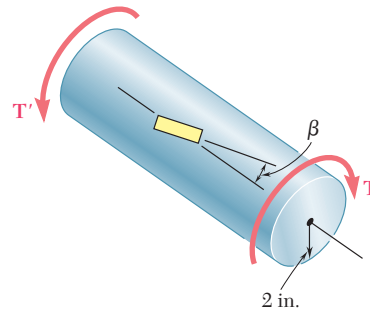


Fig. P7.150

- 7.151** Solve Prob. 7.150, assuming that the gage forms an angle $\beta = 35^\circ$ with a line parallel to the axis of the shaft.
- 7.152** A single strain gage forming an angle $\beta = 18^\circ$ with a horizontal plane is used to determine the gage pressure in the cylindrical steel tank shown. The cylindrical wall of the tank is 6-mm thick, has a 600-mm inside diameter, and is made of a steel with $E = 200$ GPa and $\nu = 0.30$. Determine the pressure in the tank indicated by a strain gage reading of 280μ .

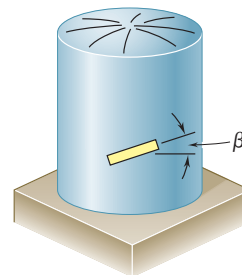


Fig. P7.152

- 7.153** Solve Prob. 7.152, assuming that the gage forms an angle $\beta = 35^\circ$ with a horizontal plane.

7.154 The given state of plane stress is known to exist on the surface of a machine component. Knowing that $E = 200$ GPa and $G = 77.2$ GPa, determine the direction and magnitude of the three principal strains (a) by determining the corresponding state of strain [use Eq. (2.43) and Eq. (2.38)] and then using Mohr's circle for strain, (b) by using Mohr's circle for stress to determine the principal planes and principal stresses and then determining the corresponding strains.

7.155 The following state of strain has been determined on the surface of a cast-iron machine part:

$$\epsilon_x = -720\mu \quad \epsilon_y = -400\mu \quad \gamma_{xy} = +660\mu$$

Knowing that $E = 69$ GPa and $G = 28$ GPa, determine the principal planes and principal stresses (a) by determining the corresponding state of plane stress [use Eq. (2.36), Eq. (2.43), and the first two equations of Prob. 2.72] and then using Mohr's circle for stress, (b) by using Mohr's circle for strain to determine the orientation and magnitude of the principal strains and then determine the corresponding stresses.

7.156 A centric axial force \mathbf{P} and a horizontal force \mathbf{Q}_x are both applied at point C of the rectangular bar shown. A 45° strain rosette on the surface of the bar at point A indicates the following strains:

$$\begin{aligned} \epsilon_1 &= -60 \times 10^{-6} \text{ in./in.} & \epsilon_2 &= +240 \times 10^{-6} \text{ in./in.} \\ \epsilon_3 &= +200 \times 10^{-6} \text{ in./in.} \end{aligned}$$

Knowing that $E = 29 \times 10^6$ psi and $\nu = 0.30$, determine the magnitudes of \mathbf{P} and \mathbf{Q}_x .

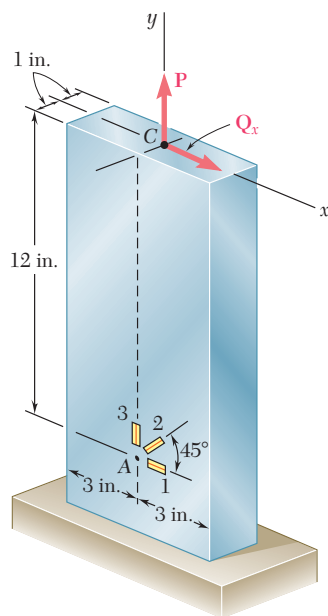


Fig. P7.156

7.157 Solve Prob. 7.156, assuming that the rosette at point A indicates the following strains:

$$\begin{aligned} \epsilon_1 &= -30 \times 10^{-6} \text{ in./in.} & \epsilon_2 &= +250 \times 10^{-6} \text{ in./in.} \\ \epsilon_3 &= +100 \times 10^{-6} \text{ in./in.} \end{aligned}$$

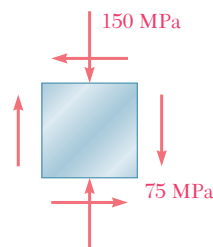


Fig. P7.154

REVIEW AND SUMMARY

The first part of this chapter was devoted to a study of the *transformation of stress* under a rotation of axes and to its application to the solution of engineering problems, and the second part to a similar study of the *transformation of strain*.

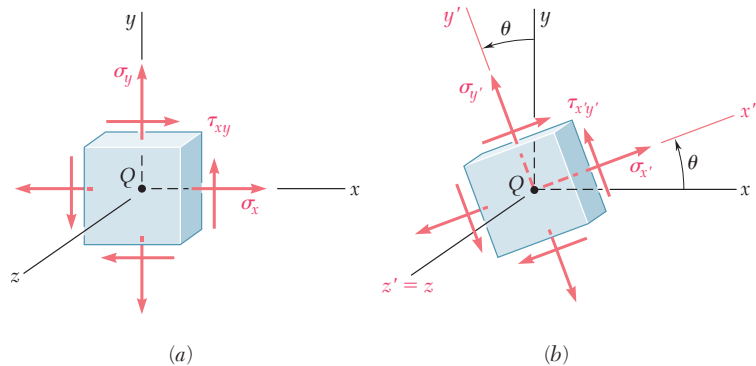


Fig. 7.77

Transformation of plane stress

Considering first a state of *plane stress* at a given point Q [Sec. 7.2] and denoting by σ_x , σ_y , and τ_{xy} the stress components associated with the element shown in Fig. 7.77a, we derived the following formulas defining the components $\sigma_{x'}$, $\sigma_{y'}$, and $\tau_{x'y'}$ associated with that element after it had been rotated through an angle θ about the z axis (Fig. 7.77b):

$$\sigma_{x'} = \frac{\sigma_x + \sigma_y}{2} + \frac{\sigma_x - \sigma_y}{2} \cos 2\theta + \tau_{xy} \sin 2\theta \quad (7.5)$$

$$\sigma_{y'} = \frac{\sigma_x + \sigma_y}{2} - \frac{\sigma_x - \sigma_y}{2} \cos 2\theta - \tau_{xy} \sin 2\theta \quad (7.7)$$

$$\tau_{x'y'} = -\frac{\sigma_x - \sigma_y}{2} \sin 2\theta + \tau_{xy} \cos 2\theta \quad (7.6)$$

In Sec. 7.3, we determined the values θ_p of the angle of rotation which correspond to the maximum and minimum values of the normal stress at point Q . We wrote

$$\tan 2\theta_p = \frac{2\tau_{xy}}{\sigma_x - \sigma_y} \quad (7.12)$$

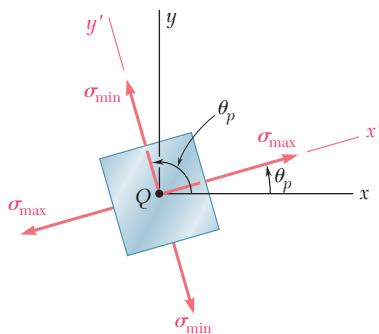


Fig. 7.78

Principal planes. Principal stresses

The two values obtained for θ_p are 90° apart (Fig. 7.78) and define the *principal planes of stress* at point Q . The corresponding values

of the normal stress are called the *principal stresses* at Q ; we obtained

$$\sigma_{\max, \min} = \frac{\sigma_x + \sigma_y}{2} \pm \sqrt{\left(\frac{\sigma_x - \sigma_y}{2}\right)^2 + \tau_{xy}^2} \quad (7.14)$$

We also noted that the corresponding value of the shearing stress is zero. Next, we determined the values θ_s of the angle θ for which the largest value of the shearing stress occurs. We wrote

$$\tan 2\theta_s = -\frac{\sigma_x - \sigma_y}{2\tau_{xy}} \quad (7.15)$$

The two values obtained for θ_s are 90° apart (Fig. 7.79). We also noted that the planes of maximum shearing stress are at 45° to the principal planes. The maximum value of the shearing stress for a rotation in the plane of stress is

$$\tau_{\max} = \sqrt{\left(\frac{\sigma_x - \sigma_y}{2}\right)^2 + \tau_{xy}^2} \quad (7.16)$$

and the corresponding value of the normal stresses is

$$\sigma' = \sigma_{\text{ave}} = \frac{\sigma_x + \sigma_y}{2} \quad (7.17)$$

We saw in Sec. 7.4 that *Mohr's circle* provides an alternative method, based on simple geometric considerations, for the analysis of the

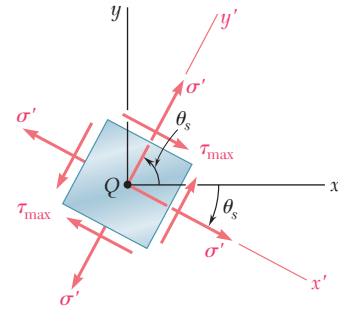


Fig. 7.79

Maximum in-plane shearing stress

Mohr's circle for stress

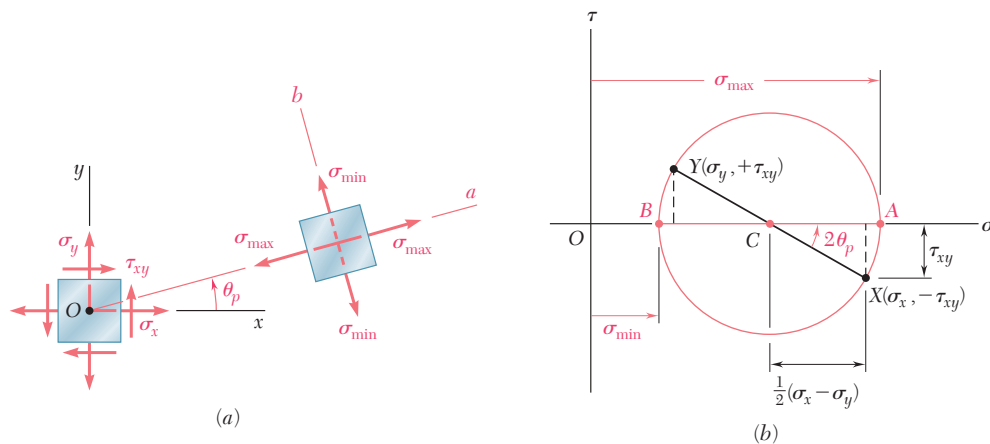


Fig. 7.80

transformation of plane stress. Given the state of stress shown in black in Fig. 7.80a, we plot point X of coordinates $\sigma_x, -\tau_{xy}$ and point Y of coordinates $\sigma_y, +\tau_{xy}$ (Fig. 7.80b). Drawing the circle of diameter XY , we obtain Mohr's circle. The abscissas of the points of intersection A and B of the circle with the horizontal axis represent the principal stresses, and the angle of rotation bringing the diameter XY into AB is twice the angle θ_p defining the principal planes in Fig. 7.80a, with both angles having the same sense. We also noted that diameter DE defines the maximum shearing stress and the orientation of the corresponding plane (Fig. 7.81) [Example 7.02, Sample Probs. 7.2 and 7.3].

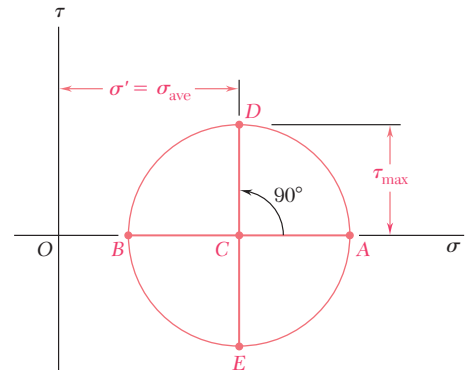


Fig. 7.81

General state of stress

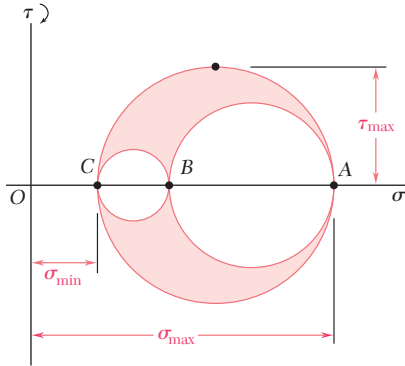


Fig. 7.82

Considering a *general state of stress* characterized by six stress components [Sec. 7.5], we showed that the normal stress on a plane of arbitrary orientation can be expressed as a quadratic form of the direction cosines of the normal to that plane. This proves the existence of three *principal axes of stress* and three *principal stresses* at any given point. Rotating a small cubic element about each of the three principal axes [Sec. 7.6], we drew the corresponding Mohr's circles that yield the values of σ_{\max} , σ_{\min} , and τ_{\max} (Fig. 7.82). In the particular case of *plane stress*, and if the x and y axes are selected in the plane of stress, point C coincides with the origin O . If A and B are located on opposite sides of O , the maximum shearing stress is equal to the maximum “in-plane” shearing stress as determined in Secs. 7.3 or 7.4. If A and B are located on the same side of O , this will not be the case. If $\sigma_a > \sigma_b > 0$, for instance the maximum shearing stress is equal to $\frac{1}{2}\sigma_a$ and corresponds to a rotation out of the plane of stress (Fig. 7.83).

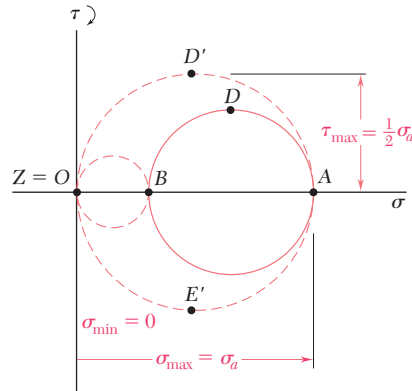


Fig. 7.83

Yield criteria for ductile materials

Yield criteria for ductile materials under plane stress were developed in Sec. 7.7. To predict whether a structural or machine component will fail at some critical point due to yield in the material, we first determine the principal stresses σ_a and σ_b at that point for the given loading condition. We then plot the point of coordinates σ_a and σ_b . If this point falls within a certain area, the component is safe; if it falls outside, the component will fail. The area used with the maximum-shearing-strength criterion is shown in Fig. 7.84 and the area used with the maximum-distortion-energy criterion in Fig. 7.85. We note that both areas depend upon the value of the yield strength σ_Y of the material.

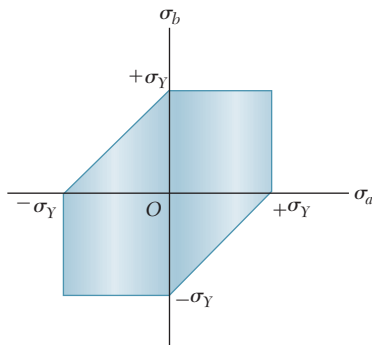


Fig. 7.84

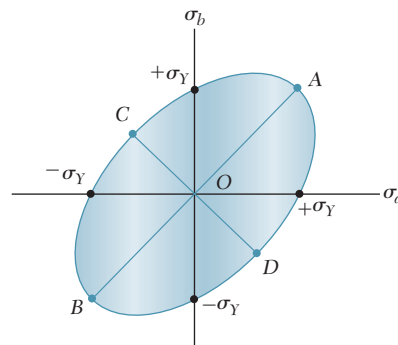


Fig. 7.85

Fracture criteria for brittle materials under plane stress were developed in Sec. 7.8 in a similar fashion. The most commonly used is *Mohr's criterion*, which utilizes the results of various types of test available for a given material. The shaded area shown in Fig. 7.86 is used when the ultimate strengths σ_{UT} and σ_{UC} have been determined, respectively, from a tension and a compression test. Again, the principal stresses σ_a and σ_b are determined at a given point of the structural or machine component being investigated. If the corresponding point falls within the shaded area, the component is safe; if it falls outside, the component will rupture.

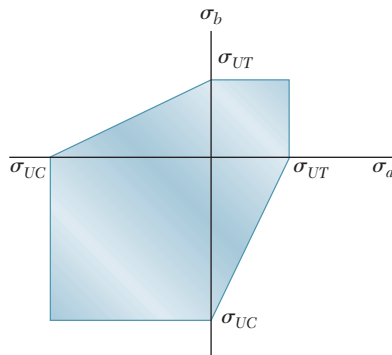


Fig. 7.86

In Sec. 7.9, we discussed the stresses in *thin-walled pressure vessels* and derived formulas relating the stresses in the walls of the vessels and the *gage pressure* p in the fluid they contain. In the case of a *cylindrical vessel* of inside radius r and thickness t (Fig. 7.87), we obtained the following expressions for the *hoop stress* σ_1 and the *longitudinal stress* σ_2 :

$$\sigma_1 = \frac{pr}{t} \quad \sigma_2 = \frac{pr}{2t} \quad (7.30, 7.31)$$

We also found that the *maximum shearing stress* occurs out of the plane of stress and is

$$\tau_{\max} = \sigma_2 = \frac{pr}{2t} \quad (7.34)$$

In the case of a *spherical vessel* of inside radius r and thickness t (Fig. 7.88), we found that the two principal stresses are equal:

$$\sigma_1 = \sigma_2 = \frac{pr}{2t} \quad (7.36)$$

Again, the *maximum shearing stress* occurs out of the plane of stress; it is

$$\tau_{\max} = \frac{1}{2}\sigma_1 = \frac{pr}{4t} \quad (7.37)$$

Fracture criteria for brittle materials

Cylindrical pressure vessels

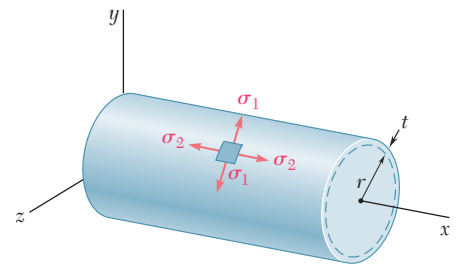


Fig. 7.87

Spherical pressure vessels

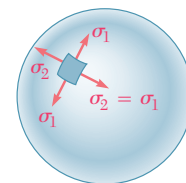


Fig. 7.88

Transformation of plane strain

The last part of the chapter was devoted to the *transformation of strain*. In Secs. 7.10 and 7.11, we discussed the transformation of *plane strain* and introduced *Mohr's circle for plane strain*. The discussion was similar to the corresponding discussion of the transformation of stress, except that, where the shearing stress τ was used, we now used $\frac{1}{2}\gamma$, that is, *half the shearing strain*. The formulas obtained for the transformation of strain under a rotation of axes through an angle θ were

$$\epsilon_{x'} = \frac{\epsilon_x + \epsilon_y}{2} + \frac{\epsilon_x - \epsilon_y}{2} \cos 2\theta + \frac{\gamma_{xy}}{2} \sin 2\theta \quad (7.44)$$

$$\epsilon_{y'} = \frac{\epsilon_x + \epsilon_y}{2} - \frac{\epsilon_x - \epsilon_y}{2} \cos 2\theta - \frac{\gamma_{xy}}{2} \sin 2\theta \quad (7.45)$$

$$\gamma_{x'y'} = -(\epsilon_x - \epsilon_y) \sin 2\theta + \gamma_{xy} \cos 2\theta \quad (7.49)$$

Using Mohr's circle for strain (Fig. 7.89), we also obtained the following relations defining the angle of rotation θ_p corresponding to the *principal axes of strain* and the values of the *principal strains* ϵ_{\max} and ϵ_{\min} :

$$\tan 2\theta_p = \frac{\gamma_{xy}}{\epsilon_x - \epsilon_y} \quad (7.52)$$

$$\epsilon_{\max} = \epsilon_{\text{ave}} + R \quad \text{and} \quad \epsilon_{\min} = \epsilon_{\text{ave}} - R \quad (7.51)$$

where

$$\epsilon_{\text{ave}} = \frac{\epsilon_x + \epsilon_y}{2} \quad \text{and} \quad R = \sqrt{\left(\frac{\epsilon_x - \epsilon_y}{2}\right)^2 + \left(\frac{\gamma_{xy}}{2}\right)^2} \quad (7.50)$$

The *maximum shearing strain* for a rotation in the plane of strain was found to be

$$\gamma_{\max(\text{in plane})} = 2R = \sqrt{(\epsilon_x - \epsilon_y)^2 + \gamma_{xy}^2} \quad (7.53)$$

Section 7.12 was devoted to the three-dimensional analysis of strain, with application to the determination of the maximum shearing strain in the particular cases of plane strain and plane stress. In the case of *plane stress*, we also found that the principal strain ϵ_c in a direction perpendicular to the plane of stress could be expressed as follows in terms of the “in-plane” principal strains ϵ_a and ϵ_b :

$$\epsilon_c = -\frac{\nu}{1 - \nu}(\epsilon_a + \epsilon_b) \quad (7.59)$$

Finally, we discussed in Sec. 7.13 the use of *strain gages* to measure the normal strain on the surface of a structural element or machine component. Considering a *strain rosette* consisting of three gages aligned along lines forming respectively, angles θ_1 , θ_2 , and θ_3 with the x axis (Fig. 7.90), we wrote the following relations among the measurements ϵ_1 , ϵ_2 , ϵ_3 of the gages and the components ϵ_x , ϵ_y , γ_{xy} characterizing the state of strain at that point:

$$\begin{aligned} \epsilon_1 &= \epsilon_x \cos^2 \theta_1 + \epsilon_y \sin^2 \theta_1 + \gamma_{xy} \sin \theta_1 \cos \theta_1 \\ \epsilon_2 &= \epsilon_x \cos^2 \theta_2 + \epsilon_y \sin^2 \theta_2 + \gamma_{xy} \sin \theta_2 \cos \theta_2 \\ \epsilon_3 &= \epsilon_x \cos^2 \theta_3 + \epsilon_y \sin^2 \theta_3 + \gamma_{xy} \sin \theta_3 \cos \theta_3 \end{aligned} \quad (7.60)$$

These equations can be solved for ϵ_x , ϵ_y , and γ_{xy} , once ϵ_1 , ϵ_2 , and ϵ_3 have been determined.

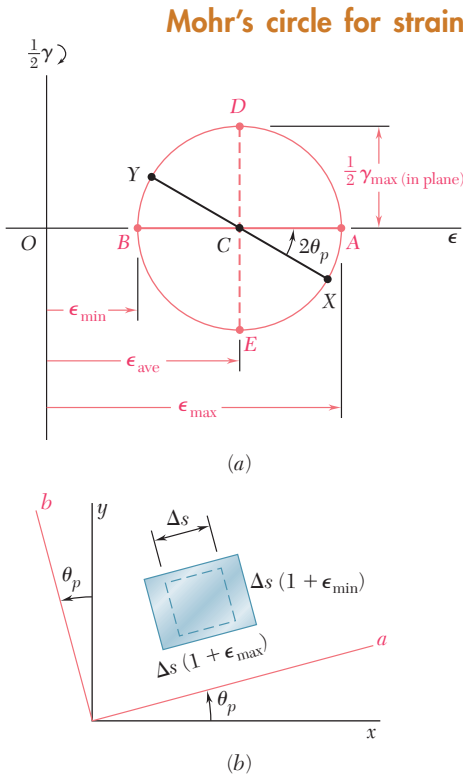


Fig. 7.89

Strain gages. Strain rosette

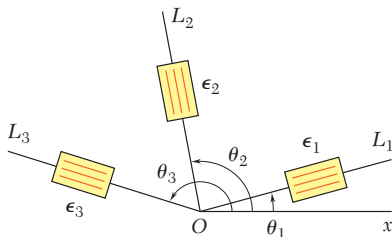


Fig. 7.90

REVIEW PROBLEMS

- 7.158** Two wooden members of 80×120 -mm uniform rectangular cross section are joined by the simple glued scarf splice shown. Knowing that $\beta = 22^\circ$ and that the maximum allowable stresses in the joint are, respectively, 400 kPa in tension (perpendicular to the splice) and 600 kPa in shear (parallel to the splice), determine the largest centric load \mathbf{P} that can be applied.

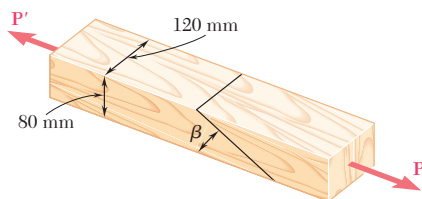


Fig. P7.158 and P7.159

- 7.159** Two wooden members of 80×120 -mm uniform rectangular cross section are joined by the simple glued scarf splice shown. Knowing that $\beta = 25^\circ$ and that centric loads of magnitude $P = 10$ kN are applied to the members as shown, determine (a) the in-plane shearing stress parallel to the splice, (b) the normal stress perpendicular to the splice.

- 7.160** The centric force \mathbf{P} is applied to a short post as shown. Knowing that the stresses on plane $a-a$ are $\sigma = -15$ ksi and $\tau = 5$ ksi, determine (a) the angle β that plane $a-a$ forms with the horizontal, (b) the maximum compressive stress in the post.

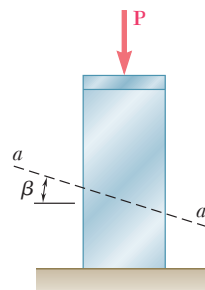


Fig. P7.160

- 7.161** Determine the principal planes and the principal stresses for the state of plane stress resulting from the superposition of the two states of stress shown.

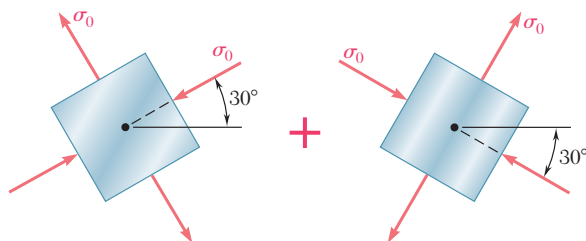


Fig. P7.161

- 7.162** For the state of stress shown, determine the maximum shearing stress when (a) $\sigma_z = +24$ MPa, (b) $\sigma_z = -24$ MPa, (c) $\sigma_z = 0$.

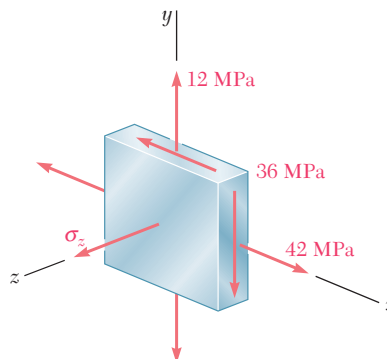


Fig. P7.162

- 7.163** For the state of stress shown, determine the maximum shearing stress when (a) $\tau_{yz} = 17.5$ ksi, (b) $\tau_{yz} = 8$ ksi, (c) $\tau_{yz} = 0$.

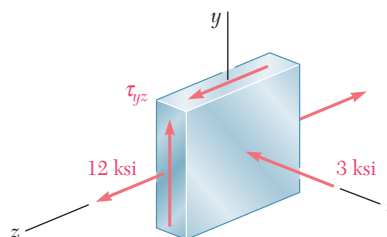


Fig. P7.163

- 7.164** The state of plane stress shown occurs in a machine component made of a steel with $\sigma_Y = 30$ ksi. Using the maximum-distortion-energy criterion, determine whether yield will occur when (a) $\tau_{xy} = 6$ ksi, (b) $\tau_{xy} = 12$ ksi, (c) $\tau_{xy} = 14$ ksi. If yield does not occur, determine the corresponding factor of safety.

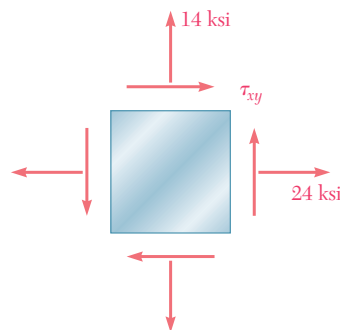


Fig. P7.164

7.165 A torque of magnitude $T = 12 \text{ kN} \cdot \text{m}$ is applied to the end of a tank containing compressed air under a pressure of 8 MPa. Knowing that the tank has a 180-mm inner diameter and a 12-mm wall thickness, determine the maximum normal stress and the maximum shearing stress in the tank.

7.166 The tank shown has a 180-mm inner diameter and a 12-mm wall thickness. Knowing that the tank contains compressed air under a pressure of 8 MPa, determine the magnitude T of the applied torque for which the maximum normal stress is 75 MPa.

7.167 The brass pipe AD is fitted with a jacket used to apply a hydrostatic pressure of 500 psi to portion BC of the pipe. Knowing that the pressure inside the pipe is 100 psi, determine the maximum normal stress in the pipe.

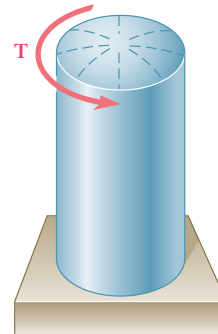


Fig. P7.165 and P7.166

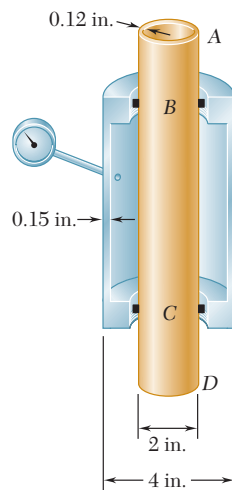


Fig. P7.167

7.168 For the assembly of Prob. 7.167, determine the normal stress in the jacket (*a*) in a direction perpendicular to the longitudinal axis of the jacket, (*b*) in a direction parallel to that axis.

7.169 Determine the largest in-plane normal strain, knowing that the following strains have been obtained by the use of the rosette shown:

$$\begin{aligned}\epsilon_1 &= -50 \times 10^{-6} \text{ in./in.} & \epsilon_2 &= +360 \times 10^{-6} \text{ in./in.} \\ \epsilon_3 &= +315 \times 10^{-6} \text{ in./in.}\end{aligned}$$

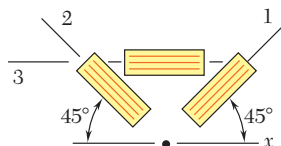


Fig. P7.169

COMPUTER PROBLEMS

The following problems are to be solved with a computer.

7.C1 A state of plane stress is defined by the stress components σ_x , σ_y , and τ_{xy} associated with the element shown in Fig. P7.C1a. (a) Write a computer program that can be used to calculate the stress components $\sigma_{x'}$, $\sigma_{y'}$, and $\tau_{x'y'}$ associated with the element after it has rotated through an angle θ about the z axis (Fig. P7.C1b). (b) Use this program to solve Probs. 7.13 through 7.16.

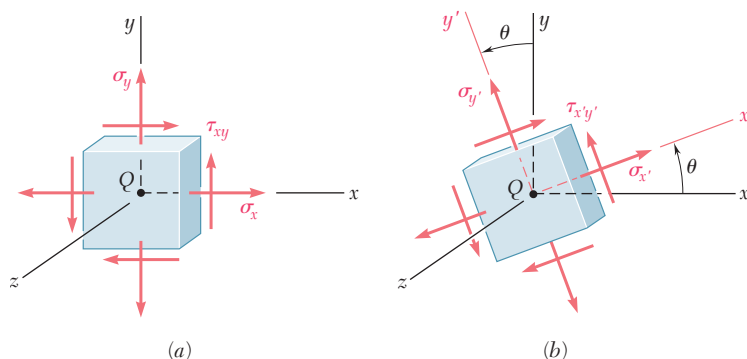


Fig. P7.C1

7.C2 A state of plane stress is defined by the stress components σ_x , σ_y , and τ_{xy} associated with the element shown in Fig. P7.C1a. (a) Write a computer program that can be used to calculate the principal axes, the principal stresses, the maximum in-plane shearing stress, and the maximum shearing stress. (b) Use this program to solve Probs. 7.5, 7.9, 7.68, and 7.69.

7.C3 (a) Write a computer program that, for a given state of plane stress and a given yield strength of a ductile material, can be used to determine whether the material will yield. The program should use both the maximum shearing-strength criterion and the maximum-distortion-energy criterion. It should also print the values of the principal stresses and, if the material does not yield, calculate the factor of safety. (b) Use this program to solve Probs. 7.81, 7.82, and 7.164.

7.C4 (a) Write a computer program based on Mohr's fracture criterion for brittle materials that, for a given state of plane stress and given values of the ultimate strength of the material in tension and compression, can be used to determine whether rupture will occur. The program should also print the values of the principal stresses. (b) Use this program to solve Probs. 7.91 and 7.92 and to check the answers to Probs. 7.93 and 7.94.

7.C5 A state of plane strain is defined by the strain components ϵ_x , ϵ_y , and γ_{xy} associated with the x and y axes. (a) Write a computer program that can be used to calculate the strain components $\epsilon_{x'}$, $\epsilon_{y'}$, and $\gamma_{x'y'}$ associated with the frame of reference $x'y'$ obtained by rotating the x and y axes through an angle θ . (b) Use this program to solve Probs. 7.129 and 7.131.

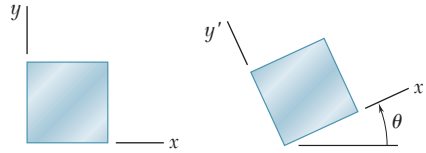


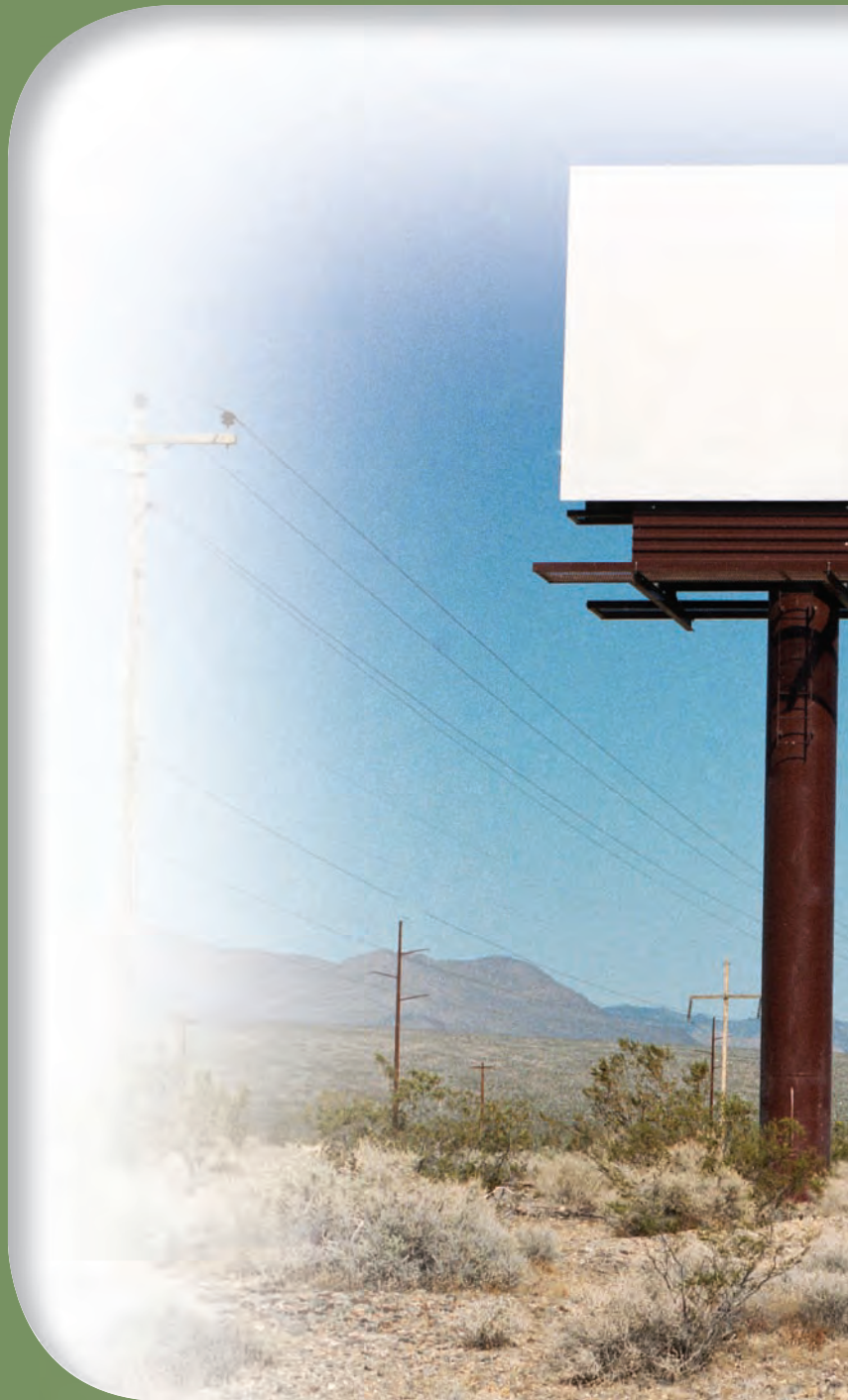
Fig. P7.C5

7.C6 A state of strain is defined by the strain components ϵ_x , ϵ_y , and γ_{xy} associated with the x and y axes. (a) Write a computer program that can be used to determine the orientation and magnitude of the principal strains, the maximum in-plane shearing strain, and the maximum shearing strain. (b) Use this program to solve Probs. 7.136 through 7.139.

7.C7 A state of plane strain is defined by the strain components ϵ_x , ϵ_y , and γ_{xy} measured at a point. (a) Write a computer program that can be used to determine the orientation and magnitude of the principal strains, the maximum in-plane shearing strain, and the magnitude of the shearing strain. (b) Use this program to solve Probs. 7.140 through 7.143.

7.C8 A rosette consisting of three gages forming, respectively, angles of θ_1 , θ_2 , and θ_3 with the x axis is attached to the free surface of a machine component made of a material with a given Poisson's ratio ν . (a) Write a computer program that, for given readings ϵ_1 , ϵ_2 , and ϵ_3 of the gages, can be used to calculate the strain components associated with the x and y axes and to determine the orientation and magnitude of the three principal strains, the maximum in-plane shearing strain, and the maximum shearing strain. (b) Use this program to solve Probs. 7.144, 7.145, 7.146, and 7.169.

Due to gravity and wind load, the post supporting the sign shown is subjected simultaneously to compression, bending, and torsion. In this chapter you will learn to determine the stresses created by such combined loadings in structures and machine components.



C H A P T E R

8

Principal Stresses under a Given Loading



Chapter 8 Principal Stresses under a Given Loading

- *8.1 Introduction
- *8.2 Principal Stresses in a Beam
- *8.3 Design of Transmission Shafts
- *8.4 Stresses under Combined Loadings

*8.1 INTRODUCTION

In the first part of this chapter, you will apply to the design of beams and shafts the knowledge that you acquired in Chap. 7 on the transformation of stresses. In the second part of the chapter, you will learn how to determine the principal stresses in structural members and machine elements under given loading conditions.

In Chap. 5 you learned to calculate the maximum normal stress σ_m occurring in a beam under a transverse loading (Fig. 8.1a) and check whether this value exceeded the allowable stress σ_{all} for the given material. If it did, the design of the beam was not acceptable. While the danger for a brittle material is actually to fail in tension, the danger for a ductile material is to fail in shear (Fig. 8.1b). The fact that $\sigma_m > \sigma_{all}$ indicates that $|M|_{max}$ is too large for the cross section selected, but does not provide any information on the actual mechanism of failure. Similarly, the fact that $\tau_m > \tau_{all}$ simply indicates that $|V|_{max}$ is too large for the cross section selected. While the danger for a ductile material is actually to fail in shear (Fig. 8.2a), the danger for a brittle material is to fail in tension under the principal stresses (Fig. 8.2b). The distribution of the principal stresses in a beam will be discussed in Sec. 8.2.

Depending upon the shape of the cross section of the beam and the value of the shear V in the critical section where $|M| = |M|_{max}$, it may happen that the largest value of the normal stress will not occur at the top or bottom of the section, but at some other point within the section. As you will see in Sec. 8.2, a combination of large values of σ_x and τ_{xy} near the junction of the web and the flanges of a W-beam or an S-beam can result in a value of the principal stress σ_{max} (Fig. 8.3) that is larger than the value of σ_m on the surface of the beam.

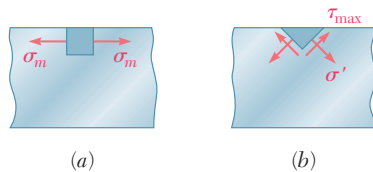


Fig. 8.1

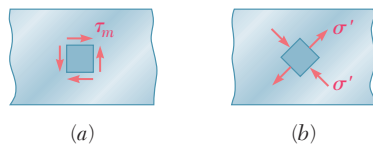


Fig. 8.2

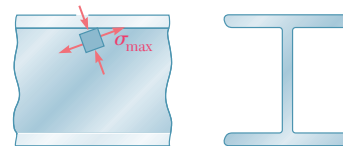


Fig. 8.3 Principal stresses at the junction of a flange and web in an I-shaped beam.

Section 8.3 will be devoted to the design of transmission shafts subjected to transverse loads as well as to torques. The effect of both the normal stresses due to bending and the shearing stresses due to torsion will be taken into account.

In Sec. 8.4 you will learn to determine the stresses at a given point K of a body of arbitrary shape subjected to a combined loading. First, you will reduce the given loading to forces and couples in the section containing K . Next, you will calculate the normal and shearing stresses at K . Finally, using one of the methods for the transformation of stresses that you learned in Chap. 7, you will determine the principal planes, principal stresses, and maximum shearing stress at K .

*8.2 PRINCIPAL STRESSES IN A BEAM

Consider a prismatic beam AB subjected to some arbitrary transverse loading (Fig. 8.4). We denote by V and M , respectively, the shear and bending moment in a section through a given point C . We recall from Chaps. 5 and 6 that, within the elastic limit, the stresses exerted on a small element with faces perpendicular, respectively, to the x and y axes reduce to the normal stresses $\sigma_m = Mc/I$ if the element is at the free surface of the beam, and to the shearing stresses $\tau_m = VQ/It$ if the element is at the neutral surface (Fig. 8.5).

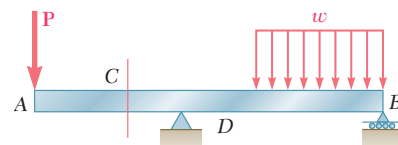


Fig. 8.4 Transversely loaded prismatic beam.

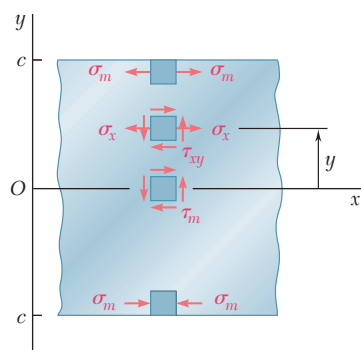


Fig. 8.5 Stress elements at selected points of a beam.

At any other point of the cross section, an element of material is subjected simultaneously to the normal stresses

$$\sigma_x = -\frac{My}{I} \quad (8.1)$$

where y is the distance from the neutral surface and I the centroidal moment of inertia of the section, and to the shearing stresses

$$\tau_{xy} = -\frac{VQ}{It} \quad (8.2)$$

where Q is the first moment about the neutral axis of the portion of the cross-sectional area located above the point where the stresses are computed, and t the width of the cross section at that point. Using either of the methods of analysis presented in Chap. 7, we can obtain the principal stresses at any point of the cross section (Fig. 8.6).

The following question now arises: Can the maximum normal stress σ_{\max} at some point within the cross section be larger than the value of $\sigma_m = Mc/I$ computed at the surface of the beam? If it can, then the determination of the largest normal stress in the beam will involve a great deal more than the computation of $|M|_{\max}$ and the use of Eq. (8.1). We can obtain an answer to this question by investigating the distribution of the principal stresses in a narrow

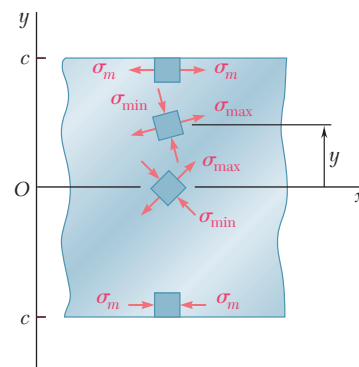


Fig. 8.6 Principal stresses at selected points of a beam.

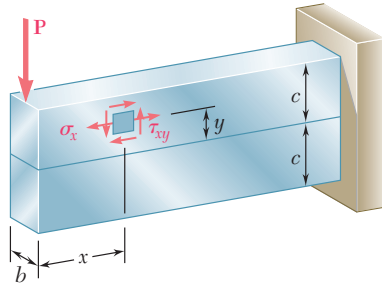


Fig. 8.7 Narrow rectangular cantilever beam supporting a single concentrated load.

rectangular cantilever beam subjected to a concentrated load \mathbf{P} at its free end (Fig. 8.7). We recall from Sec. 6.5 that the normal and shearing stresses at a distance x from the load \mathbf{P} and a distance y above the neutral surface are given, respectively, by Eq. (6.13) and Eq. (6.12). Since the moment of inertia of the cross section is

$$I = \frac{bh^3}{12} = \frac{(bh)(2c)^2}{12} = \frac{Ac^2}{3}$$

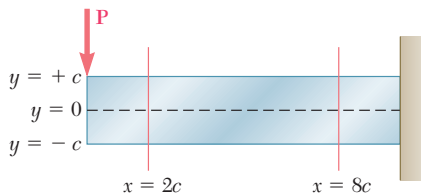
where A is the cross-sectional area and c the half-depth of the beam, we write

$$\sigma_x = \frac{Pxy}{I} = \frac{Pxy}{\frac{1}{3}Ac^2} = 3 \frac{P}{A} \frac{xy}{c^2} \quad (8.3)$$

and

$$\tau_{xy} = \frac{3}{2} \frac{P}{A} \left(1 - \frac{y^2}{c^2} \right) \quad (8.4)$$

Using the method of Sec. 7.3 or Sec. 7.4, the value of σ_{\max} can be determined at any point of the beam. Figure 8.8 shows the results of the computation of the ratios σ_{\max}/σ_m and σ_{\min}/σ_m in two sections of the beam, corresponding respectively to $x = 2c$ and $x = 8c$. In



y/c	$x = 2c$		$x = 8c$	
	σ_{\min}/σ_m	σ_{\max}/σ_m	σ_{\min}/σ_m	σ_{\max}/σ_m
1.0	0	1.000	0	1.000
0.8	-0.010	0.810	-0.001	0.801
0.6	-0.040	0.640	-0.003	0.603
0.4	-0.090	0.490	-0.007	0.407
0.2	-0.160	0.360	-0.017	0.217
0	-0.250	0.250	-0.063	0.063
-0.2	-0.360	0.160	-0.217	0.017
-0.4	-0.490	0.090	-0.407	0.007
-0.6	-0.640	0.040	-0.603	0.003
-0.8	-0.810	0.010	-0.801	0.001
-1.0	-1.000	0	-1.000	0

Fig. 8.8 Distribution of principal stresses in two transverse sections of a rectangular cantilever beam supporting a single concentrated load.

each section, these ratios have been determined at 11 different points, and the orientation of the principal axes has been indicated at each point.†

It is clear that σ_{\max} does not exceed σ_m in either of the two sections considered in Fig. 8.8 and that, if it does exceed σ_m elsewhere, it will be in sections close to the load \mathbf{P} , where σ_m is small compared to τ_m .‡ But, for sections close to the load \mathbf{P} , Saint-Venant's principle does not apply, Eqs. (8.3) and (8.4) cease to be valid, except in the very unlikely case of a load distributed parabolically over the end section (cf. Sec. 6.5), and more advanced methods of analysis taking into account the effect of stress concentrations should be used. We thus conclude that, for beams of rectangular cross section, and within the scope of the theory presented in this text, the maximum normal stress can be obtained from Eq. (8.1).

In Fig. 8.8 the directions of the principal axes were determined at 11 points in each of the two sections considered. If this analysis were extended to a larger number of sections and a larger number of points in each section, it would be possible to draw two orthogonal systems of curves on the side of the beam (Fig. 8.9). One system would consist of curves tangent to the principal axes corresponding to σ_{\max} and the other of curves tangent to the principal axes corresponding to σ_{\min} . The curves obtained in this manner are known as the *stress trajectories*. A trajectory of the first group (solid lines) defines at each of its points the direction of the largest tensile stress, while a trajectory of the second group (dashed lines) defines the direction of the largest compressive stress.§

The conclusion we have reached for beams of rectangular cross section, that the maximum normal stress in the beam can be obtained from Eq. (8.1), remains valid for many beams of nonrectangular cross section. However, when the width of the cross section varies in such a way that large shearing stresses τ_{xy} will occur at points close to the surface of the beam, where σ_x is also large, a value of the principal stress σ_{\max} larger than σ_m may result at such points. One should be particularly aware of this possibility when selecting W-beams or S-beams, and calculate the principal stress σ_{\max} at the junctions b and d of the web with the flanges of the beam (Fig. 8.10). This is done by determining σ_x and τ_{xy} at that point from Eqs. (8.1) and (8.2), respectively, and using either of the methods of analysis of Chap. 7 to obtain σ_{\max} (see Sample Prob. 8.1). An alternative procedure, used in design to select an acceptable section, consists of using for τ_{xy} the maximum value of the shearing stress in the section, $\tau_{\max} = V/A_{\text{web}}$, given by Eq. (6.11) of Sec. 6.4. This leads to a slightly larger, and thus conservative, value of the principal stress σ_{\max} at the junction of the web with the flanges of the beam (see Sample Prob. 8.2).

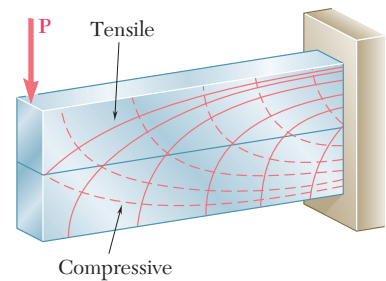


Fig. 8.9 Stress trajectories.

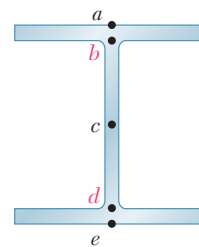


Fig. 8.10 Key stress analysis locations in I-shaped beams.

†See Prob. 8.C2, which refers to a program that can be written to obtain the results shown in Fig. 8.8.

‡As will be verified in Prob. 8.C2, σ_{\max} exceeds σ_m if $x \leq 0.544c$.

§A brittle material, such as concrete, will fail in tension along planes that are perpendicular to the tensile-stress trajectories. Thus, to be effective, steel reinforcing bars should be placed so that they intersect these planes. On the other hand, stiffeners attached to the web of a plate girder will be effective in preventing buckling only if they intersect planes perpendicular to the compressive-stress trajectories.

***8.3 DESIGN OF TRANSMISSION SHAFTS**

When we discussed the design of transmission shafts in Sec. 3.7, we considered only the stresses due to the torques exerted on the shafts. However, if the power is transferred to and from the shaft by means of gears or sprocket wheels (Fig. 8.11*a*), the forces exerted on the gear teeth or sprockets are equivalent to force-couple systems applied at the centers of the corresponding cross sections (Fig. 8.11*b*). This means that the shaft is subjected to a transverse loading, as well as to a torsional loading.

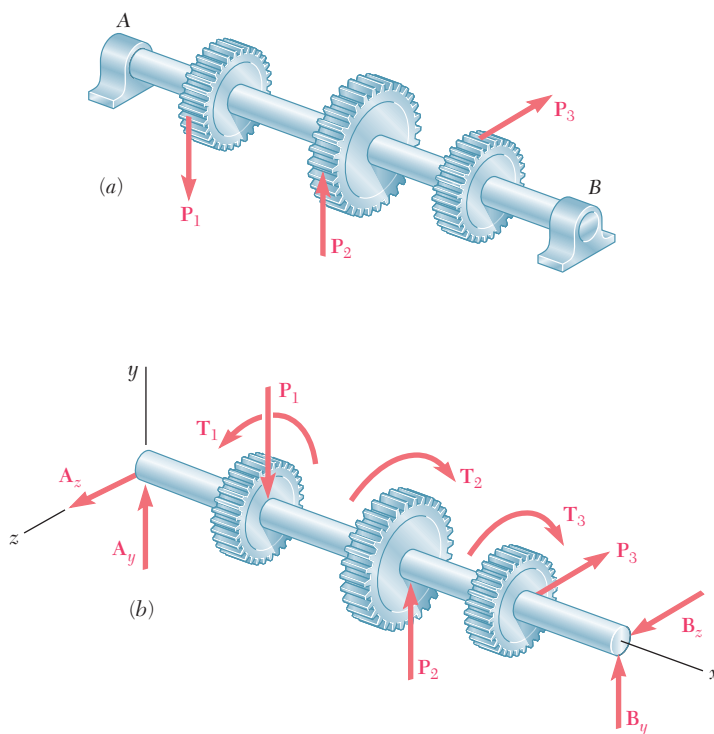


Fig. 8.11 Loadings on gear-shaft systems.

The shearing stresses produced in the shaft by the transverse loads are usually much smaller than those produced by the torques and will be neglected in this analysis.[†] The normal stresses due to the transverse loads, however, may be quite large and, as you will see presently, their contribution to the maximum shearing stress τ_{\max} should be taken into account.

[†]For an application where the shearing stresses produced by the transverse loads must be considered, see Probs. 8.21 and 8.22.

Consider the cross section of the shaft at some point C . We represent the torque \mathbf{T} and the bending couples \mathbf{M}_y and \mathbf{M}_z acting, respectively, in a horizontal and a vertical plane by the couple vectors shown (Fig. 8.12a). Since any diameter of the section is a principal axis of inertia for the section, we can replace \mathbf{M}_y and \mathbf{M}_z by their resultant \mathbf{M} (Fig. 8.12b) in order to compute the normal stresses σ_x exerted on the section. We thus find that σ_x is maximum at the end of the diameter perpendicular to the vector representing \mathbf{M} (Fig. 8.13). Recalling that the values of the normal stresses at that point are, respectively, $\sigma_m = Mc/I$ and zero, while the shearing stress is $\tau_m = Tc/J$, we plot the corresponding points X and Y on a Mohr-circle diagram (Fig. 8.14) and determine the value of the maximum shearing stress:

$$\tau_{\max} = R = \sqrt{\left(\frac{\sigma_m}{2}\right)^2 + (\tau_m)^2} = \sqrt{\left(\frac{Mc}{2I}\right)^2 + \left(\frac{Tc}{J}\right)^2}$$

Recalling that, for a circular or annular cross section, $2I = J$, we write

$$\tau_{\max} = \frac{c}{J} \sqrt{M^2 + T^2} \quad (8.5)$$

It follows that the minimum allowable value of the ratio J/c for the cross section of the shaft is

$$\frac{J}{c} = \frac{(\sqrt{M^2 + T^2})_{\max}}{\tau_{\text{all}}} \quad (8.6)$$

where the numerator in the right-hand member of the expression obtained represents the maximum value of $\sqrt{M^2 + T^2}$ in the shaft, and τ_{all} the allowable shearing stress. Expressing the bending moment M in terms of its components in the two coordinate planes, we can also write

$$\frac{J}{c} = \frac{(\sqrt{M_y^2 + M_z^2 + T^2})_{\max}}{\tau_{\text{all}}} \quad (8.7)$$

Equations (8.6) and (8.7) can be used to design both solid and hollow circular shafts and should be compared with Eq. (3.22) of Sec. 3.7, which was obtained under the assumption of a torsional loading only.

The determination of the maximum value of $\sqrt{M_y^2 + M_z^2 + T^2}$ will be facilitated if the bending-moment diagrams corresponding to M_y and M_z are drawn, as well as a third diagram representing the values of T along the shaft (see Sample Prob. 8.3).

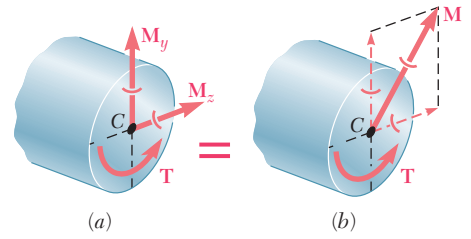


Fig. 8.12 Resultant loading on the cross section of a shaft.

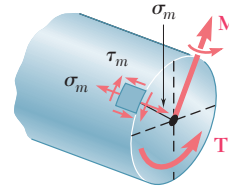


Fig. 8.13 Maximum stress element.

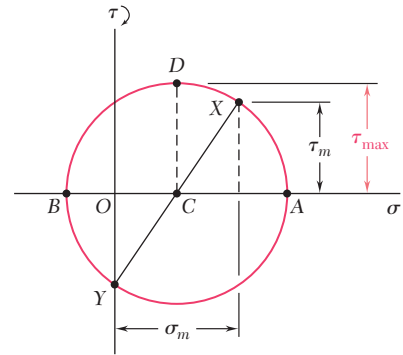
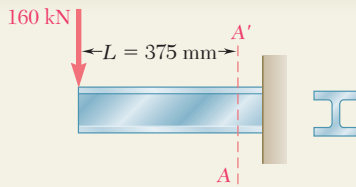


Fig. 8.14 Mohr's circle analysis.



SAMPLE PROBLEM 8.1

A 160-kN force is applied as shown at the end of a W200 × 52 rolled-steel beam. Neglecting the effect of fillets and of stress concentrations, determine whether the normal stresses in the beam satisfy a design specification that they be equal to or less than 150 MPa at section A-A'.

SOLUTION

Shear and Bending Moment. At section A-A', we have

$$M_A = (160 \text{ kN})(0.375 \text{ m}) = 60 \text{ kN} \cdot \text{m}$$

$$V_A = 160 \text{ kN}$$

Normal Stresses on Transverse Plane. Referring to the table of *Properties of Rolled-Steel Shapes* in Appendix C, we obtain the data shown and then determine the stresses σ_a and σ_b .

At point a :

$$\sigma_a = \frac{M_A}{S} = \frac{60 \text{ kN} \cdot \text{m}}{511 \times 10^{-6} \text{ m}^3} = 117.4 \text{ MPa}$$

At point b :

$$\sigma_b = \sigma_a \frac{y_b}{c} = (117.4 \text{ MPa}) \frac{90.4 \text{ mm}}{103 \text{ mm}} = 103.0 \text{ MPa}$$

We note that all normal stresses on the transverse plane are less than 150 MPa.

Shearing Stresses on Transverse Plane

At point a :

$$Q = 0 \quad \tau_a = 0$$

At point b :

$$Q = (206 \times 12.6)(96.7) = 251.0 \times 10^3 \text{ mm}^3 = 251.0 \times 10^{-6} \text{ m}^3$$

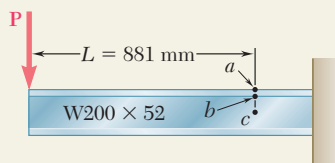
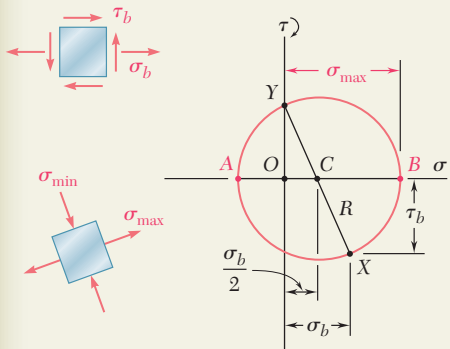
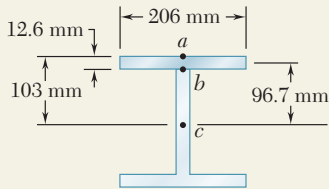
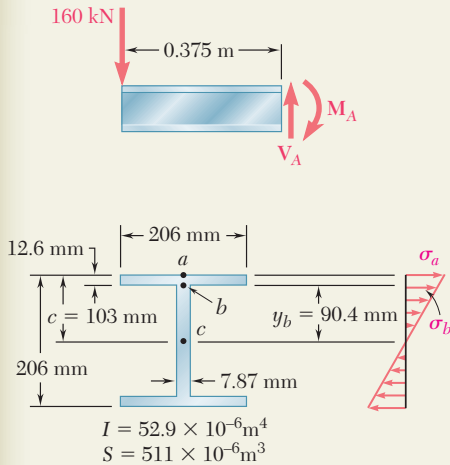
$$\tau_b = \frac{V_A Q}{I t} = \frac{(160 \text{ kN})(251.0 \times 10^{-6} \text{ m}^3)}{(52.9 \times 10^{-6} \text{ m}^4)(0.00787 \text{ m})} = 96.5 \text{ MPa}$$

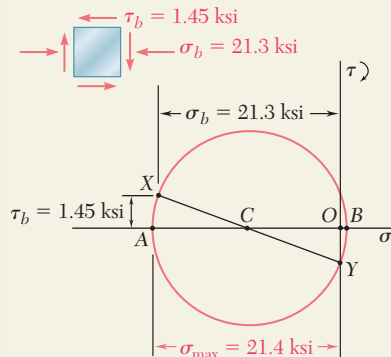
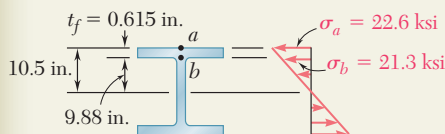
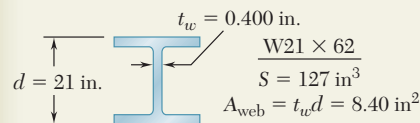
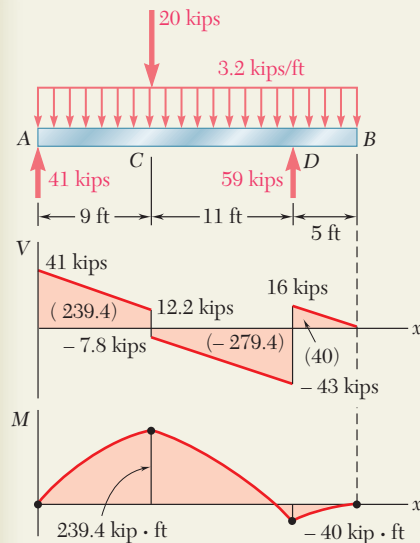
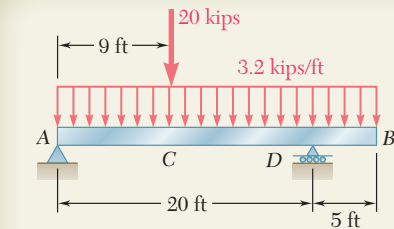
Principal Stress at Point b . The state of stress at point b consists of the normal stress $\sigma_b = 103.0 \text{ MPa}$ and the shearing stress $\tau_b = 96.5 \text{ MPa}$. We draw Mohr's circle and find

$$\begin{aligned} \sigma_{\max} &= \frac{1}{2} \sigma_b + R = \frac{1}{2} \sigma_b + \sqrt{\left(\frac{1}{2} \sigma_b\right)^2 + \tau_b^2} \\ &= \frac{103.0}{2} + \sqrt{\left(\frac{103.0}{2}\right)^2 + (96.5)^2} \\ \sigma_{\max} &= 160.9 \text{ MPa} \end{aligned}$$

The specification, $\sigma_{\max} \leq 150 \text{ MPa}$, is *not* satisfied ◀

Comment. For this beam and loading, the principal stress at point b is 36% larger than the normal stress at point a . For $L \geq 881 \text{ mm}$, the maximum normal stress would occur at point a .





SAMPLE PROBLEM 8.2

The overhanging beam AB supports a uniformly distributed load of 3.2 kips/ft and a concentrated load of 20 kips at C . Knowing that for the grade of steel to be used $\sigma_{\text{all}} = 24$ ksi and $\tau_{\text{all}} = 14.5$ ksi, select the wide-flange shape that should be used.

SOLUTION

Reactions at A and D . We draw the free-body diagram of the beam. From the equilibrium equations $\Sigma M_D = 0$ and $\Sigma M_A = 0$ we find the values of R_A and R_D shown in the diagram.

Shear and Bending-Moment Diagrams. Using the methods of Secs. 5.2 and 5.3, we draw the diagrams and observe that

$$|M|_{\text{max}} = 239.4 \text{ kip} \cdot \text{ft} = 2873 \text{ kip} \cdot \text{in.} \quad |V|_{\text{max}} = 43 \text{ kips}$$

Section Modulus. For $|M|_{\text{max}} = 2873 \text{ kip} \cdot \text{in.}$ and $\sigma_{\text{all}} = 24$ ksi, the minimum acceptable section modulus of the rolled-steel shape is

$$S_{\text{min}} = \frac{|M|_{\text{max}}}{\sigma_{\text{all}}} = \frac{2873 \text{ kip} \cdot \text{in.}}{24 \text{ ksi}} = 119.7 \text{ in}^3$$

Selection of Wide-Flange Shape. From the table of *Properties of Rolled-Steel Shapes* in Appendix C, we compile a list of the lightest shapes of a given depth that have a section modulus larger than S_{min} .

Shape	S (in^3)
W24 \times 68	154
W21 \times 62	127
W18 \times 76	146
W16 \times 77	134
W14 \times 82	123
W12 \times 96	131

We now select the lightest shape available, namely

W21 \times 62 ◀

Shearing Stress. Since we are designing the beam, we will conservatively assume that the maximum shear is uniformly distributed over the web area of a W21 \times 62. We write

$$\tau_m = \frac{V_{\text{max}}}{A_{\text{web}}} = \frac{43 \text{ kips}}{8.40 \text{ in}^2} = 5.12 \text{ ksi} < 14.5 \text{ ksi} \quad (\text{OK})$$

Principal Stress at Point b . We check that the maximum principal stress at point b in the critical section where M is maximum does not exceed $\sigma_{\text{all}} = 24$ ksi. We write

$$\sigma_a = \frac{M_{\text{max}}}{S} = \frac{2873 \text{ kip} \cdot \text{in.}}{127 \text{ in}^3} = 22.6 \text{ ksi}$$

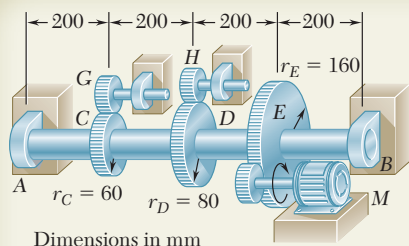
$$\sigma_b = \sigma_a \frac{y_b}{c} = (22.6 \text{ ksi}) \frac{9.88 \text{ in.}}{10.50 \text{ in.}} = 21.3 \text{ ksi}$$

$$\text{Conservatively, } \tau_b = \frac{V}{A_{\text{web}}} = \frac{12.2 \text{ kips}}{8.40 \text{ in}^2} = 1.45 \text{ ksi}$$

We draw Mohr's circle and find

$$\sigma_{\text{max}} = \frac{1}{2} \sigma_b + R = \frac{21.3 \text{ ksi}}{2} + \sqrt{\left(\frac{21.3 \text{ ksi}}{2}\right)^2 + (1.45 \text{ ksi})^2}$$

$$\sigma_{\text{max}} = 21.4 \text{ ksi} \leq 24 \text{ ksi} \quad (\text{OK}) \quad \blacktriangleleft$$



SAMPLE PROBLEM 8.3

The solid shaft AB rotates at 480 rpm and transmits 30 kW from the motor M to machine tools connected to gears G and H ; 20 kW is taken off at gear G and 10 kW at gear H . Knowing that $\tau_{\text{all}} = 50$ MPa, determine the smallest permissible diameter for shaft AB .

SOLUTION

Torques Exerted on Gears. Observing that $f = 480 \text{ rpm} = 8 \text{ Hz}$, we determine the torque exerted on gear E :

$$T_E = \frac{P}{2\pi f} = \frac{30 \text{ kW}}{2\pi(8 \text{ Hz})} = 597 \text{ N} \cdot \text{m}$$

The corresponding tangential force acting on the gear is

$$F_E = \frac{T_E}{r_E} = \frac{597 \text{ N} \cdot \text{m}}{0.16 \text{ m}} = 3.73 \text{ kN}$$

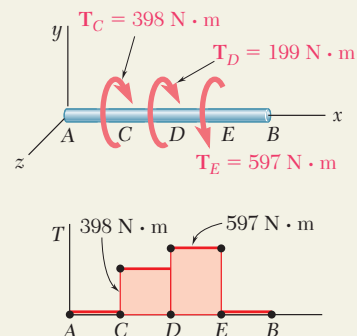
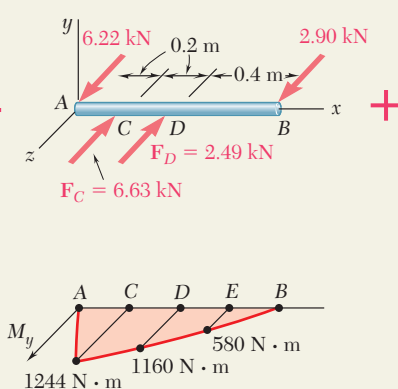
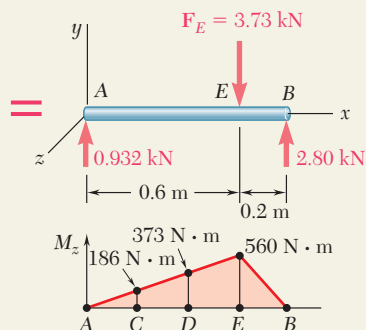
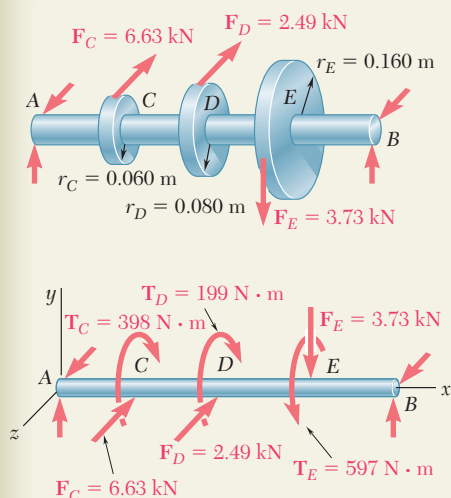
A similar analysis of gears C and D yields

$$T_C = \frac{20 \text{ kW}}{2\pi(8 \text{ Hz})} = 398 \text{ N} \cdot \text{m} \quad F_C = 6.63 \text{ kN}$$

$$T_D = \frac{10 \text{ kW}}{2\pi(8 \text{ Hz})} = 199 \text{ N} \cdot \text{m} \quad F_D = 2.49 \text{ kN}$$

We now replace the forces on the gears by equivalent force-couple systems.

Bending-Moment and Torque Diagrams



Critical Transverse Section. By computing $\sqrt{M_y^2 + M_z^2 + T^2}$ at all potentially critical sections, we find that its maximum value occurs just to the right of D :

$$\sqrt{M_y^2 + M_z^2 + T^2}_{\text{max}} = \sqrt{(1160)^2 + (373)^2 + (597)^2} = 1357 \text{ N} \cdot \text{m}$$

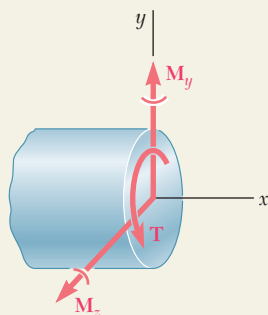
Diameter of Shaft. For $\tau_{\text{all}} = 50$ MPa, Eq. (7.32) yields

$$\frac{J}{c} = \frac{\sqrt{M_y^2 + M_z^2 + T^2}_{\text{max}}}{\tau_{\text{all}}} = \frac{1357 \text{ N} \cdot \text{m}}{50 \text{ MPa}} = 27.14 \times 10^{-6} \text{ m}^3$$

For a solid circular shaft of radius c , we have

$$\frac{J}{c} = \frac{\pi}{2} c^3 = 27.14 \times 10^{-6} \quad c = 0.02585 \text{ m} = 25.85 \text{ mm}$$

$$\text{Diameter} = 2c = 51.7 \text{ mm} \quad \blacktriangleleft$$



PROBLEMS

8.1 A W10 × 39 rolled-steel beam supports a load \mathbf{P} as shown. Knowing that $P = 45$ kips, $a = 10$ in., and $\sigma_{\text{all}} = 18$ ksi, determine (a) the maximum value of the normal stress σ_m in the beam, (b) the maximum value of the principal stress σ_{max} at the junction of the flange and web, (c) whether the specified shape is acceptable as far as these two stresses are concerned.

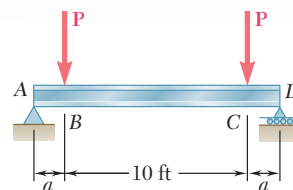


Fig. P8.1

8.2 Solve Prob. 8.1, assuming that $P = 22.5$ kips and $a = 20$ in.

8.3 An overhanging W920 × 449 rolled-steel beam supports a load \mathbf{P} as shown. Knowing that $P = 700$ kN, $a = 2.5$ m, and $\sigma_{\text{all}} = 100$ MPa, determine (a) the maximum value of the normal stress σ_m in the beam, (b) the maximum value of the principal stress σ_{max} at the junction of the flange and web, (c) whether the specified shape is acceptable as far as these two stresses are concerned.

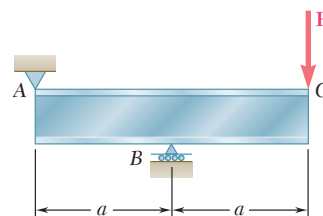


Fig. P8.3

8.4 Solve Prob. 8.3, assuming that $P = 850$ kN and $a = 2.0$ m.

8.5 and 8.6 (a) Knowing that $\sigma_{\text{all}} = 24$ ksi and $\tau_{\text{all}} = 14.5$ ksi, select the most economical wide-flange shape that should be used to support the loading shown. (b) Determine the values to be expected for σ_m , τ_m , and the principal stress σ_{max} at the junction of a flange and the web of the selected beam.

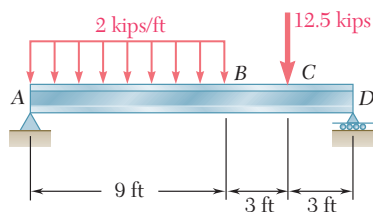


Fig. P8.5

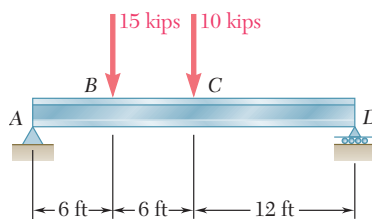


Fig. P8.6

8.7 and 8.8 (a) Knowing that $\sigma_{\text{all}} = 160$ MPa and $\tau_{\text{all}} = 100$ MPa, select the most economical metric wide-flange shape that should be used to support the loading shown. (b) Determine the values to be expected for σ_m , τ_m , and the principal stress σ_{max} at the junction of a flange and the web of the selected beam.

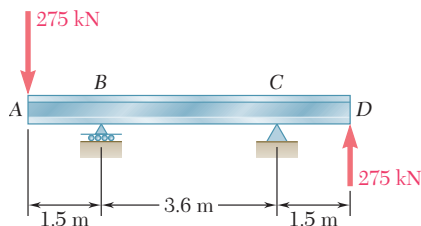


Fig. P8.7

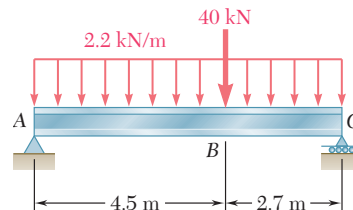


Fig. P8.8

8.9 through 8.14 Each of the following problems refers to a rolled-steel shape selected in a problem of Chap. 5 to support a given loading at a minimal cost while satisfying the requirement $\sigma_m \leq \sigma_{all}$. For the selected design, determine (a) the actual value of σ_m in the beam, (b) the maximum value of the principal stress σ_{max} at the junction of a flange and the web.

8.9 Loading of Prob. 5.73 and selected W530 \times 66 shape.

8.10 Loading of Prob. 5.74 and selected W530 \times 92 shape.

8.11 Loading of Prob. 5.77 and selected S15 \times 42.9 shape.

8.12 Loading of Prob. 5.78 and selected S12 \times 31.8 shape.

8.13 Loading of Prob. 5.75 and selected S460 \times 81.4 shape.

8.14 Loading of Prob. 5.76 and selected S510 \times 98.2 shape.

8.15 The vertical force P_1 and the horizontal force P_2 are applied as shown to disks welded to the solid shaft AD. Knowing that the diameter of the shaft is 1.75 in. and that $\tau_{all} = 8$ ksi, determine the largest permissible magnitude of the force P_2 .

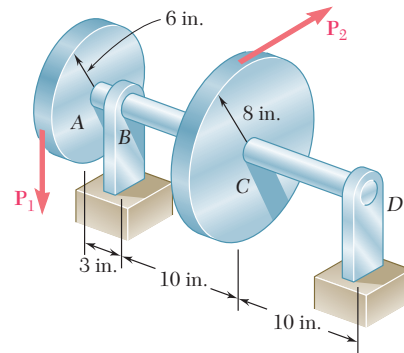


Fig. P8.15

8.16 The two 500-lb forces are vertical and the force P is parallel to the z axis. Knowing that $\tau_{all} = 8$ ksi, determine the smallest permissible diameter of the solid shaft AE.

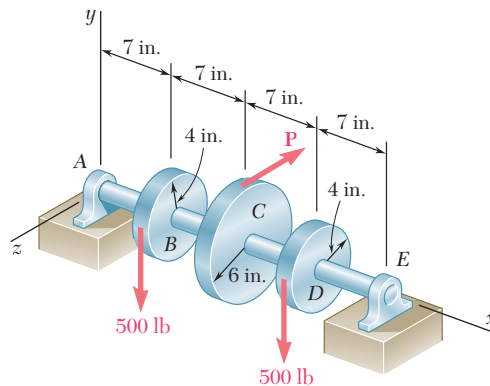


Fig. P8.16

8.17 For the gear-and-shaft system and loading of Prob. 8.16, determine the smallest permissible diameter of shaft AE, knowing that the shaft is hollow and has an inner diameter that is $\frac{2}{3}$ the outer diameter.

8.18 The 4-kN force is parallel to the x axis, and the force Q is parallel to the z axis. The shaft AD is hollow. Knowing that the inner diameter is half the outer diameter and that $\tau_{all} = 60$ MPa, determine the smallest permissible outer diameter of the shaft.

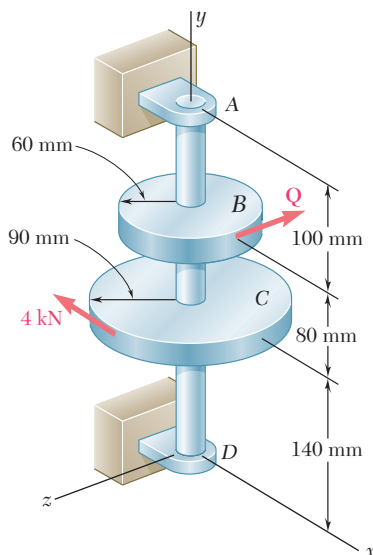


Fig. P8.18

- 8.19** Neglecting the effect of fillets and of stress concentrations, determine the smallest permissible diameters of the solid rods BC and CD . Use $\tau_{\text{all}} = 60 \text{ MPa}$.

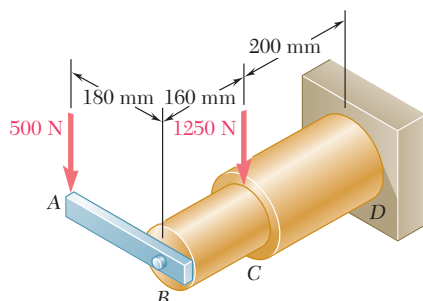


Fig. P8.19 and P8.20

- 8.20** Knowing that rods BC and CD are of diameter 24 mm and 36 mm, respectively, determine the maximum shearing stress in each rod. Neglect the effect of fillets and of stress concentrations.

- 8.21** It was stated in Sec. 8.3 that the shearing stresses produced in a shaft by the transverse loads are usually much smaller than those produced by the torques. In the preceding problems their effect was ignored and it was assumed that the maximum shearing stress in a given section occurred at point H (Fig. P8.21a) and was equal to the expression obtained in Eq. (8.5), namely,

$$\tau_H = \frac{c}{J} \sqrt{M^2 + T^2}$$

Show that the maximum shearing stress at point K (Fig. P8.21b), where the effect of the shear V is greatest, can be expressed as

$$\tau_K = \frac{c}{J} \sqrt{(M \cos \beta)^2 + \left(\frac{2}{3}cV + T\right)^2}$$

where β is the angle between the vectors \mathbf{V} and \mathbf{M} . It is clear that the effect of the shear V cannot be ignored when $\tau_K \geq \tau_H$. (Hint: Only the component of \mathbf{M} along \mathbf{V} contributes to the shearing stress at K .)

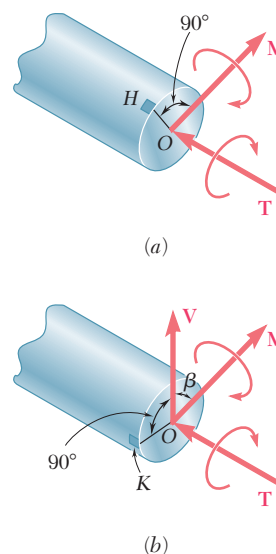


Fig. P8.21

- 8.22** Assuming that the magnitudes of the forces applied to disks A and C of Prob. 8.15 are, respectively, $P_1 = 1080 \text{ lb}$ and $P_2 = 810 \text{ lb}$, and using the expressions given in Prob. 8.21, determine the values of τ_H and τ_K in a section (a) just to the left of B , (b) just to the left of C .

- 8.23** The solid shafts ABC and DEF and the gears shown are used to transmit 20 hp from the motor M to a machine tool connected to shaft DEF . Knowing that the motor rotates at 240 rpm and that $\tau_{\text{all}} = 7.5 \text{ ksi}$, determine the smallest permissible diameter of (a) shaft ABC , (b) shaft DEF .

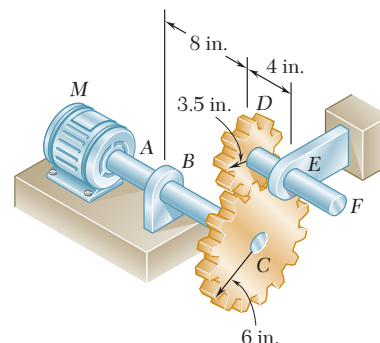


Fig. P8.23

- 8.24** Solve Prob. 8.23, assuming that the motor rotates at 360 rpm.

- 8.25** The solid shaft AB rotates at 360 rpm and transmits 20 kW from the motor M to machine tools connected to gears E and F . Knowing that $\tau_{\text{all}} = 45$ MPa and assuming that 10 kW is taken off at each gear, determine the smallest permissible diameter of shaft AB .

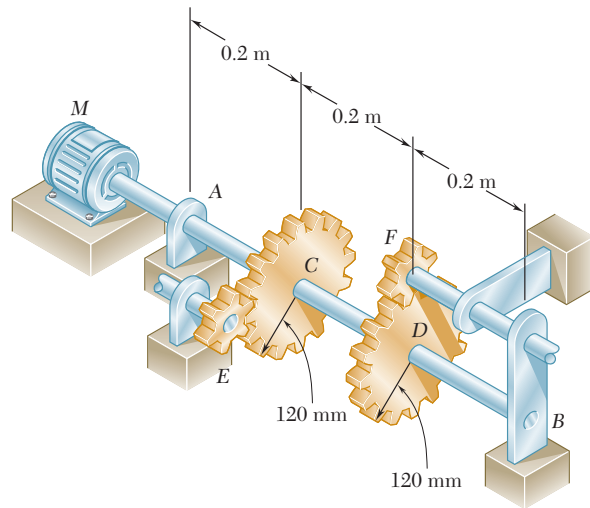


Fig. P8.25

- 8.26** Solve Prob. 8.25, assuming that the entire 20 kW is taken off at gear E .
- 8.27** The solid shaft ABC and the gears shown are used to transmit 10 kW from the motor M to a machine tool connected to gear D . Knowing that the motor rotates at 240 rpm and that $\tau_{\text{all}} = 60$ MPa, determine the smallest permissible diameter of shaft ABC .

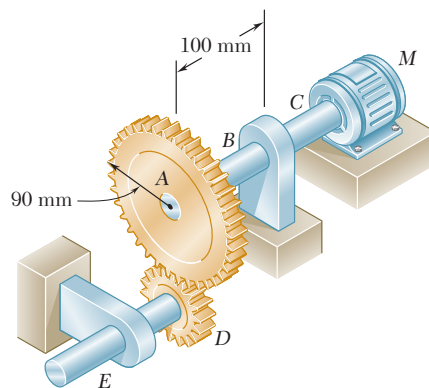


Fig. P8.27

- 8.28** Assuming that shaft ABC of Prob. 8.27 is hollow and has an outer diameter of 50 mm, determine the largest permissible inner diameter of the shaft.

- 8.29** The solid shaft AE rotates at 600 rpm and transmits 60 hp from the motor M to machine tools connected to gears G and H . Knowing that $\tau_{\text{all}} = 8$ ksi and that 40 hp is taken off at gear G and 20 hp is taken off at gear H , determine the smallest permissible diameter of shaft AE .

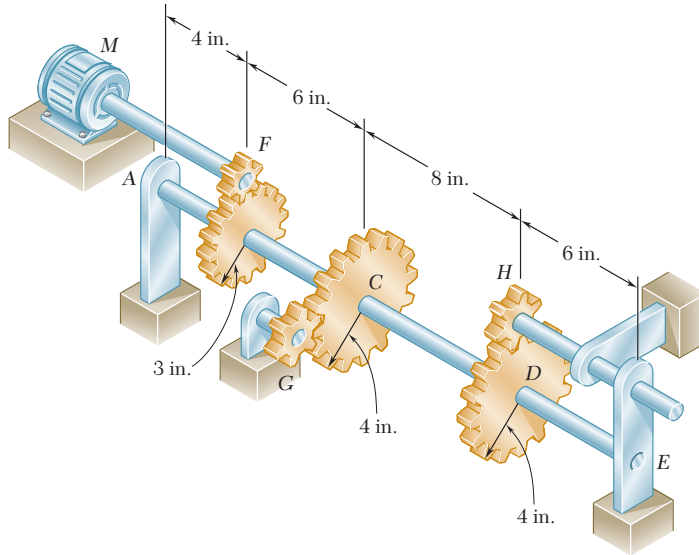


Fig. P8.29

- 8.30** Solve Prob. 8.29, assuming that 30 hp is taken off at gear G and 30 hp is taken off at gear H .

*8.4 STRESSES UNDER COMBINED LOADINGS

In Chaps. 1 and 2 you learned to determine the stresses caused by a centric axial load. In Chap. 3, you analyzed the distribution of stresses in a cylindrical member subjected to a twisting couple. In Chap. 4, you determined the stresses caused by bending couples and, in Chaps. 5 and 6, the stresses produced by transverse loads. As you will see presently, you can combine the knowledge you have acquired to determine the stresses in slender structural members or machine components under fairly general loading conditions.

Consider, for example, the bent member $ABDE$ of circular cross section that is subjected to several forces (Fig. 8.15). In order to determine the stresses produced at points H or K by the given loads, we first pass a section through these points and determine the force-couple system at the centroid C of the section that is required to maintain the equilibrium of portion ABC .† This system represents the internal forces in the section and, in general, consists of three

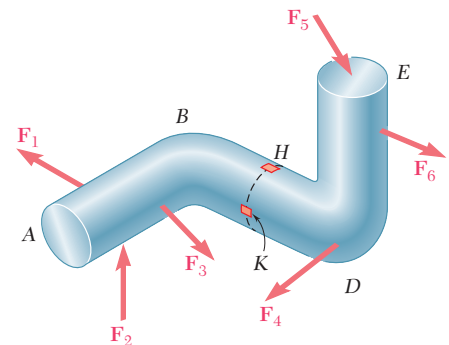


Fig. 8.15 Member $ABDE$ subjected to several forces.

†The force-couple system at C can also be defined as *equivalent to the forces acting on the portion of the member located to the right of the section* (see Example 8.01).

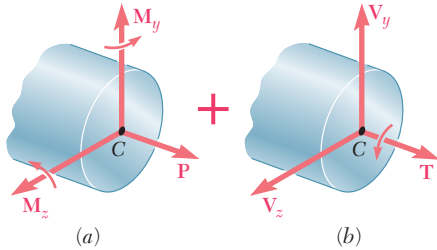


Fig. 8.17 Internal forces separated into (a) those causing normal stresses (b) those causing shearing stresses.

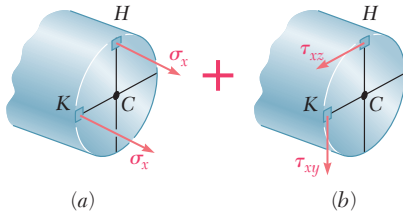


Fig. 8.18 Normal stresses and shearing stresses.

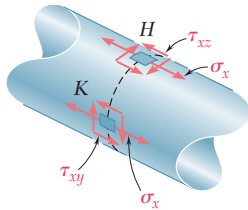


Fig. 8.19 Combined stresses.

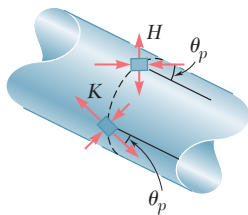


Fig. 8.20 Principal stresses and orientation of principal planes.

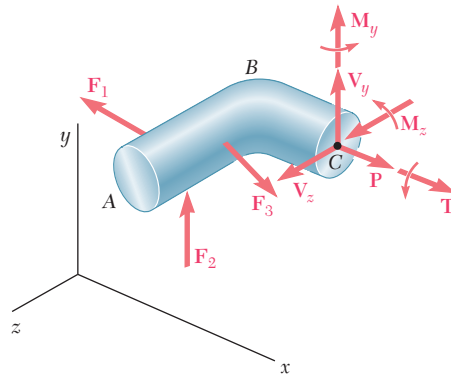


Fig. 8.16 Determination of internal forces at the section for stress analysis.

force components and three couple vectors that will be assumed directed as shown (Fig. 8.16).

The force \mathbf{P} is a centric axial force that produces normal stresses in the section. The couple vectors \mathbf{M}_y and \mathbf{M}_z cause the member to bend and also produce normal stresses in the section. They have therefore been grouped with the force \mathbf{P} in part *a* of Fig. 8.17 and the sums σ_x of the normal stresses they produce at points *H* and *K* have been shown in part *a* of Fig. 8.18. These stresses can be determined as shown in Sec. 4.14.

On the other hand, the twisting couple \mathbf{T} and the shearing forces \mathbf{V}_y and \mathbf{V}_z produce shearing stresses in the section. The sums τ_{xy} and τ_{xz} of the components of the shearing stresses they produce at points *H* and *K* have been shown in part *b* of Fig. 8.18 and can be determined as indicated in Secs. 3.4 and 6.3.† The normal and shearing stresses shown in parts *a* and *b* of Fig. 8.18 can now be combined and displayed at points *H* and *K* on the surface of the member (Fig. 8.19).

The principal stresses and the orientation of the principal planes at points *H* and *K* can be determined from the values of σ_x , τ_{xy} , and τ_{xz} at each of these points by one of the methods presented in Chap. 7 (Fig. 8.20). The values of the maximum shearing stress at each of these points and the corresponding planes can be found in a similar way.

The results obtained in this section are valid only to the extent that the conditions of applicability of the superposition principle (Sec. 2.12) and of Saint-Venant's principle (Sec. 2.17) are met. This means that the stresses involved must not exceed the proportional limit of the material, that the deformations due to one of the loadings must not affect the determination of the stresses due to the others, and that the section used in your analysis must not be too close to the points of application of the given forces. It is clear from the first of these requirements that the method presented here cannot be applied to plastic deformations.

†Note that your present knowledge allows you to determine the effect of the twisting couple \mathbf{T} only in the cases of circular shafts, of members with a rectangular cross section (Sec. 3.12), or of thin-walled hollow members (Sec. 3.13).

Two forces \mathbf{P}_1 and \mathbf{P}_2 , of magnitude $P_1 = 15 \text{ kN}$ and $P_2 = 18 \text{ kN}$, are applied as shown to the end A of bar AB, which is welded to a cylindrical member BD of radius $c = 20 \text{ mm}$ (Fig. 8.21). Knowing that the distance from A to the axis of member BD is $a = 50 \text{ mm}$ and assuming that all stresses remain below the proportional limit of the material, determine (a) the normal and shearing stresses at point K of the transverse section of member BD located at a distance $b = 60 \text{ mm}$ from end B, (b) the principal axes and principal stresses at K, (c) the maximum shearing stress at K.

EXAMPLE 8.01

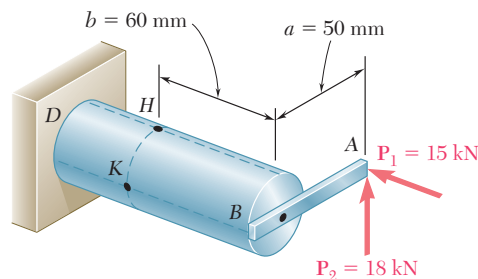


Fig. 8.21

Internal Forces in Given Section. We first replace the forces \mathbf{P}_1 and \mathbf{P}_2 by an equivalent system of forces and couples applied at the center C of the section containing point K (Fig. 8.22). This system, which represents the internal forces in the section, consists of the following forces and couples:

1. A centric axial force \mathbf{F} equal to the force \mathbf{P}_1 , of magnitude

$$F = P_1 = 15 \text{ kN}$$

2. A shearing force \mathbf{V} equal to the force \mathbf{P}_2 , of magnitude

$$V = P_2 = 18 \text{ kN}$$

3. A twisting couple \mathbf{T} of torque T equal to the moment of \mathbf{P}_2 about the axis of member BD:

$$T = P_2 a = (18 \text{ kN})(50 \text{ mm}) = 900 \text{ N} \cdot \text{m}$$

4. A bending couple \mathbf{M}_y , of moment M_y equal to the moment of \mathbf{P}_1 about a vertical axis through C:

$$M_y = P_1 a = (15 \text{ kN})(50 \text{ mm}) = 750 \text{ N} \cdot \text{m}$$

5. A bending couple \mathbf{M}_z , of moment M_z equal to the moment of \mathbf{P}_2 about a transverse, horizontal axis through C:

$$M_z = P_2 b = (18 \text{ kN})(60 \text{ mm}) = 1080 \text{ N} \cdot \text{m}$$

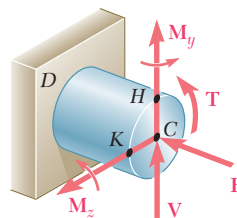


Fig. 8.22

The results obtained are shown in Fig. 8.23.

a. Normal and Shearing Stresses at Point K. Each of the forces and couples shown in Fig. 8.23 can produce a normal or shearing stress at point K. Our purpose is to compute separately each of these stresses, and then to add the normal stresses and add the shearing stresses. But we must first determine the geometric properties of the section.

Geometric Properties of the Section We have

$$\begin{aligned} A &= \pi c^2 = \pi (0.020 \text{ m})^2 = 1.257 \times 10^{-3} \text{ m}^2 \\ I_y &= I_z = \frac{1}{4} \pi c^4 = \frac{1}{4} \pi (0.020 \text{ m})^4 = 125.7 \times 10^{-9} \text{ m}^4 \\ J_C &= \frac{1}{2} \pi c^4 = \frac{1}{2} \pi (0.020 \text{ m})^4 = 251.3 \times 10^{-9} \text{ m}^4 \end{aligned}$$

We also determine the first moment Q and the width t of the area of the cross section located above the z axis. Recalling that $\bar{y} = 4c/3\pi$ for a semicircle of radius c , we have

$$\begin{aligned} Q &= A \bar{y} = \left(\frac{1}{2} \pi c^2 \right) \left(\frac{4c}{3\pi} \right) = \frac{2}{3} c^3 = \frac{2}{3} (0.020 \text{ m})^3 \\ &= 5.33 \times 10^{-6} \text{ m}^3 \end{aligned}$$

and

$$t = 2c = 2(0.020 \text{ m}) = 0.040 \text{ m}$$

Normal Stresses. We observe that normal stresses are produced at K by the centric force \mathbf{F} and the bending couple \mathbf{M}_y , but that the couple \mathbf{M}_z

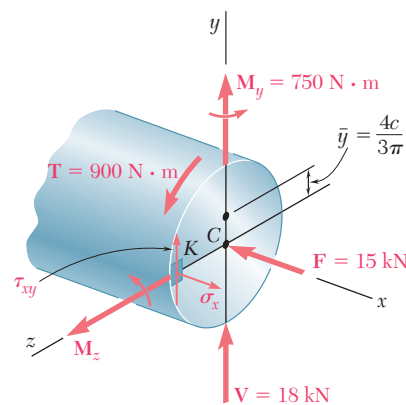


Fig. 8.23

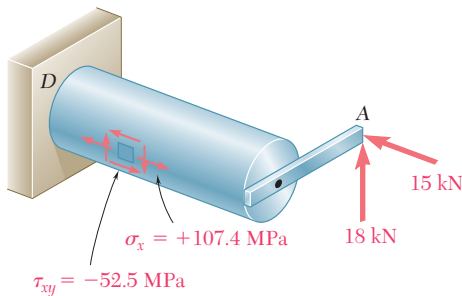


Fig. 8.24

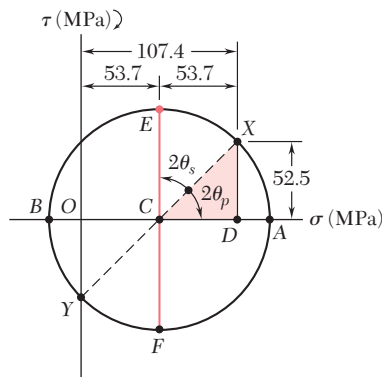


Fig. 8.25

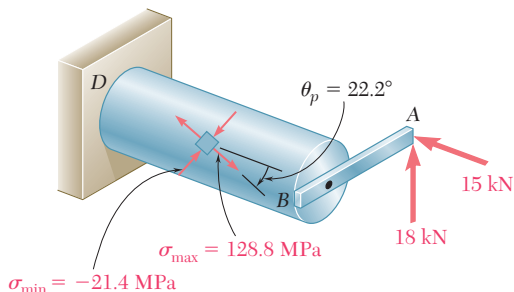


Fig. 8.26

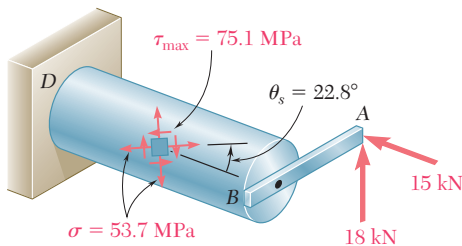


Fig. 8.27

does not produce any stress at K , since K is located on the neutral axis corresponding to that couple. Determining each sign from Fig. 8.23, we write

$$\begin{aligned}\sigma_x &= -\frac{F}{A} + \frac{M_y c}{I_y} = -11.9 \text{ MPa} + \frac{(750 \text{ N} \cdot \text{m})(0.020 \text{ m})}{125.7 \times 10^{-9} \text{ m}^4} \\ &= -11.9 \text{ MPa} + 119.3 \text{ MPa} \\ \sigma_x &= +107.4 \text{ MPa}\end{aligned}$$

Shearing Stresses. These consist of the shearing stress $(\tau_{xy})_V$ due to the vertical shear \mathbf{V} and of the shearing stress $(\tau_{xy})_{\text{twist}}$ caused by the torque \mathbf{T} . Recalling the values obtained for Q , t , I_z , and J_C , we write

$$\begin{aligned}(\tau_{xy})_V &= +\frac{VQ}{I_z t} = +\frac{(18 \times 10^3 \text{ N})(5.33 \times 10^{-6} \text{ m}^3)}{(125.7 \times 10^{-9} \text{ m}^4)(0.040 \text{ m})} \\ &= +19.1 \text{ MPa}\end{aligned}$$

$$(\tau_{xy})_{\text{twist}} = -\frac{Tc}{J_C} = -\frac{(900 \text{ N} \cdot \text{m})(0.020 \text{ m})}{251.3 \times 10^{-9} \text{ m}^4} = -71.6 \text{ MPa}$$

Adding these two expressions, we obtain τ_{xy} at point K .

$$\begin{aligned}\tau_{xy} &= (\tau_{xy})_V + (\tau_{xy})_{\text{twist}} = +19.1 \text{ MPa} - 71.6 \text{ MPa} \\ \tau_{xy} &= -52.5 \text{ MPa}\end{aligned}$$

In Fig. 8.24, the normal stress σ_x and the shearing stresses and τ_{xy} have been shown acting on a square element located at K on the surface of the cylindrical member. Note that shearing stresses acting on the longitudinal sides of the element have been included.

b. Principal Planes and Principal Stresses at Point K . We can use either of the two methods of Chap. 7 to determine the principal planes and principal stresses at K . Selecting Mohr's circle, we plot point X of coordinates $\sigma_x = +107.4 \text{ MPa}$ and $-\tau_{xy} = +52.5 \text{ MPa}$ and point Y of coordinates $\sigma_y = 0$ and $+\tau_{xy} = -52.5 \text{ MPa}$ and draw the circle of diameter XY (Fig. 8.25). Observing that

$$OC = CD = \frac{1}{2}(107.4) = 53.7 \text{ MPa} \quad DX = 52.5 \text{ MPa}$$

we determine the orientation of the principal planes:

$$\begin{aligned}\tan 2\theta_p &= \frac{DX}{CD} = \frac{52.5}{53.7} = 0.97765 \quad 2\theta_p = 44.4^\circ \downarrow \\ \theta_p &= 22.2^\circ \downarrow\end{aligned}$$

We now determine the radius of the circle,

$$R = \sqrt{(53.7)^2 + (52.5)^2} = 75.1 \text{ MPa}$$

and the principal stresses,

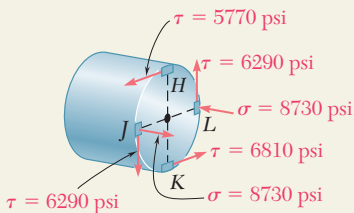
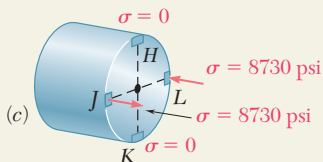
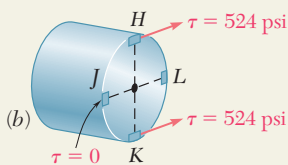
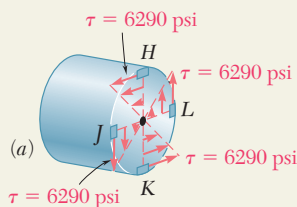
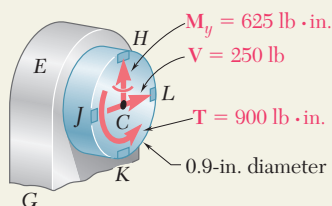
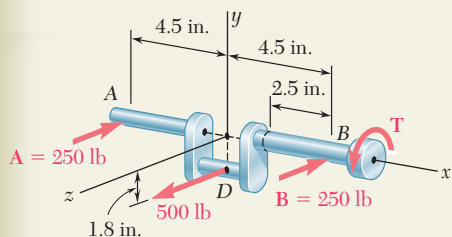
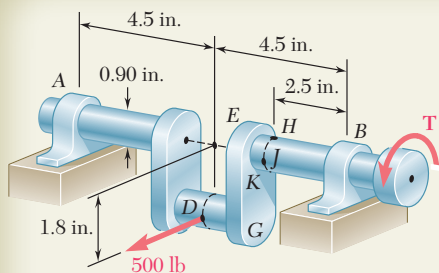
$$\begin{aligned}\sigma_{\max} &= OC + R = 53.7 + 75.1 = 128.8 \text{ MPa} \\ \sigma_{\min} &= OC - R = 53.7 - 75.1 = -21.4 \text{ MPa}\end{aligned}$$

The results obtained are shown in Fig. 8.26.

c. Maximum Shearing Stress at Point K . This stress corresponds to points E and F in Fig. 8.25. We have

$$\tau_{\max} = CE = R = 75.1 \text{ MPa}$$

Observing that $2\theta_s = 90^\circ - 2\theta_p = 90^\circ - 44.4^\circ = 45.6^\circ$, we conclude that the planes of maximum shearing stress form an angle $\theta_p = 22.8^\circ \uparrow$ with the horizontal. The corresponding element is shown in Fig. 8.27. Note that the normal stresses acting on this element are represented by OC in Fig. 8.25 and are thus equal to $+53.7 \text{ MPa}$.



SAMPLE PROBLEM 8.4

A horizontal 500-lb force acts at point *D* of crankshaft *AB* which is held in static equilibrium by a twisting couple **T** and by reactions at *A* and *B*. Knowing that the bearings are self-aligning and exert no couples on the shaft, determine the normal and shearing stresses at points *H*, *J*, *K*, and *L* located at the ends of the vertical and horizontal diameters of a transverse section located 2.5 in. to the left of bearing *B*.

SOLUTION

Free Body. Entire Crankshaft. $A = B = 250$ lb

$$+\uparrow \Sigma M_x = 0: \quad -(500 \text{ lb})(1.8 \text{ in.}) + T = 0 \quad T = 900 \text{ lb} \cdot \text{in.}$$

Internal Forces in Transverse Section. We replace the reaction **B** and the twisting couple **T** by an equivalent force-couple system at the center *C* of the transverse section containing *H*, *J*, *K*, and *L*.

$$V = B = 250 \text{ lb} \quad T = 900 \text{ lb} \cdot \text{in.}$$

$$M_y = (250 \text{ lb})(2.5 \text{ in.}) = 625 \text{ lb} \cdot \text{in.}$$

The geometric properties of the 0.9-in.-diameter section are

$$A = \pi(0.45 \text{ in.})^2 = 0.636 \text{ in}^2 \quad I = \frac{1}{4}\pi(0.45 \text{ in.})^4 = 32.2 \times 10^{-3} \text{ in}^4$$

$$J = \frac{1}{2}\pi(0.45 \text{ in.})^4 = 64.4 \times 10^{-3} \text{ in}^4$$

Stresses Produced by Twisting Couple T. Using Eq. (3.8), we determine the shearing stresses at points *H*, *J*, *K*, and *L* and show them in Fig. (a).

$$\tau = \frac{Tc}{J} = \frac{(900 \text{ lb} \cdot \text{in.})(0.45 \text{ in.})}{64.4 \times 10^{-3} \text{ in}^4} = 6290 \text{ psi}$$

Stresses Produced by Shearing Force V. The shearing force **V** produces no shearing stresses at points *J* and *L*. At points *H* and *K* we first compute *Q* for a semicircle about a vertical diameter and then determine the shearing stress produced by the shear force $V = 250$ lb. These stresses are shown in Fig. (b).

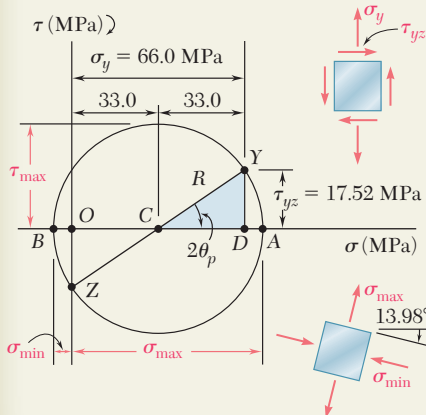
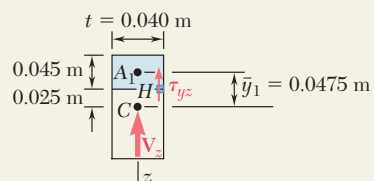
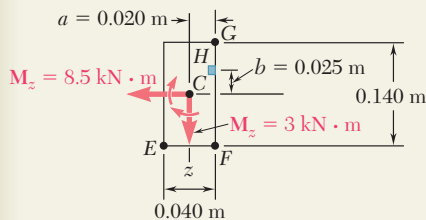
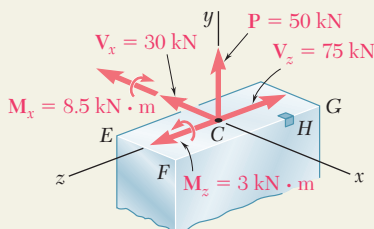
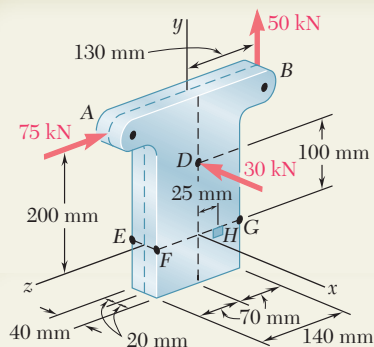
$$Q = \left(\frac{1}{2}\pi c^2\right)\left(\frac{4c}{3\pi}\right) = \frac{2}{3}c^3 = \frac{2}{3}(0.45 \text{ in.})^3 = 60.7 \times 10^{-3} \text{ in}^3$$

$$\tau = \frac{VQ}{It} = \frac{(250 \text{ lb})(60.7 \times 10^{-3} \text{ in}^3)}{(32.2 \times 10^{-3} \text{ in}^4)(0.9 \text{ in.})} = 524 \text{ psi}$$

Stresses Produced by the Bending Couple M_y . Since the bending couple M_y acts in a horizontal plane, it produces no stresses at *H* and *K*. Using Eq. (4.15), we determine the normal stresses at points *J* and *L* and show them in Fig. (c).

$$\sigma = \frac{|M_y|c}{I} = \frac{(625 \text{ lb} \cdot \text{in.})(0.45 \text{ in.})}{32.2 \times 10^{-3} \text{ in}^4} = 8730 \text{ psi}$$

Summary. We add the stresses shown and obtain the total normal and shearing stresses at points *H*, *J*, *K*, and *L*.



SAMPLE PROBLEM 8.5

Three forces are applied as shown at points A, B, and D of a short steel post. Knowing that the horizontal cross section of the post is a 40×140 -mm rectangle, determine the principal stresses, principal planes and maximum shearing stress at point H.

SOLUTION

Internal Forces in Section EFG. We replace the three applied forces by an equivalent force-couple system at the center C of the rectangular section EFG. We have

$$\begin{aligned} V_x &= -30 \text{ kN} & P &= 50 \text{ kN} & V_z &= -75 \text{ kN} \\ M_x &= (50 \text{ kN})(0.130 \text{ m}) - (75 \text{ kN})(0.200 \text{ m}) = -8.5 \text{ kN} \cdot \text{m} \\ M_y &= 0 & M_z &= (30 \text{ kN})(0.100 \text{ m}) = 3 \text{ kN} \cdot \text{m} \end{aligned}$$

We note that there is no twisting couple about the y axis. The geometric properties of the rectangular section are

$$\begin{aligned} A &= (0.040 \text{ m})(0.140 \text{ m}) = 5.6 \times 10^{-3} \text{ m}^2 \\ I_x &= \frac{1}{12}(0.040 \text{ m})(0.140 \text{ m})^3 = 9.15 \times 10^{-6} \text{ m}^4 \\ I_z &= \frac{1}{12}(0.140 \text{ m})(0.040 \text{ m})^3 = 0.747 \times 10^{-6} \text{ m}^4 \end{aligned}$$

Normal Stress at H. We note that normal stresses σ_y are produced by the centric force \mathbf{P} and by the bending couples \mathbf{M}_x and \mathbf{M}_z . We determine the sign of each stress by carefully examining the sketch of the force-couple system at C.

$$\begin{aligned} \sigma_y &= +\frac{P}{A} + \frac{|M_z|a}{I_z} - \frac{|M_x|b}{I_x} \\ &= \frac{50 \text{ kN}}{5.6 \times 10^{-3} \text{ m}^2} + \frac{(3 \text{ kN} \cdot \text{m})(0.020 \text{ m})}{0.747 \times 10^{-6} \text{ m}^4} - \frac{(8.5 \text{ kN} \cdot \text{m})(0.025 \text{ m})}{9.15 \times 10^{-6} \text{ m}^4} \\ \sigma_y &= 8.93 \text{ MPa} + 80.3 \text{ MPa} - 23.2 \text{ MPa} \quad \sigma_y = 66.0 \text{ MPa} \end{aligned}$$

Shearing Stress at H. Considering first the shearing force \mathbf{V}_x , we note that $Q = 0$ with respect to the z axis, since H is on the edge of the cross section. Thus \mathbf{V}_x produces no shearing stress at H. The shearing force \mathbf{V}_z does produce a shearing stress at H and we write

$$\begin{aligned} Q &= A_1 \bar{y}_1 = [(0.040 \text{ m})(0.045 \text{ m})](0.0475 \text{ m}) = 85.5 \times 10^{-6} \text{ m}^3 \\ \tau_{yz} &= \frac{V_z Q}{I_z t} = \frac{(75 \text{ kN})(85.5 \times 10^{-6} \text{ m}^3)}{(9.15 \times 10^{-6} \text{ m}^4)(0.040 \text{ m})} \quad \tau_{yz} = 17.52 \text{ MPa} \end{aligned}$$

Principal Stresses, Principal Planes, and Maximum Shearing Stress at H. We draw Mohr's circle for the stresses at point H

$$\tan 2\theta_p = \frac{17.52}{33.0} \quad 2\theta_p = 27.96^\circ \quad \theta_p = 13.98^\circ$$

$$\begin{aligned} R &= \sqrt{(33.0)^2 + (17.52)^2} = 37.4 \text{ MPa} & \tau_{\max} &= 37.4 \text{ MPa} \\ \sigma_{\max} &= OA = OC + R = 33.0 + 37.4 & \sigma_{\max} &= 70.4 \text{ MPa} \\ \sigma_{\min} &= OB = OC - R = 33.0 - 37.4 & \sigma_{\min} &= -7.4 \text{ MPa} \end{aligned}$$

PROBLEMS

- 8.31** A 6-kip force is applied to the machine element AB as shown. Knowing that the uniform thickness of the element is 0.8 in., determine the normal and shearing stresses at (a) point a , (b) point b , (c) point c .

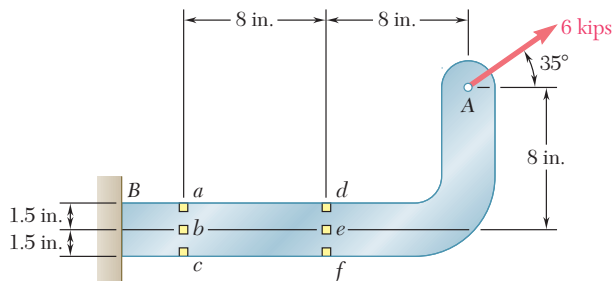


Fig. P8.31 and P8.32

- 8.32** A 6-kip force is applied to the machine element AB as shown. Knowing that the uniform thickness of the element is 0.8 in., determine the normal and shearing stresses at (a) point d , (b) point e , (c) point f .

- 8.33** For the bracket and loading shown, determine the normal and shearing stresses at (a) point a , (b) point b .

- 8.34 through 8.36** Member AB has a uniform rectangular cross section of 10×24 mm. For the loading shown, determine the normal and shearing stresses at (a) point H , (b) point K .

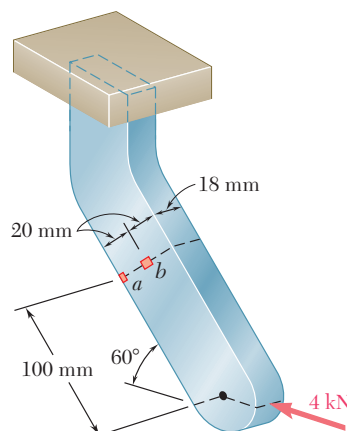


Fig. P8.33

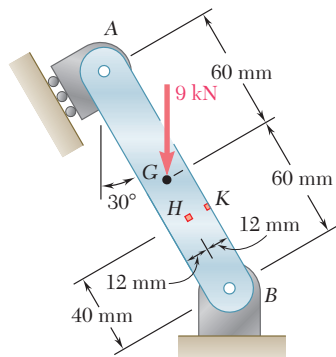


Fig. P8.34

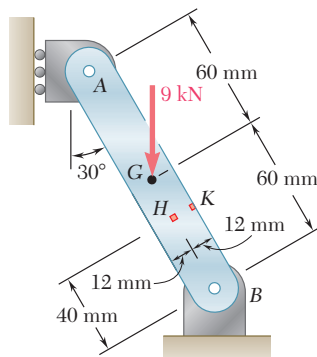


Fig. P8.35

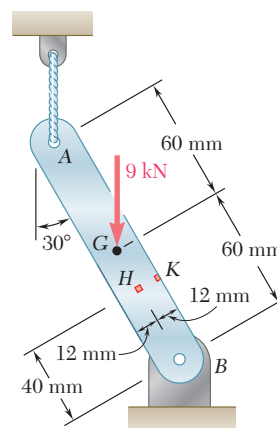


Fig. P8.36

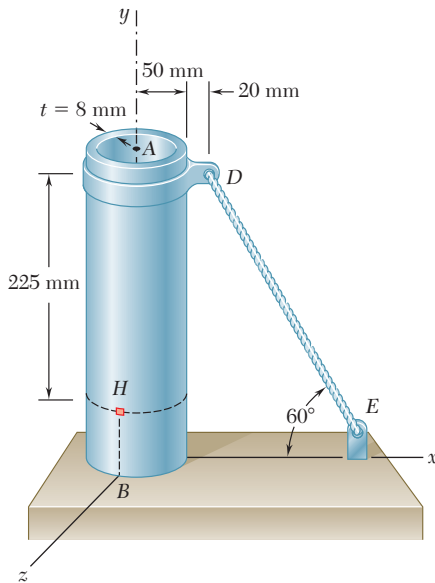


Fig. P8.38

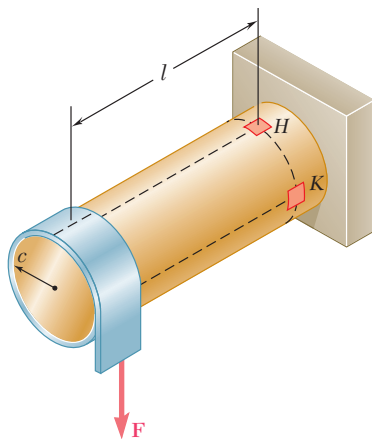


Fig. P8.40

8.37 Several forces are applied to the pipe assembly shown. Knowing that the pipe has inner and outer diameters equal to 1.61 and 1.90 in., respectively, determine the normal and shearing stresses at (a) point H, (b) point K.

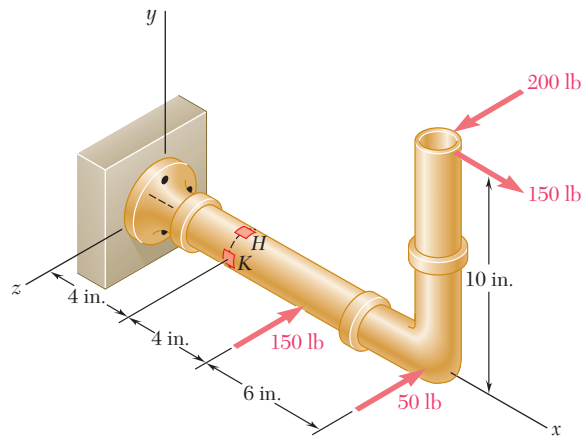


Fig. P8.37

8.38 The steel pile AB has a 100-mm outer diameter and an 8-mm wall thickness. Knowing that the tension in the cable is 40 kN, determine the normal and shearing stresses at point H.

8.39 The billboard shown weighs 8000 lb and is supported by a structural tube that has a 15-in. outer diameter and a 0.5-in. wall thickness. At a time when the resultant of the wind pressure is 3 kips, located at the center C of the billboard, determine the normal and shearing stresses at point H.

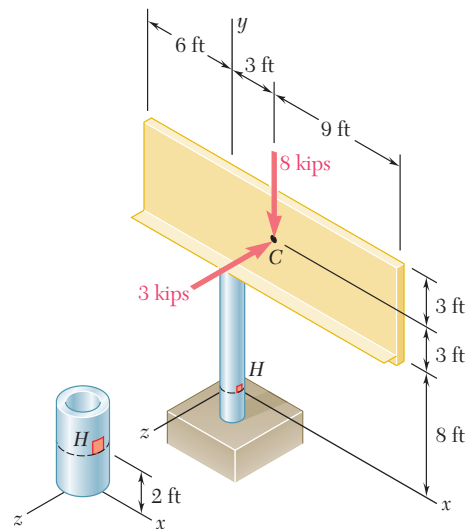


Fig. P8.39

8.40 A thin strap is wrapped around a solid rod of radius $c = 20$ mm as shown. Knowing that $l = 100$ mm and $F = 5$ kN, determine the normal and shearing stresses at (a) point H, (b) point K.

8.41 A vertical force \mathbf{P} of magnitude 60 lb is applied to the crank at point A. Knowing that the shaft BDE has a diameter of 0.75 in., determine the principal stresses and the maximum shearing stress at point H located at the top of the shaft, 2 in. to the right of support D.

8.42 A 13-kN force is applied as shown to the 60-mm-diameter cast-iron post ABD. At point H, determine (a) the principal stresses and principal planes, (b) the maximum shearing stress.

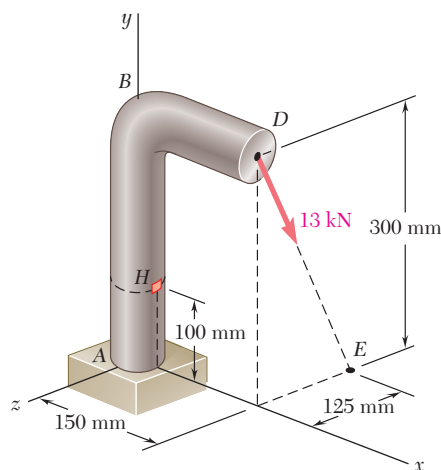


Fig. P8.42

8.43 A 10-kN force and a 1.4-kN · m couple are applied at the top of the 65-mm diameter brass post shown. Determine the principal stresses and maximum shearing stress at (a) point H, (b) point K.

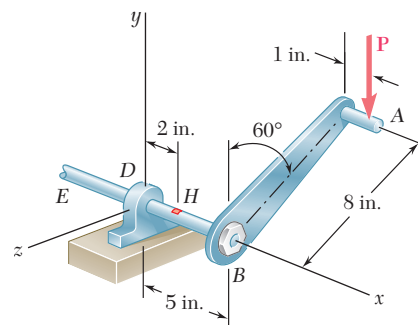


Fig. P8.41

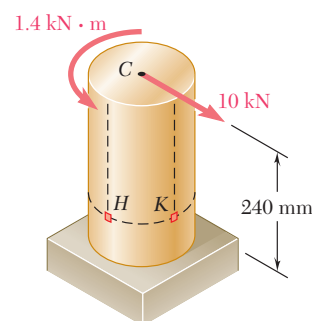


Fig. P8.43

8.44 Forces are applied at points A and B of the solid cast-iron bracket shown. Knowing that the bracket has a diameter of 0.8 in., determine the principal stresses and the maximum shearing stress at (a) point H, (b) point K.

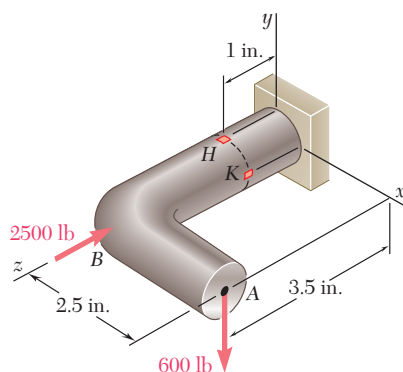


Fig. P8.44

8.45 Three forces are applied to the bar shown. Determine the normal and shearing stresses at (a) point a, (b) point b, (c) point c.

8.46 Solve Prob. 8.45, assuming that $h = 12$ in.

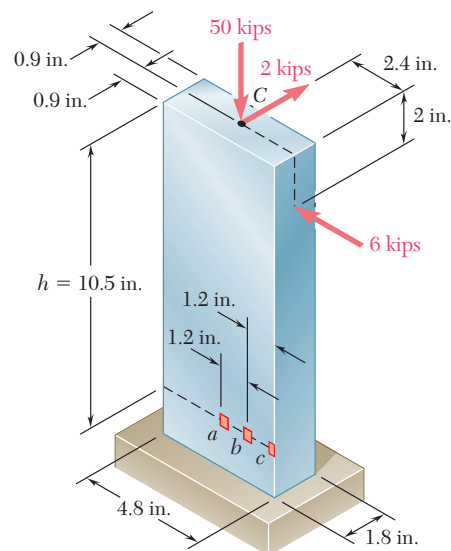


Fig. P8.45

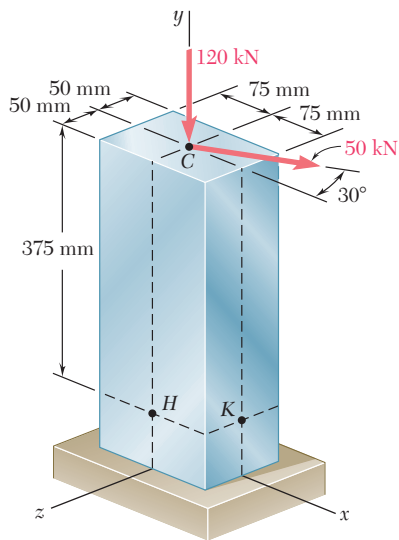


Fig. P8.49 and P8.50

8.47 Three forces are applied to the bar shown. Determine the normal and shearing stresses at (a) point *a*, (b) point *b*, (c) point *c*.

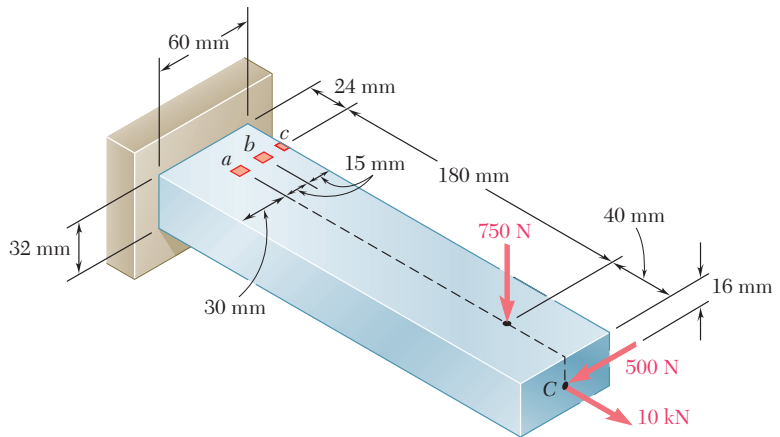


Fig. P8.47

8.48 Solve Prob. 8.47, assuming that the 750-N force is directed vertically upward.

8.49 For the post and loading shown, determine the principal stresses, principal planes, and maximum shearing stress at point *H*.

8.50 For the post and loading shown, determine the principal stresses, principal planes, and maximum shearing stress at point *K*.

8.51 Two forces are applied to the small post *BD* as shown. Knowing that the vertical portion of the post has a cross section of 1.5×2.4 in., determine the principal stresses, principal planes, and maximum shearing stress at point *H*.

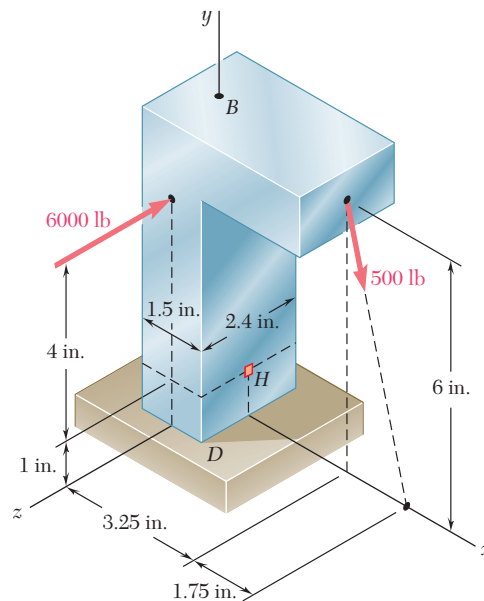


Fig. P8.51

8.52 Solve Prob. 8.51, assuming that the magnitude of the 6000-lb force is reduced to 1500 lb.

8.53 Three steel plates, each 13 mm thick, are welded together to form a cantilever beam. For the loading shown, determine the normal and shearing stresses at points a and b .

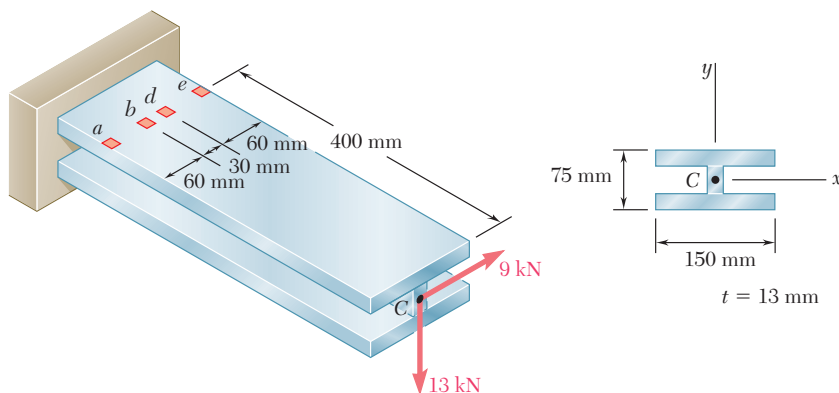


Fig. P8.53 and P8.54

8.54 Three steel plates, each 13 mm thick, are welded together to form a cantilever beam. For the loading shown, determine the normal and shearing stresses at points d and e .

8.55 Two forces are applied to a $W8 \times 28$ rolled-steel beam as shown. Determine the principal stresses and maximum shearing stress at point a .

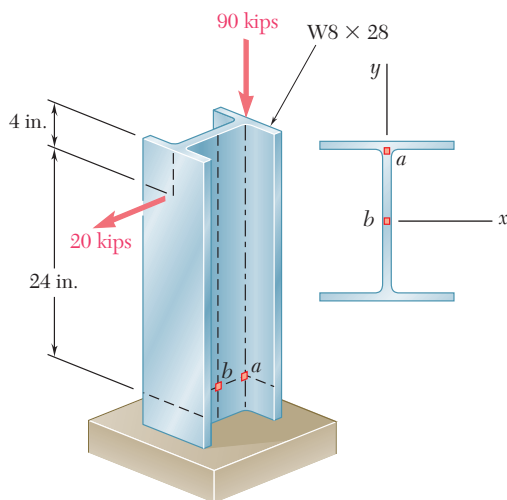


Fig. P8.55 and P8.56

8.56 Two forces are applied to a $W8 \times 28$ rolled-steel beam as shown. Determine the principal stresses and maximum shearing stress at point b .

- 8.57** Two forces \mathbf{P}_1 and \mathbf{P}_2 are applied as shown in directions perpendicular to the longitudinal axis of a W310 \times 60 beam. Knowing that $\mathbf{P}_1 = 25$ kN and $\mathbf{P}_2 = 24$ kN, determine the principal stresses and the maximum shearing stress at point a .

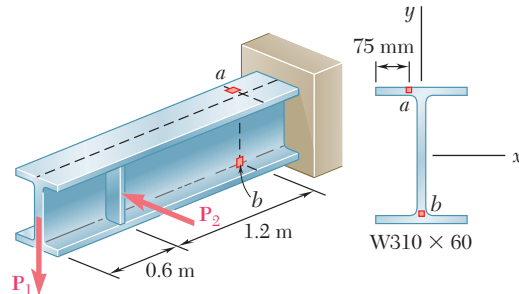


Fig. P8.57 and P8.58

- 8.58** Two forces \mathbf{P}_1 and \mathbf{P}_2 are applied as shown in directions perpendicular to the longitudinal axis of a W310 \times 60 beam. Knowing that $\mathbf{P}_1 = 25$ kN and $\mathbf{P}_2 = 24$ kN, determine the principal stresses and the maximum shearing stress at point b .

- 8.59** A vertical force \mathbf{P} is applied at the center of the free end of cantilever beam AB . (a) If the beam is installed with the web vertical ($\beta = 0$) and with its longitudinal axis AB horizontal, determine the magnitude of the force \mathbf{P} for which the normal stress at point a is $+120$ MPa. (b) Solve part a , assuming that the beam is installed with $\beta = 3^\circ$.

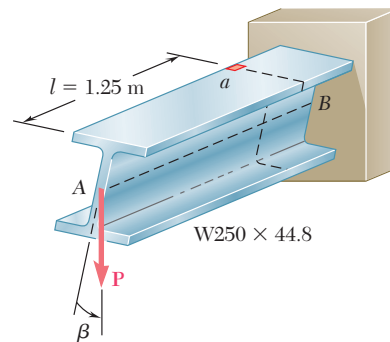


Fig. P8.59

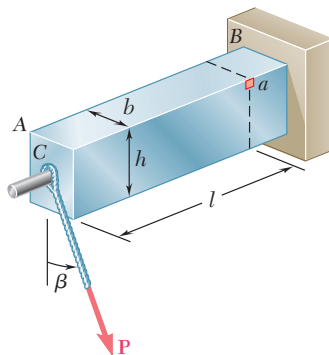


Fig. P8.60

- 8.60** A force \mathbf{P} is applied to a cantilever beam by means of a cable attached to a bolt located at the center of the free end of the beam. Knowing that \mathbf{P} acts in a direction perpendicular to the longitudinal axis of the beam, determine (a) the normal stress at point a in terms of P , b , h , l , and β , (b) the values of β for which the normal stress at a is zero.

- *8.61** A 5-kN force \mathbf{P} is applied to a wire that is wrapped around bar AB as shown. Knowing that the cross section of the bar is a square of side $d = 40$ mm, determine the principal stresses and the maximum shearing stress at point a .

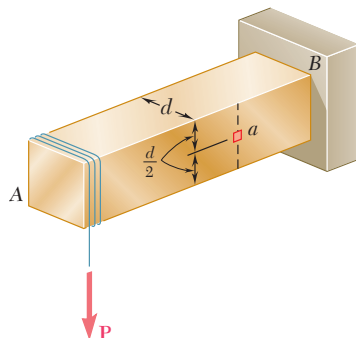


Fig. P8.61

- *8.62** Knowing that the structural tube shown has a uniform wall thickness of 0.3 in., determine the principal stresses, principal planes, and maximum shearing stress at (a) point H , (b) point K .

- *8.63** The structural tube shown has a uniform wall thickness of 0.3 in. Knowing that the 15-kip load is applied 0.15 in. above the base of the tube, determine the shearing stress at (a) point a , (b) point b .

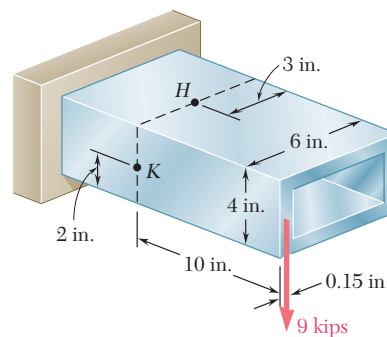


Fig. P8.62

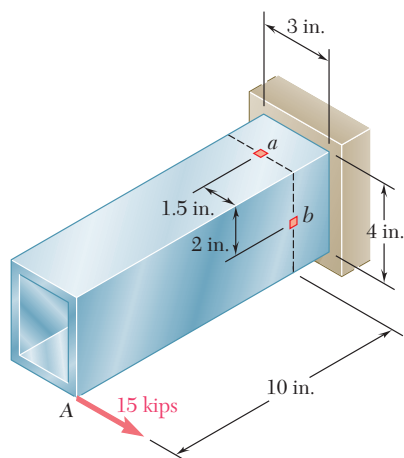


Fig. P8.63

- *8.64** For the tube and loading of Prob. 8.63, determine the principal stresses and the maximum shearing stress at point b .

REVIEW AND SUMMARY

This chapter was devoted to the determination of the principal stresses in beams, transmission shafts, and bodies of arbitrary shape subjected to combined loadings.

We first recalled in Sec. 8.2 the two fundamental relations derived in Chaps. 5 and 6 for the normal stress σ_x and the shearing stress τ_{xy} at any given point of a cross section of a prismatic beam,

$$\sigma_x = -\frac{My}{I} \quad \tau_{xy} = -\frac{VQ}{It} \quad (8.1, 8.2)$$

where V = shear in the section

M = bending moment in the section

y = distance of the point from the neutral surface

I = centroidal moment of inertia of the cross section

Q = first moment about the neutral axis of the portion of the cross section located above the given point

t = width of the cross section at the given point

Principal planes and principal stresses in a beam

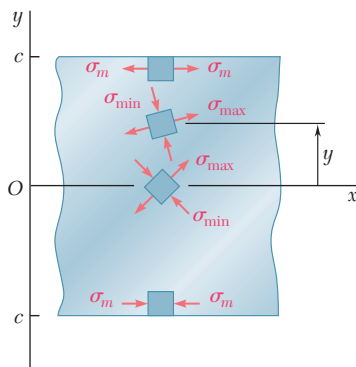


Fig. 8.28

Using one of the methods presented in Chap. 7 for the transformation of stresses, we were able to obtain the principal planes and principal stresses at the given point (Fig. 8.28).

We investigated the distribution of the principal stresses in a narrow rectangular cantilever beam subjected to a concentrated load P at its free end and found that in any given transverse section—except close to the point of application of the load—the maximum principal stress σ_{\max} did not exceed the maximum normal stress σ_m occurring at the surface of the beam.

While this conclusion remains valid for many beams of non-rectangular cross section, it may not hold for W-beams or S-beams, where σ_{\max} at the junctions b and d of the web with the flanges of the beam (Fig. 8.29) may exceed the value of σ_m occurring at points a and e . Therefore, the design of a rolled-steel beam should include the computation of the maximum principal stress at these points. (See Sample Probs. 8.1 and 8.2.)

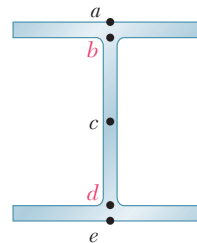


Fig. 8.29

In Sec. 8.3, we considered the design of *transmission shafts* subjected to *transverse loads* as well as to torques. Taking into account the effect of both the normal stresses due to the bending moment M and the shearing stresses due to the torque T in any given transverse section of a cylindrical shaft (either solid or hollow), we found that the minimum allowable value of the ratio J/c for the cross section was

$$\frac{J}{c} = \frac{(\sqrt{M^2 + T^2})_{\max}}{\tau_{\text{all}}} \quad (8.6)$$

In preceding chapters, you learned to determine the stresses in prismatic members caused by axial loadings (Chaps. 1 and 2), torsion (Chap. 3), bending (Chap. 4), and transverse loadings (Chaps. 5 and 6). In the second part of this chapter (Sec. 8.4), we combined this knowledge to determine stresses under more general loading conditions.

Design of transmission shafts under transverse loads

Stresses under general loading conditions

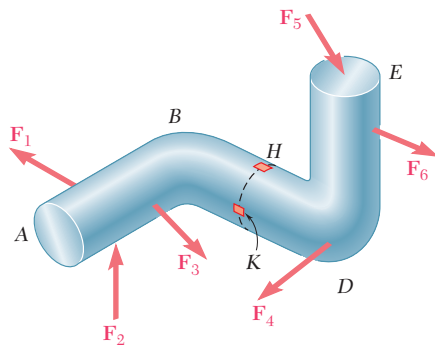


Fig. 8.30

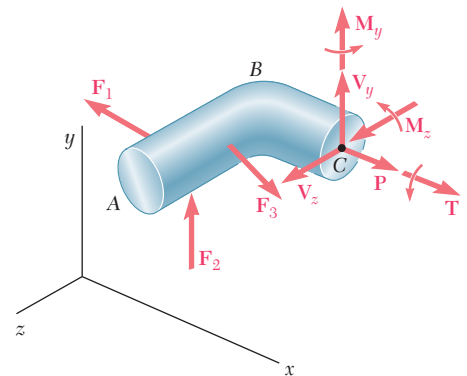


Fig. 8.31

For instance, to determine the stresses at point H or K of the bent member shown in Fig. 8.30, we passed a section through these points and replaced the applied loads by an equivalent force-couple system at the centroid C of the section (Fig. 8.31). The normal and shearing stresses produced at H or K by each of the forces and couples applied at C were determined and then combined to obtain the resulting normal stress σ_x and the resulting shearing stresses τ_{xy} and τ_{xz} at H or K . Finally, the principal stresses, the orientation of the principal planes, and the maximum shearing stress at point H or K were determined by one of the methods presented in Chap. 7 from the values obtained for σ_x , τ_{xy} , and τ_{xz} .

REVIEW PROBLEMS

- 8.65** (a) Knowing that $\sigma_{\text{all}} = 24$ ksi and $\tau_{\text{all}} = 14.5$ ksi, select the most economical wide-flange shape that should be used to support the loading shown. (b) Determine the values to be expected for σ_m , τ_m , and the principal stress σ_{max} at the junction of a flange and the web of the selected beam.

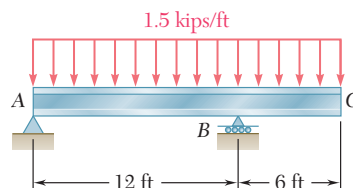


Fig. P8.65

- 8.66** Determine the smallest allowable diameter of the solid shaft ABCD, knowing that $\tau_{\text{all}} = 60$ MPa and that the radius of disk B is $r = 80$ mm.

- 8.67** Using the notation of Sec. 8.3 and neglecting the effect of shear stresses caused by transverse loads, show that the maximum normal stress in a circular shaft can be expressed as follows:

$$\sigma_{\text{max}} = \frac{C}{J} [(M_y^2 + M_z^2)^{\frac{1}{2}} + (M_y^2 + M_z^2 + T^2)^{\frac{1}{2}}]_{\text{max}}$$

- 8.68** The solid shaft AB rotates at 450 rpm and transmits 20 kW from the motor M to machine tools connected to gears F and G. Knowing that $\tau_{\text{all}} = 55$ MPa and assuming that 8 kW is taken off at gear F and 12 kW is taken off at gear G, determine the smallest permissible diameter of shaft AB.

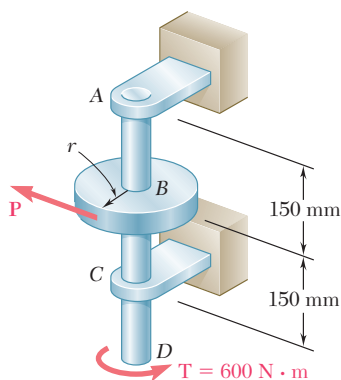


Fig. P8.66

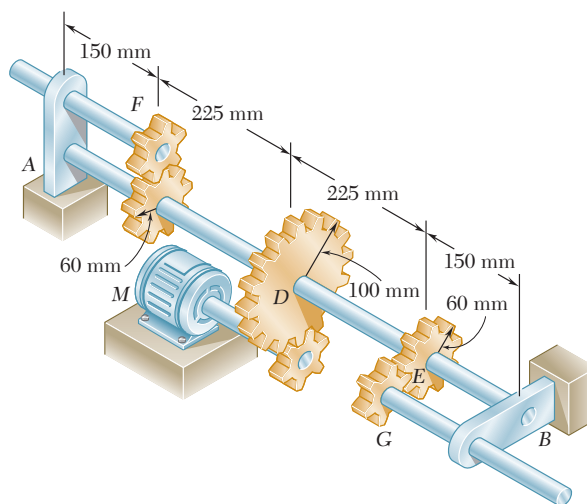


Fig. P8.68

- 8.69** Two 1.2-kip forces are applied to an L-shaped machine element AB as shown. Determine the normal and shearing stresses at (a) point a , (b) point b , (c) point c .

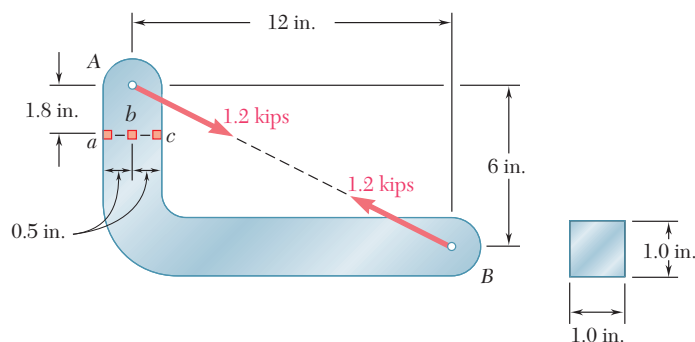


Fig. P8.69

- 8.70** Two forces are applied to the pipe AB as shown. Knowing that the pipe has inner and outer diameters equal to 35 and 42 mm, respectively, determine the normal and shearing stresses at (a) point a , (b) point b .

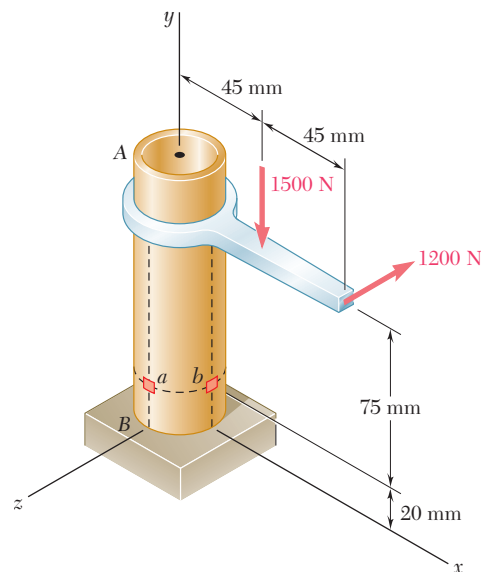


Fig. P8.70

- 8.71** A close-coiled spring is made of a circular wire of radius r that is formed into a helix of radius R . Determine the maximum shearing stress produced by the two equal and opposite forces \mathbf{P} and \mathbf{P}' . (Hint: First determine the shear \mathbf{V} and the torque \mathbf{T} in a transverse cross section.)

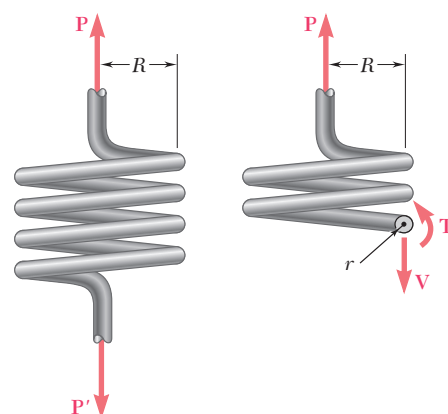


Fig. P8.71

- 8.72** Three forces are applied to a 4-in.-diameter plate that is attached to the solid 1.8-in. diameter shaft AB . At point H , determine (a) the principal stresses and principal planes, (b) the maximum shearing stress.

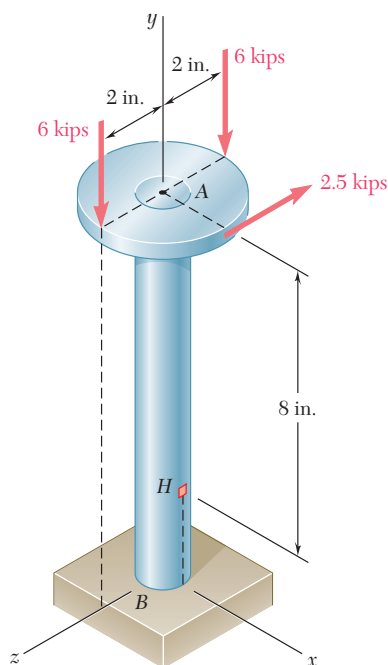


Fig. P8.72

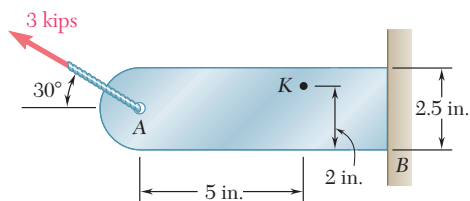


Fig. P8.73

8.73 Knowing that the bracket AB has a uniform thickness of $\frac{5}{8}$ in., determine (a) the principal planes and principal stresses at point K , (b) the maximum shearing stress at point K .

8.74 Three forces are applied to the machine component ABD as shown. Knowing that the cross section containing point H is a 20×40 -mm rectangle, determine the principal stresses and the maximum shearing stress at point H .

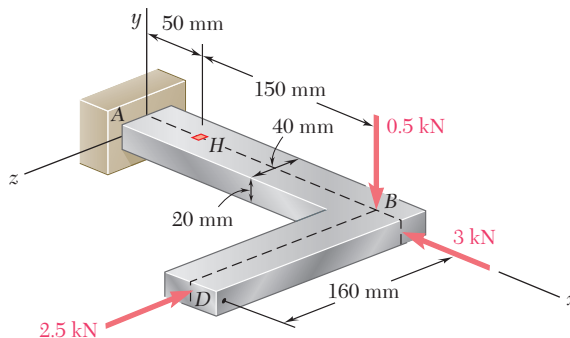


Fig. P8.74

8.75 Knowing that the structural tube shown has a uniform wall thickness of 0.25 in., determine the normal and shearing stresses at the three points indicated.

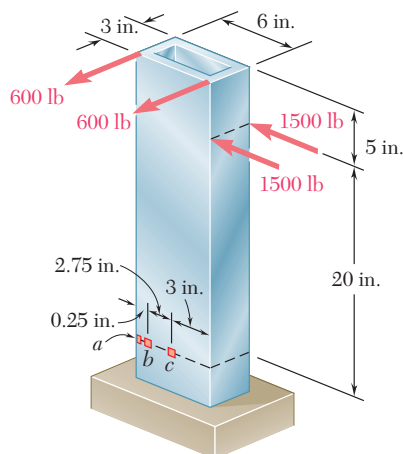


Fig. P8.75

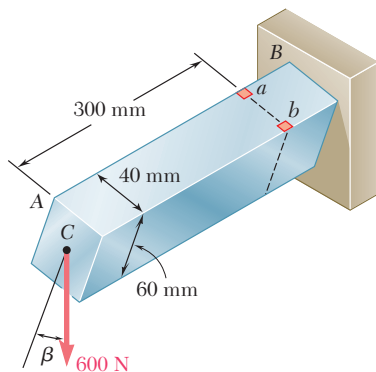


Fig. P8.76

8.76 The cantilever beam AB will be installed so that the 60-mm side forms an angle β between 0 and 90° with the vertical. Knowing that the 600-N vertical force is applied at the center of the free end of the beam, determine the normal stress at point a when (a) $\beta = 0$, (b) $\beta = 90^\circ$. (c) Also, determine the value of β for which the normal stress at point a is a maximum and the corresponding value of that stress.

COMPUTER PROBLEMS

The following problems are designed to be solved with a computer.

8.C1 Let us assume that the shear V and the bending moment M have been determined in a given section of a rolled-steel beam. Write a computer program to calculate in that section, from the data available in Appendix C, (a) the maximum normal stress σ_m , (b) the principal stress σ_{\max} at the junction of a flange and the web. Use this program to solve parts *a* and *b* of the following problems:

- (1) Prob. 8.1 (Use $V = 45$ kips and $M = 450$ kip \cdot in.)
- (2) Prob. 8.2 (Use $V = 22.5$ kips and $M = 450$ kip \cdot in.)
- (3) Prob. 8.3 (Use $V = 700$ kN and $M = 1750$ kN \cdot m)
- (4) Prob. 8.4 (Use $V = 850$ kN and $M = 1700$ kN \cdot m)

8.C2 A cantilever beam AB with a rectangular cross section of width b and depth $2c$ supports a single concentrated load P at its end A . Write a computer program to calculate, for any values of x/c and y/c , (a) the ratios σ_{\max}/σ_m and σ_{\min}/σ_m , where σ_{\max} and σ_{\min} are the principal stresses at point $K(x, y)$ and σ_m the maximum normal stress in the same transverse section, (b) the angle θ_p that the principal planes at K form with a transverse and a horizontal plane through K . Use this program to check the values shown in Fig. 8.8 and to verify that σ_{\max} exceeds σ_m if $x \leq 0.544c$, as indicated in the second footnote on page 517.

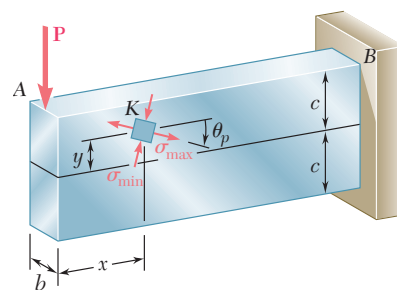


Fig. P8.C2

8.C3 Disks D_1, D_2, \dots, D_n are attached as shown in Fig. 8.C3 to the solid shaft AB of length L , uniform diameter d , and allowable shearing stress τ_{all} . Forces P_1, P_2, \dots, P_n of known magnitude (except for one of them) are applied to the disks, either at the top or bottom of its vertical diameter, or at the left or right end of its horizontal diameter. Denoting by r_i the radius of disk D_i and by c_i its distance from the support at A , write a computer program to calculate (a) the magnitude of the unknown force P_i , (b) the smallest permissible value of the diameter d of shaft AB . Use this program to solve Prob. 8.18.

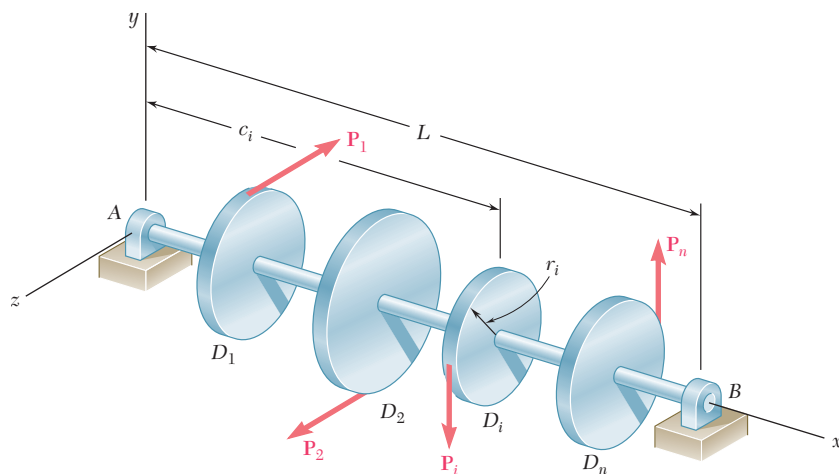


Fig. P8.C3

8.C4 The solid shaft AB of length L , uniform diameter d , and allowable shearing stress τ_{all} rotates at a given speed expressed in rpm (Fig. 8.C4). Gears G_1, G_2, \dots, G_n are attached to the shaft and each of these gears meshes with another gear (not shown), either at the top or bottom of its vertical diameter, or at the left or right end of its horizontal diameter. One of these gears is connected to a motor and the rest of them to various machine tools. Denoting by r_i the radius of disk G_i , by c_i its distance from the support at A , and by P_i the power transmitted to that gear (+ sign) or taken off that gear (− sign), write a computer program to calculate the smallest permissible value of the diameter d of shaft AB . Use this program to solve Probs. 8.27 and 8.68.

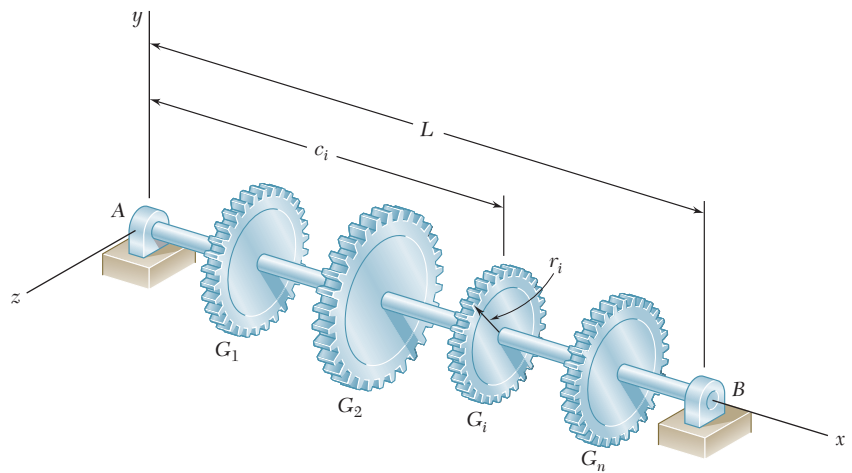


Fig. P8.C4

8.C5 Write a computer program that can be used to calculate the normal and shearing stresses at points with given coordinates y and z located on the surface of a machine part having a rectangular cross section. The internal forces are known to be equivalent to the force-couple system shown. Write the program so that the loads and dimensions can be expressed in either SI or U.S. customary units. Use this program to solve (a) Prob. 8.45b, (b) Prob. 8.47a.

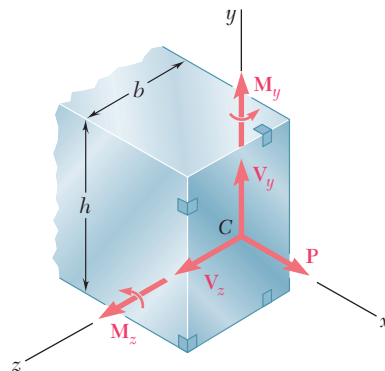


Fig. P8.C5

8.C6 Member AB has a rectangular cross section of 10×24 mm. For the loading shown, write a computer program that can be used to determine the normal and shearing stresses at points H and K for values of d from 0 to 120 mm, using 15-mm increments. Use this program to solve Prob. 8.35.

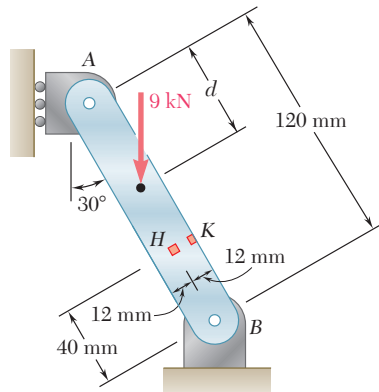


Fig. P8.C6

***8.C7** The structural tube shown has a uniform wall thickness of 0.3 in. A 9-kip force is applied at a bar (not shown) that is welded to the end of the tube. Write a computer program that can be used to determine, for any given value of c , the principal stresses, principal planes, and maximum shearing stress at point H for values of d from -3 in. to 3 in., using one-inch increments. Use this program to solve Prob. 8.62a.

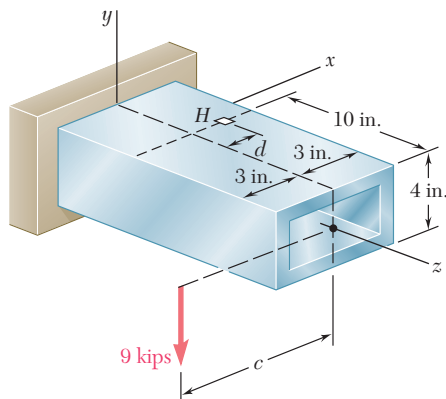


Fig. P8.C7

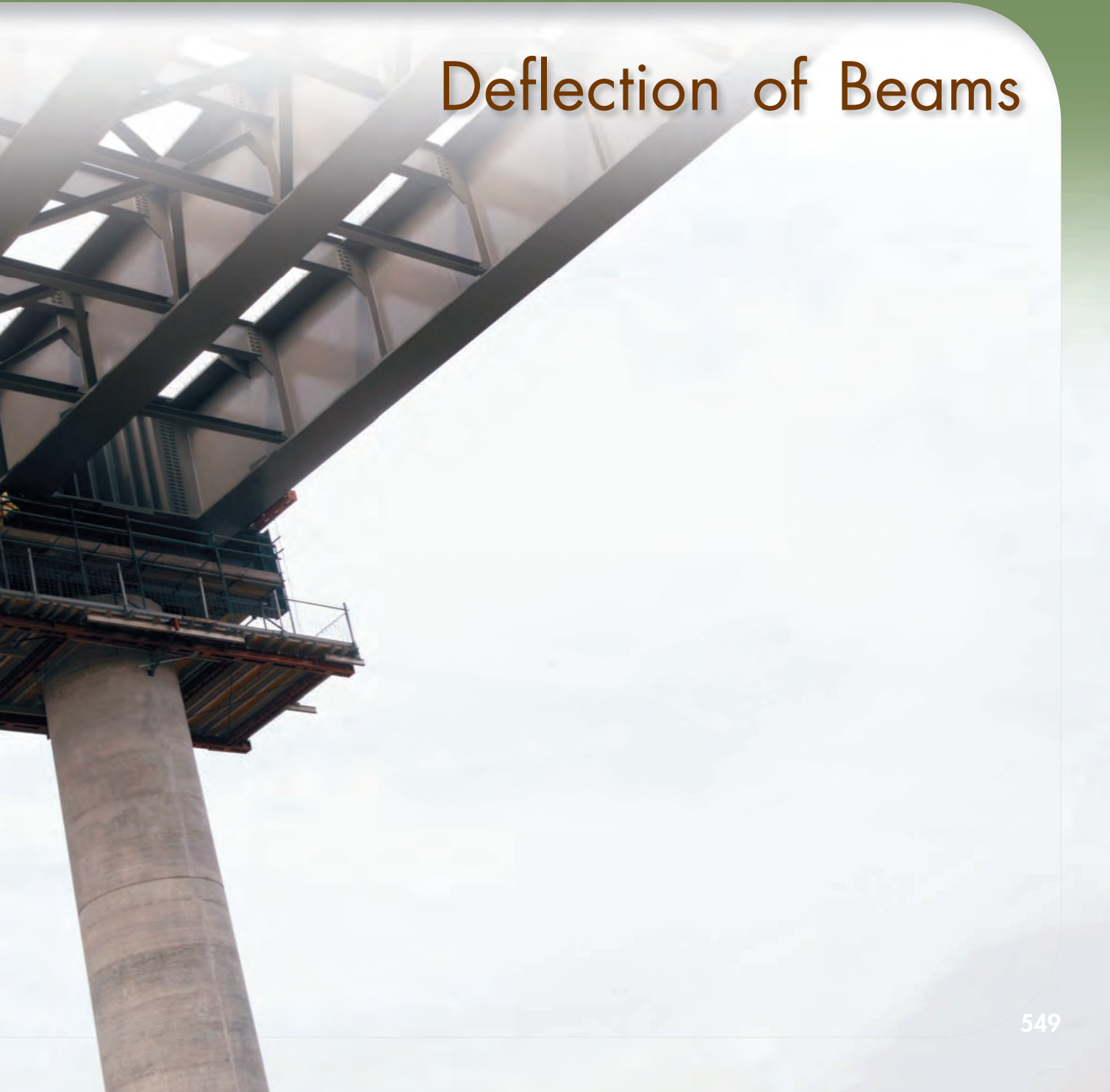
The photo shows a multiple-girder bridge during construction. The design of the steel girders is based on both strength considerations and deflection evaluations.



C H A P T E R

9

Deflection of Beams



Chapter 9 Deflection of Beams

- 9.1 Introduction
- 9.2 Deformation of a Beam under Transverse Loading
- 9.3 Equation of the Elastic Curve
- *9.4 Direct Determination of the Elastic Curve from the Load Distribution
- 9.5 Statically Indeterminate Beams
- *9.6 Using Singularity Functions to Determine the Slope and Deflection of a Beam
- 9.7 Method of Superposition
- 9.8 Application of Superposition to Statically Indeterminate Beams
- *9.9 Moment-Area Theorems
- *9.10 Application to Cantilever Beams and Beams with Symmetric Loadings
- *9.11 Bending-Moment Diagrams by Parts
- *9.12 Application of Moment-Area Theorems to Beams with Unsymmetric Loadings
- *9.13 Maximum Deflection
- *9.14 Use of Moment-Area Theorems with Statically Indeterminate Beams

9.1 INTRODUCTION

In the preceding chapter we learned to design beams for strength. In this chapter we will be concerned with another aspect in the design of beams, namely, the determination of the *deflection*. Of particular interest is the determination of the *maximum deflection* of a beam under a given loading, since the design specifications of a beam will generally include a maximum allowable value for its deflection. Also of interest is that a knowledge of the deflections is required to analyze *indeterminate beams*. These are beams in which the number of reactions at the supports exceeds the number of equilibrium equations available to determine these unknowns.

We saw in Sec. 4.4 that a prismatic beam subjected to pure bending is bent into an arc of circle and that, within the elastic range, the curvature of the neutral surface can be expressed as

$$\frac{1}{\rho} = \frac{M}{EI} \quad (4.21)$$

where M is the bending moment, E the modulus of elasticity, and I the moment of inertia of the cross section about its neutral axis.

When a beam is subjected to a transverse loading, Eq. (4.21) remains valid for any given transverse section, provided that Saint-Venant's principle applies. However, both the bending moment and the curvature of the neutral surface will vary from section to section. Denoting by x the distance of the section from the left end of the beam, we write

$$\frac{1}{\rho} = \frac{M(x)}{EI} \quad (9.1)$$

The knowledge of the curvature at various points of the beam will enable us to draw some general conclusions regarding the deformation of the beam under loading (Sec. 9.2).

To determine the slope and deflection of the beam at any given point, we first derive the following second-order linear differential equation, which governs the *elastic curve* characterizing the shape of the deformed beam (Sec. 9.3):

$$\frac{d^2y}{dx^2} = \frac{M(x)}{EI}$$

If the bending moment can be represented for all values of x by a single function $M(x)$, as in the case of the beams and loadings shown in Fig. 9.1, the slope $\theta = dy/dx$ and the deflection y at any point of the beam may be obtained through two successive integrations. The two constants of integration introduced in the process will be determined from the boundary conditions indicated in the figure.

However, if different analytical functions are required to represent the bending moment in various portions of the beam, different differential equations will also be required, leading to

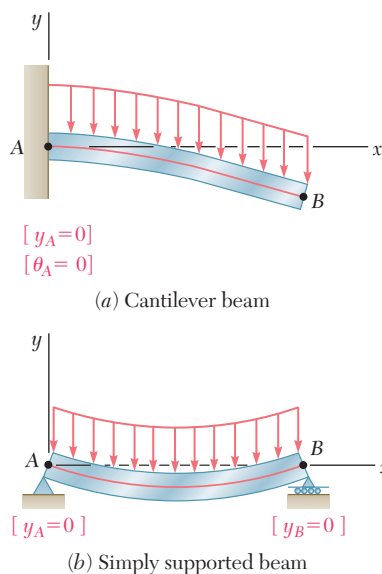


Fig. 9.1 Situations where bending moment can be given by a single function $M(x)$.

different functions defining the elastic curve in the various portions of the beam. In the case of the beam and loading of Fig. 9.2, for example, two differential equations are required, one for the portion of beam AD and the other for the portion DB . The first equation yields the functions θ_1 and y_1 , and the second the functions θ_2 and y_2 . Altogether, four constants of integration must be determined; two will be obtained by writing that the deflection is zero at A and B , and the other two by expressing that the portions of beam AD and DB have the same slope and the same deflection at D .

You will observe in Sec. 9.4 that in the case of a beam supporting a distributed load $w(x)$, the elastic curve can be obtained directly from $w(x)$ through four successive integrations. The constants introduced in this process will be determined from the boundary values of V , M , θ , and y .

In Sec. 9.5, we will discuss *statically indeterminate beams* where the reactions at the supports involve four or more unknowns. The three equilibrium equations must be supplemented with equations obtained from the boundary conditions imposed by the supports.

The method described earlier for the determination of the elastic curve when several functions are required to represent the bending moment M can be quite laborious, since it requires matching slopes and deflections at every transition point. You will see in Sec. 9.6 that the use of *singularity functions* (previously discussed in Sec. 5.5) considerably simplifies the determination of θ and y at any point of the beam.

The next part of the chapter (Secs. 9.7 and 9.8) is devoted to the *method of superposition*, which consists of determining separately, and then adding, the slope and deflection caused by the various loads applied to a beam. This procedure can be facilitated by the use of the table in Appendix D, which gives the slopes and deflections of beams for various loadings and types of support.

In Sec. 9.9, certain geometric properties of the elastic curve will be used to determine the deflection and slope of a beam at a given point. Instead of expressing the bending moment as a function $M(x)$ and integrating this function analytically, the diagram representing the variation of M/EI over the length of the beam will be drawn and two moment-area theorems will be derived. The *first moment-area theorem* will enable us to calculate the angle between the tangents to the beam at two points; the *second moment-area theorem* will be used to calculate the vertical distance from a point on the beam to a tangent at a second point.

The moment-area theorems will be used in Sec. 9.10 to determine the slope and deflection at selected points of cantilever beams and beams with symmetric loadings. In Sec. 9.11 you will find that in many cases the areas and moments of areas defined by the M/EI diagram may be more easily determined if you draw the *bending-moment diagram by parts*. As you study the moment-area method, you will observe that this method is particularly effective in the case of *beams of variable cross section*.

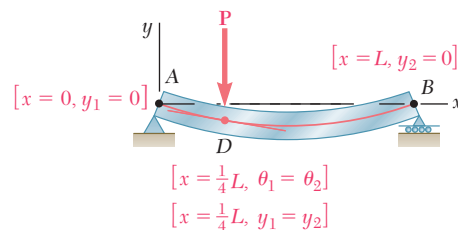


Fig. 9.2 Situation where two sets of equations are required.

Beams with unsymmetric loadings and overhanging beams will be considered in Sec. 9.12. Since for an unsymmetric loading the maximum deflection does not occur at the center of a beam, you will learn in Sec. 9.13 how to locate the point where the tangent is horizontal in order to determine the *maximum deflection*. Section 9.14 will be devoted to the solution of problems involving *statically indeterminate beams*.

9.2 DEFORMATION OF A BEAM UNDER TRANSVERSE LOADING

At the beginning of this chapter, we recalled Eq. (4.21) of Sec. 4.4, which relates the curvature of the neutral surface and the bending moment in a beam in pure bending. We pointed out that this equation remains valid for any given transverse section of a beam subjected to a transverse loading, provided that Saint-Venant's principle applies. However, both the bending moment and the curvature of the neutral surface will vary from section to section. Denoting by x the distance of the section from the left end of the beam, we write

$$\frac{1}{\rho} = \frac{M(x)}{EI} \quad (9.1)$$

Consider, for example, a cantilever beam AB of length L subjected to a concentrated load \mathbf{P} at its free end A (Fig. 9.3a). We have $M(x) = -Px$ and, substituting into (9.1),

$$\frac{1}{\rho} = -\frac{Px}{EI}$$

which shows that the curvature of the neutral surface varies linearly with x , from zero at A , where ρ_A itself is infinite, to $-PL/EI$ at B , where $|\rho_B| = EI/PL$ (Fig. 9.3b).

Consider now the overhanging beam AD of Fig. 9.4a that supports two concentrated loads as shown. From the free-body diagram of the beam (Fig. 9.4b), we find that the reactions at the supports are $R_A = 1 \text{ kN}$ and $R_C = 5 \text{ kN}$, respectively, and draw the corresponding bending-moment diagram (Fig. 9.5a). We note from the diagram that M , and thus the curvature of the beam, are both zero at each end of the beam, and also at a point E located at $x = 4 \text{ m}$. Between A and E the bending moment is positive and the beam is concave upward;

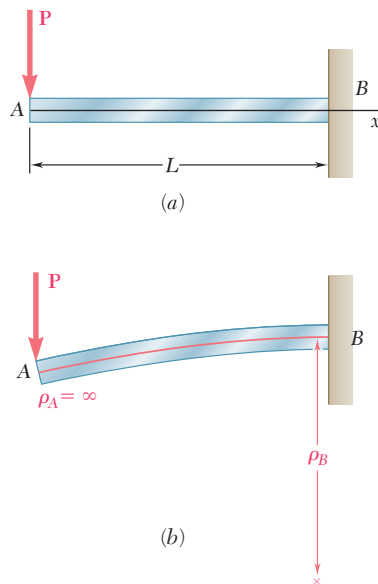


Fig. 9.3 Cantilever beam with concentrated load.

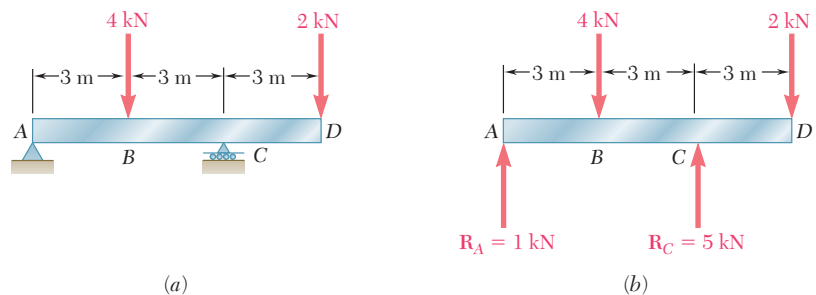


Fig. 9.4 Overhanging beam with two concentrated loads.

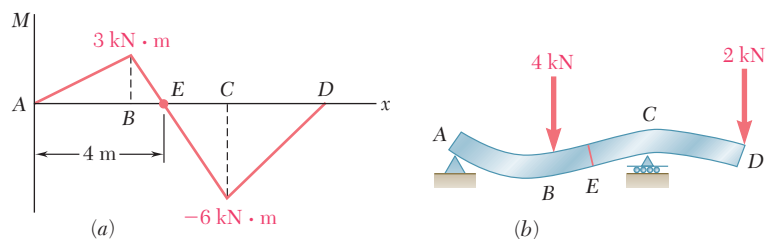


Fig. 9.5 Moment-curvature relationship for beam of Fig. 9.4.

between E and D the bending moment is negative and the beam is concave downward (Fig. 9.5b). We also note that the largest value of the curvature (i.e., the smallest value of the radius of curvature) occurs at the support C , where $|M|$ is maximum.

From the information obtained on its curvature, we get a fairly good idea of the shape of the deformed beam. However, the analysis and design of a beam usually require more precise information on the *deflection* and the *slope* of the beam at various points. Of particular importance is the knowledge of the *maximum deflection* of the beam. In the next section Eq. (9.1) will be used to obtain a relation between the deflection y measured at a given point Q on the axis of the beam and the distance x of that point from some fixed origin (Fig. 9.6). The relation obtained is the equation of the *elastic curve*, i.e., the equation of the curve into which the axis of the beam is transformed under the given loading (Fig. 9.6b).†

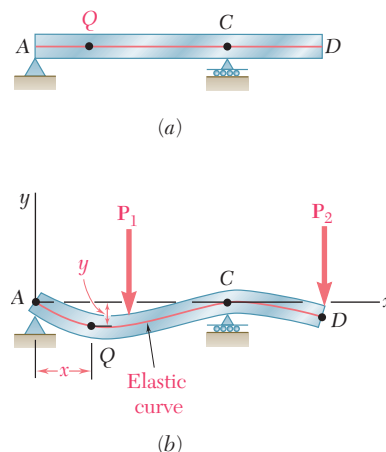


Fig. 9.6 Elastic curve for beam of Fig. 9.4.

9.3 EQUATION OF THE ELASTIC CURVE

We first recall from elementary calculus that the curvature of a plane curve at a point $Q(x, y)$ of the curve can be expressed as

$$\frac{1}{\rho} = \frac{\frac{d^2y}{dx^2}}{\left[1 + \left(\frac{dy}{dx}\right)^2\right]^{3/2}} \quad (9.2)$$

where dy/dx and d^2y/dx^2 are the first and second derivatives of the function $y(x)$ represented by that curve. But, in the case of the elastic curve of a beam, the slope dy/dx is very small, and its square is negligible compared to unity. We write, therefore,

$$\frac{1}{\rho} = \frac{d^2y}{dx^2} \quad (9.3)$$

Substituting for $1/\rho$ from (9.3) into (9.1), we have

$$\frac{d^2y}{dx^2} = \frac{M(x)}{EI} \quad (9.4)$$

†It should be noted that, in this chapter, y represents a vertical displacement, while it was used in previous chapters to represent the distance of a given point in a transverse section from the neutral axis of that section.

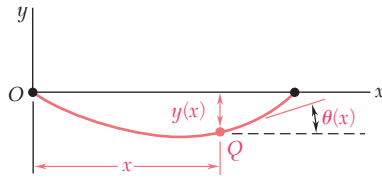


Fig. 9.7 Slope $\theta(x)$ of tangent to the elastic curve.

The equation obtained is a second-order linear differential equation; it is the governing differential equation for the elastic curve.

The product EI is known as the *flexural rigidity* and, if it varies along the beam, as in the case of a beam of varying depth, we must express it as a function of x before proceeding to integrate Eq. (9.4). However, in the case of a prismatic beam, which is the case considered here, the flexural rigidity is constant. We may thus multiply both members of Eq. (8.4) by EI and integrate in x . We write

$$EI \frac{dy}{dx} = \int_0^x M(x) dx + C_1 \quad (9.5)$$

where C_1 is a constant of integration. Denoting by $\theta(x)$ the angle, measured in radians, that the tangent to the elastic curve at Q forms with the horizontal (Fig. 9.7), and recalling that this angle is very small, we have

$$\frac{dy}{dx} = \tan \theta \approx \theta(x)$$

Thus, we write Eq. (9.5) in the alternative form

$$EI \theta(x) = \int_0^x M(x) dx + C_1 \quad (9.5')$$

Integrating both members of Eq. (9.5) in x , we have

$$\begin{aligned} EI y &= \int_0^x \left[\int_0^x M(x) dx + C_1 \right] dx + C_2 \\ EI y &= \int_0^x dx \int_0^x M(x) dx + C_1 x + C_2 \end{aligned} \quad (9.6)$$

where C_2 is a second constant, and where the first term in the right-hand member represents the function of x obtained by integrating twice in x the bending moment $M(x)$. If it were not for the fact that the constants C_1 and C_2 are as yet undetermined, Eq. (9.6) would define the deflection of the beam at any given point Q , and Eq. (9.5) or (9.5') would similarly define the slope of the beam at Q .

The constants C_1 and C_2 are determined from the *boundary conditions* or, more precisely, from the conditions imposed on the beam by its supports. Limiting our analysis in this section to *statically determinate beams*, i.e., to beams supported in such a way that the reactions at the supports can be obtained by the methods of statics, we note that only three types of beams need to be considered here (Fig. 9.8): (a) the *simply supported beam*, (b) the *overhanging beam*, and (c) the *cantilever beam*.

In the first two cases, the supports consist of a pin and bracket at A and of a roller at B , and require that the deflection be zero at each of these points. Letting first $x = x_A$, $y = y_A = 0$ in Eq. (9.6), and then $x = x_B$, $y = y_B = 0$ in the same equation, we obtain two equations that can be solved for C_1 and C_2 . In the case of the cantilever beam (Fig. 9.8c), we note that both the deflection and the slope at A must be zero. Letting $x = x_A$, $y = y_A = 0$ in Eq. (9.6), and $x = x_A$, $\theta = \theta_A = 0$ in Eq. (9.5'), we obtain again two equations that can be solved for C_1 and C_2 .

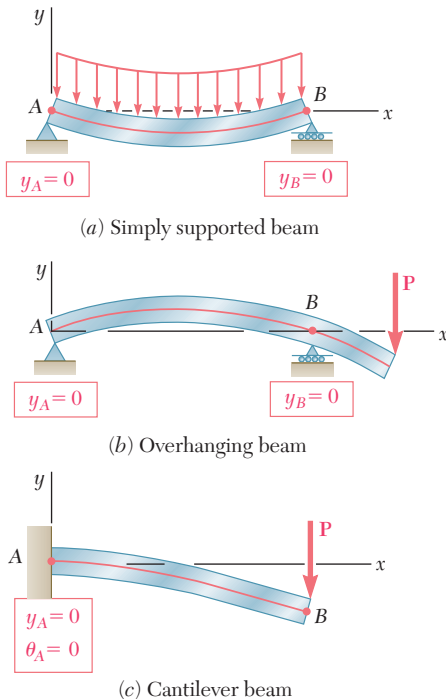


Fig. 9.8 Boundary conditions for statically determinate beams.

The cantilever beam AB is of uniform cross section and carries a load P at its free end A (Fig. 9.9). Determine the equation of the elastic curve and the deflection and slope at A .

EXAMPLE 9.01

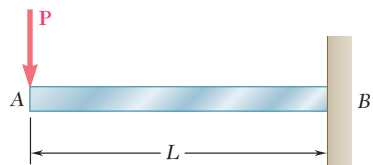


Fig. 9.9

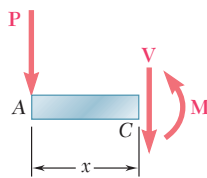


Fig. 9.10

Using the free-body diagram of the portion AC of the beam (Fig. 9.10), where C is located at a distance x from end A , we find

$$M = -Px \quad (9.7)$$

Substituting for M into Eq. (9.4) and multiplying both members by the constant EI , we write

$$EI \frac{d^2y}{dx^2} = -Px$$

Integrating in x , we obtain

$$EI \frac{dy}{dx} = -\frac{1}{2}Px^2 + C_1 \quad (9.8)$$

We now observe that at the fixed end B we have $x = L$ and $\theta = dy/dx = 0$ (Fig. 9.11). Substituting these values into (9.8) and solving for C_1 , we have

$$C_1 = \frac{1}{2}PL^2$$

which we carry back into (9.8):

$$EI \frac{dy}{dx} = -\frac{1}{2}Px^2 + \frac{1}{2}PL^2 \quad (9.9)$$

Integrating both members of Eq. (9.9), we write

$$EI y = -\frac{1}{6}Px^3 + \frac{1}{2}PL^2x + C_2 \quad (9.10)$$

But, at B we have $x = L$, $y = 0$. Substituting into (9.10), we have

$$\begin{aligned} 0 &= -\frac{1}{6}PL^3 + \frac{1}{2}PL^3 + C_2 \\ C_2 &= -\frac{1}{3}PL^3 \end{aligned}$$

Carrying the value of C_2 back into Eq. (9.10), we obtain the equation of the elastic curve:

$$EI y = -\frac{1}{6}Px^3 + \frac{1}{2}PL^2x - \frac{1}{3}PL^3$$

or

$$y = \frac{P}{6EI}(-x^3 + 3L^2x - 2L^3) \quad (9.11)$$

The deflection and slope at A are obtained by letting $x = 0$ in Eqs. (9.11) and (9.9). We find

$$y_A = -\frac{PL^3}{3EI} \quad \text{and} \quad \theta_A = \left(\frac{dy}{dx}\right)_A = \frac{PL^2}{2EI}$$

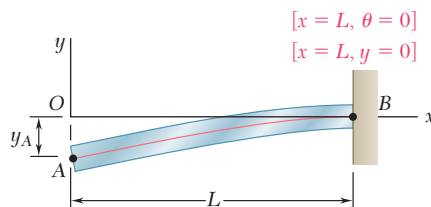


Fig. 9.11

EXAMPLE 9.02

The simply supported prismatic beam AB carries a uniformly distributed load w per unit length (Fig. 9.12). Determine the equation of the elastic curve and the maximum deflection of the beam.

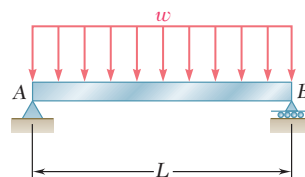


Fig. 9.12

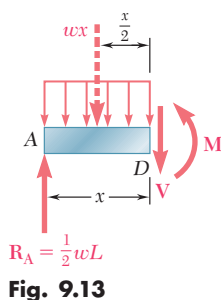


Fig. 9.13

Drawing the free-body diagram of the portion AD of the beam (Fig. 9.13) and taking moments about D , we find that

$$M = \frac{1}{2}wLx - \frac{1}{2}wx^2 \quad (9.12)$$

Substituting for M into Eq. (9.4) and multiplying both members of this equation by the constant EI , we write

$$EI \frac{d^2y}{dx^2} = -\frac{1}{2}wx^2 + \frac{1}{2}wLx \quad (9.13)$$

Integrating twice in x , we have

$$EI \frac{dy}{dx} = -\frac{1}{6}wx^3 + \frac{1}{4}wLx^2 + C_1 \quad (9.14)$$

$$EI y = -\frac{1}{24}wx^4 + \frac{1}{12}wLx^3 + C_1x + C_2 \quad (9.15)$$

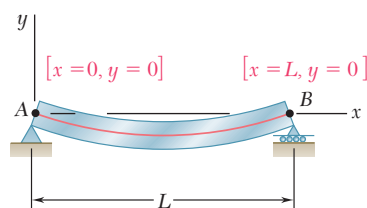


Fig. 9.14

Observing that $y = 0$ at both ends of the beam (Fig. 9.14), we first let $x = 0$ and $y = 0$ in Eq. (9.15) and obtain $C_2 = 0$. We then make $x = L$ and $y = 0$ in the same equation and write

$$0 = -\frac{1}{24}wL^4 + \frac{1}{12}wL^4 + C_1L$$

$$C_1 = -\frac{1}{24}wL^3$$

Carrying the values of C_1 and C_2 back into Eq. (9.15), we obtain the equation of the elastic curve:

$$EI y = -\frac{1}{24}wx^4 + \frac{1}{12}wLx^3 - \frac{1}{24}wL^3x$$

or

$$y = \frac{w}{24EI}(-x^4 + 2Lx^3 - L^3x) \quad (9.16)$$

Substituting into Eq. (9.14) the value obtained for C_1 , we check that the slope of the beam is zero for $x = L/2$ and that the elastic curve has a minimum at the midpoint C of the beam (Fig. 9.15). Letting $x = L/2$ in Eq. (9.16), we have

$$y_C = \frac{w}{24EI} \left(-\frac{L^4}{16} + 2L \frac{L^3}{8} - L^3 \frac{L}{2} \right) = -\frac{5wL^4}{384EI}$$

The maximum deflection or, more precisely, the maximum absolute value of the deflection, is thus

$$|y|_{\max} = \frac{5wL^4}{384EI}$$

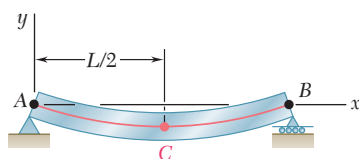


Fig. 9.15

In each of the two examples considered so far, only one free-body diagram was required to determine the bending moment in the beam. As a result, a single function of x was used to represent M throughout the beam. This, however, is not generally the case. Concentrated loads, reactions at supports, or discontinuities in a distributed load will make it necessary to divide the beam into several portions, and to represent the bending moment by a different function $M(x)$ in each of these portions of beam (Photo 9.1). Each of the functions $M(x)$ will then lead to a different expression for the slope $\theta(x)$ and for the deflection $y(x)$. Since each of the expressions obtained for the deflection must contain two constants of integration, a large number of constants will have to be determined. As you will see in the next example, the required additional boundary conditions can be obtained by observing that, while the shear and bending moment can be discontinuous at several points in a beam, the *deflection* and the *slope* of the beam *cannot be discontinuous* at any point.



Photo 9.1 A different function $M(x)$ is required in each portion of the cantilever arms.

For the prismatic beam and the loading shown (Fig. 9.16), determine the slope and deflection at point D .

We must divide the beam into two portions, AD and DB , and determine the function $y(x)$ which defines the elastic curve for each of these portions.

1. From A to D ($x < L/4$). We draw the free-body diagram of a portion of beam AE of length $x < L/4$ (Fig. 9.17). Taking moments about E , we have

$$M_1 = \frac{3P}{4}x \quad (9.17)$$

or, recalling Eq. (9.4),

$$EI \frac{d^2 y_1}{dx^2} = \frac{3}{4}Px \quad (9.18)$$

where $y_1(x)$ is the function which defines the elastic curve for *portion AD of the beam*. Integrating in x , we write

$$EI \theta_1 = EI \frac{dy_1}{dx} = \frac{3}{8}Px^2 + C_1 \quad (9.19)$$

$$EI y_1 = \frac{1}{8}Px^3 + C_1x + C_2 \quad (9.20)$$

2. From D to B ($x > L/4$). We now draw the free-body diagram of a portion of beam AE of length $x > L/4$ (Fig. 9.18) and write

$$M_2 = \frac{3P}{4}x - P\left(x - \frac{L}{4}\right) \quad (9.21)$$

EXAMPLE 9.03

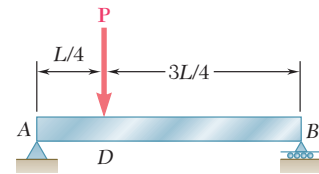


Fig. 9.16

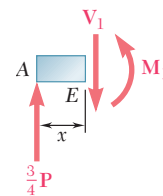


Fig. 9.17

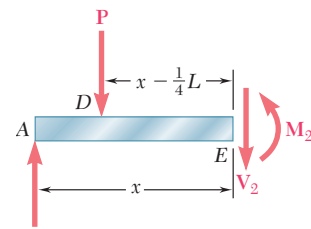


Fig. 9.18

or, recalling Eq. (9.4) and rearranging terms,

$$EI \frac{d^2 y_2}{dx^2} = -\frac{1}{4}Px + \frac{1}{4}PL \quad (9.22)$$

where $y_2(x)$ is the function which defines the elastic curve for portion *DB* of the beam. Integrating in x , we write

$$EI \theta_2 = EI \frac{dy_2}{dx} = -\frac{1}{8}Px^2 + \frac{1}{4}PLx + C_3 \quad (9.23)$$

$$EI y_2 = -\frac{1}{24}Px^3 + \frac{1}{8}PLx^2 + C_3x + C_4 \quad (9.24)$$

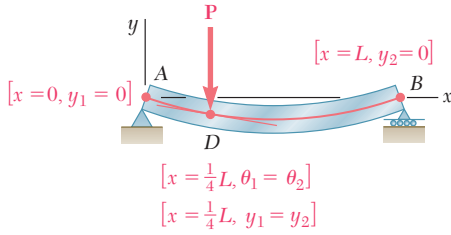


Fig. 9.19

Determination of the Constants of Integration. The conditions that must be satisfied by the constants of integration have been summarized in Fig. 9.19. At the support A, where the deflection is defined by Eq. (9.20), we must have $x = 0$ and $y_1 = 0$. At the support B, where the deflection is defined by Eq. (9.24), we must have $x = L$ and $y_2 = 0$. Also, the fact that there can be no sudden change in deflection or in slope at point *D* requires that $y_1 = y_2$ and $\theta_1 = \theta_2$ when $x = L/4$. We have therefore:

$$[x = 0, y_1 = 0], \text{ Eq. (9.20):} \quad 0 = C_2 \quad (9.25)$$

$$[x = L, y_2 = 0], \text{ Eq. (9.24):} \quad 0 = \frac{1}{12}PL^3 + C_3L + C_4 \quad (9.26)$$

$$[x = L/4, \theta_1 = \theta_2], \text{ Eqs. (9.19) and (9.23):}$$

$$\frac{3}{128}PL^2 + C_1 = \frac{7}{128}PL^2 + C_3 \quad (9.27)$$

$$[x = L/4, y_1 = y_2], \text{ Eqs. (9.20) and (9.24):}$$

$$\frac{PL^3}{512} + C_1 \frac{L}{4} = \frac{11PL^3}{1536} + C_3 \frac{L}{4} + C_4 \quad (9.28)$$

Solving these equations simultaneously, we find

$$C_1 = -\frac{7PL^2}{128}, C_2 = 0, C_3 = -\frac{11PL^2}{128}, C_4 = \frac{PL^3}{384}$$

Substituting for C_1 and C_2 into Eqs. (9.19) and (9.20), we write that for $x \leq L/4$,

$$EI \theta_1 = \frac{3}{8}Px^2 - \frac{7PL^2}{128} \quad (9.29)$$

$$EI y_1 = \frac{1}{8}Px^3 - \frac{7PL^2}{128}x \quad (9.30)$$

Letting $x = L/4$ in each of these equations, we find that the slope and deflection at point *D* are, respectively,

$$\theta_D = -\frac{PL^2}{32EI} \quad \text{and} \quad y_D = -\frac{3PL^3}{256EI}$$

We note that, since $\theta_D \neq 0$, the deflection at *D* is *not* the maximum deflection of the beam.

*9.4 DIRECT DETERMINATION OF THE ELASTIC CURVE FROM THE LOAD DISTRIBUTION

We saw in Sec. 9.3 that the equation of the elastic curve can be obtained by integrating twice the differential equation

$$\frac{d^2 y}{dx^2} = \frac{M(x)}{EI} \quad (9.4)$$

where $M(x)$ is the bending moment in the beam. We now recall from Sec. 5.3 that, when a beam supports a distributed load $w(x)$, we have $dM/dx = V$ and $dV/dx = -w$ at any point of the beam. Differentiating both members of Eq. (9.4) with respect to x and assuming EI to be constant, we have therefore

$$\frac{d^3 y}{dx^3} = \frac{1}{EI} \frac{dM}{dx} = \frac{V(x)}{EI} \quad (9.31)$$

and, differentiating again,

$$\frac{d^4 y}{dx^4} = \frac{1}{EI} \frac{dV}{dx} = -\frac{w(x)}{EI}$$

We conclude that, when a prismatic beam supports a distributed load $w(x)$, its elastic curve is governed by the fourth-order linear differential equation

$$\frac{d^4 y}{dx^4} = -\frac{w(x)}{EI} \quad (9.32)$$

Multiplying both members of Eq. (9.32) by the constant EI and integrating four times, we write

$$\begin{aligned} EI \frac{d^4 y}{dx^4} &= -w(x) \\ EI \frac{d^3 y}{dx^3} &= V(x) = -\int w(x) dx + C_1 \\ EI \frac{d^2 y}{dx^2} &= M(x) = -\int dx \int w(x) dx + C_1 x + C_2 \\ EI \frac{dy}{dx} &= EI \theta(x) = -\int dx \int dx \int w(x) dx + \frac{1}{2} C_1 x^2 + C_2 x + C_3 \\ EI y(x) &= -\int dx \int dx \int dx \int w(x) dx + \frac{1}{6} C_1 x^3 + \frac{1}{2} C_2 x^2 + C_3 x + C_4 \end{aligned} \quad (9.33)$$

The four constants of integration can be determined from the boundary conditions. These conditions include (a) the conditions imposed on the deflection or slope of the beam by its supports (cf. Sec. 9.3), and (b) the condition that V and M be zero at the free end of a cantilever beam, or that M be zero at both ends of a simply supported beam (cf. Sec. 5.3). This has been illustrated in Fig. 9.20.

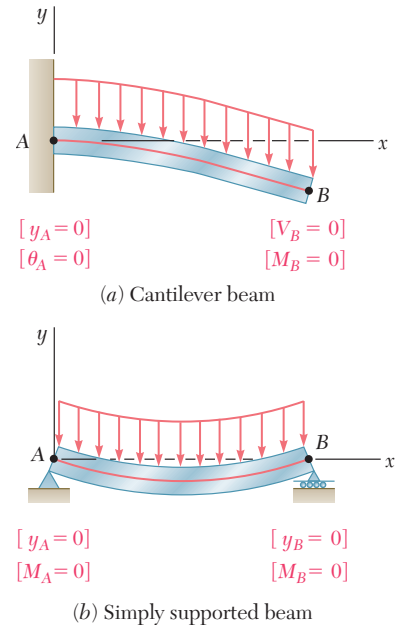


Fig. 9.20 Boundary conditions.

The method presented here can be used effectively with cantilever or simply supported beams carrying a distributed load. In the case of overhanging beams, however, the reactions at the supports will cause discontinuities in the shear, i.e., in the third derivative of y , and different functions would be required to define the elastic curve over the entire beam.

EXAMPLE 9.04

The simply supported prismatic beam AB carries a uniformly distributed load w per unit length (Fig. 9.21). Determine the equation of the elastic curve and the maximum deflection of the beam. (This is the same beam and loading as in Example 9.02.)

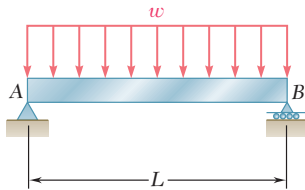
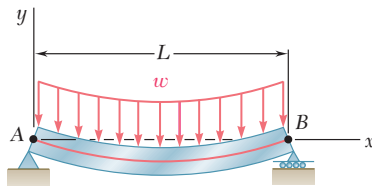


Fig. 9.21



$$\begin{aligned} [x = 0, M = 0] \\ [x = 0, y = 0] \end{aligned}$$

$$\begin{aligned} [x = L, M = 0] \\ [x = L, y = 0] \end{aligned}$$

Fig. 9.22

Since $w = \text{constant}$, the first three of Eqs. (9.33) yield

$$\begin{aligned} EI \frac{d^4 y}{dx^4} &= -w \\ EI \frac{d^3 y}{dx^3} &= V(x) = -wx + C_1 \\ EI \frac{d^2 y}{dx^2} &= M(x) = -\frac{1}{2}wx^2 + C_1x + C_2 \end{aligned} \quad (9.34)$$

Noting that the boundary conditions require that $M = 0$ at both ends of the beam (Fig. 9.22), we first let $x = 0$ and $M = 0$ in Eq. (9.34) and obtain $C_2 = 0$. We then make $x = L$ and $M = 0$ in the same equation and obtain $C_1 = \frac{1}{2}wL$.

Carrying the values of C_1 and C_2 back into Eq. (9.34), and integrating twice, we write

$$\begin{aligned} EI \frac{d^2 y}{dx^2} &= -\frac{1}{2}wx^2 + \frac{1}{2}wLx \\ EI \frac{dy}{dx} &= -\frac{1}{6}wx^3 + \frac{1}{4}wLx^2 + C_3 \\ EI y &= -\frac{1}{24}wx^4 + \frac{1}{12}wLx^3 + C_3x + C_4 \end{aligned} \quad (9.35)$$

But the boundary conditions also require that $y = 0$ at both ends of the beam. Letting $x = 0$ and $y = 0$ in Eq. (9.35), we obtain $C_4 = 0$; letting $x = L$ and $y = 0$ in the same equation, we write

$$\begin{aligned} 0 &= -\frac{1}{24}wL^4 + \frac{1}{12}wL^4 + C_3L \\ C_3 &= -\frac{1}{24}wL^3 \end{aligned}$$

Carrying the values of C_3 and C_4 back into Eq. (9.35) and dividing both members by EI , we obtain the equation of the elastic curve:

$$y = \frac{w}{24EI}(-x^4 + 2Lx^3 - L^3x) \quad (9.36)$$

The value of the maximum deflection is obtained by making $x = L/2$ in Eq. (9.36). We have

$$|y|_{\max} = \frac{5wL^4}{384EI}$$

9.5 STATICALLY INDETERMINATE BEAMS

In the preceding sections, our analysis was limited to statically determinate beams. Consider now the prismatic beam AB (Fig. 9.23a), which has a fixed end at A and is supported by a roller at B . Drawing the free-body diagram of the beam (Fig. 9.23b), we note that the reactions involve four unknowns, while only three equilibrium equations are available, namely

$$\Sigma F_x = 0 \quad \Sigma F_y = 0 \quad \Sigma M_A = 0 \quad (9.37)$$

Since only A_x can be determined from these equations, we conclude that the beam is *statically indeterminate*.

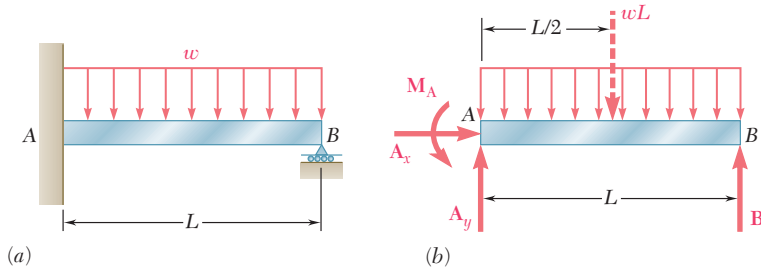


Fig. 9.23 Statically indeterminate beam.

However, we recall from Chaps. 2 and 3 that, in a statically indeterminate problem, the reactions can be obtained by considering the *deformations* of the structure involved. We should, therefore, proceed with the computation of the slope and deformation along the beam. Following the method used in Sec. 9.3, we first express the bending moment $M(x)$ at any given point of AB in terms of the distance x from A , the given load, and the unknown reactions. Integrating in x , we obtain expressions for θ and y which contain two additional unknowns, namely the constants of integration C_1 and C_2 . But altogether six equations are available to determine the reactions and the constants C_1 and C_2 ; they are the three equilibrium equations (9.37) and the three equations expressing that the boundary conditions are satisfied, i.e., that the slope and deflection at A are zero, and that the deflection at B is zero (Fig. 9.24). Thus, the reactions at the supports can be determined, and the equation of the elastic curve can be obtained.

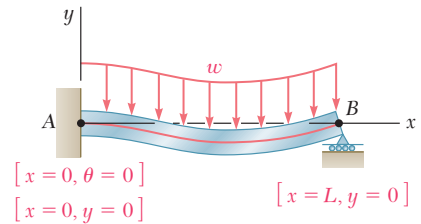


Fig. 9.24 Boundary conditions for beam of Fig. 9.23.

Determine the reactions at the supports for the prismatic beam of Fig. 9.23a.

Equilibrium Equations. From the free-body diagram of Fig. 9.23b we write

$$\begin{aligned} \pm \Sigma F_x = 0: & \quad A_x = 0 \\ + \uparrow \Sigma F_y = 0: & \quad A_y + B - wL = 0 \\ + \curvearrowright \Sigma M_A = 0: & \quad M_A + BL - \frac{1}{2}wL^2 = 0 \end{aligned} \quad (9.38)$$

EXAMPLE 9.05

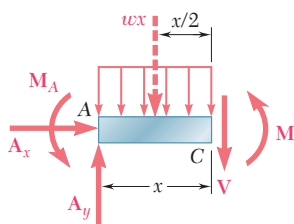


Fig. 9.25

Equation of Elastic Curve. Drawing the free-body diagram of a portion of beam AC (Fig. 9.25), we write

$$+\uparrow \Sigma M_C = 0: \quad M + \frac{1}{2}wx^2 + M_A - A_yx = 0 \quad (9.39)$$

Solving Eq. (9.39) for M and carrying into Eq. (9.4), we write

$$EI \frac{d^2y}{dx^2} = -\frac{1}{2}wx^2 + A_yx - M_A$$

Integrating in x , we have

$$EI \theta = EI \frac{dy}{dx} = -\frac{1}{6}wx^3 + \frac{1}{2}A_yx^2 - M_Ax + C_1 \quad (9.40)$$

$$EI y = -\frac{1}{24}wx^4 + \frac{1}{6}A_yx^3 - \frac{1}{2}M_Ax^2 + C_1x + C_2 \quad (9.41)$$

Referring to the boundary conditions indicated in Fig. 9.24, we make $x = 0$, $\theta = 0$ in Eq. (9.40), $x = 0$, $y = 0$ in Eq. (9.41), and conclude that $C_1 = C_2 = 0$. Thus, we rewrite Eq. (9.41) as follows:

$$EI y = -\frac{1}{24}wx^4 + \frac{1}{6}A_yx^3 - \frac{1}{2}M_Ax^2 \quad (9.42)$$

But the third boundary condition requires that $y = 0$ for $x = L$. Carrying these values into (9.42), we write

$$0 = -\frac{1}{24}wL^4 + \frac{1}{6}A_yL^3 - \frac{1}{2}M_AL^2$$

or

$$3M_A - A_yL + \frac{1}{4}wL^2 = 0 \quad (9.43)$$

Solving this equation simultaneously with the three equilibrium equations (9.38), we obtain the reactions at the supports:

$$A_x = 0 \quad A_y = \frac{5}{8}wL \quad M_A = \frac{1}{8}wL^2 \quad B = \frac{3}{8}wL$$

In the example we have just considered, there was one redundant reaction, i.e., there was one more reaction than could be determined from the equilibrium equations alone. The corresponding beam is said to be *statically indeterminate to the first degree*. Another example of a beam indeterminate to the first degree is provided in Sample Prob. 9.3. If the beam supports are such that two reactions are redundant (Fig. 9.26a), the beam is said to be *indeterminate to the second degree*. While there are now five unknown reactions (Fig. 9.26b), we find that four equations may be obtained from the boundary conditions (Fig. 9.26c). Thus, altogether seven equations are available to determine the five reactions and the two constants of integration.

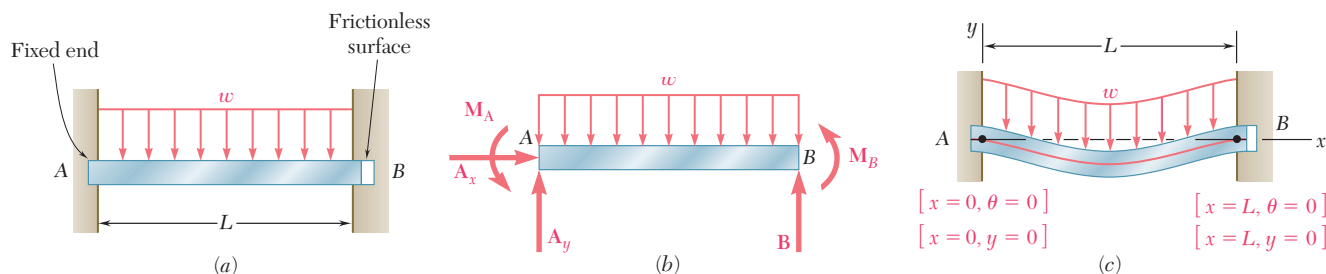
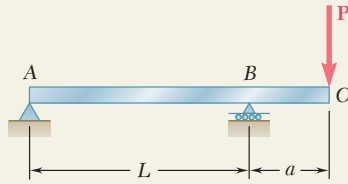


Fig. 9.26 Beam statically indeterminate to the second degree.

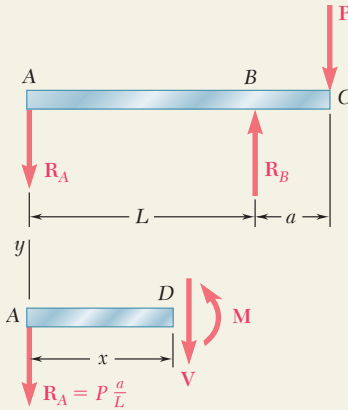
SAMPLE PROBLEM 9.1



The overhanging steel beam ABC carries a concentrated load P at end C . For portion AB of the beam, (a) derive the equation of the elastic curve, (b) determine the maximum deflection, (c) evaluate y_{\max} for the following data:

$$\begin{array}{lll} W14 \times 68 & I = 722 \text{ in}^4 & E = 29 \times 10^6 \text{ psi} \\ P = 50 \text{ kips} & L = 15 \text{ ft} = 180 \text{ in.} & a = 4 \text{ ft} = 48 \text{ in.} \end{array}$$

SOLUTION



Free-Body Diagrams. Reactions: $R_A = Pa/L \downarrow$, $R_B = P(1 + a/L) \uparrow$. Using the free-body diagram of the portion of beam AD of length x , we find

$$M = -P \frac{a}{L} x \quad (0 < x < L)$$

Differential Equation of the Elastic Curve. We use Eq. (9.4) and write

$$EI \frac{d^2 y}{dx^2} = -P \frac{a}{L} x$$

Noting that the flexural rigidity EI is constant, we integrate twice and find

$$EI \frac{dy}{dx} = -\frac{1}{2} P \frac{a}{L} x^2 + C_1 \quad (1)$$

$$EI y = -\frac{1}{6} P \frac{a}{L} x^3 + C_1 x + C_2 \quad (2)$$

Determination of Constants. For the boundary conditions shown, we have

$$[x = 0, y = 0]: \quad \text{From Eq. (2), we find} \quad C_2 = 0$$

$$[x = L, y = 0]: \quad \text{Again using Eq. (2), we write}$$

$$EI(0) = -\frac{1}{6} P \frac{a}{L} L^3 + C_1 L \quad C_1 = +\frac{1}{6} PaL$$

a. Equation of the Elastic Curve. Substituting for C_1 and C_2 into Eqs.

(1) and (2), we have

$$EI \frac{dy}{dx} = -\frac{1}{2} P \frac{a}{L} x^2 + \frac{1}{6} PaL \quad \frac{dy}{dx} = \frac{PaL}{6EI} \left[1 - 3 \left(\frac{x}{L} \right)^2 \right] \quad (3)$$

$$EI y = -\frac{1}{6} P \frac{a}{L} x^3 + \frac{1}{6} PaLx \quad y = \frac{PaL^2}{6EI} \left[\frac{x}{L} - \left(\frac{x}{L} \right)^3 \right] \quad (4) \quad \blacktriangleleft$$

b. Maximum Deflection in Portion AB. The maximum deflection

y_{\max} occurs at point E where the slope of the elastic curve is zero. Setting $dy/dx = 0$ in Eq. (3), we determine the abscissa x_m of point E :

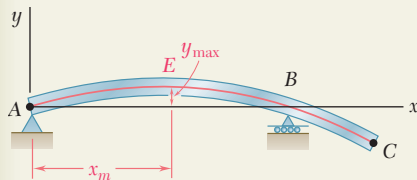
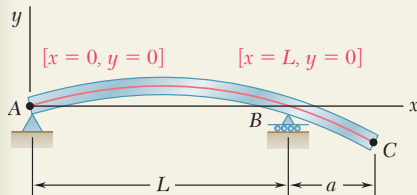
$$0 = \frac{PaL}{6EI} \left[1 - 3 \left(\frac{x_m}{L} \right)^2 \right] \quad x_m = \frac{L}{\sqrt{3}} = 0.577L$$

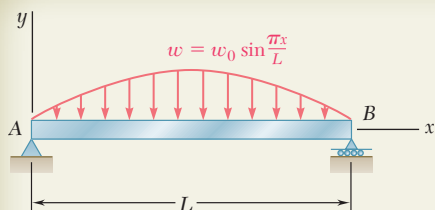
We substitute $x_m/L = 0.577$ into Eq. (4) and have

$$y_{\max} = \frac{PaL^2}{6EI} [(0.577) - (0.577)^3] \quad y_{\max} = 0.0642 \frac{PaL^2}{EI} \quad \blacktriangleleft$$

c. Evaluation of y_{\max} . For the data given, the value of y_{\max} is

$$y_{\max} = 0.0642 \frac{(50 \text{ kips})(48 \text{ in.})(180 \text{ in.})^2}{(29 \times 10^6 \text{ psi})(722 \text{ in}^4)} \quad y_{\max} = 0.238 \text{ in.} \quad \blacktriangleleft$$





SAMPLE PROBLEM 9.2

For the beam and loading shown, determine (a) the equation of the elastic curve, (b) the slope at end A, (c) the maximum deflection.

SOLUTION

Differential Equation of the Elastic Curve. From Eq. (9.32),

$$EI \frac{d^4 y}{dx^4} = -w(x) = -w_0 \sin \frac{\pi x}{L} \quad (1)$$

Integrate Eq. (1) twice:

$$EI \frac{d^3 y}{dx^3} = V = +w_0 \frac{L}{\pi} \cos \frac{\pi x}{L} + C_1 \quad (2)$$

$$EI \frac{d^2 y}{dx^2} = M = +w_0 \frac{L^2}{\pi^2} \sin \frac{\pi x}{L} + C_1 x + C_2 \quad (3)$$

Boundary Conditions:

$[x = 0, M = 0]$: From Eq. (3), we find $C_2 = 0$

$[x = L, M = 0]$: Again using Eq. (3), we write

$$0 = w_0 \frac{L^2}{\pi^2} \sin \pi + C_1 L \quad C_1 = 0$$

Thus:

$$EI \frac{d^2 y}{dx^2} = +w_0 \frac{L^2}{\pi^2} \sin \frac{\pi x}{L} \quad (4)$$

Integrate Eq. (4) twice:

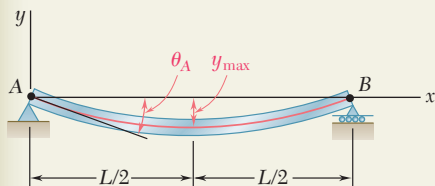
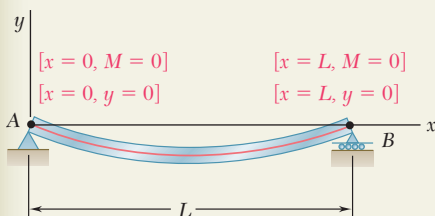
$$EI \frac{dy}{dx} = EI \theta = -w_0 \frac{L^3}{\pi^3} \cos \frac{\pi x}{L} + C_3 \quad (5)$$

$$EI y = -w_0 \frac{L^4}{\pi^4} \sin \frac{\pi x}{L} + C_3 x + C_4 \quad (6)$$

Boundary Conditions:

$[x = 0, y = 0]$: Using Eq. (6), we find $C_4 = 0$

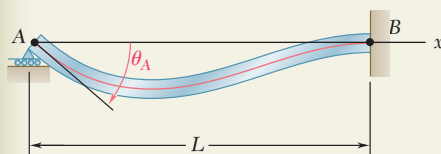
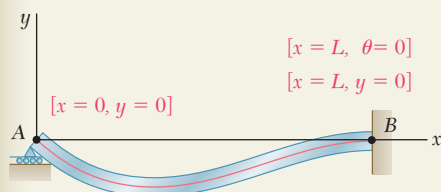
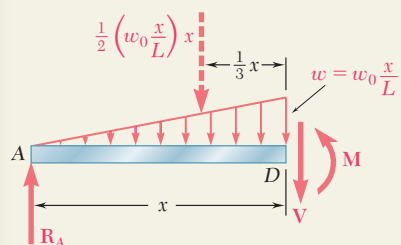
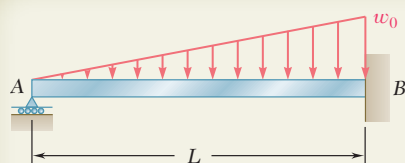
$[x = L, y = 0]$: Again using Eq. (6), we find $C_3 = 0$



a. Equation of Elastic Curve $EI y = -w_0 \frac{L^4}{\pi^4} \sin \frac{\pi x}{L}$ ◀

b. Slope at End A. For $x = 0$, we have $EI \theta_A = -w_0 \frac{L^3}{\pi^3} \cos 0$ $\theta_A = \frac{w_0 L^3}{\pi^3 EI}$ ◀

c. Maximum Deflection. For $x = \frac{1}{2}L$ $EI y_{\max} = -w_0 \frac{L^4}{\pi^4} \sin \frac{\pi}{2}$ $y_{\max} = \frac{w_0 L^4}{\pi^4 EI}$ ◀



SAMPLE PROBLEM 9.3

For the uniform beam AB , (a) determine the reaction at A , (b) derive the equation of the elastic curve, (c) determine the slope at A . (Note that the beam is statically indeterminate to the first degree.)

SOLUTION

Bending Moment. Using the free body shown, we write

$$+\downarrow \sum M_D = 0: \quad R_A x - \frac{1}{2} \left(\frac{w_0 x^2}{L} \right) \frac{x}{3} - M = 0 \quad M = R_A x - \frac{w_0 x^3}{6L}$$

Differential Equation of the Elastic Curve. We use Eq. (9.4) and write

$$EI \frac{d^2 y}{dx^2} = R_A x - \frac{w_0 x^3}{6L}$$

Noting that the flexural rigidity EI is constant, we integrate twice and find

$$EI \frac{dy}{dx} = EI \theta = \frac{1}{2} R_A x^2 - \frac{w_0 x^4}{24L} + C_1 \quad (1)$$

$$EI y = \frac{1}{6} R_A x^3 - \frac{w_0 x^5}{120L} + C_1 x + C_2 \quad (2)$$

Boundary Conditions. The three boundary conditions that must be satisfied are shown on the sketch

$$[x = 0, y = 0]: \quad C_2 = 0 \quad (3)$$

$$[x = L, \theta = 0]: \quad \frac{1}{2} R_A L^2 - \frac{w_0 L^3}{24} + C_1 = 0 \quad (4)$$

$$[x = L, y = 0]: \quad \frac{1}{6} R_A L^3 - \frac{w_0 L^4}{120} + C_1 L + C_2 = 0 \quad (5)$$

a. Reaction at A. Multiplying Eq. (4) by L , subtracting Eq. (5) member by member from the equation obtained, and noting that $C_2 = 0$, we have

$$\frac{1}{3} R_A L^3 - \frac{1}{30} w_0 L^4 = 0 \quad R_A = \frac{1}{10} w_0 L \uparrow \quad \blacktriangleleft$$

We note that the reaction is independent of E and I . Substituting $R_A = \frac{1}{10} w_0 L$ into Eq. (4), we have

$$\frac{1}{2} \left(\frac{1}{10} w_0 L \right) L^2 - \frac{1}{24} w_0 L^3 + C_1 = 0 \quad C_1 = -\frac{1}{120} w_0 L^3$$

b. Equation of the Elastic Curve. Substituting for R_A , C_1 , and C_2 into Eq. (2), we have

$$EI y = \frac{1}{6} \left(\frac{1}{10} w_0 L \right) x^3 - \frac{w_0 x^5}{120L} - \left(\frac{1}{120} w_0 L^3 \right) x$$

$$y = \frac{w_0}{120EI} (-x^5 + 2L^2 x^3 - L^4 x) \quad \blacktriangleleft$$

c. Slope at A. We differentiate the above equation with respect to x :

$$\theta = \frac{dy}{dx} = \frac{w_0}{120EI} (-5x^4 + 6L^2 x^2 - L^4)$$

Making $x = 0$, we have $\theta_A = -\frac{w_0 L^3}{120EI} \quad \theta_A = \frac{w_0 L^3}{120EI} \quad \blacktriangleleft$

PROBLEMS

In the following problems assume that the flexural rigidity EI of each beam is constant.

9.1 through 9.4 For the loading shown, determine (a) the equation of the elastic curve for the cantilever beam AB , (b) the deflection at the free end, (c) the slope at the free end.

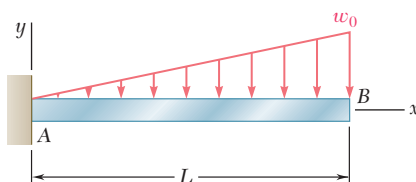


Fig. P9.1

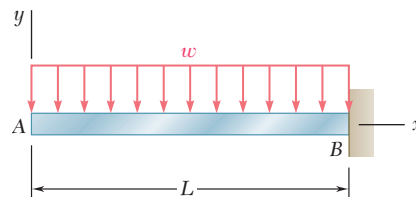


Fig. P9.2

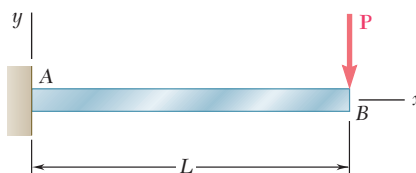


Fig. P9.3

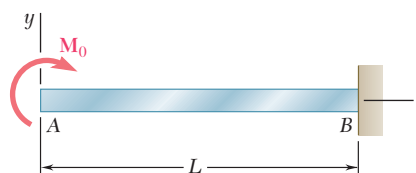


Fig. P9.4

9.5 and 9.6 For the cantilever beam and loading shown, determine (a) the equation of the elastic curve for portion AB of the beam, (b) the deflection at B , (c) the slope at B .

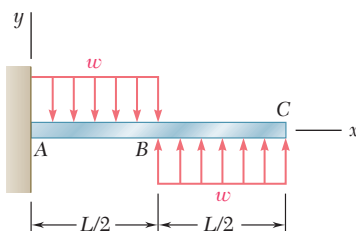


Fig. P9.5

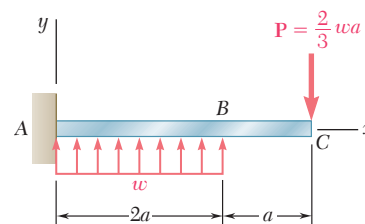


Fig. P9.6

9.7 For the beam and loading shown, determine (a) the equation of the elastic curve for portion AB of the beam, (b) the slope at A , (c) the slope at B .

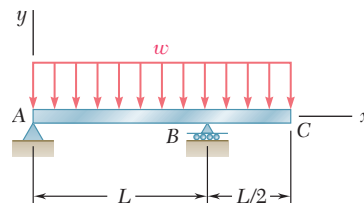


Fig. P9.7

- 9.8** For the beam and loading shown, determine (a) the equation of the elastic curve for portion AB of the beam, (b) the deflection at midspan, (c) the slope at B.

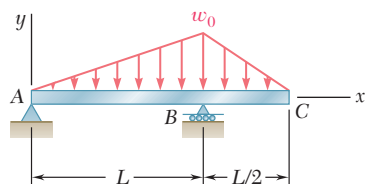


Fig. P9.8

- 9.9** Knowing that beam AB is an S200 \times 34 rolled shape and that $P = 60$ kN, $L = 2$ m, and $E = 200$ GPa, determine (a) the slope at A, (b) the deflection at C.

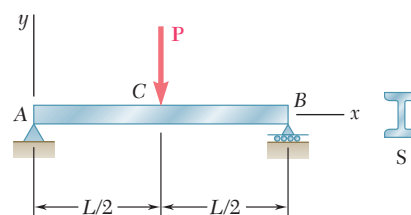


Fig. P9.9

- 9.10** Knowing that beam AB is a W10 \times 33 rolled shape and that $w_0 = 3$ kips/ft, $L = 12$ ft, and $E = 29 \times 10^6$ psi, determine (a) the slope at A, (b) the deflection at C.

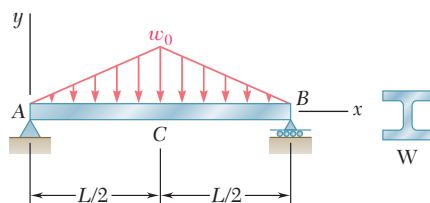


Fig. P9.10

- 9.11** (a) Determine the location and magnitude of the maximum deflection of beam AB. (b) Assuming that beam AB is a W360 \times 64, $L = 3.5$ m, and $E = 200$ GPa, calculate the maximum allowable value of the applied moment M_0 if the maximum deflection is not to exceed 1 mm.

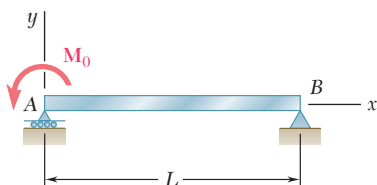


Fig. P9.11

- 9.12** For the beam and loading shown, (a) express the magnitude and location of the maximum deflection in terms of w_0 , L , E , and I . (b) Calculate the value of the maximum deflection, assuming that beam AB is a W18 \times 50 rolled shape and that $w_0 = 4.5$ kips/ft, $L = 18$ ft, and $E = 29 \times 10^6$ psi.

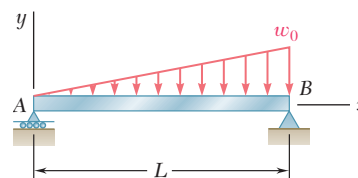


Fig. P9.12

- 9.13** For the beam and loading shown, determine the deflection at point C . Use $E = 29 \times 10^6$ psi.

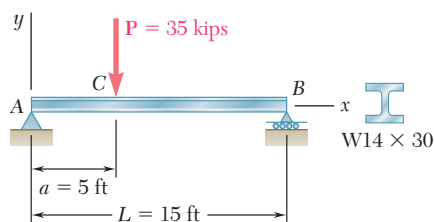


Fig. P9.13

- 9.14** For the beam and loading shown, knowing that $a = 2$ m, $w = 50$ kN/m, and $E = 200$ GPa, determine (a) the slope at support A , (b) the deflection at point C .

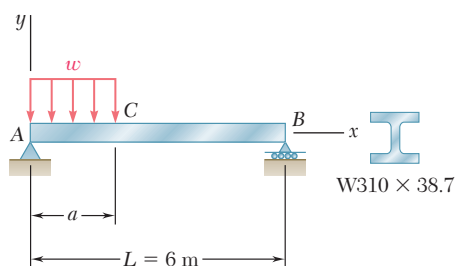


Fig. P9.14

- 9.15** For the beam and loading shown, determine the deflection at point C . Use $E = 200$ GPa.

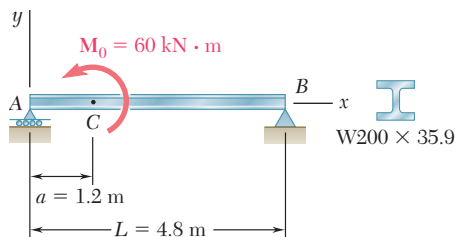


Fig. P9.15

- 9.16** Knowing that beam AE is an $S200 \times 27.4$ rolled shape and that $P = 17.5$ kN, $L = 2.5$ m, $a = 0.8$ m and $E = 200$ GPa, determine (a) the equation of the elastic curve for portion BD , (b) the deflection at the center C of the beam.

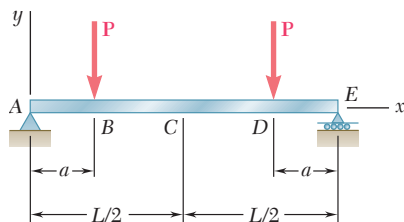


Fig. P9.16

- 9.17** For the beam and loading shown, determine (a) the equation of the elastic curve, (b) the slope at end A, (c) the deflection at the midpoint of the span.

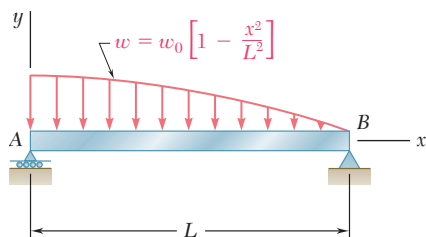


Fig. P9.17

- 9.18** For the beam and loading shown, determine (a) the equation of the elastic curve, (b) the slope at end A, (c) the deflection at the midpoint of the span.

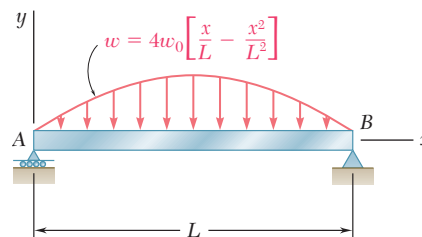


Fig. P9.18

- 9.19 through 9.22** For the beam and loading shown, determine the reaction at the roller support.

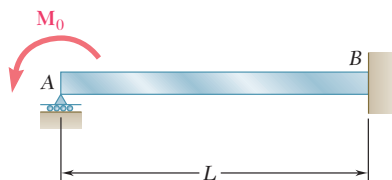


Fig. P9.19

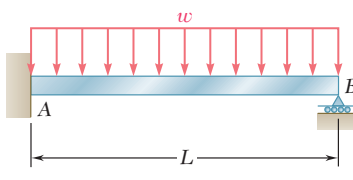


Fig. P9.20

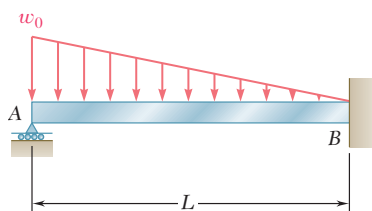


Fig. P9.21

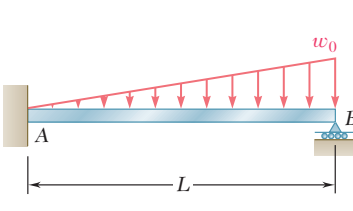


Fig. P9.22

- 9.23** For the beam shown, determine the reaction at the roller support when $w_0 = 15 \text{ kN/m}$.

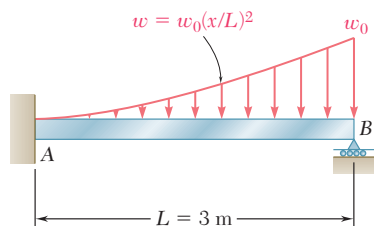


Fig. P9.23

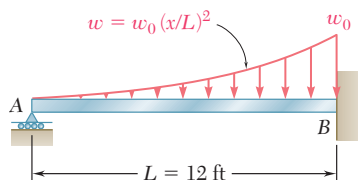


Fig. P9.24

9.24 For the beam shown, determine the reaction at the roller support when $w_0 = 6$ kips/ft.

9.25 through 9.28 Determine the reaction at the roller support and draw the bending moment diagram for the beam and loading shown.

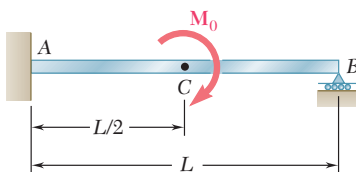


Fig. P9.25

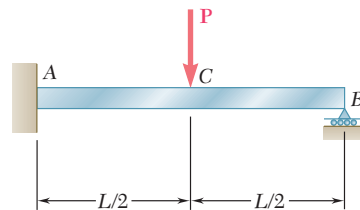


Fig. P9.26

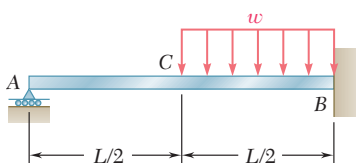


Fig. P9.27

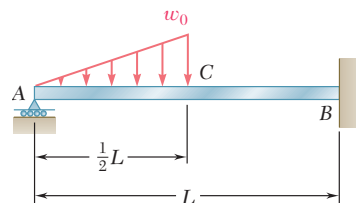


Fig. P9.28

9.29 and 9.30 Determine the reaction at the roller support and the deflection at point C.

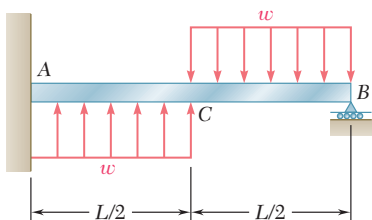


Fig. P9.29

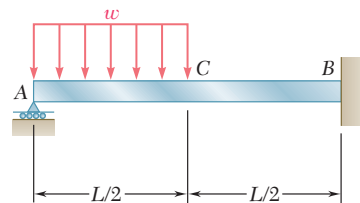


Fig. P9.30

9.31 and 9.32 Determine the reaction at the roller support and the deflection at point D if a is equal to $L/3$.

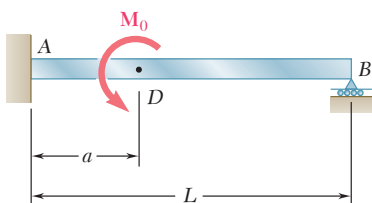


Fig. P9.31

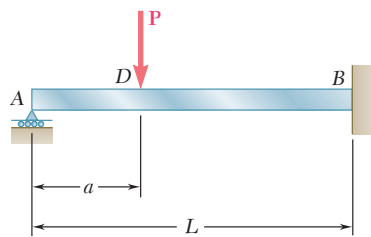


Fig. P9.32

9.33 and 9.34 Determine the reaction at A and draw the bending moment diagram for the beam and loading shown.

9.6 Using Singularity Functions to Determine the Slope and Deflection of a Beam

571

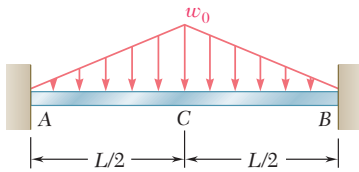


Fig. P9.33

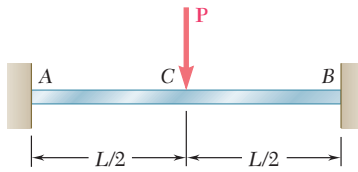


Fig. P9.34

*9.6 USING SINGULARITY FUNCTIONS TO DETERMINE THE SLOPE AND DEFLECTION OF A BEAM

Reviewing the work done so far in this chapter, we note that the integration method provides a convenient and effective way of determining the slope and deflection at any point of a prismatic beam, *as long as the bending moment can be represented by a single analytical function* $M(x)$. However, when the loading of the beam is such that two different functions are needed to represent the bending moment over the entire length of the beam, as in Example 9.03 (Fig. 9.16), four constants of integration are required, and an equal number of equations, expressing continuity conditions at point D, as well as boundary conditions at the supports A and B, must be used to determine these constants. If three or more functions were needed to represent the bending moment, additional constants and a corresponding number of additional equations would be required, resulting in rather lengthy computations. Such would be the case for the beam shown in Photo 9.2. In this section these computations will be simplified through the use of the singularity functions discussed in Sec. 5.5.



Photo 9.2 In this roof structure, each of the joists applies a concentrated load to the beam that supports it.

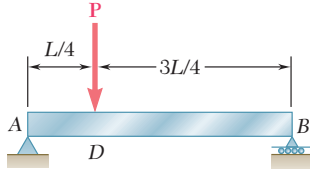


Fig. 9.16 (repeated)

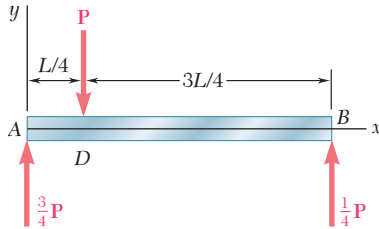


Fig. 9.27 Free-body diagram for beam of Fig. 9.16.

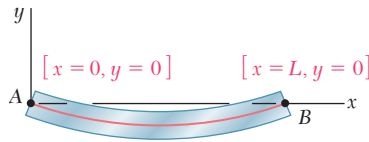


Fig. 9.28 Boundary conditions for beam of Fig. 9.16.

Let us consider again the beam and loading of Example 9.03 (Fig. 9.16) and draw the free-body diagram of that beam (Fig. 9.27). Using the appropriate singularity function, as explained in Sec. 5.5, to represent the contribution to the shear of the concentrated load P , we write

$$V(x) = \frac{3P}{4} - P\langle x - \frac{1}{4}L \rangle^0$$

Integrating in x and recalling from Sec. 5.5 that in the absence of any concentrated couple, the expression obtained for the bending moment will not contain any constant term, we have

$$M(x) = \frac{3P}{4}x - P\langle x - \frac{1}{4}L \rangle \quad (9.44)$$

Substituting for $M(x)$ from (9.44) into Eq. (9.4), we write

$$EI \frac{d^2y}{dx^2} = \frac{3P}{4}x - P\langle x - \frac{1}{4}L \rangle \quad (9.45)$$

and, integrating in x ,

$$EI \theta = EI \frac{dy}{dx} = \frac{3}{8}Px^2 - \frac{1}{2}P\langle x - \frac{1}{4}L \rangle^2 + C_1 \quad (9.46)$$

$$EI y = \frac{1}{8}Px^3 - \frac{1}{6}P\langle x - \frac{1}{4}L \rangle^3 + C_1x + C_2 \quad (9.47)^\dagger$$

The constants C_1 and C_2 can be determined from the boundary conditions shown in Fig. 9.28. Letting $x = 0, y = 0$ in Eq. (9.47), we have

$$0 = 0 - \frac{1}{6}P\langle 0 - \frac{1}{4}L \rangle^3 + 0 + C_2$$

which reduces to $C_2 = 0$, since any bracket containing a negative quantity is equal to zero. Letting now $x = L, y = 0$, and $C_2 = 0$ in Eq. (9.47), we write

$$0 = \frac{1}{8}PL^3 - \frac{1}{6}P\langle \frac{3}{4}L \rangle^3 + C_1L$$

Since the quantity between brackets is positive, the brackets can be replaced by ordinary parentheses. Solving for C_1 , we have

$$C_1 = -\frac{7PL^2}{128}$$

We check that the expressions obtained for the constants C_1 and C_2 are the same that were found earlier in Sec. 9.3. But the need for additional constants C_3 and C_4 has now been eliminated, and we do not have to write equations expressing that the slope and the deflection are continuous at point D .

[†]The continuity conditions for the slope and deflection at D are “built-in” in Eqs. (9.46) and (9.47). Indeed, the difference between the expressions for the slope θ_1 in AD and the slope θ_2 in DB is represented by the term $-\frac{1}{2}P\langle x - \frac{1}{4}L \rangle^2$ in Eq. (9.46), and this term is equal to zero at D . Similarly, the difference between the expressions for the deflection y_1 in AD and the deflection y_2 in DB is represented by the term $-\frac{1}{6}P\langle x - \frac{1}{4}L \rangle^3$ in Eq. (9.47), and this term is also equal to zero at D .

For the beam and loading shown (Fig. 9.29a) and using singularity functions, (a) express the slope and deflection as functions of the distance x from the support at A, (b) determine the deflection at the midpoint D. Use $E = 200 \text{ GPa}$ and $I = 6.87 \times 10^{-6} \text{ m}^4$.

(a) We note that the beam is loaded and supported in the same manner as the beam of Example 5.05. Referring to that example, we recall that the given distributed loading was replaced by the two equivalent open-ended loadings shown in Fig. 9.29b and that the following expressions were obtained for the shear and bending moment:

$$V(x) = -1.5\langle x - 0.6 \rangle^1 + 1.5\langle x - 1.8 \rangle^1 + 2.6 - 1.2\langle x - 0.6 \rangle^0$$

$$M(x) = -0.75\langle x - 0.6 \rangle^2 + 0.75\langle x - 1.8 \rangle^2 + 2.6x - 1.2\langle x - 0.6 \rangle^1 - 1.44\langle x - 2.6 \rangle^0$$

Integrating the last expression twice, we obtain

$$EI\theta = -0.25\langle x - 0.6 \rangle^3 + 0.25\langle x - 1.8 \rangle^3 + 1.3x^2 - 0.6\langle x - 0.6 \rangle^2 - 1.44\langle x - 2.6 \rangle^1 + C_1 \quad (9.48)$$

$$EIy = -0.0625\langle x - 0.6 \rangle^4 + 0.0625\langle x - 1.8 \rangle^4 + 0.4333x^3 - 0.2\langle x - 0.6 \rangle^3 - 0.72\langle x - 2.6 \rangle^2 + C_1x + C_2 \quad (9.49)$$

The constants C_1 and C_2 can be determined from the boundary conditions shown in Fig. 9.30. Letting $x = 0$, $y = 0$ in Eq. (9.49) and noting that all the brackets contain negative quantities and, therefore, are equal to zero, we conclude that $C_2 = 0$. Letting now $x = 3.6$, $y = 0$, and $C_2 = 0$ in Eq. (9.49), we write

$$0 = -0.0625\langle 3.0 \rangle^4 + 0.0625\langle 1.8 \rangle^4 + 0.4333(3.6)^3 - 0.2\langle 3.0 \rangle^3 - 0.72\langle 1.0 \rangle^2 + C_1(3.6) + 0$$

Since all the quantities between brackets are positive, the brackets can be replaced by ordinary parentheses. Solving for C_1 , we find $C_1 = -2.692$.

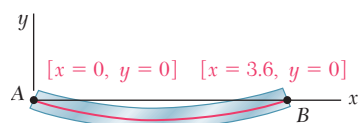


Fig. 9.30

(b) Substituting for C_1 and C_2 into Eq. (9.49) and making $x = x_D = 1.8 \text{ m}$, we find that the deflection at point D is defined by the relation

$$EIy_D = -0.0625\langle 1.2 \rangle^4 + 0.0625\langle 0 \rangle^4 + 0.4333(1.8)^3 - 0.2\langle 1.2 \rangle^3 - 0.72\langle -0.8 \rangle^2 - 2.692(1.8)$$

The last bracket contains a negative quantity and, therefore, is equal to zero. All the other brackets contain positive quantities and can be replaced by ordinary parentheses. We have

$$EIy_D = -0.0625(1.2)^4 + 0.0625(0)^4 + 0.4333(1.8)^3 - 0.2(1.2)^3 - 0 - 2.692(1.8) = -2.794$$

Recalling the given numerical values of E and I , we write

$$(200 \text{ GPa})(6.87 \times 10^{-6} \text{ m}^4)y_D = -2.794 \text{ kN} \cdot \text{m}^3$$

$$y_D = -13.64 \times 10^{-3} \text{ m} = -2.03 \text{ mm}$$

EXAMPLE 9.06

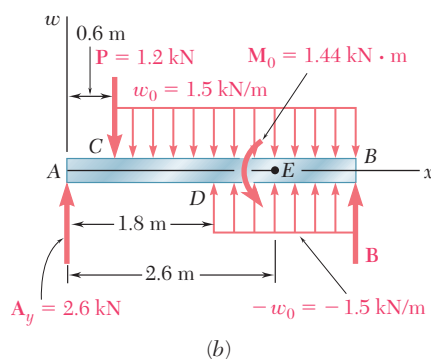
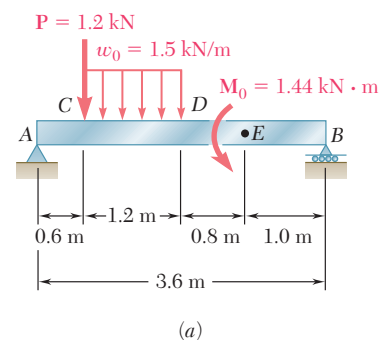
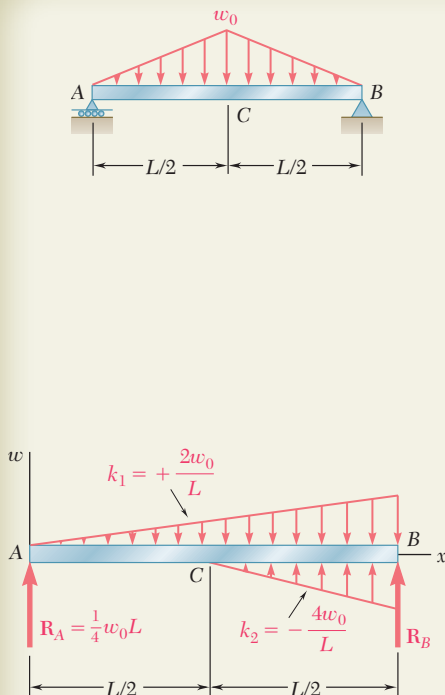


Fig. 9.29



SAMPLE PROBLEM 9.4

For the prismatic beam and loading shown, determine (a) the equation of the elastic curve, (b) the slope at A, (c) the maximum deflection.

SOLUTION

Bending Moment. The equation defining the bending moment of the beam was obtained in Sample Prob. 5.9. Using the modified loading diagram shown, we had [Eq. (3)]:

$$M(x) = -\frac{w_0}{3L}x^3 + \frac{2w_0}{3L}\langle x - \frac{1}{2}L \rangle^3 + \frac{1}{4}w_0Lx$$

a. Equation of the Elastic Curve. Using Eq. (9.4), we write

$$EI \frac{d^2y}{dx^2} = -\frac{w_0}{3L}x^3 + \frac{2w_0}{3L}\langle x - \frac{1}{2}L \rangle^3 + \frac{1}{4}w_0Lx \quad (1)$$

and, integrating twice in x ,

$$EI \theta = -\frac{w_0}{12L}x^4 + \frac{w_0}{6L}\langle x - \frac{1}{2}L \rangle^4 + \frac{w_0L}{8}x^2 + C_1 \quad (2)$$

$$EI y = -\frac{w_0}{60L}x^5 + \frac{w_0}{30L}\langle x - \frac{1}{2}L \rangle^5 + \frac{w_0L}{24}x^3 + C_1x + C_2 \quad (3)$$

Boundary Conditions.

$[x = 0, y = 0]$: Using Eq. (3) and noting that each bracket $\langle \rangle$ contains a negative quantity and, thus, is equal to zero, we find $C_2 = 0$.

$[x = L, y = 0]$: Again using Eq. (3), we write

$$0 = -\frac{w_0L^4}{60} + \frac{w_0}{30L}\left(\frac{L}{2}\right)^5 + \frac{w_0L^4}{24} + C_1L \quad C_1 = -\frac{5}{192}w_0L^3$$

Substituting C_1 and C_2 into Eqs. (2) and (3), we have

$$EI \theta = -\frac{w_0}{12L}x^4 + \frac{w_0}{6L}\langle x - \frac{1}{2}L \rangle^4 + \frac{w_0L}{8}x^2 - \frac{5}{192}w_0L^3 \quad (4)$$

$$EI y = -\frac{w_0}{60L}x^5 + \frac{w_0}{30L}\langle x - \frac{1}{2}L \rangle^5 + \frac{w_0L}{24}x^3 - \frac{5}{192}w_0L^3x \quad (5) \quad \blacktriangleleft$$

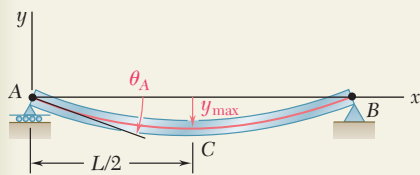
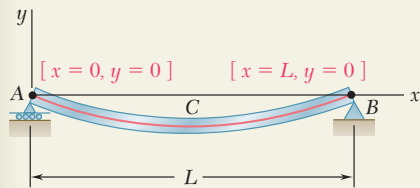
b. Slope at A. Substituting $x = 0$ into Eq. (4), we find

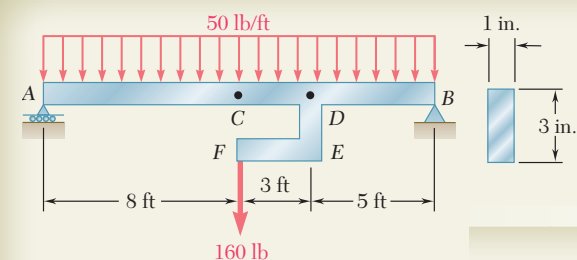
$$EI \theta_A = -\frac{5}{192}w_0L^3 \quad \theta_A = \frac{5w_0L^3}{192EI} \quad \blacktriangleleft$$

c. Maximum Deflection. Because of the symmetry of the supports and loading, the maximum deflection occurs at point C, where $x = \frac{1}{2}L$. Substituting into Eq. (5), we obtain

$$EI y_{\max} = w_0L^4 \left[-\frac{1}{60(32)} + 0 + \frac{1}{24(8)} - \frac{5}{192(2)} \right] = -\frac{w_0L^4}{120}$$

$$y_{\max} = \frac{w_0L^4}{120EI} \downarrow \quad \blacktriangleleft$$





SAMPLE PROBLEM 9.5

The rigid bar DEF is welded at point D to the uniform steel beam AB . For the loading shown, determine (a) the equation of the elastic curve of the beam, (b) the deflection at the midpoint C of the beam. Use $E = 29 \times 10^6$ psi.

SOLUTION

Bending Moment. The equation defining the bending moment of the beam was obtained in Sample Prob. 5.10. Using the modified loading diagram shown and expressing x in feet, we had [Eq. (3)]:

$$M(x) = -25x^2 + 480x - 160\langle x - 11 \rangle^1 - 480\langle x - 11 \rangle^0 \text{ lb} \cdot \text{ft}$$

a. Equation of the Elastic Curve. Using Eq. (8.4), we write

$$EI(d^2y/dx^2) = -25x^2 + 480x - 160\langle x - 11 \rangle^1 - 480\langle x - 11 \rangle^0 \text{ lb} \cdot \text{ft} \quad (1)$$

and, integrating twice in x ,

$$EI \theta = -8.333x^3 + 240x^2 - 80\langle x - 11 \rangle^2 - 480\langle x - 11 \rangle^1 + C_1 \text{ lb} \cdot \text{ft}^2 \quad (2)$$

$$EI y = -2.083x^4 + 80x^3 - 26.67\langle x - 11 \rangle^3 - 240\langle x - 11 \rangle^2 + C_1x + C_2 \text{ lb} \cdot \text{ft}^3 \quad (3)$$

Boundary Conditions.

$[x = 0, y = 0]$: Using Eq. (3) and noting that each bracket $\langle \rangle$ contains a negative quantity and, thus, is equal to zero, we find $C_2 = 0$.

$[x = 16 \text{ ft}, y = 0]$: Again using Eq. (3) and noting that each bracket contains a positive quantity and, thus, can be replaced by a parenthesis, we write

$$0 = -2.083(16)^4 + 80(16)^3 - 26.67(5)^3 - 240(5)^2 + C_1(16)$$

$$C_1 = -11.36 \times 10^3$$

Substituting the values found for C_1 and C_2 into Eq. (3), we have

$$EI y = -2.083x^4 + 80x^3 - 26.67\langle x - 11 \rangle^3 - 240\langle x - 11 \rangle^2 - 11.36 \times 10^3 x \text{ lb} \cdot \text{ft}^3 \quad (3') \quad \blacktriangleleft$$

To determine EI , we recall that $E = 29 \times 10^6$ psi and compute

$$I = \frac{1}{12}bh^3 = \frac{1}{12}(1 \text{ in.})(3 \text{ in.})^3 = 2.25 \text{ in}^4$$

$$EI = (29 \times 10^6 \text{ psi})(2.25 \text{ in}^4) = 65.25 \times 10^6 \text{ lb} \cdot \text{in}^2$$

However, since all previous computations have been carried out with feet as the unit of length, we write

$$EI = (65.25 \times 10^6 \text{ lb} \cdot \text{in}^2)(1 \text{ ft}/12 \text{ in.})^2 = 453.1 \times 10^3 \text{ lb} \cdot \text{ft}^2$$

b. Deflection at Midpoint C . Making $x = 8 \text{ ft}$ in Eq. (3'), we write

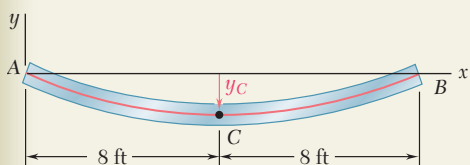
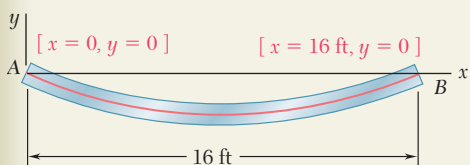
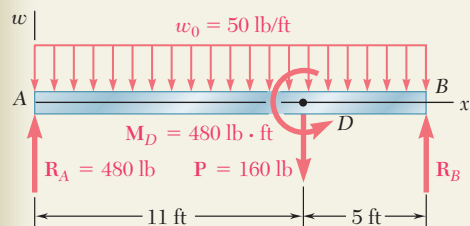
$$EI y_C = -2.083(8)^4 + 80(8)^3 - 26.67\langle -3 \rangle^3 - 240\langle -3 \rangle^2 - 11.36 \times 10^3(8)$$

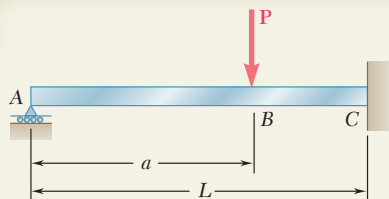
Noting that each bracket is equal to zero and substituting for EI its numerical value, we have

$$(453.1 \times 10^3 \text{ lb} \cdot \text{ft}^2)y_C = -58.45 \times 10^3 \text{ lb} \cdot \text{ft}^3$$

and, solving for y_C : $y_C = -0.1290 \text{ ft} \quad y_C = -1.548 \text{ in.} \quad \blacktriangleleft$

Note that the deflection obtained is *not* the maximum deflection.





SAMPLE PROBLEM 9.6

For the uniform beam ABC , (a) express the reaction at A in terms of P , L , a , E , and I , (b) determine the reaction at A and the deflection under the load when $a = L/2$.

SOLUTION

Reactions. For the given vertical load P the reactions are as shown. We note that they are statically indeterminate.

Shear and Bending Moment. Using a step function to represent the contribution of P to the shear, we write

$$V(x) = R_A - P\langle x - a \rangle^0$$

Integrating in x , we obtain the bending moment:

$$M(x) = R_A x - P\langle x - a \rangle^1$$

Equation of the Elastic Curve. Using Eq. (9.4), we write

$$EI \frac{d^2 y}{dx^2} = R_A x - P\langle x - a \rangle^1$$

Integrating twice in x ,

$$EI \frac{dy}{dx} = EI \theta = \frac{1}{2} R_A x^2 - \frac{1}{2} P\langle x - a \rangle^2 + C_1$$

$$EI y = \frac{1}{6} R_A x^3 - \frac{1}{6} P\langle x - a \rangle^3 + C_1 x + C_2$$

Boundary Conditions. Noting that the bracket $\langle x - a \rangle$ is equal to zero for $x = 0$, and to $(L - a)$ for $x = L$, we write

$$[x = 0, y = 0]: \quad C_2 = 0 \quad (1)$$

$$[x = L, \theta = 0]: \quad \frac{1}{2} R_A L^2 - \frac{1}{2} P(L - a)^2 + C_1 = 0 \quad (2)$$

$$[x = L, y = 0]: \quad \frac{1}{6} R_A L^3 - \frac{1}{6} P(L - a)^3 + C_1 L + C_2 = 0 \quad (3)$$

a. Reaction at A. Multiplying Eq. (2) by L , subtracting Eq. (3) member by member from the equation obtained, and noting that $C_2 = 0$, we have

$$\frac{1}{3} R_A L^3 - \frac{1}{6} P(L - a)^2 [3L - (L - a)] = 0$$

$$R_A = P \left(1 - \frac{a}{L} \right)^2 \left(1 + \frac{a}{2L} \right) \uparrow \quad \blacktriangleleft$$

We note that the reaction is independent of E and I .

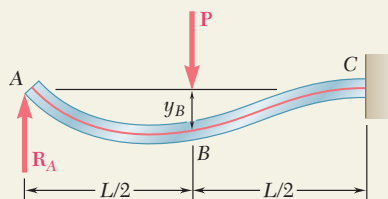
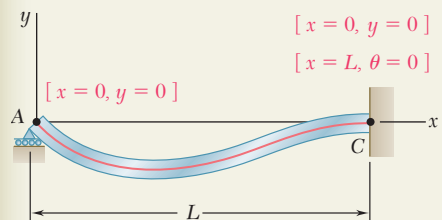
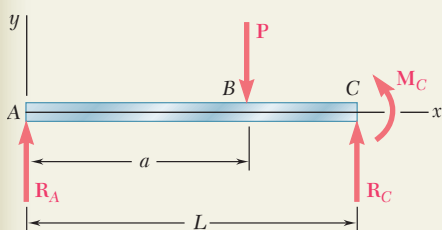
b. Reaction at A and Deflection at B when $a = \frac{1}{2}L$. Making $a = \frac{1}{2}L$ in the expression obtained for R_A , we have

$$R_A = P \left(1 - \frac{1}{2} \right)^2 \left(1 + \frac{1}{4} \right) = 5P/16 \quad R_A = \frac{5}{16} P \uparrow \quad \blacktriangleleft$$

Substituting $a = L/2$ and $R_A = 5P/16$ into Eq. (2) and solving for C_1 , we find $C_1 = -PL^2/32$. Making $x = L/2$, $C_1 = -PL^2/32$, and $C_2 = 0$ in the expression obtained for y , we have

$$y_B = -\frac{7PL^3}{768EI} \quad y_B = \frac{7PL^3}{768EI} \downarrow \quad \blacktriangleleft$$

Note that the deflection obtained is *not* the maximum deflection.



PROBLEMS

Use singularity functions to solve the following problems and assume that the flexural rigidity EI of each beam is constant.

9.35 and 9.36 For the beam and loading shown, determine (a) the equation of the elastic curve, (b) the slope at end A, (c) the deflection of point C.

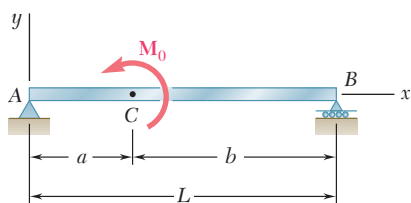


Fig. P9.35

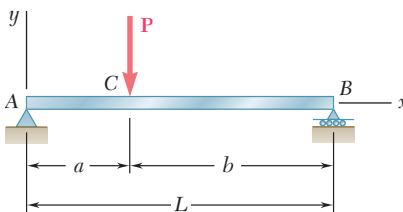


Fig. P9.36

9.37 and 9.38 For the beam and loading shown, determine (a) the equation of the elastic curve, (b) the slope at the free end, (c) the deflection of the free end.

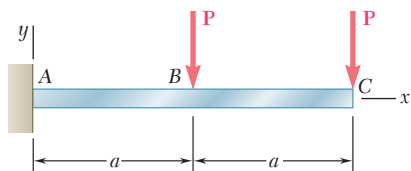


Fig. P9.37

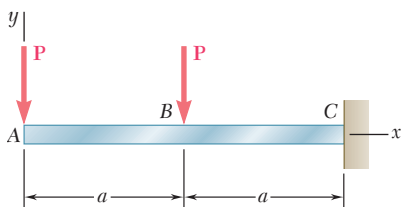


Fig. P9.38

9.39 and 9.40 For the beam and loading shown, determine (a) the deflection at end A, (b) the deflection at point C, (c) the slope at end D.

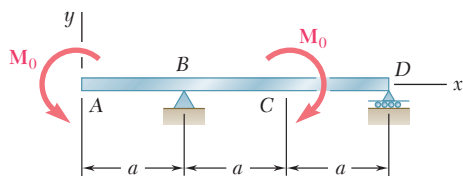


Fig. P9.39

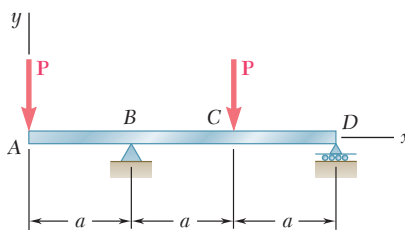


Fig. P9.40

9.41 For the beam and loading shown, determine (a) the equation of the elastic curve, (b) the deflection at the midpoint C .

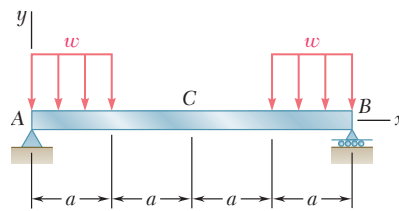


Fig. P9.41

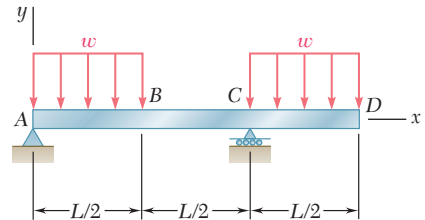


Fig. P9.42

9.42 For the beam and loading shown, determine (a) the equation of the elastic curve, (b) the deflection at point B , (c) the deflection at point D .

9.43 and 9.44 For the beam and loading shown, determine (a) the equation of the elastic curve, (b) the deflection at the midpoint C .

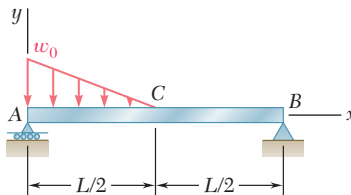


Fig. P9.43

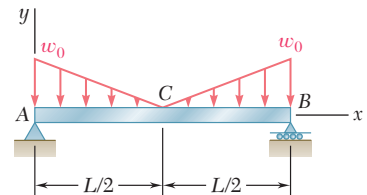


Fig. P9.44

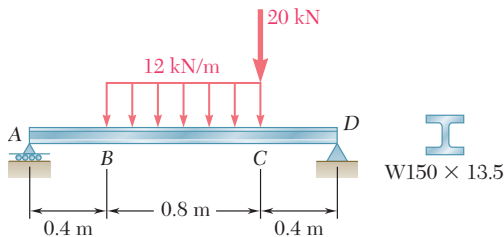


Fig. P9.45

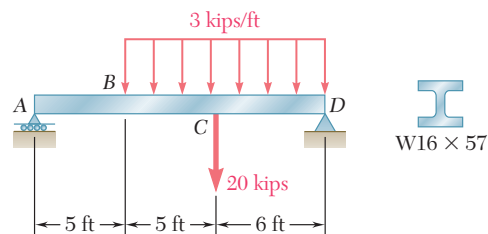


Fig. P9.46

9.46 For the beam and loading shown, determine (a) the slope at end A , (b) the deflection at point C . Use $E = 29 \times 10^6$ psi.

9.47 For the beam and loading shown, determine (a) the slope at end A , (b) the deflection at the midpoint C . Use $E = 200$ GPa.

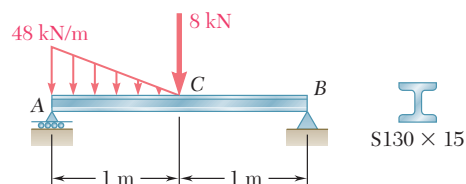


Fig. P9.47

9.48 For the timber beam and loading shown, determine (a) the slope at end A, (b) the deflection at the midpoint C. Use $E = 1.6 \times 10^6$ psi.

9.49 and 9.50 For the beam and loading shown, determine (a) the reaction at the roller support, (b) the deflection at point C.

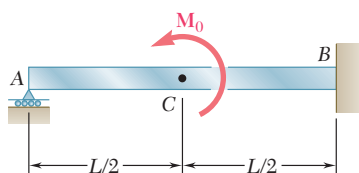


Fig. P9.49

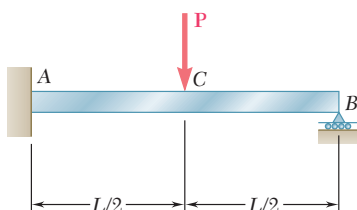


Fig. P9.50

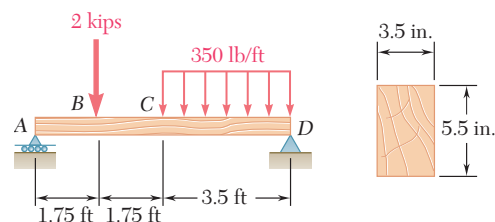


Fig. P9.48

9.51 and 9.52 For the beam and loading shown, determine (a) the reaction at the roller support, (b) the deflection at point B.

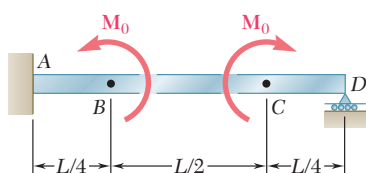


Fig. P9.51

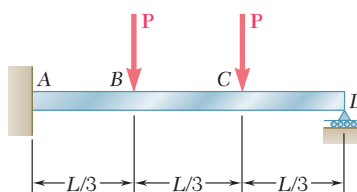


Fig. P9.52

9.53 For the beam and loading shown, determine (a) the reaction at point C, (b) the deflection at point B. Use $E = 200$ GPa.

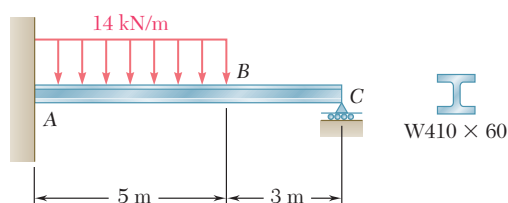


Fig. P9.53

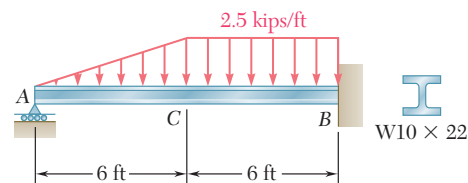


Fig. P9.54

9.54 For the beam and loading shown, determine (a) the reaction at point A, (b) the deflection at point C. Use $E = 29 \times 10^6$ psi.

9.55 For the beam and loading shown, determine (a) the reaction at point C, (b) the deflection at point B. Use $E = 29 \times 10^6$ psi.

9.56 For the beam shown and knowing that $P = 40$ kN, determine (a) the reaction at point E, (b) the deflection at point C. Use $E = 200$ GPa.

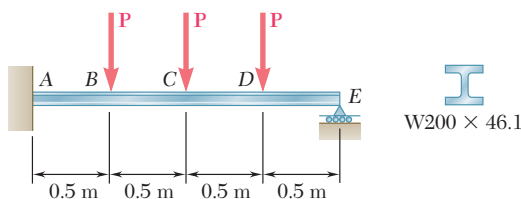


Fig. P9.56

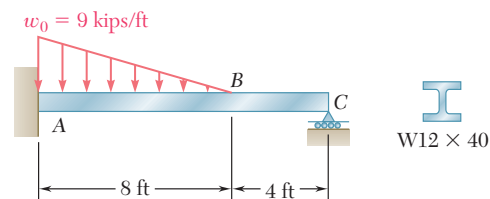


Fig. P9.55

9.57 and 9.58 For the beam and loading shown, determine (a) the reaction at point A, (b) the deflection at midpoint C.

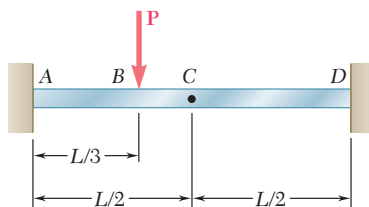


Fig. P9.57

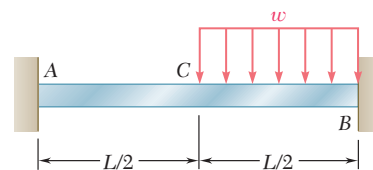


Fig. P9.58

9.59 through 9.62 For the beam and loading indicated, determine the magnitude and location of the largest downward deflection.

9.59 Beam and loading of Prob. 9.45.

9.60 Beam and loading of Prob. 9.46.

9.61 Beam and loading of Prob. 9.47.

9.62 Beam and loading of Prob. 9.48.

9.63 The rigid bars BF and DH are welded to the rolled-steel beam AE as shown. Determine for the loading shown (a) the deflection at point B, (b) the deflection at midpoint C of the beam. Use $E = 200$ GPa.

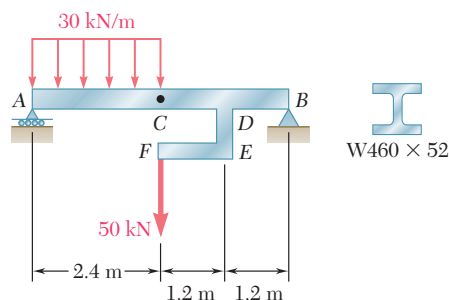


Fig. P9.64

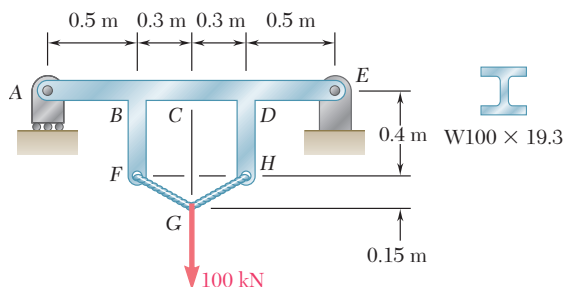


Fig. P9.63

9.64 The rigid bar DEF is welded at point D to the rolled-steel beam AB . For the loading shown, determine (a) the slope at point A, (b) the deflection at midpoint C of the beam. Use $E = 200$ GPa.

9.7 METHOD OF SUPERPOSITION

When a beam is subjected to several concentrated or distributed loads, it is often found convenient to compute separately the slope and deflection caused by each of the given loads. The slope and deflection due to the combined loads are then obtained by applying the principle of superposition (Sec. 2.12) and adding the values of the slope or deflection corresponding to the various loads.

Determine the slope and deflection at D for the beam and loading shown (Fig. 9.31), knowing that the flexural rigidity of the beam is $EI = 100 \text{ MN} \cdot \text{m}^2$.

The slope and deflection at any point of the beam can be obtained by superposing the slopes and deflections caused respectively by the concentrated load and by the distributed load (Fig. 9.32).

Since the concentrated load in Fig. 9.32b is applied at quarter span, we can use the results obtained for the beam and loading of Example 9.03 and write

$$(\theta_D)_P = -\frac{PL^2}{32EI} = -\frac{(150 \times 10^3)(8)^2}{32(100 \times 10^6)} = -3 \times 10^{-3} \text{ rad}$$

$$(y_D)_P = -\frac{3PL^3}{256EI} = -\frac{3(150 \times 10^3)(8)^3}{256(100 \times 10^6)} = -9 \times 10^{-3} \text{ m}$$

$$= -9 \text{ mm}$$

On the other hand, recalling the equation of the elastic curve obtained for a uniformly distributed load in Example 9.02, we express the deflection in Fig. 9.32c as

$$y = \frac{w}{24EI}(-x^4 + 2Lx^3 - L^3x) \quad (9.50)$$

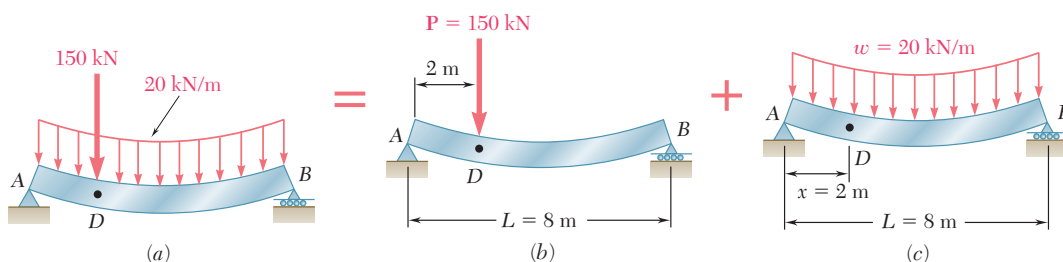


Fig. 9.32

and, differentiating with respect to x ,

$$\theta = \frac{dy}{dx} = \frac{w}{24EI}(-4x^3 + 6Lx^2 - L^3) \quad (9.51)$$

Making $w = 20 \text{ kN/m}$, $x = 2 \text{ m}$, and $L = 8 \text{ m}$ in Eqs. (9.51) and (9.50), we obtain

$$(\theta_D)_w = \frac{20 \times 10^3}{24(100 \times 10^6)}(-352) = -2.93 \times 10^{-3} \text{ rad}$$

$$(y_D)_w = \frac{20 \times 10^3}{24(100 \times 10^6)}(-912) = -7.60 \times 10^{-3} \text{ m}$$

$$= -7.60 \text{ mm}$$

Combining the slopes and deflections produced by the concentrated and the distributed loads, we have

$$\theta_D = (\theta_D)_P + (\theta_D)_w = -3 \times 10^{-3} - 2.93 \times 10^{-3}$$

$$= -5.93 \times 10^{-3} \text{ rad}$$

$$y_D = (y_D)_P + (y_D)_w = -9 \text{ mm} - 7.60 \text{ mm} = -16.60 \text{ mm}$$

EXAMPLE 9.07

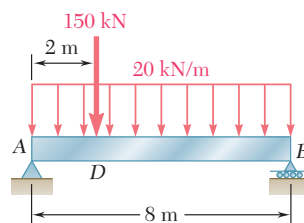


Fig. 9.31

To facilitate the task of practicing engineers, most structural and mechanical engineering handbooks include tables giving the deflections and slopes of beams for various loadings and types of support. Such a table will be found in Appendix D. We note that the slope and deflection of the beam of Fig. 9.31 could have been determined from that table. Indeed, using the information given under cases 5 and 6, we could have expressed the deflection of the beam for any value $x \leq L/4$. Taking the derivative of the expression obtained in this way would have yielded the slope of the beam over the same interval. We also note that the slope at both ends of the beam can be obtained by simply adding the corresponding values given in the table. However, the maximum deflection of the beam of Fig. 9.31 *cannot* be obtained by adding the maximum deflections of cases 5 and 6, since these deflections occur at different points of the beam.[†]

9.8 APPLICATION OF SUPERPOSITION TO STATICALLY INDETERMINATE BEAMS

We often find it convenient to use the method of superposition to determine the reactions at the supports of a statically indeterminate beam. Considering first the case of a beam indeterminate to the first degree (cf. Sec. 9.5), such as the beam shown in Photo 9.3, we follow the approach described in Sec. 2.9. We designate one of the reactions as redundant and eliminate or modify accordingly the corresponding support. The redundant reaction is then treated as an unknown load that, together with the other loads, must produce deformations that are compatible with the original supports. The slope or deflection at the point where the support has been modified or eliminated is obtained by computing separately the deformations caused by the given loads and by the redundant reaction, and by superposing the results obtained. Once the reactions at the supports have been found, the slope and deflection can be determined in the usual way at any other point of the beam.



Photo 9.3 The continuous beams supporting this highway overpass have three supports and are thus statically indeterminate.

[†]An approximate value of the maximum deflection of the beam can be obtained by plotting the values of y corresponding to various values of x . The determination of the exact location and magnitude of the maximum deflection would require setting equal to zero the expression obtained for the slope of the beam and solving this equation for x .

Determine the reactions at the supports for the prismatic beam and loading shown in Fig. 9.33. (This is the same beam and loading as in Example 9.05 of Sec. 9.5.)

EXAMPLE 9.08

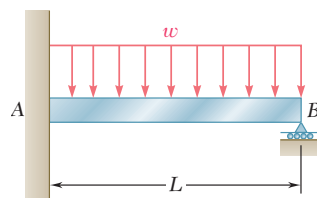


Fig. 9.33

We consider the reaction at B as redundant and release the beam from the support. The reaction \mathbf{R}_B is now considered as an unknown load (Fig. 9.34a) and will be determined from the condition that the deflection of the beam at B must be zero. The solution is carried out by considering separately the deflection $(y_B)_w$ caused at B by the uniformly distributed load w (Fig. 9.34b) and the deflection $(y_B)_R$ produced at the same point by the redundant reaction \mathbf{R}_B (Fig. 9.34c).

From the table of Appendix D (cases 2 and 1), we find that

$$(y_B)_w = -\frac{wL^4}{8EI} \quad (y_B)_R = +\frac{R_B L^3}{3EI}$$

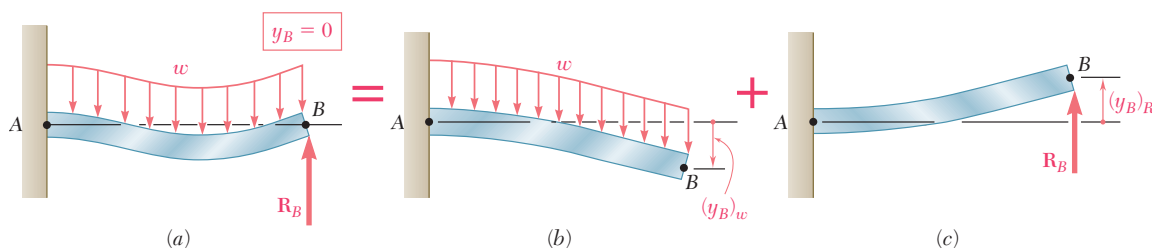


Fig. 9.34

Writing that the deflection at B is the sum of these two quantities and that it must be zero, we have

$$y_B = (y_B)_w + (y_B)_R = 0$$

$$y_B = -\frac{wL^4}{8EI} + \frac{R_B L^3}{3EI} = 0$$

and, solving for R_B , $R_B = \frac{3}{8}wL$ $\mathbf{R}_B = \frac{3}{8}wL \uparrow$

Drawing the free-body diagram of the beam (Fig. 9.35) and writing the corresponding equilibrium equations, we have

$$+\uparrow \sum F_y = 0: \quad R_A + R_B - wL = 0 \quad (9.52)$$

$$R_A = wL - R_B = wL - \frac{3}{8}wL = \frac{5}{8}wL$$

$$\mathbf{R}_A = \frac{5}{8}wL \uparrow$$

$$+\curvearrowright \sum M_A = 0: \quad M_A + R_B L - (wL)\left(\frac{1}{2}L\right) = 0 \quad (9.53)$$

$$M_A = \frac{1}{2}wL^2 - R_B L = \frac{1}{2}wL^2 - \frac{3}{8}wL^2 = \frac{1}{8}wL^2$$

$$\mathbf{M}_A = \frac{1}{8}wL^2 \curvearrowright$$

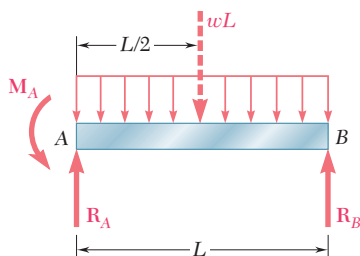


Fig. 9.35

Alternative Solution. We may consider the couple exerted at the fixed end A as redundant and replace the fixed end by a pin-and-bracket support. The couple \mathbf{M}_A is now considered as an unknown load (Fig. 9.36a) and will be determined from the condition that the slope of the beam at A must be zero. The solution is carried out by considering separately the slope $(\theta_A)_w$ caused at A by the uniformly distributed load w (Fig. 9.36b) and the slope $(\theta_A)_M$ produced at the same point by the unknown couple \mathbf{M}_A (Fig. 9.36c).

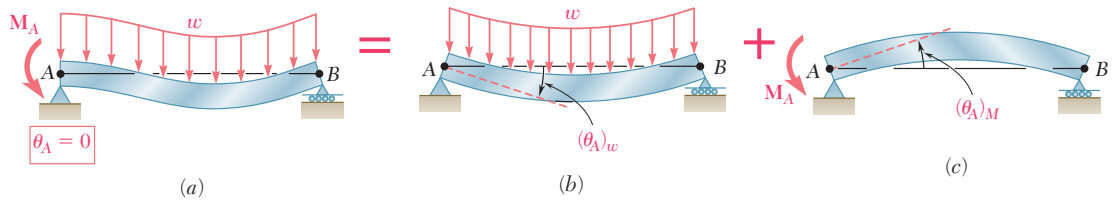


Fig. 9.36

Using the table of Appendix D (cases 6 and 7), and noting that in case 7, A and B must be interchanged, we find that

$$(\theta_A)_w = -\frac{wL^3}{24EI} \quad (\theta_A)_M = \frac{M_AL}{3EI}$$

Writing that the slope at A is the sum of these two quantities and that it must be zero, we have

$$\theta_A = (\theta_A)_w + (\theta_A)_M = 0$$

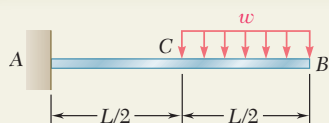
$$\theta_A = -\frac{wL^3}{24EI} + \frac{M_AL}{3EI} = 0$$

and, solving for M_A ,

$$M_A = \frac{1}{8}wL^2 \quad \mathbf{M}_A = \frac{1}{8}wL^2 \mathbf{j}$$

The values of R_A and R_B may then be found from the equilibrium equations (9.52) and (9.53).

The beam considered in the preceding example was indeterminate to the first degree. In the case of a beam indeterminate to the second degree (cf. Sec. 9.5), two reactions must be designated as redundant, and the corresponding supports must be eliminated or modified accordingly. The redundant reactions are then treated as unknown loads which, simultaneously and together with the other loads, must produce deformations which are compatible with the original supports. (See Sample Prob. 9.9.)

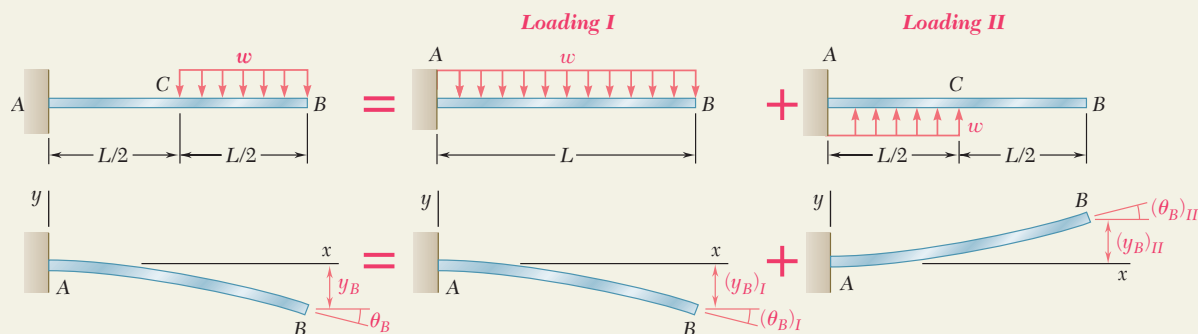


SAMPLE PROBLEM 9.7

For the beam and loading shown, determine the slope and deflection at point B.

SOLUTION

Principle of Superposition. The given loading can be obtained by superposing the loadings shown in the following “picture equation.” The beam AB is, of course, the same in each part of the figure.



For each of the loadings I and II, we now determine the slope and deflection at B by using the table of *Beam Deflections and Slopes* in Appendix D.

Loading I

$$(\theta_B)_I = -\frac{wL^3}{6EI} \qquad (y_B)_I = -\frac{wL^4}{8EI}$$

Loading II

$$(\theta_C)_{II} = +\frac{w(L/2)^3}{6EI} = +\frac{wL^3}{48EI} \qquad (y_C)_{II} = +\frac{w(L/2)^4}{8EI} = +\frac{wL^4}{128EI}$$

In portion CB, the bending moment for loading II is zero and thus the elastic curve is a straight line.

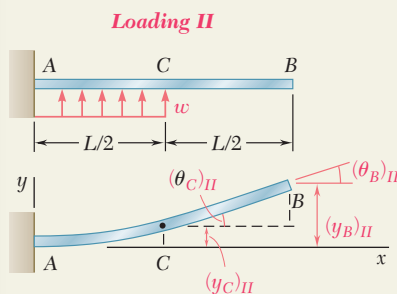
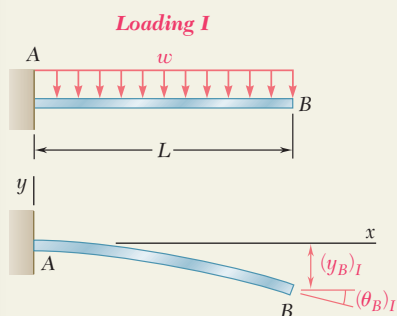
$$\begin{aligned} (\theta_B)_{II} &= (\theta_C)_{II} = +\frac{wL^3}{48EI} & (y_B)_{II} &= (y_C)_{II} + (\theta_C)_{II}\left(\frac{L}{2}\right) \\ & & &= \frac{wL^4}{128EI} + \frac{wL^3}{48EI}\left(\frac{L}{2}\right) = +\frac{7wL^4}{384EI} \end{aligned}$$

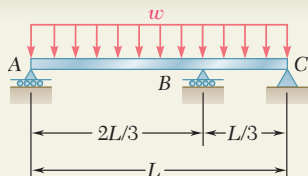
Slope at Point B

$$\theta_B = (\theta_B)_I + (\theta_B)_{II} = -\frac{wL^3}{6EI} + \frac{wL^3}{48EI} = -\frac{7wL^3}{48EI} \quad \theta_B = \frac{7wL^3}{48EI} \quad \swarrow \blacktriangleleft$$

Deflection at B

$$y_B = (y_B)_I + (y_B)_{II} = -\frac{wL^4}{8EI} + \frac{7wL^4}{384EI} = -\frac{41wL^4}{384EI} \quad y_B = \frac{41wL^4}{384EI} \quad \downarrow \blacktriangleleft$$



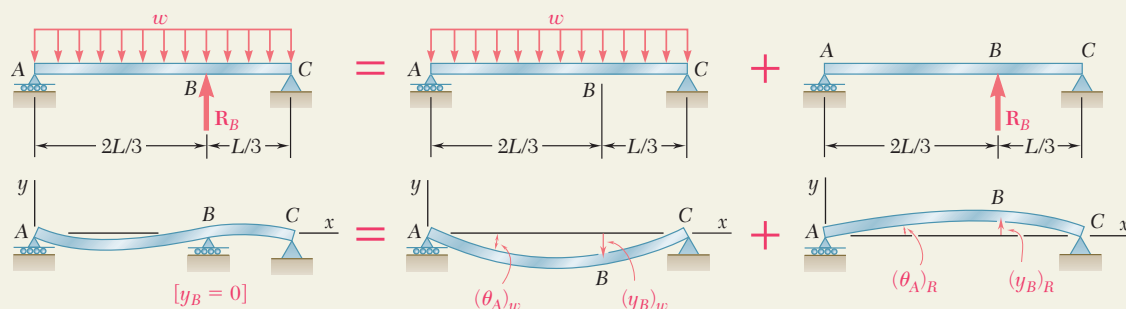


SAMPLE PROBLEM 9.8

For the uniform beam and loading shown, determine (a) the reaction at each support, (b) the slope at end A.

SOLUTION

Principle of Superposition. The reaction \mathbf{R}_B is designated as redundant and considered as an unknown load. The deflections due to the distributed load and to the reaction \mathbf{R}_B are considered separately as shown below.



For each loading the deflection at point B is found by using the table of *Beam Deflections and Slopes* in Appendix D.

Distributed Loading. We use case 6, Appendix D

$$y = -\frac{w}{24EI} (x^4 - 2Lx^3 + L^3x)$$

At point B, $x = \frac{2}{3}L$:

$$(y_B)_w = -\frac{w}{24EI} \left[\left(\frac{2}{3}L \right)^4 - 2L \left(\frac{2}{3}L \right)^3 + L^3 \left(\frac{2}{3}L \right) \right] = -0.01132 \frac{wL^4}{EI}$$

Redundant Reaction Loading. From case 5, Appendix D, with $a = \frac{2}{3}L$ and $b = \frac{1}{3}L$, we have

$$(y_B)_R = -\frac{Pa^2b^2}{3EIL} + \frac{R_B}{3EIL} \left(\frac{2}{3}L \right)^2 \left(\frac{L}{3} \right)^2 = 0.01646 \frac{R_B L^3}{EI}$$

a. Reactions at Supports. Recalling that $y_B = 0$, we write

$$y_B = (y_B)_w + (y_B)_R$$

$$0 = -0.01132 \frac{wL^4}{EI} + 0.01646 \frac{R_B L^3}{EI} \quad \mathbf{R_B = 0.688wL \uparrow} \quad \blacktriangleleft$$

Since the reaction R_B is now known, we may use the methods of statics to determine the other reactions: $\mathbf{R_A = 0.271wL \uparrow} \quad \mathbf{R_C = 0.0413wL \uparrow} \quad \blacktriangleleft$

b. Slope at End A. Referring again to Appendix D, we have

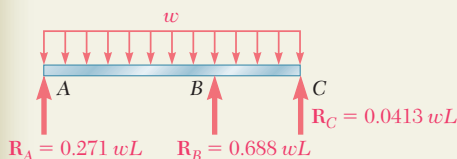
$$\text{Distributed Loading.} \quad (\theta_A)_w = -\frac{wL^3}{24EI} = -0.04167 \frac{wL^3}{EI}$$

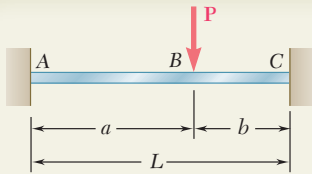
Redundant Reaction Loading. For $P = -R_B = -0.688wL$ and $b = \frac{1}{3}L$

$$(\theta_A)_R = -\frac{Pb(L^2 - b^2)}{6EIL} = +\frac{0.688wL}{6EIL} \left(\frac{L}{3} \right) \left[L^2 - \left(\frac{L}{3} \right)^2 \right] \quad (\theta_A)_R = 0.03398 \frac{wL^3}{EI}$$

Finally, $\theta_A = (\theta_A)_w + (\theta_A)_R$

$$\theta_A = -0.04167 \frac{wL^3}{EI} + 0.03398 \frac{wL^3}{EI} = -0.00769 \frac{wL^3}{EI} \quad \theta_A = 0.00769 \frac{wL^3}{EI} \quad \blacktriangleleft$$



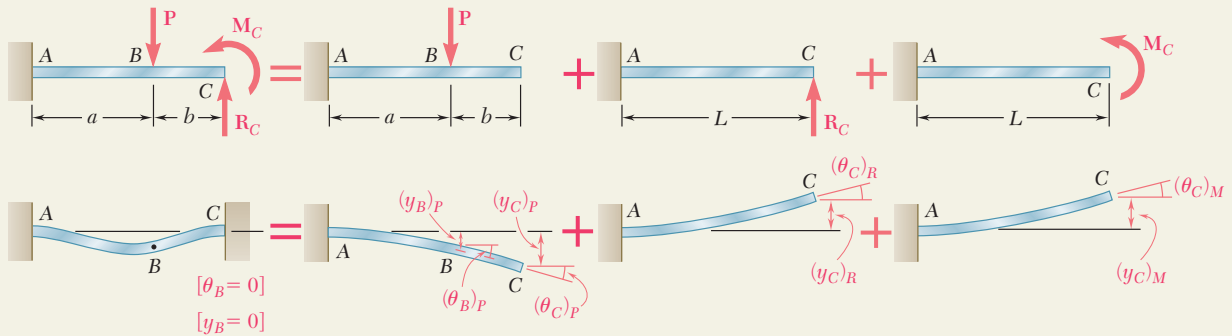


SAMPLE PROBLEM 9.9

For the beam and loading shown, determine the reaction at the fixed support C.

SOLUTION

Principle of Superposition. Assuming the axial force in the beam to be zero, the beam ABC is indeterminate to the second degree and we choose two reaction components as redundant, namely, the vertical force R_C and the couple M_C . The deformations caused by the given load P , the force R_C , and the couple M_C will be considered separately as shown.



For each load, the slope and deflection at point C will be found by using the table of *Beam Deflections and Slopes* in Appendix D.

Load P . We note that, for this loading, portion BC of the beam is straight.

$$(\theta_C)_P = (\theta_B)_P = -\frac{Pa^2}{2EI} \quad (y_C)_P = (y_B)_P + (\theta_B)_P b = -\frac{Pa^3}{3EI} - \frac{Pa^2}{2EI}b = -\frac{Pa^2}{6EI}(2a + 3b)$$

$$\text{Force } R_C \quad (\theta_C)_R = +\frac{R_C L^2}{2EI} \quad (y_C)_R = +\frac{R_C L^3}{3EI}$$

$$\text{Couple } M_C \quad (\theta_C)_M = +\frac{M_C L}{EI} \quad (y_C)_M = +\frac{M_C L^2}{2EI}$$

Boundary Conditions. At end C the slope and deflection must be zero:

$$[x = L, \theta_C = 0]: \quad \theta_C = (\theta_C)_P + (\theta_C)_R + (\theta_C)_M = 0 = -\frac{Pa^2}{2EI} + \frac{R_C L^2}{2EI} + \frac{M_C L}{EI} \quad (1)$$

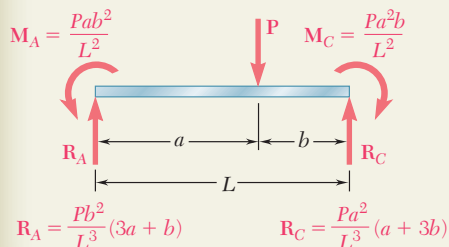
$$[x = L, y_C = 0]: \quad y_C = (y_C)_P + (y_C)_R + (y_C)_M = 0 = -\frac{Pa^2}{6EI}(2a + 3b) + \frac{R_C L^3}{3EI} + \frac{M_C L^2}{2EI} \quad (2)$$

Reaction Components at C. Solving simultaneously Eqs. (1) and (2), we find after reductions

$$R_C = +\frac{Pa^2}{L^3}(a + 3b) \quad R_C = \frac{Pa^2}{L^3}(a + 3b) \uparrow \blacktriangleleft$$

$$M_C = -\frac{Pa^2 b}{L^2} \quad M_C = \frac{Pa^2 b}{L^2} \downarrow \blacktriangleleft$$

Using the methods of statics, we can now determine the reaction at A.



PROBLEMS

Use the method of superposition to solve the following problems and assume that the flexural rigidity EI of each beam is constant.

9.65 through 9.68 For the cantilever beam and loading shown, determine the slope and deflection at the free end.

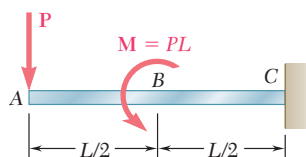


Fig. P9.65

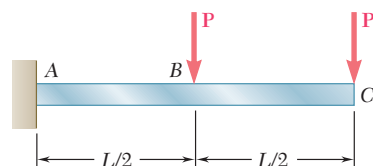


Fig. P9.66

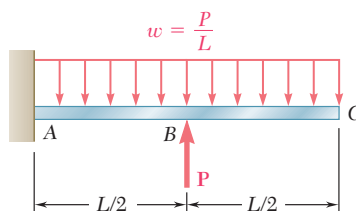


Fig. P9.67

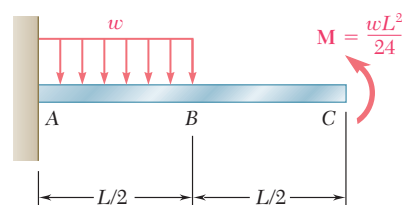


Fig. P9.68

9.69 through 9.72 For the beam and loading shown, determine (a) the deflection at C, (b) the slope at end A.

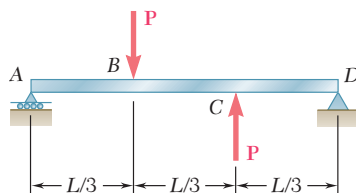


Fig. P9.69

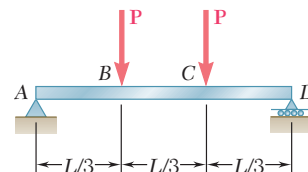


Fig. P9.70

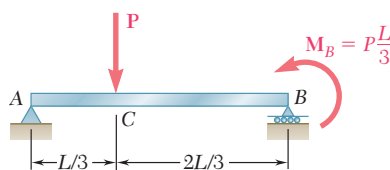


Fig. P9.71

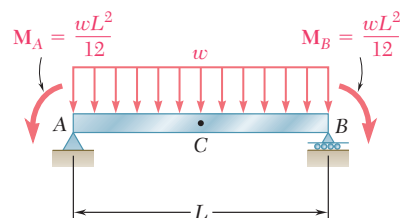


Fig. P9.72

- 9.73** For the cantilever beam and loading shown, determine the slope and deflection at end C . Use $E = 200$ GPa.

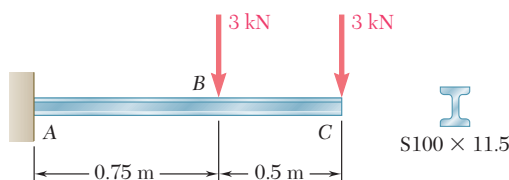


Fig. P9.73 and P9.74

- 9.74** For the cantilever beam and loading shown, determine the slope and deflection at point B . Use $E = 200$ GPa.

- 9.75** For the cantilever beam and loading shown, determine the slope and deflection at end A . Use $E = 29 \times 10^6$ psi.

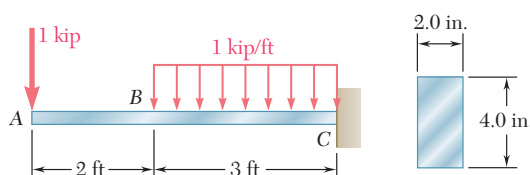


Fig. P9.75 and P9.76

- 9.76** For the cantilever beam and loading shown, determine the slope and deflection at point B . Use $E = 29 \times 10^6$ psi.

- 9.77 and 9.78** For the beam and loading shown, determine (a) the slope at end A , (b) the deflection at point C . Use $E = 200$ GPa.

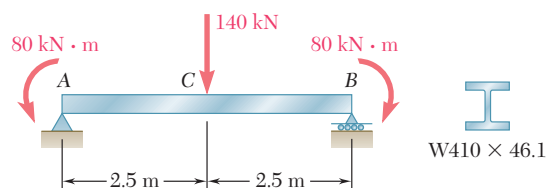


Fig. P9.77

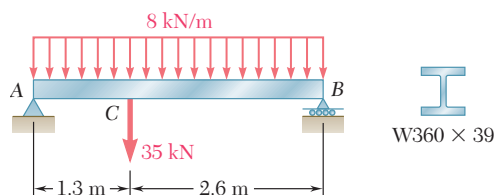


Fig. P9.78

- 9.79 and 9.80** For the uniform beam shown, determine the reaction at each of the three supports.

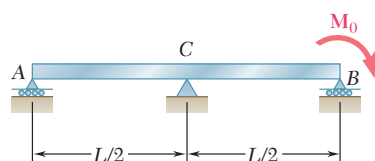


Fig. P9.79

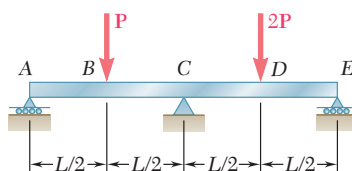


Fig. P9.80

9.81 and 9.82 For the uniform beam shown, determine (a) the reaction at A, (b) the reaction at B.

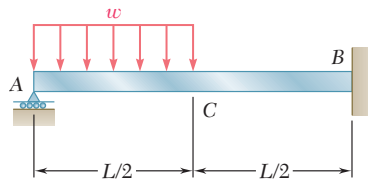


Fig. P9.81

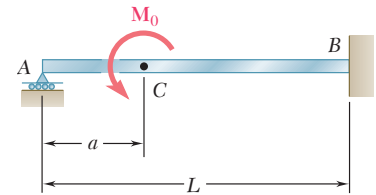


Fig. P9.82

9.83 and 9.84 For the beam shown, determine the reaction at B.

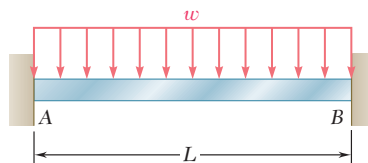


Fig. P9.83

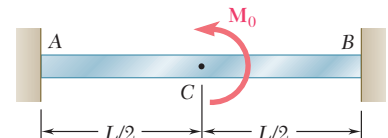


Fig. P9.84

9.85 A central beam BD is joined at hinges to two cantilever beams AB and DE . All beams have the cross section shown. For the loading shown, determine the largest w so that the deflection at C does not exceed 3 mm. Use $E = 200$ GPa.

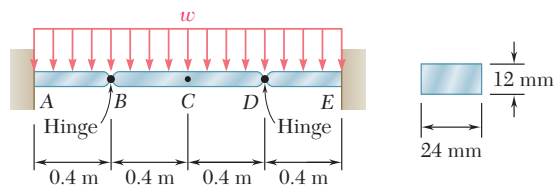


Fig. P9.85

9.86 The two beams shown have the same cross section and are joined by a hinge at C . For the loading shown, determine (a) the slope at point A, (b) the deflection at point B. Use $E = 29 \times 10^6$ psi.

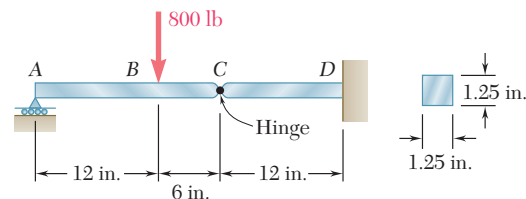


Fig. P9.86

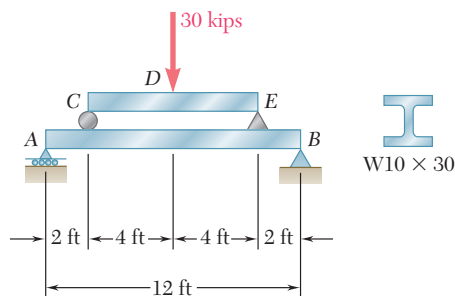


Fig. P9.87

9.87 Beam CE rests on beam AB as shown. Knowing that a $W10 \times 30$ rolled-steel shape is used for each beam, determine for the loading shown the deflection at point D . Use $E = 29 \times 10^6$ psi.

9.88 Beam AC rests on the cantilever beam DE as shown. Knowing that a $W410 \times 38.8$ rolled-steel shape is used for each beam, determine for the loading shown (a) the deflection at point B , (b) the deflection at point D . Use $E = 200$ GPa.

9.89 Before the 2-kip/ft load is applied, a gap, $\delta_0 = 0.8$ in., exists between the $W16 \times 40$ beam and the support at C . Knowing that $E = 29 \times 10^6$ psi, determine the reaction at each support after the uniformly distributed load is applied.

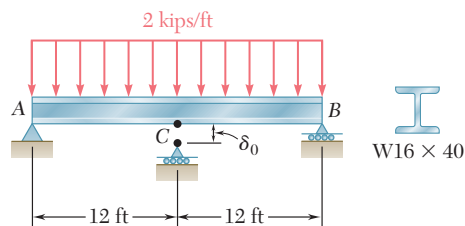


Fig. P9.89

9.90 The cantilever beam BC is attached to the steel cable AB as shown. Knowing that the cable is initially taut, determine the tension in the cable caused by the distributed load shown. Use $E = 200$ GPa.

9.91 Before the load P was applied, a gap, $\delta_0 = 0.5$ mm, existed between the cantilever beam AC and the support at B . Knowing that $E = 200$ GPa, determine the magnitude of P for which the deflection at C is 1 mm.

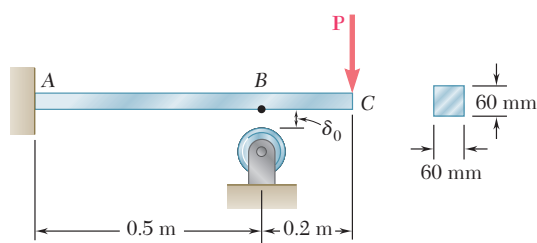


Fig. P9.91

9.92 For the loading shown, knowing that beams AC and BD have the same flexural rigidity, determine the reaction at B .

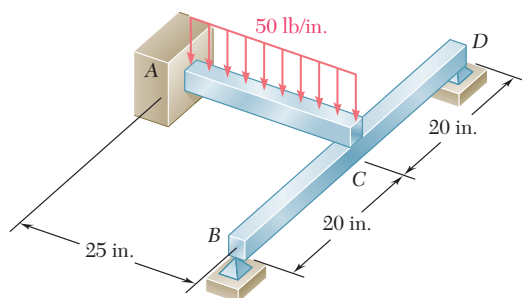


Fig. P9.92

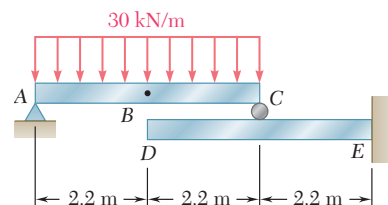


Fig. P9.88

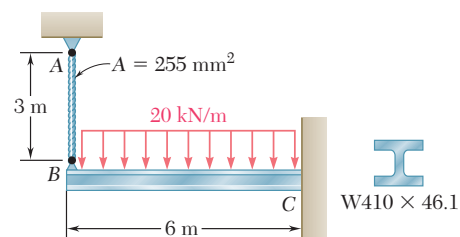


Fig. P9.90

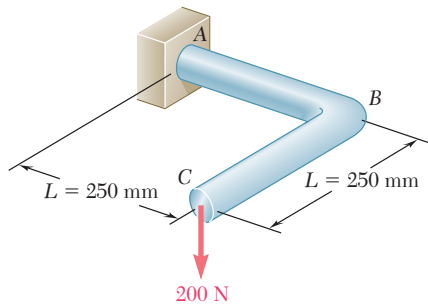


Fig. P9.94

- 9.93** A $\frac{7}{8}$ -in.-diameter rod BC is attached to the lever AB and to the fixed support at C . Lever AB has a uniform cross section $\frac{3}{8}$ in. thick and 1 in. deep. For the loading shown, determine the deflection of point A . Use $E = 29 \times 10^6$ psi and $G = 11.2 \times 10^6$ psi.

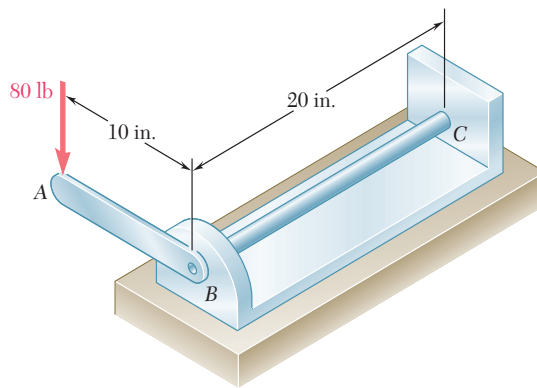


Fig. P9.93

- 9.94** A 16-mm-diameter rod has been bent into the shape shown. Determine the deflection of end C after the 200-N force is applied. Use $E = 200$ GPa and $G = 80$ GPa.

*9.9 MOMENT-AREA THEOREMS

In Sec. 9.2 through Sec. 9.6 we used a mathematical method based on the integration of a differential equation to determine the deflection and slope of a beam at any given point. The bending moment was expressed as a function $M(x)$ of the distance x measured along the beam, and two successive integrations led to the functions $\theta(x)$ and $y(x)$ representing, respectively, the slope and deflection at any point of the beam. In this section you will see how geometric properties of the elastic curve can be used to determine the deflection and slope of a beam at a specific point (Photo 9.4).



Photo 9.4 The deflections of the beams supporting the floors of a building should be taken into account in the design process.

Consider a beam AB subjected to some arbitrary loading (Fig. 9.37a). We draw the diagram representing the variation along the beam of the quantity M/EI obtained by dividing the bending moment M by the flexural rigidity EI (Fig. 9.37b). We note that, except for a difference in the scales of ordinates, this diagram will be the same as the bending-moment diagram if the flexural rigidity of the beam is constant.

Recalling Eq. (9.4) of Sec. 9.3, and the fact that $dy/dx = \theta$, we write

$$\frac{d\theta}{dx} = \frac{d^2y}{dx^2} = \frac{M}{EI}$$

or

$$d\theta = \frac{M}{EI} dx \quad (9.54)^\dagger$$

Considering two arbitrary points C and D on the beam and integrating both members of Eq. (9.54) from C to D , we write

$$\int_{\theta_C}^{\theta_D} d\theta = \int_{x_C}^{x_D} \frac{M}{EI} dx$$

or

$$\theta_D - \theta_C = \int_{x_C}^{x_D} \frac{M}{EI} dx \quad (9.55)$$

where θ_C and θ_D denote the slope at C and D , respectively (Fig. 9.37c). But the right-hand member of Eq. (9.55) represents the area under the (M/EI) diagram between C and D , and the left-hand member the angle between the tangents to the elastic curve at C and D (Fig. 9.37d). Denoting this angle by $\theta_{D/C}$, we have

$$\theta_{D/C} = \text{area under } (M/EI) \text{ diagram between } C \text{ and } D \quad (9.56)$$

This is the *first moment-area theorem*.

We note that the angle $\theta_{D/C}$ and the area under the (M/EI) diagram have the same sign. In other words, a positive area (i.e., an area located above the x axis) corresponds to a counterclockwise rotation of the tangent to the elastic curve as we move from C to D , and a negative area corresponds to a clockwise rotation.

[†]This relation can also be derived without referring to the results obtained in Sec. 9.3, by noting that the angle $d\theta$ formed by the tangents to the elastic curve at P and P' is also the angle formed by the corresponding normals to that curve (Fig. 9.38). We thus have $d\theta = ds/\rho$ where ds is the length of the arc PP' and ρ the radius of curvature at P . Substituting for $1/\rho$ from Eq. (4.21), and noting that, since the slope at P is very small, ds is equal in first approximation to the horizontal distance dx between P and P' , we write

$$d\theta = \frac{M}{EI} dx \quad (9.54)$$

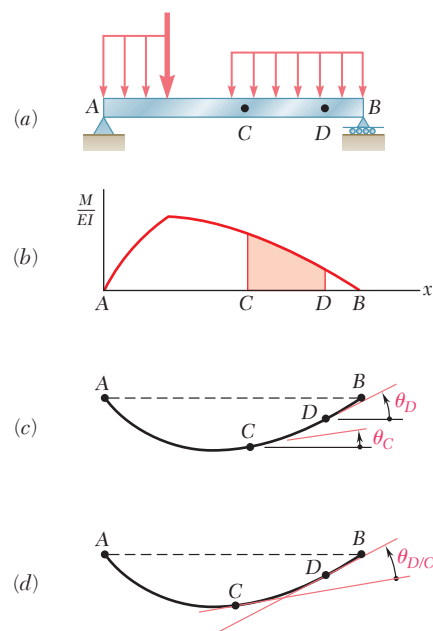


Fig. 9.37 First moment-area theorem.

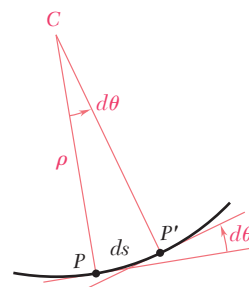


Fig. 9.38

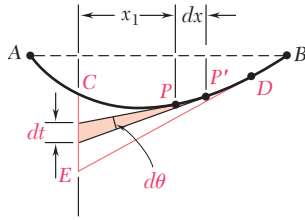


Fig. 9.39

Let us now consider two points P and P' located between C and D , and at a distance dx from each other (Fig. 9.39). The tangents to the elastic curve drawn at P and P' intercept a segment of length dt on the vertical through point C . Since the slope θ at P and the angle $d\theta$ formed by the tangents at P and P' are both small quantities, we can assume that dt is equal to the arc of circle of radius x_1 subtending the angle $d\theta$. We have, therefore,

$$dt = x_1 d\theta$$

or, substituting for $d\theta$ from Eq. (9.54),

$$dt = x_1 \frac{M}{EI} dx \quad (9.57)$$

We now integrate Eq. (9.57) from C to D . We note that, as point P describes the elastic curve from C to D , the tangent at P sweeps the vertical through C from C to E . The integral of the left-hand member is thus equal to the vertical distance from C to the tangent at D . This distance is denoted by $t_{C/D}$ and is called the *tangential deviation of C with respect to D* . We have, therefore,

$$t_{C/D} = \int_{x_C}^{x_D} x_1 \frac{M}{EI} dx \quad (9.58)$$

We now observe that $(M/EI) dx$ represents an element of area under the (M/EI) diagram, and $x_1 (M/EI) dx$ the first moment of that element with respect to a vertical axis through C (Fig. 9.40). The right-hand member in Eq. (9.58), thus, represents the first moment with respect to that axis of the area located under the (M/EI) diagram between C and D .

We can, therefore, state the *second moment-area theorem* as follows: *The tangential deviation $t_{C/D}$ of C with respect to D is equal to the first moment with respect to a vertical axis through C of the area under the (M/EI) diagram between C and D .*

Recalling that the first moment of an area with respect to an axis is equal to the product of the area and of the distance from its centroid to that axis, we may also express the second moment-area theorem as follows:

$$t_{C/D} = (\text{area between } C \text{ and } D) \bar{x}_1 \quad (9.59)$$

where the area refers to the area under the (M/EI) diagram, and where \bar{x}_1 is the distance from the centroid of the area to the vertical axis through C (Fig. 9.41a).

Care should be taken to distinguish between the tangential deviation of C with respect to D , denoted by $t_{C/D}$, and the tangential deviation of D with respect to C , which is denoted by $t_{D/C}$. The tangential deviation $t_{D/C}$ represents the vertical distance from D to the tangent to the elastic curve at C , and is obtained by multiplying the area under the (M/EI) diagram by the distance \bar{x}_2 from its centroid to the vertical axis through D (Fig. 9.41b):

$$t_{D/C} = (\text{area between } C \text{ and } D) \bar{x}_2 \quad (9.60)$$

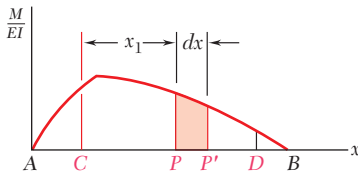
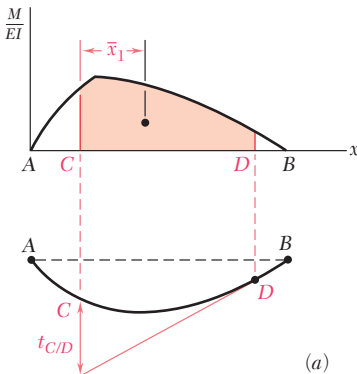
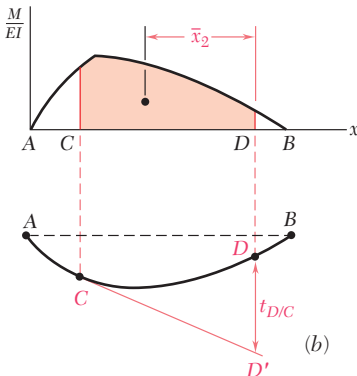


Fig. 9.40



(a)



(b)

Fig. 9.41 Second moment-area theorem.

We note that, if an area under the (M/EI) diagram is located above the x axis, its first moment with respect to a vertical axis will be positive; if it is located below the x axis, its first moment will be negative. We check from Fig. 9.41, that a point with a *positive* tangential deviation is located *above* the corresponding tangent, while a point with a *negative* tangential deviation would be located *below* that tangent.

*9.10 APPLICATION TO CANTILEVER BEAMS AND BEAMS WITH SYMMETRIC LOADINGS

We recall that the first moment-area theorem derived in the preceding section defines the angle $\theta_{D/C}$ between the tangents at two points C and D of the elastic curve. Thus, the angle θ_D that the tangent at D forms with the horizontal, i.e., the slope at D , can be obtained only if the slope at C is known. Similarly, the second moment-area theorem defines the vertical distance of one point of the elastic curve from the tangent at another point. The tangential deviation $t_{D/C}$, therefore, will help us locate point D only if the tangent at C is known. We conclude that the two moment-area theorems can be applied effectively to the determination of slopes and deflections only if a certain *reference tangent* to the elastic curve has first been determined.

In the case of a *cantilever beam* (Fig. 9.42), the tangent to the elastic curve at the fixed end A is known and can be used as the reference tangent. Since $\theta_A = 0$, the slope of the beam at any point D is $\theta_D = \theta_{D/A}$ and can be obtained by the first moment-area theorem. On the other hand, the deflection y_D of point D is equal to the tangential deviation $t_{D/A}$ measured from the horizontal reference tangent at A and can be obtained by the second moment-area theorem.

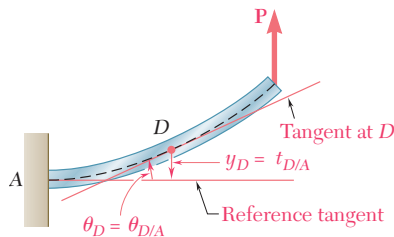


Fig. 9.42 Application of moment-area method to cantilever beams.

In the case of a simply supported beam AB with a *symmetric loading* (Fig. 9.43a) or in the case of an overhanging symmetric beam with a symmetric loading (see Sample Prob. 9.11), the tangent at the center C of the beam must be horizontal by reason of symmetry and can be used as the reference tangent (Fig. 9.43b). Since $\theta_C = 0$, the slope at the support B is $\theta_B = \theta_{B/C}$ and can be obtained by the first moment-area theorem. We also note that $|y|_{\max}$ is equal to the tangential deviation $t_{B/C}$ and can, therefore, be obtained by the second moment-area theorem. The slope at any other point D of the beam (Fig. 9.43c) is found in a similar fashion, and the deflection at D can be expressed as $y_D = t_{D/C} - t_{B/C}$.

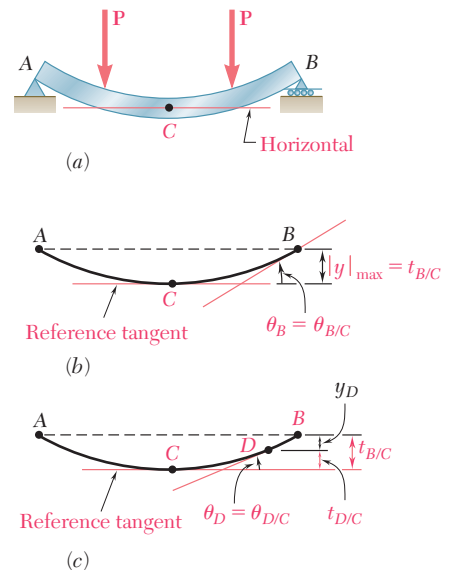
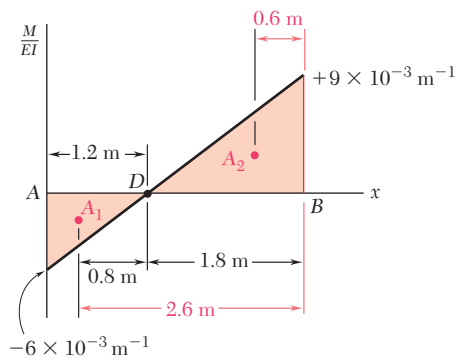
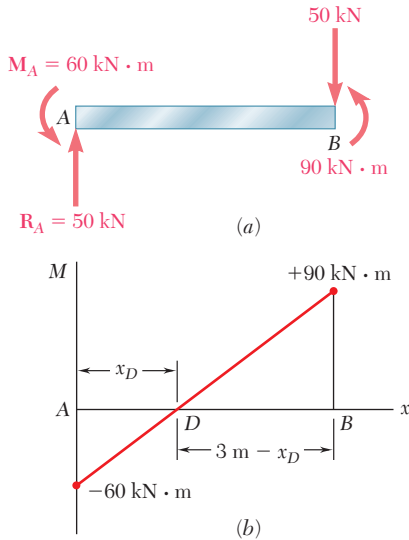
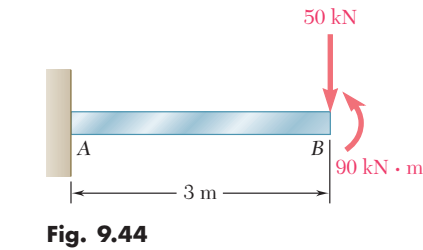


Fig. 9.43 Application of moment-area method to simply supported beams with symmetric loadings.

EXAMPLE 9.09

Determine the slope and deflection at end B of the prismatic cantilever beam AB when it is loaded as shown (Fig. 9.44), knowing that the flexural rigidity of the beam is $EI = 10 \text{ MN} \cdot \text{m}^2$.



We first draw the free-body diagram of the beam (Fig. 9.45a). Summing vertical components and moments about A , we find that the reaction at the fixed end A consists of a 50 kN upward vertical force \mathbf{R}_A and a $60 \text{ kN} \cdot \text{m}$ counterclockwise couple \mathbf{M}_A . Next, we draw the bending-moment diagram (Fig. 9.45b) and determine from similar triangles the distance x_D from the end A to the point D of the beam where $M = 0$:

$$\frac{x_D}{60} = \frac{3 - x_D}{90} = \frac{3}{150} \quad x_D = 1.2 \text{ m}$$

Dividing by the flexural rigidity EI the values obtained for M , we draw the (M/EI) diagram (Fig. 9.46) and compute the areas corresponding respectively to the segments AD and DB , assigning a positive sign to the area located above the x axis, and a negative sign to the area located below that axis. Using the first moment-area theorem, we write

$$\begin{aligned} \theta_{B/A} &= \theta_B - \theta_A = \text{area from } A \text{ to } B = A_1 + A_2 \\ &= -\frac{1}{2}(1.2 \text{ m})(6 \times 10^{-3} \text{ m}^{-1}) + \frac{1}{2}(1.8 \text{ m})(9 \times 10^{-3} \text{ m}^{-1}) \\ &= -3.6 \times 10^{-3} + 8.1 \times 10^{-3} \\ &= +4.5 \times 10^{-3} \text{ rad} \end{aligned}$$

and, since $\theta_A = 0$,

$$\theta_B = +4.5 \times 10^{-3} \text{ rad}$$

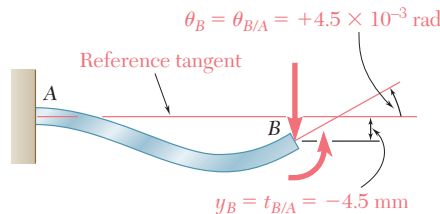
Using now the second moment-area theorem, we write that the tangential deviation $t_{B/A}$ is equal to the first moment about a vertical axis through B of the total area between A and B . Expressing the moment of each partial area as the product of that area and of the distance from its centroid to the axis through B , we have

$$\begin{aligned} t_{B/A} &= A_1(2.6 \text{ m}) + A_2(0.6 \text{ m}) \\ &= (-3.6 \times 10^{-3})(2.6 \text{ m}) + (8.1 \times 10^{-3})(0.6 \text{ m}) \\ &= -9.36 \text{ mm} + 4.86 \text{ mm} = -4.50 \text{ mm} \end{aligned}$$

Since the reference tangent at A is horizontal, the deflection at B is equal to $t_{B/A}$ and we have

$$y_B = t_{B/A} = -4.50 \text{ mm}$$

The deflected beam has been sketched in Fig. 9.47.



In many applications the determination of the angle $\theta_{D/C}$ and of the tangential deviation $t_{D/C}$ is simplified if the effect of each load is evaluated independently. A separate (M/EI) diagram is drawn for each load, and the angle $\theta_{D/C}$ is obtained by adding algebraically the areas under the various diagrams. Similarly, the tangential deviation $t_{D/C}$ is obtained by adding the first moments of these areas about a vertical axis through D . A bending-moment or (M/EI) diagram plotted in this fashion is said to be *drawn by parts*.

When a bending-moment or (M/EI) diagram is drawn by parts, the various areas defined by the diagram consist of simple geometric shapes, such as rectangles, triangles, and parabolic spandrels. For convenience, the areas and centroids of these various shapes have been indicated in Fig. 9.48.

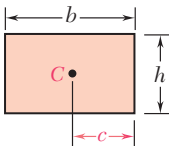
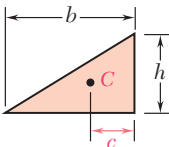
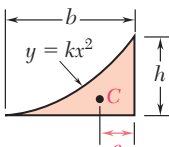
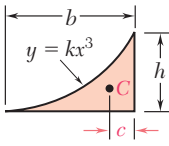
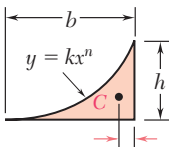
Shape		Area	c
Rectangle		bh	$\frac{b}{2}$
Triangle		$\frac{bh}{2}$	$\frac{b}{3}$
Parabolic spandrel		$\frac{bh}{3}$	$\frac{b}{4}$
Cubic spandrel		$\frac{bh}{4}$	$\frac{b}{5}$
General spandrel		$\frac{bh}{n+1}$	$\frac{b}{n+2}$

Fig. 9.48 Areas and centroids of common shapes.

EXAMPLE 9.10

Determine the slope and deflection at end B of the prismatic beam of Example 9.09, drawing the bending-moment diagram by parts.

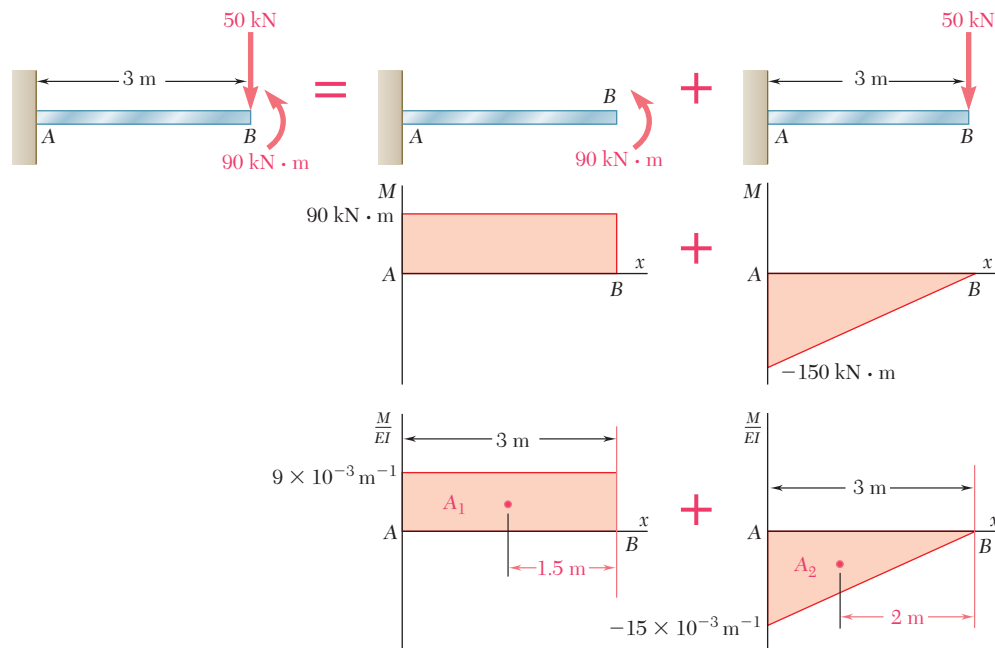


Fig. 9.49

We replace the given loading by the two equivalent loadings shown in Fig. 9.49, and draw the corresponding bending-moment and (M/EI) diagrams from right to left, starting at the free end B .

Applying the first moment-area theorem, and recalling that $\theta_A = 0$, we write

$$\begin{aligned}\theta_B &= \theta_{B/A} = A_1 + A_2 \\ &= (9 \times 10^{-3} \text{ m}^{-1})(3 \text{ m}) - \frac{1}{2}(15 \times 10^{-3} \text{ m}^{-1})(3 \text{ m}) \\ &= 27 \times 10^{-3} - 22.5 \times 10^{-3} = 4.5 \times 10^{-3} \text{ rad}\end{aligned}$$

Applying the second moment-area theorem, we compute the first moment of each area about a vertical axis through B and write

$$\begin{aligned}y_B &= t_{B/A} = A_1(1.5 \text{ m}) + A_2(2 \text{ m}) \\ &= (27 \times 10^{-3})(1.5 \text{ m}) - (22.5 \times 10^{-3})(2 \text{ m}) \\ &= 40.5 \text{ mm} - 45 \text{ mm} = -4.5 \text{ mm}\end{aligned}$$

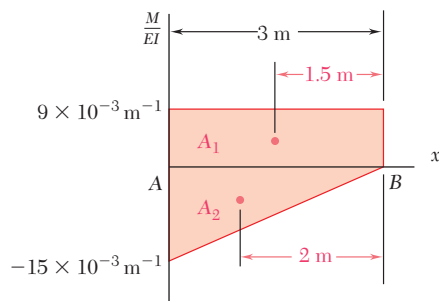


Fig. 9.50

It is convenient, in practice, to group into a single drawing the two portions of the (M/EI) diagram (Fig. 9.50).

For the prismatic beam AB and the loading shown (Fig. 9.51), determine the slope at a support and the maximum deflection.

EXAMPLE 9.11

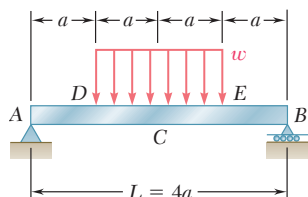


Fig. 9.51

We first sketch the deflected beam (Fig. 9.52). Since the tangent at the center C of the beam is horizontal, it will be used as the reference tangent, and we have $|y|_{\max} = t_{A/C}$. On the other hand, since $\theta_C = 0$, we write

$$\theta_{C/A} = \theta_C - \theta_A = -\theta_A \quad \text{or} \quad \theta_A = -\theta_{C/A}$$

From the free-body diagram of the beam (Fig. 9.53), we find that

$$R_A = R_B = wa$$

Next, we draw the shear and bending-moment diagrams for the portion AC of the beam. We draw these diagrams by parts, considering separately the effects of the reaction \mathbf{R}_A and of the distributed load. However, for convenience, the two parts of each diagram have been plotted together (Fig. 9.54). We recall from Sec. 5.3 that, the distributed load being uniform, the corresponding parts of the shear and bending-moment diagrams will be, respectively, linear and parabolic. The area and centroid of the triangle and of the parabolic spandrel can be obtained by referring to Fig. 9.48. The areas of the triangle and spandrel are found to be, respectively,

$$A_1 = \frac{1}{2}(2a)\left(\frac{2wa^2}{EI}\right) = \frac{2wa^3}{EI}$$

and

$$A_2 = -\frac{1}{3}(a)\left(\frac{wa^2}{2EI}\right) = -\frac{wa^3}{6EI}$$

Applying the first moment-area theorem, we write

$$\theta_{C/A} = A_1 + A_2 = \frac{2wa^3}{EI} - \frac{wa^3}{6EI} = \frac{11wa^3}{6EI}$$

Recalling from Figs. 9.51 and 9.52 that $a = \frac{1}{4}L$ and $\theta_A = -\theta_{C/A}$, we have

$$\theta_A = -\frac{11wa^3}{6EI} = -\frac{11wL^3}{384EI}$$

Applying now the second moment-area theorem, we write

$$t_{A/C} = A_1 \frac{4a}{3} + A_2 \frac{7a}{4} = \left(\frac{2wa^3}{EI}\right) \frac{4a}{3} + \left(-\frac{wa^3}{6EI}\right) \frac{7a}{4} = \frac{19wa^4}{8EI}$$

and

$$|y|_{\max} = t_{A/C} = \frac{19wa^4}{8EI} = \frac{19wL^4}{2048EI}$$

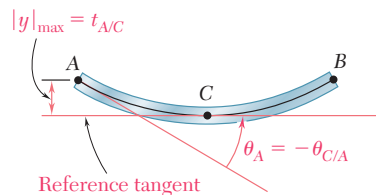


Fig. 9.52

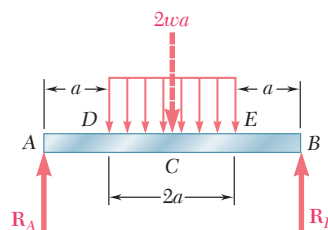


Fig. 9.53

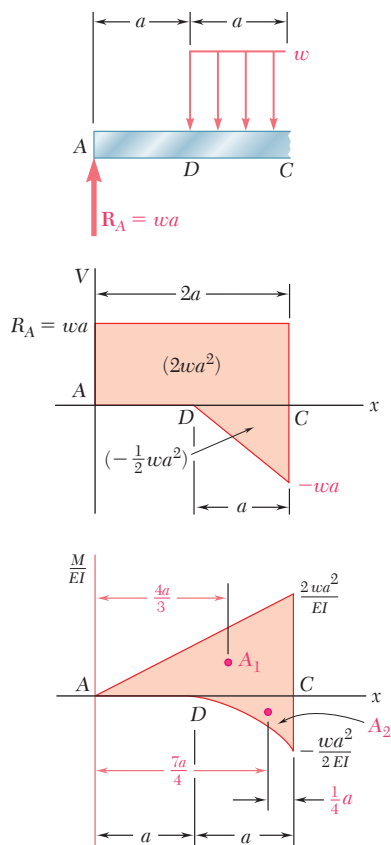
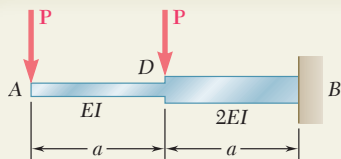


Fig. 9.54



SAMPLE PROBLEM 9.10

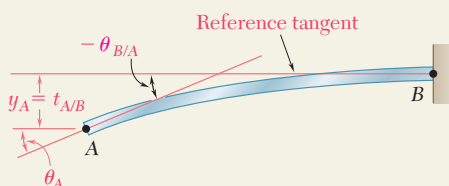
The prismatic rods AD and DB are welded together to form the cantilever beam ADB . Knowing that the flexural rigidity is EI in portion AD of the beam and $2EI$ in portion DB , determine, for the loading shown, the slope and deflection at end A .

SOLUTION

(M/EI) Diagram. We first draw the bending-moment diagram for the beam and then obtain the (M/EI) diagram by dividing the value of M at each point of the beam by the corresponding value of the flexural rigidity.

Reference Tangent. We choose the horizontal tangent at the fixed end B as the reference tangent. Since $\theta_B = 0$ and $y_B = 0$, we note that

$$\theta_A = -\theta_{B/A} \quad y_A = t_{A/B}$$



Slope at A. Dividing the (M/EI) diagram into the three triangular portions shown, we write

$$A_1 = -\frac{1}{2} \frac{Pa}{EI} a = -\frac{Pa^2}{2EI}$$

$$A_2 = -\frac{1}{2} \frac{Pa}{2EI} a = -\frac{Pa^2}{4EI}$$

$$A_3 = -\frac{1}{2} \frac{3Pa}{2EI} a = -\frac{3Pa^2}{4EI}$$

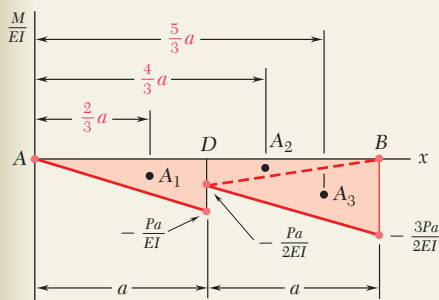
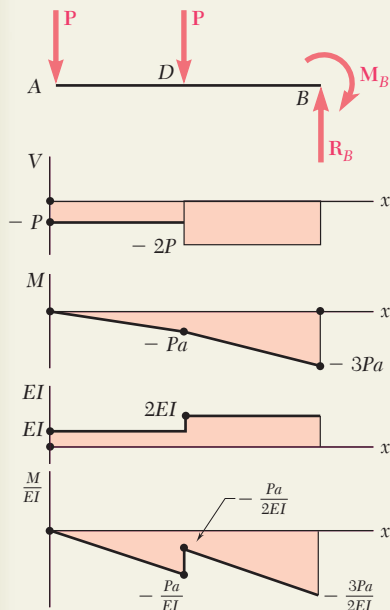
Using the first moment-area theorem, we have

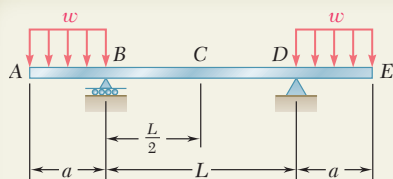
$$\theta_{B/A} = A_1 + A_2 + A_3 = -\frac{Pa^2}{2EI} - \frac{Pa^2}{4EI} - \frac{3Pa^2}{4EI} = -\frac{3Pa^2}{2EI}$$

$$\theta_A = -\theta_{B/A} = +\frac{3Pa^2}{2EI} \quad \theta_A = \frac{3Pa^2}{2EI} \quad \swarrow \blacktriangleleft$$

Deflection at A. Using the second moment-area theorem, we have

$$\begin{aligned} y_A = t_{A/B} &= A_1 \left(\frac{2}{3} a \right) + A_2 \left(\frac{4}{3} a \right) + A_3 \left(\frac{5}{3} a \right) \\ &= \left(-\frac{Pa^2}{2EI} \right) \frac{2a}{3} + \left(-\frac{Pa^2}{4EI} \right) \frac{4a}{3} + \left(-\frac{3Pa^2}{4EI} \right) \frac{5a}{3} \\ y_A &= -\frac{23Pa^3}{12EI} \quad y_A = \frac{23Pa^3}{12EI} \quad \downarrow \blacktriangleleft \end{aligned}$$





SAMPLE PROBLEM 9.11

For the prismatic beam and loading shown, determine the slope and deflection at end E.

SOLUTION

(M/EI) Diagram. From a free-body diagram of the beam, we determine the reactions and then draw the shear and bending-moment diagrams. Since the flexural rigidity of the beam is constant, we divide each value of M by EI and obtain the (M/EI) diagram shown.

Reference Tangent. Since the beam and its loading are symmetric with respect to the midpoint C, the tangent at C is horizontal and is used as the reference tangent. Referring to the sketch, we observe that, since $\theta_C = 0$,

$$\theta_E = \theta_C + \theta_{E/C} = \theta_{E/C} \quad (1)$$

$$y_E = t_{E/C} - t_{D/C} \quad (2)$$

Slope at E. Referring to the (M/EI) diagram and using the first moment-area theorem, we write

$$A_1 = -\frac{wa^2}{2EI} \left(\frac{L}{2} \right) = -\frac{wa^2L}{4EI}$$

$$A_2 = -\frac{1}{3} \left(\frac{wa^2}{2EI} \right) (a) = -\frac{wa^3}{6EI}$$

Using Eq. (1), we have

$$\theta_E = \theta_{E/C} = A_1 + A_2 = -\frac{wa^2L}{4EI} - \frac{wa^3}{6EI}$$

$$\theta_E = -\frac{wa^2}{12EI} (3L + 2a) \quad \theta_E = \frac{wa^2}{12EI} (3L + 2a) \searrow \blacktriangleleft$$

Deflection at E. Using the second moment-area theorem, we write

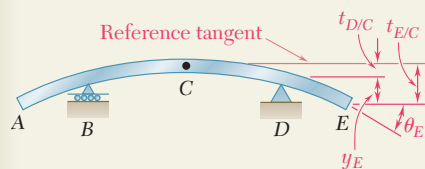
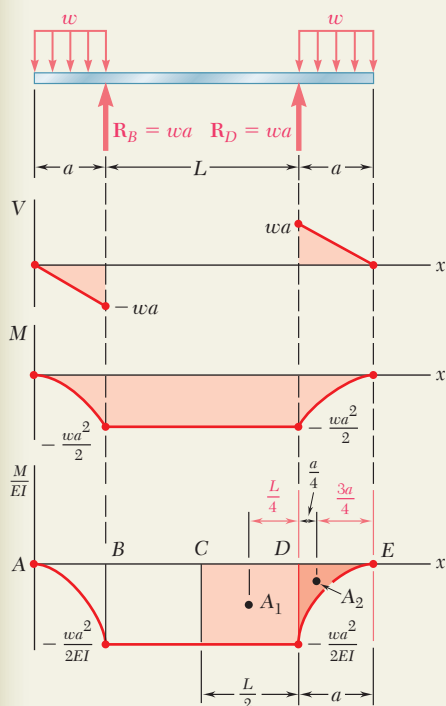
$$t_{D/C} = A_1 \frac{L}{4} = \left(-\frac{wa^2L}{4EI} \right) \frac{L}{4} = -\frac{wa^2L^2}{16EI}$$

$$\begin{aligned} t_{E/C} &= A_1 \left(a + \frac{L}{4} \right) + A_2 \left(\frac{3a}{4} \right) \\ &= \left(-\frac{wa^2L}{4EI} \right) \left(a + \frac{L}{4} \right) + \left(-\frac{wa^3}{6EI} \right) \left(\frac{3a}{4} \right) \\ &= -\frac{wa^3L}{4EI} - \frac{wa^2L^2}{16EI} - \frac{wa^4}{8EI} \end{aligned}$$

Using Eq. (2), we have

$$y_E = t_{E/C} - t_{D/C} = -\frac{wa^3L}{4EI} - \frac{wa^4}{8EI}$$

$$y_E = -\frac{wa^3}{8EI} (2L + a) \quad y_E = \frac{wa^3}{8EI} (2L + a) \downarrow \blacktriangleleft$$



PROBLEMS

Use the moment-area method to solve the following problems.

9.95 through 9.98 For the uniform cantilever beam and loading shown, determine (a) the slope at the free end, (b) the deflection at the free end.

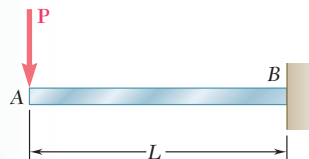


Fig. P9.95

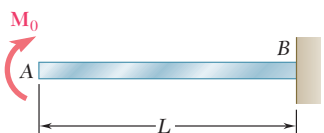


Fig. P9.96

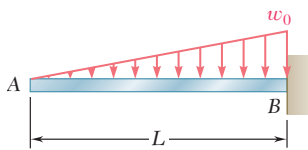


Fig. P9.97

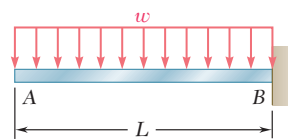


Fig. P9.98

9.99 and 9.100 For the uniform cantilever beam and loading shown, determine the slope and deflection at (a) point B, (b) point C.

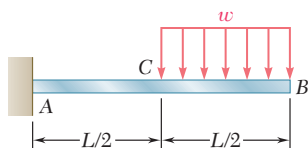


Fig. P9.99

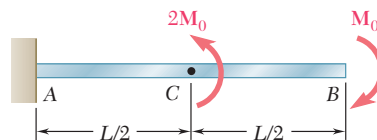


Fig. P9.100

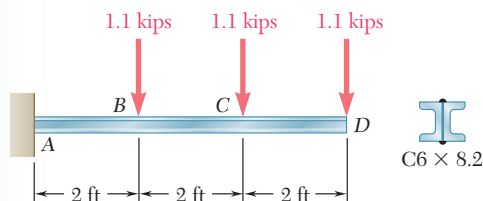


Fig. P9.101

9.101 Two C6 \times 8.2 channels are welded back to back and loaded as shown. Knowing that $E = 29 \times 10^6$ psi, determine (a) the slope at point D, (b) the deflection at point D.

9.102 For the cantilever beam and loading shown, determine (a) the slope at point A, (b) the deflection at point A. Use $E = 200$ GPa.

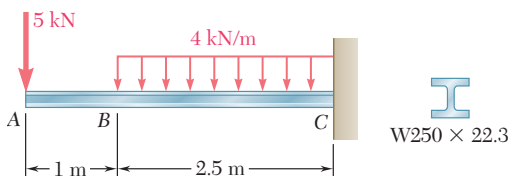


Fig. P9.102

9.103 For the cantilever beam and loading shown, determine (a) the slope at point B, (b) the deflection at point B. Use $E = 29 \times 10^6$ psi.

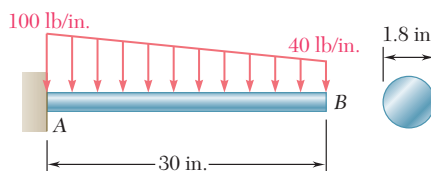


Fig. P9.103

9.104 For the cantilever beam and loading shown, determine (a) the slope at point A, (b) the deflection at point A. Use $E = 200$ GPa.

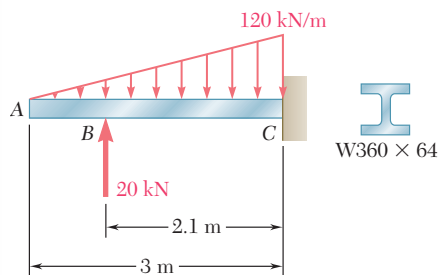


Fig. P9.104

- 9.105** For the cantilever beam and loading shown, determine (a) the slope at point C, (b) the deflection at point C.

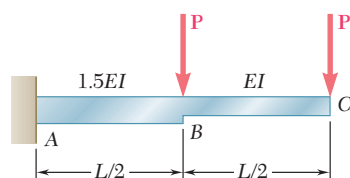


Fig. P9.105

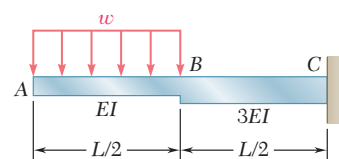


Fig. P9.106

- 9.106** For the cantilever beam and loading shown, determine (a) the slope at point A, (b) the deflection at point A.

- 9.107** Two cover plates are welded to the rolled-steel beam as shown. Using $E = 29 \times 10^6$ psi, determine (a) the slope at end C, (b) the deflection at end C.

- 9.108** Two cover plates are welded to the rolled-steel beam as shown. Using $E = 200$ GPa, determine (a) the slope at end A, (b) the deflection at end A.

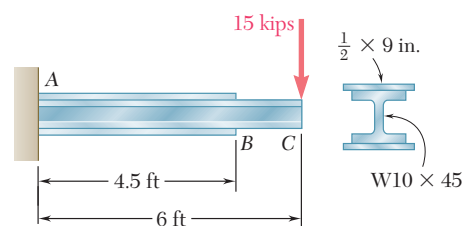


Fig. P9.107

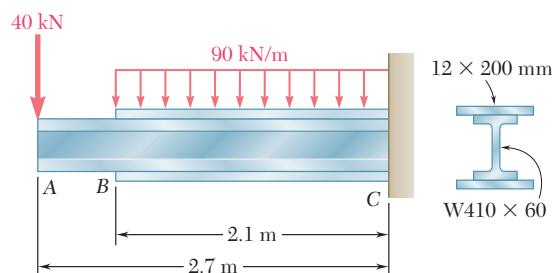


Fig. P9.108

- 9.109 through 9.114** For the prismatic beam and loading shown, determine (a) the slope at end A, (b) the deflection at the center C of the beam.

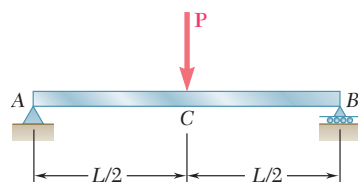


Fig. P9.109

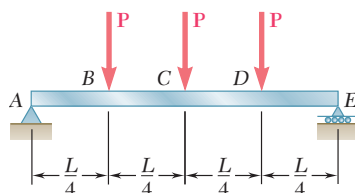


Fig. P9.110

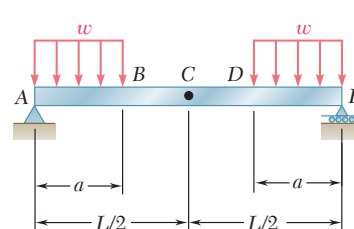


Fig. P9.111

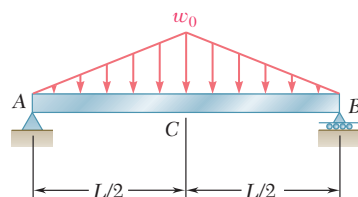


Fig. P9.112

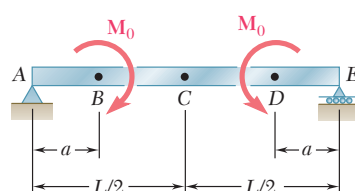


Fig. P9.113

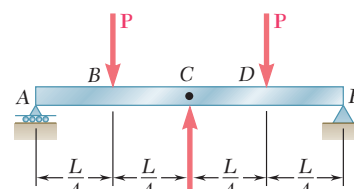


Fig. P9.114

9.115 and 9.116 For the beam and loading shown, determine (a) the slope at end A, (b) the deflection at the center C of the beam.

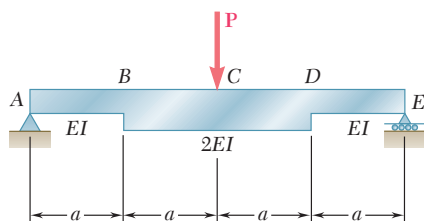


Fig. P9.115

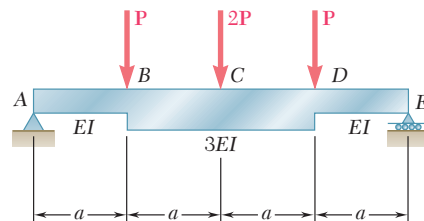


Fig. P9.116

9.117 For the beam and loading shown and knowing that $w = 8 \text{ kN/m}$, determine (a) the slope at end A, (b) the deflection at midpoint C. Use $E = 200 \text{ GPa}$.

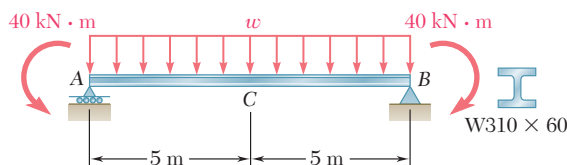


Fig. P9.117

9.118 and 9.119 For the beam and loading shown, determine (a) the slope at end A, (b) the deflection at the midpoint of the beam. Use $E = 200 \text{ GPa}$.

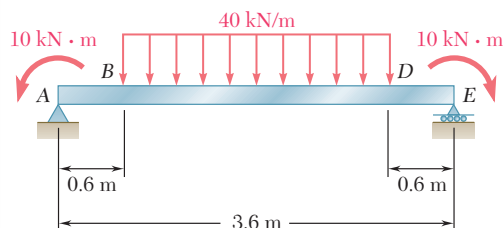


Fig. P9.118

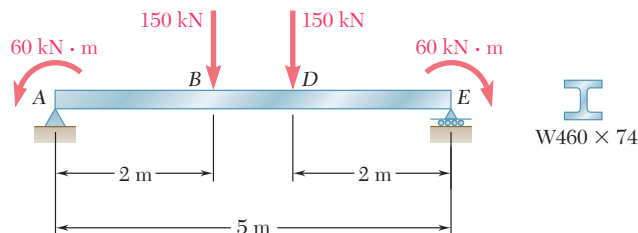


Fig. P9.119

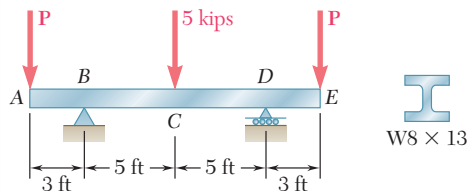


Fig. P9.120

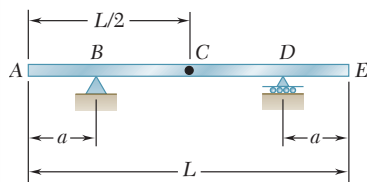


Fig. P9.123 and P9.124

9.120 Knowing that $P = 4 \text{ kips}$, determine (a) the slope at end A, (b) the deflection at the midpoint C of the beam. Use $E = 29 \times 10^6 \text{ psi}$.

9.121 For the beam and loading of Prob. 9.117, determine the value of w for which the deflection is zero at the midpoint C of the beam. Use $E = 200 \text{ GPa}$.

9.122 For the beam and loading of Prob. 9.120, determine the magnitude of the forces P for which the deflection is zero at end A of the beam. Use $E = 29 \times 10^6 \text{ psi}$.

***9.123** A uniform rod AE is to be supported at two points B and D. Determine the distance a for which the slope at ends A and E is zero.

***9.124** A uniform rod AE is to be supported at two points B and D. Determine the distance a from the ends of the rod to the points of support, if the downward deflections of points A, C, and E are to be equal.

*9.12 APPLICATION OF MOMENT-AREA THEOREMS TO BEAMS WITH UNSYMMETRIC LOADINGS

We saw in Sec. 9.10 that, when a simply supported or overhanging beam carries a symmetric load, the tangent at the center C of the beam is horizontal and can be used as the reference tangent. When a simply supported or overhanging beam carries an unsymmetric load, it is generally not possible to determine by inspection the point of the beam where the tangent is horizontal. Other means must then be found for locating a reference tangent, i.e., a tangent of known slope to be used in applying either of the two moment-area theorems.

It is usually most convenient to select the reference tangent at one of the beam supports. Considering, for example, the tangent at the support A of the simply supported beam AB (Fig. 9.55), we determine its slope by computing the tangential deviation $t_{B/A}$ of the support B with respect to A , and dividing $t_{B/A}$ by the distance L between the supports. Recalling that the tangential deviation of a point located above the tangent is positive, we write

$$\theta_A = -\frac{t_{B/A}}{L} \quad (9.61)$$

Once the slope of the reference tangent has been found, the slope θ_D of the beam at any point D (Fig. 9.56) can be determined by using the first moment-area theorem to obtain $\theta_{D/A}$, and then writing

$$\theta_D = \theta_A + \theta_{D/A} \quad (9.62)$$

The tangential deviation $t_{D/A}$ of D with respect to the support A can be obtained from the second moment-area theorem. We note that $t_{D/A}$ is equal to the segment ED (Fig. 9.57) and represents the vertical distance of D from the reference tangent. On the other hand, the deflection y_D of point D represents the vertical distance of D from the horizontal line AB (Fig. 9.58). Since y_D is equal in

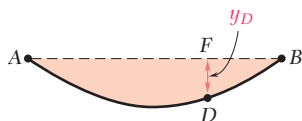


Fig. 9.58

magnitude to the segment FD , it can be expressed as the difference between EF and ED (Fig. 9.59). Observing from the similar triangles AFE and ABH that

$$\frac{EF}{x} = \frac{HB}{L} \quad \text{or} \quad EF = \frac{x}{L} t_{B/A}$$

and recalling the sign conventions used for deflections and tangential deviations, we write

$$y_D = ED - EF = t_{D/A} - \frac{x}{L} t_{B/A} \quad (9.63)$$

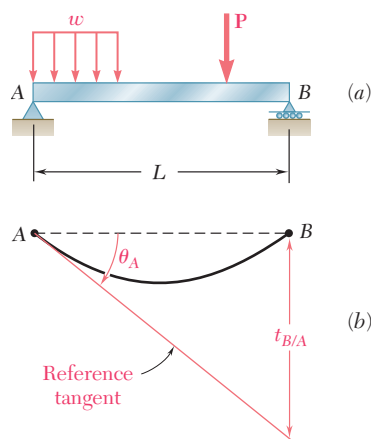


Fig. 9.55

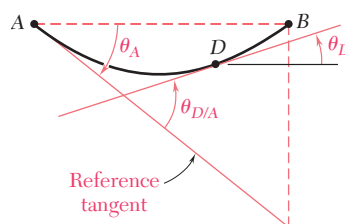


Fig. 9.56

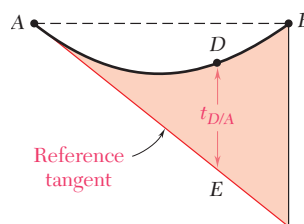


Fig. 9.57

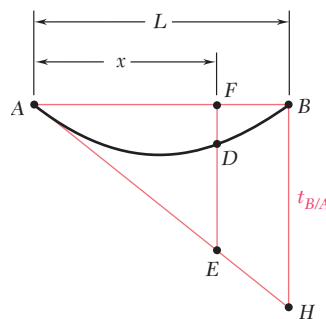


Fig. 9.59

EXAMPLE 9.12

For the prismatic beam and loading shown (Fig. 9.60), determine the slope and deflection at point D .

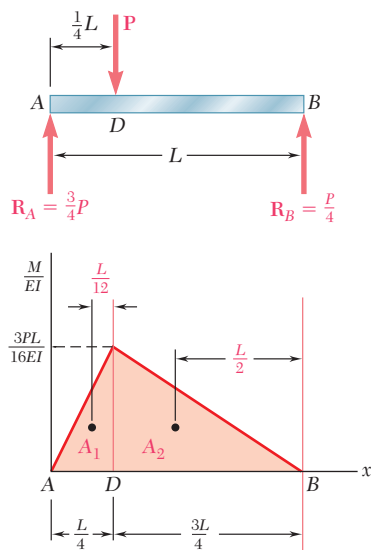


Fig. 9.61

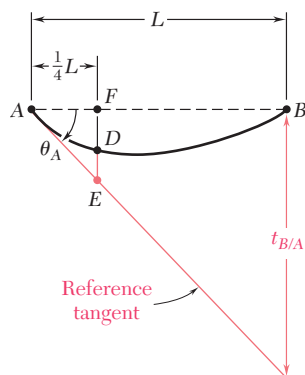


Fig. 9.62

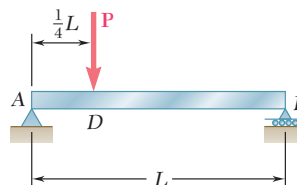


Fig. 9.60

Reference Tangent at Support A. We compute the reactions at the supports and draw the (M/EI) diagram (Fig. 9.61). We determine the tangential deviation $t_{B/A}$ of the support B with respect to the support A by applying the second moment-area theorem and computing the moments about a vertical axis through B of the areas A_1 and A_2 . We have

$$A_1 = \frac{1}{2} \frac{L}{4} \frac{3PL}{16EI} = \frac{3PL^2}{128EI} \quad A_2 = \frac{1}{2} \frac{3L}{4} \frac{3PL}{16EI} = \frac{9PL^2}{128EI}$$

$$t_{B/A} = A_1 \left(\frac{L}{12} + \frac{3L}{4} \right) + A_2 \left(\frac{L}{2} \right)$$

$$= \frac{3PL^2}{128EI} \frac{10L}{12} + \frac{9PL^2}{128EI} \frac{L}{2} = \frac{7PL^3}{128EI}$$

The slope of the reference tangent at A (Fig. 9.62) is

$$\theta_A = -\frac{t_{B/A}}{L} = -\frac{7PL^2}{128EI}$$

Slope at D . Applying the first moment-area theorem from A to D , we write

$$\theta_{D/A} = A_1 = \frac{3PL^2}{128EI}$$

Thus, the slope at D is

$$\theta_D = \theta_A + \theta_{D/A} = -\frac{7PL^2}{128EI} + \frac{3PL^2}{128EI} = -\frac{PL^2}{32EI}$$

Deflection at D . We first determine the tangential deviation $DE = t_{D/A}$ by computing the moment of the area A_1 about a vertical axis through D :

$$DE = t_{D/A} = A_1 \left(\frac{L}{12} \right) = \frac{3PL^2}{128EI} \frac{L}{12} = \frac{PL^3}{512EI}$$

The deflection at D is equal to the difference between the segments DE and EF (Fig. 9.62). We have

$$y_D = DE - EF = t_{D/A} - \frac{1}{4} t_{B/A}$$

$$= \frac{PL^3}{512EI} - \frac{1}{4} \frac{7PL^3}{128EI}$$

$$y_D = -\frac{3PL^3}{256EI} = -0.01172PL^3/EI$$

When a simply supported or overhanging beam carries an unsymmetric load, the maximum deflection generally does not occur at the center of the beam. This will be the case for the beams used in the bridge shown in Photo 9.5, which is being crossed by the truck.



Photo 9.5 The deflections of the beams used for the bridge must be reviewed for different possible positions of the truck.

To determine the maximum deflection of such a beam, we should locate the point K of the beam where the tangent is horizontal, and compute the deflection at that point.

Our analysis must begin with the determination of a reference tangent at one of the supports. If support A is selected, the slope θ_A of the tangent at A is obtained by the method indicated in the preceding section, i.e., by computing the tangential deviation $t_{B/A}$ of support B with respect to A and dividing that quantity by the distance L between the two supports.

Since the slope θ_K at point K is zero (Fig. 9.63a), we must have

$$\theta_{K/A} = \theta_K - \theta_A = 0 - \theta_A = -\theta_A$$

Recalling the first moment-area theorem, we conclude that point K may be determined by measuring under the (M/EI) diagram an area equal to $\theta_{K/A} = -\theta_A$ (Fig. 9.63b).

Observing that the maximum deflection $|y|_{\max}$ is equal to the tangential deviation $t_{A/K}$ of support A with respect to K (Fig. 9.63a), we can obtain $|y|_{\max}$ by computing the first moment with respect to the vertical axis through A of the area between A and K (Fig. 9.63b).

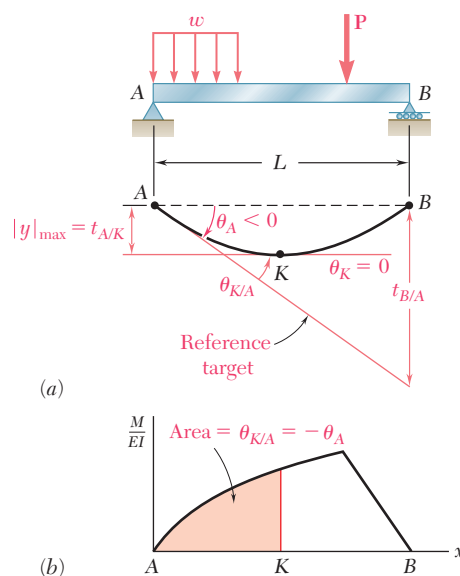


Fig. 9.63 Determination of maximum deflection using moment-area method.

EXAMPLE 9.13

Determine the maximum deflection of the beam of Example 9.12.

Determination of Point K Where Slope Is Zero. We recall from Example 9.12 that the slope at point D, where the load is applied, is negative. It follows that point K, where the slope is zero, is located between D and the support B (Fig. 9.64). Our computations, therefore, will be simplified if we relate the slope at K to the slope at B, rather than to the slope at A.

Since the slope at A has already been determined in Example 9.12, the slope at B is obtained by writing

$$\begin{aligned}\theta_B &= \theta_A + \theta_{B/A} = \theta_A + A_1 + A_2 \\ \theta_B &= -\frac{7PL^2}{128EI} + \frac{3PL^2}{128EI} + \frac{9PL^2}{128EI} = \frac{5PL^2}{128EI}\end{aligned}$$

Observing that the bending moment at a distance u from end B is $M = \frac{1}{4}Pu$ (Fig. 9.65a), we express the area A' located between K and B under the (M/EI) diagram (Fig. 9.65b) as

$$A' = \frac{1}{2} \frac{Pu}{4EI} u = \frac{Pu^2}{8EI}$$

By the first moment-area theorem, we have

$$\theta_{B/K} = \theta_B - \theta_K = A'$$

and, since $\theta_K = 0$,

$$\theta_B = A'$$

Substituting the values obtained for θ_B and A' , we write

$$\frac{5PL^2}{128EI} = \frac{Pu^2}{8EI}$$

and, solving for u ,

$$u = \frac{\sqrt{5}}{4} L = 0.559L$$

Thus, the distance from the support A to point K is

$$AK = L - 0.559L = 0.441L$$

Maximum Deflection. The maximum deflection $|y|_{\max}$ is equal to the tangential deviation $t_{B/K}$ and, thus, to the first moment of the area A' about a vertical axis through B (Fig. 9.65b). We write

$$|y|_{\max} = t_{B/K} = A' \left(\frac{2u}{3} \right) = \frac{Pu^2}{8EI} \left(\frac{2u}{3} \right) = \frac{Pu^3}{12EI}$$

Substituting the value obtained for u , we have

$$|y|_{\max} = \frac{P}{12EI} \left(\frac{\sqrt{5}}{4} L \right)^3 = 0.01456 PL^3/EI$$

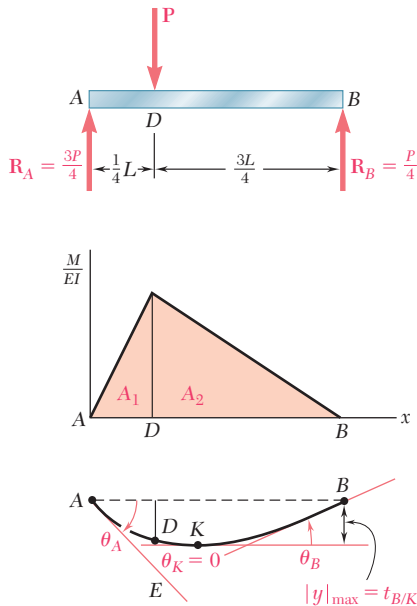


Fig. 9.64

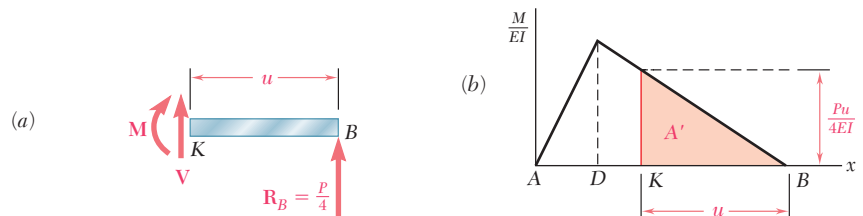


Fig. 9.65

*9.14 USE OF MOMENT-AREA THEOREMS WITH STATICALLY INDETERMINATE BEAMS

The reactions at the supports of a statically indeterminate beam can be determined by the moment-area method in much the same way that was described in Sec. 9.8. In the case of a beam indeterminate to the first degree, for example, we designate one of the reactions as redundant and eliminate or modify accordingly the corresponding support. The redundant reaction is then treated as an unknown load, which, together with the other loads, must produce deformations that are compatible with the original supports. The compatibility condition is usually expressed by writing that the tangential deviation of one support with respect to another either is zero or has a predetermined value.

Two separate free-body diagrams of the beam are drawn. One shows *the given loads and the corresponding reactions* at the supports that have not been eliminated; the other shows *the redundant reaction and the corresponding reactions* at the same supports (see Example 9.14). An M/EI diagram is then drawn for each of the two loadings, and the desired tangential deviations are obtained by the second moment-area theorem. Superposing the results obtained, we express the required compatibility condition and determine the redundant reaction. The other reactions are obtained from the free-body diagram of beam.

Once the reactions at the supports have been determined, the slope and deflection may be obtained by the moment-area method at any other point of the beam.

Determine the reaction at the supports for the prismatic beam and loading shown (Fig. 9.66).

EXAMPLE 9.14

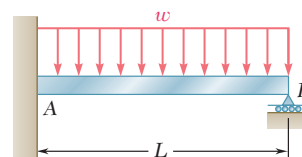


Fig. 9.66

We consider the couple exerted at the fixed end A as redundant and replace the fixed end by a pin-and-bracket support. The couple M_A is now considered as an unknown load (Fig. 9.67a) and will be determined from the condition that the tangent to the beam at A must be horizontal. It follows that this tangent must pass through the support B and, thus, that the tangential deviation $t_{B/A}$ of B with respect to A must be zero. The solution is carried out by computing separately the tangential deviation $(t_{B/A})_w$ caused by the uniformly distributed load w (Fig. 9.67b) and the tangential deviation $(t_{B/A})_M$ produced by the unknown couple M_A (Fig. 9.67c).

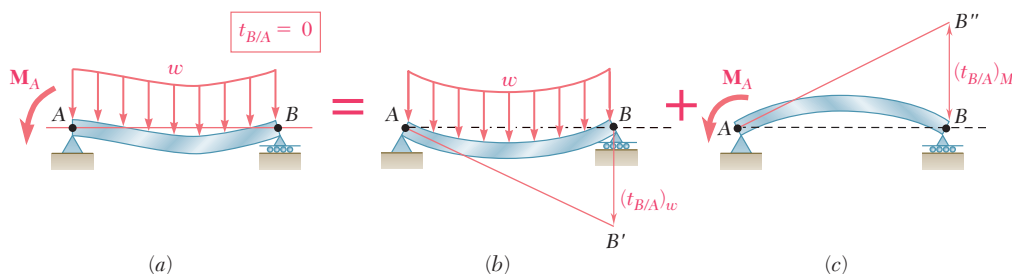


Fig. 9.67

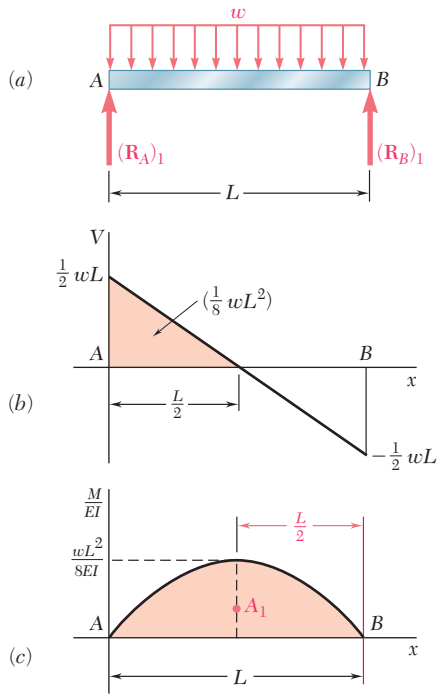


Fig. 9.68

Considering first the free-body diagram of the beam under the known distributed load w (Fig. 9.68a), we determine the corresponding reactions at the supports A and B. We have

$$(\mathbf{R}_A)_1 = (\mathbf{R}_B)_1 = \frac{1}{2}wL \uparrow \quad (9.64)$$

We can now draw the corresponding shear and (M/EI) diagrams (Figs. 9.68b and c). Observing that M/EI is represented by an arc of parabola, and recalling the formula, $A = \frac{2}{3}bh$, for the area under a parabola, we compute the first moment of this area about a vertical axis through B and write

$$(t_{B/A})_w = A_1 \left(\frac{L}{2} \right) = \left(\frac{2}{3} L \frac{wL^2}{8EI} \right) \left(\frac{L}{2} \right) = \frac{wL^4}{24EI} \quad (9.65)$$

Considering next the free-body diagram of the beam when it is subjected to the unknown couple \mathbf{M}_A (Fig. 9.69a), we determine the corresponding reactions at A and B:

$$(\mathbf{R}_A)_2 = \frac{M_A}{L} \uparrow \quad (\mathbf{R}_B)_2 = \frac{M_A}{L} \downarrow \quad (9.66)$$

Drawing the corresponding (M/EI) diagram (Fig. 9.69b), we apply again the second moment-area theorem and write

$$(t_{B/A})_M = A_2 \left(\frac{2L}{3} \right) = \left(-\frac{1}{2} L \frac{M_A}{EI} \right) \left(\frac{2L}{3} \right) = -\frac{M_A L^2}{3EI} \quad (9.67)$$

Combining the results obtained in (9.65) and (9.67), and expressing that the resulting tangential deviation $t_{B/A}$ must be zero (Fig. 9.67), we have

$$\begin{aligned} t_{B/A} &= (t_{B/A})_w + (t_{B/A})_M = 0 \\ \frac{wL^4}{24EI} - \frac{M_A L^2}{3EI} &= 0 \end{aligned}$$

and, solving for M_A ,

$$M_A = +\frac{1}{8}wL^2 \quad \mathbf{M}_A = \frac{1}{8}wL^2 \uparrow$$

Substituting for M_A into (9.66), and recalling (9.64), we obtain the values of R_A and R_B :

$$R_A = (R_A)_1 + (R_A)_2 = \frac{1}{2}wL + \frac{1}{8}wL = \frac{5}{8}wL$$

$$R_B = (R_B)_1 + (R_B)_2 = \frac{1}{2}wL - \frac{1}{8}wL = \frac{3}{8}wL$$

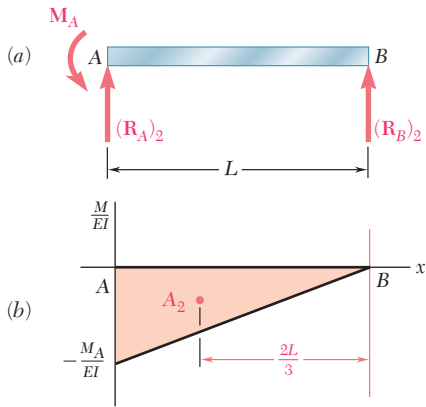
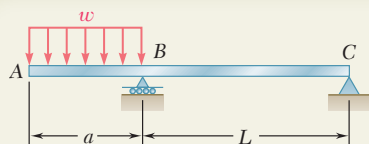


Fig. 9.69

In the example we have just considered, there was a single redundant reaction, i.e., the beam was *statically indeterminate to the first degree*. The *moment-area theorems* can also be used when there are additional redundant reactions. As discussed in Sec. 9.5, it is then necessary to write additional equations. Thus for a beam that is *statically indeterminate to the second degree*, it would be necessary to select two redundants and write two equations considering the *deformations* of the structure involved.



SAMPLE PROBLEM 9.12

For the beam and loading shown, (a) determine the deflection at end A, (b) evaluate y_A for the following data:

$$W10 \times 33; I = 171 \text{ in}^4$$

$$E = 29 \times 10^6 \text{ psi}$$

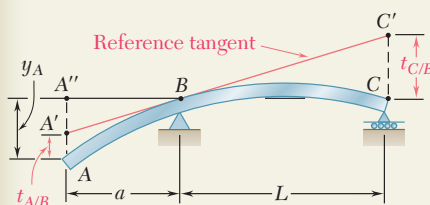
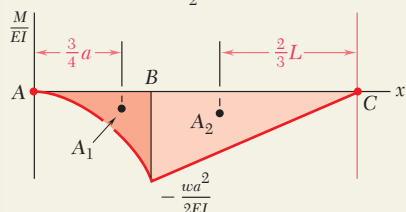
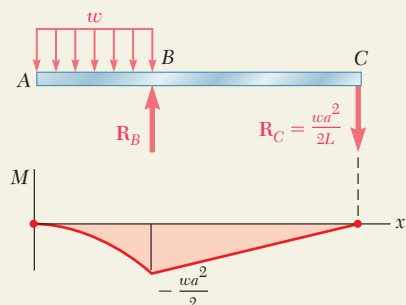
$$a = 3 \text{ ft} = 36 \text{ in.}$$

$$L = 5.5 \text{ ft} = 66 \text{ in.}$$

$$w = 13.5 \text{ kips/ft} = 1125 \text{ lb/in.}$$

SOLUTION

(M/EI) Diagram. We first draw the bending-moment diagram. Since the flexural rigidity EI is constant, we obtain the (M/EI) diagram shown, which consists of a parabolic spandrel of area A_1 and a triangle of area A_2 .



$$A_1 = \frac{1}{3} \left(-\frac{wa^2}{2EI} \right) a = -\frac{wa^3}{6EI}$$

$$A_2 = \frac{1}{2} \left(-\frac{wa^2}{2EI} \right) L = -\frac{wa^2L}{4EI}$$

Reference Tangent at B. The reference tangent is drawn at point B as shown. Using the second moment-area theorem, we determine the tangential deviation of C with respect to B:

$$t_{C/B} = A_2 \frac{2L}{3} = \left(-\frac{wa^2L}{4EI} \right) \frac{2L}{3} = -\frac{wa^2L^2}{6EI}$$

From the similar triangles $A''A'B$ and $CC'B$, we find

$$A''A' = t_{C/B} \left(\frac{a}{L} \right) = -\frac{wa^2L^2}{6EI} \left(\frac{a}{L} \right) = -\frac{wa^3L}{6EI}$$

Again using the second moment-area theorem, we write

$$t_{A/B} = A_1 \frac{3a}{4} = \left(-\frac{wa^3}{6EI} \right) \frac{3a}{4} = -\frac{wa^4}{8EI}$$

a. Deflection at End A

$$y_A = A''A' + t_{A/B} = -\frac{wa^3L}{6EI} - \frac{wa^4}{8EI} = -\frac{wa^4}{8EI} \left(\frac{4L}{3a} + 1 \right)$$

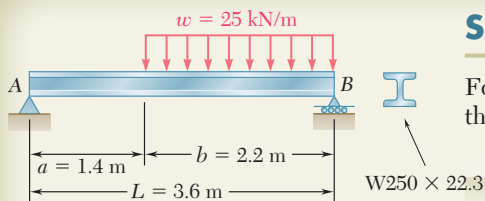
$$y_A = \frac{wa^4}{8EI} \left(1 + \frac{4L}{3a} \right) \downarrow$$

b. Evaluation of y_A .

Substituting the data given, we write

$$y_A = \frac{(1125 \text{ lb/in.})(36 \text{ in.})^4}{8(29 \times 10^6 \text{ lb/in}^2)(171 \text{ in}^4)} \left(1 + \frac{4}{3} \frac{66 \text{ in.}}{36 \text{ in.}} \right)$$

$$y_A = 0.1641 \text{ in.} \downarrow$$



SAMPLE PROBLEM 9.13

For the beam and loading shown, determine the magnitude and location of the largest deflection. Use $E = 200$ GPa.

SOLUTION

Reactions. Using the free-body diagram of the entire beam, we find

$$\mathbf{R}_A = 16.81 \text{ kN } \uparrow \quad \mathbf{R}_B = 38.2 \text{ kN } \uparrow$$

(M/EI) Diagram. We draw the (M/EI) diagram by parts, considering separately the effects of the reaction \mathbf{R}_A and of the distributed load. The areas of the triangle and of the spandrel are

$$A_1 = \frac{1}{2} \frac{R_A L}{EI} = \frac{R_A L^2}{2EI} \quad A_2 = \frac{1}{3} \left(-\frac{wb^2}{2EI} \right) b = -\frac{wb^3}{6EI}$$

Reference Tangent. The tangent to the beam at support A is chosen as the reference tangent. Using the second moment-area theorem, we determine the tangential deviation $t_{B/A}$ of support B with respect to support A:

$$t_{B/A} = A_1 \frac{L}{3} + A_2 \frac{b}{4} = \left(\frac{R_A L^2}{2EI} \right) \frac{L}{3} + \left(-\frac{wb^3}{6EI} \right) \frac{b}{4} = \frac{R_A L^3}{6EI} - \frac{wb^4}{24EI}$$

Slope at A

$$\theta_A = -\frac{t_{B/A}}{L} = -\left(\frac{R_A L^2}{6EI} - \frac{wb^4}{24EIL} \right) \quad (1)$$

Largest Deflection. The largest deflection occurs at point K, where the slope of the beam is zero. We write therefore

$$\theta_K = \theta_A + \theta_{K/A} = 0 \quad (2)$$

$$\text{But} \quad \theta_{K/A} = A_3 + A_4 = \frac{R_A x_m^2}{2EI} - \frac{w}{6EI} (x_m - a)^3 \quad (3)$$

We substitute for θ_A and $\theta_{K/A}$ from Eqs. (1) and (3) into Eq. (2):

$$-\left(\frac{R_A L^2}{6EI} - \frac{wb^4}{24EIL} \right) + \left[\frac{R_A x_m^2}{2EI} - \frac{w}{6EI} (x_m - a)^3 \right] = 0$$

Substituting the numerical data, we have

$$-29.53 \frac{10^3}{EI} + 8.405 x_m^2 \frac{10^3}{EI} - 4.167 (x_m - 1.4)^3 \frac{10^3}{EI} = 0$$

Solving by trial and error for x_m , we find

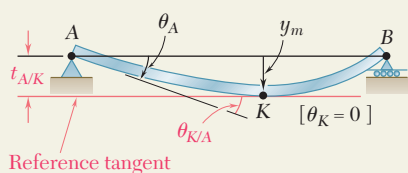
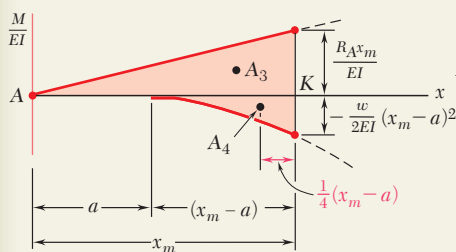
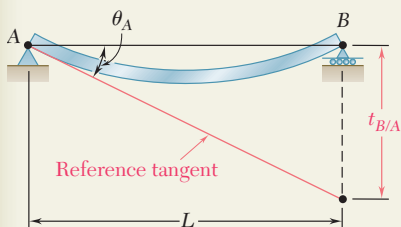
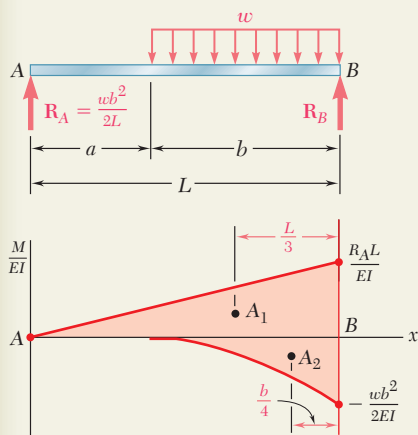
$$x_m = 1.890 \text{ m} \quad \blacktriangleleft$$

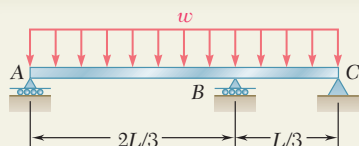
Computing the moments of A_3 and A_4 about a vertical axis through A, we have

$$\begin{aligned} |y|_m &= t_{A/K} = A_3 \frac{2x_m}{3} + A_4 \left[a + \frac{3}{4} (x_m - a) \right] \\ &= \frac{R_A x_m^3}{3EI} - \frac{wa}{6EI} (x_m - a)^3 - \frac{w}{8EI} (x_m - a)^4 \end{aligned}$$

Using the given data, $R_A = 16.81$ kN, and $I = 28.7 \times 10^{-6} \text{ m}^4$, we find

$$y_m = 6.44 \text{ mm} \quad \blacktriangleleft$$



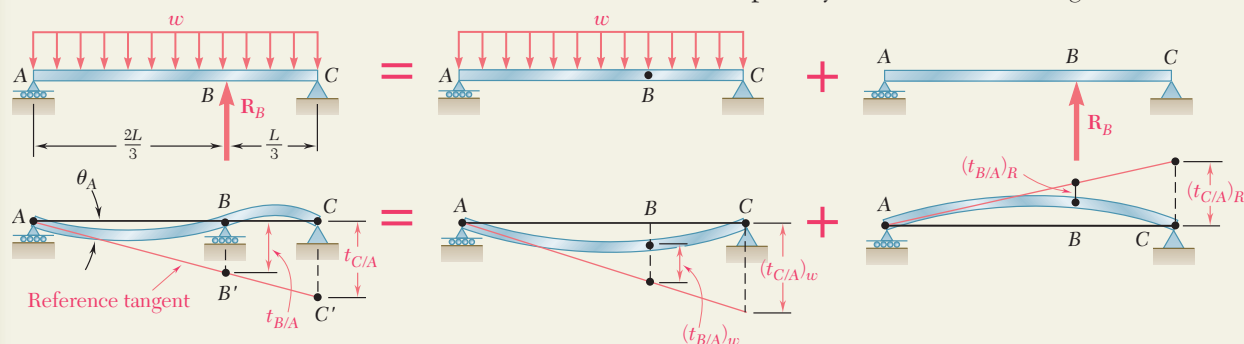


SAMPLE PROBLEM 9.14

For the uniform beam and loading shown, determine the reaction at B.

SOLUTION

The beam is indeterminate to the first degree. We choose the reaction R_B as redundant and consider separately the distributed loading and the redundant reaction loading.

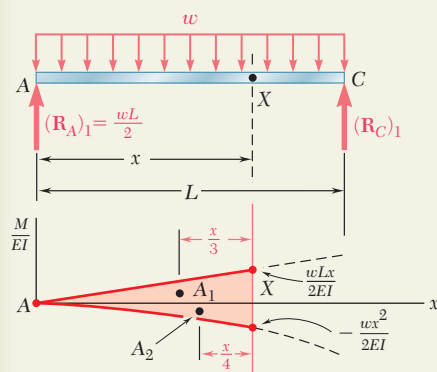


We next select the tangent at A as the reference tangent. From the similar triangles ABB' and ACC' , we find that

$$\frac{t_{C/A}}{L} = \frac{t_{B/A}}{\frac{2}{3}L} \quad t_{C/A} = \frac{3}{2}t_{B/A} \quad (1)$$

For each loading, we draw the (M/EI) diagram and then determine the tangential deviations of B and C with respect to A.

Distributed Loading. Considering the (M/EI) diagram from end A to an arbitrary point X, we write



$$(t_{X/A})_w = A_1 \frac{x}{3} + A_2 \frac{x}{4} = \left(\frac{1}{2} \frac{wLx}{2EI} x \right) \frac{x}{3} + \left(-\frac{1}{3} \frac{wx^2}{2EI} x \right) \frac{x}{4} = \frac{wx^3}{24EI} (2L - x)$$

Letting successively $x = L$ and $x = \frac{2}{3}L$, we have

$$(t_{C/A})_w = \frac{wL^4}{24EI} \quad (t_{B/A})_w = \frac{4}{243} \frac{wL^4}{EI}$$

Redundant Reaction Loading

$$(t_{C/A})_R = A_3 \frac{L}{9} + A_4 \frac{L}{3} = \left(\frac{1}{2} \frac{R_B L}{3EI} \frac{L}{3} \right) \frac{L}{9} + \left(-\frac{1}{2} \frac{R_B L}{3EI} L \right) \frac{L}{3} = -\frac{4}{81} \frac{R_B L^3}{EI}$$

$$(t_{B/A})_R = A_5 \frac{2L}{9} = \left[-\frac{1}{2} \frac{2R_B L}{9EI} \left(\frac{2L}{3} \right) \right] \frac{2L}{9} = -\frac{4}{243} \frac{R_B L^3}{EI}$$

Combined Loading. Adding the results obtained, we write

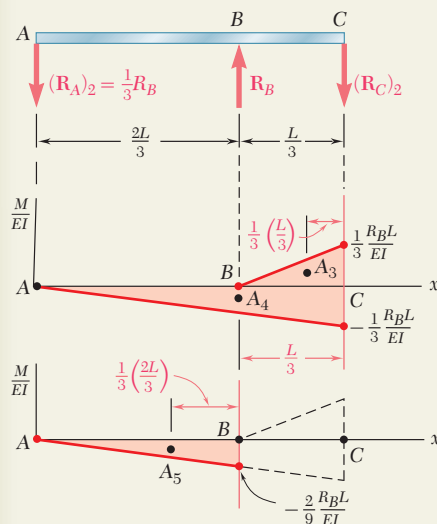
$$t_{C/A} = \frac{wL^4}{24EI} - \frac{4}{81} \frac{R_B L^3}{EI} \quad t_{B/A} = \frac{4}{243} \frac{(wL^4 - R_B L^3)}{EI}$$

Reaction at B. Substituting for $t_{C/A}$ and $t_{B/A}$ into Eq. (1), we have

$$\left(\frac{wL^4}{24EI} - \frac{4}{81} \frac{R_B L^3}{EI} \right) = \frac{3}{2} \left[\frac{4}{243} \frac{(wL^4 - R_B L^3)}{EI} \right]$$

$$R_B = 0.6875wL$$

$$R_B = 0.688wL \quad \blacktriangleleft$$



PROBLEMS

Use the moment-area method to solve the following problems.

9.125 through 9.128 For the prismatic beam and loading shown, determine (a) the deflection at point D, (b) the slope at end A.

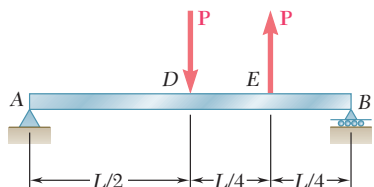


Fig. P9.125

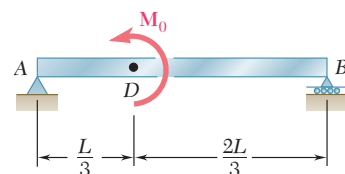


Fig. P9.126

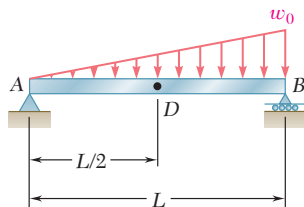


Fig. P9.127

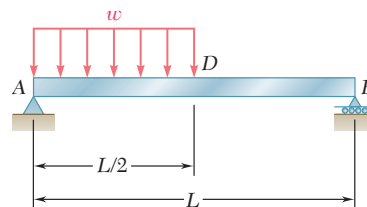


Fig. P9.128

9.129 and 9.130 For the beam and loading shown, determine (a) the slope at end A, (b) the deflection at point D. Use $E = 200 \text{ GPa}$.

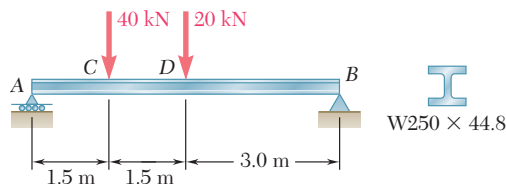


Fig. P9.129

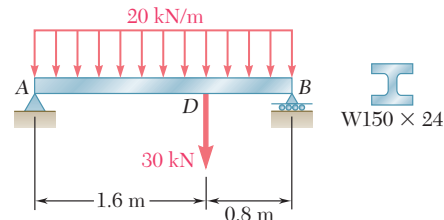


Fig. P9.130

9.131 For the beam and loading shown, determine (a) the slope at point A, (b) the deflection at point E. Use $E = 29 \times 10^6 \text{ psi}$.

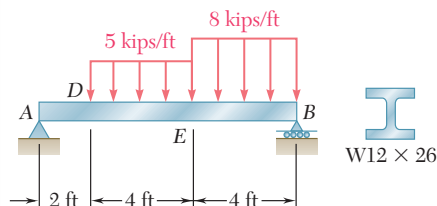


Fig. P9.131

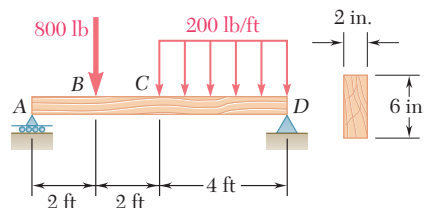


Fig. P9.132

9.132 For the timber beam and loading shown, determine (a) the slope at point A, (b) the deflection at point C. Use $E = 1.7 \times 10^6 \text{ psi}$.

- 9.133** For the beam and loading shown, determine (a) the slope at point A, (b) the deflection at point D.

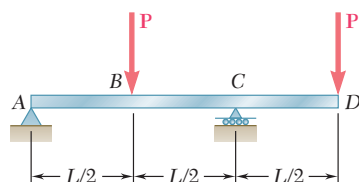


Fig. P9.133

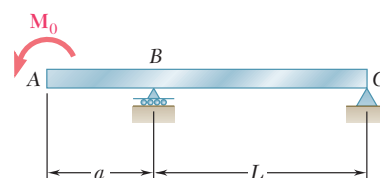


Fig. P9.134

- 9.134** For the beam and loading shown, determine (a) the slope at point A, (b) the deflection at point A.

- 9.135** For the beam and loading shown, determine (a) the slope at point C, (b) the deflection at point D. Use $E = 29 \times 10^6$ psi.

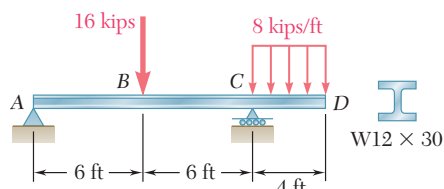


Fig. P9.135

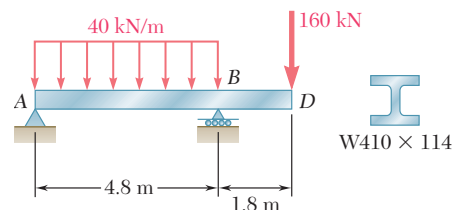


Fig. P9.136

- 9.136** For the beam and loading shown, determine (a) the slope at point B, (b) the deflection at point D. Use $E = 200$ GPa.

- 9.137** Knowing that the beam AB is made of a solid steel rod of diameter $d = 0.75$ in., determine for the loading shown (a) the slope at point D, (b) the deflection at point A. Use $E = 29 \times 10^6$ psi.

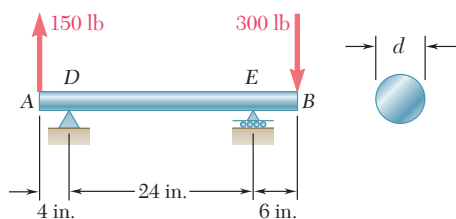


Fig. P9.137

- 9.138** Knowing that the beam AD is made of a solid steel bar, determine (a) the slope at point B, (b) the deflection at point A. Use $E = 200$ GPa.

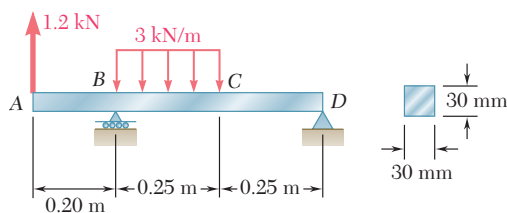


Fig. P9.138

9.139 For the beam and loading shown, determine the deflection (a) at point D , (b) at point E .

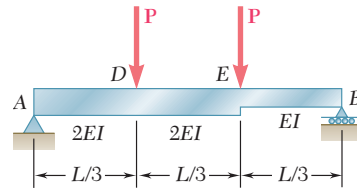


Fig. P9.139

9.140 For the beam and loading shown, determine (a) the slope at end A , (b) the slope at end B , (c) the deflection at the midpoint C .

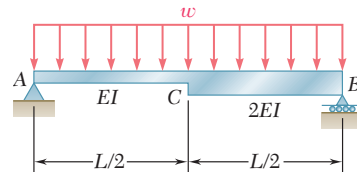


Fig. P9.140

9.141 through 9.144 For the beam and loading shown, determine the magnitude and location of the largest downward deflection.

9.141 Beam and loading of Prob. 9.125

9.142 Beam and loading of Prob. 9.127

9.143 Beam and loading of Prob. 9.129

9.144 Beam and loading of Prob. 9.131

9.145 For the beam and loading of Prob. 9.136, determine the largest upward deflection in span AB .

9.146 For the beam and loading of Prob. 9.137, determine the largest upward deflection in span DE .

9.147 through 9.150 For the beam and loading shown, determine the reaction at the roller support.

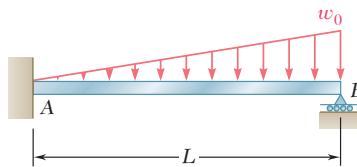


Fig. P9.147

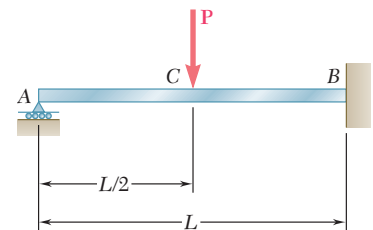


Fig. P9.148

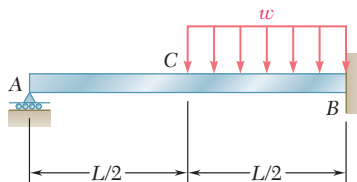


Fig. P9.149

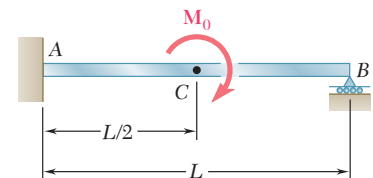


Fig. P9.150

9.151 and 9.152 For the beam and loading shown, determine the reaction at each support.

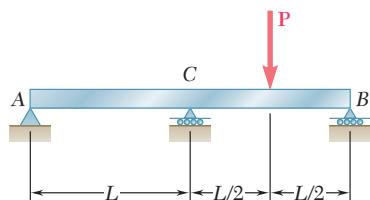


Fig. P9.151

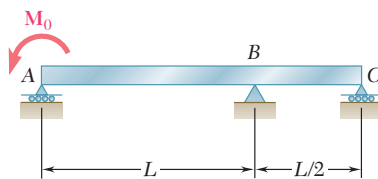


Fig. P9.152

9.153 Determine the reaction at the roller support and draw the bending-moment diagram for the beam and loading shown.

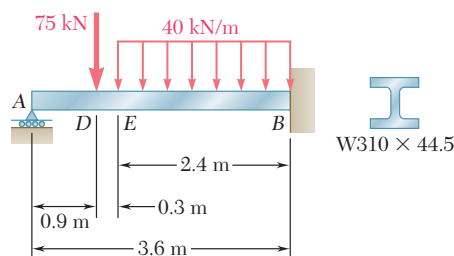


Fig. P9.153

9.154 Determine the reaction at the roller support and draw the bending-moment diagram for the beam and loading shown.

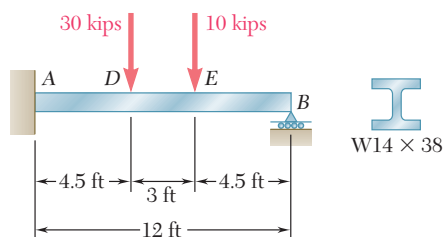


Fig. P9.154

9.155 For the beam and loading shown, determine the spring constant k for which the force in the spring is equal to one-third of the total load on the beam.

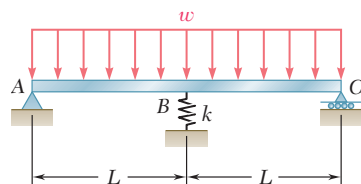


Fig. P9.155 and P9.156

9.156 For the beam and loading shown, determine the spring constant k for which the bending moment at B is $M_B = -wL^2/10$.

REVIEW AND SUMMARY

This chapter was devoted to the determination of slopes and deflections of beams under transverse loadings. Two approaches were used. First we used a mathematical method based on the method of integration of a differential equation to get the slopes and deflections at any point along the beam. We then used the *moment-area method* to find the slopes and deflections at a given point along the beam. Particular emphasis was placed on the computation of the maximum deflection of a beam under a given loading. We also applied these methods for determining deflections to the analysis of *indeterminate beams*, those in which the number of reactions at the supports exceeds the number of equilibrium equations available to determine these unknowns.

Deformation of a beam under transverse loading

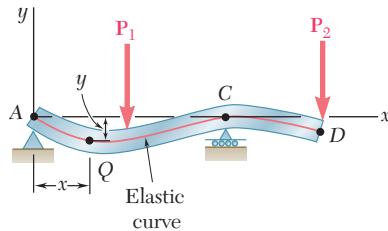


Fig. 9.70

We noted in Sec. 9.2 that Eq. (4.21) of Sec. 4.4, which relates the curvature $1/\rho$ of the neutral surface and the bending moment M in a prismatic beam in pure bending, can be applied to a beam under a transverse loading, but that both M and $1/\rho$ will vary from section to section. Denoting by x the distance from the left end of the beam, we wrote

$$\frac{1}{\rho} = \frac{M(x)}{EI} \quad (9.1)$$

This equation enabled us to determine the radius of curvature of the neutral surface for any value of x and to draw some general conclusions regarding the shape of the deformed beam.

In Sec. 9.3, we discussed how to obtain a relation between the deflection y of a beam, measured at a given point Q , and the distance x of that point from some fixed origin (Fig. 9.70). Such a relation defines the *elastic curve* of a beam. Expressing the curvature $1/\rho$ in terms of the derivatives of the function $y(x)$ and substituting into (9.1), we obtained the following second-order linear differential equation:

$$\frac{d^2y}{dx^2} = \frac{M(x)}{EI} \quad (9.4)$$

Integrating this equation twice, we obtained the following expressions defining the slope $\theta(x) = dy/dx$ and the deflection $y(x)$, respectively:

$$EI \frac{dy}{dx} = \int_0^x M(x) dx + C_1 \quad (9.5)$$

$$EI y = \int_0^x dx \int_0^x M(x) dx + C_1 x + C_2 \quad (9.6)$$

The product EI is known as the *flexural rigidity* of the beam; C_1 and C_2 are two constants of integration that can be determined from the *boundary conditions* imposed on the beam by its supports (Fig. 9.71) [Example 9.01]. The maximum deflection can then be obtained by determining the value of x for which the slope is zero and the corresponding value of y [Example 9.02, Sample Prob. 9.1].

Boundary conditions

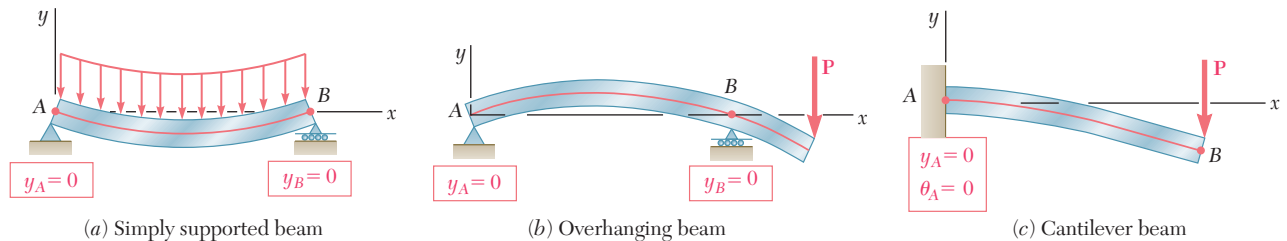


Fig. 9.71 Boundary conditions for statically determinate beams.

When the loading is such that different analytical functions are required to represent the bending moment in various portions of the beam, then different differential equations are also required, leading to different functions representing the slope $\theta(x)$ and the deflection $y(x)$ in the various portions of the beam. In the case of the beam and loading considered in Example 9.03 (Fig. 9.72), two differential equations were required, one for the portion of beam AD and the other for the portion DB . The first equation yielded the functions θ_1 and y_1 , and the second the functions θ_2 and y_2 . Altogether, four constants of integration had to be determined; two were obtained by writing that the deflections at A and B were zero, and the other two by expressing that the portions of beam AD and DB had the same slope and the same deflection at D .

Elastic curve defined by different functions

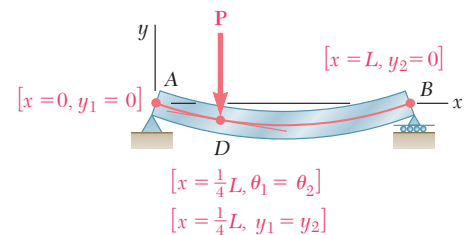


Fig. 9.72

We observed in Sec. 9.4 that in the case of a beam supporting a distributed load $w(x)$, the elastic curve can be determined directly from $w(x)$ through four successive integrations yielding V , M , θ , and y in that order. For the cantilever beam of Fig. 9.73a and the simply supported beam of Fig. 9.73b, the resulting four constants of integration can be determined from the four boundary conditions indicated in each part of the figure [Example 9.04, Sample Prob. 9.2].

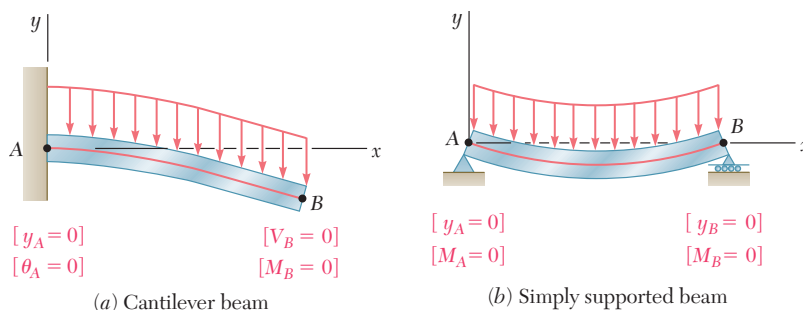


Fig. 9.73 Boundary conditions for beams carrying a distributed load.

Statically indeterminate beams

In Sec. 9.5, we discussed *statically indeterminate beams*, i.e., beams supported in such a way that the reactions at the supports involved four or more unknowns. Since only three equilibrium equations are available to determine these unknowns, the equilibrium equations had to be supplemented by equations obtained from the boundary conditions imposed by the supports. In the case of the beam of Fig 9.74, we noted that the reactions at the supports involved four

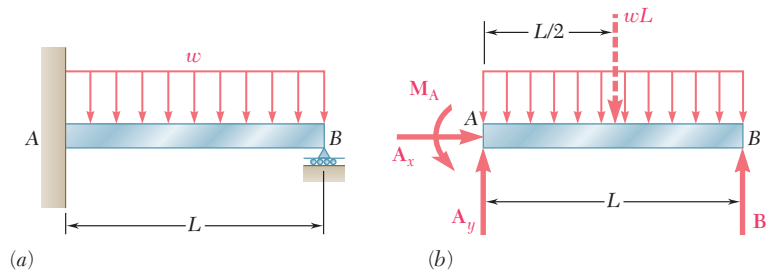


Fig. 9.74

unknowns, namely, M_A , A_x , A_y , and B . Such a beam is said to be *indeterminate to the first degree*. (If five unknowns were involved, the beam would be indeterminate to the *second degree*.) Expressing the bending moment $M(x)$ in terms of the four unknowns and integrating twice [Example 9.05], we determined the slope $\theta(x)$ and the deflection $y(x)$ in terms of the same unknowns and the constants of integration C_1 and C_2 . The six unknowns involved in this computation were obtained by solving simultaneously the three equilibrium equations for the free body of Fig. 9.74b and the three equations expressing that $\theta = 0$, $y = 0$ for $x = 0$, and that $y = 0$ for $x = L$ (Fig. 9.75) [see also Sample Prob. 9.3].

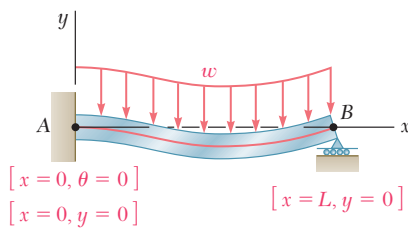


Fig. 9.75

Use of singularity functions

The integration method provides an effective way for determining the slope and deflection at any point of a prismatic beam, as long as the bending moment M can be represented by a single analytical function. However, when several functions are required to represent M over the entire length of the beam, this method can become quite laborious, since it requires matching slopes and deflections at every transition point. We saw in Sec. 9.6 that the use of *singularity functions* (previously introduced in Sec. 5.5) considerably simplifies the determination of θ and y at any point of the beam. Considering again the beam of Example 9.03 (Fig. 9.76) and drawing its free-body diagram (Fig. 9.77), we expressed the shear at any point of the beam as

$$V(x) = \frac{3P}{4} - P \langle x - \frac{1}{4}L \rangle^0$$

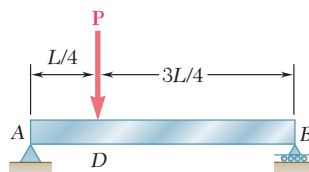


Fig. 9.76

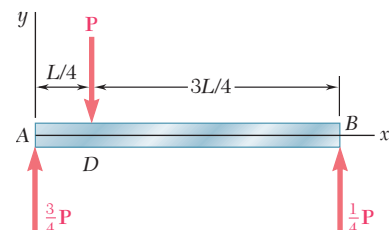


Fig. 9.77

where the step function $\langle x - \frac{1}{4}L \rangle^0$ is equal to zero when the quantity inside the brackets $\langle \rangle$ is negative, and equal to one otherwise. Integrating three times, we obtained successively

$$M(x) = \frac{3P}{4}x - P\langle x - \frac{1}{4}L \rangle \quad (9.44)$$

$$EI \theta = EI \frac{dy}{dx} = \frac{3}{8}Px^2 - \frac{1}{2}P\langle x - \frac{1}{4}L \rangle^2 + C_1 \quad (9.46)$$

$$EI y = \frac{1}{8}Px^3 - \frac{1}{6}P\langle x - \frac{1}{4}L \rangle^3 + C_1x + C_2 \quad (9.47)$$

where the brackets $\langle \rangle$ should be replaced by zero when the quantity inside is negative, and by ordinary parentheses otherwise. The constants C_1 and C_2 were determined from the boundary conditions shown in Fig. 9.78 [Example 9.06; Sample Probs. 9.4, 9.5, and 9.6].

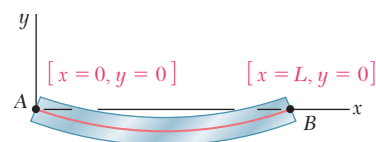


Fig. 9.78

Method of superposition

The next section was devoted to the *method of superposition*, which consists of determining separately, and then adding, the slope and deflection caused by the various loads applied to a beam [Sec. 9.7]. This procedure was facilitated by the use of the table of Appendix D, which gives the slopes and deflections of beams for various loadings and types of support [Example 9.07, Sample Prob. 9.7].

The method of superposition can be used effectively with *statically indeterminate beams* [Sec. 9.8]. In the case of the beam of Example 9.08 (Fig. 9.79), which involves four unknown reactions and is thus indeterminate to the *first degree*, the reaction at B was considered as *redundant* and the beam was released from that support. Treating the reaction R_B as an unknown load and considering separately the deflections caused at B by the given distributed load and by R_B , we wrote that the sum of these deflections was zero (Fig. 9.80). The equation obtained was solved for R_B [see also Sample Prob. 9.8]. In the case of a beam indeterminate to the *second degree*, i.e., with reactions at the supports involving five unknowns, two reactions must be designated as redundant, and the corresponding supports must be eliminated or modified accordingly [Sample Prob. 9.9].

Statically indeterminate beams by superposition

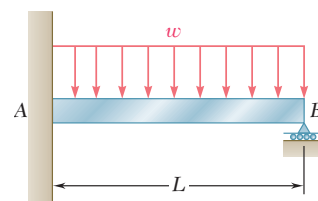


Fig. 9.79

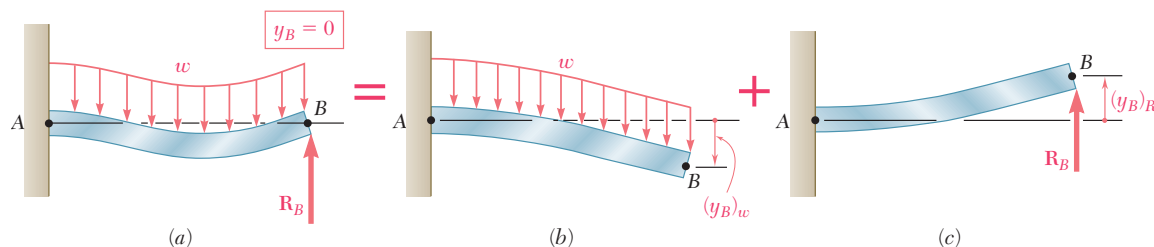


Fig. 9.80

We next studied the determination of deflections and slopes of beams using the *moment-area method*. In order to derive the *moment-area theorems* [Sec. 9.9], we first drew a diagram representing the variation along the beam of the quantity M/EI obtained by dividing the

First moment-area theorem

bending moment M by the flexural rigidity EI (Fig. 9.81). We then derived the *first moment-area theorem*, which may be stated as follows: *The area under the (M/EI) diagram between two points is equal to the angle between the tangents to the elastic curve drawn at these points.* Considering tangents at C and D , we wrote

$$\theta_{D/C} = \text{area under } (M/EI) \text{ diagram between } C \text{ and } D \quad (9.56)$$

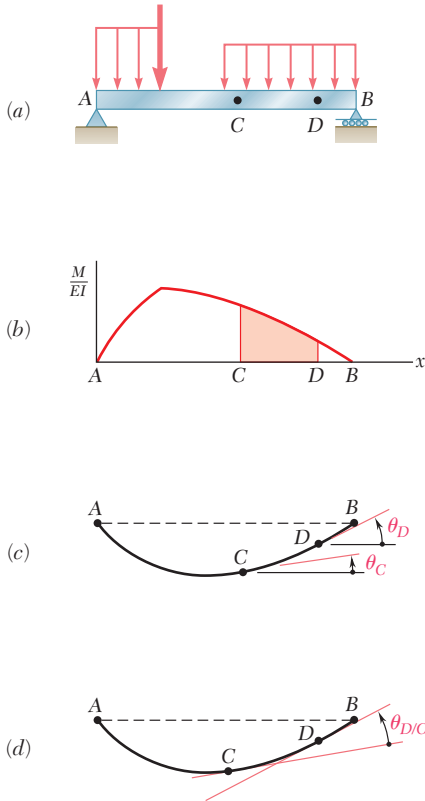


Fig. 9.81 First moment-area theorem.

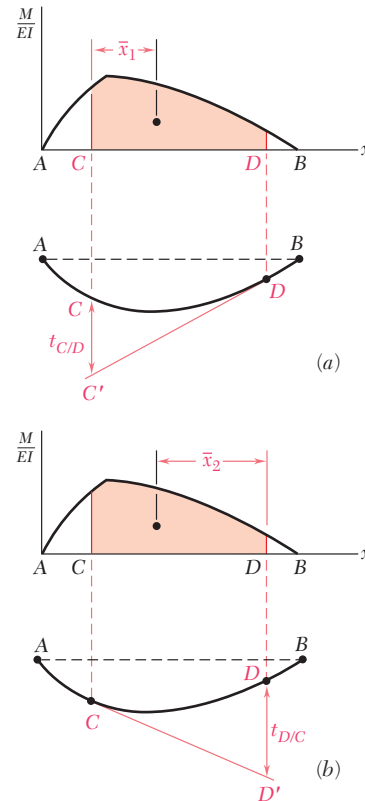


Fig. 9.82 Second moment-area theorem.

Second moment-area theorem

Again using the (M/EI) diagram and a sketch of the deflected beam (Fig. 9.82), we drew a tangent at point D and considered the vertical distance $t_{C/D}$, which is called the *tangential deviation of C with respect to D* . We then derived the second moment-area theorem, which may be stated as follows: *The tangential deviation $t_{C/D}$ of C with respect to D is equal to the first moment with respect to a vertical axis through C of the area under the (M/EI) diagram between C and D .* We were careful to distinguish between the tangential deviation of C with respect to D (Fig. 9.82a).

$$t_{C/D} = (\text{area between } C \text{ and } D) \bar{x}_1 \quad (9.59)$$

and the tangential deviation of D with respect to C (Fig. 9.82b):

$$t_{D/C} = (\text{area between } C \text{ and } D) \bar{x}_2 \quad (9.60)$$

In Sec. 9.10 we learned to determine the slope and deflection at points of *cantilever* beams and beams with *symmetric loadings*. For cantilever beams, the tangent at the fixed support is horizontal (Fig. 9.83); and for symmetrically loaded beams, the tangent is horizontal at the midpoint C of the beam (Fig. 9.84). Using the horizontal tangent as a *reference tangent*, we were able to determine slopes and deflections by using, respectively, the first and second moment-area theorems [Example 9.09, Sample Probs. 9.10 and 9.11]. We noted that to find a deflection that is not a tangential deviation (Fig. 9.84c), it is necessary to first determine which tangential deviations can be combined to obtain the desired deflection.

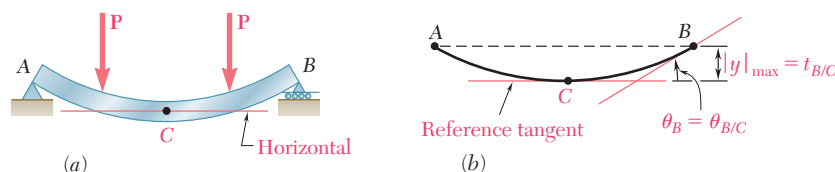


Fig. 9.84

In many cases the application of the moment-area theorems is simplified if we consider the effect of each load separately [Sec. 9.11]. To do this we drew the (M/EI) *diagram by parts* by drawing a separate (M/EI) diagram for each load. The areas and the moments of areas under the several diagrams could then be added to determine slopes and tangential deviations for the original beam and loading [Examples 9.10 and 9.11].

In Sec. 9.12 we expanded the use of the moment-area method to cover beams with *unsymmetric loadings*. Observing that locating a horizontal tangent is usually not possible, we selected a reference tangent at one of the beam supports, since the slope of that tangent can be readily determined. For example, for the beam and loading shown in Fig. 9.85, the slope of the tangent at A can be obtained by computing the

Cantilever Beams Beams with symmetric loadings

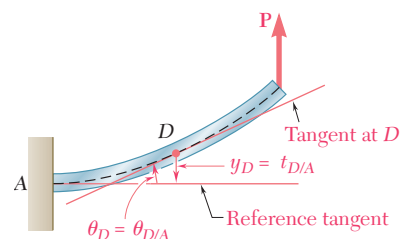
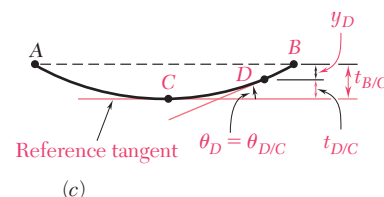


Fig. 9.83



Bending-moment diagram by parts

Unsymmetric loadings

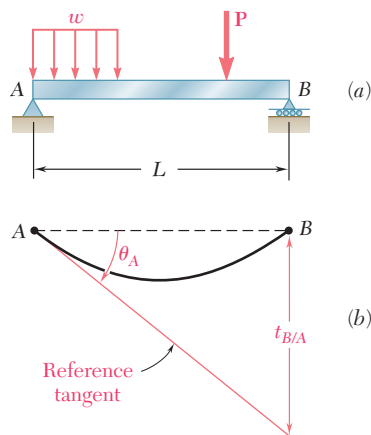


Fig. 9.85

Maximum deflection

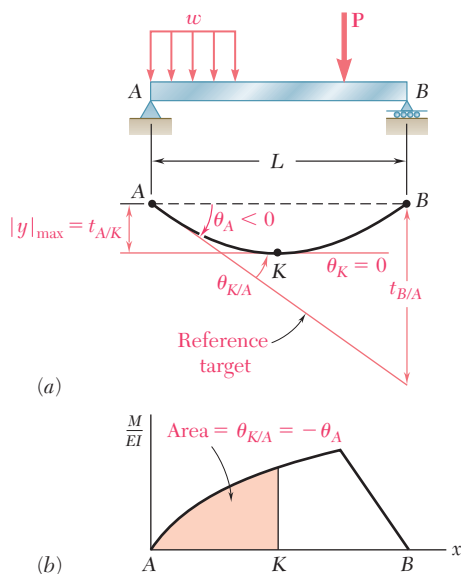


Fig. 9.86

tangential deviation $t_{B/A}$ and dividing it by the distance L between the supports A and B . Then, using both moment-area theorems and simple geometry, we could determine the slope and deflection at any point of the beam [Example 9.12, Sample Prob. 9.12].

The *maximum deflection* of an unsymmetrically loaded beam generally does not occur at midspan. The approach indicated in the preceding paragraph was used to determine point K where the maximum deflection occurs and the magnitude of that deflection [Sec. 9.13]. Observing that the slope at K is zero (Fig. 9.86), we concluded that $\theta_{K/A} = -\theta_A$. Recalling the first moment-area theorem, we determined the location of K by measuring under the (M/EI) diagram an area equal to $\theta_{K/A}$. The maximum deflection was then obtained by computing the tangential deviation $t_{A/K}$ [Sample Probs. 9.12 and 9.13].

In the last section of the chapter [Sec. 9.14] we applied the moment-area method to the analysis of *statically indeterminate beams*. Since the reactions for the beam and loading shown in Fig. 9.87 cannot be

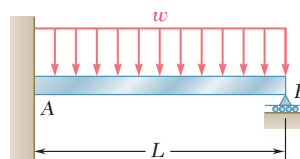


Fig. 9.87

Statically indeterminate beams

determined by statics alone, we designated one of the reactions of the beam as redundant (\mathbf{M}_A in Fig. 9.88a) and considered the redundant reaction as an unknown load. The tangential deviation of B with respect to A was considered separately for the distributed load (Fig. 9.88b) and for the redundant reaction (Fig. 9.88c). Expressing that under the combined action of the distributed load and of the couple \mathbf{M}_A the tangential deviation of B with respect to A must be zero, we wrote

$$t_{B/A} = (t_{B/A})_w + (t_{B/A})_M = 0$$

From this expression we determined the magnitude of the redundant reaction \mathbf{M}_A [Example 9.14, Sample Prob. 9.14].

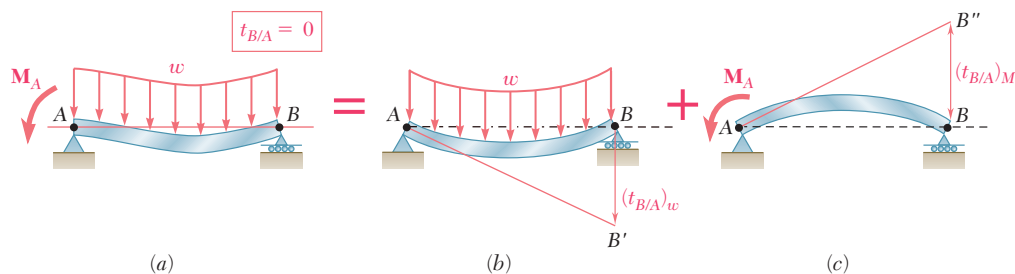


Fig. 9.88

REVIEW PROBLEMS

- 9.157** For the loading shown, determine (a) the equation of the elastic curve for the cantilever beam AB , (b) the deflection at the free end, (c) the slope at the free end.
- 9.158** (a) Determine the location and magnitude of the maximum absolute deflection in AB between A and the center of the beam. (b) Assuming that beam AB is a $W18 \times 76$ rolled shape, $M_0 = 150 \text{ kip} \cdot \text{ft}$ and $E = 29 \times 10^6 \text{ psi}$, determine the maximum allowable length L so that the maximum deflection does not exceed 0.05 in.

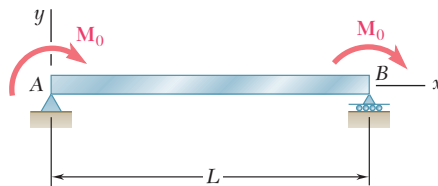


Fig. P9.158

- 9.159** For the beam and loading shown, determine (a) the equation of the elastic curve, (b) the deflection at the free end.
- 9.160** Determine the reaction at A and draw the bending moment diagram for the beam and loading shown.

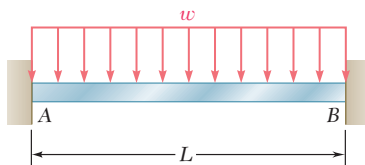


Fig. P9.160

- 9.161** For the beam and loading shown, determine (a) the slope at end A , (b) the deflection at point B . Use $E = 29 \times 10^6 \text{ psi}$.
- 9.162** The rigid bar BDE is welded at point B to the rolled-steel beam AC . For the loading shown, determine (a) the slope at point A , (b) the deflection at point B . Use $E = 200 \text{ GPa}$.

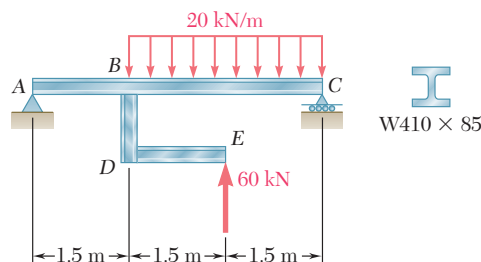


Fig. P9.162

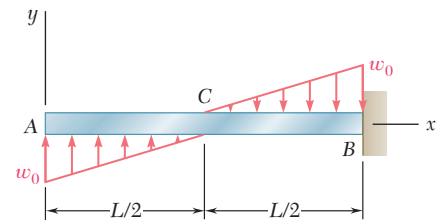


Fig. P9.157

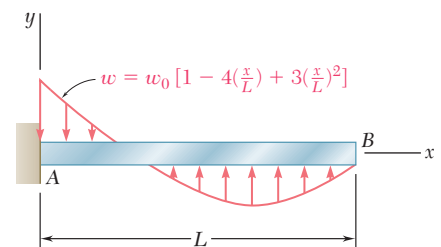


Fig. P9.159

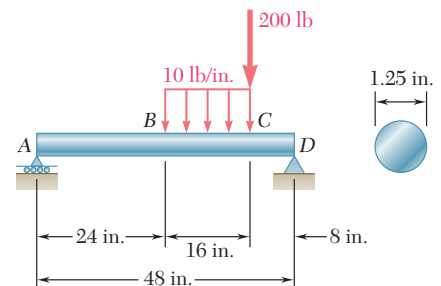


Fig. P9.161

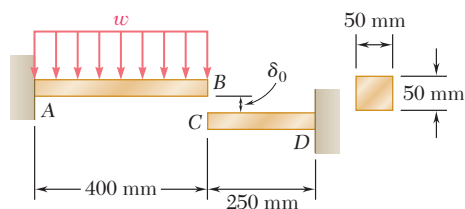


Fig. P9.163

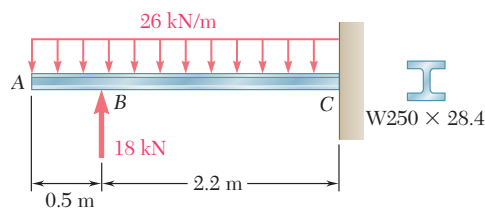


Fig. P9.165

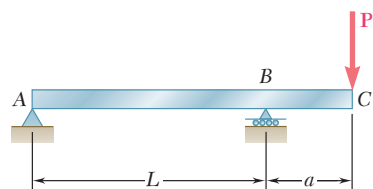


Fig. P9.167

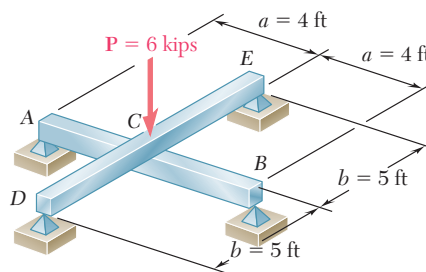


Fig. P9.164

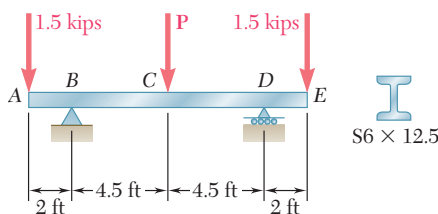


Fig. P9.166

9.163 Before the uniformly distributed load w is applied, a gap, $\delta_0 = 1.2$ mm, exists between the ends of the cantilever bars AB and CD . Knowing that $E = 105$ GPa and $w = 30$ kN/m, determine (a) the reaction at A , (b) the reaction at D .

9.164 For the loading shown, and knowing that beams AB and DE have the same flexural rigidity, determine the reaction (a) at B , (b) at E .

9.165 For the cantilever beam and loading shown, determine (a) the slope at point A , (b) the deflection at point A . Use $E = 200$ GPa.

9.166 Knowing that the magnitude of the load P is 7 kips, determine (a) the slope at end A , (b) the deflection at end A , (c) the deflection at midpoint C of the beam. Use $E = 29 \times 10^6$ psi.

9.167 For the beam and loading shown, determine (a) the slope at point C , (b) the deflection at point C .

9.168 A hydraulic jack can be used to raise point B of the cantilever beam ABC . The beam was originally straight, horizontal, and unloaded. A 20-kN load was then applied at point C , causing this point to move down. Determine (a) how much point B should be raised to return point C to its original position, (b) the final value of the reaction at B . Use $E = 200$ GPa.

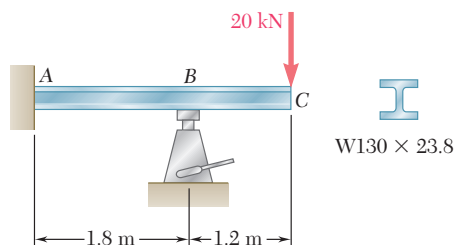


Fig. P9.168

COMPUTER PROBLEMS

The following problems are designed to be solved with a computer.

9.C1 Several concentrated loads can be applied to the cantilever beam AB . Write a computer program to calculate the slope and deflection of beam AB from $x = 0$ to $x = L$, using given increments Δx . Apply this program with increments $\Delta x = 50$ mm to the beam and loading of Prob. 9.73 and Prob. 9.74.

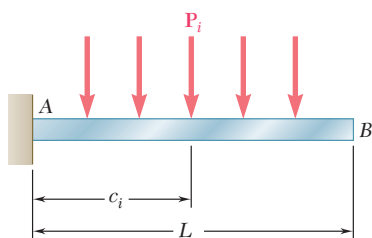


Fig. P9.C1

9.C2 The 22-ft beam AB consists of a $W21 \times 62$ rolled-steel shape and supports a 3.5-kip/ft distributed load as shown. Write a computer program and use it to calculate for values of a from 0 to 22 ft, using 1-ft increments, (a) the slope and deflection at D , (b) the location and magnitude of the maximum deflection. Use $E = 29 \times 10^6$ psi.

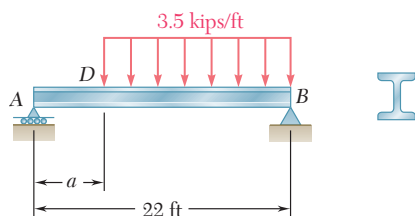


Fig. P9.C2

9.C3 The cantilever beam AB carries the distributed loads shown. Write a computer program to calculate the slope and deflection of beam AB from $x = 0$ to $x = L$ using given increments Δx . Apply this program with increments $\Delta x = 100$ mm, assuming that $L = 2.4$ m, $w = 36$ kN/m, and (a) $a = 0.6$ m, (b) $a = 1.2$ m, (c) $a = 1.8$ m. Use $E = 200$ GPa.

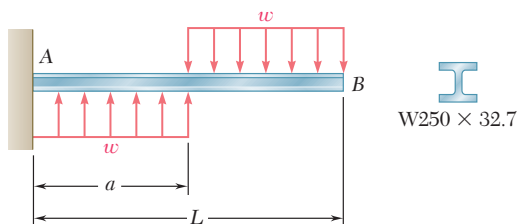


Fig. P9.C3

9.C4 The simple beam AB is of constant flexural rigidity EI and carries several concentrated loads as shown. Using the *Method of Integration*, write a computer program that can be used to calculate the slope and deflection at points along the beam from $x = 0$ to $x = L$ using given increments Δx . Apply this program to the beam and loading of (a) Prob. 9.13 with $\Delta x = 1$ ft, (b) Prob. 9.16 with $\Delta x = 0.05$ m, (c) Prob. 9.129 with $\Delta x = 0.25$ m.

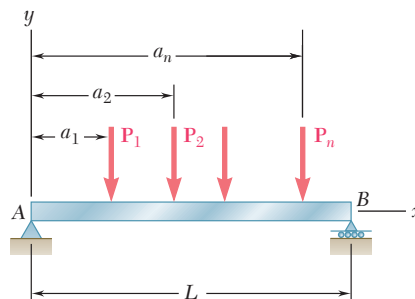


Fig. P9.C4

9.C5 The supports of beam AB consist of a fixed support at end A and a roller support located at point D . Write a computer program that can be used to calculate the slope and deflection at the free end of the beam for values of a from 0 to L using given increments Δa . Apply this program to calculate the slope and deflection at point B for each of the following cases:

	L	ΔL	w	E	Shape
(a)	12 ft	0.5 ft	1.6 k/ft	29×10^6 psi	W16 \times 57
(b)	3 m	0.2 m	18 kN/m	200 GPa	W460 \times 113

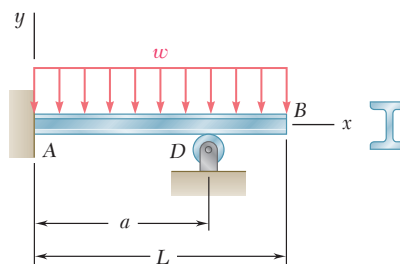


Fig. P9.C5

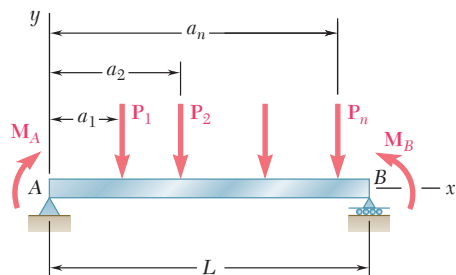


Fig. P9.C6

9.C6 For the beam and loading shown, use the *Moment-Area Method* to write a computer program to calculate the slope and deflection at points along the beam from $x = 0$ to $x = L$ using given increments Δx . Apply this program to calculate the slope and deflection at each concentrated load for the beam of (a) Prob. 9.77 with $\Delta x = 0.5$ m, (b) Prob. 9.119 with $\Delta x = 0.5$ m.

9.C7 Two 52-kN loads are maintained 2.5 m apart as they are moved slowly across beam AB . Write a computer program to calculate the deflection at the midpoint C of the beam for values of x from 0 to 9 m, using 0.5-m increments. Use $E = 200$ GPa.

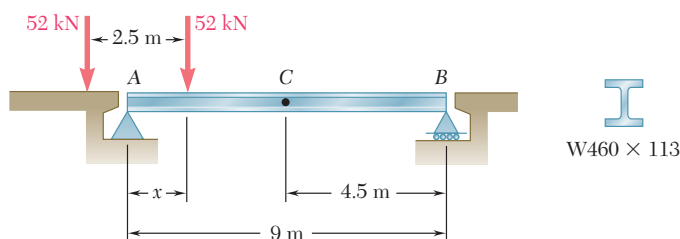


Fig. P9.C7

9.C8 A uniformly distributed load w and several distributed loads P_i may be applied to beam AB . Write a computer program to determine the reaction at the roller support and apply this program to the beam and loading of (a) Prob. 9.53a, (b) Prob. 9.154.

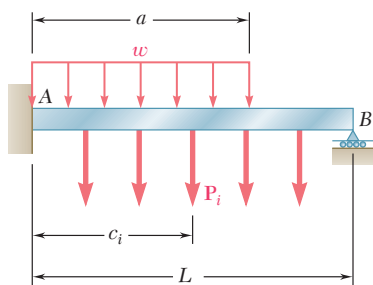


Fig. P9.C8

The curved pedestrian bridge is supported by a series of columns. The analysis and design of members supporting axial compressive loads will be discussed in this chapter.



10

CHAPTER

Columns



Chapter 10 Columns

- 10.1 Introduction
- 10.2 Stability of Structures
- 10.3 Euler's Formula for Pin-Ended Columns
- 10.4 Extension of Euler's Formula to Columns with Other End Conditions
- *10.5 Eccentric Loading; the Secant Formula
- 10.6 Design of Columns under a Centric Load
- 10.7 Design of Columns under an Eccentric Load

10.1 INTRODUCTION

In the preceding chapters, we had two primary concerns: (1) the strength of the structure, i.e., its ability to support a specified load without experiencing excessive stress; (2) the ability of the structure to support a specified load without undergoing unacceptable deformations. In this chapter, our concern will be with the stability of the structure, i.e., with its ability to support a given load without experiencing a sudden change in its configuration. Our discussion will relate chiefly to columns, i.e., to the analysis and design of vertical prismatic members supporting axial loads.

In Sec. 10.2, the stability of a simplified model of a column, consisting of two rigid rods connected by a pin and a spring and supporting a load \mathbf{P} , will first be considered. You will observe that if its equilibrium is disturbed, this system will return to its original equilibrium position as long as P does not exceed a certain value P_{cr} , called the *critical load*. However, if $P > P_{cr}$, the system will move away from its original position and settle in a new position of equilibrium. In the first case, the system is said to be *stable*, and in the second case, it is said to be *unstable*.

In Sec. 10.3, you will begin the study of the *stability of elastic columns* by considering a pin-ended column subjected to a centric axial load. *Euler's formula* for the critical load of the column will be derived and from that formula the corresponding critical normal stress in the column will be determined. By applying a factor of safety to the critical load, you will be able to determine the allowable load that can be applied to a pin-ended column.

In Sec. 10.4, the analysis of the stability of columns with different end conditions will be considered. You will simplify these analyses by learning how to determine the *effective length* of a column, i.e., the length of a pin-ended column having the same critical load.

In Sec. 10.5, you will consider columns supporting eccentric axial loads; these columns have transverse deflections for all magnitudes of the load. An expression for the maximum deflection under a given load will be derived and used to determine the maximum normal stress in the column. Finally, the *secant formula* which relates the average and maximum stresses in a column will be developed.

In the first sections of the chapter, each column is initially assumed to be a straight homogeneous prism. In the last part of the chapter, you will consider real columns which are designed and analyzed using empirical formulas set forth by professional organizations. In Sec. 10.6, formulas will be presented for the allowable stress in columns made of steel, aluminum, or wood and subjected to a centric axial load. In the last section of the chapter (Sec. 10.7), the design of columns under an eccentric axial load will be considered.

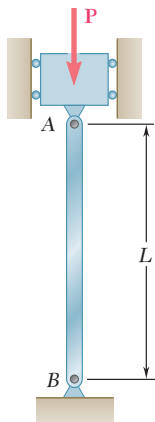


Fig. 10.1 Column.

10.2 STABILITY OF STRUCTURES

Suppose we are to design a column AB of length L to support a given load \mathbf{P} (Fig. 10.1). The column will be pin-connected at both ends and we assume that \mathbf{P} is a centric axial load. If the cross-sectional

area A of the column is selected so that the value $\sigma = P/A$ of the stress on a transverse section is less than the allowable stress σ_{all} for the material used, and if the deformation $\delta = PL/AE$ falls within the given specifications, we might conclude that the column has been properly designed. However, it may happen that, as the load is applied, the column will *buckle*; instead of remaining straight, it will suddenly become sharply curved (Fig. 10.2). Photo 10.1 shows a column that has been loaded so that it is no longer straight; the column has buckled. Clearly, a column that buckles under the load it is to support is not properly designed.



Photo 10.1 Laboratory test showing a buckled column.

Before getting into the actual discussion of the stability of elastic columns, some insight will be gained on the problem by considering a simplified model consisting of two rigid rods AC and BC connected at C by a pin and a torsional spring of constant K (Fig. 10.3).



Fig. 10.2 Buckled column.

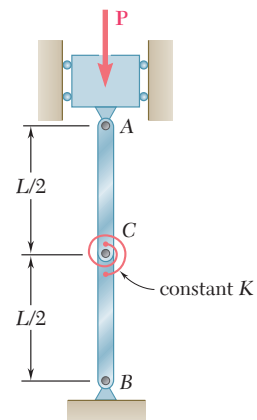


Fig. 10.3 Column model.

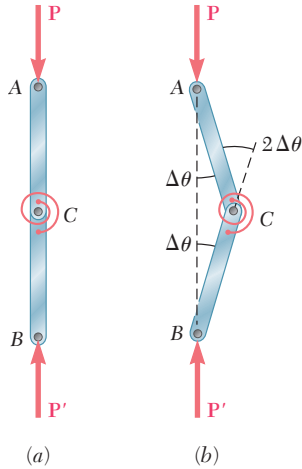


Fig. 10.4

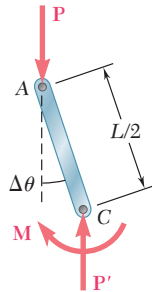


Fig. 10.5

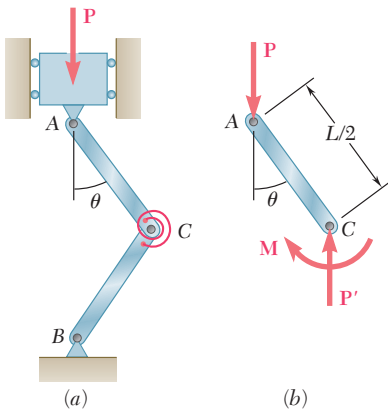


Fig. 10.6 Column model in buckled position.

If the two rods and the two forces \mathbf{P} and \mathbf{P}' are perfectly aligned, the system will remain in the position of equilibrium shown in Fig. 10.4a as long as it is not disturbed. But suppose that we move C slightly to the right, so that each rod now forms a small angle $\Delta\theta$ with the vertical (Fig. 10.4b). Will the system return to its original equilibrium position, or will it move further away from that position? In the first case, the system is said to be *stable*, and in the second case, it is said to be *unstable*.

To determine whether the two-rod system is stable or unstable, we consider the forces acting on rod AC (Fig. 10.5). These forces consist of two couples, namely the couple formed by \mathbf{P} and \mathbf{P}' , of moment $P(L/2) \sin \Delta\theta$, which tends to move the rod away from the vertical, and the couple \mathbf{M} exerted by the spring, which tends to bring the rod back into its original vertical position. Since the angle of deflection of the spring is $2\Delta\theta$, the moment of the couple \mathbf{M} is $M = K(2\Delta\theta)$. If the moment of the second couple is larger than the moment of the first couple, the system tends to return to its original equilibrium position; the system is stable. If the moment of the first couple is larger than the moment of the second couple, the system tends to move away from its original equilibrium position; the system is unstable. The value of the load for which the two couples balance each other is called the *critical load* and is denoted by P_{cr} . We have

$$P_{cr}(L/2) \sin \Delta\theta = K(2\Delta\theta) \quad (10.1)$$

or, since $\sin \Delta\theta \approx \Delta\theta$,

$$P_{cr} = 4K/L \quad (10.2)$$

Clearly, the system is stable for $P < P_{cr}$, that is, for values of the load smaller than the critical value, and unstable for $P > P_{cr}$.

Let us assume that a load $P > P_{cr}$ has been applied to the two rods of Fig. 10.3 and that the system has been disturbed. Since $P > P_{cr}$, the system will move further away from the vertical and, after some oscillations, will settle into a new equilibrium position (Fig. 10.6a). Considering the equilibrium of the free body AC (Fig. 10.6b), we obtain an equation similar to Eq. (10.1), but involving the finite angle θ , namely

$$P(L/2) \sin \theta = K(2\theta)$$

or

$$\frac{PL}{4K} = \frac{\theta}{\sin \theta} \quad (10.3)$$

The value of θ corresponding to the equilibrium position represented in Fig. 10.6 is obtained by solving Eq. (10.3) by trial and error. But we observe that, for any positive value of θ , we have $\sin \theta < \theta$. Thus, Eq. (10.3) yields a value of θ different from zero only when the left-hand member of the equation is larger than one. Recalling Eq. (10.2), we note that this is indeed the case here, since we have assumed $P > P_{cr}$. But, if we had assumed $P < P_{cr}$, the second equilibrium position shown in Fig. 10.6 would not exist and the only

possible equilibrium position would be the position corresponding to $\theta = 0$. We thus check that, for $P < P_{cr}$, the position $\theta = 0$ must be stable.

This observation applies to structures and mechanical systems in general, and will be used in the next section, where the stability of elastic columns will be discussed.

10.3 EULER'S FORMULA FOR PIN-ENDED COLUMNS

Returning to the column AB considered in the preceding section (Fig. 10.1), we propose to determine the critical value of the load P , i.e., the value P_{cr} of the load for which the position shown in Fig. 10.1 ceases to be stable. If $P > P_{cr}$, the slightest misalignment or disturbance will cause the column to buckle, i.e., to assume a curved shape as shown in Fig. 10.2.

Our approach will be to determine the conditions under which the configuration of Fig. 10.2 is possible. Since a column can be considered as a beam placed in a vertical position and subjected to an axial load, we proceed as in Chap. 9 and denote by x the distance from end A of the column to a given point Q of its elastic curve, and by y the deflection of that point (Fig. 10.7a). It follows that the x axis will be vertical and directed downward, and the y axis horizontal and directed to the right. Considering the equilibrium of the free body AQ (Fig. 10.7b), we find that the bending moment at Q is $M = -Py$. Substituting this value for M in Eq. (9.4) of Sec. 9.3, we write

$$\frac{d^2y}{dx^2} = \frac{M}{EI} = -\frac{P}{EI}y \quad (10.4)$$

or, transposing the last term,

$$\frac{d^2y}{dx^2} + \frac{P}{EI}y = 0 \quad (10.5)$$

This equation is a linear, homogeneous differential equation of the second order with constant coefficients. Setting

$$p^2 = \frac{P}{EI} \quad (10.6)$$

we write Eq. (10.5) in the form

$$\frac{d^2y}{dx^2} + p^2y = 0 \quad (10.7)$$

which is the same as that of the differential equation for simple harmonic motion except, of course, that the independent variable is now the distance x instead of the time t . The general solution of Eq. (10.7) is

$$y = A \sin px + B \cos px \quad (10.8)$$

as we easily check by computing d^2y/dx^2 and substituting for y and d^2y/dx^2 into Eq. (10.7).

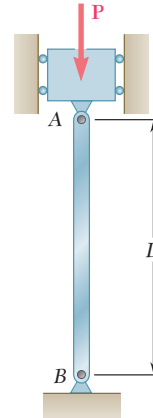


Fig. 10.1 Column (repeated)

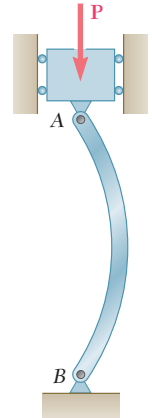


Fig. 10.2 Buckled column (repeated)

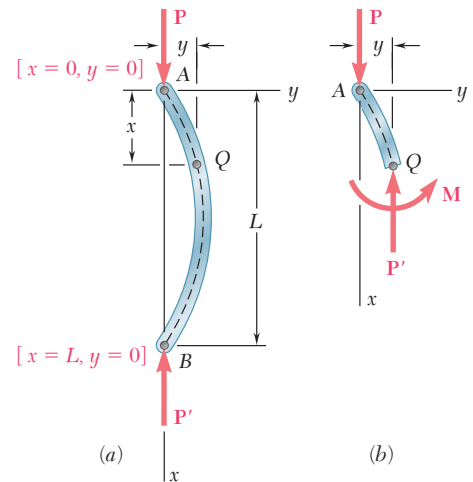


Fig. 10.7 Column in buckled position.

Recalling the boundary conditions that must be satisfied at ends A and B of the column (Fig. 10.7a), we first make $x = 0$, $y = 0$ in Eq. (10.8) and find that $B = 0$. Substituting next $x = L$, $y = 0$, we obtain

$$A \sin pL = 0 \quad (10.9)$$

This equation is satisfied either if $A = 0$, or if $\sin pL = 0$. If the first of these conditions is satisfied, Eq. (10.8) reduces to $y = 0$ and the column is straight (Fig. 10.1). For the second condition to be satisfied, we must have $pL = n\pi$ or, substituting for p from (10.6) and solving for P ,

$$P = \frac{n^2 \pi^2 EI}{L^2} \quad (10.10)$$

The smallest of the values of P defined by Eq. (10.10) is that corresponding to $n = 1$. We thus have

$$P_{\text{cr}} = \frac{\pi^2 EI}{L^2} \quad (10.11)$$

The expression obtained is known as *Euler's formula*, after the Swiss mathematician Leonhard Euler (1707–1783). Substituting this expression for P into Eq. (10.6) and the value obtained for p into Eq. (10.8), and recalling that $B = 0$, we write

$$y = A \sin \frac{\pi x}{L} \quad (10.12)$$

which is the equation of the elastic curve after the column has buckled (Fig. 10.2). We note that the value of the maximum deflection, $y_m = A$, is indeterminate. This is due to the fact that the differential equation (10.5) is a linearized approximation of the actual governing differential equation for the elastic curve.†

If $P < P_{\text{cr}}$, the condition $\sin pL = 0$ cannot be satisfied, and the solution given by Eq. (10.12) does not exist. We must then have $A = 0$, and the only possible configuration for the column is a straight one. Thus, for $P < P_{\text{cr}}$ the straight configuration of Fig. 10.1 is stable.

In the case of a column with a circular or square cross section, the moment of inertia I of the cross section is the same about any centroidal axis, and the column is as likely to buckle in one plane as another, except for the restraints that can be imposed by the end connections. For other shapes of cross section, the critical load should be computed by making $I = I_{\text{min}}$ in Eq. (10.11); if buckling occurs, it will take place in a plane perpendicular to the corresponding principal axis of inertia.

The value of the stress corresponding to the critical load is called the *critical stress* and is denoted by σ_{cr} . Recalling Eq. (10.11)

†We recall that the equation $d^2y/dx^2 = M/EI$ was obtained in Sec. 9.3 by assuming that the slope dy/dx of the beam could be neglected and that the exact expression given in Eq. (9.3) for the curvature of the beam could be replaced by $1/\rho = d^2y/dx^2$.

and setting $I = Ar^2$, where A is the cross-sectional area and r its radius of gyration, we have

$$\sigma_{\text{cr}} = \frac{P_{\text{cr}}}{A} = \frac{\pi^2 E A r^2}{A L^2}$$

or

$$\sigma_{\text{cr}} = \frac{\pi^2 E}{(L/r)^2} \quad (10.13)$$

The quantity L/r is called the *slenderness ratio* of the column. It is clear, in view of the remark of the preceding paragraph, that the minimum value of the radius of gyration r should be used in computing the slenderness ratio and the critical stress in a column.

Equation (10.13) shows that the critical stress is proportional to the modulus of elasticity of the material, and inversely proportional to the square of the slenderness ratio of the column. The plot of σ_{cr} versus L/r is shown in Fig. 10.8 for structural steel, assuming $E = 200$ GPa and $\sigma_Y = 250$ MPa. We should keep in mind that no factor of safety has been used in plotting σ_{cr} . We also note that, if the value obtained for σ_{cr} from Eq. (10.13) or from the curve of Fig. 10.8 is larger than the yield strength σ_Y , this value is of no interest to us, since the column will yield in compression and cease to be elastic before it has a chance to buckle.

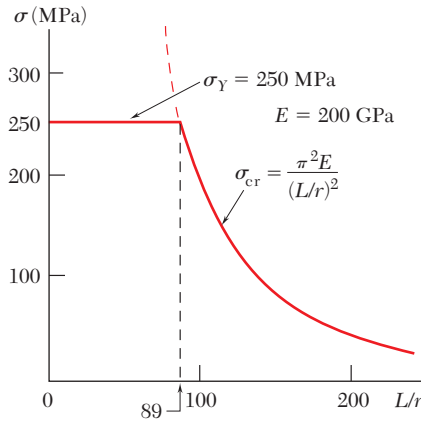


Fig. 10.8 Plot of critical stress.

Our analysis of the behavior of a column has been based so far on the assumption of a perfectly aligned centric load. In practice, this is seldom the case, and in Sec. 10.5 the effect of the eccentricity of the loading is taken into account. This approach will lead to a smoother transition from the buckling failure of long, slender columns to the compression failure of short, stubby columns. It will also provide us with a more realistic view of the relation between the slenderness ratio of a column and the load that causes it to fail.

EXAMPLE 10.01

A 2-m-long pin-ended column of square cross section is to be made of wood. Assuming $E = 13$ GPa, $\sigma_{\text{all}} = 12$ MPa, and using a factor of safety of 2.5 in computing Euler's critical load for buckling, determine the size of the cross section if the column is to safely support (a) a 100-kN load, (b) a 200-kN load.

(a) For the 100-kN Load. Using the given factor of safety, we make

$$P_{\text{cr}} = 2.5(100 \text{ kN}) = 250 \text{ kN} \quad L = 2 \text{ m} \quad E = 13 \text{ GPa}$$

in Euler's formula (10.11) and solve for I . We have

$$I = \frac{P_{\text{cr}} L^2}{\pi^2 E} = \frac{(250 \times 10^3 \text{ N})(2 \text{ m})^2}{\pi^2 (13 \times 10^9 \text{ Pa})} = 7.794 \times 10^{-6} \text{ m}^4$$

Recalling that, for a square of side a , we have $I = a^4/12$, we write

$$\frac{a^4}{12} = 7.794 \times 10^{-6} \text{ m}^4 \quad a = 98.3 \text{ mm} \approx 100 \text{ mm}$$

We check the value of the normal stress in the column:

$$\sigma = \frac{P}{A} = \frac{100 \text{ kN}}{(0.100 \text{ m})^2} = 10 \text{ MPa}$$

Since σ is smaller than the allowable stress, a 100×100 -mm cross section is acceptable.

(b) For the 200-kN Load. Solving again Eq. (10.11) for I , but making now $P_{\text{cr}} = 2.5(200) = 500$ kN, we have

$$I = 15.588 \times 10^{-6} \text{ m}^4$$
$$\frac{a^4}{12} = 15.588 \times 10^{-6} \quad a = 116.95 \text{ mm}$$

The value of the normal stress is

$$\sigma = \frac{P}{A} = \frac{200 \text{ kN}}{(0.11695 \text{ m})^2} = 14.62 \text{ MPa}$$

Since this value is larger than the allowable stress, the dimension obtained is not acceptable, and we must select the cross section on the basis of its resistance to compression. We write

$$A = \frac{P}{\sigma_{\text{all}}} = \frac{200 \text{ kN}}{12 \text{ MPa}} = 16.67 \times 10^{-3} \text{ m}^2$$
$$a^2 = 16.67 \times 10^{-3} \text{ m}^2 \quad a = 129.1 \text{ mm}$$

A 130×130 -mm cross section is acceptable.

10.4 EXTENSION OF EULER'S FORMULA TO COLUMNS WITH OTHER END CONDITIONS

Euler's formula (10.11) was derived in the preceding section for a column that was pin-connected at both ends. Now the critical load P_{cr} will be determined for columns with different end conditions.

In the case of a column with one free end A supporting a load \mathbf{P} and one fixed end B (Fig. 10.9a), we observe that the column will behave as the upper half of a pin-connected column (Fig. 10.9b). The critical load for the column of Fig. 10.9a is thus the same as for the pin-ended column of Fig. 10.9b and can be obtained from Euler's

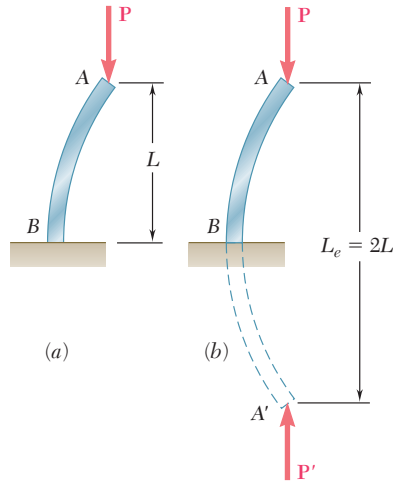


Fig. 10.9 Column with free end.

formula (10.11) by using a column length equal to twice the actual length L of the given column. We say that the *effective length* L_e of the column of Fig. 10.9 is equal to $2L$ and substitute $L_e = 2L$ in Euler's formula:

$$P_{cr} = \frac{\pi^2 EI}{L_e^2} \quad (10.11')$$

The critical stress is found in a similar way from the formula

$$\sigma_{cr} = \frac{\pi^2 E}{(L_e/r)^2} \quad (10.13')$$

The quantity L_e/r is referred to as the *effective slenderness ratio* of the column and, in the case considered here, is equal to $2L/r$.

Consider next a column with two fixed ends A and B supporting a load \mathbf{P} (Fig. 10.10). The symmetry of the supports and of the loading about a horizontal axis through the midpoint C requires that the shear at C and the horizontal components of the reactions at A and B be zero (Fig. 10.11). It follows that the restraints imposed upon the upper half AC of the column by the support at A and by the

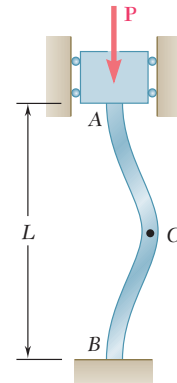


Fig. 10.10 Column with fixed ends.

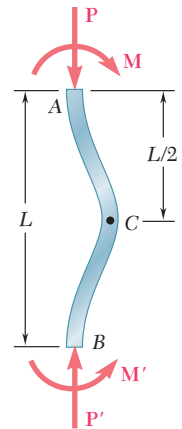


Fig. 10.11 Buckled shape of column with fixed ends.

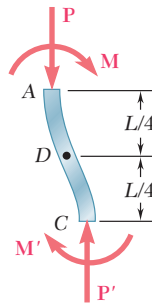


Fig. 10.12

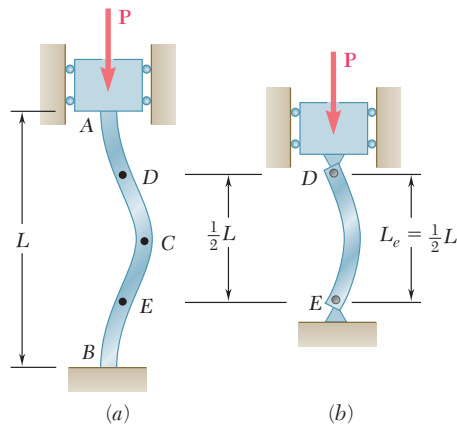


Fig. 10.13

lower half CB are identical (Fig. 10.12). Portion AC must thus be symmetric about its midpoint D , and this point must be a point of inflection, where the bending moment is zero. A similar reasoning shows that the bending moment at the midpoint E of the lower half of the column must also be zero (Fig. 10.13a). Since the bending moment at the ends of a pin-ended column is zero, it follows that the portion DE of the column of Fig. 10.13a must behave as a pin-ended column (Fig. 10.13b). We thus conclude that the effective length of a column with two fixed ends is $L_e = L/2$.

In the case of a column with one fixed end B and one pin-connected end A supporting a load \mathbf{P} (Fig. 10.14), we must write and solve the differential equation of the elastic curve to determine the effective length of the column. From the free-body diagram of the entire column (Fig. 10.15), we first note that a transverse force \mathbf{V} is exerted at end A , in addition to the axial load \mathbf{P} , and that \mathbf{V} is statically indeterminate. Considering now the free-body diagram of a portion AQ of the column (Fig. 10.16), we find that the bending moment at Q is

$$M = -Py - Vx$$

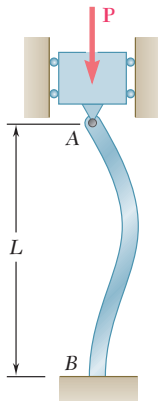


Fig. 10.14 Column with one end pin-connected and one end fixed.

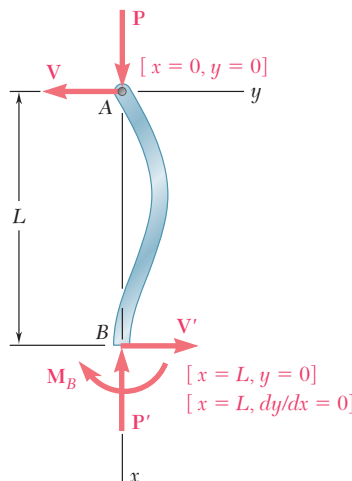


Fig. 10.15

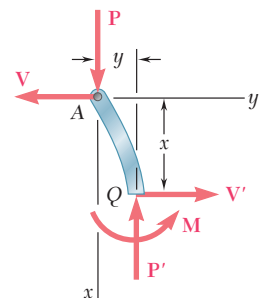


Fig. 10.16

Substituting this value into Eq. (9.4) of Sec. 9.3, we write

$$\frac{d^2y}{dx^2} = \frac{M}{EI} = -\frac{P}{EI}y - \frac{V}{EI}x$$

Transposing the term containing y and setting

$$p^2 = \frac{P}{EI} \quad (10.6)$$

as we did in Sec. 10.3, we write

$$\frac{d^2y}{dx^2} + p^2y = -\frac{V}{EI}x \quad (10.14)$$

This equation is a linear, nonhomogeneous differential equation of the second order with constant coefficients. Observing that the left-hand members of Eqs. (10.7) and (10.14) are identical, we conclude that the general solution of Eq. (10.14) can be obtained by adding a particular solution of Eq. (10.14) to the solution (10.8) obtained for Eq. (10.7). Such a particular solution is easily seen to be

$$y = -\frac{V}{p^2EI}x$$

or, recalling (10.6),

$$y = -\frac{V}{P}x \quad (10.15)$$

Adding the solutions (10.8) and (10.15), we write the general solution of Eq. (10.14) as

$$y = A \sin px + B \cos px - \frac{V}{P}x \quad (10.16)$$

The constants A and B , and the magnitude V of the unknown transverse force \mathbf{V} are obtained from the boundary conditions indicated in Fig. (10.15). Making first $x = 0$, $y = 0$ in Eq. (10.16), we find that $B = 0$. Making next $x = L$, $y = 0$, we obtain

$$A \sin pL = \frac{V}{P}L \quad (10.17)$$

Finally, computing

$$\frac{dy}{dx} = Ap \cos px - \frac{V}{P}$$

and making $x = L$, $dy/dx = 0$, we have

$$Ap \cos pL = \frac{V}{P} \quad (10.18)$$

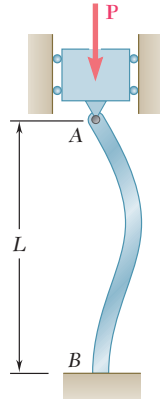


Fig. 10.14
(repeated)

Dividing (10.17) by (10.18) member by member, we conclude that a solution of the form (10.16) can exist only if

$$\tan pL = pL \quad (10.19)$$

Solving this equation by trial and error, we find that the smallest value of pL which satisfies (10.19) is

$$pL = 4.4934 \quad (10.20)$$

Carrying the value of p defined by Eq. (10.20) into Eq. (10.6) and solving for P , we obtain the critical load for the column of Fig. 10.14

$$P_{cr} = \frac{20.19EI}{L^2} \quad (10.21)$$

The effective length of the column is obtained by equating the right-hand members of Eqs. (10.11') and (10.21):

$$\frac{\pi^2 EI}{L_e^2} = \frac{20.19EI}{L^2}$$

Solving for L_e , we find that the effective length of a column with one fixed end and one pin-connected end is $L_e = 0.699L \approx 0.7L$.

The effective lengths corresponding to the various end conditions considered in this section are shown in Fig. 10.17.

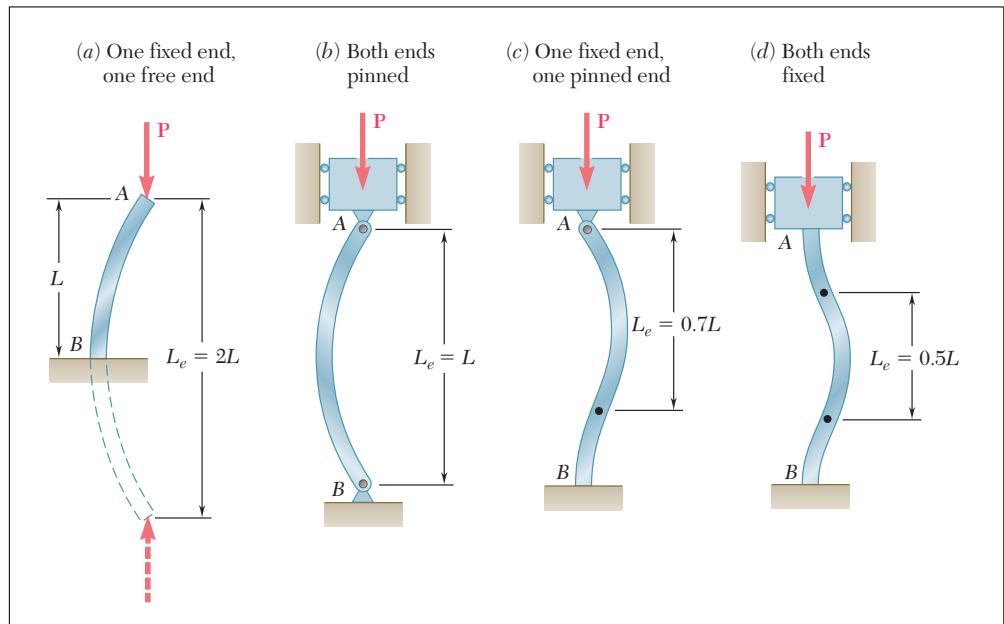
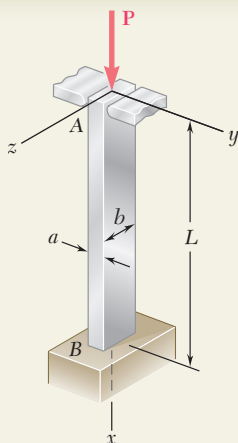


Fig. 10.17 Effective length of column for various end conditions.



SAMPLE PROBLEM 10.1

An aluminum column of length L and rectangular cross section has a fixed end B and supports a centric load at A . Two smooth and rounded fixed plates restrain end A from moving in one of the vertical planes of symmetry of the column, but allow it to move in the other plane. (a) Determine the ratio a/b of the two sides of the cross section corresponding to the most efficient design against buckling. (b) Design the most efficient cross section for the column, knowing that $L = 20$ in., $E = 10.1 \times 10^6$ psi, $P = 5$ kips, and that a factor of safety of 2.5 is required.

SOLUTION

Buckling in xy Plane. Referring to Fig. 10.17, we note that the effective length of the column with respect to buckling in this plane is $L_e = 0.7L$. The radius of gyration r_z of the cross section is obtained by writing

$$I_x = \frac{1}{12}ba^3 \quad A = ab$$

and, since $I_z = Ar_z^2$,
$$r_z^2 = \frac{I_z}{A} = \frac{\frac{1}{12}ba^3}{ab} = \frac{a^2}{12} \quad r_z = a/\sqrt{12}$$

The effective slenderness ratio of the column with respect to buckling in the xy plane is

$$\frac{L_e}{r_z} = \frac{0.7L}{a/\sqrt{12}} \quad (1)$$

Buckling in xz Plane. The effective length of the column with respect to buckling in this plane is $L_e = 2L$, and the corresponding radius of gyration is $r_y = b/\sqrt{12}$. Thus,

$$\frac{L_e}{r_y} = \frac{2L}{b/\sqrt{12}} \quad (2)$$

a. Most Efficient Design. The most efficient design is that for which the critical stresses corresponding to the two possible modes of buckling are equal. Referring to Eq. (10.13'), we note that this will be the case if the two values obtained above for the effective slenderness ratio are equal. We write

$$\frac{0.7L}{a/\sqrt{12}} = \frac{2L}{b/\sqrt{12}}$$

and, solving for the ratio a/b ,
$$\frac{a}{b} = \frac{0.7}{2} \quad \frac{a}{b} = 0.35 \quad \blacktriangleleft$$

b. Design for Given Data. Since $F.S. = 2.5$ is required,

$$P_{cr} = (F.S.)P = (2.5)(5 \text{ kips}) = 12.5 \text{ kips}$$

Using $a = 0.35b$, we have $A = ab = 0.35b^2$ and

$$\sigma_{cr} = \frac{P_{cr}}{A} = \frac{12,500 \text{ lb}}{0.35b^2}$$

Making $L = 20$ in. in Eq. (2), we have $L_e/r_y = 138.6/b$. Substituting for E , L_e/r , and σ_{cr} into Eq. (10.13'), we write

$$\sigma_{cr} = \frac{\pi^2 E}{(L_e/r)^2} \quad \frac{12,500 \text{ lb}}{0.35b^2} = \frac{\pi^2 (10.1 \times 10^6 \text{ psi})}{(138.6/b)^2}$$

$$b = 1.620 \text{ in.} \quad a = 0.35b = 0.567 \text{ in.} \quad \blacktriangleleft$$

PROBLEMS

- 10.1** Knowing that the spring at A is of constant k and that the bar AB is rigid, determine the critical load P_{cr} .

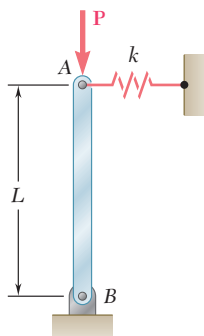


Fig. P10.1



Fig. P10.2

- 10.2** Knowing that the torsional spring at B is of constant K and that the bar AB is rigid, determine the critical load P_{cr} .

- 10.3** Two rigid bars AC and BC are connected by a pin at C as shown. Knowing that the torsional spring at B is of constant K , determine the critical load P_{cr} for the system.

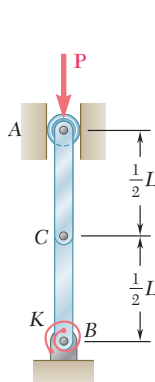


Fig. P10.3

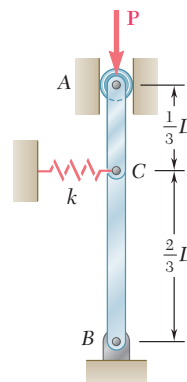


Fig. P10.4

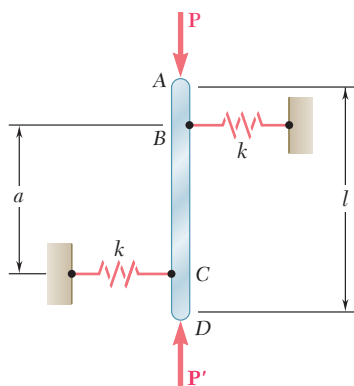


Fig. P10.5

- 10.4** Two rigid bars AC and BC are connected as shown to a spring of constant k . Knowing that the spring can act in either tension or compression, determine the critical load P_{cr} for the system.

- 10.5** The rigid bar AD is attached to two springs of constant k and is in equilibrium in the position shown. Knowing that the equal and opposite loads \mathbf{P} and \mathbf{P}' remain vertical, determine the magnitude P_{cr} of the critical load for the system. Each spring can act in either tension or compression.

10.6 The rigid rod AB is attached to a hinge at A and to two springs, each of constant k . If $h = 450$ mm, $d = 300$ mm, and $m = 200$ kg, determine the range of values of k for which the equilibrium of rod AB is stable in the position shown. Each spring can act in either tension or compression.

10.7 The rigid rod AB is attached to a hinge at A and to two springs, each of constant $k = 2$ kips/in., that can act in either tension or compression. Knowing that $h = 2$ ft, determine the critical load.

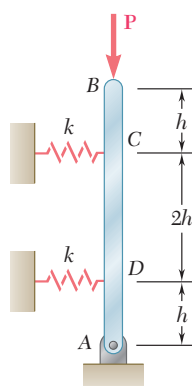


Fig. P10.7

10.8 A frame consists of four L-shaped members connected by four torsional springs, each of constant K . Knowing that equal loads \mathbf{P} are applied at points A and D as shown, determine the critical value P_{cr} of the loads applied to the frame.

10.9 Determine the critical load of a round wooden dowel that is 48 in. long and has a diameter of (a) 0.375 in., (b) 0.5 in. Use $E = 1.6 \times 10^6$ psi.

10.10 Determine the critical load of a steel tube that is 5 m long and has a 100-mm outer diameter and a 16-mm wall thickness. Use $E = 200$ GPa.

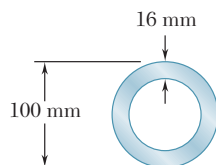


Fig. P10.10

10.11 A compression member of 20-in. effective length consists of a solid 1-in.-diameter aluminum rod. In order to reduce the weight of the member by 25%, the solid rod is replaced by a hollow rod of the cross section shown. Determine (a) the percent reduction in the critical load, (b) the value of the critical load for the hollow rod. Use $E = 10.6 \times 10^6$ psi.

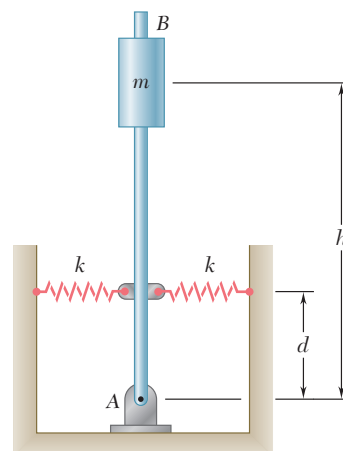


Fig. P10.6

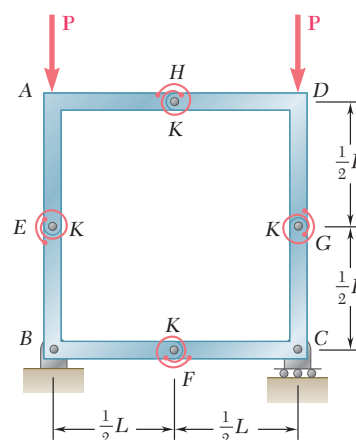


Fig. P10.8

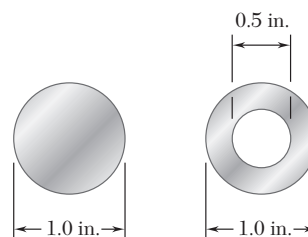


Fig. P10.11

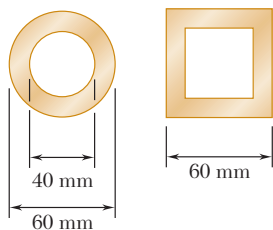


Fig. P10.12

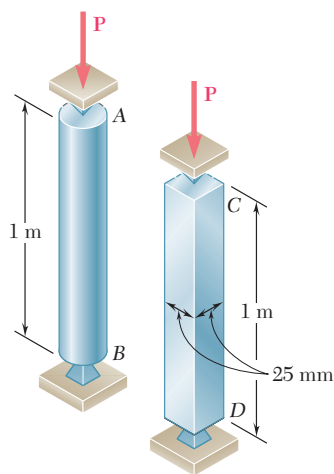


Fig. P10.14

10.12 Two brass rods used as compression members, each of 3-m effective length, have the cross sections shown. (a) Determine the wall thickness of the hollow square rod for which the rods have the same cross-sectional area. (b) Using $E = 105$ GPa, determine the critical load of each rod.

10.13 A column of effective length L can be made by gluing together identical planks in either of the arrangements shown. Determine the ratio of the critical load using the arrangement a to the critical load using the arrangement b .

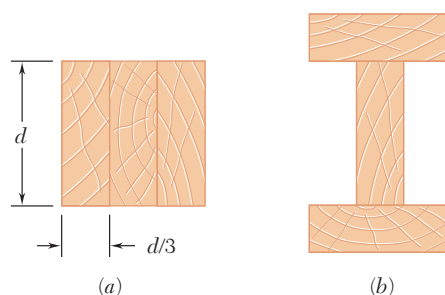


Fig. P10.13

10.14 Determine the radius of the round strut so that the round and square struts have the same cross-sectional area and compute the critical load of each strut. Use $E = 200$ GPa.

10.15 A compression member of 7-m effective length is made by welding together two L152 \times 102 \times 12.7 angles as shown. Using $E = 200$ GPa, determine the allowable centric load for the member if a factor of safety of 2.2 is required.

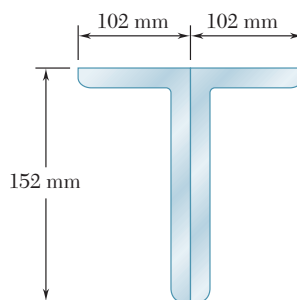


Fig. P10.15

10.16 A column of 3-m effective length is to be made by welding together two C130 \times 13 rolled-steel channels. Using $E = 200$ GPa, determine for each arrangement shown the allowable centric load if a factor of safety of 2.4 is required.

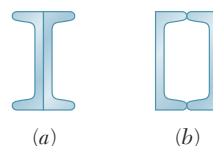


Fig. P10.16

10.17 A single compression member of 27-ft effective length is obtained by connecting two C8 \times 11.5 steel channels with lacing bars as shown. Knowing that the factor of safety is 1.85, determine the allowable centric load for the member. Use $E = 29 \times 10^6$ psi and $d = 4.0$ in.

10.18 A column of 22-ft effective length is made by welding two 9 \times 0.5-in. plates to a W8 \times 35 as shown. Determine the allowable centric load if a factor of safety of 2.3 is required. Use $E = 29 \times 10^6$ psi.

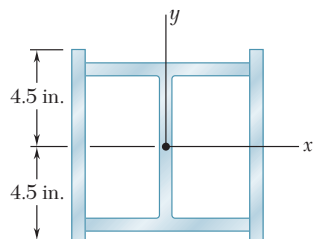


Fig. P10.18

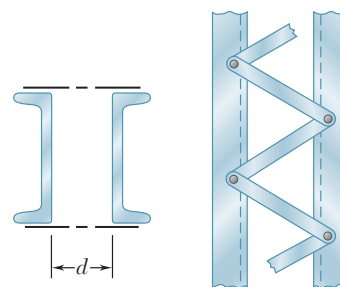


Fig. P10.17

10.19 Member AB consists of a single C130 \times 10.4 steel channel of length 2.5 m. Knowing that the pins A and B pass through the centroid of the cross section of the channel, determine the factor of safety for the load shown with respect to buckling in the plane of the figure when $\theta = 30^\circ$. Use $E = 200$ GPa.

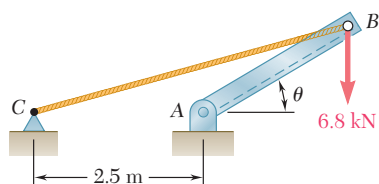


Fig. P10.19

10.20 Knowing that $P = 5.2$ kN, determine the factor of safety for the structure shown. Use $E = 200$ GPa and consider only buckling in the plane of the structure.

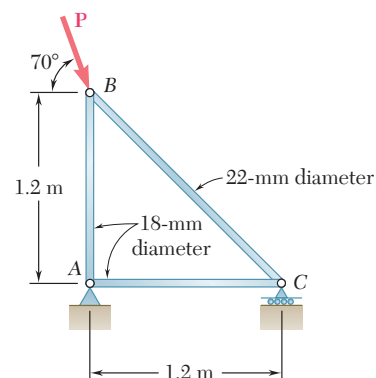


Fig. P10.20

10.21 A rigid block of mass m can be supported in each of the four ways shown. Each column consists of an aluminum tube that has a 44-mm outer diameter and a 4-mm wall thickness. Using $E = 70$ GPa and a factor of safety of 2.8, determine the allowable mass for each support condition.

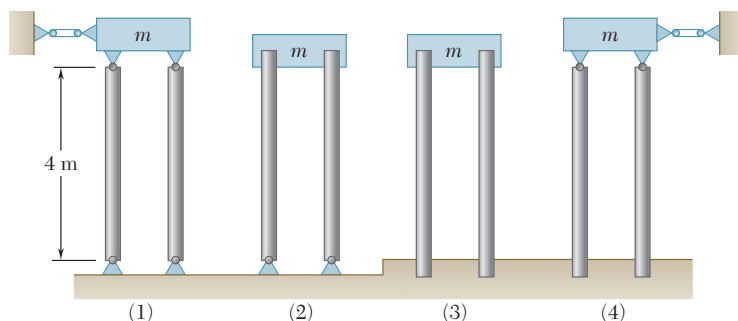


Fig. P10.21

- 10.22** Each of the five struts shown consists of a solid steel rod. (a) Knowing that the strut of Fig. (1) is of a 20-mm diameter, determine the factor of safety with respect to buckling for the loading shown. (b) Determine the diameter of each of the other struts for which the factor of safety is the same as the factor of safety obtained in part a. Use $E = 200$ GPa.

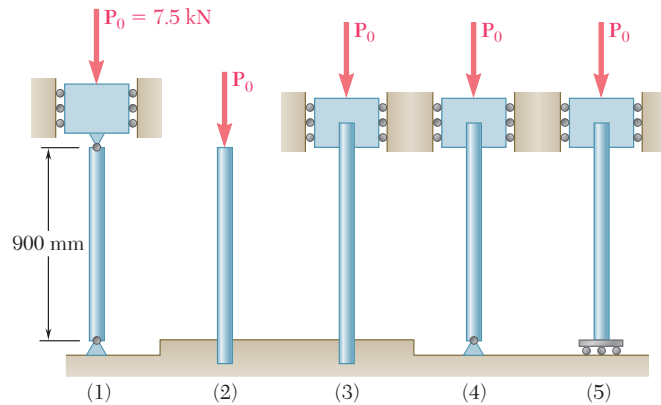


Fig. P10.22

- 10.23** A 1-in.-square aluminum strut is maintained in the position shown by a pin support at A and by sets of rollers at B and C that prevent rotation of the strut in the plane of the figure. Knowing that $L_{AB} = 3$ ft, determine (a) the largest values of L_{BC} and L_{CD} that can be used if the allowable load P is to be as large as possible, (b) the magnitude of the corresponding allowable load. Consider only buckling in the plane of the figure and use $E = 10.4 \times 10^6$ psi.

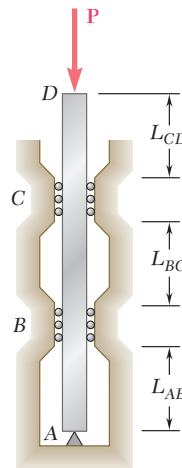


Fig. P10.23 and P10.24

- 10.24** A 1-in.-square aluminum strut is maintained in the position shown by a pin support at A and by sets of rollers at B and C that prevent rotation of the strut in the plane of the figure. Knowing that $L_{AB} = 3$ ft, $L_{BC} = 4$ ft, and $L_{CD} = 1$ ft, determine the allowable load P using a factor of safety with respect to buckling of 3.2. Consider only buckling in the plane of the figure and use $E = 10.4 \times 10^6$ psi.

- 10.25** Column AB carries a centric load \mathbf{P} of magnitude 15 kips. Cables BC and BD are taut and prevent motion of point B in the xz plane. Using Euler's formula and a factor of safety of 2.2, and neglecting the tension in the cables, determine the maximum allowable length L . Use $E = 29 \times 10^6$ psi.

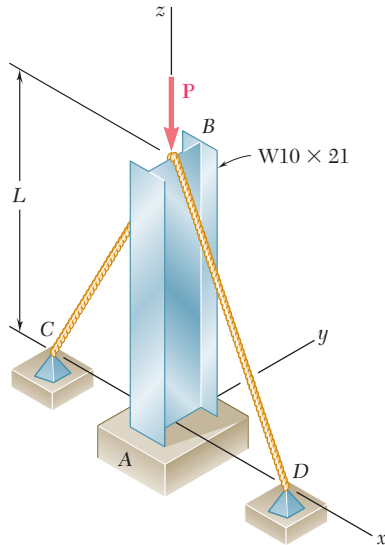


Fig. P10.25

- 10.26** A $W8 \times 21$ rolled-steel shape is used with the support and cable arrangement shown in Prob. 10.25. Knowing that $L = 24$ ft, determine the allowable centric load \mathbf{P} if a factor of safety of 2.2 is required. Use $E = 29 \times 10^6$ psi.
- 10.27** Column ABC has a uniform rectangular cross section with $b = 12$ mm and $d = 22$ mm. The column is braced in the xz plane at its midpoint C and carries a centric load \mathbf{P} of magnitude 3.8 kN. Knowing that a factor of safety of 3.2 is required, determine the largest allowable length L . Use $E = 200$ GPa.
- 10.28** Column ABC has a uniform rectangular cross section and is braced in the xz plane at its midpoint C . (a) Determine the ratio b/d for which the factor of safety is the same with respect to buckling in the xz and yz planes. (b) Using the ratio found in part a, design the cross section of the column so that the factor of safety will be 3.0 when $P = 4.4$ kN, $L = 1$ m, and $E = 200$ GPa.

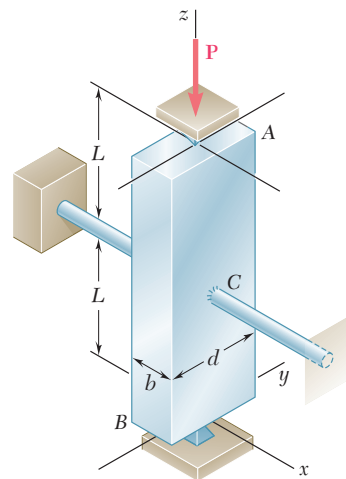


Fig. P10.27 and P10.28

*10.5 ECCENTRIC LOADING; THE SECANT FORMULA

In this section the problem of column buckling will be approached in a different way, by observing that the load \mathbf{P} applied to a column is never perfectly centric. Denoting by e the eccentricity of the load, i.e., the distance between the line of action \mathbf{P} and the axis of the

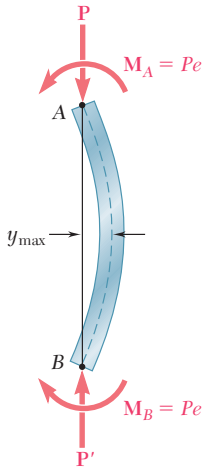


Fig. 10.19 Deflection of column with eccentric load.

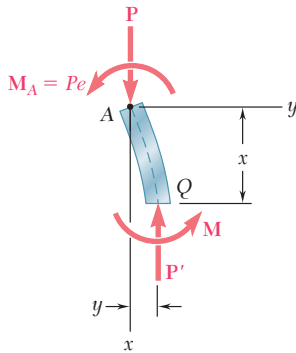


Fig. 10.20

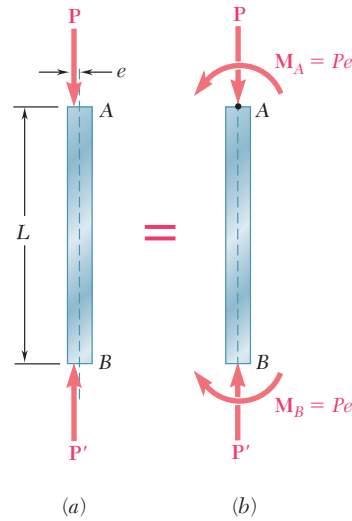


Fig. 10.18 Column with eccentric load.

column (Fig. 10.18a), we replace the given eccentric load by a centric force \mathbf{P} and a couple \mathbf{M}_A of moment $M_A = Pe$ (Fig. 10.18b). It is clear that, no matter how small the load \mathbf{P} and the eccentricity e , the couple \mathbf{M}_A will cause some bending of the column (Fig. 10.19). As the eccentric load is increased, both the couple \mathbf{M}_A and the axial force \mathbf{P} increase, and both cause the column to bend further. Viewed in this way, the problem of buckling is not a question of determining how long the column can remain straight and stable under an increasing load, but rather how much the column can be permitted to bend under the increasing load, if the allowable stress is not to be exceeded and if the deflection y_{\max} is not to become excessive.

We first write and solve the differential equation of the elastic curve, proceeding in the same manner as we did earlier in Secs. 10.3 and 10.4. Drawing the free-body diagram of a portion AQ of the column and choosing the coordinate axes as shown (Fig. 10.20), we find that the bending moment at Q is

$$M = -Py - M_A = -Py - Pe \quad (10.22)$$

Substituting the value of M into Eq. (9.4) of Sec. 9.3, we write

$$\frac{d^2y}{dx^2} = \frac{M}{EI} = -\frac{P}{EI}y - \frac{Pe}{EI}$$

Transposing the term containing y and setting

$$p^2 = \frac{P}{EI} \quad (10.6)$$

as done earlier, we write

$$\frac{d^2y}{dx^2} + p^2y = -p^2e \quad (10.23)$$

Since the left-hand member of this equation is the same as that of Eq. (10.7), which was solved in Sec. 10.3, we write the general solution of Eq. (10.23) as

$$y = A \sin px + B \cos px - e \quad (10.24)$$

where the last term is a particular solution of Eq. (10.23).

The constants A and B are obtained from the boundary conditions shown in Fig. 10.21. Making first $x = 0$, $y = 0$ in Eq. (10.24), we have

$$B = e$$

Making next $x = L$, $y = 0$, we write

$$A \sin pL = e(1 - \cos pL) \quad (10.25)$$

Recalling that

$$\sin pL = 2 \sin \frac{pL}{2} \cos \frac{pL}{2}$$

and

$$1 - \cos pL = 2 \sin^2 \frac{pL}{2}$$

and substituting into Eq. (10.25), we obtain, after reductions,

$$A = e \tan \frac{pL}{2}$$

Substituting for A and B into Eq. (10.24), we write the equation of the elastic curve:

$$y = e \left(\tan \frac{pL}{2} \sin px + \cos px - 1 \right) \quad (10.26)$$

The value of the maximum deflection is obtained by setting $x = L/2$ in Eq. (10.26). We have

$$\begin{aligned} y_{\max} &= e \left(\tan \frac{pL}{2} \sin \frac{pL}{2} + \cos \frac{pL}{2} - 1 \right) \\ &= e \left(\frac{\sin^2 \frac{pL}{2} + \cos^2 \frac{pL}{2}}{\cos \frac{pL}{2}} - 1 \right) \\ y_{\max} &= e \left(\sec \frac{pL}{2} - 1 \right) \end{aligned} \quad (10.27)$$

Recalling Eq. (10.6), we write

$$y_{\max} = e \left[\sec \left(\sqrt{\frac{P}{EI}} \frac{L}{2} \right) - 1 \right] \quad (10.28)$$

We note from the expression obtained that y_{\max} becomes infinite when

$$\sqrt{\frac{P}{EI}} \frac{L}{2} = \frac{\pi}{2} \quad (10.29)$$

While the deflection does not actually become infinite, it nevertheless becomes unacceptably large, and P should not be allowed to reach the critical value which satisfies Eq. (10.29). Solving (10.29) for P , we have

$$P_{\text{cr}} = \frac{\pi^2 EI}{L^2} \quad (10.30)$$

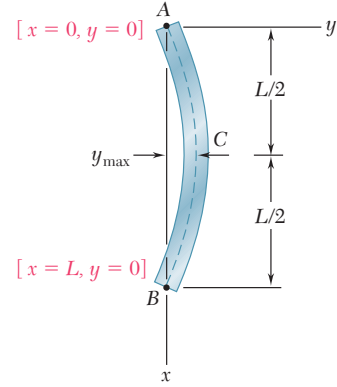


Fig. 10.21

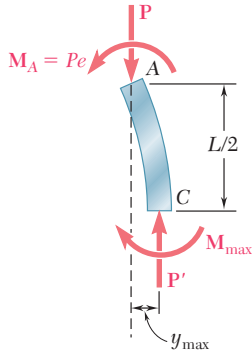


Fig. 10.22

which is the value that we obtained in Sec. 10.3 for a column under a centric load. Solving (10.30) for EI and substituting into (10.28), we can express the maximum deflection in the alternative form

$$y_{\max} = e \left(\sec \frac{\pi}{2} \sqrt{\frac{P}{P_{\text{cr}}}} - 1 \right) \quad (10.31)$$

The maximum stress σ_{\max} occurs in the section of the column where the bending moment is maximum, i.e., in the transverse section through the midpoint C , and can be obtained by adding the normal stresses due, respectively, to the axial force and the bending couple exerted on that section (cf. Sec. 4.12). We have

$$\sigma_{\max} = \frac{P}{A} + \frac{M_{\max}c}{I} \quad (10.32)$$

From the free-body diagram of the portion AC of the column (Fig. 10.22), we find that

$$M_{\max} = Py_{\max} + M_A = P(y_{\max} + e)$$

Substituting this value into (10.32) and recalling that $I = Ar^2$, we write

$$\sigma_{\max} = \frac{P}{A} \left[1 + \frac{(y_{\max} + e)c}{r^2} \right] \quad (10.33)$$

Substituting for y_{\max} the value obtained in (10.28), we write

$$\sigma_{\max} = \frac{P}{A} \left[1 + \frac{ec}{r^2} \sec \left(\sqrt{\frac{P}{EI}} \frac{L}{2} \right) \right] \quad (10.34)$$

An alternative form for σ_{\max} is obtained by substituting for y_{\max} from (10.31) into (10.33). We have

$$\sigma_{\max} = \frac{P}{A} \left(1 + \frac{ec}{r^2} \sec \frac{\pi}{2} \sqrt{\frac{P}{P_{\text{cr}}}} \right) \quad (10.35)$$

The equation obtained can be used with any end conditions, as long as the appropriate value is used for the critical load (cf. Sec. 10.4).

We note that, since σ_{\max} does not vary linearly with the load P , the principle of superposition does not apply to the determination of the stress due to the simultaneous application of several loads; the resultant load must first be computed, and then Eq. (10.34) or Eq. (10.35) can be used to determine the corresponding stress. For the same reason, any given factor of safety should be applied to the load, and not to the stress.

Making $I = Ar^2$ in Eq. (10.34) and solving for the ratio P/A in front of the bracket, we write

$$\frac{P}{A} = \frac{\sigma_{\max}}{1 + \frac{ec}{r^2} \sec \left(\frac{1}{2} \sqrt{\frac{P}{EA}} \frac{L_e}{r} \right)} \quad (10.36)$$

where the effective length is used to make the formula applicable to various end conditions. This formula is referred to as *the secant formula*; it defines the force per unit area, P/A , that causes a specified maximum stress σ_{\max} in a column of given effective slenderness ratio, L_e/r , for a given value of the ratio ec/r^2 , where e is the eccentricity of the applied load. We note that, since P/A appears in both members, it is necessary to solve a transcendental equation by trial and error to obtain the value of P/A corresponding to a given column and loading condition.

Equation (10.36) was used to draw the curves shown in Fig. 10.23*a* and *b* for a steel column, assuming the values of E and σ_Y shown in the figure. These curves make it possible to determine the load per unit area P/A , which causes the column to yield for given values of the ratios L_e/r and ec/r^2 .

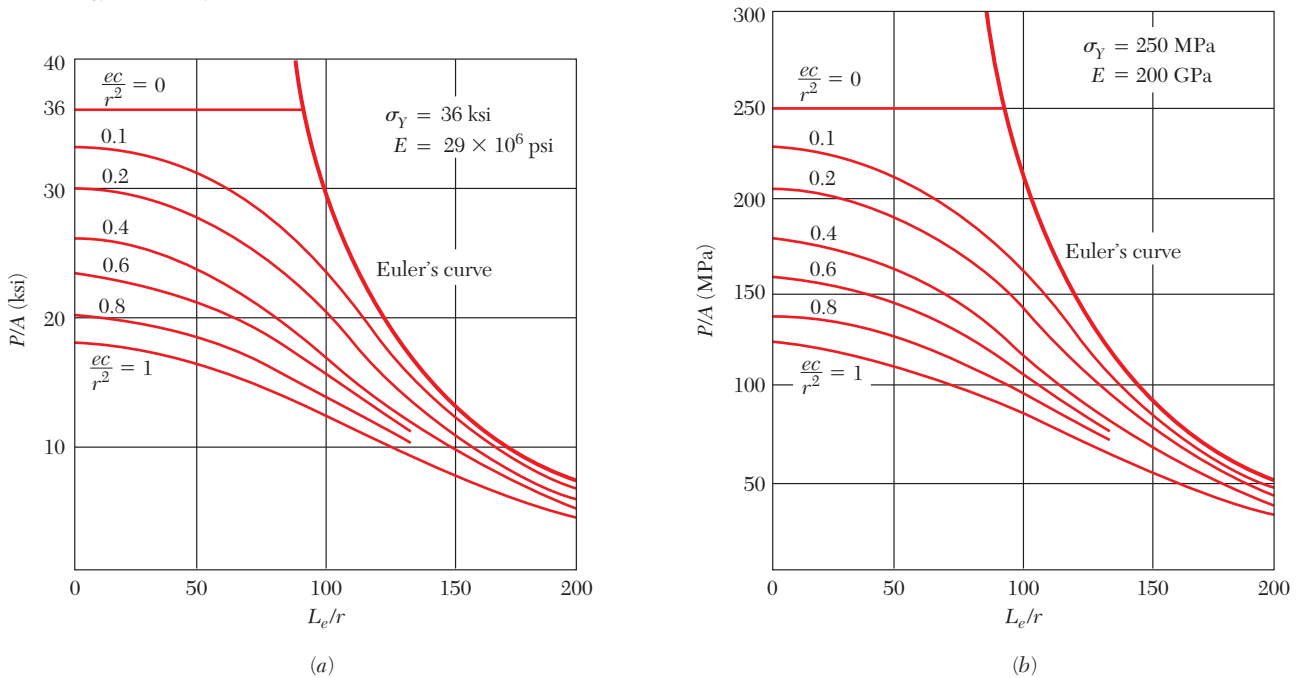
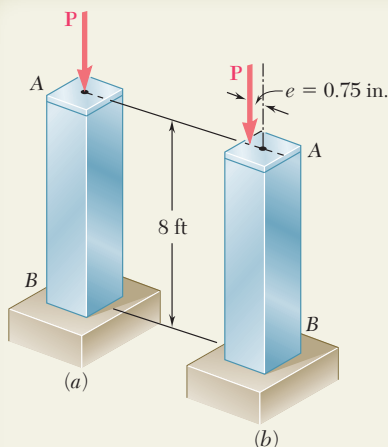


Fig. 10.23 Load per unit area, P/A , causing yield in column.

We note that, for small values of L_e/r , the secant is almost equal to 1 in Eq. (10.36), and P/A can be assumed equal to

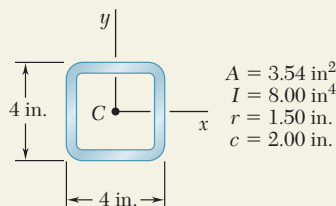
$$\frac{P}{A} = \frac{\sigma_{\max}}{1 + \frac{ec}{r^2}} \quad (10.37)$$

a value that could be obtained by neglecting the effect of the lateral deflection of the column and using the method of Sec. 4.12. On the other hand, we note from Fig. 10.23 that, for large values of L_e/r , the curves corresponding to the various values of the ratio ec/r^2 get very close to Euler's curve defined by Eq. (10.13'), and thus that the effect of the eccentricity of the loading on the value of P/A becomes negligible. The secant formula is chiefly useful for intermediate values of L_e/r . However, to use it effectively, we should know the value of the eccentricity e of the loading, and this quantity, unfortunately, is seldom known with any degree of precision.



SAMPLE PROBLEM 10.2

The uniform column AB consists of an 8-ft section of structural tubing having the cross section shown. (a) Using Euler's formula and a factor of safety of two, determine the allowable centric load for the column and the corresponding normal stress. (b) Assuming that the allowable load, found in part a, is applied as shown at a point 0.75 in. from the geometric axis of the column, determine the horizontal deflection of the top of the column and the maximum normal stress in the column. Use $E = 29 \times 10^6$ psi.



SOLUTION

Effective Length. Since the column has one end fixed and one end free, its effective length is

$$L_e = 2(8 \text{ ft}) = 16 \text{ ft} = 192 \text{ in.}$$

Critical Load. Using Euler's formula, we write

$$P_{cr} = \frac{\pi^2 EI}{L_e^2} = \frac{\pi^2 (29 \times 10^6 \text{ psi})(8.00 \text{ in}^4)}{(192 \text{ in.})^2} \quad P_{cr} = 62.1 \text{ kips}$$

a. Allowable Load and Stress. For a factor of safety of 2, we find

$$P_{all} = \frac{P_{cr}}{F.S.} = \frac{62.1 \text{ kips}}{2} \quad P_{all} = 31.1 \text{ kips} \quad \blacktriangleleft$$

and

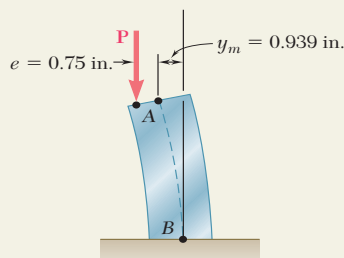
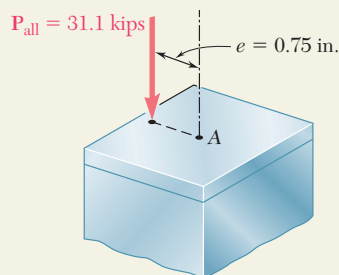
$$\sigma = \frac{P_{all}}{A} = \frac{31.1 \text{ kips}}{3.54 \text{ in}^2} \quad \sigma = 8.79 \text{ ksi} \quad \blacktriangleleft$$

b. Eccentric Load. We observe that column AB and its loading are identical to the upper half of the column of Fig. 10.19 which was used in the derivation of the secant formulas; we conclude that the formulas of Sec. 10.5 apply directly to the case considered here. Recalling that $P_{all}/P_{cr} = \frac{1}{2}$ and using Eq. (10.31), we compute the horizontal deflection of point A:

$$\begin{aligned} y_m &= e \left[\sec \left(\frac{\pi}{2} \sqrt{\frac{P}{P_{cr}}} \right) - 1 \right] = (0.75 \text{ in.}) \left[\sec \left(\frac{\pi}{2\sqrt{2}} \right) - 1 \right] \\ &= (0.75 \text{ in.})(2.252 - 1) \quad y_m = 0.939 \text{ in.} \quad \blacktriangleleft \end{aligned}$$

The maximum normal stress is obtained from Eq. (10.35):

$$\begin{aligned} \sigma_m &= \frac{P}{A} \left[1 + \frac{ec}{r^2} \sec \left(\frac{\pi}{2} \sqrt{\frac{P}{P_{cr}}} \right) \right] \\ &= \frac{31.1 \text{ kips}}{3.54 \text{ in}^2} \left[1 + \frac{(0.75 \text{ in.})(2 \text{ in.})}{(1.50 \text{ in.})^2} \sec \left(\frac{\pi}{2\sqrt{2}} \right) \right] \\ &= (8.79 \text{ ksi})[1 + 0.667(2.252)] \quad \sigma_m = 22.0 \text{ ksi} \quad \blacktriangleleft \end{aligned}$$



PROBLEMS

- 10.29** An axial load \mathbf{P} is applied to the 32-mm-diameter steel rod AB as shown. For $P = 37 \text{ kN}$ and $e = 1.2 \text{ mm}$, determine (a) the deflection at the midpoint C of the rod, (b) the maximum stress in the rod. Use $E = 200 \text{ GPa}$.

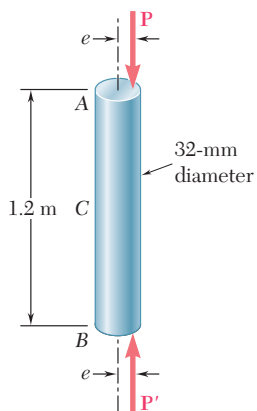


Fig. P10.29

- 10.30** An axial load $\mathbf{P} = 15 \text{ kN}$ is applied at point D that is 4 mm from the geometric axis of the square aluminum bar BC . Using $E = 70 \text{ GPa}$, determine (a) the horizontal deflection of end C , (b) the maximum stress in the column.

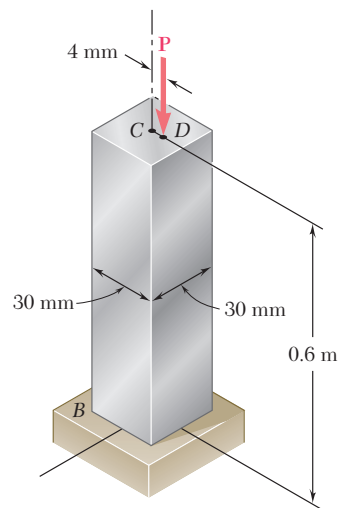


Fig. P10.30

- 10.31** The line of action of the 75-kip axial load is parallel to the geometric axis of the column AB and intersects the x axis at $x = 0.6 \text{ in.}$ Using $E = 29 \times 10^6 \text{ psi}$, determine (a) the horizontal deflection of the midpoint C of the column, (b) the maximum stress in the column.

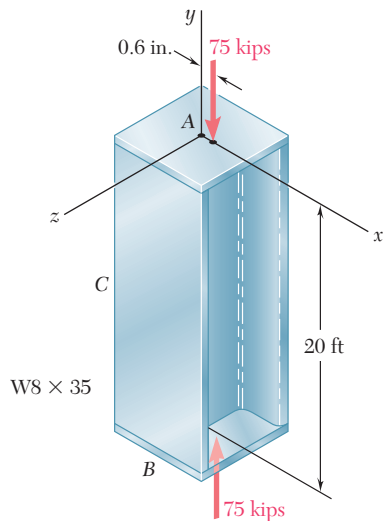


Fig. P10.31

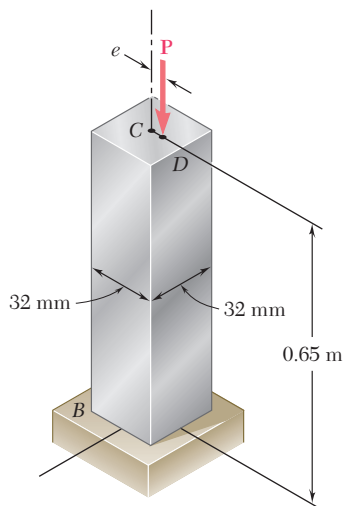


Fig. P10.32

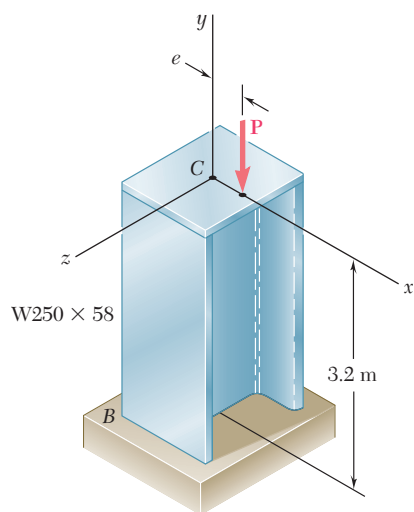


Fig. P10.34

10.32 An axial load \mathbf{P} is applied to the 32-mm-square aluminum bar BC as shown. When $P = 24$ kN, the horizontal deflection at end C is 4 mm. Using $E = 70$ GPa, determine (a) the eccentricity e of the load, (b) the maximum stress in the bar.

10.33 An axial load \mathbf{P} is applied to the 1.375-in. diameter steel rod AB as shown. When $P = 21$ kips, it is observed that the horizontal deflection at midpoint C is 0.03 in. Using $E = 29 \times 10^6$ psi, determine (a) the eccentricity e of the load, (b) the maximum stress in the rod.

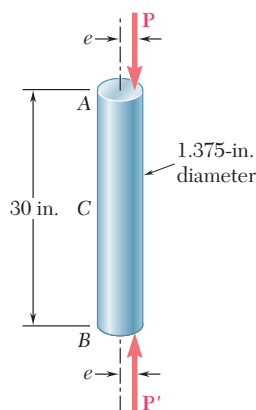


Fig. P10.33

10.34 The axial load \mathbf{P} is applied at a point located on the x axis at a distance e from the geometric axis of the rolled-steel column BC . When $P = 350$ kN, the horizontal deflection of the top of the column is 5 mm. Using $E = 200$ GPa, determine (a) the eccentricity e of the load, (b) the maximum stress in the column.

10.35 An axial load \mathbf{P} is applied at point D that is 0.25 in. from the geometric axis of the square aluminum bar BC . Using $E = 10.1 \times 10^6$ psi, determine (a) the load \mathbf{P} for which the horizontal deflection of end C is 0.50 in., (b) the corresponding maximum stress in the column.

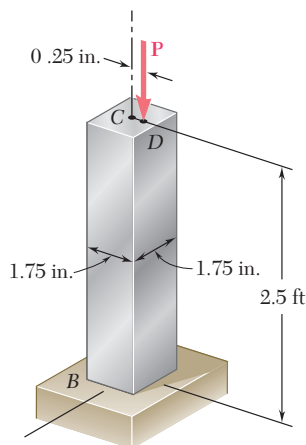


Fig. P10.35

10.36 An axial load \mathbf{P} is applied at a point located on the x axis at a distance $e = 12$ mm from the geometric axis of the $W310 \times 60$ rolled-steel column BC . Assuming that $L = 3.5$ m and using $E = 200$ GPa, determine (a) the load \mathbf{P} for which the horizontal deflection at end C is 15 mm, (b) the corresponding maximum stress in the column.

10.37 Solve Prob. 10.36, assuming that L is 4.5 m.

10.38 The line of action of an axial load \mathbf{P} is parallel to the geometric axis of the column AB and intersects the x axis at $x = 0.8$ in. Using $E = 29 \times 10^6$ psi, determine (a) the load \mathbf{P} for which the horizontal deflection of the midpoint C of the column is 0.5 in., (b) the corresponding maximum stress in the column.

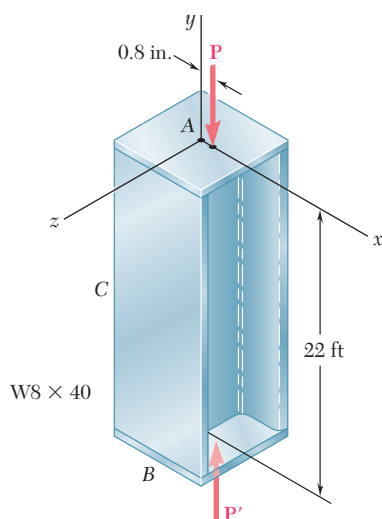


Fig. P10.38

10.39 A brass pipe having the cross section shown has an axial load \mathbf{P} applied 5 mm from its geometric axis. Using $E = 120$ GPa, determine (a) the load \mathbf{P} for which the horizontal deflection at the midpoint C is 5 mm, (b) the corresponding maximum stress in the column.

10.40 Solve Prob. 10.39, assuming that the axial load \mathbf{P} is applied 10 mm from the geometric axis of the column.

10.41 The steel bar AB has a $\frac{3}{8} \times \frac{3}{8}$ -in. square cross section and is held by pins that are a fixed distance apart and are located at a distance $e = 0.03$ in. from the geometric axis of the bar. Knowing that at temperature T_0 the pins are in contact with the bar and that the force in the bar is zero, determine the increase in temperature for which the bar will just make contact with point C if $d = 0.01$ in. Use $E = 29 \times 10^6$ psi and a coefficient of thermal expansion $\alpha = 6.5 \times 10^{-6}/^\circ\text{F}$.

10.42 For the bar of Prob. 10.41, determine the required distance d for which the bar will just make contact with point C when the temperature increases by 120°F .

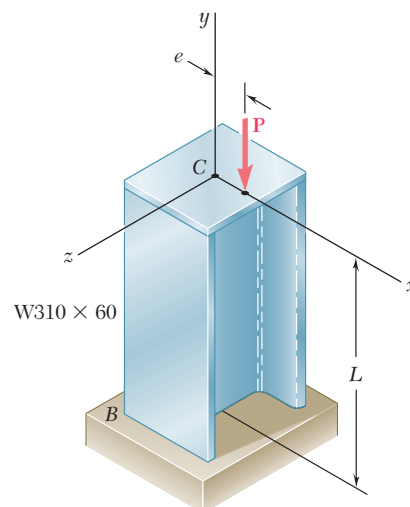


Fig. P10.36

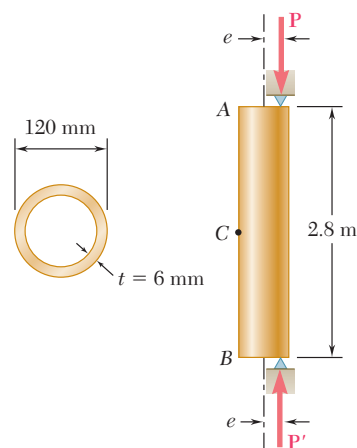


Fig. P10.39

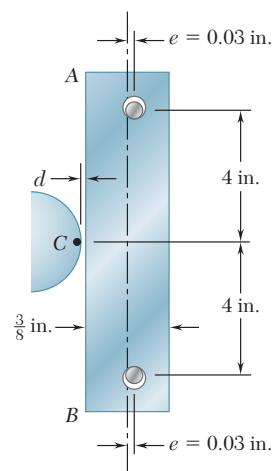


Fig. P10.41

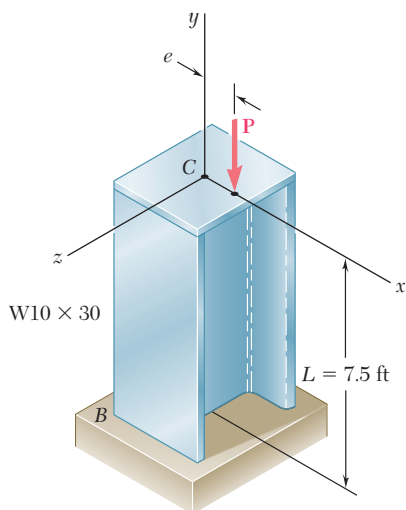


Fig. P10.43

10.43 An axial load \mathbf{P} is applied to the W10 \times 30 rolled-steel column BC that is free at its top C and fixed at its base B . Knowing that the eccentricity of the load is $e = 0.5$ in. and that for the grade of steel used $\sigma_Y = 36$ ksi and $E = 29 \times 10^6$ psi, determine (a) the magnitude of P of the allowable load when a factor of safety of 2.4 with respect to permanent deformation is required, (b) the ratio of the load found in part a to the magnitude of the allowable centric load for the column. (Hint: Since the factor of safety must be applied to the load \mathbf{P} , not to the stress, use Fig. 10.23 to determine P_Y).

10.44 Solve Prob. 10.43, assuming that the length of the column is reduced to 5 ft.

10.45 A 3.5-m-long steel tube having the cross section and properties shown is used as a column. For the grade of steel used $\sigma_Y = 250$ MPa and $E = 200$ GPa. Knowing that a factor of safety of 2.6 with respect to permanent deformation is required, determine the allowable load \mathbf{P} when the eccentricity e is (a) 15 mm, (b) 7.5 mm. (See hint of Prob. 10.43).

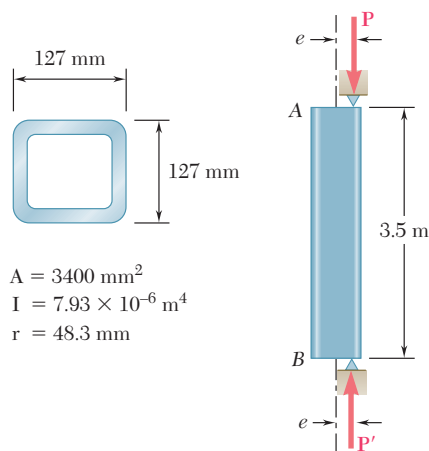


Fig. P10.45 and P10.46

10.46 Solve Prob. 10.45, assuming that the length of the tube is increased to 5 m.

10.47 A 250-kN axial load \mathbf{P} is applied to a W200 \times 35.9 rolled-steel column BC that is free at its top C and fixed at its base B . Knowing that the eccentricity of the load is $e = 6$ mm, determine the largest permissible length L if the allowable stress in the column is 80 MPa. Use $E = 200$ GPa.

10.48 A 100-kN axial load \mathbf{P} is applied to the W150 \times 18 rolled-steel column BC that is free at its top C and fixed at its base B . Knowing that the eccentricity of the load is $e = 6$ mm, determine the largest permissible length L if the allowable stress in the column is 80 MPa. Use $E = 200$ GPa.

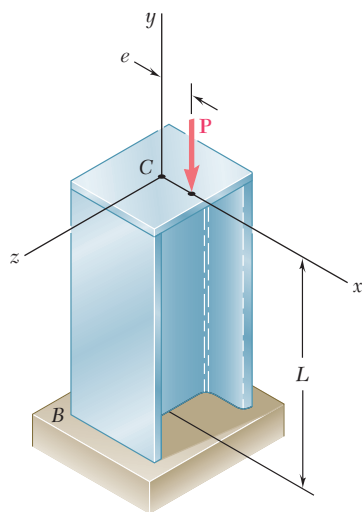


Fig. P10.47 and P10.48

- 10.49** Axial loads of magnitude $P = 20$ kips are applied parallel to the geometric axis of the $W8 \times 15$ rolled-steel column AB and intersect the x axis at a distance e from the geometric axis. Knowing that $\sigma_{\text{all}} = 12$ ksi and $E = 29 \times 10^6$ psi, determine the largest permissible length L when (a) $e = 0.25$ in., (b) $e = 0.5$ in.

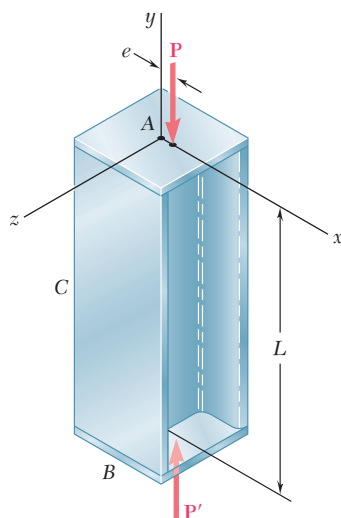


Fig. P10.49 and P10.50

- 10.50** Axial loads of magnitude $P = 135$ kips are applied parallel to the geometric axis of the $W10 \times 54$ rolled-steel column AB and intersect the x axis at a distance e from the geometric axis. Knowing that $\sigma_{\text{all}} = 12$ ksi and $E = 29 \times 10^6$ psi, determine the largest permissible length L when (a) $e = 0.25$ in., (b) $e = 0.5$ in.
- 10.51** A 12-kip axial load is applied with an eccentricity $e = 0.375$ in. to the circular steel rod BC that is free at its top C and fixed at its base B . Knowing that the stock of rods available for use have diameters in increments of $\frac{1}{8}$ in. from 1.5 in. to 3.0 in., determine the lightest rod that can be used if $\sigma_{\text{all}} = 15$ ksi. Use $E = 29 \times 10^6$ psi.

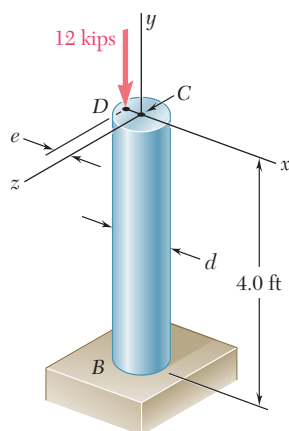


Fig. P10.51

- 10.52** Solve Prob. 10.51, assuming that the 12-kip axial load will be applied to the rod with an eccentricity $e = \frac{1}{2}d$.

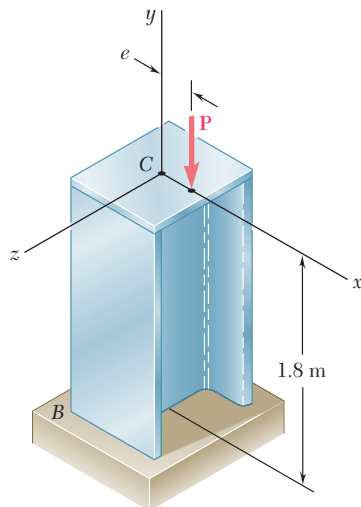


Fig. P10.53

10.53 An axial load of magnitude $P = 220$ kN is applied at a point located on the x axis at a distance $e = 6$ mm from the geometric axis of the wide-flange column BC . Knowing that $E = 200$ GPa, choose the lightest W200 shape that can be used if $\sigma_{\text{all}} = 120$ MPa.

10.54 Solve Prob. 10.53, assuming that the magnitude of the axial load is $P = 345$ kN.

10.55 Axial loads of magnitude $P = 175$ kN are applied parallel to the geometric axis of a W250 \times 44.8 rolled-steel column AB and intersect the axis at a distance $e = 12$ mm from its geometric axis. Knowing that $\sigma_Y = 250$ MPa and $E = 200$ GPa, determine the factor of safety with respect to yield. (*Hint*: Since the factor of safety must be applied to the load P , not to the stresses, use Fig. 10.23 to determine P_Y .)

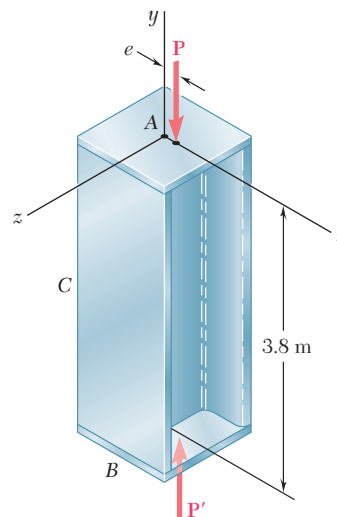


Fig. P10.55

10.56 Solve Prob. 10.55, assuming that $e = 0.16$ mm and $P = 155$ kN.

10.6 DESIGN OF COLUMNS UNDER A CENTRIC LOAD

In the preceding sections, we have determined the critical load of a column by using Euler's formula, and we have investigated the deformations and stresses in eccentrically loaded columns by using the secant formula. In each case we assumed that all stresses remained below the proportional limit and that the column was initially a straight homogeneous prism. Real columns fall short of such an idealization, and in practice the design of columns is based on empirical formulas that reflect the results of numerous laboratory tests.

Over the last century, many steel columns have been tested by applying to them a centric axial load and increasing the load until failure occurred. The results of such tests are represented in

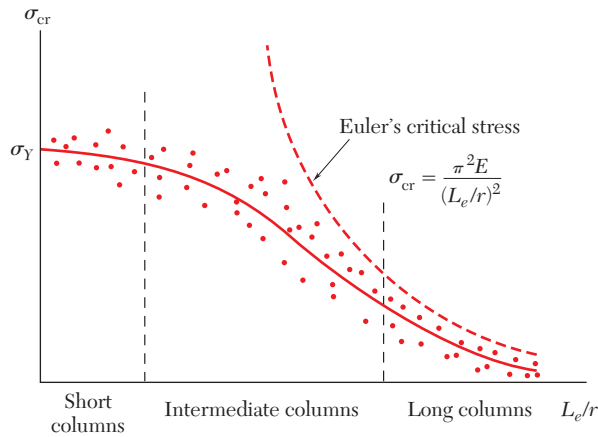


Fig. 10.24 Plot of test data for steel columns.

Fig. 10.24 where, for each of many tests, a point has been plotted with its ordinate equal to the normal stress σ_{cr} at failure, and its abscissa equal to the corresponding value of the effective slenderness ratio, L_e/r . Although there is considerable scatter in the test results, regions corresponding to three types of failure can be observed. For long columns, where L_e/r is large, failure is closely predicted by Euler's formula, and the value of σ_{cr} is observed to depend on the modulus of elasticity E of the steel used, but not on its yield strength σ_Y . For very short columns and compression blocks, failure occurs essentially as a result of yield, and we have $\sigma_{cr} \approx \sigma_Y$. Columns of intermediate length comprise those cases where failure is dependent on both σ_Y and E . In this range, column failure is an extremely complex phenomenon, and test data have been used extensively to guide the development of specifications and design formulas.

Empirical formulas that express an allowable stress or critical stress in terms of the effective slenderness ratio were first introduced over a century ago, and since then have undergone a continuous process of refinement and improvement. Typical empirical formulas previously used to approximate test data are shown in Fig. 10.25. It is not always feasible to use a single formula for all values of L_e/r . Most design specifications use different formulas, each with a definite range of applicability. In each case we must check that the formula we propose to use is applicable for the value of L_e/r for the

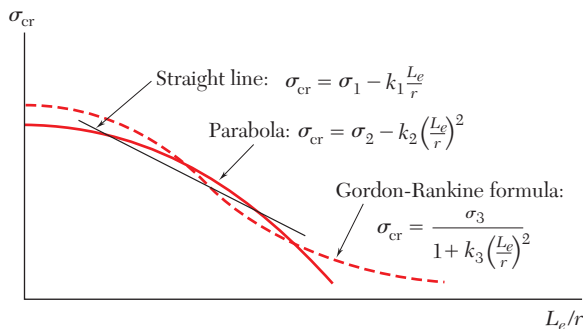


Fig. 10.25 Plots of empirical formulas for column critical stress.

column involved. Furthermore, we must determine whether the formula provides the value of the critical stress for the column, in which case we must apply the appropriate factor of safety, or whether it provides directly an allowable stress.

Specific formulas for the design of steel, aluminum and wood columns under centric loading will now be considered. Photo 10.2 shows examples of columns that would be designed using these formulas. The design for the three different materials using *Allowable Stress Design* is first presented. This is followed with the formulas needed for the design of steel columns based on *Load and Resistance Factor Design*.†

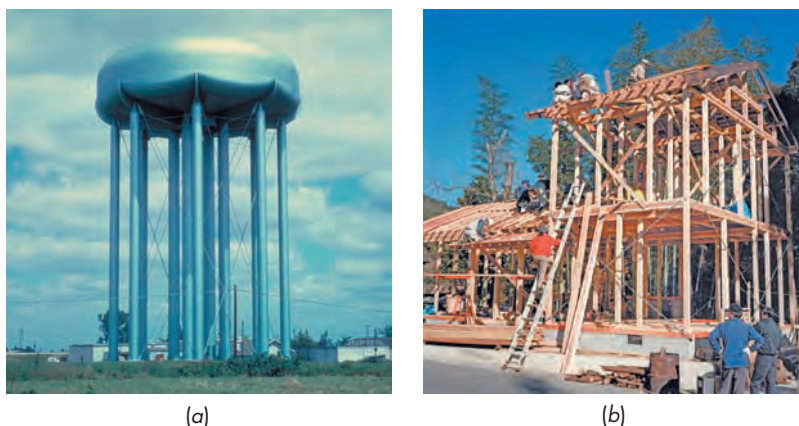


Photo 10.2 The water tank in (a) is supported by steel columns and the building under construction in (b) is framed with wood columns.

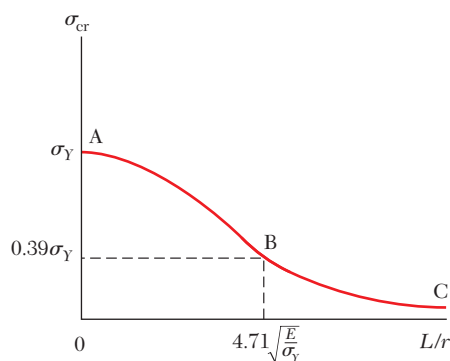


Fig. 10.26 Steel column design.

Structural Steel—Allowable Stress Design. The formulas most widely used for the allowable stress design of steel columns under a centric load are found in the Specification for Structural Steel Buildings of the American Institute of Steel Construction.‡ As we shall see, an exponential expression is used to predict σ_{all} for columns of short and intermediate lengths, and an Euler-based relation is used for long columns. The design relations are developed in two steps:

1. First a curve representing the variation of σ_{cr} with L/r is obtained (Fig. 10.26). It is important to note that this curve does not incorporate any factor of safety.§ The portion AB of this curve is defined by the equation

$$\sigma_{cr} = [0.658^{(\sigma_Y/\sigma_e)}] \sigma_Y \quad (10.38)$$

†In specific design formulas, the letter L will always refer to the effective length of the column.

‡*Manual of Steel Construction*, 13th ed., American Institute of Steel Construction, Chicago, 2005.

§In the *Specification for Structural Steel for Buildings*, the symbol F is used for stresses.

$$\sigma_e = \frac{\pi^2 E}{(L/r)^2} \quad (10.39)$$

The portion BC is defined by the equation

$$\sigma_{cr} = 0.877 \sigma_e \quad (10.40)$$

We note that when $L/r = 0$, $\sigma_{cr} = \sigma_Y$ in Eq. (10.38). At point B , Eq. (10.38) joins Eq. (10.40). The value of slenderness L/r at the junction between the two equations is

$$\frac{L}{r} = 4.71 \sqrt{\frac{E}{\sigma_Y}} \quad (10.41)$$

If L/r is smaller than the value in Eq. (10.41), σ_{cr} is determined from Eq. (10.38), and if L/r is greater, σ_{cr} is determined from Eq. (10.40). At the value of the slenderness L/r specified in Eq. (10.41), the stress $\sigma_e = 0.44 \sigma_Y$. Using Eq. (10.40), $\sigma_{cr} = 0.877 (0.44 \sigma_Y) = 0.39 \sigma_Y$.

2. A factor of safety must be introduced to obtain the final AISC design formulas. The factor of safety specified by the specification is 1.67. Thus

$$\sigma_{all} = \frac{\sigma_{cr}}{1.67} \quad (10.42)$$

The formulas obtained can be used with SI or U.S. customary units.

We observe that, by using Eqs. (10.38), (10.40), (10.41), and (10.42), we can determine the allowable axial stress for a given grade of steel and any given value of L/r . The procedure is to first compute the value of L/r at the intersection between the two equations from Eq. (10.41). For given values of L/r smaller than that in Eq. (10.41), we use Eqs. (10.38) and (10.42) to calculate σ_{all} , and for values greater than that in Eq. (10.41), we use Eqs. (10.40) and (10.42) to calculate σ_{all} . Figure 10.27 provides a general illustration of how σ_e varies as a function of L/r for different grades of structural steel.

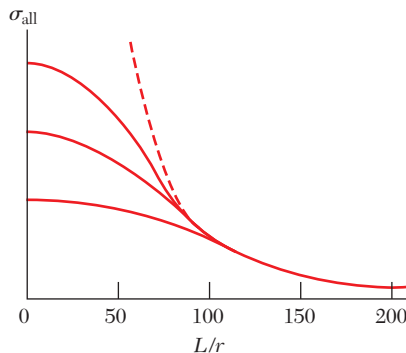


Fig. 10.27 Steel column design for different grades of steel.

EXAMPLE 10.02

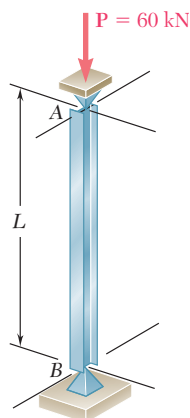


Fig. 10.28

Determine the longest unsupported length L for which the $S100 \times 11.5$ rolled-steel compression member AB can safely carry the centric load shown (Fig. 10.28). Assume $\sigma_Y = 250$ MPa and $E = 200$ GPa.

From Appendix C we find that, for an $S100 \times 11.5$ shape,

$$A = 1460 \text{ mm}^2 \quad r_x = 41.7 \text{ mm} \quad r_y = 14.6 \text{ mm}$$

If the 60-kN load is to be safely supported, we must have

$$\sigma_{\text{all}} = \frac{P}{A} = \frac{60 \times 10^3 \text{ N}}{1460 \times 10^{-6} \text{ m}^2} = 41.1 \times 10^6 \text{ Pa}$$

We must compute the critical stress σ_{cr} . Assuming L/r is larger than the slenderness specified by Eq. (10.41), we use Eq. (10.40) with (10.39) and write

$$\begin{aligned} \sigma_{\text{cr}} &= 0.877 \sigma_e = 0.877 \frac{\pi^2 E}{(L/r)^2} \\ &= 0.877 \frac{\pi^2 (200 \times 10^9 \text{ Pa})}{(L/r)^2} = \frac{1.731 \times 10^{12} \text{ Pa}}{(L/r)^2} \end{aligned}$$

Using this expression in Eq. (10.42) for σ_{all} , we write

$$\sigma_{\text{all}} = \frac{\sigma_{\text{cr}}}{1.67} = \frac{1.037 \times 10^{12} \text{ Pa}}{(L/r)^2}$$

Equating this expression to the required value of σ_{all} , we write

$$\frac{1.037 \times 10^{12} \text{ Pa}}{(L/r)^2} = 41.1 \times 10^6 \text{ Pa} \quad L/r = 158.8$$

The slenderness ratio from Eq. (10.41) is

$$\frac{L}{r} = 4.71 \sqrt{\frac{200 \times 10^9}{250 \times 10^6}} = 133.2$$

Our assumption that L/r is greater than this slenderness ratio was correct. Choosing the smaller of the two radii of gyration, we have

$$\frac{L}{r_y} = \frac{L}{14.6 \times 10^{-3} \text{ m}} = 158.8 \quad L = 2.32 \text{ m}$$

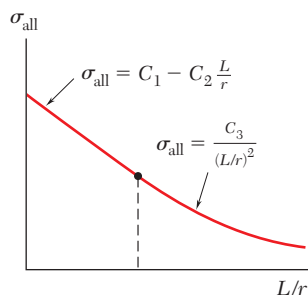


Fig. 10.29 Aluminum column design.

Aluminum. Many aluminum alloys are available for use in structural and machine construction. For most columns the specifications of the Aluminum Association† provide two formulas for the allowable stress in columns under centric loading. The variation of σ_{all} with L/r defined by these formulas is shown in Fig. 10.29. We note that for short columns a linear relation between σ_{all} with L/r is used and for long columns an Euler-type formula is used. Specific formulas for use in the design of buildings and similar structures are given below in both SI and U.S. customary units for two commonly used alloys.

†Specifications for Aluminum Structures, Aluminum Association, Inc., Washington, D.C., 2010.

Alloy 6061-T6:

$$L/r < 66: \quad \sigma_{\text{all}} = [20.3 - 0.127(L/r)] \text{ ksi} \quad (10.43)$$

$$= [140 - 0.874(L/r)] \text{ MPa} \quad (10.43')$$

$$L/r \geq 66: \quad \sigma_{\text{all}} = \frac{51,400 \text{ ksi}}{(L/r)^2} = \frac{354 \times 10^3 \text{ MPa}}{(L/r)^2} \quad (10.44)$$

Alloy 2014-T6:

$$L/r < 55: \quad \sigma_{\text{all}} = [30.9 - 0.229(L/r)] \text{ ksi} \quad (10.45)$$

$$= [213 - 1.577(L/r)] \text{ MPa} \quad (10.45')$$

$$L/r \geq 55: \quad \sigma_{\text{all}} = \frac{55,400 \text{ ksi}}{(L/r)^2} = \frac{382 \times 10^3 \text{ MPa}}{(L/r)^2} \quad (10.46)$$

Wood. For the design of wood columns the specifications of the American Forest & Paper Association† provides a single equation that can be used to obtain the allowable stress for short, intermediate, and long columns under centric loading. For a column with a *rectangular* cross section of sides b and d , where $d < b$, the variation of σ_{all} with L/d is shown in Fig. 10.30.

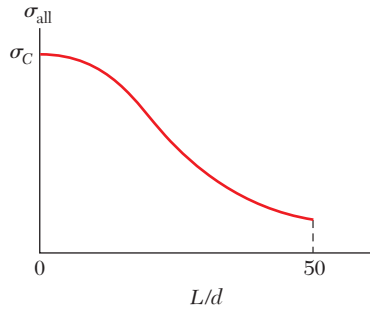


Fig. 10.30 Wood column design.

For solid columns made from a single piece of wood or made by gluing laminations together, the allowable stress σ_{all} is

$$\sigma_{\text{all}} = \sigma_C C_P \quad (10.47)$$

where σ_C is the adjusted allowable stress for compression parallel to the grain.‡ Adjustments used to obtain σ_C are included in the specifications to account for different variations, such as in the load duration. The column stability factor C_P accounts for the column length and is defined by the following equation:

$$C_P = \frac{1 + (\sigma_{CE}/\sigma_C)}{2c} - \sqrt{\left[\frac{1 + (\sigma_{CE}/\sigma_C)}{2c} \right]^2 - \frac{\sigma_{CE}/\sigma_C}{c}} \quad (10.48)$$

†*National Design Specification for Wood Construction*, American Forest & Paper Association, American Wood Council, Washington, D.C., 2005.

‡In the *National Design Specification for Wood Construction*, the symbol F is used for stresses.

The parameter c accounts for the type of column, and it is equal to 0.8 for sawn lumber columns and 0.90 for glued laminated wood columns. The value of σ_{CE} is defined as

$$\sigma_{CE} = \frac{0.822E}{(L/d)^2} \quad (10.49)$$

Where E is an adjusted modulus of elasticity for column buckling. Columns in which L/d exceeds 50 are not permitted by the *National Design Specification for Wood Construction*.

EXAMPLE 10.03

Knowing that column AB (Fig. 10.31) has an effective length of 14 ft, and that it must safely carry a 32-kip load, design the column using a square glued laminated cross section. The adjusted modulus of elasticity for the wood is $E = 800 \times 10^3$ psi, and the adjusted allowable stress for compression parallel to the grain is $\sigma_C = 1060$ psi.

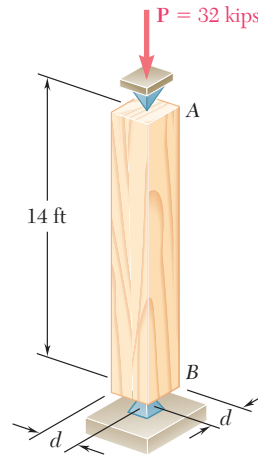


Fig. 10.31

We note that $c = 0.90$ for glued laminated wood columns. We must compute the value of σ_{CE} . Using Eq. (10.49) we write

$$\sigma_{CE} = \frac{0.822E}{(L/d)^2} = \frac{0.822(800 \times 10^3 \text{ psi})}{(168 \text{ in.}/d)^2} = 23.299d^2 \text{ psi}$$

We then use Eq. (10.48) to express the column stability factor in terms of d , with $(\sigma_{CE}/\sigma_C) = (23.299d^2/1.060 \times 10^3) = 21.98 \times 10^{-3} d^2$,

$$\begin{aligned} C_P &= \frac{1 + (\sigma_{CE}/\sigma_C)}{2c} - \sqrt{\left[\frac{1 + (\sigma_{CE}/\sigma_C)}{2c} \right]^2 - \frac{\sigma_{CE}/\sigma_C}{c}} \\ &= \frac{1 + 21.98 \times 10^{-3} d^2}{2(0.90)} - \sqrt{\left[\frac{1 + 21.98 \times 10^{-3} d^2}{2(0.90)} \right]^2 - \frac{21.98 \times 10^{-3} d^2}{0.90}} \end{aligned}$$

Since the column must carry 32 kips, which is equal to $\sigma_c d^2$, we use Eq. (10.47) to write

$$\sigma_{\text{all}} = \frac{32 \text{ kips}}{d^2} = \sigma_c C_P = 1.060 C_P$$

Solving this equation for C_P and substituting the value obtained into the previous equation, we write

$$\frac{30.19}{d^2} = \frac{1 + 21.98 \times 10^{-3} d^2}{2(0.90)} - \sqrt{\left[\frac{1 + 21.98 \times 10^{-3} d^2}{2(0.90)} \right]^2 - \frac{21.98 \times 10^{-3} d^2}{0.90}}$$

Solving for d by trial and error yields $d = 6.45$ in.

***Structural Steel—Load and Resistance Factor Design.** As we saw in Sec. 1.13, an alternative method of design is based on the determination of the load at which the structure ceases to be useful. Design is based on the inequality given by Eq. (1.26):

$$\gamma_D P_D + \gamma_L P_L \leq \phi P_U \quad (1.26)$$

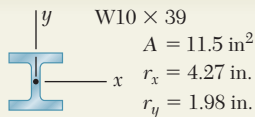
The approach used for the design of steel columns under a centric load using Load and Resistance Factor Design with the AISC Specification is similar to that for Allowable Stress Design. Using the critical stress σ_{cr} , the ultimate load P_U is defined as

$$P_U = \sigma_{cr} A \quad (10.50)$$

The determination of the critical stress σ_{cr} follows the same approach used for Allowable Stress Design. This requires using Eq. (10.41) to determine the slenderness at the junction between Eqs. (10.38) and Eq. (10.40). If the specified slenderness L/r is smaller than the value from Eq. (10.41), Eq. (10.38) governs, and if it is larger, Eq. (10.40) governs. The equations can be used with SI or U.S. customary units.

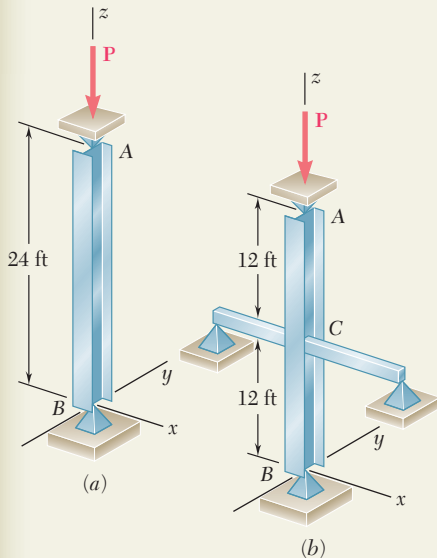
We observe that, by using Eq. (10.50) with Eq. (1.26), we can determine if the design is acceptable. The procedure is to first determine the slenderness ratio from Eq. (10.41). For values of L/r smaller than this slenderness, the *ultimate load* P_U for use with Eq. (1.26) is obtained from Eq. (10.50), using σ_{cr} determined from Eq. (10.38). For values of L/r larger than this slenderness, the *ultimate load* P_U is obtained by using Eq. (10.50) with Eq. (10.40). The Load and Resistance Factor Design Specification of the American Institute of Steel Construction specifies that the *resistance factor* ϕ is 0.90.

Note: The design formulas presented throughout Sec. 10.6 are intended to provide examples of different design approaches. These formulas do not provide all the requirements that are needed for many designs, and the student should refer to the appropriate design specifications before attempting actual designs.



SAMPLE PROBLEM 10.3

Column AB consists of a W10 × 39 rolled-steel shape made of a grade of steel for which $\sigma_Y = 36 \text{ ksi}$ and $E = 29 \times 10^6 \text{ psi}$. Determine the allowable centric load \mathbf{P} (a) if the effective length of the column is 24 ft in all directions, (b) if bracing is provided to prevent the movement of the midpoint C in the xz plane. (Assume that the movement of point C in the yz plane is not affected by the bracing.)



SOLUTION

We first compute the value of the slenderness ratio from Eq. 10.41 corresponding to the given yield strength $\sigma_Y = 36 \text{ ksi}$.

$$\frac{L}{r} = 4.71 \sqrt{\frac{29 \times 10^6}{36 \times 10^3}} = 133.7$$

a. Effective Length = 24 ft. Since $r_y < r_x$, buckling will take place in the xz plane. For $L = 24 \text{ ft}$ and $r = r_y = 1.98 \text{ in.}$, the slenderness ratio is

$$\frac{L}{r_y} = \frac{(24 \times 12) \text{ in.}}{1.98 \text{ in.}} = \frac{288 \text{ in.}}{1.98 \text{ in.}} = 145.5$$

Since $L/r > 133.7$, we use Eq. (10.39) in Eq. (10.40) to determine σ_{cr}

$$\sigma_{cr} = 0.877 \sigma_e = 0.877 \frac{\pi^2 E}{(L/r)^2} = 0.877 \frac{\pi^2 (29 \times 10^3 \text{ ksi})}{(145.5)^2} = 11.86 \text{ ksi}$$

The allowable stress, determined using Eq. (10.42), and P_{all} are

$$\sigma_{all} = \frac{\sigma_{cr}}{1.67} = \frac{11.86 \text{ ksi}}{1.67} = 7.10 \text{ ksi}$$

$$P_{all} = \sigma_{all} A = (7.10 \text{ ksi})(11.5 \text{ in}^2) = 81.7 \text{ kips}$$

b. Bracing at Midpoint C. Since bracing prevents movement of point C in the xz plane but not in the yz plane, we must compute the slenderness ratio corresponding to buckling in each plane and determine which is larger.

xz Plane: Effective length = 12 ft = 144 in., $r = r_y = 1.98 \text{ in.}$

$$L/r = (144 \text{ in.})/(1.98 \text{ in.}) = 72.7$$

yz Plane: Effective length = 24 ft = 288 in., $r = r_x = 4.27 \text{ in.}$

$$L/r = (288 \text{ in.})/(4.27 \text{ in.}) = 67.4$$

Since the larger slenderness ratio corresponds to a smaller allowable load, we choose $L/r = 72.7$. Since this is smaller than $L/r = 133.7$, we use Eqs. (10.39) and (10.38) to determine σ_{cr}

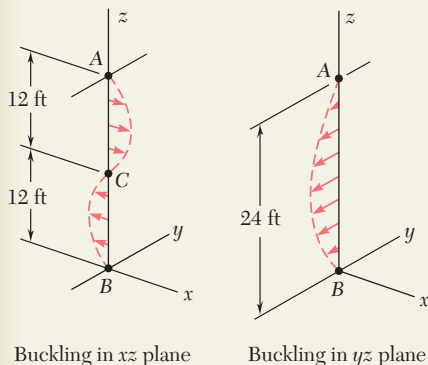
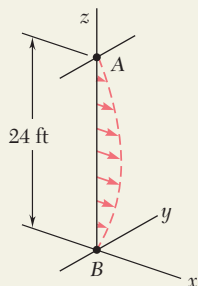
$$\sigma_e = \frac{\pi^2 E}{(L/r)^2} = \frac{\pi^2 (29 \times 10^3 \text{ ksi})}{(72.7)^2} = 54.1 \text{ ksi}$$

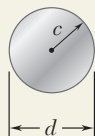
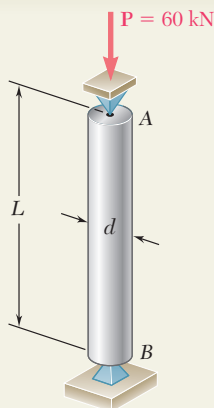
$$\sigma_{cr} = [0.658^{(\sigma_Y/\sigma_e)}] F_Y = [0.658^{(36 \text{ ksi}/54.1 \text{ ksi})}] 36 \text{ ksi} = 27.3 \text{ ksi}$$

We now calculate the allowable stress using Eq. (10.42) and the allowable load.

$$\sigma_{all} = \frac{\sigma_{cr}}{1.67} = \frac{27.3 \text{ ksi}}{1.67} = 16.32 \text{ ksi}$$

$$P_{all} = \sigma_{all} A = (16.32 \text{ ksi})(11.5 \text{ in}^2) \quad P_{all} = 187.7 \text{ kips}$$





SAMPLE PROBLEM 10.4

Using the aluminum alloy 2014-T6, determine the smallest diameter rod that can be used to support the centric load $P = 60$ kN if (a) $L = 750$ mm, (b) $L = 300$ mm.

SOLUTION

For the cross section of a solid circular rod, we have

$$I = \frac{\pi}{4}c^4 \quad A = \pi c^2 \quad r = \sqrt{\frac{I}{A}} = \sqrt{\frac{\pi c^4/4}{\pi c^2}} = \frac{c}{2}$$

a. Length of 750 mm. Since the diameter of the rod is not known, a value of L/r must be assumed; we *assume* that $L/r > 55$ and use Eq. (10.46). For the centric load P , we have $\sigma = P/A$ and write

$$\begin{aligned} \frac{P}{A} = \sigma_{\text{all}} &= \frac{382 \times 10^3 \text{ MPa}}{(L/r)^2} \\ \frac{60 \times 10^3 \text{ N}}{\pi c^2} &= \frac{382 \times 10^9 \text{ Pa}}{\left(\frac{0.750 \text{ m}}{c/2}\right)^2} \\ c^4 &= 112.5 \times 10^{-9} \text{ m}^4 \quad c = 18.31 \text{ mm} \end{aligned}$$

For $c = 18.44$ mm, the slenderness ratio is

$$\frac{L}{r} = \frac{L}{c/2} = \frac{750 \text{ mm}}{(18.31 \text{ mm})/2} = 81.9 > 55$$

Our assumption is correct, and for $L = 750$ mm, the required diameter is

$$d = 2c = 2(18.31 \text{ mm}) \quad d = 36.6 \text{ mm} \quad \blacktriangleleft$$

b. Length of 300 mm. We again *assume* that $L/r > 55$. Using Eq. (10.46), and following the procedure used in part a, we find that $c = 11.58$ mm and $L/r = 51.8$. Since L/r is less than 55, our assumption is wrong; we now assume that $L/r < 55$ and use Eq. (10.45') for the design of this rod.

$$\begin{aligned} \frac{P}{A} = \sigma_{\text{all}} &= \left[213 - 1.577 \left(\frac{L}{r} \right) \right] \text{ MPa} \\ \frac{60 \times 10^3 \text{ N}}{\pi c^2} &= \left[213 - 1.577 \left(\frac{0.3 \text{ m}}{c/2} \right) \right] 10^6 \text{ Pa} \\ c &= 11.95 \text{ mm} \end{aligned}$$

For $c = 11.95$ mm, the slenderness ratio is

$$\frac{L}{r} = \frac{L}{c/2} = \frac{300 \text{ mm}}{(11.95 \text{ mm})/2} = 50.2$$

Our second assumption that $L/r < 55$ is correct. For $L = 300$ mm, the required diameter is

$$d = 2c = 2(11.95 \text{ mm}) \quad d = 23.9 \text{ mm} \quad \blacktriangleleft$$

PROBLEMS

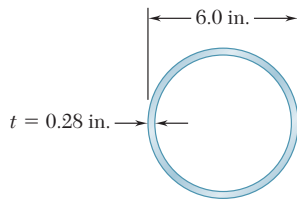


Fig. P10.59

10.57 Using allowable stress design, determine the allowable centric load for a column of 6-m effective length that is made from the following rolled-steel shape: (a) W200 \times 35.9, (b) W200 \times 86. Use $\sigma_Y = 250$ MPa and $E = 200$ GPa.

10.58 A W8 \times 31 rolled-steel shape is used for a column of 21-ft effective length. Using allowable stress design, determine the allowable centric load if the yield strength of the grade of steel used is (a) $\sigma_Y = 36$ ksi, (b) $\sigma_Y = 50$ ksi. Use $E = 29 \times 10^6$ psi.

10.59 A steel pipe having the cross section shown is used as a column. Using the allowable stress design determine the allowable centric load if the effective length of the column is (a) 18 ft, (b) 26 ft. Use $\sigma_Y = 36$ ksi and $E = 29 \times 10^6$ psi.

10.60 A column is made from half of a W360 \times 216 rolled-steel shape, with the geometric properties as shown. Using allowable stress design, determine the allowable centric load if the effective length of the column is (a) 4.0 m, (b) 6.5 m. Use $\sigma_Y = 345$ MPa and $E = 200$ GPa.

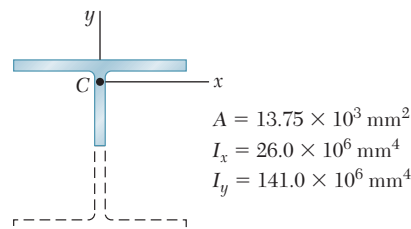


Fig. P10.60

10.61 A compression member has the cross section shown and an effective length of 5 ft. Knowing that the aluminum alloy used is 2014-T6, determine the allowable centric load.

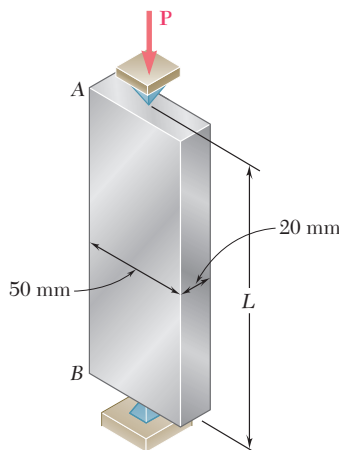


Fig. P10.62

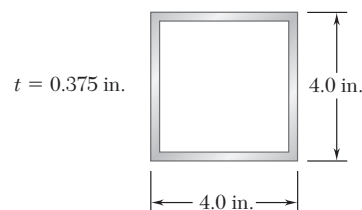


Fig. P10.61

10.62 Using the aluminum alloy 2014-T6, determine the largest allowable length of the aluminum bar AB for a centric load P of magnitude (a) 150 kN, (b) 90 kN, (c) 25 kN.

10.63 A sawn lumber column with a 7.5×5.5 -in. cross section has an 18-ft effective length. Knowing that for the grade of wood used the adjusted allowable stress for compression parallel to the grain is $\sigma_C = 1200$ psi and that the adjusted modulus $E = 470 \times 10^3$ psi, determine the maximum allowable centric load for the column.

10.64 A column having a 3.5-m effective length is made of sawn lumber with a 114×140 -mm cross section. Knowing that for the grade of wood used the adjusted allowable stress for compression parallel to the grain is $\sigma_C = 7.6$ MPa and the adjusted modulus $E = 2.8$ GPa, determine the maximum allowable centric load for the column.

10.65 A compression member of 8.2-ft effective length is obtained by bolting together two $L5 \times 3 \times \frac{1}{2}$ -in. steel angles as shown. Using allowable stress design, determine the allowable centric load for the column. Use $\sigma_Y = 36$ ksi and $E = 29 \times 10^6$ psi.



Fig. P10.65

10.66 and 10.67 A compression member of 9-m effective length is obtained by welding two 10-mm-thick steel plates to a $W250 \times 80$ rolled-steel shape as shown. Knowing that $\sigma_Y = 345$ MPa and $E = 200$ GPa and using allowable stress design, determine the allowable centric load for the compression member.



Fig. P10.66

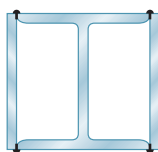


Fig. P10.67

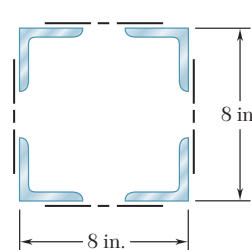
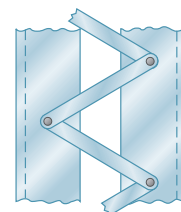


Fig. P10.68



10.68 A column of 18-ft effective length is obtained by connecting four $L3 \times 3 \times \frac{3}{8}$ -in. steel angles with lacing bars as shown. Using allowable stress design, determine the allowable centric load for the column. Use $\sigma_Y = 36$ ksi and $E = 29 \times 10^6$ psi.

10.69 An aluminum structural tube is reinforced by bolting two plates to it as shown for use as a column of 1.7-m effective length. Knowing that all material is aluminum alloy 2014-T6, determine the maximum allowable centric load.

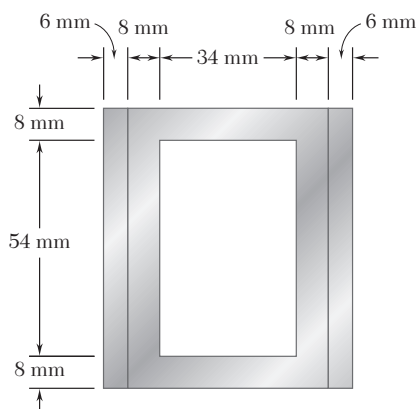


Fig. P10.69

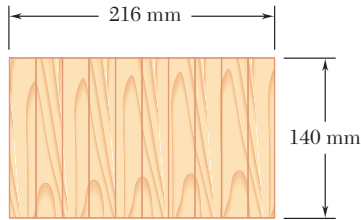


Fig. P10.70

10.70 A rectangular column with a 4.4-m effective length is made of glued laminated wood. Knowing that for the grade of wood used the adjusted allowable stress for compression parallel to the grain is $\sigma_C = 8.3$ MPa and the adjusted modulus $E = 4.6$ GPa, determine the maximum allowable centric load for the column.

10.71 For a rod made of the aluminum alloy 2014-T6, select the smallest square cross section that may be used if the rod is to carry a 55-kip centric load.

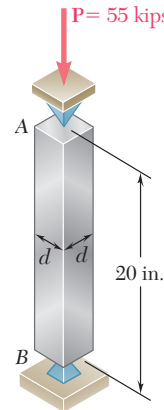


Fig. P10.71

10.72 An aluminum tube of 90-mm outer diameter is to carry a centric load of 120 kN. Knowing that the stock of tubes available for use are made of alloy 2014-T6 and with wall thicknesses in increments of 3 mm from 6 mm to 15 mm, determine the lightest tube that can be used.

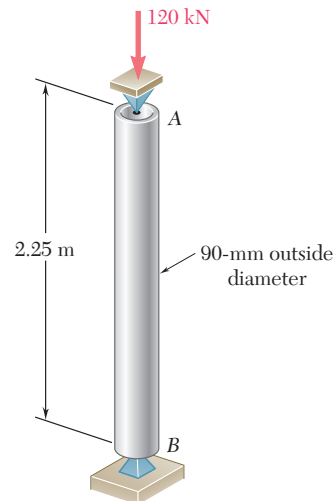


Fig. P10.72

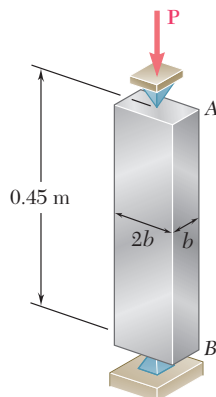


Fig. P10.73

10.73 A 72-kN centric load must be supported by an aluminum column as shown. Using the aluminum alloy 6061-T6, determine the minimum dimension b that can be used.

10.74 The glued laminated column shown is free at its top A and fixed at its base B . Using wood that has an adjusted allowable stress for compression parallel to the grain $\sigma_C = 9.2$ MPa and an adjusted modulus of elasticity $E = 5.7$ GPa, determine the smallest cross section that can support a centric load of 62 kN.

10.75 An 18-kip centric load is applied to a rectangular sawn lumber column of 22-ft effective length. Using sawn lumber for which the adjusted allowable stress for compression parallel to the grain is $\sigma_C = 1050$ psi and the adjusted modulus is $E = 440 \times 10^3$ psi, determine the smallest cross section that can be used. Use $b = 2d$.

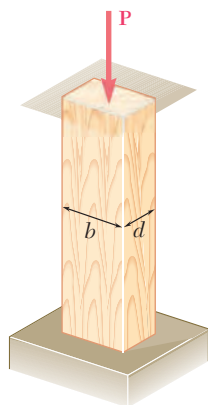


Fig. P10.75

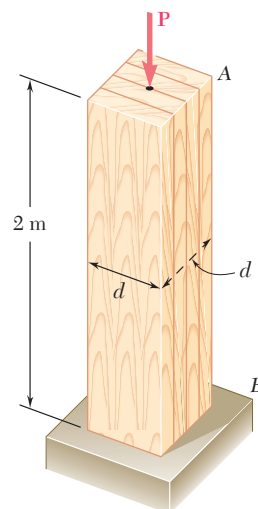


Fig. P10.74

10.76 A glue laminated column of 3-m effective length is to be made from boards of 24×100 -mm cross section. Knowing that for the grade of wood used, $E = 11$ GPa and the adjusted allowable stress for compression parallel to the grain is $\sigma_C = 9$ MPa, determine the number of boards that must be used to support the centric load shown when (a) $P = 34$ kN, (b) $P = 17$ kN.

10.77 A column of 4.5-m effective length must carry a centric load of 900 kN. Knowing that $\sigma_Y = 345$ MPa and $E = 200$ GPa, use allowable stress design to select the wide-flange shape of 250-mm nominal depth that should be used.

10.78 A column of 4.6-m effective length must carry a centric load of 525 kN. Knowing that $\sigma_Y = 345$ MPa and $E = 200$ GPa, use allowable stress design to select the wide-flange shape of 200-mm nominal depth that should be used.

10.79 A column of 22.5-ft effective length must carry a centric load of 288 kips. Using allowable stress design, select the wide-flange shape of 14-in. nominal depth that should be used. Use $\sigma_Y = 50$ ksi and $E = 29 \times 10^6$ psi.

10.80 A square steel tube having the cross section shown is used as a column of 26-ft effective length to carry a centric load of 65 kips. Knowing that the tubes available for use are made with wall thicknesses ranging from $\frac{1}{4}$ in. to $\frac{3}{4}$ in. in increments of $\frac{1}{16}$ in., use allowable stress design to determine the lightest tube that can be used. Use $\sigma_Y = 36$ ksi and $E = 29 \times 10^6$ psi.

10.81 Solve Prob. 10.80, assuming that the effective length of the column is decreased to 20 ft.

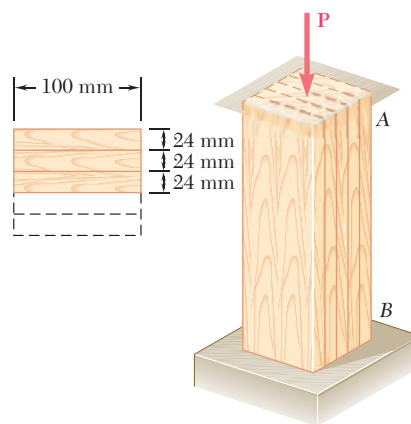


Fig. P10.76

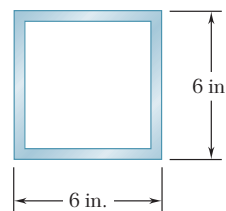


Fig. P10.80

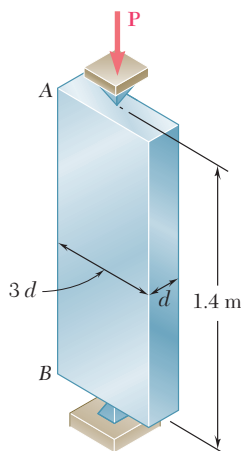


Fig. P10.82

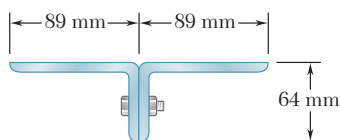


Fig. P10.84

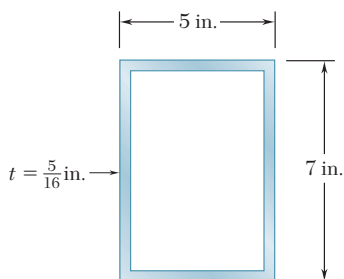


Fig. P10.86

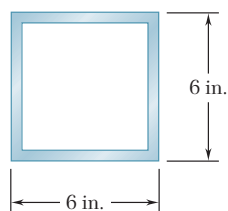


Fig. P10.88

10.82 A centric load P must be supported by the steel bar AB . Using allowable stress design, determine the smallest dimension d of the cross section that can be used when (a) $P = 108$ kN, (b) $P = 166$ kN. Use $\sigma_Y = 250$ MPa and $E = 200$ GPa.

10.83 Two $3\frac{1}{2} \times 2\frac{1}{2}$ -in. angles are bolted together as shown for use as a column of 6-ft effective length to carry a centric load of 54 kips. Knowing that the angles available have thicknesses of $\frac{1}{4}$, $\frac{3}{8}$, and $\frac{1}{2}$ in., use allowable stress design to determine the lightest angles that can be used. Use $\sigma_Y = 36$ ksi and $E = 29 \times 10^6$ psi.

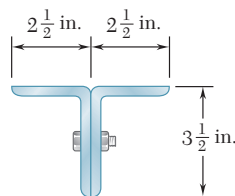


Fig. P10.83

10.84 Two 89×64 -mm angles are bolted together as shown for use as a column of 2.4-m effective length to carry a centric load of 180 kN. Knowing that the angles available have thicknesses of 6.4 mm, 9.5 mm, and 12.7 mm, use allowable stress design to determine the lightest angles that can be used. Use $\sigma_Y = 250$ MPa and $E = 200$ GPa.

***10.85** A column with a 5.8-m effective length supports a centric load, with ratio of dead to live load equal to 1.35. The dead load factor is $\gamma_D = 1.2$, the live load factor $\gamma_L = 1.6$, and the resistance factor $\phi = 0.90$. Use load and resistance factor design to determine the allowable centric dead and live loads if the column is made of the following rolled-steel shape: (a) W250 \times 67, (b) W360 \times 101. Use $\sigma_Y = 345$ MPa and $E = 200$ GPa.

***10.86** A rectangular steel tube having the cross section shown is used as a column of 14.5-ft effective length. Knowing that $\sigma_Y = 36$ ksi and $E = 29 \times 10^6$ psi., use load and resistance factor design to determine the largest centric live load that can be applied if the centric dead load is 54 kips. Use a dead load factor $\gamma_D = 1.2$, a live load factor $\gamma_L = 1.6$ and the resistance factor $\phi = 0.90$.

***10.87** A steel column of 5.5-m effective length must carry a centric dead load of 310 kN and a centric live load of 375 kN. Knowing that $\sigma_Y = 250$ MPa and $E = 200$ GPa, use load and resistance factor design to select the wide-flange shape of 310-mm nominal depth that should be used. The dead load factor $\gamma_D = 1.2$, the live load factor $\gamma_L = 1.6$, and the resistance factor $\phi = 0.90$.

***10.88** The steel tube having the cross section shown is used as a column of 15-ft effective length to carry a centric dead load of 51 kips and a centric live load of 58 kips. Knowing that the tubes available for use are made with wall thicknesses in increments of $\frac{1}{16}$ in. from $\frac{3}{16}$ in. to $\frac{3}{8}$ in., use load and resistance factor design to determine the lightest tube that can be used. Use $\sigma_Y = 36$ ksi and $E = 29 \times 10^6$ psi. The dead load factor $\gamma_D = 1.2$, the live load factor $\gamma_L = 1.6$, and the resistance factor $\phi = 0.90$.

10.7 DESIGN OF COLUMNS UNDER AN ECCENTRIC LOAD

In this section, the design of columns subjected to an eccentric load will be considered. You will see how the empirical formulas developed in the preceding section for columns under a centric load can be modified and used when the load \mathbf{P} applied to the column has an eccentricity e which is known.

We first recall from Sec. 4.12 that an eccentric axial load \mathbf{P} applied in a plane of symmetry of the column can be replaced by an equivalent system consisting of a centric load \mathbf{P} and a couple \mathbf{M} of moment $M = Pe$, where e is the distance from the line of action of the load to the longitudinal axis of the column (Fig. 10.32). The normal stresses exerted on a transverse section of the column can then be obtained by superposing the stresses due, respectively, to the centric load \mathbf{P} and to the couple \mathbf{M} (Fig. 10.33), provided that

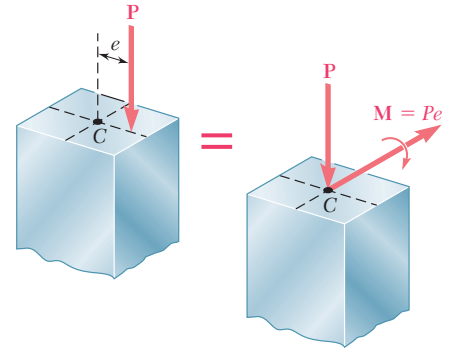


Fig. 10.32 Column with eccentric load.

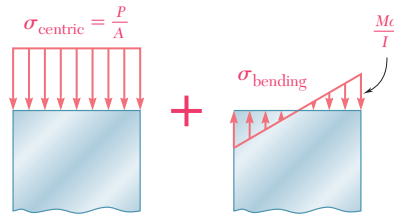


Fig. 10.33 Stresses on column transverse section.

the section considered is not too close to either end of the column, and as long as the stresses involved do not exceed the proportional limit of the material. The normal stresses due to the eccentric load \mathbf{P} can thus be expressed as

$$\sigma = \sigma_{\text{centric}} + \sigma_{\text{bending}} \quad (10.51)$$

Recalling the results obtained in Sec. 4.12, we find that the maximum compressive stress in the column is

$$\sigma_{\text{max}} = \frac{P}{A} + \frac{Mc}{I} \quad (10.52)$$

In a properly designed column, the maximum stress defined by Eq. (10.52) should not exceed the allowable stress for the column. Two alternative approaches can be used to satisfy this requirement, namely, the *allowable-stress method* and the *interaction method*.

a. Allowable-Stress Method. This method is based on the assumption that the allowable stress for an eccentrically loaded column is the same as if the column were centrically loaded. We must have, therefore, $\sigma_{\text{max}} \leq \sigma_{\text{all}}$, where σ_{all} is the allowable stress under a centric load, or substituting for σ_{max} from Eq. (10.52)

$$\frac{P}{A} + \frac{Mc}{I} \leq \sigma_{\text{all}} \quad (10.53)$$

The allowable stress is obtained from the formulas of Sec. 10.6 which, for a given material, express σ_{all} as a function of the slenderness ratio of the column. The major engineering codes require that the largest value of the slenderness ratio of the column be used to determine the allowable stress, whether or not this value corresponds to the actual plane of bending. This requirement sometimes results in an overly conservative design.

EXAMPLE 10.04

A column with a 2-in.-square cross section and 28-in. effective length is made of the aluminum alloy 2014-T6. Using the allowable-stress method, determine the maximum load P that can be safely supported with an eccentricity of 0.8 in.

We first compute the radius of gyration r using the given data

$$A = (2 \text{ in.})^2 = 4 \text{ in}^2 \quad I = \frac{1}{12}(2 \text{ in.})^4 = 1.333 \text{ in}^4$$

$$r = \sqrt{\frac{I}{A}} = \sqrt{\frac{1.333 \text{ in}^4}{4 \text{ in}^2}} = 0.5774 \text{ in.}$$

We next compute $L/r = (28 \text{ in.})/(0.5774 \text{ in.}) = 48.50$.

Since $L/r < 55$, we use Eq. (10.48) to determine the allowable stress for the aluminum column subjected to a centric load. We have

$$\sigma_{\text{all}} = [30.9 - 0.229(48.50)] = 19.79 \text{ ksi}$$

We now use Eq. (10.53) with $M = Pe$ and $c = \frac{1}{2}(2 \text{ in.}) = 1 \text{ in.}$ to determine the allowable load:

$$\frac{P}{4 \text{ in}^2} + \frac{P(0.8 \text{ in.})(1 \text{ in.})}{1.333 \text{ in}^4} \leq 19.79 \text{ ksi}$$

$$P \leq 23.3 \text{ kips}$$

The maximum load that can be safely applied is $P = 23.3 \text{ kips}$.

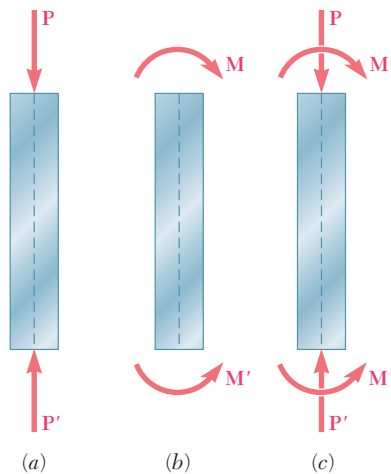


Fig. 10.34 Column load possibilities.

b. Interaction Method. We recall that the allowable stress for a column subjected to a centric load (Fig. 10.34a) is generally smaller than the allowable stress for a column in pure bending (Fig. 10.34b), since the former takes into account the possibility of buckling. Therefore, when we use the allowable-stress method to design an eccentrically loaded column and write that the sum of the stresses due to the centric load \mathbf{P} and the bending couple \mathbf{M} (Fig. 10.34c) must not exceed the allowable stress for a centrically loaded column, the resulting design is generally overly conservative. An improved method of design can be developed by rewriting Eq. 10.53 in the form

$$\frac{P/A}{\sigma_{\text{all}}} + \frac{Mc/I}{\sigma_{\text{all}}} \leq 1 \quad (10.54)$$

and substituting for σ_{all} in the first and second terms the values of the allowable stress which correspond, respectively, to the

centric loading of Fig. 10.34a and to the pure bending of Fig. 10.34b. We have

$$\frac{P/A}{(\sigma_{\text{all}})_{\text{centric}}} + \frac{Mc/I}{(\sigma_{\text{all}})_{\text{bending}}} \leq 1 \quad (10.55)$$

The type of formula obtained is known as an *interaction formula*.

We note that, when $M = 0$, the use of this formula results in the design of a centrically loaded column by the method of Sec. 10.6. On the other hand, when $P = 0$, the use of the formula results in the design of a beam in pure bending by the method of Chap. 4. When P and M are both different from zero, the interaction formula results in a design that takes into account the capacity of the member to resist bending as well as axial loading. In all cases, $(\sigma_{\text{all}})_{\text{centric}}$ will be determined by using the largest slenderness ratio of the column, regardless of the plane in which bending takes place.†

When the eccentric load \mathbf{P} is not applied in a plane of symmetry of the column, it causes bending about both of the principal axes of the cross section. We recall from Sec. 4.14 that the load \mathbf{P} can then be replaced by a centric load \mathbf{P} and two couples represented by the couple vectors \mathbf{M}_x and \mathbf{M}_z shown in Fig. 10.35. The interaction formula to be used in this case is

$$\frac{P/A}{(\sigma_{\text{all}})_{\text{centric}}} + \frac{|M_x|z_{\text{max}}/I_x}{(\sigma_{\text{all}})_{\text{bending}}} + \frac{|M_z|x_{\text{max}}/I_z}{(\sigma_{\text{all}})_{\text{bending}}} \leq 1 \quad (10.56)$$

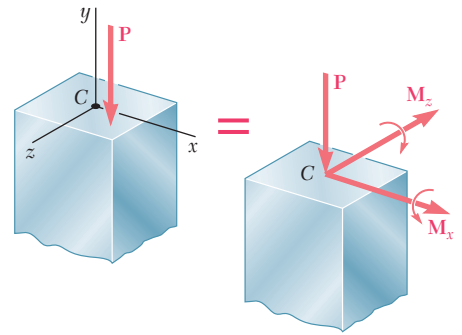


Fig. 10.35 Column with eccentric load.

Use the interaction method to determine the maximum load P that can be safely supported by the column of Example 10.04 with an eccentricity of 0.8 in. The allowable stress in bending is 24 ksi.

EXAMPLE 10.05

The value of $(\sigma_{\text{all}})_{\text{centric}}$ has already been determined in Example 10.04. We have

$$(\sigma_{\text{all}})_{\text{centric}} = 19.79 \text{ ksi} \quad (\sigma_{\text{all}})_{\text{bending}} = 24 \text{ ksi}$$

Substituting these values into Eq. (10.55), we write

$$\frac{P/A}{19.79 \text{ ksi}} + \frac{Mc/I}{24 \text{ ksi}} \leq 1.0$$

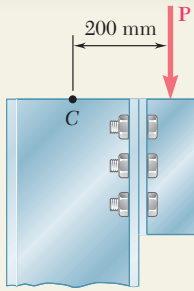
Using the numerical data from Example 10.04, we write

$$\frac{P/4}{19.79 \text{ ksi}} + \frac{P(0.8)(1.0)/1.333}{24 \text{ ksi}} \leq 1.0$$

$$P \leq 26.6 \text{ kips}$$

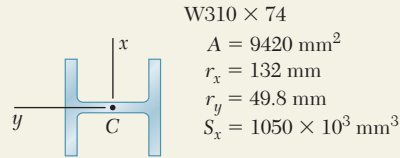
The maximum load that can be safely applied is thus $P = 26.6$ kips.

†This procedure is required by all major codes for the design of steel, aluminum, and timber compression members. In addition, many specifications call for the use of an additional factor in the second term of Eq. (10.55); this factor takes into account the additional stresses resulting from the deflection of the column due to bending.



SAMPLE PROBLEM 10.5

Using the allowable-stress method, determine the largest load **P** that can be safely carried by a W310 × 74 steel column of 4.5-m effective length. Use $E = 200$ GPa and $\sigma_Y = 250$ MPa.



SOLUTION

The largest slenderness ratio of the column is $L/r_y = (4.5 \text{ m})/(0.0498 \text{ m}) = 90.4$. Using Eq. (10.41) with $E = 200$ GPa and $\sigma_Y = 250$ MPa, we find that the slenderness ratio at the junction between the two equations for σ_{cr} is $L/r = 133.2$. Thus, we use Eqs. (10.38) and (10.39) and find that $\sigma_{cr} = 162.2$ MPa. Using Eq. (10.42), the allowable stress is

$$(\sigma_{\text{all}})_{\text{centric}} = 162.2/1.67 = 97.1 \text{ MPa}$$

For the given column and loading, we have

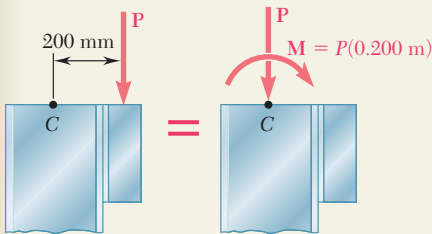
$$\frac{P}{A} = \frac{P}{9.42 \times 10^{-3} \text{ m}^2} \quad \frac{Mc}{I} = \frac{M}{S} = \frac{P(0.200 \text{ m})}{1.050 \times 10^{-3} \text{ m}^3}$$

Substituting into Eq. (10.58), we write

$$\frac{P}{9.42 \times 10^{-3} \text{ m}^2} + \frac{P(0.200 \text{ m})}{1.050 \times 10^{-3} \text{ m}^3} \leq 97.1 \text{ MPa} \quad P \leq 327 \text{ kN}$$

The largest allowable load **P** is thus

$$\mathbf{P = 327 \text{ kN} \downarrow}$$



SAMPLE PROBLEM 10.6

Using the interaction method, solve Sample Prob. 10.5. Assume $(\sigma_{\text{all}})_{\text{bending}} = 150$ MPa.

SOLUTION

Using Eq. (10.60), we write

$$\frac{P/A}{(\sigma_{\text{all}})_{\text{centric}}} + \frac{Mc/I}{(\sigma_{\text{all}})_{\text{bending}}} \leq 1$$

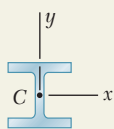
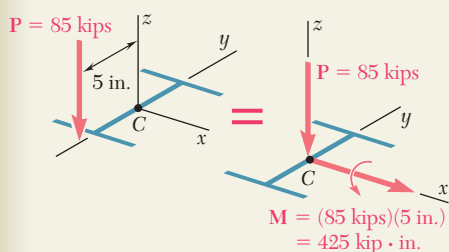
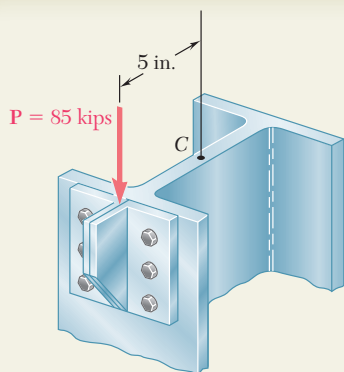
Substituting the given allowable bending stress and the allowable centric stress found in Sample Prob. 10.5, as well as the other given data, we have

$$\frac{P/(9.42 \times 10^{-3} \text{ m}^2)}{97.1 \times 10^6 \text{ Pa}} + \frac{P(0.200 \text{ m})/(1.050 \times 10^{-3} \text{ m}^3)}{150 \times 10^6 \text{ Pa}} \leq 1$$

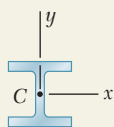
$$\mathbf{P \leq 423 \text{ kN}}$$

The largest allowable load **P** is thus

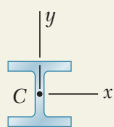
$$\mathbf{P = 423 \text{ kN} \downarrow}$$



W8 × 35
 $A = 10.3 \text{ in}^2$
 $r_x = 3.51 \text{ in.}$
 $r_y = 2.03 \text{ in.}$
 $S_x = 31.2 \text{ in}^3$
 $L = 16 \text{ ft} = 192 \text{ in.}$



W8 × 48
 $A = 14.1 \text{ in}^2$
 $r_x = 3.61 \text{ in.}$
 $r_y = 2.08 \text{ in.}$
 $S_x = 43.2 \text{ in}^3$
 $L = 16 \text{ ft} = 192 \text{ in.}$



W8 × 40
 $A = 11.7 \text{ in}^2$
 $r_x = 3.53 \text{ in.}$
 $r_y = 2.04 \text{ in.}$
 $S_x = 35.5 \text{ in}^3$
 $L = 16 \text{ ft} = 192 \text{ in.}$

SAMPLE PROBLEM 10.7

A steel column having an effective length of 16 ft is loaded eccentrically as shown. Using the interaction method, select the wide-flange shape of 8-in. nominal depth that should be used. Assume $E = 29 \times 10^6 \text{ psi}$ and $\sigma_Y = 36 \text{ ksi}$, and use an allowable stress in bending of 22 ksi.

SOLUTION

So that we can select a trial section, we use the allowable-stress method with $\sigma_{\text{all}} = 22 \text{ ksi}$ and write

$$\sigma_{\text{all}} = \frac{P}{A} + \frac{Mc}{I_x} = \frac{P}{A} + \frac{Mc}{Ar_x^2} \quad (1)$$

From Appendix C we observe for shapes of 8-in. nominal depth that $c \approx 4 \text{ in.}$ and $r_x \approx 3.5 \text{ in.}$ Substituting into Eq. (1), we have

$$22 \text{ ksi} = \frac{85 \text{ kips}}{A} + \frac{(425 \text{ kip} \cdot \text{in.})(4 \text{ in.})}{A(3.5 \text{ in.})^2} \quad A \approx 10.2 \text{ in}^2$$

We select for a first trial shape: W8 × 35.

Trial 1: W8 × 35. The allowable stresses are

Allowable Bending Stress: (see data) $(\sigma_{\text{all}})_{\text{bending}} = 22 \text{ ksi}$

Allowable Concentric Stress: The largest slenderness ratio of the column is $L/r_y = (192 \text{ in.})/(2.03 \text{ in.}) = 94.6$. Using Eq. (10.41) with $E = 29 \times 10^6 \text{ psi}$ and $\sigma_Y = 36 \text{ ksi}$, we find that the slenderness ratio at the junction between the two equations for σ_{cr} is $L/r = 133.7$. Thus, we use Eqs. (10.38) and (10.39) and find that $\sigma_{cr} = 22.5 \text{ ksi}$. Using Eq. (10.42), the allowable stress is

$$(\sigma_{\text{all}})_{\text{centric}} = 22.5/1.67 = 13.46 \text{ ksi}$$

For the W8 × 35 trial shape, we have

$$\frac{P}{A} = \frac{85 \text{ kips}}{10.3 \text{ in}^2} = 8.25 \text{ ksi} \quad \frac{Mc}{I} = \frac{M}{S_x} = \frac{425 \text{ kip} \cdot \text{in.}}{31.2 \text{ in}^3} = 13.62 \text{ ksi}$$

With this data we find that the left-hand member of Eq. (10.60) is

$$\frac{P/A}{(\sigma_{\text{all}})_{\text{centric}}} + \frac{Mc/I}{(\sigma_{\text{all}})_{\text{bending}}} = \frac{8.25 \text{ ksi}}{13.46 \text{ ksi}} + \frac{13.62 \text{ ksi}}{22 \text{ ksi}} = 1.232$$

Since $1.232 > 1.000$, the requirement expressed by the interaction formula is not satisfied; we must select a larger trial shape.

Trial 2: W8 × 48. Following the procedure used in trial 1, we write

$$\frac{L}{r_y} = \frac{192 \text{ in.}}{2.08 \text{ in.}} = 92.3 \quad (\sigma_{\text{all}})_{\text{centric}} = 13.76 \text{ ksi}$$

$$\frac{P}{A} = \frac{85 \text{ kips}}{14.1 \text{ in}^2} = 6.03 \text{ ksi} \quad \frac{Mc}{I} = \frac{M}{S_x} = \frac{425 \text{ kip} \cdot \text{in.}}{43.2 \text{ in}^3} = 9.84 \text{ ksi}$$

Substituting into Eq. (10.60) gives

$$\frac{P/A}{(\sigma_{\text{all}})_{\text{centric}}} + \frac{Mc/I}{(\sigma_{\text{all}})_{\text{bending}}} = \frac{6.03 \text{ ksi}}{13.76 \text{ ksi}} + \frac{9.82 \text{ ksi}}{22 \text{ ksi}} = 0.885 < 1.000$$

The W8 × 48 shape is satisfactory but may be unnecessarily large.

Trial 3: W8 × 40. Following again the same procedure, we find that the interaction formula is not satisfied.

Selection of Shape. The shape to be used is

W8 × 48 ◀

PROBLEMS

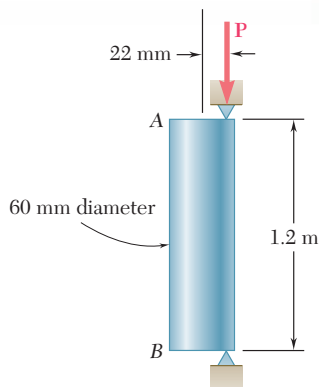


Fig. P10.89

10.89 An eccentric load is applied at a point 22 mm from the geometric axis of a 60-mm-diameter rod made of a steel for which $\sigma_Y = 250$ MPa and $E = 200$ GPa. Using the allowable-stress method, determine the allowable load **P**.

10.90 Solve Prob. 10.89, assuming that the load is applied at a point 40 mm from the geometric axis and that the effective length is 0.9 m.

10.91 A column of 5.5-m effective length is made of the aluminum alloy 2014-T6, for which the allowable stress in bending is 220 MPa. Using the interaction method, determine the allowable load **P**, knowing that the eccentricity is (a) $e = 0$, (b) $e = 40$ mm.

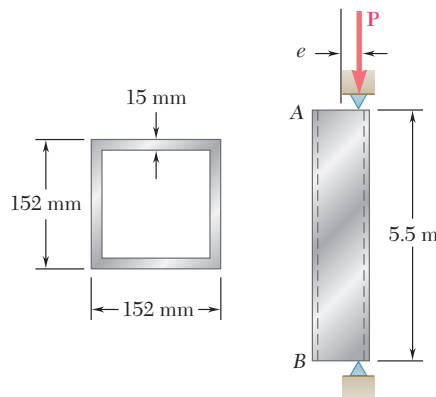


Fig. P10.91

10.92 Solve Prob. 10.91, assuming that the effective length of the column is 3.0 m.

10.93 A sawn-lumber column of 5.0×7.5 -in. cross section has an effective length of 8.5 ft. The grade of wood used has an adjusted allowable stress for compression parallel to the grain $\sigma_C = 1180$ psi and an adjusted modulus $E = 440 \times 10^3$ psi. Using the allowable-stress method, determine the largest eccentric load **P** that can be applied when (a) $e = 0.5$ in., (b) $e = 1.0$ in.

10.94 Solve Prob. 10.93 using the interaction method and an allowable stress in bending of 1300 psi.

10.95 A column of 14-ft effective length consists of a section of steel tubing having the cross section shown. Using the allowable-stress method, determine the maximum allowable eccentricity e if (a) $P = 55$ kips, (b) $P = 35$ kips. Use $\sigma_Y = 36$ ksi and $E = 29 \times 10^6$ psi.

10.96 Solve Prob. 10.95, assuming that the effective length of the column is increased to 18 ft and that (a) $P = 28$ kips, (b) $P = 18$ kips.

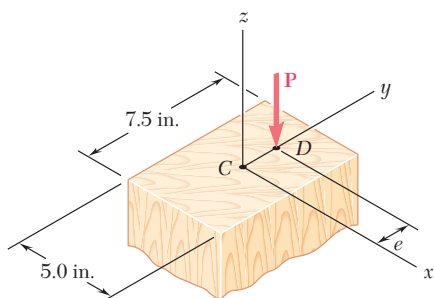


Fig. P10.93

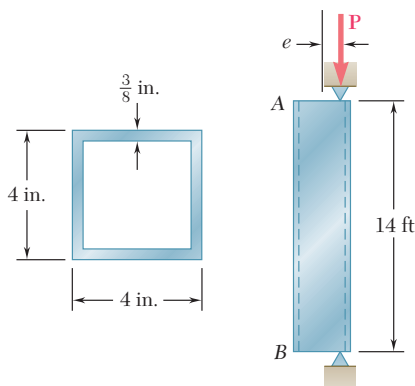


Fig. P10.95

10.97 The compression member AB is made of a steel for which $\sigma_Y = 250$ MPa and $E = 200$ GPa. It is free at its top A and fixed at its base B . Using the allowable-stress method, determine the largest allowable eccentricity e_x , knowing that (a) $e_y = 0$, (b) $e_y = 8$ mm.

10.98 The compression member AB is made of a steel for which $\sigma_Y = 250$ MPa and $E = 200$ GPa. It is free at its top A and fixed at its base B . Using the interaction method with an allowable bending stress equal to 120 MPa and knowing that the eccentricities e_x and e_y are equal, determine their largest allowable common value.

10.99 An eccentric load $P = 10$ kips is applied at a point 0.8 in. from the geometric axis of a 2-in.-diameter rod made of the aluminum alloy 6061-T6. Using the interaction method and an allowable stress in bending of 21 ksi, determine the largest allowable effective length L that can be used.

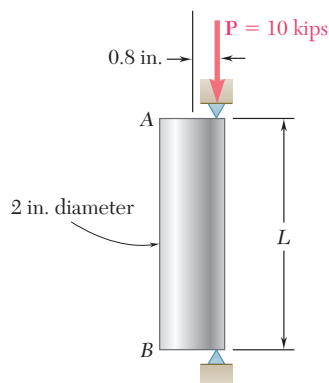


Fig. P10.99

10.100 Solve Prob. 10.99, assuming that the aluminum alloy used is 2014-T6 and that the allowable stress in bending is 24 ksi.

10.101 A rectangular column is made of a grade of sawn wood that has an adjusted allowable stress for compression parallel to the grain $\sigma_C = 8.3$ MPa and an adjusted modulus of elasticity $E = 11.1$ GPa. Using the allowable-stress method, determine the largest allowable effective length L that can be used.

10.102 Solve Prob. 10.101, assuming that $P = 105$ kN.

10.103 An 11-kip vertical load P is applied at the midpoint of one edge of the square cross section of the steel compression member AB , which is free at its top A and fixed at its base B . Knowing that for the grade of steel used $\sigma_Y = 36$ ksi and $E = 29 \times 10^6$ psi, and using the allowable-stress method, determine the smallest allowable dimension d .

10.104 Solve Prob. 10.103, assuming that the vertical load P is applied at the corner of the cross section.

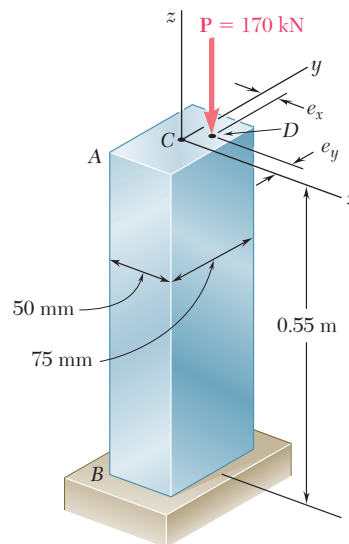


Fig. P10.97 and P10.98

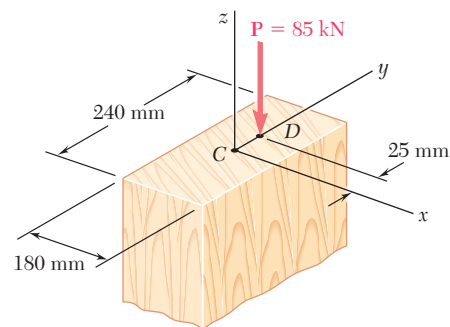


Fig. P10.101

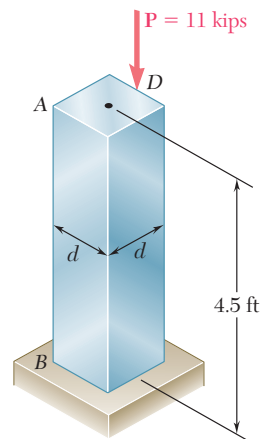


Fig. P10.103

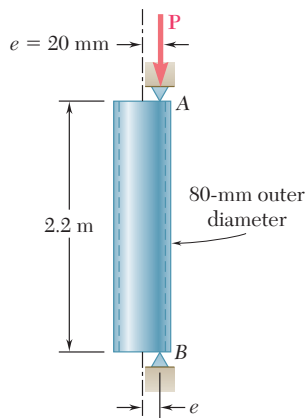


Fig. P10.105

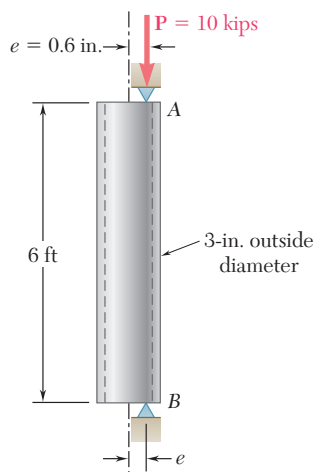


Fig. P10.109

10.105 A steel tube of 80-mm outer diameter is to carry a 93-kN load P with an eccentricity of 20 mm. The tubes available for use are made with wall thicknesses in increments of 3 mm from 6 mm to 15 mm. Using the allowable-stress method, determine the lightest tube that can be used. Assume $E = 200$ GPa and $\sigma_Y = 250$ MPa.

10.106 Solve Prob. 10.105, using the interaction method with $P = 165$ kN, $e = 15$ mm, and an allowable stress in bending of 150 MPa.

10.107 A compression member of rectangular cross section has an effective length of 0.9 m and is made of the aluminum alloy 2014-T6 for which the allowable stress in bending is 160 MPa. Using the interaction method, determine the smallest dimension d of the cross section that can be used when $e = 10$ mm.

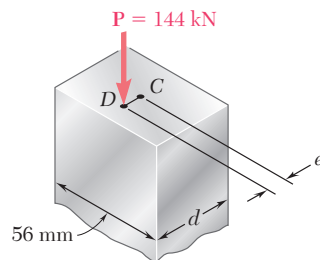


Fig. P10.107

10.108 Solve Prob. 10.107, assuming that $e = 5$ mm.

10.109 An aluminum tube of 3-in. outside diameter is to carry a load of 10 kips having an eccentricity $e = 0.6$ in. Knowing that the stock of tubes available for use are made of alloy 2014-T6 and have wall thicknesses in increments of $\frac{1}{16}$ in. up to $\frac{1}{2}$ in. determine the lightest tube that can be used. Use the allowable-stress method.

10.110 Solve Prob. 10.109, using the interaction method of design with an allowable stress in bending of 25 ksi.

10.111 A sawn lumber column of rectangular cross section has a 2.2-m effective length and supports a 41-kN load as shown. The sizes available for use have b equal to 90 mm, 140 mm, 190 mm, and 240 mm. The grade of wood has an adjusted allowable stress for compression parallel to the grain $\sigma_C = 8.1$ MPa and an adjusted modulus $E = 8.3$ GPa. Using the allowable-stress method, determine the lightest section that can be used.

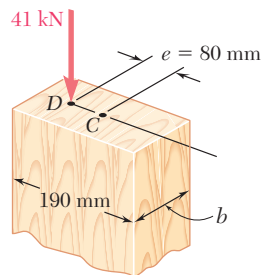


Fig. P10.111

10.112 Solve Prob. 10.111, assuming that $e = 40$ mm.

- 10.113** A steel column having a 24-ft effective length is loaded eccentrically as shown. Using the allowable-stress method, select the wide-flange shape of 14-in. nominal depth that should be used. Use $\sigma_Y = 36$ ksi and $E = 29 \times 10^6$ psi.

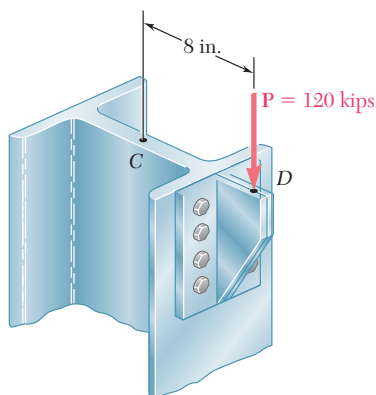


Fig. P10.113

- 10.114** Solve Prob. 10.113 using the interaction method, assuming that $\sigma_Y = 50$ ksi and the allowable stress in bending is 30 ksi.
- 10.115** A steel column of 7.2-m effective length is to support an 83-kN eccentric load \mathbf{P} at a point D , located on the x axis as shown. Using the allowable-stress method, select the wide-flange shape of 250-mm nominal depth that should be used. Use $E = 200$ GPa and $\sigma_Y = 250$ MPa.

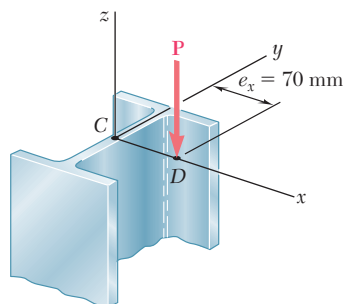


Fig. P10.115

- 10.116** A steel compression member of 5.8-m effective length is to support a 296-kN eccentric load \mathbf{P} . Using the interaction method, select the wide-flange shape of 200-mm nominal depth that should be used. Use $E = 200$ GPa, $\sigma_Y = 250$ MPa, and $\sigma_{all} = 150$ MPa in bending.

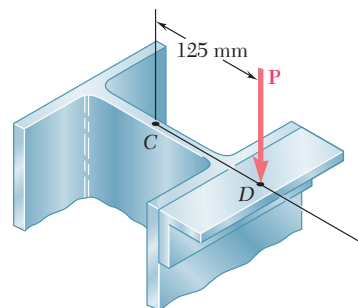


Fig. P10.116

REVIEW AND SUMMARY

Critical load

This chapter was devoted to the design and analysis of columns, i.e., prismatic members supporting axial loads. In order to gain insight into the behavior of columns, we first considered in Sec. 10.2 the equilibrium of a simple model and found that for values of the load P exceeding a certain value P_{cr} , called the *critical load*, two equilibrium positions of the model were possible: the original position with zero transverse deflections and a second position involving deflections that could be quite large. This led us to conclude that the first equilibrium position was unstable for $P > P_{cr}$, and stable for $P < P_{cr}$, since in the latter case it was the only possible equilibrium position.

In Sec. 10.3, we considered a pin-ended column of length L and of constant flexural rigidity EI subjected to an axial centric load P . Assuming that the column had buckled (Fig. 10.36), we noted that the bending moment at point Q was equal to $-Py$ and wrote

$$\frac{d^2y}{dx^2} = \frac{M}{EI} = -\frac{P}{EI}y \quad (10.4)$$

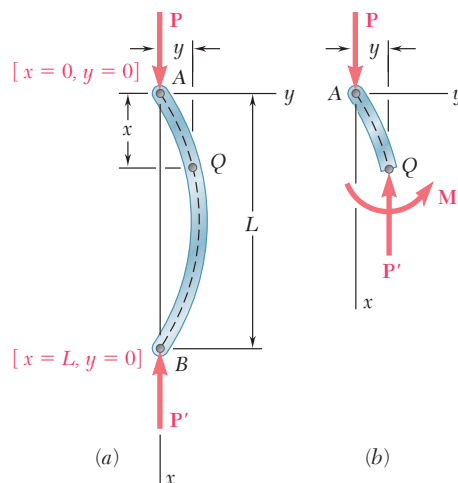


Fig. 10.36

Euler's formula

Solving this differential equation, subject to the boundary conditions corresponding to a pin-ended column, we determined the smallest load P for which buckling can take place. This load, known as the *critical load* and denoted by P_{cr} , is given by *Euler's formula*:

$$P_{cr} = \frac{\pi^2 EI}{L^2} \quad (10.11)$$

where L is the length of the column. For this load or any larger load, the equilibrium of the column is unstable and transverse deflections will occur.

Denoting the cross-sectional area of the column by A and its radius of gyration by r , we determined the critical stress σ_{cr} corresponding to the critical load P_{cr} :

$$\sigma_{cr} = \frac{\pi^2 E}{(L/r)^2} \quad (10.13)$$

The quantity L/r is called the *slenderness ratio* and we plotted σ_{cr} as a function of L/r (Fig. 10.37). Since our analysis was based on stresses remaining below the yield strength of the material, we noted that the column would fail by yielding when $\sigma_{cr} > \sigma_Y$.

In Sec. 10.4, we discussed the critical load of columns with various end conditions and wrote

$$P_{cr} = \frac{\pi^2 EI}{L_e^2} \quad (10.11')$$

where L_e is the *effective length* of the column, i.e., the length of an equivalent pin-ended column. The effective lengths of several columns with various end conditions were calculated and shown in Fig. 10.17 on page 642.

In Sec. 10.5, we considered columns supporting an *eccentric axial load*. For a pin-ended column subjected to a load P applied with an eccentricity e , we replaced the load by a centric axial load and a couple of moment $M_A = Pe$ (Figs. 10.38 and 10.39) and derived the following expression for the maximum transverse deflection:

$$y_{\max} = e \left[\sec \left(\sqrt{\frac{P}{EI}} \frac{L}{2} \right) - 1 \right] \quad (10.28)$$

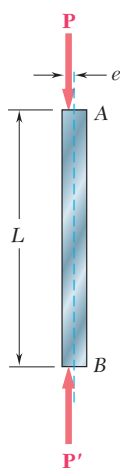


Fig. 10.38

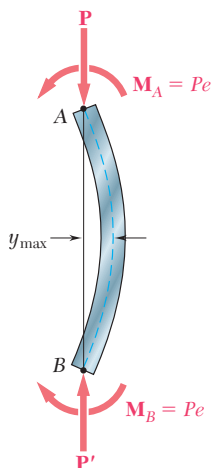


Fig. 10.39

Slenderness ratio

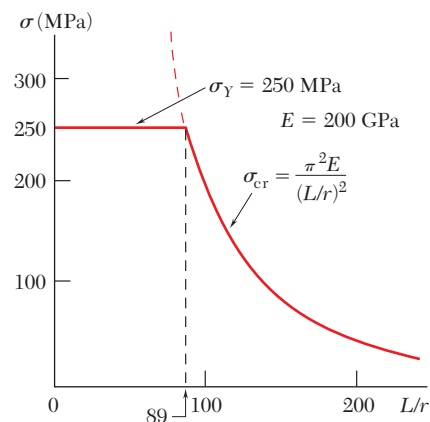


Fig. 10.37

Effective length

Eccentric axial load. Secant formula.

We then determined the maximum stress in the column, and from the expression obtained for that stress, we derived the *secant formula*:

$$\frac{P}{A} = \frac{\sigma_{\max}}{1 + \frac{ec}{r^2} \sec\left(\frac{1}{2}\sqrt{\frac{P}{EA}} \frac{L_e}{r}\right)} \quad (10.36)$$

This equation can be solved for the force per unit area, P/A , that causes a specified maximum stress σ_{\max} in a pin-ended column or any other column of effective slenderness ratio L_e/r .

Design of real columns

Centrally loaded columns

In the first part of the chapter we considered each column as a straight homogeneous prism. Since imperfections exist in all real columns, the *design of real columns* is done by using empirical formulas based on laboratory tests and set forth in specifications and codes issued by professional organizations. In Sec. 10.6, we discussed the design of *centrally loaded columns* made of steel, aluminum, or wood. For each material, the design of the column was based on formulas expressing the allowable stress as a function of the slenderness ratio L/r of the column. For structural steel, we also discussed the alternative method of *Load and Resistance Factor Design*.

Eccentrically loaded columns

Allowable-stress method

In the last section of the chapter [Sec. 10.7], we studied two methods used for the design of columns under an *eccentric* load. The first method was the *allowable-stress method*, a conservative method in which it is assumed that the allowable stress is the same as if the column were centrally loaded. The allowable-stress method requires that the following inequality be satisfied:

$$\frac{P}{A} + \frac{Mc}{I} \leq \sigma_{\text{all}} \quad (10.53)$$

Interaction method

The second method was the *interaction method*, a method used in most modern specifications. In this method the allowable stress for a centrally loaded column is used for the portion of the total stress due to the axial load and the allowable stress in bending for the stress due to bending. Thus, the inequality to be satisfied is

$$\frac{P/A}{(\sigma_{\text{all}})_{\text{centric}}} + \frac{Mc/I}{(\sigma_{\text{all}})_{\text{bending}}} \leq 1 \quad (10.55)$$

REVIEW PROBLEMS

- 10.117** The rigid bar AD is attached to two springs of constant k and is in equilibrium in the position shown. Knowing that the equal and opposite loads \mathbf{P} and \mathbf{P}' remain horizontal, determine the magnitude P_{cr} of the critical load for the system.
- 10.118** The steel rod BC is attached to the rigid bar AB and to the fixed support at C . Knowing that $G = 11.2 \times 10^6$ psi, determine the diameter of rod BC for which the critical load P_{cr} of the system is 80 lb.

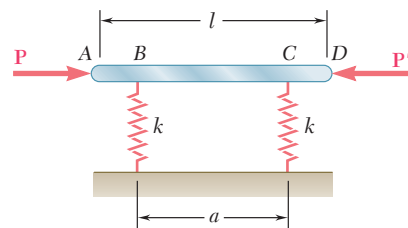


Fig. P10.117

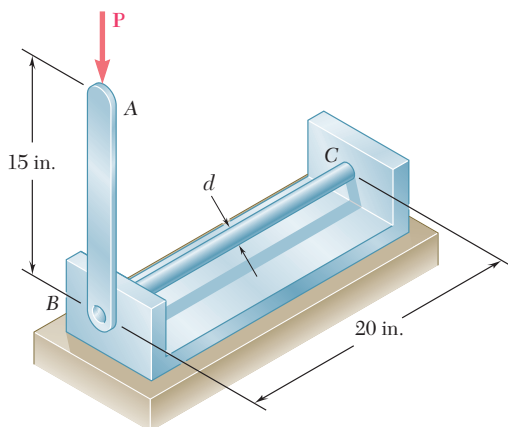
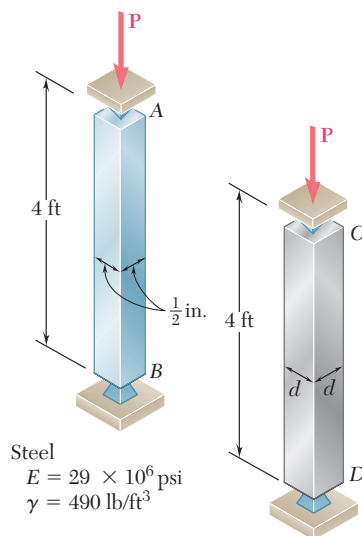


Fig. P10.118

- 10.119** Determine (a) the critical load for the steel strut, (b) the dimension d for which the aluminum strut will have the same critical load. (c) Express the weight of the aluminum strut as a percent of the weight of the steel strut.
- 10.120** Supports A and B of the pin-ended column shown are at a fixed distance L from each other. Knowing that at a temperature T_0 the force in the column is zero and that buckling occurs when the temperature is $T_1 = T_0 + \Delta T$, express ΔT in terms of b , L and the coefficient of thermal expansion α .



Steel
 $E = 29 \times 10^6$ psi
 $\gamma = 490$ lb/ft³

Aluminum
 $E = 10.1 \times 10^6$ psi
 $\gamma = 170$ lb/ft³

Fig. P10.119

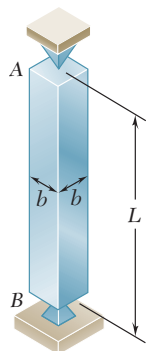


Fig. P10.120

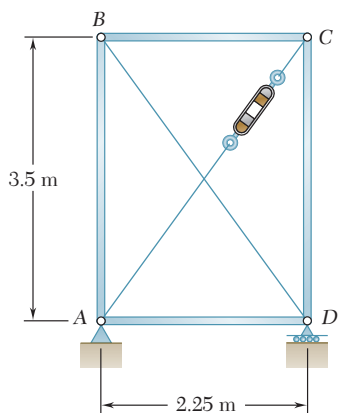


Fig. P10.121

10.121 Members AB and CD are 30-mm-diameter steel rods, and members BC and AD are 22-mm-diameter steel rods. When the turnbuckle is tightened, the diagonal member AC is put in tension. Knowing that a factor of safety with respect to buckling of 2.75 is required, determine the largest allowable tension in AC . Use $E = 200$ GPa and consider only buckling in the plane of the structure.

10.122 The uniform aluminum bar AB has a 20×36 -mm rectangular cross section and is supported by pins and brackets as shown. Each end of the bar may rotate freely about a horizontal axis through the pin, but rotation about a vertical axis is prevented by the brackets. Using $E = 70$ GPa, determine the allowable centric load P if a factor of safety of 2.5 is required.

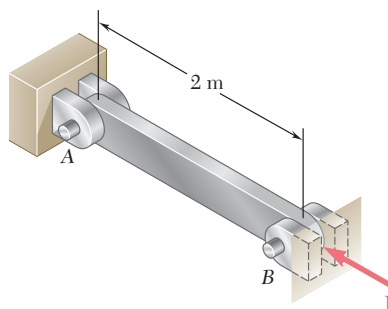


Fig. P10.122

10.123 A column with the cross section shown has a 13.5-ft effective length. Using allowable stress design, determine the largest centric load that can be applied to the column. Use $\sigma_Y = 36$ ksi and $E = 29 \times 10^6$ psi.

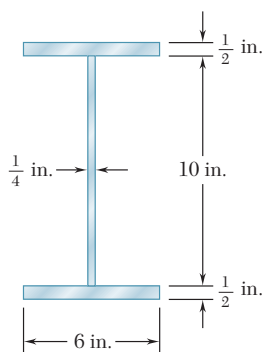


Fig. P10.123

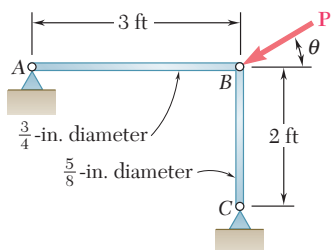


Fig. P10.124

10.124 (a) Considering only buckling in the plane of the structure shown and using Euler's formula, determine the value of θ between 0 and 90° for which the allowable magnitude of the load P is maximum. (b) Determine the corresponding maximum value of P knowing that a factor of safety of 3.2 is required. Use $E = 29 \times 10^6$ psi.

10.125 An axial load \mathbf{P} of magnitude 560 kN is applied at a point on the x axis at a distance $e = 6$ mm from the geometric axis of the $W200 \times 46.1$ rolled-steel column BC . Using $E = 200$ GPa, determine (a) the horizontal deflection of end C , (b) the maximum stress in the column.

10.126 A column of 17-ft effective length must carry a centric load of 235 kips. Using allowable stress design, select the wide-flange shape of 10-in. nominal depth that should be used. Use $\sigma_Y = 36$ ksi and $E = 29 \times 10^6$ psi.

10.127 Bar AB is free at its end A and fixed at its base B . Determine the allowable centric load \mathbf{P} if the aluminum alloy is (a) 6061-T6, (b) 2014-T6.

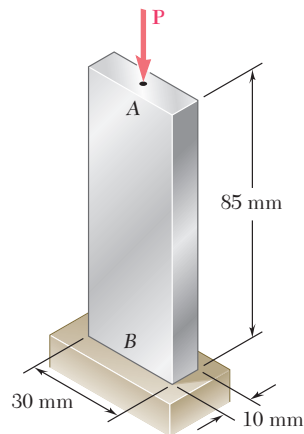


Fig. P10.127

10.128 A 43-kip axial load \mathbf{P} is applied to the rolled-steel column BC at a point on the x axis at a distance $e = 2.5$ in. from the geometric axis of the column. Using the allowable-stress method, select the wide-flange shape of 8-in. nominal depth that should be used. Use $E = 29 \times 10^6$ psi and $\sigma_Y = 36$ ksi.

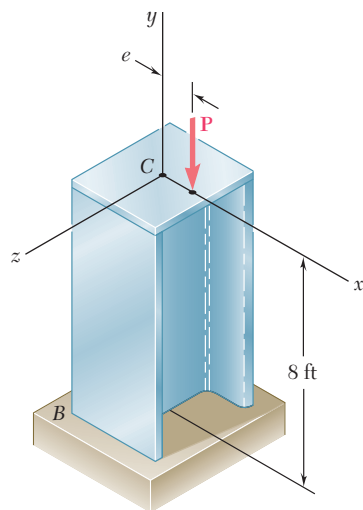


Fig. P10.128

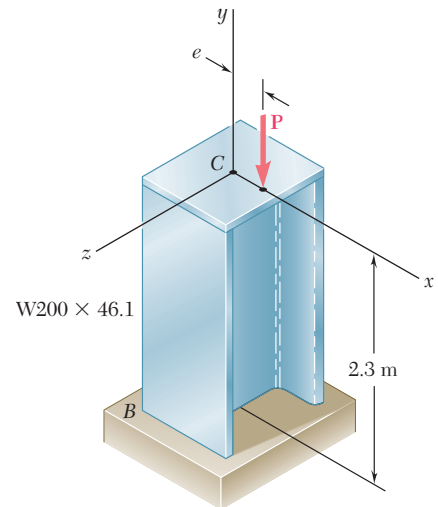


Fig. P10.125

COMPUTER PROBLEMS

The following problems are designed to be solved with a computer.

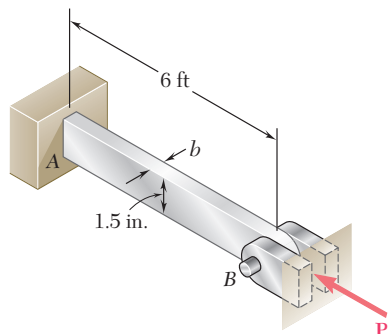


Fig. P10.C2

10.C1 A solid steel rod having an effective length of 500 mm is to be used as a compression strut to carry a centric load P . For the grade of steel used, $E = 200$ GPa and $\sigma_Y = 245$ MPa. Knowing that a factor of safety of 2.8 is required and using Euler's formula, write a computer program and use it to calculate the allowable centric load P_{all} for values of the radius of the rod from 6 mm to 24 mm, using 2-mm increments.

10.C2 An aluminum bar is fixed at end A and supported at end B so that it is free to rotate about a horizontal axis through the pin. Rotation about a vertical axis at end B is prevented by the brackets. Knowing that $E = 10.1 \times 10^6$ psi, use Euler's formula with a factor of safety of 2.5 to determine the allowable centric load P for values of b from 0.75 in. to 1.5 in., using 0.125-in. increments.

10.C3 The pin-ended members AB and BC consist of sections of aluminum pipe of 120-mm outer diameter and 10-mm wall thickness. Knowing that a factor of safety of 3.5 is required, determine the mass m of the largest block that can be supported by the cable arrangement shown for values of h from 4 m to 8 m, using 0.25-m increments. Use $E = 70$ GPa and consider only buckling in the plane of the structure.

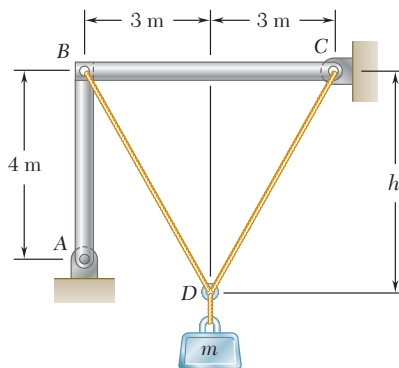


Fig. P10.C3

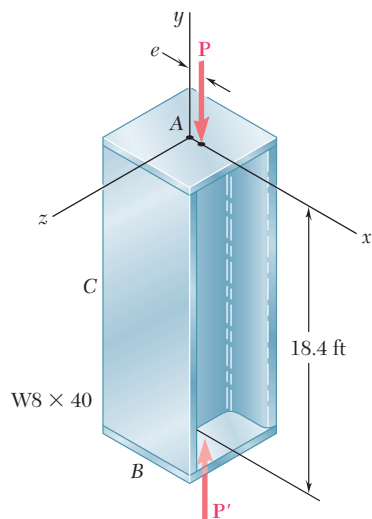


Fig. P10.C4

10.C4 An axial load P is applied at a point located on the x axis at a distance $e = 0.5$ in. from the geometric axis of the W8 \times 40 rolled-steel column AB. Using $E = 29 \times 10^6$ psi, write a computer program and use it to calculate for values of P from 25 to 75 kips, using 5-kip increments, (a) the horizontal deflection at the midpoint C, (b) the maximum stress in the column.

10.C5 A column of effective length L is made from a rolled-steel shape and carries a centric axial load \mathbf{P} . The yield strength for the grade of steel used is denoted by σ_Y , the modulus of elasticity by E , the cross-sectional area of the selected shape by A , and its smallest radius of gyration by r . Using the AISC design formulas for allowable stress design, write a computer program that can be used with either SI or U.S. customary units to determine the allowable load \mathbf{P} . Use this program to solve (a) Prob. 10.57, (b) Prob. 10.58, (c) Prob. 10.60.

10.C6 A column of effective length L is made from a rolled-steel shape and is loaded eccentrically as shown. The yield strength of the grade of steel used is denoted by σ_Y , the allowable stress in bending by σ_{all} , the modulus of elasticity by E , the cross-sectional area of the selected shape by A , and its smallest radius of gyration by r . Write a computer program that can be used with either SI or U.S. customary units to determine the allowable load \mathbf{P} , using either the allowable-stress method or the interaction method. Use this program to check the given answer for (a) Prob. 10.113, (b) Prob. 10.114.

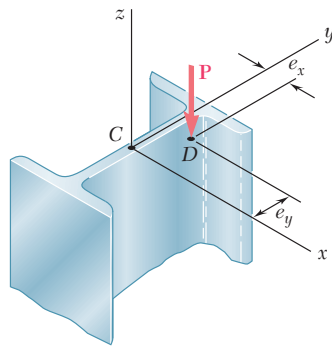


Fig. P10.C6

As the diver comes down on the diving board the potential energy due to his elevation above the board will be converted into strain energy due to the bending of the board. The normal and shearing stresses resulting from energy loadings will be determined in this chapter.



11

C H A P T E R

Energy Methods



Chapter 11 Energy Methods

- 11.1 Introduction
- 11.2 Strain Energy
- 11.3 Strain-Energy Density
- 11.4 Elastic Strain Energy for Normal Stresses
- 11.5 Elastic Strain Energy for Shearing Stresses
- 11.6 Strain Energy for a General State of Stress
- 11.7 Impact Loading
- 11.8 Design for Impact Loads
- 11.9 Work and Energy under a Single Load
- 11.10 Deflection under a Single Load By the Work-Energy Method
- *11.11 Work and Energy under Several Loads
- *11.12 Castigliano's Theorem
- *11.13 Deflections by Castigliano's Theorem
- *11.14 Statically Indeterminate Structures

11.1 INTRODUCTION

In the previous chapter we were concerned with the relations existing between forces and deformations under various loading conditions. Our analysis was based on two fundamental concepts, the concept of stress (Chap. 1) and the concept of strain (Chap. 2). A third important concept, the concept of *strain energy*, will now be introduced.

In Sec. 11.2, the *strain energy* of a member will be defined as the increase in energy associated with the deformation of the member. You will see that the strain energy is equal to the work done by a slowly increasing load applied to the member. The *strain-energy density* of a material will be defined as the strain energy per unit volume; it will be seen that it is equal to the area under the stress-strain diagram of the material (Sec. 11.3). From the stress-strain diagram of a material two additional properties will be defined, namely, the *modulus of toughness* and the *modulus of resilience* of the material.

In Sec. 11.4 the elastic strain energy associated with *normal stresses* will be discussed, first in members under axial loading and then in members in bending. Later you will consider the elastic strain energy associated with shearing stresses such as occur in torsional loadings of shafts and in transverse loadings of beams (Sec. 11.5). Strain energy for a *general state of stress* will be considered in Sec. 11.6, where the *maximum-distortion-energy criterion* for yielding will be derived.

The effect of *impact loading* on members will be considered in Sec. 11.7. You will learn to calculate both the *maximum stress* and the *maximum deflection* caused by a moving mass impacting on a member. Properties that increase the ability of a structure to withstand impact loads effectively will be discussed in Sec. 11.8.

In Sec. 11.9 the elastic strain of a member subjected to a *single concentrated load* will be calculated, and in Sec. 11.10 the deflection at the point of application of a single load will be determined.

The last portion of the chapter will be devoted to the determination of the strain energy of structures subjected to *several loads* (Sec. 11.11). *Castigliano's theorem* will be derived in Sec. 11.12 and used in Sec. 11.13 to determine the deflection at a given point of a structure subjected to several loads. In the last section Castigliano's theorem will be applied to the analysis of indeterminate structures (Sec. 11.14).

11.2 STRAIN ENERGY

Consider a rod BC of length L and uniform cross-sectional area A , which is attached at B to a fixed support, and subjected at C to a *slowly increasing* axial load P (Fig. 11.1). As we noted in Sec. 2.2, by plotting the magnitude P of the load against the deformation x of the rod, we obtain a certain load-deformation diagram (Fig. 11.2) that is characteristic of the rod BC .

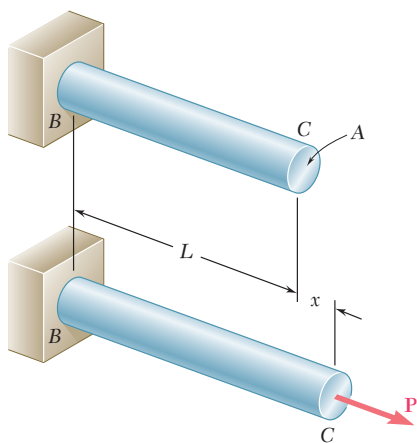


Fig. 11.1 Axially loaded rod.

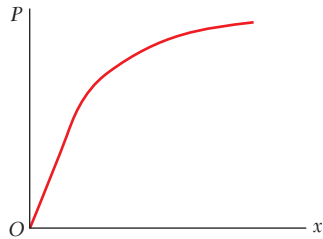


Fig. 11.2 Load-deformation diagram.

Let us now consider the work dU done by the load \mathbf{P} as the rod elongates by a small amount dx . This *elementary work* is equal to the product of the magnitude P of the load and of the small elongation dx . We write

$$dU = P \, dx \quad (11.1)$$

and note that the expression obtained is equal to the element of area of width dx located under the load-deformation diagram (Fig. 11.3). The *total work* U done by the load as the rod undergoes a deformation x_1 is thus

$$U = \int_0^{x_1} P \, dx$$

and is equal to the area under the load-deformation diagram between $x = 0$ and $x = x_1$.

The work done by the load \mathbf{P} as it is slowly applied to the rod must result in the increase of some energy associated with the deformation of the rod. This energy is referred to as the *strain energy* of the rod. We have, by definition,

$$\text{Strain energy} = U = \int_0^{x_1} P \, dx \quad (11.2)$$

We recall that work and energy should be expressed in units obtained by multiplying units of length by units of force. Thus, if SI metric units are used, work and energy are expressed in $\text{N} \cdot \text{m}$; this unit is called a *joule* (J). If U.S. customary units are used, work and energy are expressed in $\text{ft} \cdot \text{lb}$ or in $\text{in} \cdot \text{lb}$.

In the case of a linear and elastic deformation, the portion of the load-deformation diagram involved can be represented by a straight line of equation $P = kx$ (Fig. 11.4). Substituting for P in Eq. (11.2), we have

$$U = \int_0^{x_1} kx \, dx = \frac{1}{2} kx_1^2$$

or

$$U = \frac{1}{2} P_1 x_1 \quad (11.3)$$

where P_1 is the value of the load corresponding to the deformation x_1 .

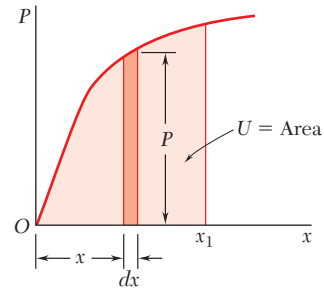


Fig. 11.3 Work due to load \mathbf{P} .

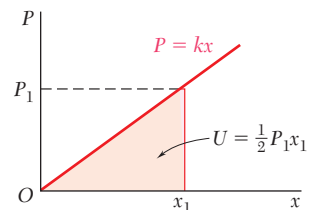


Fig. 11.4 Work due to linear, elastic deformation.

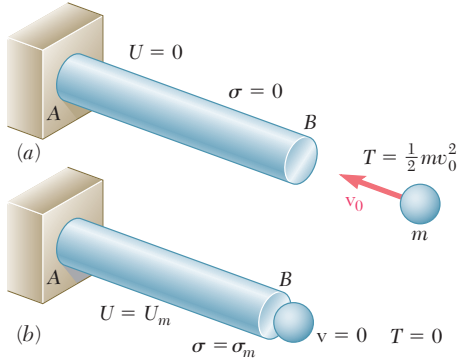


Fig. 11.5 Rod subject to impact loading.

The concept of strain energy is particularly useful in the determination of the effects of impact loadings on structures or machine components. Consider, for example, a body of mass m moving with a velocity \mathbf{v}_0 which strikes the end B of a rod AB (Fig. 11.5a). Neglecting the inertia of the elements of the rod, and assuming no dissipation of energy during the impact, we find that the maximum strain energy U_m acquired by the rod (Fig. 11.5b) is equal to the original kinetic energy $T = \frac{1}{2}mv_0^2$ of the moving body. We then determine the value P_m of the static load which would have produced the same strain energy in the rod, and obtain the value σ_m of the largest stress occurring in the rod by dividing P_m by the cross-sectional area of the rod.

11.3 STRAIN-ENERGY DENSITY

As we noted in Sec. 2.2, the load-deformation diagram for a rod BC depends upon the length L and the cross-sectional area A of the rod. The strain energy U defined by Eq. (11.2), therefore, will also depend upon the dimensions of the rod. In order to eliminate the effect of size from our discussion and direct our attention to the properties of the material, the strain energy per unit volume will be considered. Dividing the strain energy U by the volume $V = AL$ of the rod (Fig. 11.1), and using Eq. (11.2), we have

$$\frac{U}{V} = \int_0^{x_1} \frac{P}{A} \frac{dx}{L}$$

Recalling that P/A represents the normal stress σ_x in the rod, and x/L the normal strain ϵ_x , we write

$$\frac{U}{V} = \int_0^{\epsilon_1} \sigma_x d\epsilon_x$$

where ϵ_1 denotes the value of the strain corresponding to the elongation x_1 . The strain energy per unit volume, U/V , is referred to as the *strain-energy density* and will be denoted by the letter u . We have, therefore,

$$\text{Strain-energy density} = u = \int_0^{\epsilon_1} \sigma_x d\epsilon_x \quad (11.4)$$

The strain-energy density u is expressed in units obtained by dividing units of energy by units of volume. Thus, if SI metric units are used, the strain-energy density is expressed in J/m^3 or its multiples kJ/m^3 and MJ/m^3 ; if U.S. customary units are used, it is expressed in $\text{in} \cdot \text{lb/in}^3$.†

†We note that 1 J/m^3 and 1 Pa are both equal to 1 N/m^2 , while $1 \text{ in} \cdot \text{lb/in}^3$ and 1 psi are both equal to 1 lb/in^2 . Thus, strain-energy density and stress are dimensionally equal and could be expressed in the same units.

Referring to Fig. 11.6, we note that the strain-energy density u is equal to the area under the stress-strain curve, measured from $\epsilon_x = 0$ to $\epsilon_x = \epsilon_1$. If the material is unloaded, the stress returns to zero, but there is a permanent deformation represented by the strain ϵ_p , and only the portion of the strain energy per unit volume corresponding to the triangular area is recovered. The remainder of the energy spent in deforming the material is dissipated in the form of heat.

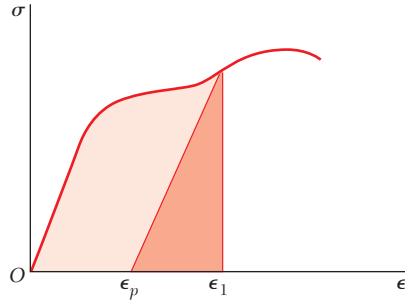


Fig. 11.6 Strain energy.

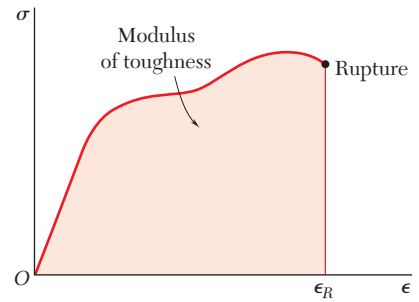


Fig. 11.7 Modulus of toughness.

The value of the strain-energy density obtained by setting $\epsilon_1 = \epsilon_R$ in Eq. (11.4), where ϵ_R is the strain at rupture, is known as the *modulus of toughness* of the material. It is equal to the area under the entire stress-strain diagram (Fig. 11.7) and represents the energy per unit volume required to cause the material to rupture. It is clear that the toughness of a material is related to its ductility as well as to its ultimate strength (Sec. 2.3), and that the capacity of a structure to withstand an impact load depends upon the toughness of the material used (Photo 11.1).

If the stress σ_x remains within the proportional limit of the material, Hooke's law applies and we write

$$\sigma_x = E\epsilon_x \quad (11.5)$$

Substituting for σ_x from (11.5) into (11.4), we have

$$u = \int_0^{\epsilon_1} E\epsilon_x d\epsilon_x = \frac{E\epsilon_1^2}{2} \quad (11.6)$$

or, using Eq. (11.5) to express ϵ_1 in terms of the corresponding stress σ_1 ,

$$u = \frac{\sigma_1^2}{2E} \quad (11.7)$$

The value u_Y of the strain-energy density obtained by setting $\sigma_1 = \sigma_Y$ in Eq. (11.7), where σ_Y is the yield strength, is called the *modulus of resilience* of the material. We have

$$u_Y = \frac{\sigma_Y^2}{2E} \quad (11.8)$$



Photo 11.1 The railroad coupler is made of a ductile steel that has a large modulus of toughness.

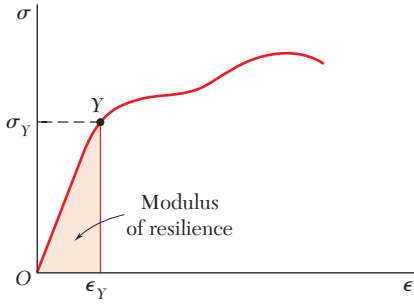


Fig. 11.8 Modulus of resilience.

The modulus of resilience is equal to the area under the straight-line portion OY of the stress-strain diagram (Fig. 11.8) and represents the energy per unit volume that the material can absorb without yielding. The capacity of a structure to withstand an impact load without being permanently deformed clearly depends upon the resilience of the material used.

Since the modulus of toughness and the modulus of resilience represent characteristic values of the strain-energy density of the material considered, they are both expressed in J/m^3 or its multiples if SI units are used, and in $\text{in} \cdot \text{lb/in}^3$ if U.S. customary units are used.†

11.4 ELASTIC STRAIN ENERGY FOR NORMAL STRESSES

Since the rod considered in the preceding section was subjected to uniformly distributed stresses σ_x , the strain-energy density was constant throughout the rod and could be defined as the ratio U/V of the strain energy U and the volume V of the rod. In a structural element or machine part with a nonuniform stress distribution, the strain-energy density u can be defined by considering the strain energy of a small element of material of volume ΔV and writing

$$u = \lim_{\Delta V \rightarrow 0} \frac{\Delta U}{\Delta V}$$

or

$$u = \frac{dU}{dV} \quad (11.9)$$

The expression obtained for u in Sec. 11.3 in terms of σ_x and ϵ_x remains valid, i.e., we still have

$$u = \int_0^{\epsilon_x} \sigma_x d\epsilon_x \quad (11.10)$$

but the stress σ_x , the strain ϵ_x , and the strain-energy density u will generally vary from point to point.

For values of σ_x within the proportional limit, we may set $\sigma_x = E\epsilon_x$ in Eq. (11.10) and write

$$u = \frac{1}{2}E\epsilon_x^2 = \frac{1}{2}\sigma_x\epsilon_x = \frac{1}{2}\frac{\sigma_x^2}{E} \quad (11.11)$$

The value of the strain energy U of a body subjected to uniaxial normal stresses can be obtained by substituting for u from Eq. (11.11) into Eq. (11.9) and integrating both members. We have

$$U = \int \frac{\sigma_x^2}{2E} dV \quad (11.12)$$

The expression obtained is valid only for elastic deformations and is referred to as the *elastic strain energy* of the body.

†However, referring to the footnote on page 696, we note that the modulus of toughness and the modulus of resilience could be expressed in the same units as stress.

Strain Energy under Axial Loading. We recall from Sec. 2.17 that, when a rod is subjected to a centric axial loading, the normal stresses σ_x can be assumed uniformly distributed in any given transverse section. Denoting by A the area of the section located at a distance x from the end B of the rod (Fig. 11.9), and by P the internal force in that section, we write $\sigma_x = P/A$. Substituting for σ_x into Eq. (11.12), we have

$$U = \int \frac{P^2}{2EA^2} dV \quad (11.13)$$

or, setting $dV = A dx$,

$$U = \int_0^L \frac{P^2}{2AE} dx \quad (11.13)$$

In the case of a rod of uniform cross section subjected at its ends to equal and opposite forces of magnitude P (Fig. 11.10), Eq. (11.13) yields

$$U = \frac{P^2 L}{2AE} \quad (11.14)$$

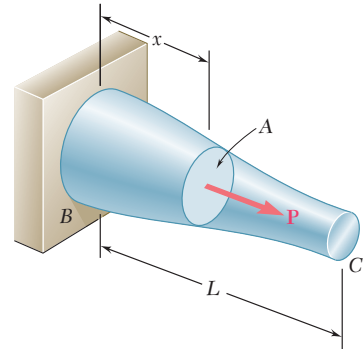


Fig. 11.9 Rod with centric axial load.

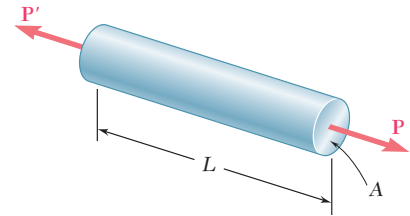


Fig. 11.10

A rod consists of two portions BC and CD of the same material and same length, but of different cross sections (Fig. 11.11). Determine the strain energy of the rod when it is subjected to a centric axial load P , expressing the result in terms of P , L , E , the cross-sectional area A of portion CD , and the ratio n of the two diameters.

We use Eq. (11.14) to compute the strain energy of each of the two portions, and add the expressions obtained:

$$U_n = \frac{P^2(\frac{1}{2}L)}{2AE} + \frac{P^2(\frac{1}{2}L)}{2(n^2A)E} = \frac{P^2L}{4AE} \left(1 + \frac{1}{n^2} \right)$$

or

$$U_n = \frac{1 + n^2}{2n^2} \frac{P^2L}{2AE} \quad (11.15)$$

We check that, for $n = 1$, we have

$$U_1 = \frac{P^2L}{2AE}$$

which is the expression given in Eq. (11.14) for a rod of length L and uniform cross section of area A . We also note that, for $n > 1$, we have $U_n < U_1$; for example, when $n = 2$, we have $U_2 = (\frac{5}{8})U_1$. Since the maximum stress occurs in portion CD of the rod and is equal to $\sigma_{\max} = P/A$, it follows that, for a given allowable stress, increasing the diameter of portion BC of the rod results in a *decrease* of the overall energy-absorbing capacity of the rod. Unnecessary changes in cross-sectional area should therefore be avoided in the design of members that may be subjected to loadings, such as impact loadings, where the energy-absorbing capacity of the member is critical.

EXAMPLE 11.01

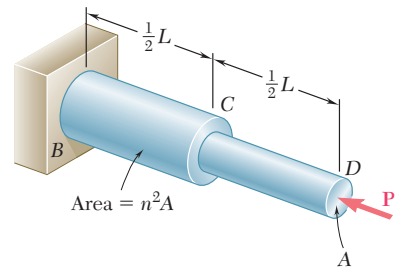


Fig. 11.11

EXAMPLE 11.02

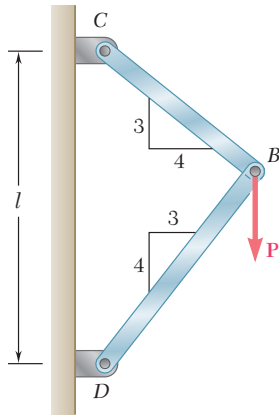


Fig. 11.12

A load P is supported at B by two rods of the same material and of the same uniform cross section of area A (Fig. 11.12). Determine the strain energy of the system.

Denoting by F_{BC} and F_{BD} , respectively, the forces in members BC and BD , and recalling Eq. (11.14), we express the strain energy of the system as

$$U = \frac{F_{BC}^2(BC)}{2AE} + \frac{F_{BD}^2(BD)}{2AE} \quad (11.16)$$

But we note from Fig. 11.12 that

$$BC = 0.6l \quad BD = 0.8l$$

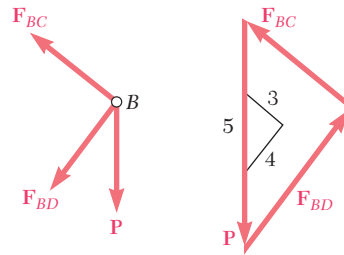


Fig. 11.13

and from the free-body diagram of pin B and the corresponding force triangle (Fig. 11.13) that

$$F_{BC} = +0.6P \quad F_{BD} = -0.8P$$

Substituting into Eq. (11.16), we have

$$U = \frac{P^2 l [(0.6)^3 + (0.8)^3]}{2AE} = 0.364 \frac{P^2 l}{AE}$$

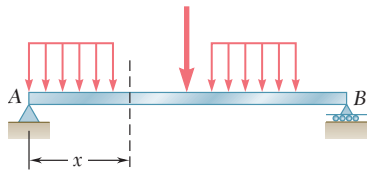


Fig. 11.14 Beam subject to transverse loads.

Strain Energy in Bending. Consider a beam AB subjected to a given loading (Fig. 11.14), and let M be the bending moment at a distance x from end A . Neglecting for the time being the effect of shear, and taking into account only the normal stresses $\sigma_x = My/I$, we substitute this expression into Eq. (11.12) and write

$$U = \int \frac{\sigma_x^2}{2E} dV = \int \frac{M^2 y^2}{2EI^2} dV$$

Setting $dV = dA dx$, where dA represents an element of the cross-sectional area, and recalling that $M^2/2EI^2$ is a function of x alone, we have

$$U = \int_0^L \frac{M^2}{2EI^2} \left(\int y^2 dA \right) dx$$

Recalling that the integral within the parentheses represents the moment of inertia I of the cross section about its neutral axis, we write

$$U = \int_0^L \frac{M^2}{2EI} dx \quad (11.17)$$

Determine the strain energy of the prismatic cantilever beam AB (Fig. 11.15), taking into account only the effect of the normal stresses.

The bending moment at a distance x from end A is $M = -Px$. Substituting this expression into Eq. (11.17), we write

$$U = \int_0^L \frac{P^2 x^2}{2EI} dx = \frac{P^2 L^3}{6EI}$$

EXAMPLE 11.03

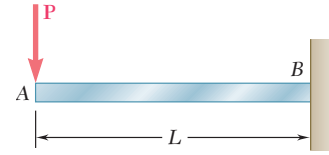


Fig. 11.15

11.5 ELASTIC STRAIN ENERGY FOR SHEARING STRESSES

When a material is subjected to plane shearing stresses τ_{xy} , the strain-energy density at a given point can be expressed as

$$u = \int_0^{\gamma_{xy}} \tau_{xy} d\gamma_{xy} \quad (11.18)$$

where γ_{xy} is the shearing strain corresponding to τ_{xy} (Fig. 11.16a). We note that the strain-energy density u is equal to the area under the shearing-stress-strain diagram (Fig. 11.16b).

For values of τ_{xy} within the proportional limit, we have $\tau_{xy} = G\gamma_{xy}$, where G is the modulus of rigidity of the material. Substituting for τ_{xy} into Eq. (11.18) and performing the integration, we write

$$u = \frac{1}{2} G \gamma_{xy}^2 = \frac{1}{2} \tau_{xy} \gamma_{xy} = \frac{\tau_{xy}^2}{2G} \quad (11.19)$$

The value of the strain energy U of a body subjected to plane shearing stresses can be obtained by recalling from Sec. 11.4 that

$$u = \frac{dU}{dV} \quad (11.9)$$

Substituting for u from Eq. (11.19) into Eq. (11.9) and integrating both members, we have

$$U = \int \frac{\tau_{xy}^2}{2G} dV \quad (11.20)$$

This expression defines the elastic strain associated with the shear deformations of the body. Like the similar expression obtained in Sec. 11.4 for uniaxial normal stresses, it is valid only for elastic deformations.

Strain Energy in Torsion. Consider a shaft BC of length L subjected to one or several twisting couples. Denoting by J the polar moment of inertia of the cross section located at a distance x from B (Fig. 11.17), and by T the internal torque in that section, we recall

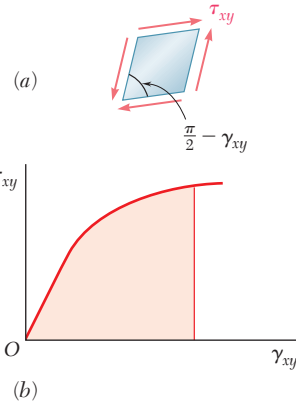


Fig. 11.16 Strain energy due to shear.

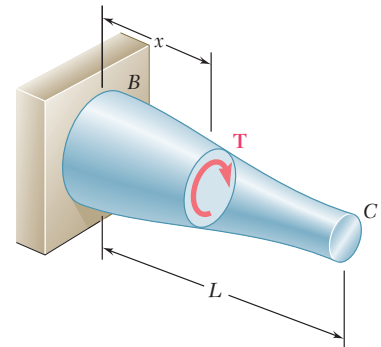


Fig. 11.17 Shaft subject to torque.

that the shearing stresses in the section are $\tau_{xy} = T\rho/J$. Substituting for τ_{xy} into Eq. (11.20), we have

$$U = \int \frac{\tau_{xy}^2}{2G} dV = \int \frac{T^2 \rho^2}{2GJ^2} dV$$

Setting $dV = dA dx$, where dA represents an element of the cross-sectional area, and observing that $T^2/2GJ^2$ is a function of x alone, we write

$$U = \int_0^L \frac{T^2}{2GJ^2} \left(\int \rho^2 dA \right) dx$$

Recalling that the integral within the parentheses represents the polar moment of inertia J of the cross section, we have

$$U = \int_0^L \frac{T^2}{2GJ} dx \quad (11.21)$$

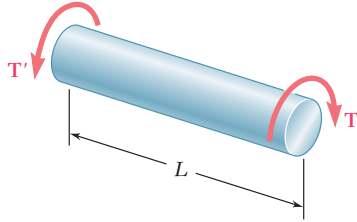


Fig. 11.18

In the case of a shaft of uniform cross section subjected at its ends to equal and opposite couples of magnitude T (Fig. 11.18), Eq. (11.21) yields

$$U = \frac{T^2 L}{2GJ} \quad (11.22)$$

EXAMPLE 11.04

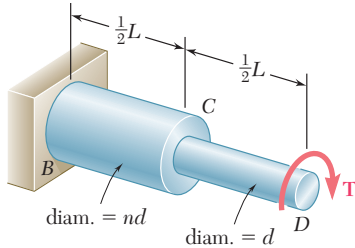


Fig. 11.19

A circular shaft consists of two portions BC and CD of the same material and same length, but of different cross sections (Fig. 11.19). Determine the strain energy of the shaft when it is subjected to a twisting couple T at end D , expressing the result in terms of T , L , G , the polar moment of inertia J of the smaller cross section, and the ratio n of the two diameters.

We use Eq. (11.22) to compute the strain energy of each of the two portions of shaft, and add the expressions obtained. Noting that the polar moment of inertia of portion BC is equal to $n^4 J$, we write

$$U_n = \frac{T^2(\frac{1}{2}L)}{2GJ} + \frac{T^2(\frac{1}{2}L)}{2G(n^4 J)} = \frac{T^2 L}{4GJ} \left(1 + \frac{1}{n^4} \right)$$

or

$$U_n = \frac{1 + n^4}{2n^4} \frac{T^2 L}{2GJ} \quad (11.23)$$

We check that, for $n = 1$, we have

$$U_1 = \frac{T^2 L}{2GJ}$$

which is the expression given in Eq. (11.22) for a shaft of length L and uniform cross section. We also note that, for $n > 1$, we have $U_n < U_1$; for example, when $n = 2$, we have $U_2 = (\frac{17}{32})U_1$. Since the maximum shearing stress occurs in the portion CD of the shaft and is proportional to the torque T , we note as we did earlier in the case of the axial loading of a rod that, for a given allowable stress, increasing the diameter of portion BC of the shaft results in a *decrease* of the overall energy-absorbing capacity of the shaft.

Strain Energy under Transverse Loading. In Sec. 11.4 we obtained an expression for the strain energy of a beam subjected to a transverse loading. However, in deriving that expression we took into account only the effect of the normal stresses due to bending and neglected the effect of the shearing stresses. In Example 11.05 both types of stresses will be taken into account.

Determine the strain energy of the rectangular cantilever beam AB (Fig. 11.20), taking into account the effect of both normal and shearing stresses.

We first recall from Example 11.03 that the strain energy due to the normal stresses σ_x is

$$U_\sigma = \frac{P^2 L^3}{6EI}$$

To determine the strain energy U_τ due to the shearing stresses τ_{xy} , we recall Eq. (6.9) of Sec. 6.4 and find that, for a beam with a rectangular cross section of width b and depth h ,

$$\tau_{xy} = \frac{3}{2} \frac{V}{A} \left(1 - \frac{y^2}{c^2} \right) = \frac{3}{2} \frac{P}{bh} \left(1 - \frac{y^2}{c^2} \right)$$

Substituting for τ_{xy} into Eq. (11.20), we write

$$U_\tau = \frac{1}{2G} \left(\frac{3}{2} \frac{P}{bh} \right)^2 \iint \left(1 - \frac{y^2}{c^2} \right)^2 dV$$

or, setting $dV = b \, dy \, dx$, and after reductions,

$$U_\tau = \frac{9P^2}{8Gbh^2} \int_{-c}^c \left(1 - 2\frac{y^2}{c^2} + \frac{y^4}{c^4} \right) dy \int_0^L dx$$

Performing the integrations, and recalling that $c = h/2$, we have

$$U_\tau = \frac{9P^2 L}{8Gbh^2} \left[y - \frac{2}{3} \frac{y^3}{c^2} + \frac{1}{5} \frac{y^5}{c^4} \right]_{-c}^+ = \frac{3P^2 L}{5Gbh} = \frac{3P^2 L}{5GA}$$

The total strain energy of the beam is thus

$$U = U_\sigma + U_\tau = \frac{P^2 L^3}{6EI} + \frac{3P^2 L}{5GA}$$

or, noting that $I/A = h^2/12$ and factoring the expression for U_σ ,

$$U = \frac{P^2 L^3}{6EI} \left(1 + \frac{3Eh^2}{10GL^2} \right) = U_\sigma \left(1 + \frac{3Eh^2}{10GL^2} \right) \quad (11.24)$$

Recalling from Sec. 2.14 that $G \geq E/3$, we conclude that the parenthesis in the expression obtained is less than $1 + 0.9(h/L)^2$ and, thus, that the relative error is less than $0.9(h/L)^2$ when the effect of shear is neglected. For a beam with a ratio h/L less than $\frac{1}{10}$, the percentage error is less than 0.9%. It is therefore customary in engineering practice to neglect the effect of shear in computing the strain energy of slender beams.

EXAMPLE 11.05

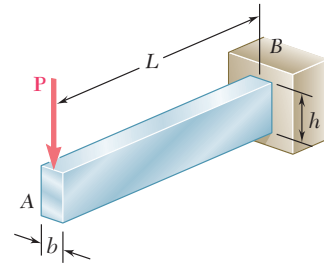


Fig. 11.20

11.6 STRAIN ENERGY FOR A GENERAL STATE OF STRESS

In the preceding sections, we determined the strain energy of a body in a state of uniaxial stress (Sec. 11.4) and in a state of plane shearing stress (Sec. 11.5). In the case of a body in a general state of stress characterized by the six stress components σ_x , σ_y , σ_z , τ_{xy} , τ_{yz} , and τ_{zx} , the strain-energy density can be obtained by adding the expressions given in Eqs. (11.10) and (11.18), as well as the four other expressions obtained through a permutation of the subscripts.

In the case of the elastic deformation of an isotropic body, each of the six stress-strain relations involved is linear, and the strain-energy density can be expressed as

$$u = \frac{1}{2}(\sigma_x \epsilon_x + \sigma_y \epsilon_y + \sigma_z \epsilon_z + \tau_{xy} \gamma_{xy} + \tau_{yz} \gamma_{yz} + \tau_{zx} \gamma_{zx}) \quad (11.25)$$

Recalling the relations (2.38) obtained in Sec. 2.14, and substituting for the strain components into (11.25), we have, for the most general state of stress at a given point of an elastic isotropic body,

$$u = \frac{1}{2E} [\sigma_x^2 + \sigma_y^2 + \sigma_z^2 - 2\nu(\sigma_x \sigma_y + \sigma_y \sigma_z + \sigma_z \sigma_x)] + \frac{1}{2G} (\tau_{xy}^2 + \tau_{yz}^2 + \tau_{zx}^2) \quad (11.26)$$

If the principal axes at the given point are used as coordinate axes, the shearing stresses become zero and Eq. (11.26) reduces to

$$u = \frac{1}{2E} [\sigma_a^2 + \sigma_b^2 + \sigma_c^2 - 2\nu(\sigma_a \sigma_b + \sigma_b \sigma_c + \sigma_c \sigma_a)] \quad (11.27)$$

where σ_a , σ_b , and σ_c are the principal stresses at the given point.

We now recall from Sec. 7.7 that one of the criteria used to predict whether a given state of stress will cause a ductile material to yield, namely, the maximum-distortion-energy criterion, is based on the determination of the energy per unit volume associated with the distortion, or change in shape, of that material. Let us, therefore, attempt to separate the strain-energy density u at a given point into two parts, a part u_v associated with a change in volume of the material at that point, and a part u_d associated with a distortion, or change in shape, of the material at the same point. We write

$$u = u_v + u_d \quad (11.28)$$

In order to determine u_v and u_d , we introduce the *average value* $\bar{\sigma}$ of the principal stresses at the point considered,

$$\bar{\sigma} = \frac{\sigma_a + \sigma_b + \sigma_c}{3} \quad (11.29)$$

and set

$$\sigma_a = \bar{\sigma} + \sigma'_a \quad \sigma_b = \bar{\sigma} + \sigma'_b \quad \sigma_c = \bar{\sigma} + \sigma'_c \quad (11.30)$$

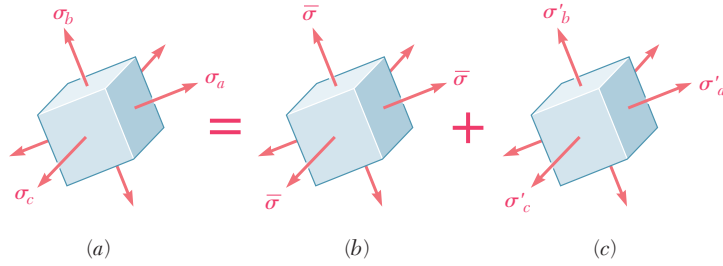


Fig. 11.21 Element subject to multiaxial stress.

Thus, the given state of stress (Fig. 11.21a) can be obtained by superposing the states of stress shown in Fig. 11.21b and c. We note that the state of stress described in Fig. 11.21b tends to change the volume of the element of material, but not its shape, since all the faces of the element are subjected to the same stress $\bar{\sigma}$. On the other hand, it follows from Eqs. (11.29) and (11.30) that

$$\sigma'_a + \sigma'_b + \sigma'_c = 0 \quad (11.31)$$

which indicates that some of the stresses shown in Fig. 11.21c are tensile and others compressive. Thus, this state of stress tends to change the shape of the element. However, it does not tend to change its volume. Indeed, recalling Eq. (2.31) of Sec. 2.13, we note that the dilatation e (i.e., the change in volume per unit volume) caused by this state of stress is

$$e = \frac{1 - 2\nu}{E} (\sigma'_a + \sigma'_b + \sigma'_c)$$

or $e = 0$, in view of Eq. (11.31). We conclude from these observations that the portion u_v of the strain-energy density must be associated with the state of stress shown in Fig. 11.21b, while the portion u_d must be associated with the state of stress shown in Fig. 11.21c.

It follows that the portion u_v of the strain-energy density corresponding to a change in volume of the element can be obtained by substituting $\bar{\sigma}$ for each of the principal stresses in Eq. (11.27). We have

$$u_v = \frac{1}{2E} [3\bar{\sigma}^2 - 2\nu(3\bar{\sigma}^2)] = \frac{3(1 - 2\nu)}{2E} \bar{\sigma}^2$$

or, recalling Eq. (11.29),

$$u_v = \frac{1 - 2\nu}{6E} (\sigma_a + \sigma_b + \sigma_c)^2 \quad (11.32)$$

The portion of the strain-energy density corresponding to the distortion of the element is obtained by solving Eq. (11.28) for u_d

and substituting for u and u_v from Eqs. (11.27) and (11.32), respectively. We write

$$u_d = u - u_v = \frac{1}{6E} [3(\sigma_a^2 + \sigma_b^2 + \sigma_c^2) - 6\nu(\sigma_a\sigma_b + \sigma_b\sigma_c + \sigma_c\sigma_a) - (1 - 2\nu)(\sigma_a + \sigma_b + \sigma_c)^2]$$

Expanding the square and rearranging terms, we have

$$u_d = \frac{1 + \nu}{6E} [(\sigma_a^2 - 2\sigma_a\sigma_b + \sigma_b^2) + (\sigma_b^2 - 2\sigma_b\sigma_c + \sigma_c^2) + (\sigma_c^2 - 2\sigma_c\sigma_a + \sigma_a^2)]$$

Noting that each of the parentheses inside the bracket is a perfect square, and recalling from Eq. (2.43) of Sec. 2.15 that the coefficient in front of the bracket is equal to $1/12G$, we obtain the following expression for the portion u_d of the strain-energy density, i.e., for the distortion energy per unit volume,

$$u_d = \frac{1}{12G} [(\sigma_a - \sigma_b)^2 + (\sigma_b - \sigma_c)^2 + (\sigma_c - \sigma_a)^2] \quad (11.33)$$

In the case of *plane stress*, and assuming that the c axis is perpendicular to the plane of stress, we have $\sigma_c = 0$ and Eq. (11.33) reduces to

$$u_d = \frac{1}{6G} (\sigma_a^2 - \sigma_a\sigma_b + \sigma_b^2) \quad (11.34)$$

Considering the particular case of a tensile-test specimen, we note that, at yield, we have $\sigma_a = \sigma_Y$, $\sigma_b = 0$, and thus $(u_d)_Y = \sigma_Y^2/6G$. The maximum-distortion-energy criterion for plane stress indicates that a given state of stress is safe as long as $u_d < (u_d)_Y$ or, substituting for u_d from Eq. (11.34), as long as

$$\sigma_a^2 - \sigma_a\sigma_b + \sigma_b^2 < \sigma_Y^2 \quad (7.26)$$

which is the condition stated in Sec. 7.7 and represented graphically by the ellipse of Fig. 7.39. In the case of a general state of stress, the expression (11.33) obtained for u_d should be used. The maximum-distortion-energy criterion is then expressed by the condition.

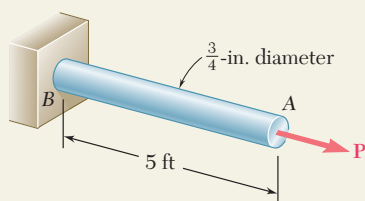
$$(\sigma_a - \sigma_b)^2 + (\sigma_b - \sigma_c)^2 + (\sigma_c - \sigma_a)^2 < 2\sigma_Y^2 \quad (11.35)$$

which indicates that a given state of stress is safe if the point of coordinates $\sigma_a, \sigma_b, \sigma_c$ is located within the surface defined by the equation

$$(\sigma_a - \sigma_b)^2 + (\sigma_b - \sigma_c)^2 + (\sigma_c - \sigma_a)^2 = 2\sigma_Y^2 \quad (11.36)$$

This surface is a circular cylinder of radius $\sqrt{2/3}\sigma_Y$ with an axis of symmetry forming equal angles with the three principal axes of stress.

SAMPLE PROBLEM 11.1



During a routine manufacturing operation, rod AB must acquire an elastic strain energy of $120 \text{ in} \cdot \text{lb}$. Using $E = 29 \times 10^6 \text{ psi}$, determine the required yield strength of the steel if the factor of safety with respect to permanent deformation is to be five.

SOLUTION

Factor of Safety. Since a factor of safety of five is required, the rod should be designed for a strain energy of

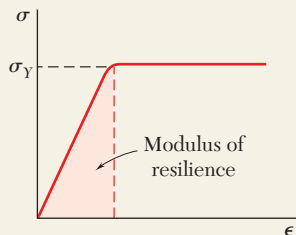
$$U = 5(120 \text{ in} \cdot \text{lb}) = 600 \text{ in} \cdot \text{lb}$$

Strain-Energy Density. The volume of the rod is

$$V = AL = \frac{\pi}{4}(0.75 \text{ in.})^2(60 \text{ in.}) = 26.5 \text{ in}^3$$

Since the rod is of uniform cross section, the required strain-energy density is

$$u = \frac{U}{V} = \frac{600 \text{ in} \cdot \text{lb}}{26.5 \text{ in}^3} = 22.6 \text{ in} \cdot \text{lb/in}^3$$

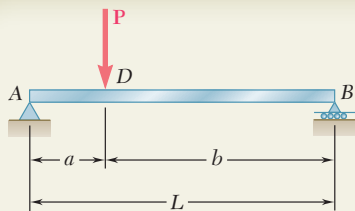


Yield Strength. We recall that the modulus of resilience is equal to the strain-energy density when the maximum stress is equal to σ_Y . Using Eq. (11.8), we write

$$u = \frac{\sigma_Y^2}{2E}$$

$$22.6 \text{ in} \cdot \text{lb/in}^3 = \frac{\sigma_Y^2}{2(29 \times 10^6 \text{ psi})} \quad \sigma_Y = 36.2 \text{ ksi} \quad \blacktriangleleft$$

Comment. It is important to note that, since energy loads are not linearly related to the stresses they produce, factors of safety associated with energy loads should be applied to the energy loads and not to the stresses.



SAMPLE PROBLEM 11.2

- (a) Taking into account only the effect of normal stresses due to bending, determine the strain energy of the prismatic beam AB for the loading shown. (b) Evaluate the strain energy, knowing that the beam is a $W10 \times 45$, $P = 40$ kips, $L = 12$ ft, $a = 3$ ft, $b = 9$ ft, and $E = 29 \times 10^6$ psi.

SOLUTION

Bending Moment. Using the free-body diagram of the entire beam, we determine the reactions

$$R_A = \frac{Pb}{L} \uparrow \quad R_B = \frac{Pa}{L} \uparrow$$

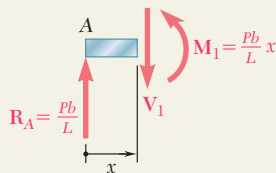
For portion AD of the beam, the bending moment is

$$M_1 = \frac{Pb}{L} x$$

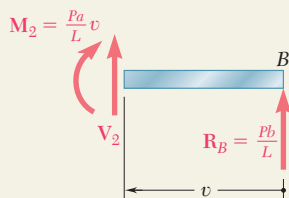
For portion DB , the bending moment at a distance v from end B is

$$M_2 = \frac{Pa}{L} v$$

From A to D :



From B to D :



a. Strain Energy. Since strain energy is a scalar quantity, we add the strain energy of portion AD to that of portion DB to obtain the total strain energy of the beam. Using Eq. (11.17), we write

$$\begin{aligned} U &= U_{AD} + U_{DB} \\ &= \int_0^a \frac{M_1^2}{2EI} dx + \int_0^b \frac{M_2^2}{2EI} dv \\ &= \frac{1}{2EI} \int_0^a \left(\frac{Pb}{L} x \right)^2 dx + \frac{1}{2EI} \int_0^b \left(\frac{Pa}{L} v \right)^2 dv \\ &= \frac{1}{2EI} \frac{P^2}{L^2} \left(\frac{b^2 a^3}{3} + \frac{a^2 b^3}{3} \right) = \frac{P^2 a^2 b^2}{6EIL^2} (a + b) \end{aligned}$$

or, since $(a + b) = L$,

$$U = \frac{P^2 a^2 b^2}{6EIL} \quad \blacktriangleleft$$

b. Evaluation of the Strain Energy. The moment of inertia of a $W10 \times 45$ rolled-steel shape is obtained from Appendix C and the given data is restated using units of kips and inches.

$$\begin{array}{ll} P = 40 \text{ kips} & L = 12 \text{ ft} = 144 \text{ in.} \\ a = 3 \text{ ft} = 36 \text{ in.} & b = 9 \text{ ft} = 108 \text{ in.} \\ E = 29 \times 10^6 \text{ psi} = 29 \times 10^3 \text{ ksi} & I = 248 \text{ in}^4 \end{array}$$

Substituting into the expression for U , we have

$$U = \frac{(40 \text{ kips})^2 (36 \text{ in.})^2 (108 \text{ in.})^2}{6(29 \times 10^3 \text{ ksi})(248 \text{ in}^4)(144 \text{ in.})} \quad U = 3.89 \text{ in} \cdot \text{kips} \quad \blacktriangleleft$$

PROBLEMS

11.1 Determine the modulus of resilience for each of the following metals:

- (a) Stainless steel
AISI 302 (annealed): $E = 190 \text{ GPa}$ $\sigma_Y = 260 \text{ MPa}$
- (b) Stainless steel 2014-T6
AISI 302 (cold-rolled): $E = 190 \text{ GPa}$ $\sigma_Y = 520 \text{ MPa}$
- (c) Malleable cast iron: $E = 165 \text{ GPa}$ $\sigma_Y = 230 \text{ MPa}$

11.2 Determine the modulus of resilience for each of the following alloys:

- (a) Titanium: $E = 16.5 \times 10^6 \text{ psi}$ $\sigma_Y = 120 \text{ ksi}$
- (b) Magnesium: $E = 6.5 \times 10^6 \text{ psi}$ $\sigma_Y = 29 \text{ ksi}$
- (c) Cupronickel (annealed) $E = 20 \times 10^6 \text{ psi}$ $\sigma_Y = 16 \text{ ksi}$

11.3 Determine the modulus of resilience for each of the following grades of structural steel:

- (a) ASTM A709 Grade 50: $\sigma_Y = 50 \text{ ksi}$
- (b) ASTM A913 Grade 65: $\sigma_Y = 65 \text{ ksi}$
- (c) ASTM A709 Grade 100: $\sigma_Y = 100 \text{ ksi}$

11.4 Determine the modulus of resilience for each of the following aluminum alloys:

- (a) 1100-H14: $E = 70 \text{ GPa}$ $\sigma_Y = 55 \text{ MPa}$
- (b) 2014-T6: $E = 72 \text{ GPa}$ $\sigma_Y = 220 \text{ MPa}$
- (c) 6061-T6: $E = 69 \text{ GPa}$ $\sigma_Y = 150 \text{ MPa}$

11.5 The stress-strain diagram shown has been drawn from data obtained during a tensile test of an aluminum alloy. Using $E = 72 \text{ GPa}$, determine (a) the modulus of resilience of the alloy, (b) the modulus of toughness of the alloy.

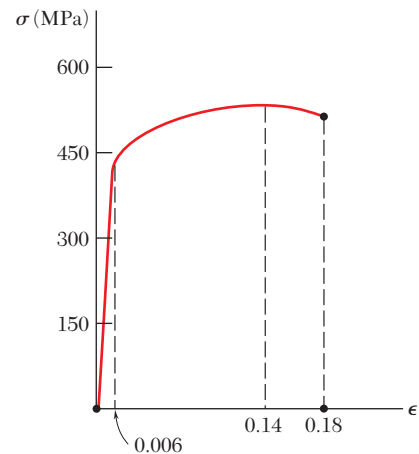


Fig. P11.5

11.6 The stress-strain diagram shown has been drawn from data obtained during a tensile test of a specimen of structural steel. Using $E = 29 \times 10^6 \text{ psi}$, determine (a) the modulus of resilience of the steel, (b) the modulus of toughness of the steel.

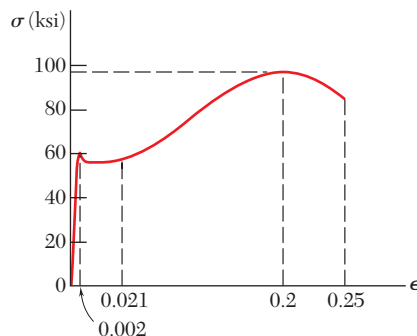


Fig. P11.6

11.7 The load-deformation diagram shown has been drawn from data obtained during a tensile test of a 0.875-in.-diameter rod of an aluminum alloy. Knowing that the deformation was measured using a 15-in. gage length, determine (a) the modulus of resilience of the alloy, (b) the modulus of toughness of the alloy.

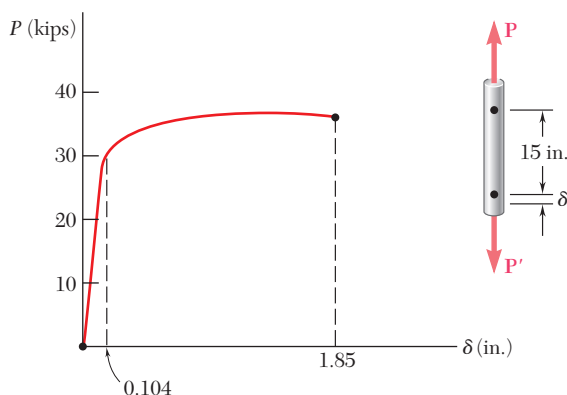


Fig. P11.7

11.8 The load-deformation diagram shown has been drawn from data obtained during a tensile test of structural steel. Knowing that the cross-sectional area of the specimen is 250 mm^2 and that the deformation was measured using a 500-mm gage length, determine (a) the modulus of resilience of the steel, (b) the modulus of toughness of the steel.

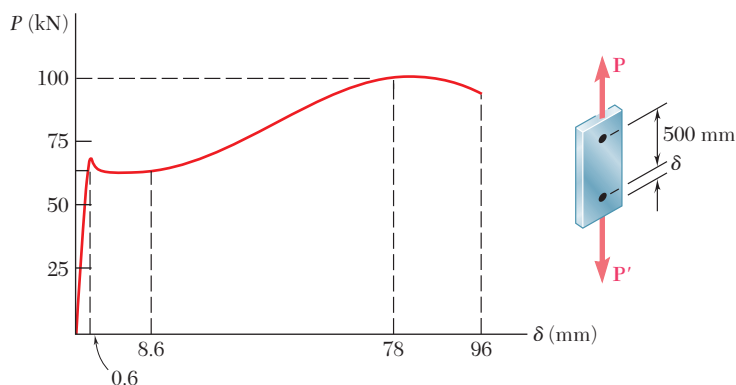


Fig. P11.8

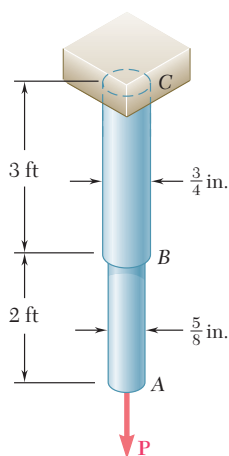


Fig. P11.9

11.9 Using $E = 29 \times 10^6 \text{ psi}$, determine (a) the strain energy of the steel rod ABC when $P = 8 \text{ kips}$, (b) the corresponding strain energy density in portions AB and BC of the rod.

11.10 Using $E = 200$ GPa, determine (a) the strain energy of the steel rod ABC when $P = 25$ kN, (b) the corresponding strain-energy density in portions AB and BC of the rod.

11.11 A 30-in. length of aluminum pipe of cross-sectional area 1.85 in² is welded to a fixed support A and to a rigid cap B. The steel rod EF, of 0.75-in. diameter, is welded to cap B. Knowing that the modulus of elasticity is 29×10^6 psi for the steel and 10.6×10^6 psi for the aluminum, determine (a) the total strain energy of the system when $P = 8$ kips, (b) the corresponding strain-energy density of the pipe CD and in the rod EF.

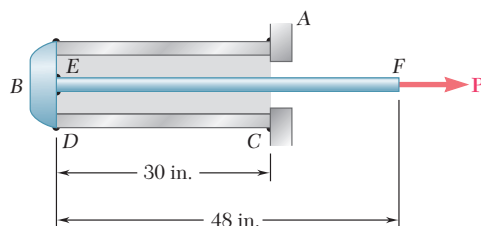


Fig. P11.11

11.12 Rod AB is made of a steel for which the yield strength is $\sigma_Y = 450$ MPa and $E = 200$ GPa; rod BC is made of an aluminum alloy for which $\sigma_Y = 280$ MPa and $E = 73$ GPa. Determine the maximum strain energy that can be acquired by the composite rod ABC without causing any permanent deformations.

11.13 A single 6-mm-diameter steel pin B is used to connect the steel strip DE to two aluminum strips, each of 20-mm width and 5-mm thickness. The modulus of elasticity is 200 GPa for the steel and 70 GPa for the aluminum. Knowing that for the pin at B the allowable shearing stress is $\tau_{\text{all}} = 85$ MPa, determine, for the loading shown, the maximum strain energy that can be acquired by the assembled strips.

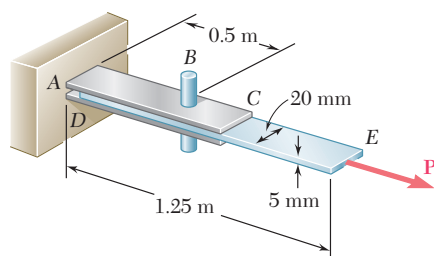


Fig. P11.13

11.14 Rod BC is made of a steel for which the yield strength is $\sigma_Y = 300$ MPa and the modulus of elasticity is $E = 200$ GPa. Knowing that a strain energy of 10 J must be acquired by the rod when the axial load P is applied, determine the diameter of the rod for which the factor of safety with respect to permanent deformation is six.

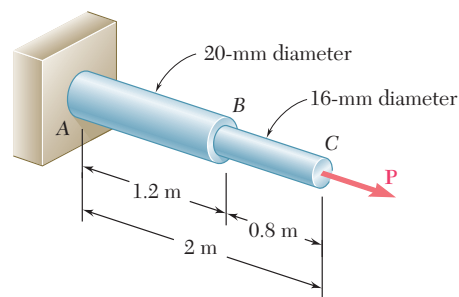


Fig. P11.10

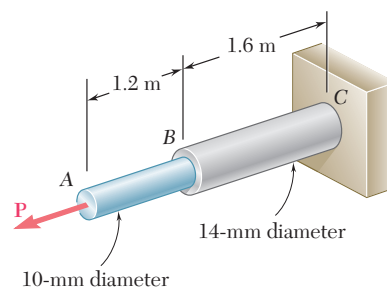


Fig. P11.12

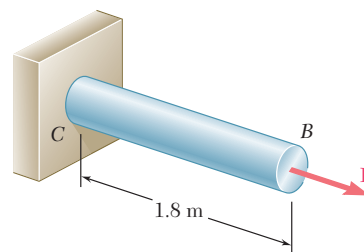


Fig. P11.14

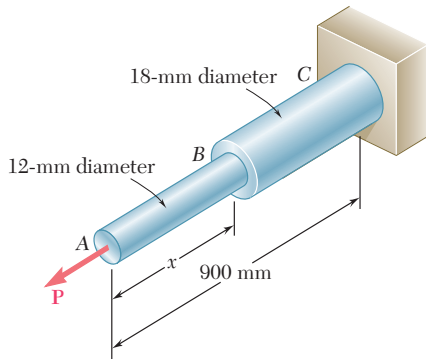


Fig. P11.15

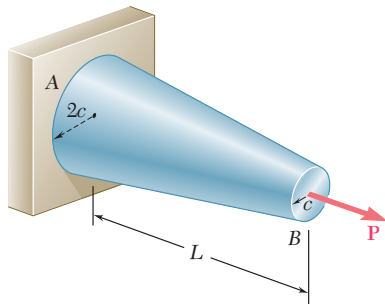


Fig. P11.17

11.15 The assembly *ABC* is made of a steel for which $E = 200 \text{ GPa}$ and $\sigma_Y = 320 \text{ MPa}$. Knowing that a strain energy of 5 J must be acquired by the assembly as the axial load \mathbf{P} is applied, determine the factor of safety with respect to permanent deformation when (a) $x = 300 \text{ mm}$, (b) $x = 600 \text{ mm}$.

11.16 Using $E = 10.6 \times 10^6 \text{ psi}$, determine by approximate means the maximum strain energy that can be acquired by the aluminum rod shown if the allowable normal stress is $\sigma_{\text{all}} = 22 \text{ ksi}$.

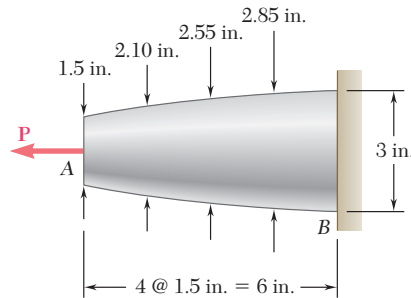


Fig. P11.16

11.17 Show by integration that the strain energy of the tapered rod *AB* is

$$U = \frac{1}{4} \frac{P^2 L}{EA_{\min}}$$

where A_{\min} is the cross-sectional area at end *B*.

11.18 through 11.21 In the truss shown, all members are made of the same material and have the uniform cross-sectional area indicated. Determine the strain energy of the truss when the load \mathbf{P} is applied.

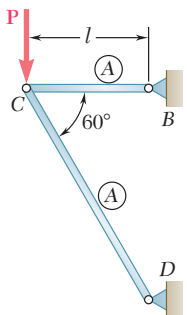


Fig. P11.18

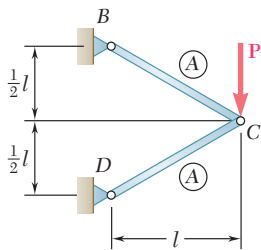


Fig. P11.19

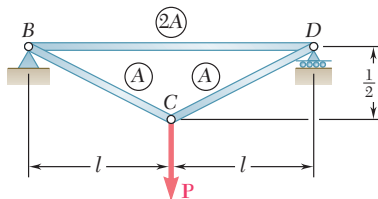


Fig. P11.20

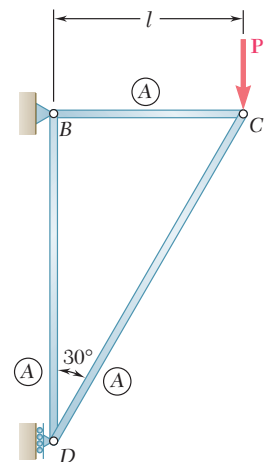


Fig. P11.21

- 11.22** Each member of the truss shown is made of steel and has the cross-sectional area shown. Using $E = 29 \times 10^6$ psi, determine the strain energy of the truss for the loading shown.

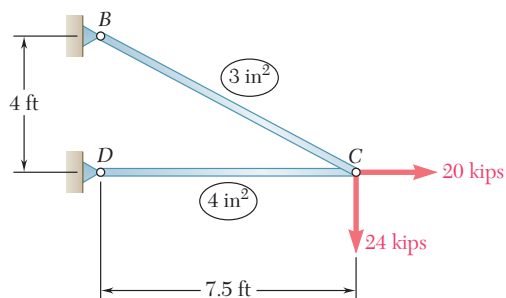


Fig. P11.22

- 11.23** Each member of the truss shown is made of aluminum and has the cross-sectional area shown. Using $E = 72$ GPa, determine the strain energy of the truss for the loading shown.

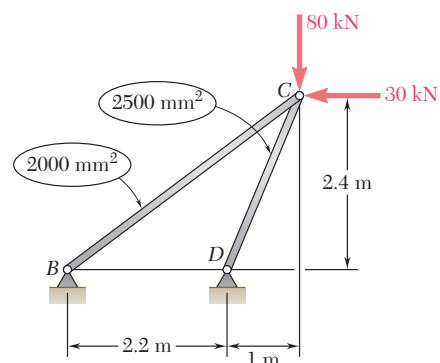


Fig. P11.23

- 11.24 through 11.27** Taking into account only the effect of normal stresses, determine the strain energy of the prismatic beam AB for the loading shown.

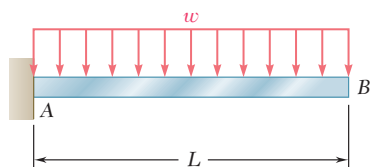


Fig. P11.24

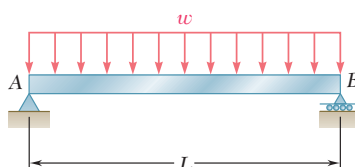


Fig. P11.25

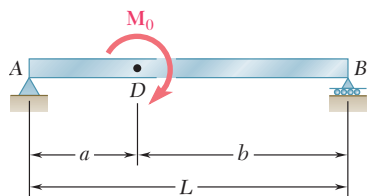


Fig. P11.26

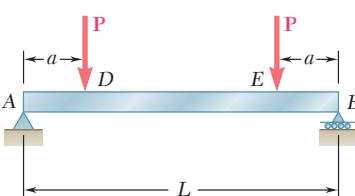


Fig. P11.27

- 11.28 and 11.29** Using $E = 200$ GPa, determine the strain energy due to bending for the steel beam and loading shown. (Ignore the effect of shearing stresses.)

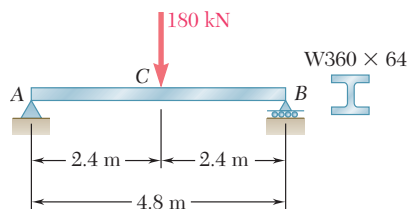


Fig. P11.28

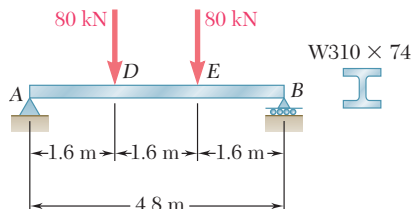


Fig. P11.29

11.30 and 11.31 Using $E = 29 \times 10^6$ psi, determine the strain energy due to bending for the steel beam and loading shown. (Ignore the effect of shearing stresses.)

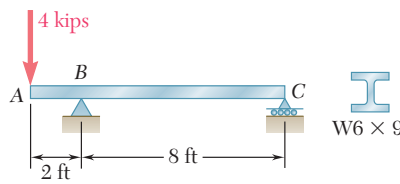


Fig. P11.30

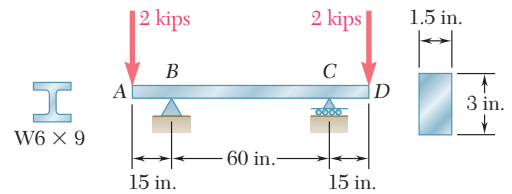


Fig. P11.31

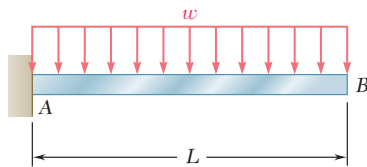


Fig. P11.32

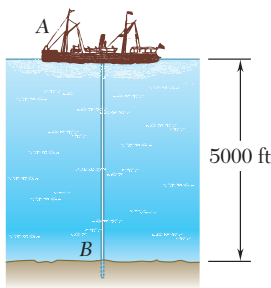


Fig. P11.33

11.32 Assuming that the prismatic beam AB has a rectangular cross section, show that for the given loading the maximum value of the strain-energy density in the beam is

$$u_{\max} = 15 \frac{U}{V}$$

where U is the strain energy of the beam and V is its volume.

11.33 The ship at A has just started to drill for oil on the ocean floor at a depth of 5000 ft. The steel drill pipe has an outer diameter of 8 in. and a uniform wall thickness of 0.5 in. Knowing that the top of the drill pipe rotates through two complete revolutions before the drill bit at B starts to operate and using $G = 11.2 \times 10^6$ psi, determine the maximum strain energy acquired by the drill pipe.

11.34 Rod AC is made of aluminum and is subjected to a torque T applied at C . Knowing that $G = 73$ GPa and that portion BC of the rod is hollow and has an inner diameter of 16 mm, determine the strain energy of the rod for a maximum shearing stress of 120 MPa.

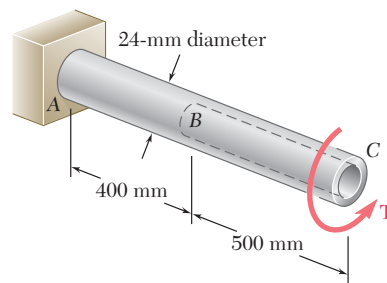


Fig. P11.34

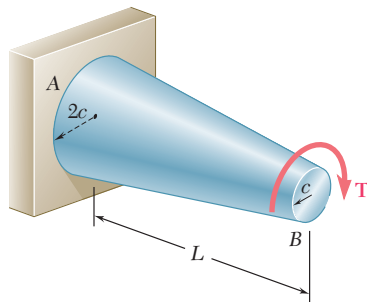


Fig. P11.35

11.35 Show by integration that the strain energy in the tapered rod AB is

$$U = \frac{7}{48} \frac{T^2 L}{G J_{\min}}$$

where J_{\min} is the polar moment of inertia of the rod at end B .

11.36 The state of stress shown occurs in a machine component made of a grade of steel for which $\sigma_Y = 65$ ksi. Using the maximum-distortion-energy criterion, determine the factor of safety associated with the yield strength when (a) $\sigma_y = +16$ ksi, (b) $\sigma_y = -16$ ksi.

11.37 The state of stress shown occurs in a machine component made of a grade of steel for which $\sigma_Y = 65$ ksi. Using the maximum-distortion-energy criterion, determine the range of values of σ_y for which the factor of safety associated with the yield strength is equal to or larger than 2.2.

11.38 The state of stress shown occurs in a machine component made of a brass for which $\sigma_Y = 160$ MPa. Using the maximum-distortion-energy criterion, determine the range of values of σ_z for which yield does not occur.

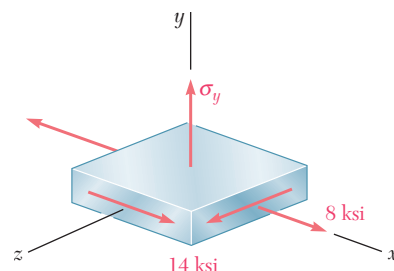


Fig. P11.36 and P11.37

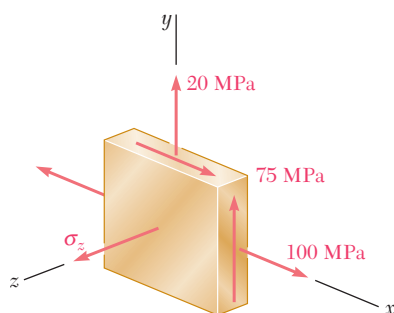


Fig. P11.38 and P11.39

11.39 The state of stress shown occurs in a machine component made of a brass for which $\sigma_Y = 160$ MPa. Using the maximum-distortion-energy criterion, determine whether yield occurs when (a) $\sigma_z = +45$ MPa, (b) $\sigma_z = -45$ MPa.

11.40 Determine the strain energy of the prismatic beam AB , taking into account the effect of both normal and shearing stresses.

***11.41** A vibration isolation support is made by bonding a rod A , of radius R_1 , and a tube B , of inner radius R_2 , to a hollow rubber cylinder. Denoting by G the modulus of rigidity of the rubber, determine the strain energy of the hollow rubber cylinder for the loading shown.

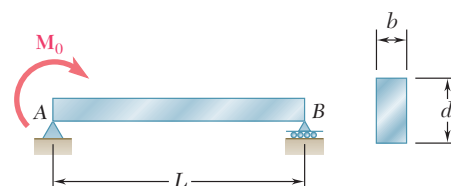


Fig. P11.40

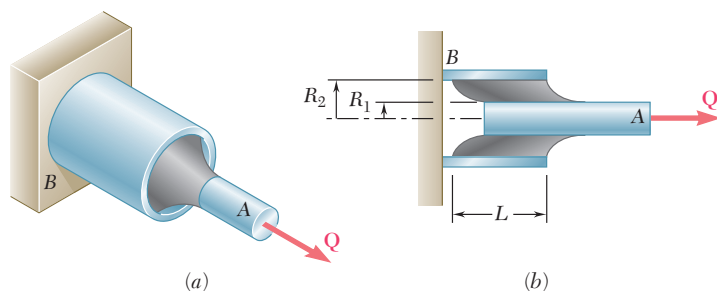


Fig. P11.41

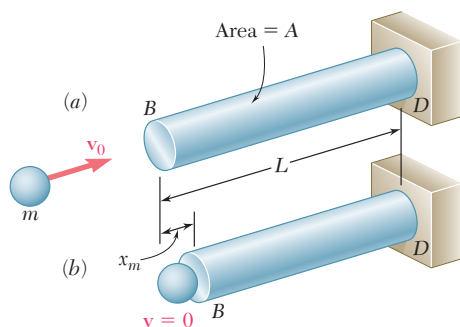


Fig. 11.22 Rod subject to impact loading.

11.7 IMPACT LOADING

Consider a rod BD of uniform cross section which is hit at its end B by a body of mass m moving with a velocity \mathbf{v}_0 (Fig. 11.22a). As the rod deforms under the impact (Fig. 11.22b), stresses develop within the rod and reach a maximum value σ_m . After vibrating for a while, the rod will come to rest, and all stresses will disappear. Such a sequence of events is referred to as an *impact loading* (Photo 11.2).

In order to determine the maximum value σ_m of the stress occurring at a given point of a structure subjected to an impact loading, we are going to make several simplifying assumptions.

First, we assume that the kinetic energy $T = \frac{1}{2}mv_0^2$ of the striking body is transferred entirely to the structure and, thus, that the strain energy U_m corresponding to the maximum deformation x_m is

$$U_m = \frac{1}{2}mv_0^2 \quad (11.37)$$

This assumption leads to the following two specific requirements:

1. No energy should be dissipated during the impact.
2. The striking body should not bounce off the structure and retain part of its energy. This, in turn, necessitates that the inertia of the structure be negligible, compared to the inertia of the striking body.

In practice, neither of these requirements is satisfied, and only part of the kinetic energy of the striking body is actually transferred to the structure. Thus, assuming that all of the kinetic energy of the striking body is transferred to the structure leads to a conservative design of that structure.

We further assume that the stress-strain diagram obtained from a static test of the material is also valid under impact loading. Thus, for an elastic deformation of the structure, we can express the maximum value of the strain energy as

$$U_m = \int \frac{\sigma_m^2}{2E} dV \quad (11.38)$$

In the case of the uniform rod of Fig. 11.22, the maximum stress σ_m has the same value throughout the rod, and we write $U_m = \sigma_m^2 V/2E$. Solving for σ_m and substituting for U_m from Eq. (11.37), we write

$$\sigma_m = \sqrt{\frac{2U_mE}{V}} = \sqrt{\frac{mv_0^2 E}{V}} \quad (11.39)$$

We note from the expression obtained that selecting a rod with a large volume V and a low modulus of elasticity E will result in a smaller value of the maximum stress σ_m for a given impact loading.

In most problems, the distribution of stresses in the structure is not uniform, and formula (11.39) does not apply. It is then convenient to determine the static load \mathbf{P}_m , which would produce the same strain energy as the impact loading, and compute from P_m the corresponding value σ_m of the largest stress occurring in the structure.



Photo 11.2 Steam alternately lifts a weight inside the pile driver and then propels it downward. This delivers a large impact load to the pile that is being driven into the ground.

A body of mass m moving with a velocity \mathbf{v}_0 hits the end B of the non-uniform rod BCD (Fig. 11.23). Knowing that the diameter of portion BC is twice the diameter of portion CD , determine the maximum value σ_m of the stress in the rod.

Making $n = 2$ in the expression (11.15) obtained in Example 11.01, we find that when rod BCD is subjected to a static load P_m , its strain energy is

$$U_m = \frac{5P_m^2 L}{16AE} \quad (11.40)$$

where A is the cross-sectional area of portion CD of the rod. Solving Eq. (11.40) for P_m , we find that the static load that produces in the rod the same strain energy as the given impact loading is

$$P_m = \sqrt{\frac{16}{5} \frac{U_m AE}{L}}$$

where U_m is given by Eq. (11.37). The largest stress occurs in portion CD of the rod. Dividing P_m by the area A of that portion, we have

$$\sigma_m = \frac{P_m}{A} = \sqrt{\frac{16}{5} \frac{U_m E}{AL}} \quad (11.41)$$

or, substituting for U_m from Eq. (11.37),

$$\sigma_m = \sqrt{\frac{8}{5} \frac{mv_0^2 E}{AL}} = 1.265 \sqrt{\frac{mv_0^2 E}{AL}}$$

Comparing this value with the value obtained for σ_m in the case of the uniform rod of Fig. 11.22 and making $V = AL$ in Eq. (11.39), we note that the maximum stress in the rod of variable cross section is 26.5% larger than in the lighter uniform rod. Thus, as we observed earlier in our discussion of Example 11.01, increasing the diameter of portion BC of the rod results in a *decrease* of the energy-absorbing capacity of the rod.

EXAMPLE 11.06

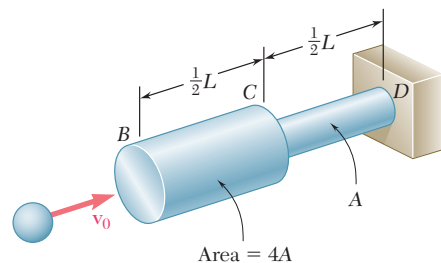


Fig. 11.23

A block of weight W is dropped from a height h onto the free end of the cantilever beam AB (Fig. 11.24). Determine the maximum value of the stress in the beam.

As it falls through the distance h , the potential energy Wh of the block is transformed into kinetic energy. As a result of the impact, the kinetic energy in turn is transformed into strain energy. We have, therefore,†

$$U_m = Wh \quad (11.42)$$

†The total distance through which the block drops is actually $h + y_m$, where y_m is the maximum deflection of the end of the beam. Thus, a more accurate expression for U_m (see Sample Prob. 11.3) is

$$U_m = W(h + y_m) \quad (11.42')$$

However, when $h \gg y_m$ we may neglect y_m and use Eq. (11.42).

EXAMPLE 11.07

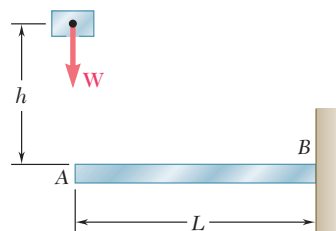


Fig. 11.24

Recalling the expression obtained for the strain energy of the cantilever beam AB in Example 11.03 and neglecting the effect of shear, we write

$$U_m = \frac{P_m^2 L^3}{6EI}$$

Solving this equation for P_m , we find that the static force that produces in the beam the same strain energy is

$$P_m = \sqrt{\frac{6U_m EI}{L^3}} \quad (11.43)$$

The maximum stress σ_m occurs at the fixed end B and is

$$\sigma_m = \frac{|M|c}{I} = \frac{P_m L c}{I}$$

Substituting for P_m from (11.43), we write

$$\sigma_m = \sqrt{\frac{6U_m E}{L(I/c^2)}} \quad (11.44)$$

or, recalling (11.42),

$$\sigma_m = \sqrt{\frac{6WhE}{L(I/c^2)}}$$

11.8 DESIGN FOR IMPACT LOADS

Let us now compare the values obtained in the preceding section for the maximum stress σ_m (a) in the rod of uniform cross section of Fig. 11.22, (b) in the rod of variable cross section of Example 11.06, and (c) in the cantilever beam of Example 11.07, assuming that the last has a circular cross section of radius c .

(a) We first recall from Eq. (11.39) that, if U_m denotes the amount of energy transferred to the rod as a result of the impact loading, the maximum stress in the rod of uniform cross section is

$$\sigma_m = \sqrt{\frac{2U_m E}{V}} \quad (11.45a)$$

where V is the volume of the rod.

(b) Considering next the rod of Example 11.06 and observing that the volume of the rod is

$$V = 4A(L/2) + A(L/2) = 5AL/2$$

we substitute $AL = 2V/5$ into Eq. (11.41) and write

$$\sigma_m = \sqrt{\frac{8U_m E}{V}} \quad (11.45b)$$

(c) Finally, recalling that $I = \frac{1}{4}\pi c^4$ for a beam of circular cross section, we note that

$$L(I/c^2) = L(\frac{1}{4}\pi c^4/c^2) = \frac{1}{4}(\pi c^2 L) = \frac{1}{4}V$$

where V denotes the volume of the beam. Substituting into Eq. (11.44), we express the maximum stress in the cantilever beam of Example 11.07 as

$$\sigma_m = \sqrt{\frac{24U_mE}{V}} \quad (11.45c)$$

We note that, in each case, the maximum stress σ_m is proportional to the square root of the modulus of elasticity of the material and inversely proportional to the square root of the volume of the member. Assuming all three members to have the same volume and to be of the same material, we also note that, for a given value of the absorbed energy, the uniform rod will experience the lowest maximum stress, and the cantilever beam the highest one.

This observation can be explained by the fact that, the distribution of stresses being uniform in case *a*, the strain energy will be uniformly distributed throughout the rod. In case *b*, on the other hand, the stresses in portion *BC* of the rod are only 25% as large as the stresses in portion *CD*. This uneven distribution of the stresses and of the strain energy results in a maximum stress σ_m twice as large as the corresponding stress in the uniform rod. Finally, in case *c*, where the cantilever beam is subjected to a transverse impact loading, the stresses vary linearly along the beam as well as across a transverse section. The very uneven resulting distribution of strain energy causes the maximum stress σ_m to be 3.46 times larger than if the same member had been loaded axially as in case *a*.

The properties noted in the three specific cases discussed in this section are quite general and can be observed in all types of structures and impact loadings. We thus conclude that a structure designed to withstand effectively an impact load should

1. Have a large volume
2. Be made of a material with a low modulus of elasticity and a high yield strength
3. Be shaped so that the stresses are distributed as evenly as possible throughout the structure

11.9 WORK AND ENERGY UNDER A SINGLE LOAD

When we first introduced the concept of strain energy at the beginning of this chapter, we considered the work done by an axial load \mathbf{P} applied to the end of a rod of uniform cross section (Fig. 11.1). We defined the strain energy of the rod for an elongation x_1 as the work of the load \mathbf{P} as it is slowly increased from 0 to the value P_1 corresponding to x_1 . We wrote

$$\text{Strain energy} = U = \int_0^{x_1} P \, dx \quad (11.2)$$

In the case of an elastic deformation, the work of the load \mathbf{P} , and thus the strain energy of the rod, were expressed as

$$U = \frac{1}{2}P_1x_1 \quad (11.3)$$

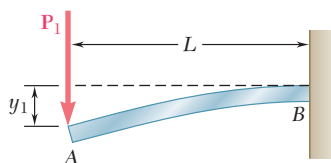


Fig. 11.25 Cantilever beam with load P_1 .

Later, in Secs. 11.4 and 11.5, we computed the strain energy of structural members under various loading conditions by determining the strain-energy density u at every point of the member and integrating u over the entire member.

However, when a structure or member is subjected to a *single concentrated load*, it is possible to use Eq. (11.3) to evaluate its elastic strain energy, provided, of course, that the relation between the load and the resulting deformation is known. For instance, in the case of the cantilever beam of Example 11.03 (Fig. 11.25), we write

$$U = \frac{1}{2} P_1 y_1$$

and, substituting for y_1 the value obtained from the table of *Beam Deflections and Slopes* of Appendix D,

$$U = \frac{1}{2} P_1 \left(\frac{P_1 L^3}{3EI} \right) = \frac{P_1^2 L^3}{6EI} \quad (11.46)$$

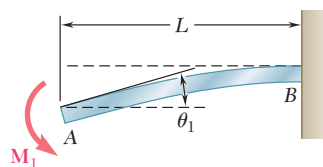


Fig. 11.26 Cantilever beam with couple M_1 .

A similar approach can be used to determine the strain energy of a structure or member subjected to a *single couple*. Recalling that the elementary work of a couple of moment M is $M d\theta$, where $d\theta$ is a small angle, we find, since M and θ are linearly related, that the elastic strain energy of a cantilever beam AB subjected to a single couple M_1 at its end A (Fig. 11.26) can be expressed as

$$U = \int_0^{\theta_1} M d\theta = \frac{1}{2} M_1 \theta_1 \quad (11.47)$$

where θ_1 is the slope of the beam at A . Substituting for θ_1 the value obtained from Appendix D, we write

$$U = \frac{1}{2} M_1 \left(\frac{M_1 L}{EI} \right) = \frac{M_1^2 L}{2EI} \quad (11.48)$$

In a similar way, the elastic strain energy of a uniform circular shaft AB of length L subjected at its end B to a single torque T_1 (Fig. 11.27) can be expressed as

$$U = \int_0^{\phi_1} T d\phi = \frac{1}{2} T_1 \phi_1 \quad (11.49)$$

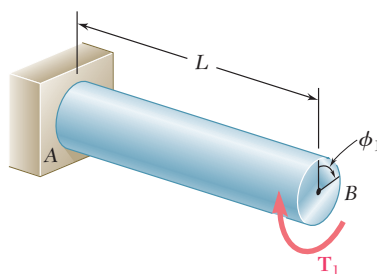


Fig. 11.27 Shaft with Torque T_1 .

Substituting for the angle of twist ϕ_1 from Eq. (3.16), we verify that

$$U = \frac{1}{2} T_1 \left(\frac{T_1 L}{JG} \right) = \frac{T_1^2 L}{2JG}$$

as previously obtained in Sec. 11.5.

The method presented in this section may simplify the solution of many impact-loading problems. In Example 11.08, the crash of an automobile into a barrier (Photo 11.3) is considered by using a simplified model consisting of a block and a simple beam.



Photo 11.3 As the automobile crashed into the barrier, considerable energy was dissipated as heat during the permanent deformation of the automobile and the barrier. *Source:* Crash test photo courtesy of Sec-Envel and L.I.E.R., France.

A block of mass m moving with a velocity \mathbf{v}_0 hits squarely the prismatic member AB at its midpoint C (Fig. 11.28). Determine (a) the equivalent static load P_m , (b) the maximum stress σ_m in the member, and (c) the maximum deflection x_m at point C .

(a) Equivalent Static Load. The maximum strain energy of the member is equal to the kinetic energy of the block before impact. We have

$$U_m = \frac{1}{2} m v_0^2 \quad (11.50)$$

On the other hand, expressing U_m as the work of the equivalent horizontal static load as it is slowly applied at the midpoint C of the member, we write

$$U_m = \frac{1}{2} P_m x_m \quad (11.51)$$

where x_m is the deflection of C corresponding to the static load P_m . From the table of *Beam Deflections and Slopes* of Appendix D, we find that

$$x_m = \frac{P_m L^3}{48EI} \quad (11.52)$$

EXAMPLE 11.08

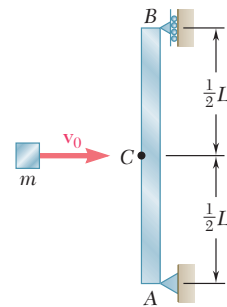


Fig. 11.28

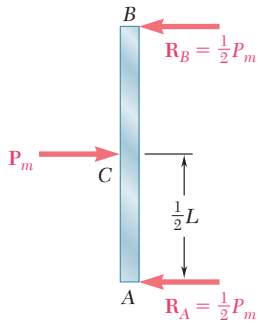


Fig. 11.29

Substituting for x_m from (11.52) into (11.51), we write

$$U_m = \frac{1}{2} \frac{P_m^2 L^3}{48EI}$$

Solving for P_m and recalling Eq. (11.50), we find that the static load equivalent to the given impact loading is

$$P_m = \sqrt{\frac{96U_m EI}{L^3}} = \sqrt{\frac{48mv_0^2 EI}{L^3}} \quad (11.53)$$

(b) Maximum Stress. Drawing the free-body diagram of the member (Fig. 11.29), we find that the maximum value of the bending moment occurs at C and is $M_{\max} = P_m L/4$. The maximum stress, therefore, occurs in a transverse section through C and is equal to

$$\sigma_m = \frac{M_{\max} c}{I} = \frac{P_m L c}{4I}$$

Substituting for P_m from (11.53), we write

$$\sigma_m = \sqrt{\frac{3mv_0^2 EI}{L(I/c)^2}}$$

(c) Maximum Deflection. Substituting into Eq. (11.52) the expression obtained for P_m in (11.53), we have

$$x_m = \frac{L^3}{48EI} \sqrt{\frac{48mv_0^2 EI}{L^3}} = \sqrt{\frac{mv_0^2 L^3}{48EI}}$$

11.10 DEFLECTION UNDER A SINGLE LOAD BY THE WORK-ENERGY METHOD

We saw in the preceding section that, if the deflection x_1 of a structure or member under a single concentrated load \mathbf{P}_1 is known, the corresponding strain energy U is obtained by writing

$$U = \frac{1}{2} P_1 x_1 \quad (11.3)$$

A similar expression for the strain energy of a structural member under a single couple \mathbf{M}_1 is:

$$U = \frac{1}{2} M_1 \theta_1 \quad (11.47)$$

Conversely, if the strain energy U of a structure or member subjected to a single concentrated load \mathbf{P}_1 or couple \mathbf{M}_1 is known, Eq. (11.3) or (11.47) can be used to determine the corresponding deflection x_1 or angle θ_1 . In order to determine the deflection under a single load applied to a structure consisting of several component parts, it is easier, rather than use one of the methods of Chap. 9, to first compute the strain energy of the structure by integrating the strain-energy density over its various parts, as was done in Secs. 11.4 and 11.5, and then use either Eq. (11.3) or Eq. (11.47) to obtain the desired deflection. Similarly, the angle of twist ϕ_1 of a composite shaft can be obtained by integrating the

strain-energy density over the various parts of the shaft and solving Eq. (11.49) for ϕ_1 .

It should be kept in mind that the method presented in this section can be used *only if the given structure is subjected to a single concentrated load or couple*. The strain energy of a structure subjected to several loads *cannot* be determined by computing the work of each load as if it were applied independently to the structure (see Sec. 11.11). We can also observe that, even if it were possible to compute the strain energy of the structure in this manner, only one equation would be available to determine the deflections corresponding to the various loads. In Secs. 11.12 and 11.13, another method based on the concept of strain energy is presented, one that can be used to determine the deflection or slope at a given point of a structure, even when that structure is subjected simultaneously to several concentrated loads, distributed loads, or couples.

A load \mathbf{P} is supported at B by two uniform rods of the same cross-sectional area A (Fig. 11.30). Determine the vertical deflection of point B .

The strain energy of the system under the given load was determined in Example 11.02. Equating the expression obtained for U to the work of the load, we write

$$U = 0.364 \frac{P^2 l}{AE} = \frac{1}{2} P y_B$$

and, solving for the vertical deflection of B ,

$$y_B = 0.728 \frac{Pl}{AE}$$

Remark. We should note that, once the forces in the two rods have been obtained (see Example 11.02), the deformations $\delta_{B/C}$ and $\delta_{B/D}$ of the rods could be obtained by the method of Chap. 2. Determining the vertical deflection of point B from these deformations, however, would require a careful geometric analysis of the various displacements involved. The strain-energy method used here makes such an analysis unnecessary.

EXAMPLE 11.09

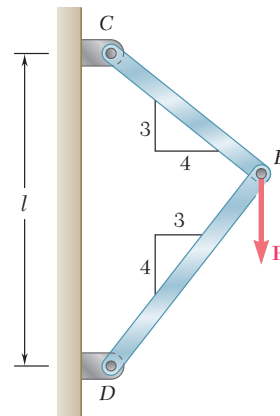


Fig. 11.30

Determine the deflection of end A of the cantilever beam AB (Fig. 11.31), taking into account the effect of (a) the normal stresses only, (b) both the normal and shearing stresses.

(a) Effect of Normal Stresses. The work of the force \mathbf{P} as it is slowly applied to A is

$$U = \frac{1}{2} P y_A$$

Substituting for U the expression obtained for the strain energy of the beam in Example 11.03, where only the effect of the normal stresses was considered, we write

$$\frac{P^2 L^3}{6EI} = \frac{1}{2} P y_A$$

EXAMPLE 11.10

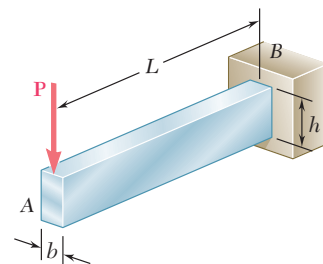


Fig. 11.31

and, solving for y_A ,

$$y_A = \frac{PL^3}{3EI}$$

(b) Effect of Normal and Shearing Stresses. We now substitute for U the expression (11.24) obtained in Example 11.05, where the effects of both the normal and shearing stresses were taken into account. We have

$$\frac{P^2 L^3}{6EI} \left(1 + \frac{3Eh^2}{10GL^2} \right) = \frac{1}{2} P y_A$$

and, solving for y_A ,

$$y_A = \frac{PL^3}{3EI} \left(1 + \frac{3Eh^2}{10GL^2} \right)$$

We note that the relative error when the effect of shear is neglected is the same that was obtained in Example 11.05, i.e., less than $0.9(h/L)^2$. As we indicated then, this is less than 0.9% for a beam with a ratio h/L less than $\frac{1}{10}$.

EXAMPLE 11.11

A torque \mathbf{T} is applied at the end D of shaft BCD (Fig. 11.32). Knowing that both portions of the shaft are of the same material and same length, but that the diameter of BC is twice the diameter of CD , determine the angle of twist for the entire shaft.

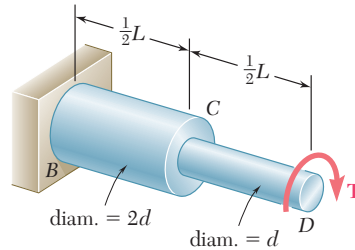


Fig. 11.32

The strain energy of a similar shaft was determined in Example 11.04 by breaking the shaft into its component parts BC and CD . Making $n = 2$ in Eq. (11.23), we have

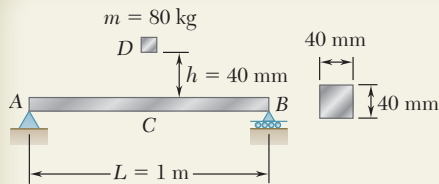
$$U = \frac{17}{32} \frac{T^2 L}{2GJ}$$

where G is the modulus of rigidity of the material and J the polar moment of inertia of portion CD of the shaft. Setting U equal to the work of the torque as it is slowly applied to end D , and recalling Eq. (11.49), we write

$$\frac{17}{32} \frac{T^2 L}{2GJ} = \frac{1}{2} T \phi_{D/B}$$

and, solving for the angle of twist $\phi_{D/B}$,

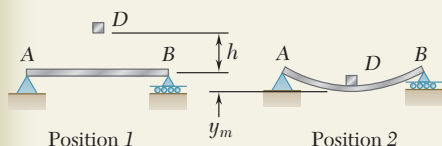
$$\phi_{D/B} = \frac{17TL}{32GJ}$$



SAMPLE PROBLEM 11.3

The block D of mass m is released from rest and falls a distance h before it strikes the midpoint C of the aluminum beam AB . Using $E = 73$ GPa, determine (a) the maximum deflection of point C , (b) the maximum stress that occurs in the beam.

SOLUTION



Principle of Work and Energy. Since the block is released from rest, we note that in position 1 both the kinetic energy and the strain energy are zero. In position 2, where the maximum deflection y_m occurs, the kinetic energy is again zero. Referring to the table of *Beam Deflections and Slopes* of Appendix D, we find the expression for y_m shown. The strain energy of the beam in position 2 is

$$U_2 = \frac{1}{2} P_m y_m = \frac{1}{2} \frac{48EI}{L^3} y_m^2 \quad U_2 = \frac{24EI}{L^3} y_m^2$$

We observe that the work done by the weight \mathbf{W} of the block is $W(h + y_m)$. Equating the strain energy of the beam to the work done by \mathbf{W} , we have

$$\frac{24EI}{L^3} y_m^2 = W(h + y_m) \quad (1)$$

From Appendix D

$$y_m = \frac{P_m L^3}{48EI} \quad P_m = \frac{48EI}{L^3} y_m$$

a. Maximum Deflection of Point C. From the given data we have

$$EI = (73 \times 10^9 \text{ Pa}) \frac{1}{12} (0.04 \text{ m})^4 = 15.573 \times 10^3 \text{ N} \cdot \text{m}^2$$

$$L = 1 \text{ m} \quad h = 0.040 \text{ m} \quad W = mg = (80 \text{ kg})(9.81 \text{ m/s}^2) = 784.8 \text{ N}$$

Substituting into Eq. (1), we obtain and solve the quadratic equation

$$(373.8 \times 10^3) y_m^2 - 784.8 y_m - 31.39 = 0 \quad y_m = 10.27 \text{ mm} \quad \blacktriangleleft$$

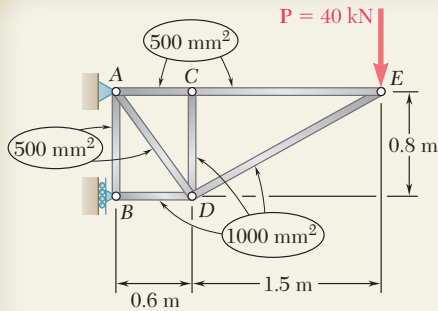
b. Maximum Stress. The value of P_m is

$$P_m = \frac{48EI}{L^3} y_m = \frac{48(15.573 \times 10^3 \text{ N} \cdot \text{m})}{(1 \text{ m})^3} (0.01027 \text{ m}) \quad P_m = 7677 \text{ N}$$

Recalling that $\sigma_m = M_{\max} c / I$ and $M_{\max} = \frac{1}{4} P_m L$, we write

$$\sigma_m = \frac{(\frac{1}{4} P_m L) c}{I} = \frac{\frac{1}{4} (7677 \text{ N}) (1 \text{ m}) (0.020 \text{ m})}{\frac{1}{12} (0.040 \text{ m})^4} \quad \sigma_m = 179.9 \text{ MPa} \quad \blacktriangleleft$$

An approximation for the work done by the weight of the block can be obtained by omitting y_m from the expression for the work and from the right-hand member of Eq. (1), as was done in Example 11.07. If this approximation is used here, we find $y_m = 9.16$ mm; the error is 10.8%. However, if an 8-kg block is dropped from a height of 400 mm, producing the same value of Wh , omitting y_m from the right-hand member of Eq. (1) results in an error of only 1.2%. A further discussion of this approximation is given in Prob. 11.70.

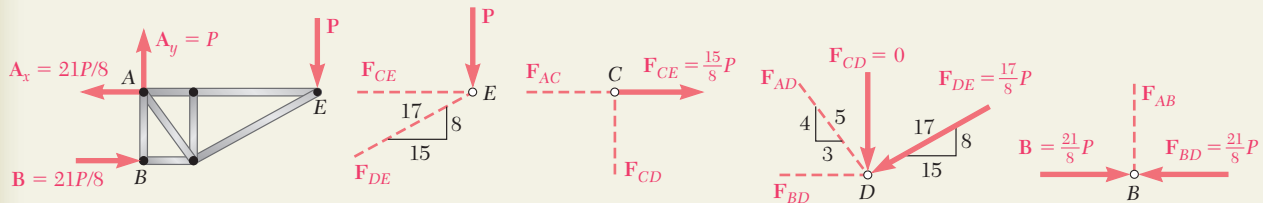


SAMPLE PROBLEM 11.4

Members of the truss shown consist of sections of aluminum pipe with the cross-sectional areas indicated. Using $E = 73 \text{ GPa}$, determine the vertical deflection of point E caused by the load \mathbf{P} .

SOLUTION

Axial Forces in Truss Members. The reactions are found by using the free-body diagram of the entire truss. We then consider in sequence the equilibrium of joints, E , C , D , and B . At each joint we determine the forces indicated by dashed lines. At joint B , the equation $\Sigma F_x = 0$ provides a check of our computations.



$$\begin{array}{llll} \Sigma F_y = 0: F_{DE} = -\frac{17}{8}P & \Sigma F_x = 0: F_{AC} = +\frac{15}{8}P & \Sigma F_y = 0: F_{AD} = +\frac{5}{4}P & \Sigma F_y = 0: F_{AB} = 0 \\ \Sigma F_x = 0: F_{CE} = +\frac{15}{8}P & \Sigma F_y = 0: F_{CD} = 0 & \Sigma F_x = 0: F_{BD} = -\frac{21}{8}P & \Sigma F_x = 0: (\text{Checks}) \end{array}$$

Strain Energy. Noting that E is the same for all members, we express the strain energy of the truss as follows

$$U = \sum \frac{F_i^2 L_i}{2A_i E} = \frac{1}{2E} \sum \frac{F_i^2 L_i}{A_i} \quad (1)$$

Member	F_i	$L_i, \text{ m}$	$A_i, \text{ m}^2$	$\frac{F_i^2 L_i}{A_i}$
AB	0	0.8	500×10^{-6}	0
AC	$+15P/8$	0.6	500×10^{-6}	$4\,219P^2$
AD	$+5P/4$	1.0	500×10^{-6}	$3\,125P^2$
BD	$-21P/8$	0.6	1000×10^{-6}	$4\,134P^2$
CD	0	0.8	1000×10^{-6}	0
CE	$+15P/8$	1.5	500×10^{-6}	$10\,547P^2$
DE	$-17P/8$	1.7	1000×10^{-6}	$7\,677P^2$

where F_i is the force in a given member as indicated in the following table and where the summation is extended over all members of the truss.

$$\sum \frac{F_i^2 L_i}{A_i} = 29\,700P^2$$

Returning to Eq. (1), we have

$$U = (1/2E)(29.7 \times 10^3 P^2).$$

Principle of Work-Energy. We recall that the work done by the load \mathbf{P} as it is gradually applied is $\frac{1}{2}Py_E$. Equating the work done by \mathbf{P} to the strain energy U and recalling that $E = 73 \text{ GPa}$ and $P = 40 \text{ kN}$, we have

$$\begin{aligned} \frac{1}{2}Py_E &= U & \frac{1}{2}Py_E &= \frac{1}{2E}(29.7 \times 10^3 P^2) \\ y_E &= \frac{1}{E}(29.7 \times 10^3 P) = \frac{(29.7 \times 10^3)(40 \times 10^3)}{73 \times 10^9} \\ y_E &= 16.27 \times 10^{-3} \text{ m} & y_E &= 16.27 \text{ mm} \downarrow \end{aligned}$$

PROBLEMS

11.42 The cylindrical block E has a speed $v_0 = 16$ ft/s when it strikes squarely the yoke BD that is attached to the $\frac{7}{8}$ -in.-diameter rods AB and CD . Knowing that the rods are made of a steel for which $\sigma_Y = 50$ ksi and $E = 29 \times 10^6$ psi, determine the weight of block E for which the factor of safety is five with respect to permanent deformation of the rods.

11.43 The 18-lb cylindrical block E has a horizontal velocity v_0 when it strikes squarely the yoke BD that is attached to the $\frac{7}{8}$ -in.-diameter rods AB and CD . Knowing that the rods are made of a steel for which $\sigma_Y = 50$ ksi and $E = 29 \times 10^6$ psi, determine the maximum allowable speed v_0 if the rods are not to be permanently deformed.

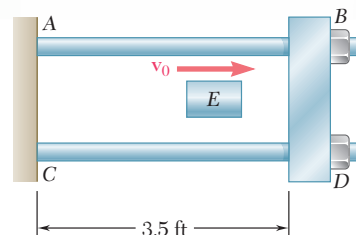


Fig. P11.42 and P11.43

11.44 Collar D is released from rest in the position shown and is stopped by a small plate attached at end C of the vertical rod ABC . Determine the mass of the collar for which the maximum normal stress in portion BC is 125 MPa.

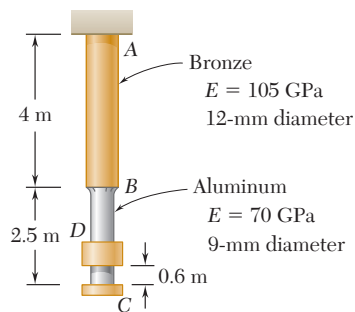


Fig. P11.44

11.45 Solve Prob. 11.44, assuming that both portions of rod ABC are made of aluminum.

11.46 The 48-kg collar G is released from rest in the position shown and is stopped by plate BDF that is attached to the 20-mm-diameter steel rod CD and to the 15-mm-diameter steel rods AB and EF . Knowing that for the grade of steel used $\sigma_{all} = 180$ MPa and $E = 200$ GPa, determine the largest allowable distance h .

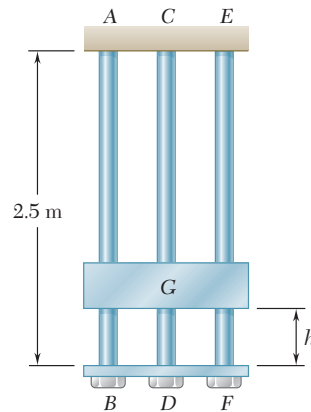


Fig. P11.46

11.47 Solve Prob. 11.46, assuming that the 20-mm-diameter steel rod CD is replaced by a 20-mm-diameter rod made of an aluminum alloy for which $\sigma_{all} = 150$ MPa and $E = 75$ GPa.

11.48 The steel beam AB is struck squarely at its midpoint C by a 45-kg block moving horizontally with a speed $v_0 = 2$ m/s. Using $E = 200$ GPa, determine (a) the equivalent static load, (b) the maximum normal stress in the beam, (c) the maximum deflection of the midpoint C of the beam.

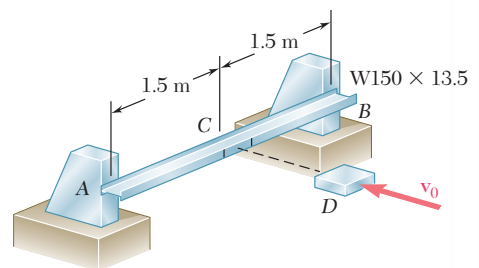


Fig. P11.48

11.49 Solve Prob. 11.48, assuming that the $W150 \times 13.5$ rolled-steel beam is rotated by 90° about its longitudinal axis so that its web is vertical.

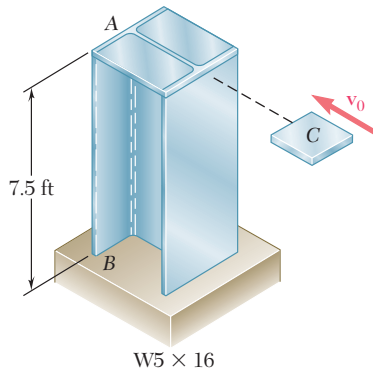


Fig. P11.50

11.50 A 25-lb block C moving horizontally with at velocity v_0 hits the post AB squarely as shown. Using $E = 29 \times 10^6$ psi, determine the largest speed v_0 for which the maximum normal stress in the pipe does not exceed 18 ksi.

11.51 Solve Prob. 11.50, assuming that the post AB has been rotated 90° about its longitudinal axis.

11.52 and 11.53 The 2-kg block D is dropped from the position shown onto the end of a 16-mm-diameter rod. Knowing that $E = 200$ GPa, determine (a) the maximum deflection of end A , (b) the maximum bending moment in the rod, (c) the maximum normal stress in the rod.

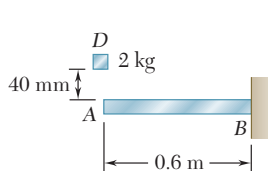


Fig. P11.52

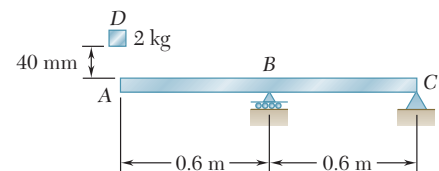


Fig. P11.53

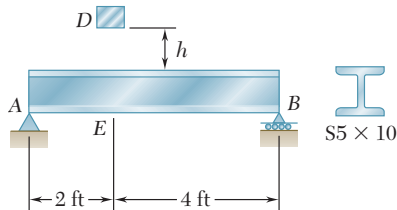


Fig. P11.54

11.54 The 45-lb block D is dropped from a height $h = 0.6$ ft onto the steel beam AB . Knowing that $E = 29 \times 10^6$ psi, determine (a) the maximum deflection at point E , (b) the maximum normal stress in the beam.

11.55 Solve Prob. 11.54, assuming that a $W4 \times 13$ rolled-steel shape is used for beam AB .

11.56 A block of weight W is dropped from a height h onto the horizontal beam AB and hits it at point D . (a) Show that the maximum deflection y_m at point D can be expressed as

$$y_m = y_{st} \left(1 + \sqrt{1 + \frac{2h}{y_{st}}} \right)$$

where y_{st} represents the deflection at D caused by a static load W applied at that point and where the quantity in parenthesis is referred to as the *impact factor*. (b) Compute the impact factor for the beam and the impact of Prob. 11.52.

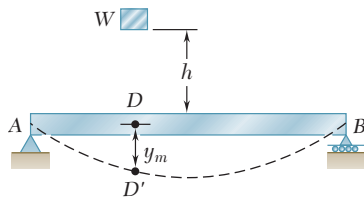


Fig. P11.56 and P11.57

11.57 A block of weight W is dropped from a height h onto the horizontal beam AB and hits point D . (a) Denoting by y_m the exact value of the maximum deflection at D and by y'_m the value obtained by neglecting the effect of this deflection on the change in potential energy of the block, show that the absolute value of the relative error is $(y'_m - y_m)/y_m$, never exceeding $y'_m/2h$. (b) Check the result obtained in part a by solving part a of Prob. 11.52 without taking y_m into account when determining the change in potential energy of the load, and comparing the answer obtained in this way with the exact answer to that problem.

11.58 and 11.59 Using the method of work and energy, determine the deflection at point D caused by the load P .

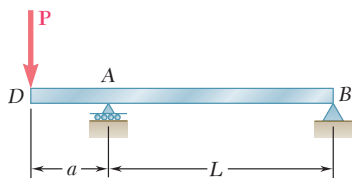


Fig. P11.58

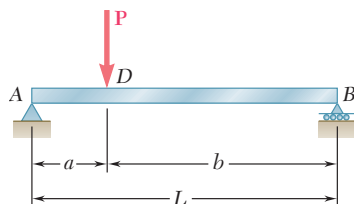


Fig. P11.59

11.60 and 11.61 Using the method of work and energy, determine the slope at point D caused by the couple M_0 .

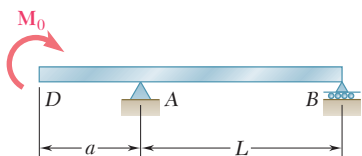


Fig. P11.60

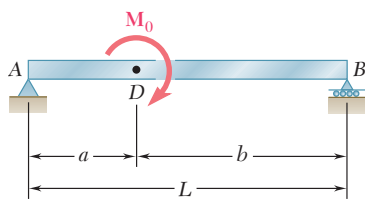


Fig. P11.61

11.62 and 11.63 Using the method of work and energy, determine the deflection at point C caused by the load P .

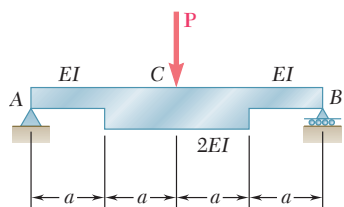


Fig. P11.62

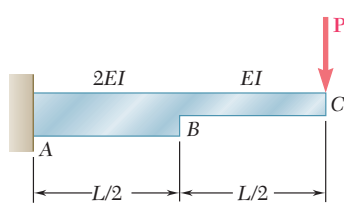


Fig. P11.63

11.64 Using the method of work and energy, determine the slope at point A caused by the couple M_0 .

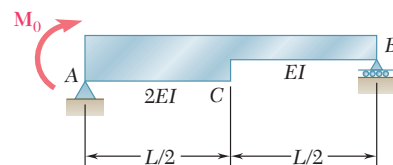


Fig. P11.64

11.65 Using the method of work and energy, determine the slope at point D caused by the couple M_0 .

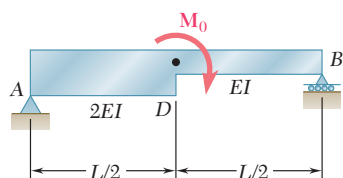


Fig. P11.65

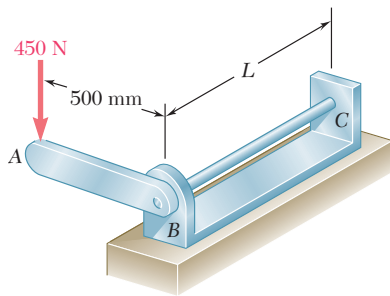


Fig. P11.67 and P11.68

- 11.66** Torques of the same magnitude T are applied to the steel shafts AB and CD . Using the method of work and energy, determine the length L of the hollow portion of shaft CD for which the angle of twist at C is equal to 1.25 times the angle of twist at A .

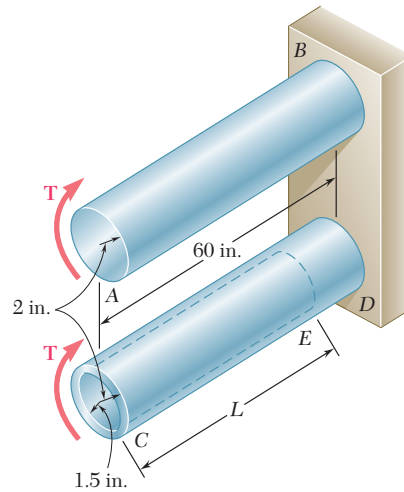


Fig. P11.66

- 11.67** The 20-mm diameter steel rod BC is attached to the lever AB and to the fixed support C . The uniform steel lever is 10 mm thick and 30 mm deep. Using the method of work and energy, determine the deflection of point A when $L = 600$ mm. Use $E = 200$ GPa and $G = 77.2$ GPa.
- 11.68** The 20-mm diameter steel rod BC is attached to the lever AB and to the fixed support C . The uniform steel lever is 10 mm thick and 30 mm deep. Using the method of work and energy, determine the length L of the rod BC for which the deflection at point A is 40 mm. Use $E = 200$ GPa and $G = 77.2$ GPa.
- 11.69** Two solid steel shafts are connected by the gears shown. Using the method of work and energy, determine the angle through which end D rotates when $T = 820$ N · m. Use $G = 77.2$ GPa.

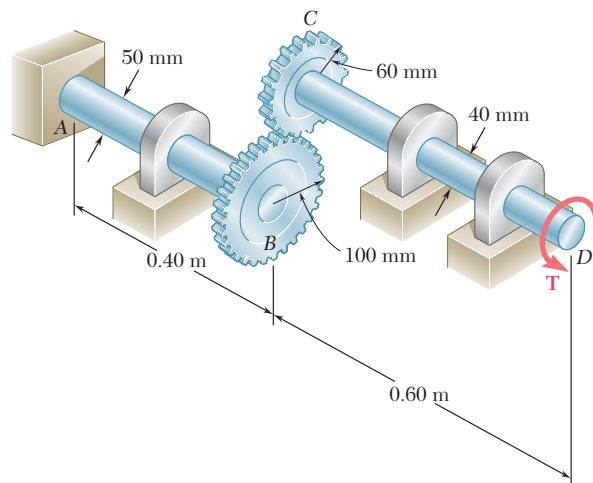


Fig. P11.69

- 11.70** The thin-walled hollow cylindrical member AB has a noncircular cross section of nonuniform thickness. Using the expression given in Eq. (3.53) of Sec. 3.13, and the expression for the strain-energy density given in Eq. (11.19), show that the angle of twist of member AB is

$$\phi = \frac{TL}{4\bar{a}^2G} \oint \frac{ds}{t}$$

where ds is an element of the center line of the wall cross section and \bar{a} is the area enclosed by that center line.

- 11.71** Each member of the truss shown has a uniform cross-sectional area A . Using the method of work and energy, determine the vertical deflection of the point of application of the load P .

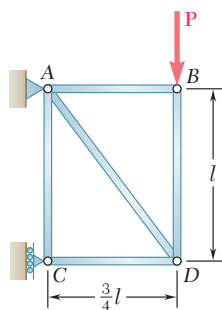


Fig. P11.71

- 11.72** Each member of the truss shown is made of steel and has a cross-sectional area of 400 mm^2 . Using $E = 200 \text{ GPa}$, determine the deflection of point D caused by the 16-kN load.
- 11.73** Each member of the truss shown is made of steel and has a cross-sectional area of 5 in^2 . Using $E = 29 \times 10^6 \text{ psi}$, determine the vertical deflection of point B caused by the 20-kip load.

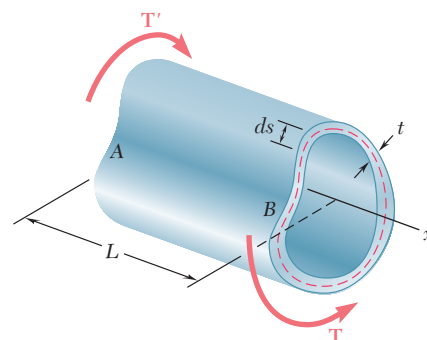


Fig. P11.70

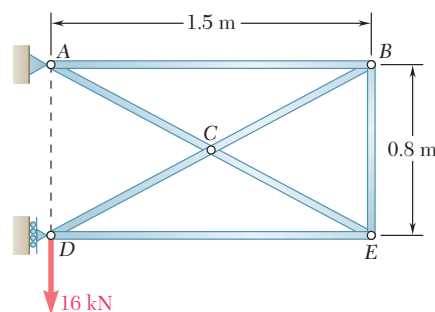


Fig. P11.72

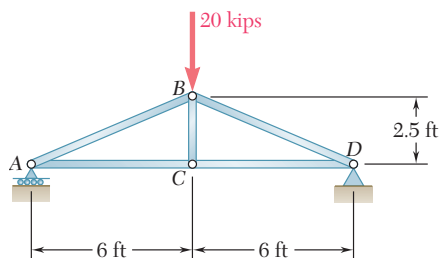


Fig. P11.73

- 11.74** Each member of the truss shown is made of steel and has a uniform cross-sectional area of 5 in^2 . Using $E = 29 \times 10^6 \text{ psi}$, determine the vertical deflection of joint C caused by the application of the 15-kip load.

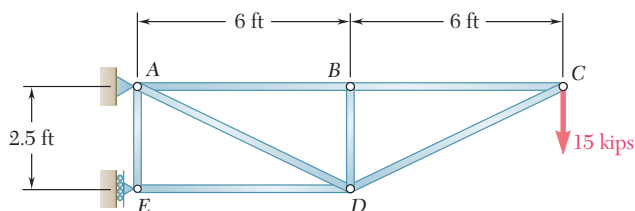


Fig. P11.74

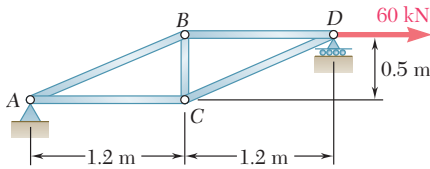


Fig. P11.75

11.75 Each member of the truss shown is made of steel; the cross-sectional area of member BC is 800 mm^2 and for all other members the cross-sectional area is 400 mm^2 . Using $E = 200 \text{ GPa}$, determine the deflection of point D caused by the 60-kN load.

11.76 The steel rod BC has a 24-mm diameter and the steel cable $ABDCA$ has a 12-mm diameter. Using $E = 200 \text{ GPa}$, determine the deflection of joint D caused by the 12-kN load.

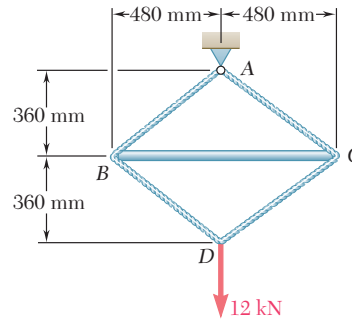


Fig. P11.76

*11.11 WORK AND ENERGY UNDER SEVERAL LOADS

In this section, the strain energy of a structure subjected to several loads will be considered and will be expressed in terms of the loads and the resulting deflections.

Consider an elastic beam AB subjected to two concentrated loads \mathbf{P}_1 and \mathbf{P}_2 . The strain energy of the beam is equal to the work of \mathbf{P}_1 and \mathbf{P}_2 as they are slowly applied to the beam at C_1 and C_2 , respectively (Fig. 11.33). However, in order to evaluate this work, we must first express the deflections x_1 and x_2 in terms of the loads \mathbf{P}_1 and \mathbf{P}_2 .

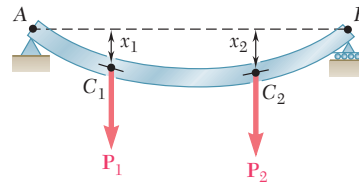


Fig. 11.33 Beam with multiple loads.

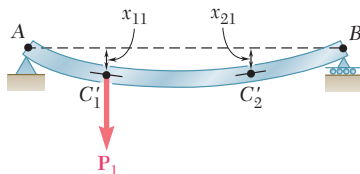


Fig. 11.34

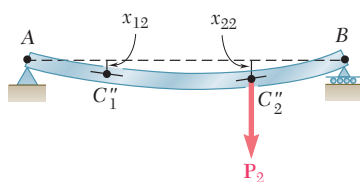


Fig. 11.35

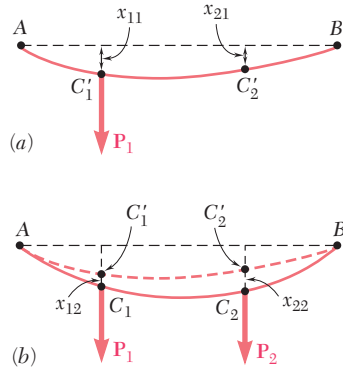
Let us assume that only \mathbf{P}_1 is applied to the beam (Fig. 11.34). We note that both C_1 and C_2 are deflected and that their deflections are proportional to the load \mathbf{P}_1 . Denoting these deflections by x_{11} and x_{21} , respectively, we write

$$x_{11} = \alpha_{11}P_1 \quad x_{21} = \alpha_{21}P_1 \quad (11.54)$$

where α_{11} and α_{21} are constants called *influence coefficients*. These constants represent the deflections of C_1 and C_2 , respectively, when a unit load is applied at C_1 and are characteristics of the beam AB .

Let us now assume that only \mathbf{P}_2 is applied to the beam (Fig. 11.35). Denoting by x_{12} and x_{22} , respectively, the resulting deflections of C_1 and C_2 , we write

$$x_{12} = \alpha_{12}P_2 \quad x_{22} = \alpha_{22}P_2 \quad (11.55)$$

**Fig. 11.36**

where α_{12} and α_{22} are the influence coefficients representing the deflections of C_1 and C_2 , respectively, when a unit load is applied at C_2 . Applying the principle of superposition, we express the deflections x_1 and x_2 of C_1 and C_2 when both loads are applied (Fig. 11.33) as

$$x_1 = x_{11} + x_{12} = \alpha_{11}P_1 + \alpha_{12}P_2 \quad (11.56)$$

$$x_2 = x_{21} + x_{22} = \alpha_{21}P_1 + \alpha_{22}P_2 \quad (11.57)$$

To compute the work done by \mathbf{P}_1 and \mathbf{P}_2 , and thus the strain energy of the beam, it is convenient to assume that \mathbf{P}_1 is first applied slowly at C_1 (Fig. 11.36a). Recalling the first of Eqs. (11.54), we express the work of \mathbf{P}_1 as

$$\frac{1}{2}P_1x_{11} = \frac{1}{2}P_1(\alpha_{11}P_1) = \frac{1}{2}\alpha_{11}P_1^2 \quad (11.58)$$

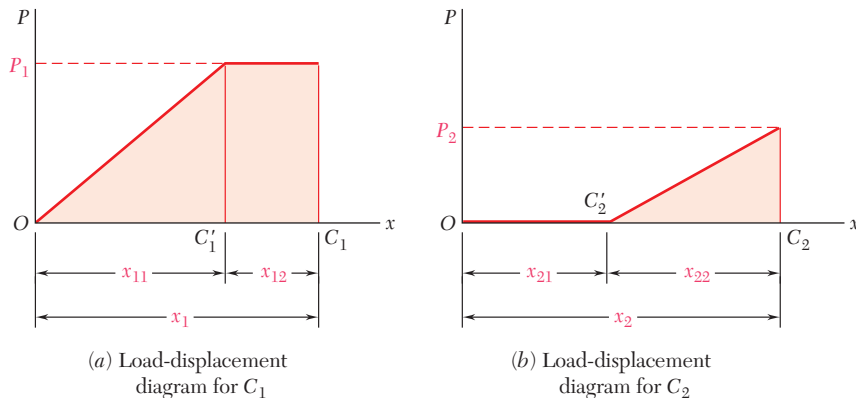
and note that \mathbf{P}_2 does no work while C_2 moves through x_{21} , since it has not yet been applied to the beam.

Now we slowly apply \mathbf{P}_2 at C_2 (Fig. 11.36b); recalling the second of Eqs. (11.55), we express the work of \mathbf{P}_2 as

$$\frac{1}{2}P_2x_{22} = \frac{1}{2}P_2(\alpha_{22}P_2) = \frac{1}{2}\alpha_{22}P_2^2 \quad (11.59)$$

But, as \mathbf{P}_2 is slowly applied at C_2 , the point of application of \mathbf{P}_1 moves through x_{12} from C'_1 to C_1 , and the load \mathbf{P}_1 does work. Since \mathbf{P}_1 is *fully applied* during this displacement (Fig. 11.37), its work is equal to P_1x_{12} or, recalling the first of Eqs. (11.55),

$$P_1x_{12} = P_1(\alpha_{12}P_2) = \alpha_{12}P_1P_2 \quad (11.60)$$

**Fig. 11.37** Load-displacement diagrams.

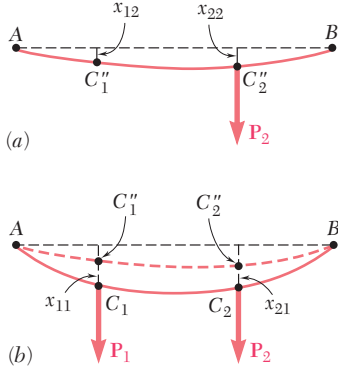


Fig. 11.38

Adding the expressions obtained in (11.58), (11.59), and (11.60), we express the strain energy of the beam under the loads \mathbf{P}_1 and \mathbf{P}_2 as

$$U = \frac{1}{2}(\alpha_{11}P_1^2 + 2\alpha_{12}P_1P_2 + \alpha_{22}P_2^2) \quad (11.61)$$

If the load \mathbf{P}_2 had first been applied to the beam (Fig. 11.38a), and then the load \mathbf{P}_1 (Fig. 11.38b), the work done by each load would have been as shown in Fig. 11.39. Calculations similar to those we have just carried out would lead to the following alternative expression for the strain energy of the beam:

$$U = \frac{1}{2}(\alpha_{22}P_2^2 + 2\alpha_{21}P_2P_1 + \alpha_{11}P_1^2) \quad (11.62)$$

Equating the right-hand members of Eqs. (11.61) and (11.62), we find that $\alpha_{12} = \alpha_{21}$, and thus conclude that the deflection produced at C_1 by a unit load applied at C_2 is equal to the deflection produced at C_2 by a unit load applied at C_1 . This is known as *Maxwell's reciprocal theorem*, after the British physicist James Clerk Maxwell (1831–1879).

While we are now able to express the strain energy U of a structure subjected to several loads as a function of these loads, we cannot use the method of Sec. 11.10 to determine the deflection of such a structure. Indeed, computing the strain energy U by integrating the strain-energy density u over the structure and substituting the expression obtained into (11.61) would yield only one equation, which clearly could not be solved for the various coefficients α .

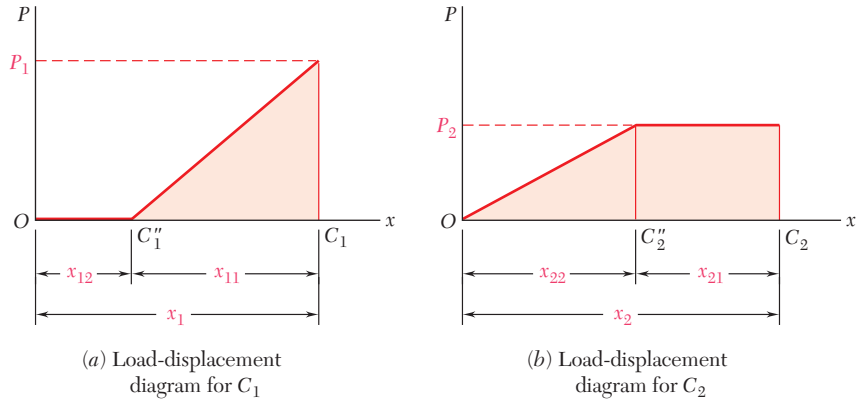


Fig. 11.39 Alternative load-displacement diagrams.

*11.12 CASTIGLIANO'S THEOREM

We recall the expression obtained in the preceding section for the strain energy of an elastic structure subjected to two loads \mathbf{P}_1 and \mathbf{P}_2 :

$$U = \frac{1}{2}(\alpha_{11}P_1^2 + 2\alpha_{12}P_1P_2 + \alpha_{22}P_2^2) \quad (11.61)$$

where α_{11} , α_{12} , and α_{22} are the influence coefficients associated with the points of application C_1 and C_2 of the two loads. Differentiating both members of Eq. (11.61) with respect to P_1 and recalling Eq. (11.56), we write

$$\frac{\partial U}{\partial P_1} = \alpha_{11}P_1 + \alpha_{12}P_2 = x_1 \quad (11.63)$$

Differentiating both members of Eq. (11.61) with respect to P_2 , recalling Eq. (11.57), and keeping in mind that $\alpha_{12} = \alpha_{21}$, we have

$$\frac{\partial U}{\partial P_2} = \alpha_{12}P_1 + \alpha_{22}P_2 = x_2 \quad (11.64)$$

More generally, if an elastic structure is subjected to n loads $\mathbf{P}_1, \mathbf{P}_2, \dots, \mathbf{P}_n$, the deflection x_j of the point of application of \mathbf{P}_j , measured along the line of action of \mathbf{P}_j , can be expressed as the partial derivative of the strain energy of the structure with respect to the load \mathbf{P}_j . We write

$$x_j = \frac{\partial U}{\partial P_j} \quad (11.65)$$

This is *Castigliano's theorem*, named after the Italian engineer Alberto Castigliano (1847–1884) who first stated it.[†]

Recalling that the work of a couple \mathbf{M} is $\frac{1}{2}M\theta$, where θ is the angle of rotation at the point where the couple is slowly applied, we note that Castigliano's theorem may be used to determine the slope of a beam at the point of application of a couple \mathbf{M}_j . We have

$$\theta_j = \frac{\partial U}{\partial M_j} \quad (11.68)$$

Similarly, the angle of twist ϕ_j in a section of a shaft where a torque \mathbf{T}_j is slowly applied is obtained by differentiating the strain energy of the shaft with respect to T_j :

$$\phi_j = \frac{\partial U}{\partial T_j} \quad (11.69)$$

[†]In the case of an elastic structure subjected to n loads $\mathbf{P}_1, \mathbf{P}_2, \dots, \mathbf{P}_n$, the deflection of the point of application of \mathbf{P}_j , measured along the line of action of \mathbf{P}_j , can be expressed as

$$x_j = \sum_k \alpha_{jk}P_k \quad (11.66)$$

and the strain energy of the structure is found to be

$$U = \frac{1}{2} \sum_i \sum_k \alpha_{ik}P_iP_k \quad (11.67)$$

Differentiating U with respect to P_j , and observing that P_j is found in terms corresponding to either $i = j$ or $k = j$, we write

$$\frac{\partial U}{\partial P_j} = \frac{1}{2} \sum_k \alpha_{jk}P_k + \frac{1}{2} \sum_i \alpha_{ij}P_i$$

or, since $\alpha_{ij} = \alpha_{ji}$,

$$\frac{\partial U}{\partial P_j} = \frac{1}{2} \sum_k \alpha_{jk}P_k + \frac{1}{2} \sum_i \alpha_{ji}P_i = \sum_k \alpha_{jk}P_k$$

Recalling Eq. (11.66), we verify that

$$x_j = \frac{\partial U}{\partial P_j} \quad (11.65)$$

***11.13 DEFLECTIONS BY CASTIGLIANO'S THEOREM**

We saw in the preceding section that the deflection x_j of a structure at the point of application of a load \mathbf{P}_j can be determined by computing the partial derivative $\partial U / \partial P_j$ of the strain energy U of the structure. As we recall from Secs. 11.4 and 11.5, the strain energy U is obtained by integrating or summing over the structure the strain energy of each element of the structure. The calculation by Castigliano's theorem of the deflection x_j is simplified if the differentiation with respect to the load P_j is carried out before the integration or summation.

In the case of a beam, for example, we recall from Sec. 11.4 that

$$U = \int_0^L \frac{M^2}{2EI} dx \quad (11.17)$$

and determine the deflection x_j of the point of application of the load \mathbf{P}_j by writing

$$x_j = \frac{\partial U}{\partial P_j} = \int_0^L \frac{M}{EI} \frac{\partial M}{\partial P_j} dx \quad (11.70)$$

In the case of a truss consisting of n uniform members of length L_i , cross-sectional area A_i , and internal force F_i , we recall Eq. (11.14) and express the strain energy U of the truss as

$$U = \sum_{i=1}^n \frac{F_i^2 L_i}{2A_i E} \quad (11.71)$$

The deflection x_j of the point of application of the load \mathbf{P}_j is obtained by differentiating with respect to P_j each term of the sum. We write

$$x_j = \frac{\partial U}{\partial P_j} = \sum_{i=1}^n \frac{F_i L_i}{A_i E} \frac{\partial F_i}{\partial P_j} \quad (11.72)$$

EXAMPLE 11.12

The cantilever beam AB supports a uniformly distributed load w and a concentrated load \mathbf{P} as shown (Fig. 11.40). Knowing that $L = 2$ m, $w = 4$ kN/m, $P = 6$ kN, and $EI = 5$ MN \cdot m², determine the deflection at A .

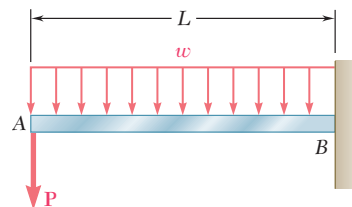


Fig. 11.40

The deflection y_A of the point A where the load \mathbf{P} is applied is obtained from Eq. (11.70). Since \mathbf{P} is vertical and directed downward, y_A represents a vertical deflection and is positive downward. We have

$$y_A = \frac{\partial U}{\partial P} = \int_0^L \frac{M}{EI} \frac{\partial M}{\partial P} dx \quad (11.73)$$

The bending moment M at a distance x from A is

$$M = -(Px + \frac{1}{2}wx^2) \quad (11.74)$$

and its derivative with respect to P is

$$\frac{\partial M}{\partial P} = -x$$

Substituting for M and $\partial M/\partial P$ into Eq. (11.73), we write

$$\begin{aligned} y_A &= \frac{1}{EI} \int_0^L \left(Px^2 + \frac{1}{2}wx^3 \right) dx \\ y_A &= \frac{1}{EI} \left(\frac{PL^3}{3} + \frac{wL^4}{8} \right) \end{aligned} \quad (11.75)$$

Substituting the given data, we have

$$\begin{aligned} y_A &= \frac{1}{5 \times 10^6 \text{ N} \cdot \text{m}^2} \left[\frac{(6 \times 10^3 \text{ N})(2 \text{ m})^3}{3} + \frac{(4 \times 10^3 \text{ N/m})(2 \text{ m})^4}{8} \right] \\ y_A &= 4.8 \times 10^{-3} \text{ m} \quad y_A = 4.8 \text{ mm} \downarrow \end{aligned}$$

We note that the computation of the partial derivative $\partial M/\partial P$ could not have been carried out if the numerical value of P had been substituted for P in the expression (11.74) for the bending moment.

We can observe that the deflection x_j of a structure at a given point C_j can be obtained by the direct application of Castigliano's theorem only if a load \mathbf{P}_j happens to be applied at C_j in the direction in which x_j is to be determined. When no load is applied at C_j , or when a load is applied in a direction other than the desired one, we can still obtain the deflection x_j by Castigliano's theorem if we use the following procedure: We apply a fictitious or "dummy" load \mathbf{Q}_j at C_j in the direction in which the deflection x_j is to be determined and use Castigliano's theorem to obtain the deflection

$$x_j = \frac{\partial U}{\partial Q_j} \quad (11.76)$$

due to \mathbf{Q}_j and the actual loads. Making $Q_j = 0$ in Eq. (11.76) yields the deflection at C_j in the desired direction under the given loading.

The slope θ_j of a beam at a point C_j can be determined in a similar manner by applying a fictitious couple \mathbf{M}_j at C_j , computing the partial derivative $\partial U/\partial M_j$, and making $M_j = 0$ in the expression obtained.

EXAMPLE 11.13

The cantilever beam AB supports a uniformly distributed load w (Fig. 11.41). Determine the deflection and slope at A .

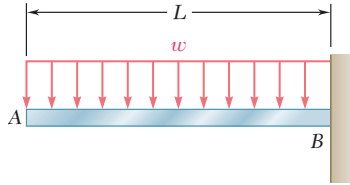


Fig. 11.41

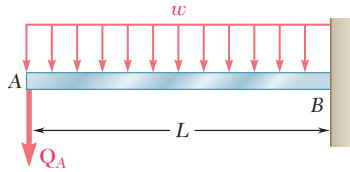


Fig. 11.42

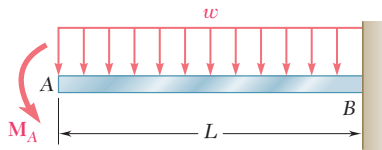


Fig. 11.43

Deflection at A. We apply a dummy downward load Q_A at A (Fig. 11.42) and write

$$y_A = \frac{\partial U}{\partial Q_A} = \int_0^L \frac{M}{EI} \frac{\partial M}{\partial Q_A} dx \quad (11.77)$$

The bending moment M at a distance x from A is

$$M = -Q_A x - \frac{1}{2} w x^2 \quad (11.78)$$

and its derivative with respect to Q_A is

$$\frac{\partial M}{\partial Q_A} = -x \quad (11.79)$$

Substituting for M and $\partial M/\partial Q_A$ from (11.78) and (11.79) into (11.77), and making $Q_A = 0$, we obtain the deflection at A for the given loading:

$$y_A = \frac{1}{EI} \int_0^L \left(-\frac{1}{2} w x^2\right)(-x) dx = +\frac{wL^4}{8EI}$$

Since the dummy load was directed downward, the positive sign indicates that

$$y_A = \frac{wL^4}{8EI} \downarrow$$

Slope at A. We apply a dummy counterclockwise couple M_A at A (Fig. 11.43) and write

$$\theta_A = \frac{\partial U}{\partial M_A}$$

Recalling Eq. (11.17), we have

$$\theta_A = \frac{\partial}{\partial M_A} \int_0^L \frac{M^2}{2EI} dx = \int_0^L \frac{M}{EI} \frac{\partial M}{\partial M_A} dx \quad (11.80)$$

The bending moment M at a distance x from A is

$$M = -M_A - \frac{1}{2} w x^2 \quad (11.81)$$

and its derivative with respect to M_A is

$$\frac{\partial M}{\partial M_A} = -1 \quad (11.82)$$

Substituting for M and $\partial M/\partial M_A$ from (11.81) and (11.82) into (11.80), and making $M_A = 0$, we obtain the slope at A for the given loading:

$$\theta_A = \frac{1}{EI} \int_0^L \left(-\frac{1}{2} w x^2\right)(-1) dx = +\frac{wL^3}{6EI}$$

Since the dummy couple was counterclockwise, the positive sign indicates that the angle θ_A is also counterclockwise:

$$\theta_A = \frac{wL^3}{6EI} \curvearrowright$$

A load \mathbf{P} is supported at B by two rods of the same material and of the same cross-sectional area A (Fig. 11.44). Determine the horizontal and vertical deflection of point B .

We apply a dummy horizontal load \mathbf{Q} at B (Fig. 11.45). From Castigliano's theorem we have

$$x_B = \frac{\partial U}{\partial Q} \quad y_B = \frac{\partial U}{\partial P}$$

Recalling from Sec. 11.4 the expression (11.14) for the strain energy of a rod, we write

$$U = \frac{F_{BC}^2(BC)}{2AE} + \frac{F_{BD}^2(BD)}{2AE}$$

where F_{BC} and F_{BD} represent the forces in BC and BD , respectively. We have, therefore,

$$x_B = \frac{\partial U}{\partial Q} = \frac{F_{BC}(BC)}{AE} \frac{\partial F_{BC}}{\partial Q} + \frac{F_{BD}(BD)}{AE} \frac{\partial F_{BD}}{\partial Q} \quad (11.83)$$

and

$$y_B = \frac{\partial U}{\partial P} = \frac{F_{BC}(BC)}{AE} \frac{\partial F_{BC}}{\partial P} + \frac{F_{BD}(BD)}{AE} \frac{\partial F_{BD}}{\partial P} \quad (11.84)$$

From the free-body diagram of pin B (Fig. 11.46), we obtain

$$F_{BC} = 0.6P + 0.8Q \quad F_{BD} = -0.8P + 0.6Q \quad (11.85)$$

Differentiating these expressions with respect to Q and P , we write

$$\begin{aligned} \frac{\partial F_{BC}}{\partial Q} &= 0.8 & \frac{\partial F_{BD}}{\partial Q} &= 0.6 \\ \frac{\partial F_{BC}}{\partial P} &= 0.6 & \frac{\partial F_{BD}}{\partial P} &= -0.8 \end{aligned} \quad (11.86)$$

Substituting from (11.85) and (11.86) into both (11.83) and (11.84), making $Q = 0$, and noting that $BC = 0.6l$ and $BD = 0.8l$, we obtain the horizontal and vertical deflections of point B under the given load \mathbf{P} :

$$\begin{aligned} x_B &= \frac{(0.6P)(0.6l)}{AE}(0.8) + \frac{(-0.8P)(0.8l)}{AE}(0.6) \\ &= -0.096 \frac{Pl}{AE} \\ y_B &= \frac{(0.6P)(0.6l)}{AE}(0.6) + \frac{(-0.8P)(0.8l)}{AE}(-0.8) \\ &= +0.728 \frac{Pl}{AE} \end{aligned}$$

Referring to the directions of the loads \mathbf{Q} and \mathbf{P} , we conclude that

$$x_B = 0.096 \frac{Pl}{AE} \leftarrow \quad y_B = 0.728 \frac{Pl}{AE} \downarrow$$

We check that the expression obtained for the vertical deflection of B is the same that was found in Example 11.09.

EXAMPLE 11.14

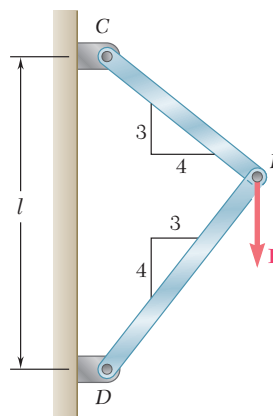


Fig. 11.44

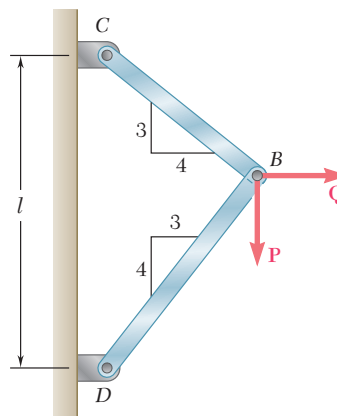


Fig. 11.45

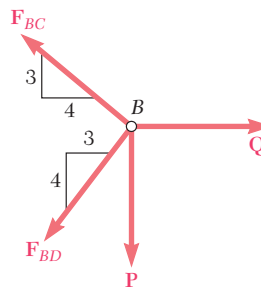


Fig. 11.46

*11.14 STATICALLY INDETERMINATE STRUCTURES

The reactions at the supports of a statically indeterminate elastic structure can be determined by Castigliano's theorem. In the case of a structure indeterminate to the first degree, for example, we designate one of the reactions as redundant and eliminate or modify accordingly the corresponding support. The redundant reaction is then treated as an unknown load that, together with the other loads, must produce deformations that are compatible with the original supports. We first calculate the strain energy U of the structure due to the combined action of the given loads and the redundant reaction. Observing that the partial derivative of U with respect to the redundant reaction represents the deflection (or slope) at the support that has been eliminated or modified, we then set this derivative equal to zero and solve the equation obtained for the redundant reaction.† The remaining reactions can be obtained from the equations of statics.

†This is in the case of a rigid support allowing no deflection. For other types of support, the partial derivative of U should be set equal to the allowed deflection.

EXAMPLE 11.15

Determine the reactions at the supports for the prismatic beam and loading shown (Fig. 11.47).

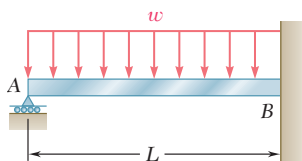


Fig. 11.47

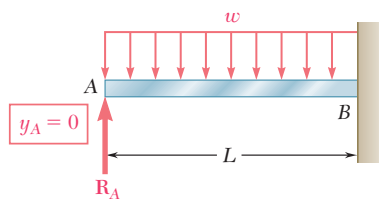


Fig. 11.48

The beam is statically indeterminate to the first degree. We consider the reaction at A as redundant and release the beam from that support. The reaction \mathbf{R}_A is now considered as an unknown load (Fig. 11.48) and will be determined from the condition that the deflection y_A at A must be zero. By Castigliano's theorem $y_A = \partial U / \partial R_A$, where U is the strain energy of the beam under the distributed load and the redundant reaction. Recalling Eq. (11.70), we write

$$y_A = \frac{\partial U}{\partial R_A} = \int_0^L \frac{M}{EI} \frac{\partial M}{\partial R_A} dx \quad (11.87)$$

We now express the bending moment M for the loading of Fig. 11.48. The bending moment at a distance x from A is

$$M = R_A x - \frac{1}{2} w x^2 \quad (11.88)$$

and its derivative with respect to R_A is

$$\frac{\partial M}{\partial R_A} = x \quad (11.89)$$

Substituting for M and $\partial M / \partial R_A$ from (11.88) and (11.89) into (11.87), we write

$$y_A = \frac{1}{EI} \int_0^L \left(R_A x^2 - \frac{1}{2} w x^3 \right) dx = \frac{1}{EI} \left(\frac{R_A L^3}{3} - \frac{w L^4}{8} \right)$$

Setting $y_A = 0$ and solving for R_A , we have

$$R_A = \frac{3}{8} w L \quad \mathbf{R}_A = \frac{3}{8} w L \uparrow$$

From the conditions of equilibrium for the beam, we find that the reaction at B consists of the following force and couple:

$$\mathbf{R}_B = \frac{5}{8} w L \uparrow \quad \mathbf{M}_B = \frac{1}{8} w L^2 \downarrow$$

A load \mathbf{P} is supported at B by three rods of the same material and the same cross-sectional area A (Fig. 11.49). Determine the force in each rod.

EXAMPLE 11.16

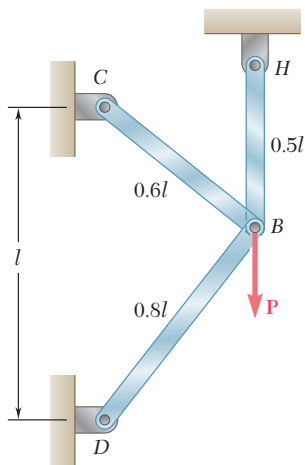


Fig. 11.49

The structure is statically indeterminate to the first degree. We consider the reaction at H as redundant and release rod BH from its support at H . The reaction \mathbf{R}_H is now considered as an unknown load (Fig. 11.50) and will be determined from the condition that the deflection y_H of point H must be zero. By Castigliano's theorem $y_H = \partial U / \partial R_H$, where U is the strain energy of the three-rod system under the load \mathbf{P} and the redundant reaction \mathbf{R}_H . Recalling Eq. (11.72), we write

$$y_H = \frac{F_{BC}(BC)}{AE} \frac{\partial F_{BC}}{\partial R_H} + \frac{F_{BD}(BD)}{AE} \frac{\partial F_{BD}}{\partial R_H} + \frac{F_{BH}(BH)}{AE} \frac{\partial F_{BH}}{\partial R_H} \quad (11.90)$$

We note that the force in rod BH is equal to R_H and write

$$F_{BH} = R_H \quad (11.91)$$

Then, from the free-body diagram of pin B (Fig. 11.51), we obtain

$$F_{BC} = 0.6P - 0.6R_H \quad F_{BD} = 0.8R_H - 0.8P \quad (11.92)$$

Differentiating with respect to R_H the force in each rod, we write

$$\frac{\partial F_{BC}}{\partial R_H} = -0.6 \quad \frac{\partial F_{BD}}{\partial R_H} = 0.8 \quad \frac{\partial F_{BH}}{\partial R_H} = 1 \quad (11.93)$$

Substituting from (11.91), (11.92), and (11.93) into (11.90), and noting that the lengths BC , BD , and BH are, respectively, equal to $0.6l$, $0.8l$, and $0.5l$, we write

$$y_H = \frac{1}{AE} [(0.6P - 0.6R_H)(0.6l)(-0.6) + (0.8R_H - 0.8P)(0.8l)(0.8) + R_H(0.5l)(1)]$$

Setting $y_H = 0$, we obtain

$$1.228R_H - 0.728P = 0$$

and, solving for R_H ,

$$R_H = 0.593P$$

Carrying this value into Eqs. (11.91) and (11.92), we obtain the forces in the three rods:

$$F_{BC} = +0.244P \quad F_{BD} = -0.326P \quad F_{BH} = +0.593P$$

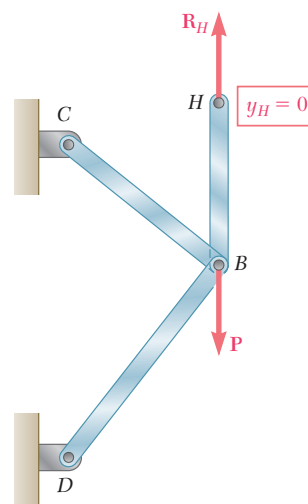


Fig. 11.50

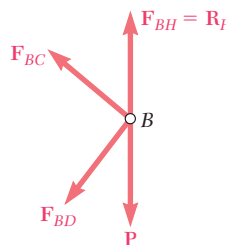
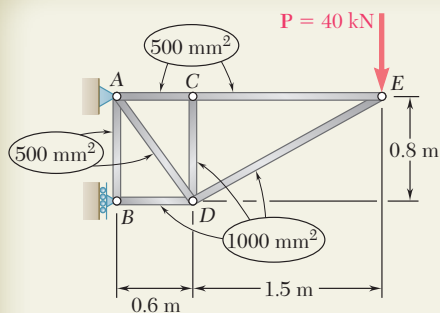


Fig. 11.51



SAMPLE PROBLEM 11.5

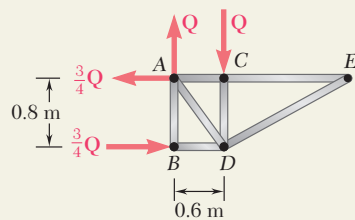
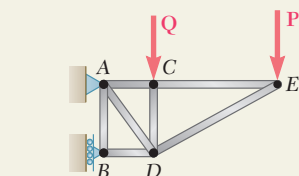
For the truss and loading of Sample Prob. 11.4, determine the vertical deflection of joint C.

SOLUTION

Castigliano's Theorem. Since no vertical load is applied at joint C, we introduce the dummy load Q as shown. Using Castigliano's theorem, and denoting by F_i the force in a given member i caused by the combined loading of P and Q , we have, since $E = \text{constant}$,

$$y_C = \sum \left(\frac{F_i L_i}{A_i E} \right) \frac{\partial F_i}{\partial Q} = \frac{1}{E} \sum \left(\frac{F_i L_i}{A_i} \right) \frac{\partial F_i}{\partial Q} \quad (1)$$

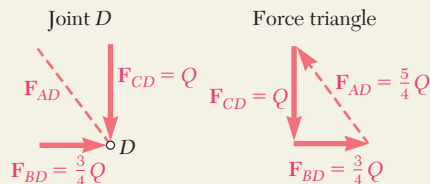
Force in Members. Considering in sequence the equilibrium of joints E, C, B, and D, we determine the force in each member caused by load Q .



Joint E: $F_{CE} = F_{DE} = 0$

Joint C: $F_{AC} = 0; F_{CD} = -Q$

Joint B: $F_{AB} = 0; F_{BD} = -\frac{3}{4}Q$



The force in each member caused by the load P was previously found in Sample Prob. 11.4. The total force in each member under the combined action of Q and P is shown in the following table. Forming $\partial F_i / \partial Q$ for each member, we then compute $(F_i L_i / A_i)(\partial F_i / \partial Q)$ as indicated in the table.

Member	F_i	$\partial F_i / \partial Q$	$L_i, \text{ m}$	$A_i, \text{ m}^2$	$\left(\frac{F_i L_i}{A_i} \right) \frac{\partial F_i}{\partial Q}$
AB	0	0	0.8	500×10^{-6}	0
AC	$+15P/8$	0	0.6	500×10^{-6}	0
AD	$+5P/4 + 5Q/4$	$\frac{5}{4}$	1.0	500×10^{-6}	$+3125P + 3125Q$
BD	$-21P/8 - 3Q/4$	$-\frac{3}{4}$	0.6	1000×10^{-6}	$+1181P + 338Q$
CD	$-Q$	-1	0.8	1000×10^{-6}	$+ 800Q$
CE	$+15P/8$	0	1.5	500×10^{-6}	0
DE	$-17P/8$	0	1.7	1000×10^{-6}	0

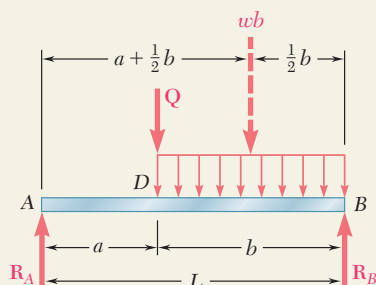
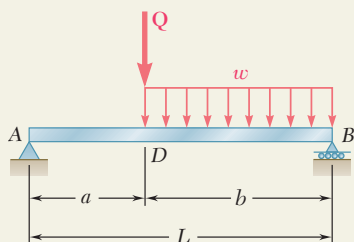
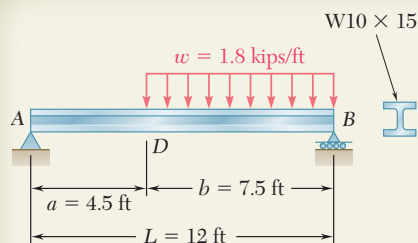
$$\sum \left(\frac{F_i L_i}{A_i} \right) \frac{\partial F_i}{\partial Q} = 4306P + 4263Q$$

Deflection of C. Substituting into Eq. (1), we have

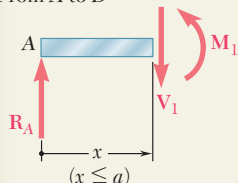
$$y_C = \frac{1}{E} \sum \left(\frac{F_i L_i}{A_i} \right) \frac{\partial F_i}{\partial Q} = \frac{1}{E} (4306P + 4263Q)$$

Since the load Q is not part of the original loading, we set $Q = 0$. Substituting the given data, $P = 40 \text{ kN}$ and $E = 73 \text{ GPa}$, we find

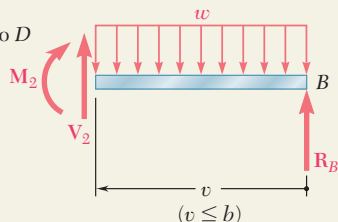
$$y_C = \frac{4306 (40 \times 10^3 \text{ N})}{73 \times 10^9 \text{ Pa}} = 2.36 \times 10^{-3} \text{ m} \quad y_C = 2.36 \text{ mm} \downarrow$$



From A to D



From B to D



SAMPLE PROBLEM 11.6

For the beam and loading shown, determine the deflection at point D. Use $E = 29 \times 10^6$ psi.

SOLUTION

Castigliano's Theorem. Since the given loading does not include a vertical load at point D, we introduce the dummy load Q as shown. Using Castigliano's theorem and noting that EI is constant, we write

$$y_D = \int \frac{M}{EI} \left(\frac{\partial M}{\partial Q} \right) dx = \frac{1}{EI} \int M \left(\frac{\partial M}{\partial Q} \right) dx \quad (1)$$

The integration will be performed separately for portions AD and DB.

Reactions. Using the free-body diagram of the entire beam, we find

$$R_A = \frac{wb^2}{2L} + Q \frac{b}{L} \uparrow \quad R_B = \frac{wb(a + \frac{1}{2}b)}{L} + Q \frac{a}{L} \uparrow$$

Portion AD of Beam. Using the free body shown, we find

$$M_1 = R_A x = \left(\frac{wb^2}{2L} + Q \frac{b}{L} \right) x \quad \frac{\partial M_1}{\partial Q} = + \frac{bx}{L}$$

Substituting into Eq. (1) and integrating from A to D gives

$$\frac{1}{EI} \int M_1 \frac{\partial M_1}{\partial Q} dx = \frac{1}{EI} \int_0^a R_A x \left(\frac{bx}{L} \right) dx = \frac{R_A a^3 b}{3EI L}$$

We substitute for R_A and then set the dummy load Q equal to zero.

$$\frac{1}{EI} \int M_1 \frac{\partial M_1}{\partial Q} dx = \frac{wa^3 b^3}{6EIL^2} \quad (2)$$

Portion DB of Beam. Using the free body shown, we find that the bending moment at a distance v from end B is

$$M_2 = R_B v - \frac{wv^2}{2} = \left[\frac{wb(a + \frac{1}{2}b)}{L} + Q \frac{a}{L} \right] v - \frac{wv^2}{2} \quad \frac{\partial M_2}{\partial Q} = + \frac{av}{L}$$

Substituting into Eq. (1) and integrating from point B where $v = 0$, to point D where $v = b$, we write

$$\frac{1}{EI} \int M_2 \frac{\partial M_2}{\partial Q} dv = \frac{1}{EI} \int_0^b \left(R_B v - \frac{wv^2}{2} \right) \left(\frac{av}{L} \right) dv = \frac{R_B ab^3}{3EI L} - \frac{wab^4}{8EI L}$$

Substituting for R_B and setting $Q = 0$,

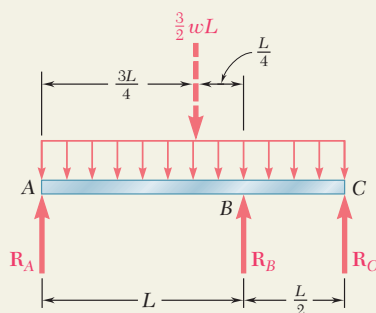
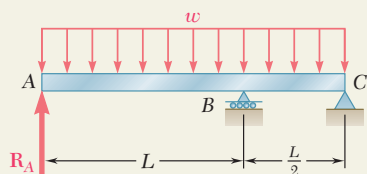
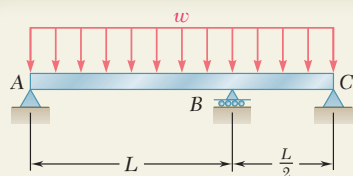
$$\frac{1}{EI} \int M_2 \frac{\partial M_2}{\partial Q} dv = \left[\frac{wb(a + \frac{1}{2}b)}{L} \right] \frac{ab^3}{3EI L} - \frac{wab^4}{8EI L} = \frac{5a^2 b^4 + ab^5}{24EIL^2} w \quad (3)$$

Deflection at Point D. Recalling Eqs. (1), (2), and (3), we have

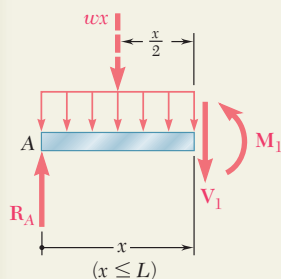
$$y_D = \frac{wab^3}{24EIL^2} (4a^2 + 5ab + b^2) = \frac{wab^3}{24EIL^2} (4a + b)(a + b) = \frac{wab^3}{24EIL^2} (4a + b)$$

From Appendix C we find that $I = 68.9 \text{ in}^4$ for a W10 \times 15. Substituting for I , w , a , b , and L their numerical values, we obtain

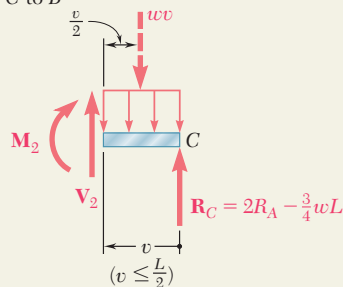
$$y_D = 0.262 \text{ in.} \downarrow$$



From A to B



From C to B



SAMPLE PROBLEM 11.7

For the uniform beam and loading shown, determine the reactions at the supports.

SOLUTION

Castigliano's Theorem. The beam is indeterminate to the first degree and we choose the reaction \mathbf{R}_A as redundant. Using Castigliano's theorem, we determine the deflection at A due to the combined action of \mathbf{R}_A and the distributed load. Since EI is constant, we write

$$y_A = \int \frac{M}{EI} \left(\frac{\partial M}{\partial R_A} \right) dx = \frac{1}{EI} \int M \frac{\partial M}{\partial R_A} dx \quad (1)$$

The integration will be performed separately for portions AB and BC of the beam. Finally, \mathbf{R}_A is obtained by setting y_A equal to zero.

Free Body: Entire Beam. We express the reactions at B and C in terms of R_A and the distributed load

$$R_B = \frac{9}{4} wL - 3R_A \quad R_C = 2R_A - \frac{3}{4} wL \quad (2)$$

Portion AB of Beam. Using the free-body diagram shown, we find

$$M_1 = R_A x - \frac{wx^2}{2} \quad \frac{\partial M_1}{\partial R_A} = x$$

Substituting into Eq. (1) and integrating from A to B, we have

$$\frac{1}{EI} \int M_1 \frac{\partial M_1}{\partial R_A} dx = \frac{1}{EI} \int_0^L \left(R_A x^2 - \frac{wx^3}{2} \right) dx = \frac{1}{EI} \left(\frac{R_A L^3}{3} - \frac{wL^4}{8} \right) \quad (3)$$

Portion BC of Beam. We have

$$M_2 = \left(2R_A - \frac{3}{4} wL \right) v - \frac{wv^2}{2} \quad \frac{\partial M_2}{\partial R_A} = 2v$$

Substituting into Eq. (1) and integrating from C, where $v = 0$, to B, where $v = \frac{1}{2}L$, we have

$$\begin{aligned} \frac{1}{EI} \int M_2 \frac{\partial M_2}{\partial R_A} dv &= \frac{1}{EI} \int_0^{L/2} \left(4R_A v^2 - \frac{3}{2} wL v^2 - wv^3 \right) dv \\ &= \frac{1}{EI} \left(\frac{R_A L^3}{6} - \frac{wL^4}{16} - \frac{wL^4}{64} \right) = \frac{1}{EI} \left(\frac{R_A L^3}{6} - \frac{5wL^4}{64} \right) \end{aligned} \quad (4)$$

Reaction at A. Adding the expressions obtained in (3) and (4), we determine y_A and set it equal to zero

$$y_A = \frac{1}{EI} \left(\frac{R_A L^3}{3} - \frac{wL^4}{8} \right) + \frac{1}{EI} \left(\frac{R_A L^3}{6} - \frac{5wL^4}{64} \right) = 0$$

Solving for R_A ,

$$R_A = \frac{13}{32} wL \quad R_A = \frac{13}{32} wL \uparrow \quad \blacktriangleleft$$

Reactions at B and C. Substituting for R_A into Eqs. (2), we obtain

$$R_B = \frac{33}{32} wL \uparrow \quad R_C = \frac{wL}{16} \uparrow \quad \blacktriangleleft$$

PROBLEMS

11.77 through 11.79 Using the information in Appendix D, compute the work of the loads as they are applied to the beam (a) if the load \mathbf{P} is applied first, (b) if the couple \mathbf{M} is applied first.

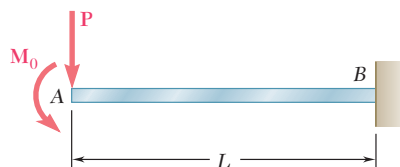


Fig. P11.77

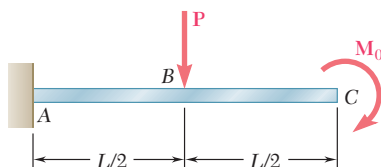


Fig. P11.78

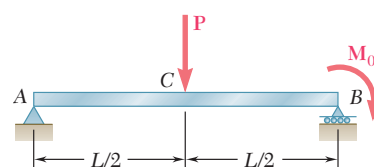


Fig. P11.79

11.80 through 11.82 For the beam and loading shown, (a) compute the work of the loads as they are applied successively to the beam, using the information provided in Appendix D, (b) compute the strain energy of the beam by the method of Sec. 11.4 and show that it is equal to the work obtained in part a.

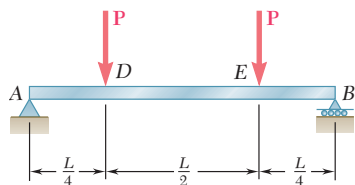


Fig. P11.80

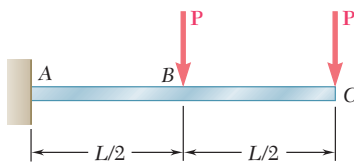


Fig. P11.81

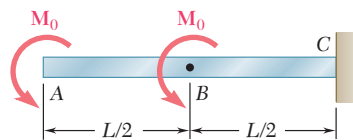


Fig. P11.82

11.83 and 11.84 For the prismatic beam shown, determine the deflection of point D.

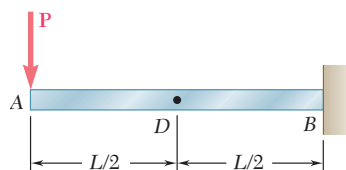


Fig. P11.83 and P11.85

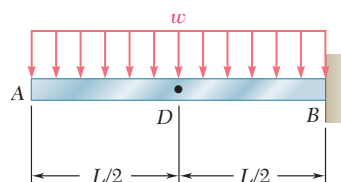


Fig. P11.84 and P11.86

11.85 and 11.86 For the prismatic beam shown, determine the slope at point D.

11.87 and 11.88 For the prismatic beam shown, determine the deflection at point D.

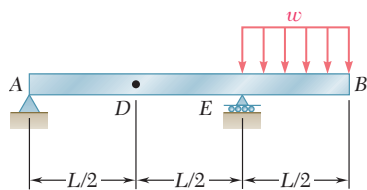


Fig. P11.87 and P11.89

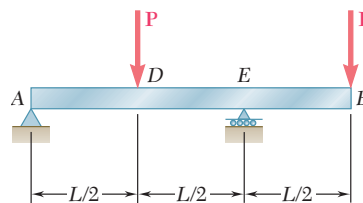
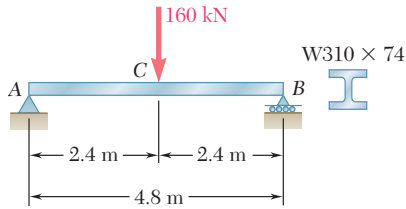


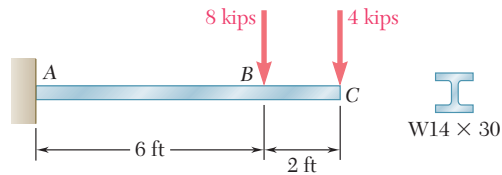
Fig. P11.88 and P11.90

11.89 and 11.90 For the prismatic beam shown, determine the slope at point D.

**Fig. P11.91**

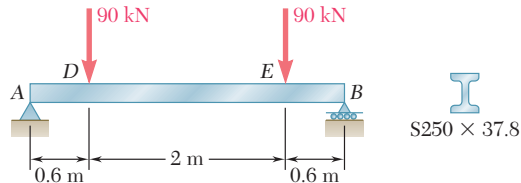
11.91 For the beam and loading shown, determine the slope at end A. Use $E = 200 \text{ GPa}$.

11.92 For the beam and loading shown, determine the slope at end C. Use $E = 29 \times 10^6 \text{ psi}$.

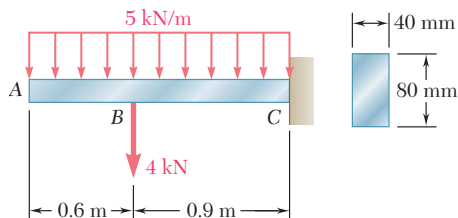
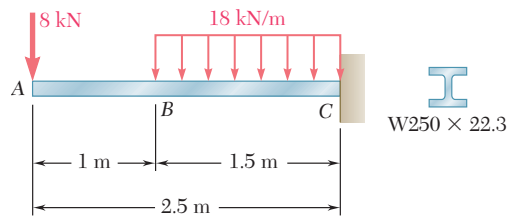
**Fig. P11.92 and P11.93**

11.93 For the beam and loading shown, determine the deflection at end C. Use $E = 29 \times 10^6 \text{ psi}$.

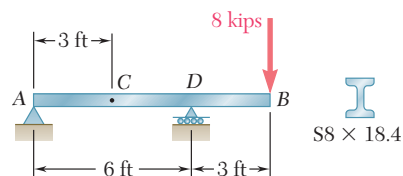
11.94 For the beam and loading shown, determine the deflection at point D. Use $E = 200 \text{ GPa}$.

**Fig. P11.94**

11.95 and 11.96 For the beam and loading shown, determine the deflection at point B. Use $E = 200 \text{ GPa}$.

**Fig. P11.95****Fig. P11.96**

11.97 For the beam and loading shown, determine the deflection at point C. Use $E = 29 \times 10^6 \text{ psi}$.

**Fig. P11.97 and P11.98**

11.98 For the beam and loading shown, determine the slope at end A. Use $E = 29 \times 10^6 \text{ psi}$.

11.99 and 11.100 For the truss and loading shown, determine the horizontal and vertical deflection of joint C .

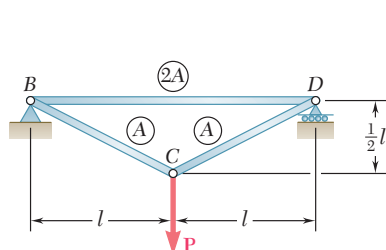


Fig. P11.99

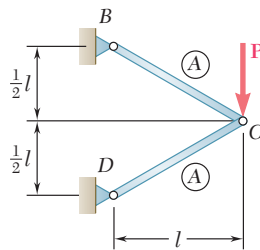


Fig. P11.100

11.101 and 11.102 Each member of the truss shown is made of steel and has a cross-sectional area of 500 mm^2 . Using $E = 200\text{ GPa}$, determine the deflection indicated.

11.101 Vertical deflection of joint B .

11.102 Horizontal deflection of joint B .

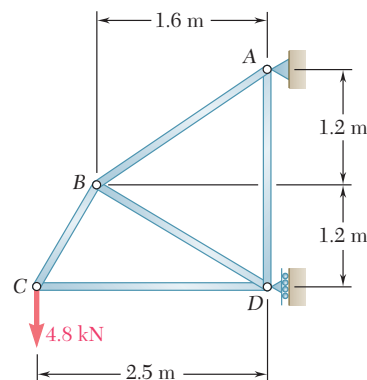


Fig. P11.101 and P11.102

11.103 and 11.104 Each member of the truss shown is made of steel and has the cross-sectional area shown. Using $E = 29 \times 10^6\text{ psi}$, determine the deflection indicated.

11.103 Vertical deflection of joint C .

11.104 Horizontal deflection of joint C .

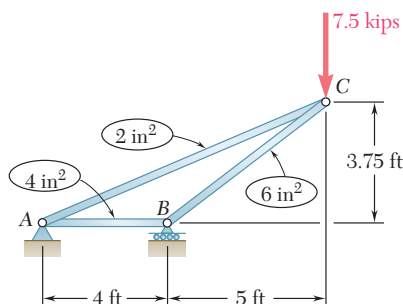


Fig. P11.103 and P11.104

11.105 Two rods AB and BC of the same flexural rigidity EI are welded together at B . For the loading shown, determine (a) the deflection of point C , (b) the slope of member BC at point C .

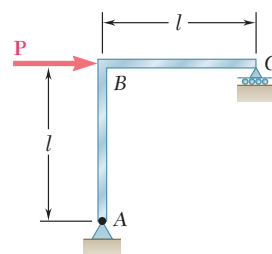


Fig. P11.105

11.106 A uniform rod of flexural rigidity EI is bent and loaded as shown. Determine (a) the horizontal deflection of point D , (b) the slope at point D .

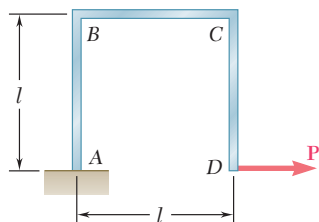


Fig. P11.106 and P11.107

11.107 A uniform rod of flexural rigidity EI is bent and loaded as shown. Determine (a) the vertical deflection of point D , (b) the slope of BC at point C .

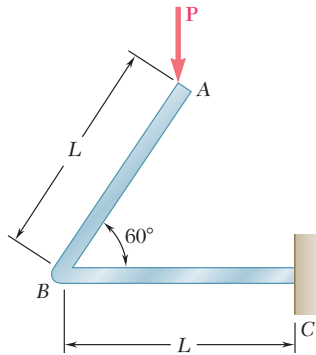


Fig. P11.108

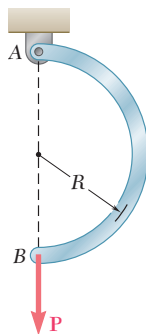


Fig. P11.110

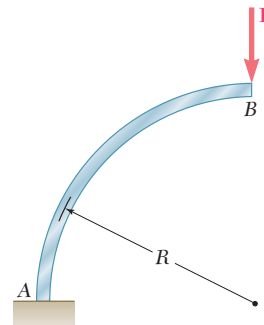


Fig. P11.109

11.108 A uniform rod of flexural rigidity EI is bent and loaded as shown. Determine (a) the vertical deflection of point A, (b) the horizontal deflection of point A.

11.109 For the beam and loading shown and using Castigliano's theorem, determine (a) the horizontal deflection of point B, (b) the vertical deflection of point B.

11.110 For the uniform rod and loading shown and using Castigliano's theorem, determine the deflection of point B.

11.111 through 11.114 Determine the reaction at the roller support and draw the bending-moment diagram for the beam and loading shown.

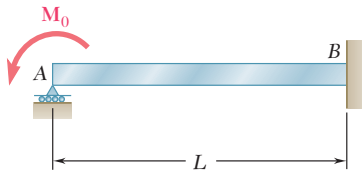


Fig. P11.111

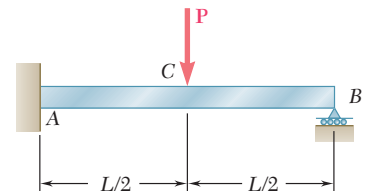


Fig. P11.112

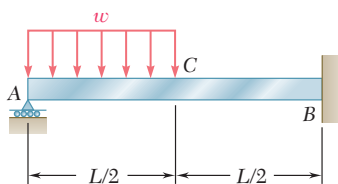


Fig. P11.113

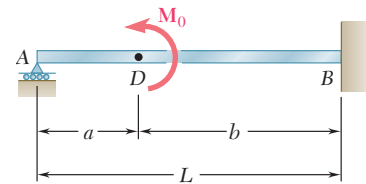


Fig. P11.114

11.115 For the uniform beam and loading shown, determine the reaction at each support.

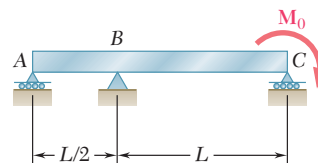


Fig. P11.115

11.116 Determine the reaction at the roller support and draw the bending-moment diagram for the beam and loading shown.

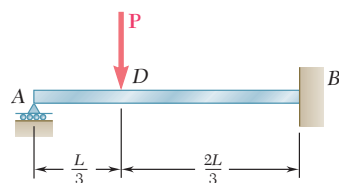


Fig. P11.116

11.117 through 11.120 Three members of the same material and same cross-sectional area are used to support the loading P . Determine the force in member BC .

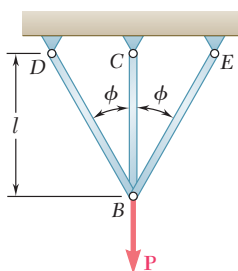


Fig. P11.117

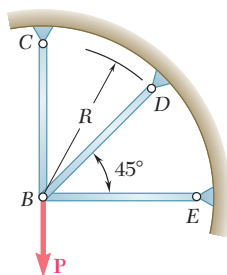


Fig. P11.118

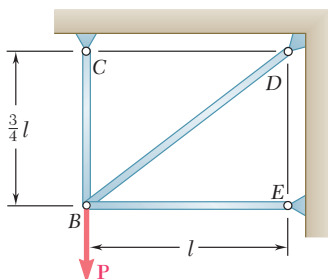


Fig. P11.119

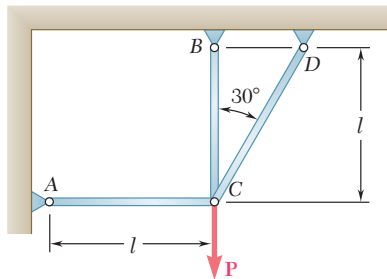


Fig. P11.120

11.121 and 11.122 Knowing that the eight members of the indeterminate truss shown have the same uniform cross-sectional area, determine the force in member AB .

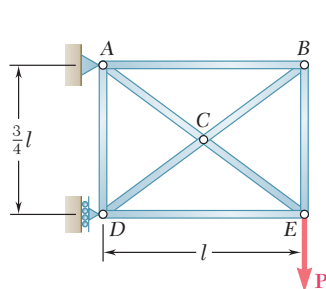


Fig. P11.121

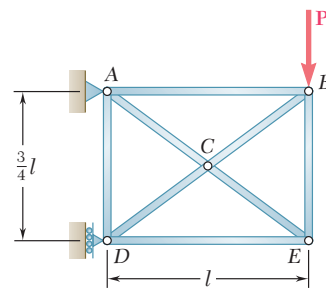


Fig. P11.122

REVIEW AND SUMMARY

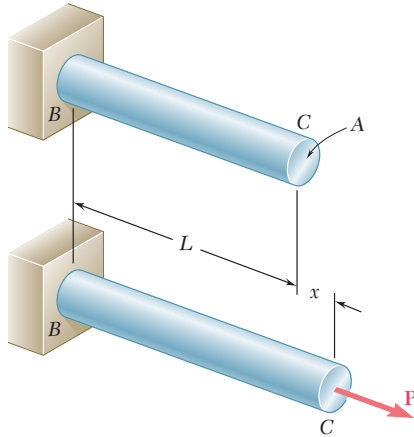


Fig. 11.52

This chapter was devoted to the study of strain energy and to the ways in which it can be used to determine the stresses and deformations in structures subjected to both static and impact loadings.

In Sec. 11.2 we considered a uniform rod subjected to a slowly increasing axial load \mathbf{P} (Fig. 11.52). We noted that the area under

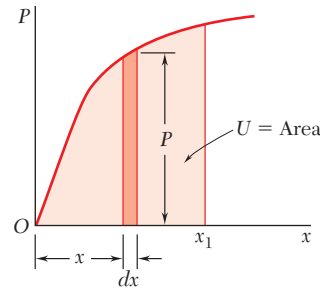


Fig. 11.53

Strain energy

the load-deformation diagram (Fig. 11.53) represents the work done by \mathbf{P} . This work is equal to the *strain energy* of the rod associated with the deformation caused by the load \mathbf{P} :

$$\text{Strain energy} = U = \int_0^{x_1} P \, dx \quad (11.2)$$

Strain-energy density

Since the stress is uniform throughout the rod, we were able to divide the strain energy by the volume of the rod and obtain the strain energy per unit volume, which we defined as the *strain-energy density* of the material [Sec. 11.3]. We found that

$$\text{Strain-energy density} = u = \int_0^{\epsilon_1} \sigma_x \, d\epsilon_x \quad (11.4)$$

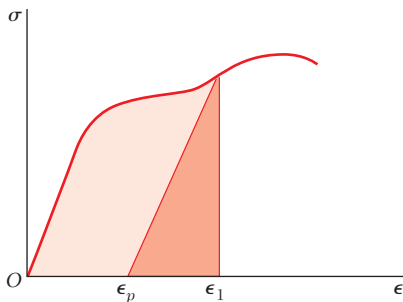


Fig. 11.54

and noted that the strain-energy density is equal to the area under the stress-strain diagram of the material (Fig. 11.54). As we saw in Sec. 11.4, Eq. (11.4) remains valid when the stresses are not uniformly distributed, but the strain-energy density will then vary from point to point. If the material is unloaded, there is a permanent strain ϵ_p and only the strain-energy density corresponding to the triangular area is recovered, the remainder of the energy having been dissipated in the form of heat during the deformation of the material.

Modulus of toughness

The area under the entire stress-strain diagram was defined as the *modulus of toughness* and is a measure of the total energy that can be acquired by the material.

If the normal stress σ remains within the proportional limit of the material, the strain-energy density u is expressed as

$$u = \frac{\sigma^2}{2E}$$

The area under the stress-strain curve from zero strain to the strain ϵ_Y at yield (Fig. 11.55) is referred to as the *modulus of resilience* of the material and represents the energy per unit volume that the material can absorb without yielding. We wrote

$$u_Y = \frac{\sigma_Y^2}{2E} \quad (11.8)$$

In Sec. 11.4 we considered the strain energy associated with *normal stresses*. We saw that if a rod of length L and *variable cross-sectional area* A is subjected at its end to a centric axial load \mathbf{P} , the strain energy of the rod is

$$U = \int_0^L \frac{P^2}{2AE} dx \quad (11.13)$$

If the rod is of *uniform cross section* of area A , the strain energy is

$$U = \frac{P^2 L}{2AE} \quad (11.14)$$

We saw that for a beam subjected to transverse loads (Fig. 11.56) the strain energy associated with the normal stresses is

$$U = \int_0^L \frac{M^2}{2EI} dx \quad (11.17)$$

where M is the bending moment and EI the flexural rigidity of the beam.

The strain energy associated with *shearing stresses* was considered in Sec. 11.5. We found that the strain-energy density for a material in pure shear is

$$u = \frac{\tau_{xy}^2}{2G} \quad (11.19)$$

where τ_{xy} is the shearing stress and G the modulus of rigidity of the material.

For a shaft of length L and uniform cross section subjected at its ends to couples of magnitude T (Fig. 11.57) the strain energy was found to be

$$U = \frac{T^2 L}{2GJ} \quad (11.22)$$

where J is the polar moment of inertia of the cross-sectional area of the shaft.

Modulus of resilience

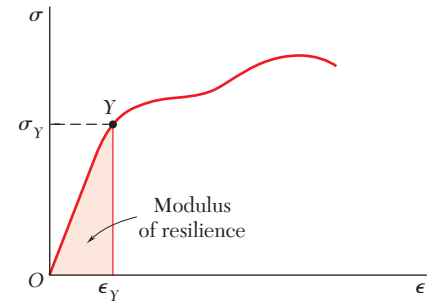


Fig. 11.55

Strain energy under axial load

Strain energy due to bending

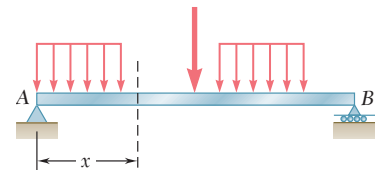


Fig. 11.56

Strain energy due to shearing stresses

Strain energy due to torsion

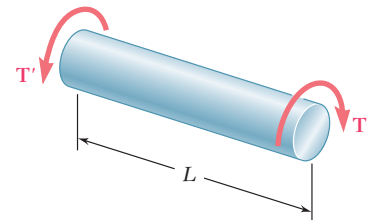


Fig. 11.57

General state of stress

In Sec. 11.6 we considered the strain energy of an elastic isotropic material under a general state of stress and expressed the strain-energy density at a given point in terms of the principal stresses σ_a , σ_b , and σ_c at that point:

$$u = \frac{1}{2E} [\sigma_a^2 + \sigma_b^2 + \sigma_c^2 - 2\nu(\sigma_a\sigma_b + \sigma_b\sigma_c + \sigma_c\sigma_a)] \quad (11.27)$$

The strain-energy density at a given point was divided into two parts: u_v , associated with a change in volume of the material at that point, and u_d , associated with a distortion of the material at the same point. We wrote $u = u_v + u_d$, where

$$u_v = \frac{1 - 2\nu}{6E} (\sigma_a + \sigma_b + \sigma_c)^2 \quad (11.32)$$

and

$$u_d = \frac{1}{12G} [(\sigma_a - \sigma_b)^2 + (\sigma_b - \sigma_c)^2 + (\sigma_c - \sigma_a)^2] \quad (11.33)$$

Using the expression obtained for u_d , we derived the maximum-distortion-energy criterion, which was used in Sec. 7.7 to predict whether a ductile material would yield under a given state of plane stress.

Impact loading

In Sec. 11.7 we considered the *impact loading* of an elastic structure being hit by a mass moving with a given velocity. We assumed that the kinetic energy of the mass is transferred entirely to the structure and defined the *equivalent static load* as the load that would cause the same deformations and stresses as are caused by the impact loading.

Equivalent static load

After discussing several examples, we noted that a structure designed to withstand effectively an impact load should be shaped in such a way that stresses are evenly distributed throughout the structure, and that the material used should have a low modulus of elasticity and a high yield strength [Sec. 11.8].

Members subjected to a single load

The strain energy of structural members subjected to a *single load* was considered in Sec. 11.9. In the case of the beam and loading of Fig. 11.58 we found that the strain energy of the beam is

$$U = \frac{P_1^2 L^3}{6EI} \quad (11.46)$$

Observing that the work done by the load \mathbf{P} is equal to $\frac{1}{2}P_1y_1$, we equated the work of the load and the strain energy of the beam and determined the deflection y_1 at the point of application of the load [Sec. 11.10 and Example 11.10].

The method just described is of limited value, since it is restricted to structures subjected to a single concentrated load and to the determination of the deflection at the point of application of that load. In the remaining sections of the chapter, we presented a

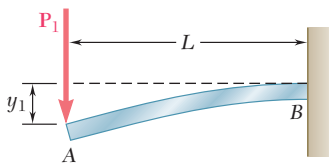


Fig. 11.58

more general method, which can be used to determine deflections at various points of structures subjected to several loads.

In Sec. 11.11 we discussed the strain energy of a structure subjected to several loads, and in Sec. 11.12 introduced *Castigliano's theorem*, which states that the deflection x_j , of the point of application of a load \mathbf{P}_j measured along the line of action of \mathbf{P}_j is equal to the partial derivative of the strain energy of the structure with respect to the load \mathbf{P}_j . We wrote

$$x_j = \frac{\partial U}{\partial P_j} \quad (11.65)$$

We also found that we could use Castigliano's theorem to determine the *slope* of a beam at the point of application of a couple \mathbf{M}_j by writing

$$\theta_j = \frac{\partial U}{\partial M_j} \quad (11.68)$$

and the *angle of twist* in a section of a shaft where a torque \mathbf{T}_j is applied by writing

$$\phi_j = \frac{\partial U}{\partial T_j} \quad (11.69)$$

In Sec. 11.13, Castigliano's theorem was applied to the determination of deflections and slopes at various points of a given structure. The use of “dummy” loads enabled us to include points where no actual load was applied. We also observed that the calculation of a deflection x_j was simplified if the differentiation with respect to the load P_j was carried out before the integration. In the case of a beam, recalling Eq. (11.17), we wrote

$$x_j = \frac{\partial U}{\partial P_j} = \int_0^L \frac{M}{EI} \frac{\partial M}{\partial P_j} dx \quad (11.70)$$

Similarly, for a truss consisting of n members, the deflection x_j at the point of application of the load \mathbf{P}_j was found by writing

$$x_j = \frac{\partial U}{\partial P_j} = \sum_{i=1}^n \frac{F_i L_i}{A_i E} \frac{\partial F_i}{\partial P_j} \quad (11.72)$$

The chapter concluded [Sec. 11.14] with the application of Castigliano's theorem to the analysis of *statically indeterminate structures* [Sample Prob. 11.7, Examples 11.15 and 11.16].

Castigliano's theorem

Indeterminate structures

REVIEW PROBLEMS

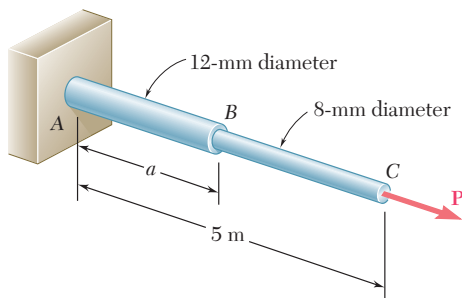


Fig. P11.123

11.123 Rods AB and BC are made of a steel for which the yield strength is $\sigma_Y = 300$ MPa and the modulus of elasticity is $E = 200$ GPa. Determine the maximum strain energy that can be acquired by the assembly without causing permanent deformation when the length a of rod AB is (a) 2 m, (b) 4 m.

11.124 Assuming that the prismatic beam AB has a rectangular cross section, show that for the given loading the maximum value of the strain-energy density in the beam is

$$u_{\max} = \frac{45}{8} \frac{U}{V}$$

where U is the strain energy of the beam and V is its volume.

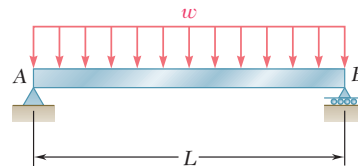


Fig. P11.124

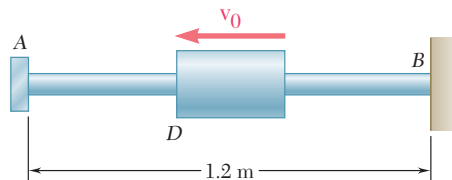


Fig. P11.125

11.125 A 5-kg collar D moves along the uniform rod AB and has a speed $v_0 = 6$ m/s when it strikes a small plate attached to end A of the rod. Using $E = 200$ GPa and knowing that the allowable stress in the rod is 250 MPa, determine the smallest diameter that can be used for the rod.

11.126 A 160-lb diver jumps from a height of 20 in. onto end C of a diving board having the uniform cross section shown. Assuming that the diver's legs remain rigid and using $E = 1.8 \times 10^6$ psi, determine (a) the maximum deflection at point C , (b) the maximum normal stress in the board, (c) the equivalent static load.

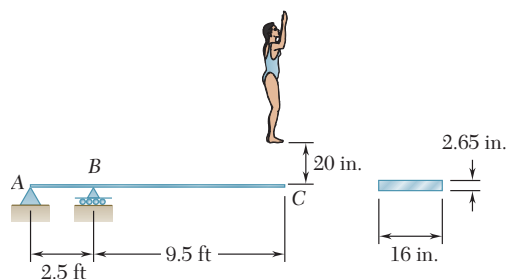


Fig. P11.126

11.127 A block of weight W is placed in contact with a beam at some given point D and released. Show that the resulting maximum deflection at point D is twice as large as the deflection due to a static load W applied at D .

- 11.128** The 12-mm-diameter steel rod ABC has been bent into the shape shown. Knowing that $E = 200$ GPa and $G = 77.2$ GPa, determine the deflection of end C caused by the 150-N force.

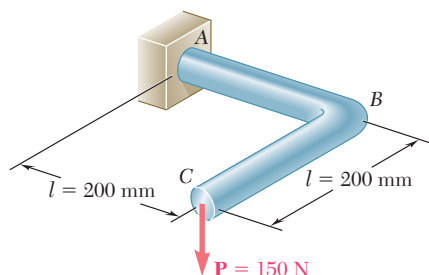


Fig. P11.128

- 11.129** Two steel shafts, each of 0.75-in diameter, are connected by the gears shown. Knowing that $G = 11.2 \times 10^6$ psi and that shaft DF is fixed at F , determine the angle through which end A rotates when a 750-lb · in. torque is applied at A . (Ignore the strain energy due to the bending of the shafts.)

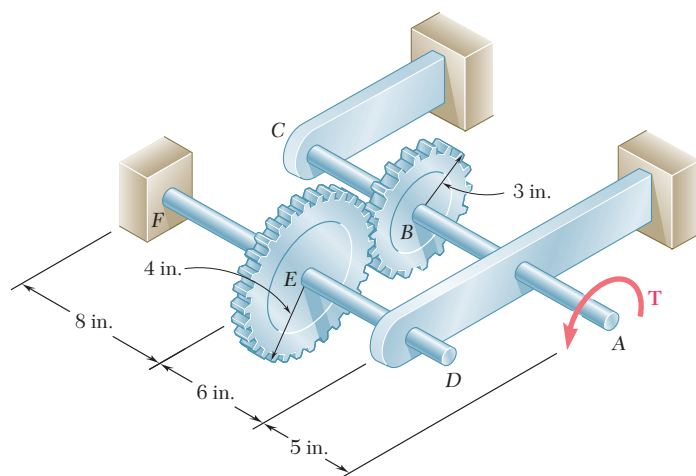


Fig. P11.129

- 11.130** Each member of the truss shown is made of steel and has a uniform cross-sectional area of 3 in^2 . Using $E = 29 \times 10^6$ psi, determine the vertical deflection of joint A caused by the application of the 24-kip load.

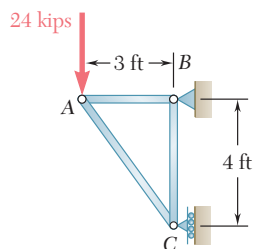


Fig. P11.130

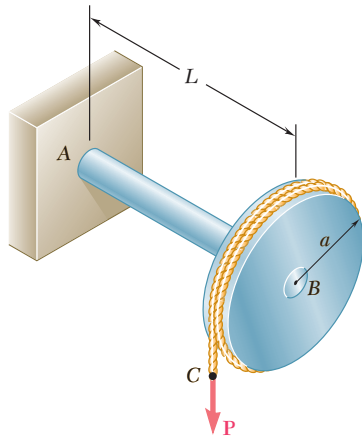


Fig. P11.131

- 11.131** A disk of radius a has been welded to end B of the solid steel shaft AB . A cable is then wrapped around the disk and a vertical force \mathbf{P} is applied to end C of the cable. Knowing that the radius of the shaft is r and neglecting the deformations of the disk and of the cable, show that the deflection of point C caused by the application of \mathbf{P} is

$$\delta_C = \frac{PL^3}{3EI} \left(1 + 1.5 \frac{Er^2}{GL^2} \right)$$

- 11.132** Three rods, each of the same flexural rigidity EI , are welded to form the frame $ABCD$. For the loading shown, determine the angle formed by the frame at point D .

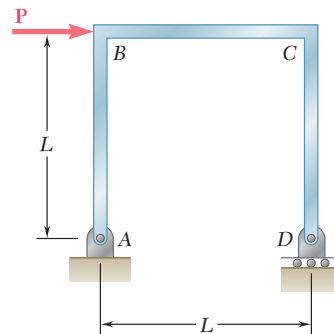


Fig. P11.132

- 11.133** The steel bar ABC has a square cross section of side 0.75 in. and is subjected to a 50-lb load \mathbf{P} . Using $E = 29 \times 10^6$ psi for rod BD and the bar, determine the deflection of point C .

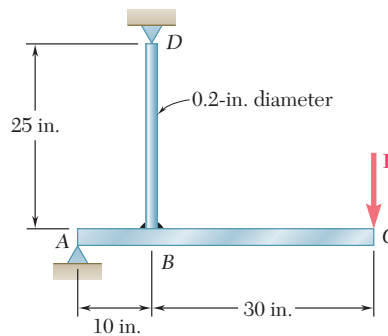


Fig. P11.133

- 11.134** For the uniform beam and loading shown, determine the reaction at each support.

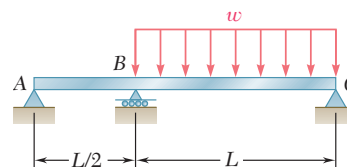


Fig. P11.134

COMPUTER PROBLEMS

The following problems are designed to be solved with a computer.

11.C1 A rod consisting of n elements, each of which is homogeneous and of uniform cross section, is subjected to a load \mathbf{P} applied at its free end. The length of element i is denoted by L_i and its diameter by d_i . (a) Denoting by E the modulus of elasticity of the material used in the rod, write a computer program that can be used to determine the strain energy acquired by the rod and the deformation measured at its free end. (b) Use this program to determine the strain energy and deformation for the rods of Probs. 11.9 and 11.10.

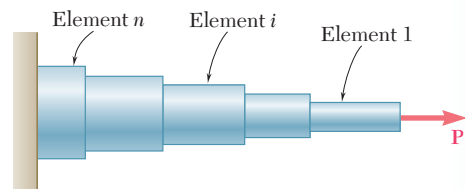


Fig. P11.C1

11.C2 Two 0.75×6 -in. cover plates are welded to a $W8 \times 18$ rolled-steel beam as shown. The 1500-lb block is to be dropped from a height $h = 2$ in. onto the beam. (a) Write a computer program to calculate the maximum normal stress on transverse sections just to the left of D and at the center of the beam for values of a from 0 to 60 in. using 5-in. increments. (b) From the values considered in part a , select the distance a for which the maximum normal stress is as small as possible. Use $E = 29 \times 10^6$ psi.

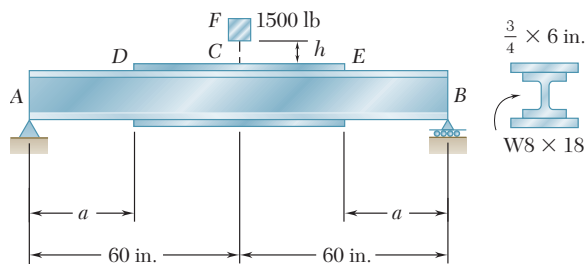


Fig. P11.C2

11.C3 The 16-kg block D is dropped from a height h onto the free end of the steel bar AB . For the steel used $\sigma_{\text{all}} = 120$ MPa and $E = 200$ GPa. (a) Write a computer program to calculate the maximum allowable height h for values of the length L from 100 mm to 1.2 m, using 100-mm increments. (b) From the values considered in part a , select the length corresponding to the largest allowable height.

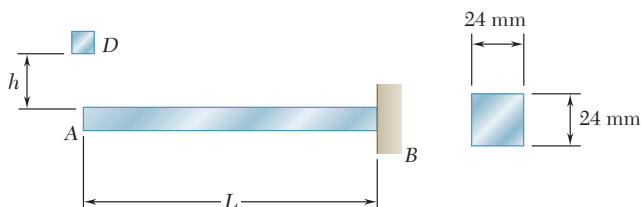


Fig. P11.C3

11.C4 The block D of mass $m = 8$ kg is dropped from a height $h = 750$ mm onto the rolled-steel beam AB . Knowing that $E = 200$ GPa, write a computer program to calculate the maximum deflection of point E and the maximum normal stress in the beam for values of a from 100 to 900 mm, using 100-mm increments.

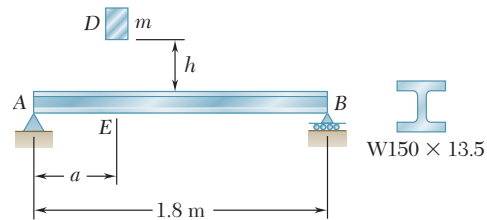


Fig. P11.C4

11.C5 The steel rods AB and BC are made of a steel for which $\sigma_Y = 300$ MPa and $E = 200$ GPa. (a) Write a computer program to calculate for values of a from 0 to 6 m, using 1-m increments, the maximum strain energy that can be acquired by the assembly without causing any permanent deformation. (b) For each value of a considered, calculate the diameter of a uniform rod of length 6 m and of the same mass as the original assembly, and the maximum strain energy that could be acquired by this uniform rod without causing permanent deformation.

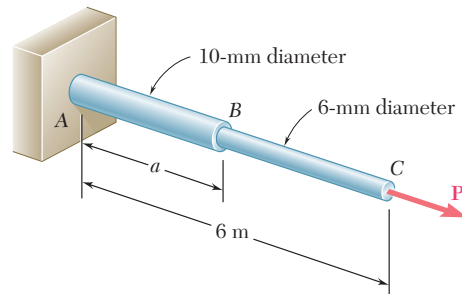


Fig. P11.C5

11.C6 A 160-lb diver jumps from a height of 20 in. onto end C of a diving board having the uniform cross section shown. Write a computer program to calculate for values of a from 10 to 50 in., using 10-in. increments, (a) the maximum deflection of point C , (b) the maximum bending moment in the board, (c) the equivalent static load. Assume that the diver's legs remain rigid and use $E = 1.8 \times 10^6$ psi.

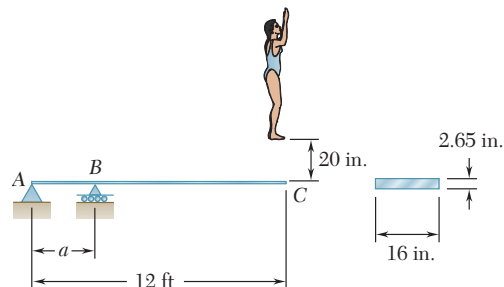


Fig. P11.C6

Appendices

- APPENDIX A** Moments of Areas A2
- APPENDIX B** Typical Properties of Selected Materials Used in Engineering A12
- APPENDIX C** Properties of Rolled-Steel Shapes† A16
- APPENDIX D** Beam Deflections and Slopes A28
- APPENDIX E** Fundamentals of Engineering Examination A29

†Courtesy of the American Institute of Steel Construction, Chicago, Illinois.

Appendix A

Moments of Areas

A.1 FIRST MOMENT OF AN AREA; CENTROID OF AN AREA

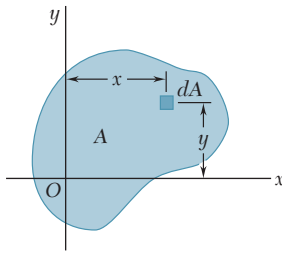


Fig. A.1

Consider an area A located in the xy plane (Fig. A.1). Denoting by x and y the coordinates of an element of area dA , we define the *first moment of the area A with respect to the x axis* as the integral

$$Q_x = \int_A y \, dA \quad (\text{A.1})$$

Similarly, the *first moment of the area A with respect to the y axis* is defined as the integral

$$Q_y = \int_A x \, dA \quad (\text{A.2})$$

We note that each of these integrals may be positive, negative, or zero, depending on the position of the coordinate axes. If SI units are used, the first moments Q_x and Q_y are expressed in m^3 or mm^3 ; if U.S. customary units are used, they are expressed in ft^3 or in^3 .

The *centroid of the area A* is defined as the point C of coordinates \bar{x} and \bar{y} (Fig. A.2), which satisfy the relations

$$\int_A x \, dA = A\bar{x} \quad \int_A y \, dA = A\bar{y} \quad (\text{A.3})$$

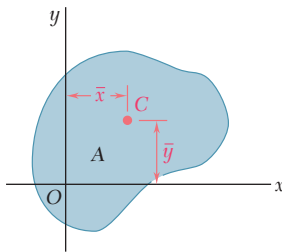


Fig. A.2

Comparing Eqs. (A.1) and (A.2) with Eqs. (A.3), we note that the first moments of the area A can be expressed as the products of the area and of the coordinates of its centroid:

$$Q_x = A\bar{y} \quad Q_y = A\bar{x} \quad (\text{A.4})$$

When an area possesses an *axis of symmetry*, the first moment of the area with respect to that axis is zero. Indeed, considering the area A of Fig. A.3, which is symmetric with respect to the y axis, we observe that to every element of area dA of abscissa x corresponds an element of area dA' of abscissa $-x$. It follows that the integral in Eq. (A.2) is zero and, thus, that $Q_y = 0$. It also follows from the first of the relations (A.3) that $\bar{x} = 0$. Thus, if an area A possesses an axis of symmetry, its centroid C is located on that axis.

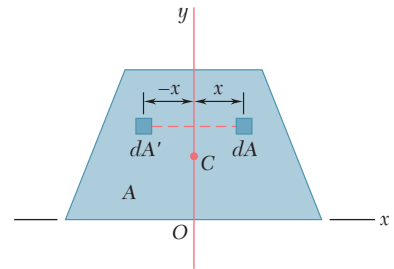


Fig. A.3

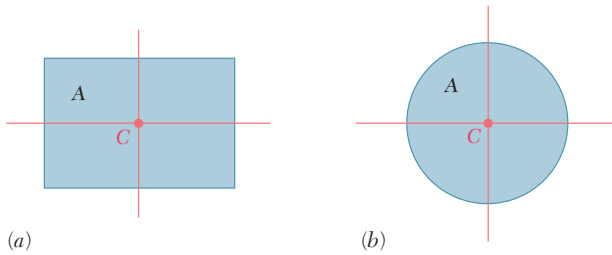


Fig. A.4

Since a rectangle possesses two axes of symmetry (Fig. A.4a), the centroid C of a rectangular area coincides with its geometric center. Similarly, the centroid of a circular area coincides with the center of the circle (Fig. A.4b).

When an area possesses a *center of symmetry* O , the first moment of the area about any axis through O is zero. Indeed, considering the area A of Fig. A.5, we observe that to every element of area dA of coordinates x and y corresponds an element of area dA' of coordinates $-x$ and $-y$. It follows that the integrals in Eqs. (A.1) and (A.2) are both zero, and that $Q_x = Q_y = 0$. It also follows from Eqs. (A.3) that $\bar{x} = \bar{y} = 0$, that is, the centroid of the area coincides with its center of symmetry.

When the centroid C of an area can be located by symmetry, the first moment of that area with respect to any given axis can be readily obtained from Eqs. (A.4). For example, in the case of the rectangular area of Fig. A.6, we have

$$Q_x = A\bar{y} = (bh)(\frac{1}{2}h) = \frac{1}{2}bh^2$$

and

$$Q_y = A\bar{x} = (bh)(\frac{1}{2}b) = \frac{1}{2}b^2h$$

In most cases, however, it is necessary to perform the integrations indicated in Eqs. (A.1) through (A.3) to determine the first moments and the centroid of a given area. While each of the integrals involved is actually a double integral, it is possible in many applications to select elements of area dA in the shape of thin horizontal or vertical strips, and thus to reduce the computations to integrations in a single variable. This is illustrated in Example A.01. Centroids of common geometric shapes are indicated in a table inside the back cover of this book.

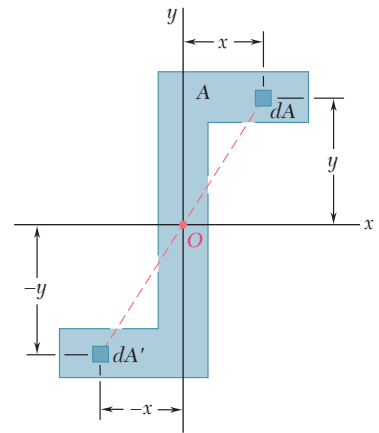


Fig. A.5

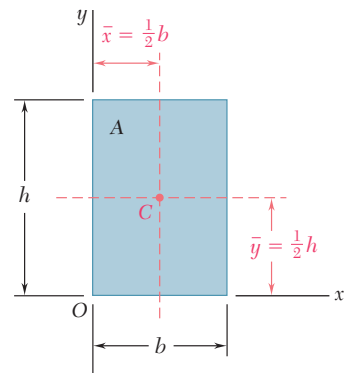


Fig. A.6

EXAMPLE A.01

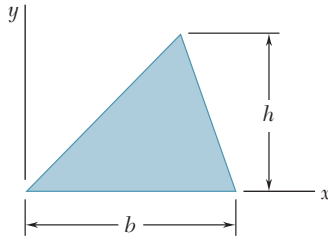


Fig. A.7

For the triangular area of Fig. A.7, determine (a) the first moment Q_x of the area with respect to the x axis, (b) the ordinate \bar{y} of the centroid of the area.

(a) First Moment Q_x . We select as an element of area a horizontal strip of length u and thickness dy , and note that all the points within the element are at the same distance y from the x axis (Fig. A.8). From similar triangles, we have

$$\frac{u}{b} = \frac{h-y}{h} \quad u = b \frac{h-y}{h}$$

and

$$dA = u \, dy = b \frac{h-y}{h} \, dy$$

The first moment of the area with respect to the x axis is

$$\begin{aligned} Q_x &= \int_A y \, dA = \int_0^h y b \frac{h-y}{h} \, dy = \frac{b}{h} \int_0^h (hy - y^2) \, dy \\ &= \frac{b}{h} \left[h \frac{y^2}{2} - \frac{y^3}{3} \right]_0^h \quad Q_x = \frac{1}{6} b h^2 \end{aligned}$$

(b) Ordinate of Centroid. Recalling the first of Eqs. (A.4) and observing that $A = \frac{1}{2}bh$, we have

$$\begin{aligned} Q_x &= A \bar{y} \quad \frac{1}{6} b h^2 = \left(\frac{1}{2} b h \right) \bar{y} \\ \bar{y} &= \frac{1}{3} h \end{aligned}$$

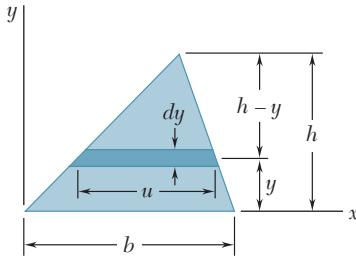
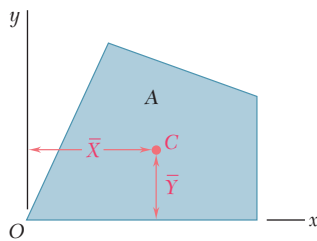


Fig. A.8

A.2 DETERMINATION OF THE FIRST MOMENT AND CENTROID OF A COMPOSITE AREA



Consider an area A , such as the trapezoidal area shown in Fig. A.9, which may be divided into simple geometric shapes. As we saw in the preceding section, the first moment Q_x of the area with respect to the x axis is represented by the integral $\int y \, dA$, which extends over the entire area A . Dividing A into its component parts A_1 , A_2 , A_3 , we write

$$Q_x = \int_A y \, dA = \int_{A_1} y \, dA + \int_{A_2} y \, dA + \int_{A_3} y \, dA$$

or, recalling the second of Eqs. (A.3),

$$Q_x = A_1 \bar{y}_1 + A_2 \bar{y}_2 + A_3 \bar{y}_3$$

where \bar{y}_1 , \bar{y}_2 , and \bar{y}_3 represent the ordinates of the centroids of the component areas. Extending this result to an arbitrary number of component areas, and noting that a similar expression may be obtained for Q_y , we write

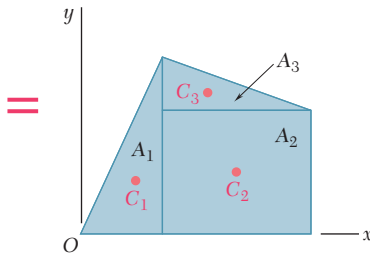


Fig. A.9

$$Q_x = \sum A_i \bar{y}_i \quad Q_y = \sum A_i \bar{x}_i \quad (\text{A.5})$$

To obtain the coordinates \bar{X} and \bar{Y} of the centroid C of the composite area A , we substitute $Q_x = A\bar{Y}$ and $Q_y = A\bar{X}$ into Eqs. (A.5). We have

$$A\bar{Y} = \sum_i A_i \bar{y}_i \quad A\bar{X} = \sum_i A_i \bar{x}_i$$

Solving for \bar{X} and \bar{Y} and recalling that the area A is the sum of the component areas A_i , we write

$$\bar{X} = \frac{\sum_i A_i \bar{x}_i}{\sum_i A_i} \quad \bar{Y} = \frac{\sum_i A_i \bar{y}_i}{\sum_i A_i} \quad (\text{A.6})$$

Locate the centroid C of the area A shown in Fig. A.10.

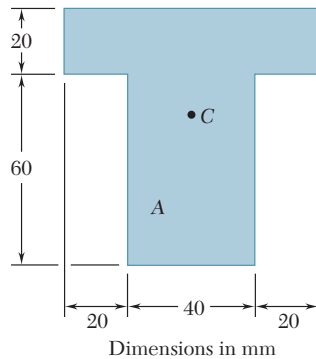


Fig. A.10

Selecting the coordinate axes shown in Fig. A.11, we note that the centroid C must be located on the y axis, since this axis is an axis of symmetry; thus, $\bar{X} = 0$.

Dividing A into its component parts A_1 and A_2 , we use the second of Eqs. (A.6) to determine the ordinate \bar{Y} of the centroid. The actual computation is best carried out in tabular form.

	Area, mm ²	\bar{y}_i , mm	$A_i \bar{y}_i$, mm ³
A_1	$(20)(80) = 1600$	70	112×10^3
A_2	$(40)(60) = 2400$	30	72×10^3
	$\sum_i A_i = 4000$		$\sum_i A_i \bar{y}_i = 184 \times 10^3$

$$\bar{Y} = \frac{\sum_i A_i \bar{y}_i}{\sum_i A_i} = \frac{184 \times 10^3 \text{ mm}^3}{4 \times 10^3 \text{ mm}^2} = 46 \text{ mm}$$

EXAMPLE A.02

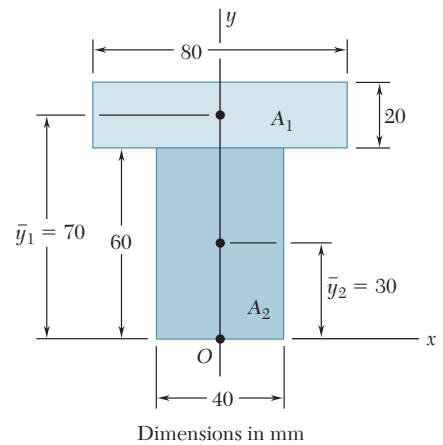


Fig. A.11

EXAMPLE A.03

Referring to the area A of Example A.02, we consider the horizontal x' axis through its centroid C . (Such an axis is called a *centroidal axis*.) Denoting by A' the portion of A located above that axis (Fig. A.12), determine the first moment of A' with respect to the x' axis.

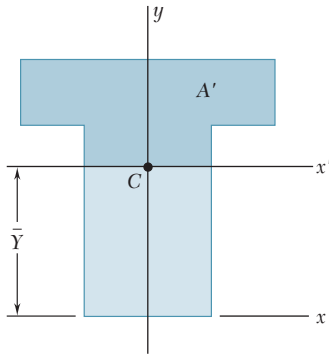


Fig. A.12

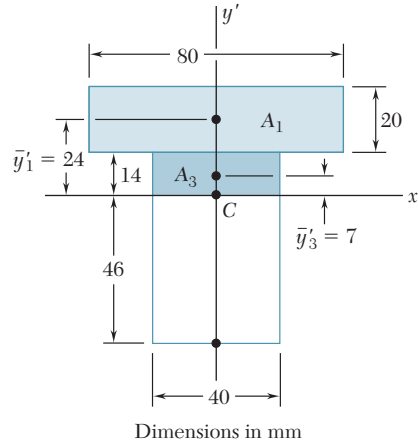


Fig. A.13

Solution. We divide the area A' into its components A_1 and A_3 (Fig. A.13). Recalling from Example A.02 that C is located 46 mm above the lower edge of A , we determine the ordinates \bar{y}'_1 and \bar{y}'_3 of A_1 and A_3 and express the first moment $Q'_{x'}$ of A' with respect to x' as follows:

$$\begin{aligned} Q'_{x'} &= A_1 \bar{y}'_1 + A_3 \bar{y}'_3 \\ &= (20 \times 80)(24) + (14 \times 40)(7) = 42.3 \times 10^3 \text{ mm}^3 \end{aligned}$$

Alternative Solution. We first note that since the centroid C of A is located on the x' axis, the first moment $Q_{x'}$ of the *entire* area A with respect to that axis is zero:

$$Q_{x'} = A \bar{y}' = A(0) = 0$$

Denoting by A'' the portion of A located below the x' axis and by $Q''_{x'}$ its first moment with respect to that axis, we have therefore

$$Q_{x'} = Q'_{x'} + Q''_{x'} = 0 \quad \text{or} \quad Q'_{x'} = -Q''_{x'}$$

which shows that the first moments of A' and A'' have the same magnitude and opposite signs. Referring to Fig. A.14, we write

$$Q''_{x'} = A_4 \bar{y}'_4 = (40 \times 46)(-23) = -42.3 \times 10^3 \text{ mm}^3$$

and

$$Q'_{x'} = -Q''_{x'} = +42.3 \times 10^3 \text{ mm}^3$$

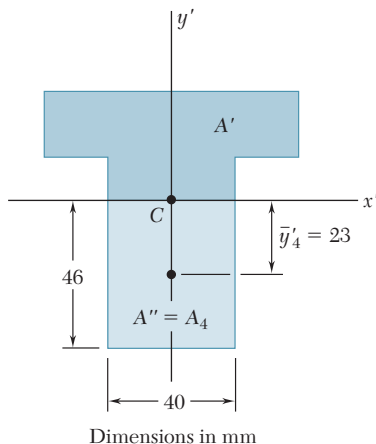


Fig. A.14

A.3 SECOND MOMENT, OR MOMENT OF INERTIA, OF AN AREA; RADIUS OF GYRATION

Consider again an area A located in the xy plane (Fig. A.1) and the element of area dA of coordinates x and y . The *second moment*, or *moment of inertia*, of the area A with respect to the x axis, and the second moment, or moment of inertia, of A with respect to the y axis are defined, respectively, as

$$I_x = \int_A y^2 dA \quad I_y = \int_A x^2 dA \quad (\text{A.7})$$

These integrals are referred to as *rectangular moments of inertia*, since they are computed from the rectangular coordinates of the element dA . While each integral is actually a double integral, it is possible in many applications to select elements of area dA in the shape of thin horizontal or vertical strips, and thus reduce the computations to integrations in a single variable. This is illustrated in Example A.04.

We now define the *polar moment of inertia* of the area A with respect to point O (Fig. A.15) as the integral

$$J_O = \int_A \rho^2 dA \quad (\text{A.8})$$

where ρ is the distance from O to the element dA . While this integral is again a double integral, it is possible in the case of a circular area to select elements of area dA in the shape of thin circular rings, and thus reduce the computation of J_O to a single integration (see Example A.05).

We note from Eqs. (A.7) and (A.8) that the moments of inertia of an area are positive quantities. If SI units are used, moments of inertia are expressed in m^4 or mm^4 ; if U.S. customary units are used, they are expressed in ft^4 or in^4 .

An important relation may be established between the polar moment of inertia J_O of a given area and the rectangular moments of inertia I_x and I_y of the same area. Noting that $\rho^2 = x^2 + y^2$, we write

$$J_O = \int_A \rho^2 dA = \int_A (x^2 + y^2) dA = \int_A y^2 dA + \int_A x^2 dA$$

or

$$J_O = I_x + I_y \quad (\text{A.9})$$

The *radius of gyration* of an area A with respect to the x axis is defined as the quantity r_x , that satisfies the relation

$$I_x = r_x^2 A \quad (\text{A.10})$$

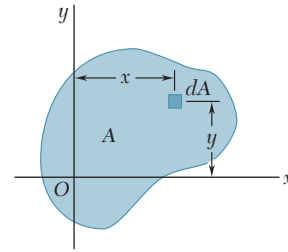


Fig. A.1 (repeated)

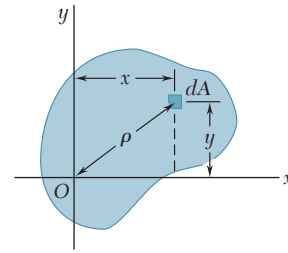


Fig. A.15

where I_x is the moment of inertia of A with respect to the x axis. Solving Eq. (A.10) for r_x , we have

$$r_x = \sqrt{\frac{I_x}{A}} \quad (\text{A.11})$$

In a similar way, we define the radii of gyration with respect to the y axis and the origin O . We write

$$I_y = r_y^2 A \quad r_y = \sqrt{\frac{I_y}{A}} \quad (\text{A.12})$$

$$J_O = r_O^2 A \quad r_O = \sqrt{\frac{J_O}{A}} \quad (\text{A.13})$$

Substituting for J_O , I_x , and I_y in terms of the corresponding radii of gyration in Eq. (A.9), we observe that

$$r_O^2 = r_x^2 + r_y^2 \quad (\text{A.14})$$

EXAMPLE A.04

For the rectangular area of Fig. A.16, determine (a) the moment of inertia I_x of the area with respect to the centroidal x axis, (b) the corresponding radius of gyration r_x .

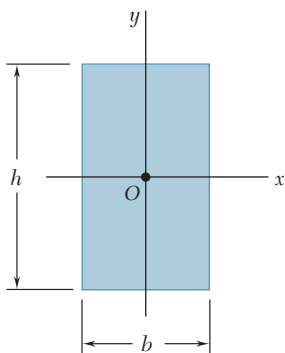


Fig. A.16

(a) Moment of Inertia I_x . We select as an element of area a horizontal strip of length b and thickness dy (Fig. A.17). Since all the points within the strip are at the same distance y from the x axis, the moment of inertia of the strip with respect to that axis is

$$dI_x = y^2 dA = y^2(b dy)$$

Integrating from $y = -h/2$ to $y = +h/2$, we write

$$\begin{aligned} I_x &= \int_A y^2 dA = \int_{-h/2}^{+h/2} y^2(b dy) = \frac{1}{3}b[y^3]_{-h/2}^{+h/2} \\ &= \frac{1}{3}b\left(\frac{h^3}{8} + \frac{h^3}{8}\right) \end{aligned}$$

or

$$I_x = \frac{1}{12}bh^3$$

(b) Radius of Gyration r_x . From Eq. (A.10), we have

$$I_x = r_x^2 A \quad \frac{1}{12}bh^3 = r_x^2(bh)$$

and, solving for r_x ,

$$r_x = h/\sqrt{12}$$

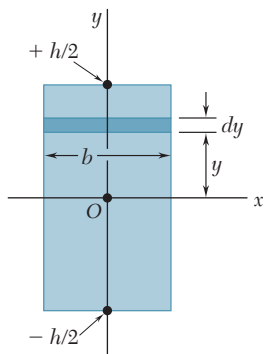


Fig. A.17

For the circular area of Fig. A.18, determine (a) the polar moment of inertia J_O , (b) the rectangular moments of inertia I_x and I_y .

(a) Polar Moment of Inertia. We select as an element of area a ring of radius ρ and thickness $d\rho$ (Fig. A.19). Since all the points within the ring are at the same distance ρ from the origin O , the polar moment of inertia of the ring is

$$dJ_O = \rho^2 dA = \rho^2(2\pi\rho d\rho)$$

Integrating in ρ from 0 to c , we write

$$J_O = \int_A \rho^2 dA = \int_0^c \rho^2(2\pi\rho d\rho) = 2\pi \int_0^c \rho^3 d\rho$$

$$J_O = \frac{1}{2}\pi c^4$$

(b) Rectangular Moments of Inertia. Because of the symmetry of the circular area, we have $I_x = I_y$. Recalling Eq. (A.9), we write

$$J_O = I_x + I_y = 2I_x \quad \frac{1}{2}\pi c^4 = 2I_x$$

and, thus,

$$I_x = I_y = \frac{1}{4}\pi c^4$$

EXAMPLE A.05

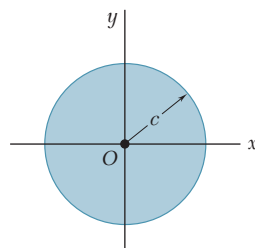


Fig. A.18

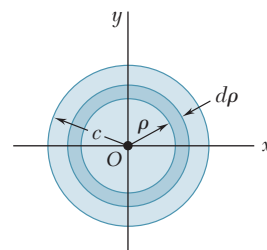


Fig. A.19

The results obtained in the preceding two examples, and the moments of inertia of other common geometric shapes, are listed in a table inside the back cover of this book.

A.4 PARALLEL-AXIS THEOREM

Consider the moment of inertia I_x of an area A with respect to an arbitrary x axis (Fig. A.20). Denoting by y the distance from an element of area dA to that axis, we recall from Sec. A.3 that

$$I_x = \int_A y^2 dA$$

Let us now draw the *centroidal* x' axis, i.e., the axis parallel to the x axis which passes through the centroid C of the area. Denoting by y' the distance from the element dA to that axis, we write $y = y' + d$, where d is the distance between the two axes. Substituting for y in the integral representing I_x , we write

$$I_x = \int_A y^2 dA = \int_A (y' + d)^2 dA$$

$$I_x = \int_A y'^2 dA + 2d \int_A y' dA + d^2 \int_A dA \quad (\text{A.15})$$

The first integral in Eq. (A.15) represents the moment of inertia $\bar{I}_{x'}$ of the area with respect to the centroidal x' axis. The second integral

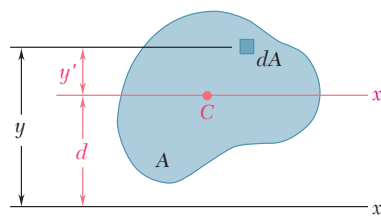


Fig. A.20

represents the first moment $Q_{x'}$ of the area with respect to the x' axis and is equal to zero, since the centroid C of the area is located on that axis. Indeed, we recall from Sec. A.1 that

$$Q_{x'} = A\bar{y}' = A(0) = 0$$

Finally, we observe that the last integral in Eq. (A.15) is equal to the total area A . We have, therefore,

$$I_x = \bar{I}_{x'} + Ad^2 \quad (\text{A.16})$$

This formula expresses that the moment of inertia I_x of an area with respect to an arbitrary x axis is equal to the moment of inertia $\bar{I}_{x'}$ of the area with respect to the centroidal x' axis parallel to the x axis, *plus* the product Ad^2 of the area A and of the square of the distance d between the two axes. This result is known as the *parallel-axis theorem*. It makes it possible to determine the moment of inertia of an area with respect to a given axis, when its moment of inertia with respect to a centroidal axis of the same direction is known. Conversely, it makes it possible to determine the moment of inertia $\bar{I}_{x'}$ of an area A with respect to a centroidal axis x' , when the moment of inertia I_x of A with respect to a parallel axis is known, by *subtracting* from I_x the product Ad^2 . We should note that the parallel-axis theorem may be used *only if one of the two axes involved is a centroidal axis*.

A similar formula may be derived, which relates the polar moment of inertia J_O of an area with respect to an arbitrary point O and the polar moment of inertia \bar{J}_C of the same area with respect to its centroid C . Denoting by d the distance between O and C , we write

$$J_O = \bar{J}_C + Ad^2 \quad (\text{A.17})$$

A.5 DETERMINATION OF THE MOMENT OF INERTIA OF A COMPOSITE AREA

Consider a composite area A made of several component parts A_1 , A_2 and so forth. Since the integral representing the moment of inertia of A may be subdivided into integrals extending over A_1 , A_2 and so forth, the moment of inertia of A with respect to a given axis will be obtained by adding the moments of inertia of the areas A_1 , A_2 , and so forth, with respect to the same axis. The moment of inertia of an area made of several of the common shapes shown in the table inside the back cover of this book may thus be obtained from the formulas given in that table. Before adding the moments of inertia of the component areas, however, the parallel-axis theorem should be used to transfer each moment of inertia to the desired axis. This is shown in Example A.06.

Determine the moment of inertia \bar{I}_x of the area shown with respect to the centroidal x axis (Fig. A.21).

EXAMPLE A.06

Location of Centroid. The centroid C of the area must first be located. However, this has already been done in Example A.02 for the given area. We recall from that example that C is located 46 mm above the lower edge of the area A .

Computation of Moment of Inertia. We divide the area A into the two rectangular areas A_1 and A_2 (Fig. A.22), and compute the moment of inertia of each area with respect to the x axis.

Rectangular Area A_1 . To obtain the moment of inertia $(I_x)_1$ of A_1 with respect to the x axis, we first compute the moment of inertia of A_1 with respect to its own centroidal axis x' . Recalling the formula derived in part *a* of Example A.04 for the centroidal moment of inertia of a rectangular area, we have

$$(\bar{I}_{x'})_1 = \frac{1}{12}bh^3 = \frac{1}{12}(80 \text{ mm})(20 \text{ mm})^3 = 53.3 \times 10^3 \text{ mm}^4$$

Using the parallel-axis theorem, we transfer the moment of inertia of A_1 from its centroidal axis x' to the parallel axis x :

$$\begin{aligned}(I_x)_1 &= (\bar{I}_{x'})_1 + A_1 d_1^2 = 53.3 \times 10^3 + (80 \times 20)(24)^2 \\ &= 975 \times 10^3 \text{ mm}^4\end{aligned}$$

Rectangular Area A_2 . Computing the moment of inertia of A_2 with respect to its centroidal axis x'' , and using the parallel-axis theorem to transfer it to the x axis, we have

$$\begin{aligned}(\bar{I}_{x''})_2 &= \frac{1}{12}bh^3 = \frac{1}{12}(40)(60)^3 = 720 \times 10^3 \text{ mm}^4 \\ (I_x)_2 &= (\bar{I}_{x''})_2 + A_2 d_2^2 = 720 \times 10^3 + (40 \times 60)(16)^2 \\ &= 1334 \times 10^3 \text{ mm}^4\end{aligned}$$

Entire Area A . Adding the values computed for the moments of inertia of A_1 and A_2 with respect to the x axis, we obtain the moment of inertia \bar{I}_x of the entire area:

$$\begin{aligned}\bar{I}_x &= (I_x)_1 + (I_x)_2 = 975 \times 10^3 + 1334 \times 10^3 \\ \bar{I}_x &= 2.31 \times 10^6 \text{ mm}^4\end{aligned}$$

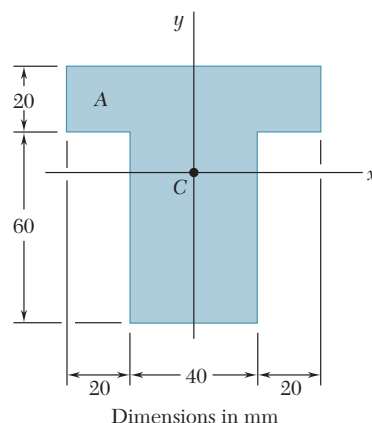


Fig. A.21

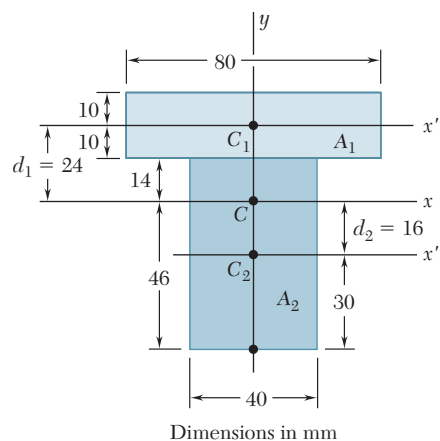


Fig. A.22

A12

APPENDIX B Typical Properties of Selected Materials Used in Engineering^{1,5} (U.S. Customary Units)

		Ultimate Strength			Yield Strength ³		Modulus of Elasticity, 10 ⁶ psi	Modulus of Rigidity, 10 ⁶ psi	Coefficient of Thermal Expansion, 10 ⁻⁶ /°F	Ductility, Percent Elongation in 2 in.
		Tension, ksi	Compression, ² ksi	Shear, ksi	Tension, ksi	Shear, ksi				
Material	Specific Weight, lb/in ³									
Steel										
Structural (ASTM-A36)	0.284	58			36	21	29	11.2	6.5	21
High-strength-low-alloy										
ASTM-A709 Grade 50	0.284	65			50		29	11.2	6.5	21
ASTM-A913 Grade 65	0.284	80			65		29	11.2	6.5	17
ASTM-A992 Grade 50	0.284	65			50		29	11.2	6.5	21
Quenched & tempered										
ASTM-A709 Grade 100	0.284	110			100		29	11.2	6.5	18
Stainless, AISI 302										
Cold-rolled	0.286	125			75		28	10.8	9.6	12
Annealed	0.286	95			38	22	28	10.8	9.6	50
Reinforcing Steel										
Medium strength	0.283	70			40		29	11	6.5	
High strength	0.283	90			60		29	11	6.5	
Cast Iron										
Gray Cast Iron										
4.5% C, ASTM A-48	0.260	25	95	35			10	4.1	6.7	0.5
Malleable Cast Iron										
2% C, 1% Si, ASTM A-47	0.264	50	90	48	33		24	9.3	6.7	10
Aluminum										
Alloy 1100-H14										
(99% Al)	0.098	16		10	14	8	10.1	3.7	13.1	9
Alloy 2014-T6	0.101	66		40	58	33	10.9	3.9	12.8	13
Alloy 2024-T4	0.101	68		41	47		10.6		12.9	19
Alloy 5456-H116	0.095	46		27	33	19	10.4		13.3	16
Alloy 6061-T6	0.098	38		24	35	20	10.1	3.7	13.1	17
Alloy 7075-T6	0.101	83		48	73		10.4	4	13.1	11
Copper										
Oxygen-free copper										
(99.9% Cu)										
Annealed	0.322	32		22	10		17	6.4	9.4	45
Hard-drawn	0.322	57		29	53		17	6.4	9.4	4
Yellow Brass										
(65% Cu, 35% Zn)										
Cold-rolled	0.306	74		43	60	36	15	5.6	11.6	8
Annealed	0.306	46		32	15	9	15	5.6	11.6	65
Red Brass										
(85% Cu, 15% Zn)										
Cold-rolled	0.316	85		46	63		17	6.4	10.4	3
Annealed	0.316	39		31	10		17	6.4	10.4	48
Tin bronze	0.318	45			21		14		10	30
(88 Cu, 8Sn, 4Zn)										
Manganese bronze	0.302	95			48		15		12	20
(63 Cu, 25 Zn, 6 Al, 3 Mn, 3 Fe)										
Aluminum bronze	0.301	90	130		40		16	6.1	9	6
(81 Cu, 4 Ni, 4 Fe, 11 Al)										

(Table continued on page A13)

APPENDIX B Typical Properties of Selected Materials Used in Engineering^{1,5} (SI Units)

A13

		Ultimate Strength			Yield Strength ³		Modulus of Elasticity, GPa	Modulus of Rigidity, GPa	Coefficient of Thermal Expansion, 10 ⁻⁶ /°C	Ductility, Percent Elongation in 50 mm
		Tension, MPa	Compression, ² MPa	Shear, MPa	Tension, MPa	Shear, MPa				
Material	Density kg/m ³									
Steel										
Structural (ASTM-A36)	7860	400			250	145	200	77.2	11.7	21
High-strength-low-alloy										
ASTM-A709 Grade 345	7860	450			345		200	77.2	11.7	21
ASTM-A913 Grade 450	7860	550			450		200	77.2	11.7	17
ASTM-A992 Grade 345	7860	450			345		200	77.2	11.7	21
Quenched & tempered										
ASTM-A709 Grade 690	7860	760			690		200	77.2	11.7	18
Stainless, AISI 302										
Cold-rolled	7920	860			520		190	75	17.3	12
Annealed	7920	655			260	150	190	75	17.3	50
Reinforcing Steel										
Medium strength	7860	480			275		200	77	11.7	
High strength	7860	620			415		200	77	11.7	
Cast Iron										
Gray Cast Iron										
4.5% C, ASTM A-48	7200	170	655	240			69	28	12.1	0.5
Malleable Cast Iron										
2% C, 1% Si, ASTM A-47	7300	345	620	330	230		165	65	12.1	10
Aluminum										
Alloy 1100-H14										
(99% Al)	2710	110		70	95	55	70	26	23.6	9
Alloy 2014-T6	2800	455		275	400	230	75	27	23.0	13
Alloy-2024-T4	2800	470		280	325		73		23.2	19
Alloy-5456-H116	2630	315		185	230	130	72		23.9	16
Alloy 6061-T6	2710	260		165	240	140	70	26	23.6	17
Alloy 7075-T6	2800	570		330	500		72	28	23.6	11
Copper										
Oxygen-free copper										
(99.9% Cu)										
Annealed	8910	220		150	70		120	44	16.9	45
Hard-drawn	8910	390		200	265		120	44	16.9	4
Yellow-Brass										
(65% Cu, 35% Zn)										
Cold-rolled	8470	510		300	410	250	105	39	20.9	8
Annealed	8470	320		220	100	60	105	39	20.9	65
Red Brass										
(85% Cu, 15% Zn)										
Cold-rolled	8740	585		320	435		120	44	18.7	3
Annealed	8740	270		210	70		120	44	18.7	48
Tin bronze	8800	310			145		95		18.0	30
(88 Cu, 8Sn, 4Zn)										
Manganese bronze	8360	655			330		105		21.6	20
(63 Cu, 25 Zn, 6 Al, 3 Mn, 3 Fe)										
Aluminum bronze	8330	620	900		275		110	42	16.2	6
(81 Cu, 4 Ni, 4 Fe, 11 Al)										

(Table continued on page A14)

A14 **APPENDIX B Typical Properties of Selected Materials Used in Engineering^{1,5}**
(U.S. Customary Units)
Continued from page A13

Material	Specific Weight, lb/in ³	Ultimate Strength			Yield Strength ³		Modulus of Elasticity, 10 ⁶ psi	Modulus of Rigidity, 10 ⁶ psi	Coefficient of Thermal Expansion, 10 ⁻⁶ /°F	Ductility, Percent Elongation in 2 in.
		Tension, ksi	Compres- sion, ² ksi	Shear, ksi	Tension, ksi	Shear, ksi				
Magnesium Alloys										
Alloy AZ80 (Forging)	0.065	50		23	36		6.5	2.4	14	6
Alloy AZ31 (Extrusion)	0.064	37		19	29		6.5	2.4	14	12
Titanium										
Alloy (6% Al, 4% V)	0.161	130			120		16.5		5.3	10
Monel Alloy 400(Ni-Cu)										
Cold-worked	0.319	98			85	50	26		7.7	22
Annealed	0.319	80			32	18	26		7.7	46
Cupronickel										
(90% Cu, 10% Ni)										
Annealed	0.323	53			16		20	7.5	9.5	35
Cold-worked	0.323	85			79		20	7.5	9.5	3
Timber, air dry										
Douglas fir	0.017	15	7.2	1.1			1.9	.1	Varies 1.7 to 2.5	
Spruce, Sitka	0.015	8.6	5.6	1.1			1.5	.07		
Shortleaf pine	0.018		7.3	1.4			1.7			
Western white pine	0.014		5.0	1.0			1.5			
Ponderosa pine	0.015	8.4	5.3	1.1			1.3			
White oak	0.025		7.4	2.0			1.8			
Red oak	0.024		6.8	1.8			1.8			
Western hemlock	0.016	13	7.2	1.3			1.6			
Shagbark hickory	0.026		9.2	2.4			2.2			
Redwood	0.015	9.4	6.1	0.9			1.3			
Concrete										
Medium strength	0.084		4.0				3.6		5.5	
High strength	0.084		6.0				4.5		5.5	
Plastics										
Nylon, type 6/6, (molding compound)	0.0412	11	14		6.5		0.4		80	50
Polycarbonate	0.0433	9.5	12.5		9		0.35		68	110
Polyester, PBT (thermoplastic)	0.0484	8	11		8		0.35		75	150
Polyester elastomer	0.0433	6.5		5.5			0.03			500
Polystyrene	0.0374	8	13		8		0.45		70	2
Vinyl, rigid PVC	0.0520	6	10		6.5		0.45		75	40
Rubber	0.033	2							90	600
Granite (Avg. values)	0.100	3	35	5			10	4	4	
Marble (Avg. values)	0.100	2	18	4			8	3	6	
Sandstone (Avg. values)	0.083	1	12	2			6	2	5	
Glass, 98% silica	0.079		7				9.6	4.1	44	

¹Properties of metals vary widely as a result of variations in composition, heat treatment, and mechanical working.

²For ductile metals the compression strength is generally assumed to be equal to the tension strength.

³Offset of 0.2 percent.

⁴Timber properties are for loading parallel to the grain.

⁵See also *Marks' Mechanical Engineering Handbook*, 10th ed., McGraw-Hill, New York, 1996; *Annual Book of ASTM*, American Society for Testing Materials, Philadelphia, Pa.; *Metals Handbook*, American Society for Metals, Metals Park, Ohio; and *Aluminum Design Manual*, The Aluminum Association, Washington, DC.

APPENDIX B Typical Properties of Selected Materials Used in Engineering^{1,5} (SI Units)

A15

Continued from page A14

Material	Density kg/m ³	Ultimate Strength			Yield Strength ³		Modulus of Elasticity, GPa	Modulus of Rigidity, GPa	Coefficient of Thermal Expansion, 10 ⁻⁶ /°C	Ductility, Percent Elongation in 50 mm
		Tension, MPa	Compres- sion, ² MPa	Shear, MPa	Tension, MPa	Shear, MPa				
Magnesium Alloys										
Alloy AZ80 (Forging)	1800	345		160	250		45	16	25.2	6
Alloy AZ31 (Extrusion)	1770	255		130	200		45	16	25.2	12
Titanium										
Alloy (6% Al, 4% V)	4730	900			830		115		9.5	10
Monel Alloy 400(Ni-Cu)										
Cold-worked	8830	675			585	345	180		13.9	22
Annealed	8830	550			220	125	180		13.9	46
Cupronickel (90% Cu, 10% Ni)										
Annealed	8940	365			110		140	52	17.1	35
Cold-worked	8940	585			545		140	52	17.1	3
Timber, air dry										
Douglas fir	470	100	50	7.6			13	0.7	Varies 3.0 to 4.5	
Spruce, Sitka	415	60	39	7.6			10	0.5		
Shortleaf pine	500		50	9.7			12			
Western white pine	390		34	7.0			10			
Ponderosa pine	415	55	36	7.6			9			
White oak	690		51	13.8			12			
Red oak	660		47	12.4			12			
Western hemlock	440	90	50	10.0			11			
Shagbark hickory	720		63	16.5			15			
Redwood	415	65	42	6.2			9			
Concrete										
Medium strength	2320		28				25		9.9	
High strength	2320		40				30		9.9	
Plastics										
Nylon, type 6/6, (molding compound)	1140	75	95		45		2.8		144	50
Polycarbonate	1200	65	85		35		2.4		122	110
Polyester, PBT (thermoplastic)	1340	55	75		55		2.4		135	150
Polyester elastomer	1200	45		40			0.2			500
Polystyrene	1030	55	90		55		3.1		125	2
Vinyl, rigid PVC	1440	40	70		45		3.1		135	40
Rubber	910	15							162	600
Granite (Avg. values)	2770	20	240	35			70	4	7.2	
Marble (Avg. values)	2770	15	125	28			55	3	10.8	
Sandstone (Avg. values)	2300	7	85	14			40	2	9.0	
Glass, 98% silica	2190		50				65	4.1	80	

¹Properties of metals vary widely as a result of variations in composition, heat treatment, and mechanical working.

²For ductile metals the compression strength is generally assumed to be equal to the tension strength.

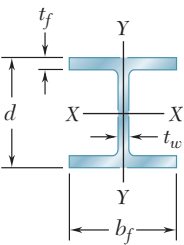
³Offset of 0.2 percent.

⁴Timber properties are for loading parallel to the grain.

⁵See also *Marks' Mechanical Engineering Handbook*, 10th ed., McGraw-Hill, New York, 1996; *Annual Book of ASTM*, American Society for Testing Materials, Philadelphia, Pa.; *Metals Handbook*, American Society of Metals, Metals Park, Ohio; and *Aluminum Design Manual*, The Aluminum Association, Washington, DC.

APPENDIX C Properties of Rolled-Steel Shapes
(U.S. Customary Units)

W Shapes
(Wide-Flange Shapes)

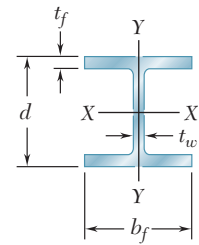


Designation†	Area <i>A</i> , in ²	Depth <i>d</i> , in.	Flange		Web Thick- ness <i>t_w</i> , in.	Axis X-X			Axis Y-Y		
			Width <i>b_f</i> , in.	Thick- ness <i>t_f</i> , in.		<i>I_x</i> , in ⁴	<i>S_x</i> , in ³	<i>r_x</i> , in.	<i>I_y</i> , in ⁴	<i>S_y</i> , in ³	<i>r_y</i> , in.
W36 × 302	88.8	37.3	16.7	1.68	0.945	21100	1130	15.4	1300	156	3.82
135	39.7	35.6	12.0	0.790	0.600	7800	439	14.0	225	37.7	2.38
W33 × 201	59.2	33.7	15.7	1.15	0.715	11600	686	14.0	749	95.2	3.56
118	34.7	32.9	11.5	0.740	0.550	5900	359	13.0	187	32.6	2.32
W30 × 173	51.0	30.4	15.0	1.07	0.655	8230	541	12.7	598	79.8	3.42
99	29.1	29.7	10.50	0.670	0.520	3990	269	11.7	128	24.5	2.10
W27 × 146	43.1	27.4	14.0	0.975	0.605	5660	414	11.5	443	63.5	3.20
84	24.8	26.70	10.0	0.640	0.460	2850	213	10.7	106	21.2	2.07
W24 × 104	30.6	24.1	12.8	0.750	0.500	3100	258	10.1	259	40.7	2.91
68	20.1	23.7	8.97	0.585	0.415	1830	154	9.55	70.4	15.7	1.87
W21 × 101	29.8	21.4	12.3	0.800	0.500	2420	227	9.02	248	40.3	2.89
62	18.3	21.0	8.24	0.615	0.400	1330	127	8.54	57.5	14.0	1.77
44	13.0	20.7	6.50	0.450	0.350	843	81.6	8.06	20.7	6.37	1.26
W18 × 106	31.1	18.7	11.2	0.940	0.590	1910	204	7.84	220	39.4	2.66
76	22.3	18.2	11.0	0.680	0.425	1330	146	7.73	152	27.6	2.61
50	14.7	18.0	7.50	0.570	0.355	800	88.9	7.38	40.1	10.7	1.65
35	10.3	17.7	6.00	0.425	0.300	510	57.6	7.04	15.3	5.12	1.22
W16 × 77	22.6	16.5	10.3	0.76	0.455	1110	134	7.00	138	26.9	2.47
57	16.8	16.4	7.12	0.715	0.430	758	92.2	6.72	43.1	12.1	1.60
40	11.8	16.0	7.00	0.505	0.305	518	64.7	6.63	28.9	8.25	1.57
31	9.13	15.9	5.53	0.440	0.275	375	47.2	6.41	12.4	4.49	1.17
26	7.68	15.7	5.50	0.345	0.250	301	38.4	6.26	9.59	3.49	1.12
W14 × 370	109	17.9	16.5	2.66	1.66	5440	607	7.07	1990	241	4.27
145	42.7	14.8	15.5	1.09	0.680	1710	232	6.33	677	87.3	3.98
82	24.0	14.3	10.1	0.855	0.510	881	123	6.05	148	29.3	2.48
68	20.0	14.0	10.0	0.720	0.415	722	103	6.01	121	24.2	2.46
53	15.6	13.9	8.06	0.660	0.370	541	77.8	5.89	57.7	14.3	1.92
43	12.6	13.7	8.00	0.530	0.305	428	62.6	5.82	45.2	11.3	1.89
38	11.2	14.1	6.77	0.515	0.310	385	54.6	5.87	26.7	7.88	1.55
30	8.85	13.8	6.73	0.385	0.270	291	42.0	5.73	19.6	5.82	1.49
26	7.69	13.9	5.03	0.420	0.255	245	35.3	5.65	8.91	3.55	1.08
22	6.49	13.7	5.00	0.335	0.230	199	29.0	5.54	7.00	2.80	1.04

†A wide-flange shape is designated by the letter W followed by the nominal depth in inches and the weight in pounds per foot.
(Table continued on page A17)

APPENDIX C Properties of Rolled-Steel Shapes (SI Units)

W Shapes (Wide-Flange Shapes)



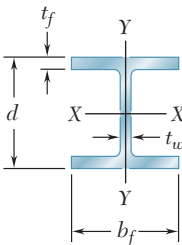
Designation†	Area A , mm ²	Depth d , mm	Flange		Web Thick- ness t_w , mm	Axis X-X			Axis Y-Y		
			Width b_f , mm	Thick- ness t_f , mm		I_x 10 ⁶ mm ⁴	S_x 10 ³ mm ³	r_x mm	I_y 10 ⁶ mm ⁴	S_y 10 ³ mm ³	r_y mm
W920 × 449	57300	947	424	42.7	24.0	8780	18500	391	541	2560	97.0
201	25600	904	305	20.1	15.2	3250	7190	356	93.7	618	60.5
W840 × 299	38200	856	399	29.2	18.2	4830	11200	356	312	1560	90.4
176	22400	836	292	18.8	14.0	2460	5880	330	77.8	534	58.9
W760 × 257	32900	772	381	27.2	16.6	3430	8870	323	249	1310	86.9
147	18800	754	267	17.0	13.2	1660	4410	297	53.3	401	53.3
W690 × 217	27800	696	356	24.8	15.4	2360	6780	292	184	1040	81.3
125	16000	678	254	16.3	11.7	1190	3490	272	44.1	347	52.6
W610 × 155	19700	612	325	19.1	12.7	1290	4230	257	108	667	73.9
101	13000	602	228	14.9	10.5	762	2520	243	29.3	257	47.5
W530 × 150	19200	544	312	20.3	12.7	1010	3720	229	103	660	73.4
92	11800	533	209	15.6	10.2	554	2080	217	23.9	229	45.0
66	8390	526	165	11.4	8.89	351	1340	205	8.62	104	32.0
W460 × 158	20100	475	284	23.9	15.0	795	3340	199	91.6	646	67.6
113	14400	462	279	17.3	10.8	554	2390	196	63.3	452	66.3
74	9480	457	191	14.5	9.02	333	1460	187	16.7	175	41.9
52	6650	450	152	10.8	7.62	212	944	179	6.37	83.9	31.0
W410 × 114	14600	419	262	19.3	11.6	462	2200	178	57.4	441	62.7
85	10800	417	181	18.2	10.9	316	1510	171	17.9	198	40.6
60	7610	406	178	12.8	7.75	216	1060	168	12.0	135	39.9
46.1	5890	404	140	11.2	6.99	156	773	163	5.16	73.6	29.7
38.8	4950	399	140	8.76	6.35	125	629	159	3.99	57.2	28.4
W360 × 551	70300	455	419	67.6	42.2	2260	9950	180	828	3950	108
216	27500	376	394	27.7	17.3	712	3800	161	282	1430	101
122	15500	363	257	21.7	13.0	367	2020	154	61.6	480	63.0
101	12900	356	254	18.3	10.5	301	1690	153	50.4	397	62.5
79	10100	353	205	16.8	9.40	225	1270	150	24.0	234	48.8
64	8130	348	203	13.5	7.75	178	1030	148	18.8	185	48.0
57.8	7230	358	172	13.1	7.87	160	895	149	11.1	129	39.4
44	5710	351	171	9.78	6.86	121	688	146	8.16	95.4	37.8
39	4960	353	128	10.7	6.48	102	578	144	3.71	58.2	27.4
32.9	4190	348	127	8.51	5.84	82.8	475	141	2.91	45.9	26.4

†A wide-flange shape is designated by the letter W followed by the nominal depth in millimeters and the mass in kilograms per meter.

(Table continued on page A18)

APPENDIX C Properties of Rolled-Steel Shapes
(U.S. Customary Units)
Continued from page A17

W Shapes
(Wide-Flange Shapes)



Designation†			Flange		Web Thick- ness t_w , in.	Axis X-X			Axis Y-Y		
			Width b_f , in.	Thick- ness t_f , in.		I_x , in ⁴	S_x , in ³	r_x , in.	I_y , in ⁴	S_y , in ³	r_y , in.
W12 × 96	28.2	12.7	12.2	0.900	0.550	833	131	5.44	270	44.4	3.09
72	21.1	12.3	12.0	0.670	0.430	597	97.4	5.31	195	32.4	3.04
50	14.6	12.2	8.08	0.640	0.370	391	64.2	5.18	56.3	13.9	1.96
40	11.7	11.9	8.01	0.515	0.295	307	51.5	5.13	44.1	11.0	1.94
35	10.3	12.5	6.56	0.520	0.300	285	45.6	5.25	24.5	7.47	1.54
30	8.79	12.3	6.52	0.440	0.260	238	38.6	5.21	20.3	6.24	1.52
26	7.65	12.2	6.49	0.380	0.230	204	33.4	5.17	17.3	5.34	1.51
22	6.48	12.3	4.03	0.425	0.260	156	25.4	4.91	4.66	2.31	0.848
16	4.71	12.0	3.99	0.265	0.220	103	17.1	4.67	2.82	1.41	0.773
W10 × 112	32.9	11.4	10.4	1.25	0.755	716	126	4.66	236	45.3	2.68
68	20.0	10.4	10.1	0.770	0.470	394	75.7	4.44	134	26.4	2.59
54	15.8	10.1	10.0	0.615	0.370	303	60.0	4.37	103	20.6	2.56
45	13.3	10.1	8.02	0.620	0.350	248	49.1	4.32	53.4	13.3	2.01
39	11.5	9.92	7.99	0.530	0.315	209	42.1	4.27	45.0	11.3	1.98
33	9.71	9.73	7.96	0.435	0.290	171	35.0	4.19	36.6	9.20	1.94
30	8.84	10.5	5.81	0.510	0.300	170	32.4	4.38	16.7	5.75	1.37
22	6.49	10.2	5.75	0.360	0.240	118	23.2	4.27	11.4	3.97	1.33
19	5.62	10.2	4.02	0.395	0.250	96.3	18.8	4.14	4.29	2.14	0.874
15	4.41	10.0	4.00	0.270	0.230	68.9	13.8	3.95	2.89	1.45	0.810
W8 × 58	17.1	8.75	8.22	0.810	0.510	228	52.0	3.65	75.1	18.3	2.10
48	14.1	8.50	8.11	0.685	0.400	184	43.2	3.61	60.9	15.0	2.08
40	11.7	8.25	8.07	0.560	0.360	146	35.5	3.53	49.1	12.2	2.04
35	10.3	8.12	8.02	0.495	0.310	127	31.2	3.51	42.6	10.6	2.03
31	9.12	8.00	8.00	0.435	0.285	110	27.5	3.47	37.1	9.27	2.02
28	8.24	8.06	6.54	0.465	0.285	98.0	24.3	3.45	21.7	6.63	1.62
24	7.08	7.93	6.50	0.400	0.245	82.7	20.9	3.42	18.3	5.63	1.61
21	6.16	8.28	5.27	0.400	0.250	75.3	18.2	3.49	9.77	3.71	1.26
18	5.26	8.14	5.25	0.330	0.230	61.9	15.2	3.43	7.97	3.04	1.23
15	4.44	8.11	4.01	0.315	0.245	48.0	11.8	3.29	3.41	1.70	0.876
13	3.84	7.99	4.00	0.255	0.230	39.6	9.91	3.21	2.73	1.37	0.843
W6 × 25	7.34	6.38	6.08	0.455	0.320	53.4	16.7	2.70	17.1	5.61	1.52
20	5.87	6.20	6.02	0.365	0.260	41.4	13.4	2.66	13.3	4.41	1.50
16	4.74	6.28	4.03	0.405	0.260	32.1	10.2	2.60	4.43	2.20	0.967
12	3.55	6.03	4.00	0.280	0.230	22.1	7.31	2.49	2.99	1.50	0.918
9	2.68	5.90	3.94	0.215	0.170	16.4	5.56	2.47	2.20	1.11	0.905
W5 × 19	5.56	5.15	5.03	0.430	0.270	26.3	10.2	2.17	9.13	3.63	1.28
16	4.71	5.01	5.00	0.360	0.240	21.4	8.55	2.13	7.51	3.00	1.26
W4 × 13	3.83	4.16	4.06	0.345	0.280	11.3	5.46	1.72	3.86	1.90	1.00

†A wide-flange shape is designated by the letter W followed by the nominal depth in inches and the weight in pounds per foot.

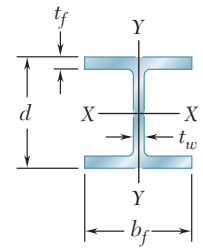
APPENDIX C Properties of Rolled-Steel Shapes

(SI Units)

Continued from page A18

W Shapes

(Wide-Flange Shapes)

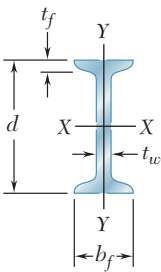


Designation†	Area A , mm ²	Depth d , mm	Flange		Web Thick- ness t_w , mm	Axis X-X			Axis Y-Y		
			Width b_f , mm	Thick- ness t_f , mm		I_x 10 ⁶ mm ⁴	S_x 10 ³ mm ³	r_x mm	I_y 10 ⁶ mm ⁴	S_y 10 ³ mm ³	r_y mm
W310 × 143	18200	323	310	22.9	14.0	347	2150	138	112	728	78.5
107	13600	312	305	17.0	10.9	248	1600	135	81.2	531	77.2
74	9420	310	205	16.3	9.40	163	1050	132	23.4	228	49.8
60	7550	302	203	13.1	7.49	128	844	130	18.4	180	49.3
52	6650	318	167	13.2	7.62	119	747	133	10.2	122	39.1
44.5	5670	312	166	11.2	6.60	99.1	633	132	8.45	102	38.6
38.7	4940	310	165	9.65	5.84	84.9	547	131	7.20	87.5	38.4
32.7	4180	312	102	10.8	6.60	64.9	416	125	1.94	37.9	21.5
23.8	3040	305	101	6.73	5.59	42.9	280	119	1.17	23.1	19.6
W250 × 167	21200	290	264	31.8	19.2	298	2060	118	98.2	742	68.1
101	12900	264	257	19.6	11.9	164	1240	113	55.8	433	65.8
80	10200	257	254	15.6	9.4	126	983	111	42.9	338	65.0
67	8580	257	204	15.7	8.89	103	805	110	22.2	218	51.1
58	7420	252	203	13.5	8.00	87.0	690	108	18.7	185	50.3
49.1	6260	247	202	11.0	7.37	71.2	574	106	15.2	151	49.3
44.8	5700	267	148	13.0	7.62	70.8	531	111	6.95	94.2	34.8
32.7	4190	259	146	9.14	6.10	49.1	380	108	4.75	65.1	33.8
28.4	3630	259	102	10.0	6.35	40.1	308	105	1.79	35.1	22.2
22.3	2850	254	102	6.86	5.84	28.7	226	100	1.20	23.8	20.6
W200 × 86	11000	222	209	20.6	13.0	94.9	852	92.7	31.3	300	53.3
71	9100	216	206	17.4	10.2	76.6	708	91.7	25.3	246	52.8
59	7550	210	205	14.2	9.14	60.8	582	89.7	20.4	200	51.8
52	6650	206	204	12.6	7.87	52.9	511	89.2	17.7	174	51.6
46.1	5880	203	203	11.0	7.24	45.8	451	88.1	15.4	152	51.3
41.7	5320	205	166	11.8	7.24	40.8	398	87.6	9.03	109	41.1
35.9	4570	201	165	10.2	6.22	34.4	342	86.9	7.62	92.3	40.9
31.3	3970	210	134	10.2	6.35	31.3	298	88.6	4.07	60.8	32.0
26.6	3390	207	133	8.38	5.84	25.8	249	87.1	3.32	49.8	31.2
22.5	2860	206	102	8.00	6.22	20.0	193	83.6	1.42	27.9	22.3
19.3	2480	203	102	6.48	5.84	16.5	162	81.5	1.14	22.5	21.4
W150 × 37.1	4740	162	154	11.6	8.13	22.2	274	68.6	7.12	91.9	38.6
29.8	3790	157	153	9.27	6.60	17.2	220	67.6	5.54	72.3	38.1
24	3060	160	102	10.3	6.60	13.4	167	66.0	1.84	36.1	24.6
18	2290	153	102	7.11	5.84	9.20	120	63.2	1.24	24.6	23.3
13.5	1730	150	100	5.46	4.32	6.83	91.1	62.7	0.916	18.2	23.0
W130 × 28.1	3590	131	128	10.9	6.86	10.9	167	55.1	3.80	59.5	32.5
23.8	3040	127	127	9.14	6.10	8.91	140	54.1	3.13	49.2	32.0
W100 × 19.3	2470	106	103	8.76	7.11	4.70	89.5	43.7	1.61	31.1	25.4

†A wide-flange shape is designated by the letter W followed by the nominal depth in millimeters and the mass in kilograms per meter.

APPENDIX C Properties of Rolled-Steel Shapes
(U.S. Customary Units)

S Shapes
(American Standard Shapes)



Designation†			Flange		Web Thick- ness t_w , in.	Axis X-X			Axis Y-Y		
			Width b_f , in.	Thick- ness t_f , in.		I_x , in ⁴	S_x , in ³	r_x , in.	I_y , in ⁴	S_y , in ³	r_y , in.
S24 × 121	35.5	24.5	8.05	1.09	0.800	3160	258	9.43	83.0	20.6	1.53
106	31.1	24.5	7.87	1.09	0.620	2940	240	9.71	76.8	19.5	1.57
100	29.3	24.0	7.25	0.870	0.745	2380	199	9.01	47.4	13.1	1.27
90	26.5	24.0	7.13	0.870	0.625	2250	187	9.21	44.7	12.5	1.30
80	23.5	24.0	7.00	0.870	0.500	2100	175	9.47	42.0	12.0	1.34
S20 × 96	28.2	20.3	7.20	0.920	0.800	1670	165	7.71	49.9	13.9	1.33
86	25.3	20.3	7.06	0.920	0.660	1570	155	7.89	46.6	13.2	1.36
75	22.0	20.0	6.39	0.795	0.635	1280	128	7.62	29.5	9.25	1.16
66	19.4	20.0	6.26	0.795	0.505	1190	119	7.83	27.5	8.78	1.19
S18 × 70	20.5	18.0	6.25	0.691	0.711	923	103	6.70	24.0	7.69	1.08
54.7	16.0	18.0	6.00	0.691	0.461	801	89.0	7.07	20.7	6.91	1.14
S15 × 50	14.7	15.0	5.64	0.622	0.550	485	64.7	5.75	15.6	5.53	1.03
42.9	12.6	15.0	5.50	0.622	0.411	446	59.4	5.95	14.3	5.19	1.06
S12 × 50	14.6	12.0	5.48	0.659	0.687	303	50.6	4.55	15.6	5.69	1.03
40.8	11.9	12.0	5.25	0.659	0.462	270	45.1	4.76	13.5	5.13	1.06
35	10.2	12.0	5.08	0.544	0.428	228	38.1	4.72	9.84	3.88	0.980
31.8	9.31	12.0	5.00	0.544	0.350	217	36.2	4.83	9.33	3.73	1.00
S10 × 35	10.3	10.0	4.94	0.491	0.594	147	29.4	3.78	8.30	3.36	0.899
25.4	7.45	10.0	4.66	0.491	0.311	123	24.6	4.07	6.73	2.89	0.950
S8 × 23	6.76	8.00	4.17	0.425	0.441	64.7	16.2	3.09	4.27	2.05	0.795
18.4	5.40	8.00	4.00	0.425	0.271	57.5	14.4	3.26	3.69	1.84	0.827
S6 × 17.2	5.06	6.00	3.57	0.359	0.465	26.2	8.74	2.28	2.29	1.28	0.673
12.5	3.66	6.00	3.33	0.359	0.232	22.0	7.34	2.45	1.80	1.08	0.702
S5 × 10	2.93	5.00	3.00	0.326	0.214	12.3	4.90	2.05	1.19	0.795	0.638
S4 × 9.5	2.79	4.00	2.80	0.293	0.326	6.76	3.38	1.56	0.887	0.635	0.564
7.7	2.26	4.00	2.66	0.293	0.193	6.05	3.03	1.64	0.748	0.562	0.576
S3 × 7.5	2.20	3.00	2.51	0.260	0.349	2.91	1.94	1.15	0.578	0.461	0.513
5.7	1.66	3.00	2.33	0.260	0.170	2.50	1.67	1.23	0.447	0.383	0.518

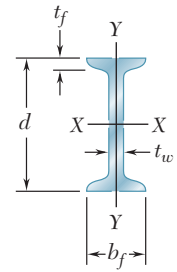
†An American Standard Beam is designated by the letter S followed by the nominal depth in inches and the weight in pounds per foot.

APPENDIX C Properties of Rolled-Steel Shapes

(SI Units)

S Shapes

(American Standard Shapes)

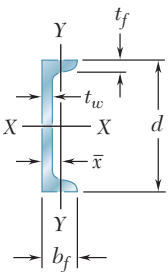


Designation†	Area A , mm ²	Depth d , mm	Flange		Web Thick- ness t_w , mm	Axis X-X			Axis Y-Y		
			Width b_f , mm	Thick- ness t_f , mm		I_x 10 ⁶ mm ⁴	S_x 10 ³ mm ³	r_x mm	I_y 10 ⁶ mm ⁴	S_y 10 ³ mm ³	r_y mm
S610 × 180	22900	622	204	27.7	20.3	1320	4230	240	34.5	338	38.9
158	20100	622	200	27.7	15.7	1220	3930	247	32.0	320	39.9
149	18900	610	184	22.1	18.9	991	3260	229	19.7	215	32.3
134	17100	610	181	22.1	15.9	937	3060	234	18.6	205	33.0
119	15200	610	178	22.1	12.7	874	2870	241	17.5	197	34.0
S510 × 143	18200	516	183	23.4	20.3	695	2700	196	20.8	228	33.8
128	16300	516	179	23.4	16.8	653	2540	200	19.4	216	34.5
112	14200	508	162	20.2	16.1	533	2100	194	12.3	152	29.5
98.2	12500	508	159	20.2	12.8	495	1950	199	11.4	144	30.2
S460 × 104	13200	457	159	17.6	18.1	384	1690	170	10.0	126	27.4
81.4	10300	457	152	17.6	11.7	333	1460	180	8.62	113	29.0
S380 × 74	9480	381	143	15.8	14.0	202	1060	146	6.49	90.6	26.2
64	8130	381	140	15.8	10.4	186	973	151	5.95	85.0	26.9
S310 × 74	9420	305	139	16.7	17.4	126	829	116	6.49	93.2	26.2
60.7	7680	305	133	16.7	11.7	112	739	121	5.62	84.1	26.9
52	6580	305	129	13.8	10.9	94.9	624	120	4.10	63.6	24.9
47.3	6010	305	127	13.8	8.89	90.3	593	123	3.88	61.1	25.4
S250 × 52	6650	254	125	12.5	15.1	61.2	482	96.0	3.45	55.1	22.8
37.8	4810	254	118	12.5	7.90	51.2	403	103	2.80	47.4	24.1
S200 × 34	4360	203	106	10.8	11.2	26.9	265	78.5	1.78	33.6	20.2
27.4	3480	203	102	10.8	6.88	23.9	236	82.8	1.54	30.2	21.0
S150 × 25.7	3260	152	90.7	9.12	11.8	10.9	143	57.9	0.953	21.0	17.1
18.6	2360	152	84.6	9.12	5.89	9.16	120	62.2	0.749	17.7	17.8
S130 × 15	1890	127	76.2	8.28	5.44	5.12	80.3	52.1	0.495	13.0	16.2
S100 × 14.1	1800	102	71.1	7.44	8.28	2.81	55.4	39.6	0.369	10.4	14.3
11.5	1460	102	67.6	7.44	4.90	2.52	49.7	41.7	0.311	9.21	14.6
S75 × 11.2	1420	76.2	63.8	6.60	8.86	1.21	31.8	29.2	0.241	7.55	13.0
8.5	1070	76.2	59.2	6.60	4.32	1.04	27.4	31.2	0.186	6.28	13.2

†An American Standard Beam is designated by the letter S followed by the nominal depth in millimeters and the mass in kilograms per meter.

APPENDIX C Properties of Rolled-Steel Shapes
(U.S. Customary Units)

C Shapes
(American Standard Channels)



Designation† Area A_f in ² Depth d_f in.			Flange		Web Thick- ness t_{w_f} in.	Axis X-X			Axis Y-Y			
			Width b_{f_f} in.	Thick- ness t_{f_f} in.								
						I_{x_f} in ⁴	S_{x_f} in ³	r_{x_f} in.	I_{y_f} in ⁴	S_{y_f} in ³	r_{y_f} in.	x_f in.
C15 × 50	14.7	15.0	3.72	0.650	0.716	404	53.8	5.24	11.0	3.77	0.865	0.799
40	11.8	15.0	3.52	0.650	0.520	348	46.5	5.45	9.17	3.34	0.883	0.778
33.9	10.0	15.0	3.40	0.650	0.400	315	42.0	5.62	8.07	3.09	0.901	0.788
C12 × 30	8.81	12.0	3.17	0.501	0.510	162	27.0	4.29	5.12	2.05	0.762	0.674
25	7.34	12.0	3.05	0.501	0.387	144	24.0	4.43	4.45	1.87	0.779	0.674
20.7	6.08	12.0	2.94	0.501	0.282	129	21.5	4.61	3.86	1.72	0.797	0.698
C10 × 30	8.81	10.0	3.03	0.436	0.673	103	20.7	3.42	3.93	1.65	0.668	0.649
25	7.34	10.0	2.89	0.436	0.526	91.1	18.2	3.52	3.34	1.47	0.675	0.617
20	5.87	10.0	2.74	0.436	0.379	78.9	15.8	3.66	2.80	1.31	0.690	0.606
15.3	4.48	10.0	2.60	0.436	0.240	67.3	13.5	3.87	2.27	1.15	0.711	0.634
C9 × 20	5.87	9.00	2.65	0.413	0.448	60.9	13.5	3.22	2.41	1.17	0.640	0.583
15	4.41	9.00	2.49	0.413	0.285	51.0	11.3	3.40	1.91	1.01	0.659	0.586
13.4	3.94	9.00	2.43	0.413	0.233	47.8	10.6	3.49	1.75	0.954	0.666	0.601
C8 × 18.7	5.51	8.00	2.53	0.390	0.487	43.9	11.0	2.82	1.97	1.01	0.598	0.565
13.7	4.04	8.00	2.34	0.390	0.303	36.1	9.02	2.99	1.52	0.848	0.613	0.554
11.5	3.37	8.00	2.26	0.390	0.220	32.5	8.14	3.11	1.31	0.775	0.623	0.572
C7 × 12.2	3.60	7.00	2.19	0.366	0.314	24.2	6.92	2.60	1.16	0.696	0.568	0.525
9.8	2.87	7.00	2.09	0.366	0.210	21.2	6.07	2.72	0.957	0.617	0.578	0.541
C6 × 13	3.81	6.00	2.16	0.343	0.437	17.3	5.78	2.13	1.05	0.638	0.524	0.514
10.5	3.08	6.00	2.03	0.343	0.314	15.1	5.04	2.22	0.860	0.561	0.529	0.500
8.2	2.39	6.00	1.92	0.343	0.200	13.1	4.35	2.34	0.687	0.488	0.536	0.512
C5 × 9	2.64	5.00	1.89	0.320	0.325	8.89	3.56	1.83	0.624	0.444	0.486	0.478
6.7	1.97	5.00	1.75	0.320	0.190	7.48	2.99	1.95	0.470	0.372	0.489	0.484
C4 × 7.2	2.13	4.00	1.72	0.296	0.321	4.58	2.29	1.47	0.425	0.337	0.447	0.459
5.4	1.58	4.00	1.58	0.296	0.184	3.85	1.92	1.56	0.312	0.277	0.444	0.457
C3 × 6	1.76	3.00	1.60	0.273	0.356	2.07	1.38	1.08	0.300	0.263	0.413	0.455
5	1.47	3.00	1.50	0.273	0.258	1.85	1.23	1.12	0.241	0.228	0.405	0.439
4.1	1.20	3.00	1.41	0.273	0.170	1.65	1.10	1.17	0.191	0.196	0.398	0.437

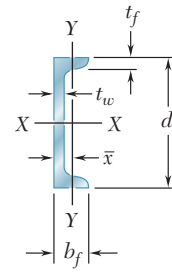
†An American Standard Channel is designated by the letter C followed by the nominal depth in inches and the weight in pounds per foot.

APPENDIX C Properties of Rolled-Steel Shapes

(SI Units)

C Shapes

(American Standard Channels)

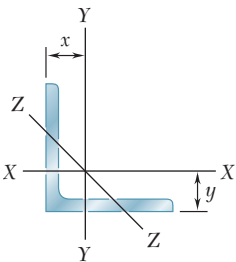


Designation†	Area A , mm ²	Depth d , mm	Flange		Web Thick- ness t_w , mm	Axis X-X			Axis Y-Y			
			Width b_f , mm	Thick- ness t_f , mm		I_x 10 ⁶ mm ⁴	S_x 10 ³ mm ³	r_x mm	I_y 10 ⁶ mm ⁴	S_y 10 ³ mm ³	r_y mm	x mm
C380 × 74	9480	381	94.5	16.5	18.2	168	882	133	4.58	61.8	22.0	20.3
60	7610	381	89.4	16.5	13.2	145	762	138	3.82	54.7	22.4	19.8
50.4	6450	381	86.4	16.5	10.2	131	688	143	3.36	50.6	22.9	20.0
C310 × 45	5680	305	80.5	12.7	13.0	67.4	442	109	2.13	33.6	19.4	17.1
37	4740	305	77.5	12.7	9.83	59.9	393	113	1.85	30.6	19.8	17.1
30.8	3920	305	74.7	12.7	7.16	53.7	352	117	1.61	28.2	20.2	17.7
C250 × 45	5680	254	77.0	11.1	17.1	42.9	339	86.9	1.64	27.0	17.0	16.5
37	4740	254	73.4	11.1	13.4	37.9	298	89.4	1.39	24.1	17.1	15.7
30	3790	254	69.6	11.1	9.63	32.8	259	93.0	1.17	21.5	17.5	15.4
22.8	2890	254	66.0	11.1	6.10	28.0	221	98.3	0.945	18.8	18.1	16.1
C230 × 30	3790	229	67.3	10.5	11.4	25.3	221	81.8	1.00	19.2	16.3	14.8
22	2850	229	63.2	10.5	7.24	21.2	185	86.4	0.795	16.6	16.7	14.9
19.9	2540	229	61.7	10.5	5.92	19.9	174	88.6	0.728	15.6	16.9	15.3
C200 × 27.9	3550	203	64.3	9.91	12.4	18.3	180	71.6	0.820	16.6	15.2	14.4
20.5	2610	203	59.4	9.91	7.70	15.0	148	75.9	0.633	13.9	15.6	14.1
17.1	2170	203	57.4	9.91	5.59	13.5	133	79.0	0.545	12.7	15.8	14.5
C180 × 18.2	2320	178	55.6	9.30	7.98	10.1	113	66.0	0.483	11.4	14.4	13.3
14.6	1850	178	53.1	9.30	5.33	8.82	100	69.1	0.398	10.1	14.7	13.7
C150 × 19.3	2460	152	54.9	8.71	11.1	7.20	94.7	54.1	0.437	10.5	13.3	13.1
15.6	1990	152	51.6	8.71	7.98	6.29	82.6	56.4	0.358	9.19	13.4	12.7
12.2	1540	152	48.8	8.71	5.08	5.45	71.3	59.4	0.286	8.00	13.6	13.0
C130 × 13	1700	127	48.0	8.13	8.26	3.70	58.3	46.5	0.260	7.28	12.3	12.1
10.4	1270	127	44.5	8.13	4.83	3.11	49.0	49.5	0.196	6.10	12.4	12.3
C100 × 10.8	1370	102	43.7	7.52	8.15	1.91	37.5	37.3	0.177	5.52	11.4	11.7
8	1020	102	40.1	7.52	4.67	1.60	31.5	39.6	0.130	4.54	11.3	11.6
C75 × 8.9	1140	76.2	40.6	6.93	9.04	0.862	22.6	27.4	0.125	4.31	10.5	11.6
7.4	948	76.2	38.1	6.93	6.55	0.770	20.2	28.4	0.100	3.74	10.3	11.2
6.1	774	76.2	35.8	6.93	4.32	0.687	18.0	29.7	0.0795	3.21	10.1	11.1

†An American Standard Channel is designated by the letter C followed by the nominal depth in millimeters and the mass in kilograms per meter.

APPENDIX C Properties of Rolled-Steel Shapes
(U.S. Customary Units)

Angles
Equal Legs



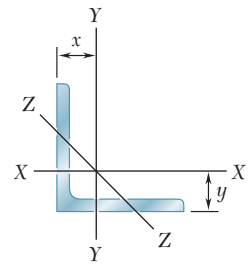
Size and Thickness, in.	Weight per Foot, lb/ft	Area, in ²	Axis X-X and Axis Y-Y				Axis Z-Z r _z , in.
			I, in ⁴	S, in ³	r, in.	x or y, in.	
L8 × 8 × 1	51.0	15.0	89.1	15.8	2.43	2.36	1.56
¾	38.9	11.4	69.9	12.2	2.46	2.26	1.57
½	26.4	7.75	48.8	8.36	2.49	2.17	1.59
L6 × 6 × 1	37.4	11.0	35.4	8.55	1.79	1.86	1.17
¾	28.7	8.46	28.1	6.64	1.82	1.77	1.17
¾	24.2	7.13	24.1	5.64	1.84	1.72	1.17
½	19.6	5.77	19.9	4.59	1.86	1.67	1.18
¾	14.9	4.38	15.4	3.51	1.87	1.62	1.19
L5 × 5 × ¾	23.6	6.94	15.7	4.52	1.50	1.52	0.972
¾	20.0	5.86	13.6	3.85	1.52	1.47	0.975
½	16.2	4.75	11.3	3.15	1.53	1.42	0.980
¾	12.3	3.61	8.76	2.41	1.55	1.37	0.986
L4 × 4 × ¾	18.5	5.44	7.62	2.79	1.18	1.27	0.774
¾	15.7	4.61	6.62	2.38	1.20	1.22	0.774
½	12.8	3.75	5.52	1.96	1.21	1.18	0.776
¾	9.80	2.86	4.32	1.50	1.23	1.13	0.779
¼	6.60	1.94	3.00	1.03	1.25	1.08	0.783
L3½ × 3½ × ½	11.1	3.25	3.63	1.48	1.05	1.05	0.679
¾	8.50	2.48	2.86	1.15	1.07	1.00	0.683
¼	5.80	1.69	2.00	0.787	1.09	0.954	0.688
L3 × 3 × ½	9.40	2.75	2.20	1.06	0.895	0.929	0.580
¾	7.20	2.11	1.75	0.825	0.910	0.884	0.581
¼	4.90	1.44	1.23	0.569	0.926	0.836	0.585
L2½ × 2½ × ½	7.70	2.25	1.22	0.716	0.735	0.803	0.481
¾	5.90	1.73	0.972	0.558	0.749	0.758	0.481
¼	4.10	1.19	0.692	0.387	0.764	0.711	0.482
¾	3.07	0.900	0.535	0.295	0.771	0.687	0.482
L2 × 2 × ¾	4.70	1.36	0.476	0.348	0.591	0.632	0.386
¼	3.19	0.938	0.346	0.244	0.605	0.586	0.387
¾	1.65	0.484	0.189	0.129	0.620	0.534	0.391

APPENDIX C Properties of Rolled-Steel Shapes

(SI Units)

Angles

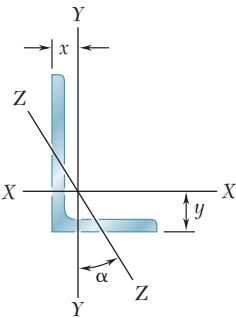
Equal Legs



Size and Thickness, mm	Mass per Meter, kg/m	Area, mm ²	Axis X-X				Axis Z-Z r_z mm
			I 10 ⁶ mm ⁴	S 10 ³ mm ³	r mm	x or y mm	
L203 × 203 × 25.4	75.9	9680	37.1	259	61.7	59.9	39.6
19	57.9	7350	29.1	200	62.5	57.4	39.9
12.7	39.3	5000	20.3	137	63.2	55.1	40.4
L152 × 152 × 25.4	55.7	7100	14.7	140	45.5	47.2	29.7
19	42.7	5460	11.7	109	46.2	45.0	29.7
15.9	36.0	4600	10.0	92.4	46.7	43.7	29.7
12.7	29.2	3720	8.28	75.2	47.2	42.4	30.0
9.5	22.2	2830	6.41	57.5	47.5	41.1	30.2
L127 × 127 × 19	35.1	4480	6.53	74.1	38.1	38.6	24.7
15.9	29.8	3780	5.66	63.1	38.6	37.3	24.8
12.7	24.1	3060	4.70	51.6	38.9	36.1	24.9
9.5	18.3	2330	3.65	39.5	39.4	34.8	25.0
L102 × 102 × 19	27.5	3510	3.17	45.7	30.0	32.3	19.7
15.9	23.4	2970	2.76	39.0	30.5	31.0	19.7
12.7	19.0	2420	2.30	32.1	30.7	30.0	19.7
9.5	14.6	1850	1.80	24.6	31.2	28.7	19.8
6.4	9.80	1250	1.25	16.9	31.8	27.4	19.9
L89 × 89 × 12.7	16.5	2100	1.51	24.3	26.7	26.7	17.2
9.5	12.6	1600	1.19	18.8	27.2	25.4	17.3
6.4	8.60	1090	0.832	12.9	27.7	24.2	17.5
L76 × 76 × 12.7	14.0	1770	0.916	17.4	22.7	23.6	14.7
9.5	10.7	1360	0.728	13.5	23.1	22.5	14.8
6.4	7.30	929	0.512	9.32	23.5	21.2	14.9
L64 × 64 × 12.7	11.4	1450	0.508	11.7	18.7	20.4	12.2
9.5	8.70	1120	0.405	9.14	19.0	19.3	12.2
6.4	6.10	768	0.288	6.34	19.4	18.1	12.2
4.8	4.60	581	0.223	4.83	19.6	17.4	12.2
L51 × 51 × 9.5	7.00	877	0.198	5.70	15.0	16.1	9.80
6.4	4.70	605	0.144	4.00	15.4	14.9	9.83
3.2	2.40	312	0.0787	2.11	15.7	13.6	9.93

APPENDIX C Properties of Rolled-Steel Shapes
(U.S. Customary Units)

Angles
Unequal Legs



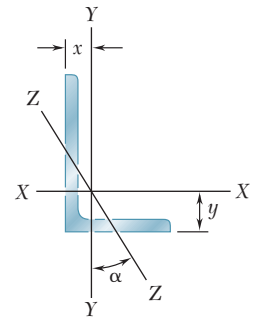
Size and Thickness, in.	Weight per Foot, lb/ft	Area, in ²	Axis X-X				Axis Y-Y				Axis Z-Z	
			<i>I</i> _x , in ⁴	<i>S</i> _x , in ³	<i>r</i> _x , in.	<i>y</i> , in.	<i>I</i> _y , in ⁴	<i>S</i> _y , in ³	<i>r</i> _y , in.	<i>x</i> , in.	<i>r</i> _z , in.	tan α
L8 × 6 × 1	44.2	13.0	80.9	15.1	2.49	2.65	38.8	8.92	1.72	1.65	1.28	0.542
¾	33.8	9.94	63.5	11.7	2.52	2.55	30.8	6.92	1.75	1.56	1.29	0.550
½	23.0	6.75	44.4	8.01	2.55	2.46	21.7	4.79	1.79	1.46	1.30	0.557
L6 × 4 × ¾	23.6	6.94	24.5	6.23	1.88	2.07	8.63	2.95	1.12	1.07	0.856	0.428
½	16.2	4.75	17.3	4.31	1.91	1.98	6.22	2.06	1.14	0.981	0.864	0.440
⅜	12.3	3.61	13.4	3.30	1.93	1.93	4.86	1.58	1.16	0.933	0.870	0.446
L5 × 3 × ½	12.8	3.75	9.43	2.89	1.58	1.74	2.55	1.13	0.824	0.746	0.642	0.357
¾	9.80	2.86	7.35	2.22	1.60	1.69	2.01	0.874	0.838	0.698	0.646	0.364
¼	6.60	1.94	5.09	1.51	1.62	1.64	1.41	0.600	0.853	0.648	0.652	0.371
L4 × 3 × ½	11.1	3.25	5.02	1.87	1.24	1.32	2.40	1.10	0.858	0.822	0.633	0.542
¾	8.50	2.48	3.94	1.44	1.26	1.27	1.89	0.851	0.873	0.775	0.636	0.551
¼	5.80	1.69	2.75	0.988	1.27	1.22	1.33	0.585	0.887	0.725	0.639	0.558
L3½ × 2½ × ½	9.40	2.75	3.24	1.41	1.08	1.20	1.36	0.756	0.701	0.701	0.532	0.485
¾	7.20	2.11	2.56	1.09	1.10	1.15	1.09	0.589	0.716	0.655	0.535	0.495
¼	4.90	1.44	1.81	0.753	1.12	1.10	0.775	0.410	0.731	0.607	0.541	0.504
L3 × 2 × ½	7.70	2.25	1.92	1.00	0.922	1.08	0.667	0.470	0.543	0.580	0.425	0.413
¾	5.90	1.73	1.54	0.779	0.937	1.03	0.539	0.368	0.555	0.535	0.426	0.426
¼	4.10	1.19	1.09	0.541	0.953	0.980	0.390	0.258	0.569	0.487	0.431	0.437
L2½ × 2 × ¾	5.30	1.55	0.914	0.546	0.766	0.826	0.513	0.361	0.574	0.578	0.419	0.612
¼	3.62	1.06	0.656	0.381	0.782	0.779	0.372	0.253	0.589	0.532	0.423	0.624

APPENDIX C Properties of Rolled-Steel Shapes

(SI Units)

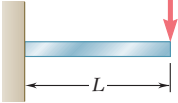
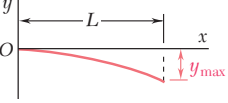
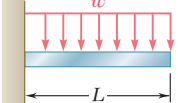
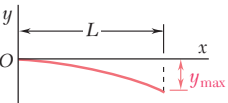
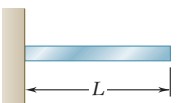
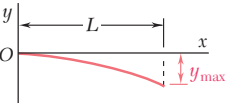
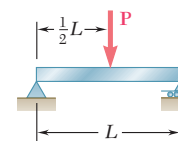
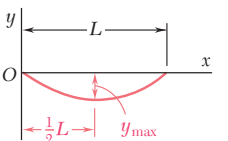
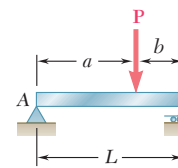
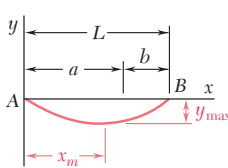
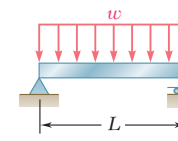
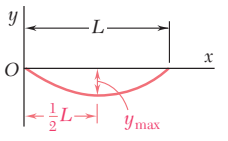
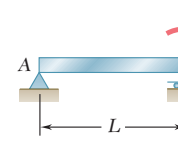
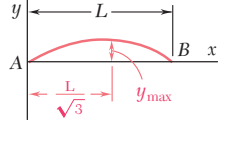
Angles

Unequal Legs



Size and Thickness, mm	Mass per Meter kg/m	Area mm ²	Axis X-X				Axis Y-Y				Axis Z-Z	
			I_x 10 ⁶ mm ⁴	S_x 10 ³ mm ³	r_x mm	y mm	I_y 10 ⁶ mm ⁴	S_y 10 ³ mm ³	r_y mm	x mm	r_z mm	$\tan \alpha$
L203 × 152 × 25.4	65.5	8390	33.7	247	63.2	67.3	16.1	146	43.7	41.9	32.5	0.542
19	50.1	6410	26.4	192	64.0	64.8	12.8	113	44.5	39.6	32.8	0.550
12.7	34.1	4350	18.5	131	64.8	62.5	9.03	78.5	45.5	37.1	33.0	0.557
L152 × 102 × 19	35.0	4480	10.2	102	47.8	52.6	3.59	48.3	28.4	27.2	21.7	0.428
12.7	24.0	3060	7.20	70.6	48.5	50.3	2.59	33.8	29.0	24.9	21.9	0.440
9.5	18.2	2330	5.58	54.1	49.0	49.0	2.02	25.9	29.5	23.7	22.1	0.446
L127 × 76 × 12.7	19.0	2420	3.93	47.4	40.1	44.2	1.06	18.5	20.9	18.9	16.3	0.357
9.5	14.5	1850	3.06	36.4	40.6	42.9	0.837	14.3	21.3	17.7	16.4	0.364
6.4	9.80	1250	2.12	24.7	41.1	41.7	0.587	9.83	21.7	16.5	16.6	0.371
L102 × 76 × 12.7	16.4	2100	2.09	30.6	31.5	33.5	0.999	18.0	21.8	20.9	16.1	0.542
9.5	12.6	1600	1.64	23.6	32.0	32.3	0.787	13.9	22.2	19.7	16.2	0.551
6.4	8.60	1090	1.14	16.2	32.3	31.0	0.554	9.59	22.5	18.4	16.2	0.558
L89 × 64 × 12.7	13.9	1770	1.35	23.1	27.4	30.5	0.566	12.4	17.8	17.8	13.5	0.485
9.5	10.7	1360	1.07	17.9	27.9	29.2	0.454	9.65	18.2	16.6	13.6	0.495
6.4	7.30	929	0.753	12.3	28.4	27.9	0.323	6.72	18.6	15.4	13.7	0.504
L76 × 51 × 12.7	11.5	1450	0.799	16.4	23.4	27.4	0.278	7.70	13.8	14.7	10.8	0.413
9.5	8.80	1120	0.641	12.8	23.8	26.2	0.224	6.03	14.1	13.6	10.8	0.426
6.4	6.10	768	0.454	8.87	24.2	24.9	0.162	4.23	14.5	12.4	10.9	0.437
L64 × 51 × 9.5	7.90	1000	0.380	8.95	19.5	21.0	0.214	5.92	14.6	14.7	10.6	0.612
6.4	5.40	684	0.273	6.24	19.9	19.8	0.155	4.15	15.0	13.5	10.7	0.624

APPENDIX D Beam Deflections and Slopes

Beam and Loading	Elastic Curve	Maximum Deflection	Slope at End	Equation of Elastic Curve
1 		$-\frac{PL^3}{3EI}$	$-\frac{PL^2}{2EI}$	$y = \frac{P}{6EI}(x^3 - 3Lx^2)$
2 		$-\frac{wL^4}{8EI}$	$-\frac{wL^3}{6EI}$	$y = -\frac{w}{24EI}(x^4 - 4Lx^3 + 6L^2x^2)$
3 		$-\frac{ML^2}{2EI}$	$-\frac{ML}{EI}$	$y = -\frac{M}{2EI}x^2$
4 		$-\frac{PL^3}{48EI}$	$\pm \frac{PL^2}{16EI}$	For $x \leq \frac{1}{2}L$: $y = \frac{P}{48EI}(4x^3 - 3L^2x)$
5 		For $a > b$: $-\frac{Pb(L^2 - b^2)^{3/2}}{9\sqrt{3}EIL}$ at $x_m = \sqrt{\frac{L^2 - b^2}{3}}$	$\theta_A = -\frac{Pb(L^2 - b^2)}{6EIL}$ $\theta_B = +\frac{Pa(L^2 - a^2)}{6EIL}$	For $x < a$: $y = \frac{Pb}{6EIL}[x^3 - (L^2 - b^2)x]$ For $x = a$: $y = -\frac{Pa^2b^2}{3EIL}$
6 		$-\frac{5wL^4}{384EI}$	$\pm \frac{wL^3}{24EI}$	$y = -\frac{w}{24EI}(x^4 - 2Lx^3 + L^3x)$
7 		$\frac{ML^2}{9\sqrt{3}EI}$	$\theta_A = +\frac{ML}{6EI}$ $\theta_B = -\frac{ML}{3EI}$	$y = -\frac{M}{6EIL}(x^3 - L^2x)$

Appendix E

Fundamentals of Engineering Examination

Engineers are required to be licensed when their work directly affects the public health, safety, and welfare. The intent is to ensure that engineers have met minimum qualifications, involving competence, ability, experience, and character. The licensing process involves an initial exam, called the *Fundamentals of Engineering Examination*, professional experience, and a second exam, called the *Principles and Practice of Engineering*. Those who successfully complete these requirements are licensed as a *Professional Engineer*. The exams are developed under the auspices of the *National Council of Examiners for Engineering and Surveying*.

The first exam, the *Fundamentals of Engineering Examination*, can be taken just before or after graduation from a four-year accredited engineering program. The exam stresses subject material in a typical undergraduate engineering program, including *Mechanics of Materials*. The topics included in the exam cover much of the material in this book. The following is a list of the main topic areas, with references to the appropriate sections in this book. Also included are problems that can be solved to review this material.

Stresses (1.3–1.8; 1.11–1.12)

Problems: 1.1, 1.7, 1.31, 1.37

Strains (2.2–2.3; 2.5–2.6; 2.8–2.11; 2.14–2.15)

Problems: 2.7, 2.19, 2.41, 2.49, 2.63, 2.68

Torsion (3.2–3.6; 3.13)

Problems: 3.6, 3.28, 3.35, 3.51, 3.132, 3.138

Bending (4.2–4.6; 4.12)

Problems: 4.11, 4.23, 4.34, 4.47, 4.104, 4.109

Shear and Bending-Moment Diagrams (5.2–5.3)

Problems: 5.6, 5.9, 5.42, 5.48

Normal Stresses in Beams (5.1–5.3)

Problems: 5.18, 5.21, 5.55, 5.61

Shear (6.2–6.4; 6.6–6.7)

Problems: 6.2, 6.12, 6.32, 6.36

Transformation of Stresses and Strains (7.2–7.4; 7.7–7.9)

Problems: 7.6, 7.13, 7.33, 7.41, 7.81, 7.87, 7.102, 7.109

Deflection of Beams (9.2–9.4; 9.7)

Problems: 9.6, 9.10, 9.72, 9.75

Columns (10.2–10.4)

Problems: 10.11, 10.21, 10.28

Strain Energy (11.2–11.4)

Problems: 11.10, 11.14, 11.19

Photo Credits

CHAPTER 1

Opener: © Construction Photography/CORBIS RF; 1.1: © Vince Streano/CORBIS; 1.2: © John DeWolf.

CHAPTER 2

Opener: © Construction Photography/CORBIS; 2.1: © John DeWolf; 2.2: Courtesy of Tinius Olsen Testing Machine Co., Inc.; 2.3, 2.4, 2.5: © John DeWolf.

CHAPTER 3

Opener: © Brownie Harris; 3.1: © 2008 Ford Motor Company; 3.2: © John DeWolf; 3.3: Courtesy of Tinius Olsen Testing Machine Co., Inc.

CHAPTER 4

Opener: © Lawrence Manning/CORBIS; 4.1: Courtesy of Flexifoil; 4.2: © Tony Freeman/Photo Edit; 4.3: © Hisham Ibrahim/Getty Images RF; 4.4: © Kevin R. Morris/CORBIS; 4.5: © Tony Freeman/Photo Edit; 4.6: © John DeWolf.

CHAPTER 5

Opener: © Mark Segal/Digital Vision/Getty Images RF; 5.1: © David Papazian/CORBIS RF; 5.2: © Godden Collection, National Information Service for Earthquake Engineering, University of California, Berkeley.

CHAPTER 6

Opener: © Godden Collection, National Information Service for Earthquake Engineering, University of California, Berkeley; 6.1:

© John DeWolf; 6.2: © Jake Wyman/Getty Images; 6.3: © Rodho/shutterstock.com.

CHAPTER 7

Opener: NASA; 7.1: © Radlund & Associates/Getty Images RF; 7.2: © Spencer C. Grant/Photo Edit; 7.3: © Clair Dunn/Alamy; 7.4: © Spencer C. Grant/Photo Edit.

CHAPTER 8

Opener: © Mark Read.

CHAPTER 9

Opener: © Construction Photography/CORBIS; 9.1: Royalty-Free/CORBIS; 9.2 and 9.3: © John DeWolf; 9.4: Courtesy of Aztec Galvenizing Services; 9.5: Royalty-Free/CORBIS.

CHAPTER 10

Opener: © Jose Manuel/Photographer's Choice RF/Getty Images; 10.1: © Courtesy of Fritz Engineering Laboratory, Lehigh University; 10.2a: © Godden Collection, National Information Service for Earthquake Engineering, University of California, Berkeley; 10.2b: © Peter Marlow/Magnum Photos.

CHAPTER 11

Opener: © Corbis Super RF/Alamy; 11.1: © Daniel Schwen; 11.2: © Tony Freeman/Photo Edit Inc.; 11.3: Courtesy of L.I.E.R. and Sec Envel.

This page intentionally left blank

Index

A

Accuracy, numerical, 17, 44
Actual deformation, 95, 99
Allowable load and allowable stress, 4
 factor of safety, 31–32, 44
 shearing stresses, 156–158
Allowable-stress method, 235
 design of columns under an eccentric load, 675–676, 685–686
Aluminum
 design of columns under a centric load, 664–665
 properties of, 58, 60, 129, A12–A13
 structural tubing, 202
American Forest & Paper Association, 665
American Institute of Steel Construction, 662, 667
American standard beams (S-beams), 231, 388
American standard channel steel (C shapes), properties of, A22–A23
American standard shape steel (S shapes), properties of, A20–A21
American wide-flange beam (W-beam), 231, 388
Analysis and design of beams for bending, 314–379
 computer problems, 378–379
 design of prismatic beams for bending, 339–349, 370, 371–372
 introduction, 316–319
 nonprismatic beams, 361–369, 373
 relations among load, shear, and bending moment, 329–339, 371
 review problems, 374–377
 shear and bending-moment diagrams, 319–328, 370–371
 summary, 370–373
 using singularity functions to determine shear and bending moment in a beam, 350–361, 372–373
Analysis and design of simple structures, 14–16
 determining bearing stresses, 16
 determining normal stress, 14–15
 determining shearing stress, 15–16
Angle of twist, 143, 145–147, 189
 adding algebraically, 161
 in elastic range, 159–163, 165, 211
Angle steel
 equal legs, A24–A25
 properties of, A24–A27
 unequal legs, A26–A27
Anisotropic materials, 63, 130
Anticlastic curvature, 234, 306

Areas. *See* Moments of areas

Average value, of stresses, 9, 42

Axes

 centroidal, A6, A9–A10

 of symmetry, A3

Axial loading

 bearing stress in connections, 13, 43

 centric, 42

 deformations under, 67–71, 101–103

 eccentric, 42, 284–293, 308

 normal stress, 9–11, 42

 shearing stress, 11–13, 43

 slowly increasing, 694

 stress and strain distribution under, 52–139

 stress and strain in, 138–139

Axisymmetry, of circular shafts, 146, 197

B

Bauschinger effect, 65

Beam deflections and slopes, 585, 720–721, 725, A28

Beam elements

 of arbitrary curved surface, longitudinal shear on, 428

 of arbitrary shape, longitudinal shear on, 399–400

 shear on the horizontal face of, 384–386, 427

Beams. *See also* Analysis and design of beams for bending

 of constant strength, 373

 nonprismatic, 318, 361–369, 373

 overhanging, 554

 simply-supported, 554

 statically indeterminate, 561–571, 620

 of variable cross section, 551

Bearing stresses, 4, 13, 16, 18, 43

 in connections, 13, 43

 determination of, 16

Bearing surfaces, 13, 43

Bend and twist, 415, 420

Bending. *See also* Pure bending

 analysis and design of beams for, 314–379

 of curved members, 294–304, 308

 of members made of several materials, 242–245, 306

 stresses due to, 419, 531, 679

Bending moment, 225, 235, 263

 relation to shear, 330–335

Bending-moment diagrams, 318–328, 333–335, 370–371

 by parts, 551, 597–604, 623

- Boundary conditions, 554, 564–565, 574–576, 619
- Breaking strength, 59
- Brittle materials, 54, 58–61, 129
 - under plane stress, fracture criteria for, 469–477, 505
 - sudden failure of, 32, 151
- Bulk modulus, 55, 96–98, 132

C

- C shapes. *See* Standard shape steel channels
- Cantilever beams, 554, 595, 623
 - and beams with symmetric loadings, 595–596, 623
- Cast iron, properties of, A12–A13
- Castigliano, Alberto, 735
- Castigliano's theorem, 694, 734–735, 753
 - deflections by, 736–739
- Center of symmetry, 421, A3
- Centric loading, 10, 223, 270
 - axial, 42
 - design of columns under, 660–674, 686
- Centroid, 236
 - of an area, A2–A4
 - of a composite area, A4–A6
- Centroidal axis, A6, A9–A10
- Centroidal moment of inertia, 236, 400, 407, 515
- Circular shafts
 - as axisymmetric, 146, 197
 - deformations in, 144–148, 184–186, 210, 212
 - made of an elastoplastic material, 186–189, 212–213
- Clebsch, A., 354
- Coefficients
 - influence, 732
 - of thermal expansion, 82, 131
- Columns, 630–691
 - computer problems, 690–691
 - critical load, 684
 - design of under a centric load, 660–674, 686
 - design of under an eccentric load, 675–683, 685–686
 - eccentric loading, 649–660, 685–686
 - effective length, 632, 685
 - Euler's formula for pin-ended columns, 635–638, 684–685
 - extension of Euler's formula to columns with other end conditions, 638–649
 - introduction, 632
 - review problems, 687–689
 - the secant formula, 632, 649–660, 685–686
 - slenderness ratio, 685
 - stability of structures, 632–635
 - summary, 684–686
- Combined loadings, stresses under, 527–539, 613
- Combined stresses, 419
- Components of stress, 4, 27–30
- Composite materials, 224
 - fiber-reinforced, stress-strain relationships for, 103–107, 134

- Compression, 227
 - modulus of, 97
- Computations, 17
 - errors in, 17
- Computer problems
 - analysis and design of beams for bending, 378–379
 - applying singularity functions to determine shear and bending moment in a beam, 355
 - axial loading, 138–139
 - columns, 690–691
 - concept of stress, 49–51
 - deflection of beams, 627–629
 - energy methods, 757–758
 - principal stresses under a given loading, 545–547
 - pure bending, 312–313
 - shearing stresses in beams and thin-walled members, 434–435
 - torsion, 218–219
 - transformations of stress and strain, 510–511
- Concentrated loads, 316
 - single, 720
- Concentric stress, 679
- Concept of stress, 2–51
 - computer problems, 49–51
- Concrete
 - maximum stress in, 249
 - properties of, 129, A14–A15
 - reinforced beams of, 245
 - stress-strain diagram for, 61
- Constant strength, 319, 362, 373
- Constants of integration, determination of, 558
- Copper, properties of, A12–A13
- Coulomb, Charles Augustin de, 469–470
- Coulomb's criterion, 469
- Creep, 64
- Critical load, 634
 - on columns, 684
- Critical stress, 636
- Cupronickel, properties of, A14–A15
- Curvature, 232
 - anticlastic, 234, 306
 - radius of, 224, 235, 263
- Curved members, bending of, 294–304, 308
- Cylindrical thin-walled pressure vessels, stresses in, 505

D

- Dead load, 33
- Deflection of beams, 70, 86–87, 548–629
 - applying cantilever beams and beams with symmetric loadings, 595–596, 623
 - applying moment-area theorems to beams with unsymmetric loadings, 605–606, 625–626
 - applying superposition to statically indeterminate beams, 582–592, 621
 - bending-moment diagrams by parts, 597–604, 623

- Deflection of beams—*Cont.*
 - boundary conditions, 619
 - by Castigliano's theorem, 736–739, 753
 - computer problems, 627–629
 - direct determination of the elastic curve from the load distribution, 559–560
 - equation of the elastic curve, 553–558, 619
 - introduction, 550–552
 - maximum, 607–608, 624, 694, 722, 725, A28
 - method of superposition, 580–582, 585–587, 621
 - moment-area theorems, 592–595, 621–622
 - review problems, 625–626
 - under a single load, 722–732
 - statically indeterminate beams, 561–571, 620
 - summary, 618–624
 - under transverse loading, 552–553, 618
 - using moment-area theorems with statically indeterminate beams, 609–617, 624
 - using singularity functions to determine, 571–580, 620–621
 - by the work-energy method, 722–732
 - Deformations, 54, 86–87, 113, 167, 225, 561, 610. *See also*
 - Elastic deformations; Plastic deformations
 - actual, 95, 99
 - under axial loading, 67–71, 101–103
 - of a beam under transverse loading, 552–553, 618
 - in a circular shaft, 144–148, 210
 - computing, 17
 - maximum, 716
 - permanent, 224
 - in a symmetric member in pure bending, 226–228
 - in a transverse cross section, 233–241, 306
 - Design considerations, 30–35. *See also* Analysis and design
 - allowable load and allowable stress, 31–32, 44
 - determination of the ultimate strength of a material, 30–31
 - factor of safety, 44
 - for impact loads, 718–719
 - load and resistance factors, 33, 44, 341–343
 - for loads, 31
 - of prismatic beams for bending, 339–349, 370–372
 - selection of an appropriate factor of safety, 31–33
 - specifications of, 33
 - of transmission shafts, 143, 176–178, 518–527, 541
 - *Design considerations, of transmission shafts, 211
 - Design of columns
 - allowable-stress method, 662–664, 675–676, 686
 - aluminum, 664–665
 - under a centric load, 660–674, 686
 - under an eccentric load, 675–683, 686
 - for greatest efficiency, 643
 - interaction method, 676–677, 686
 - with load and resistance factor design, 667–669
 - structural steel, 662–664, 667–669
 - wood, 665–667
 - Deterioration, 32
 - Determination
 - of the bearing stresses, 16
 - of constants of integration, 558
 - of elastic curve, 559–560
 - of first moment, A4–A6
 - of forces, 113, 441
 - of the moment of inertia of a composite area, A10–A11
 - of the normal stress, 14–15
 - of the shearing stress, 15–16
 - of the shearing stresses in a beam, 386–387, 428
 - of the ultimate strength of a material, 30–31, 44
 - Deviation, tangential, 594
 - Diagonal stays, 52–53
 - Diagrams
 - free-body, 4, 17–18, 34–35, 42, 70–71
 - loading, 357
 - of shear, 319–328, 333–335, 342–343, 370–371
 - of shear and bending-moment, 319–328, 370–371, 597–604, 623
 - of stress-strain relationships, 54, 56–61, 129, 186, 716
 - Dilatation, 97, 132
 - bulk modulus, 96–98, 132
 - Dimensionless quantities, 56
 - Discontinuity, 350
 - Displacement, relative, 69
 - Distributed loading, 316, 613
 - Distribution of stresses
 - in a narrow rectangular beam, 390–399, 428
 - over the section, 418–419
 - statically indeterminate, 10
 - Double shear, 13
 - Ductile materials, 54, 58–60, 129, 151
 - under plane stress, yield criteria for, 467–469, 504
- ## E
- Eccentric axial loading, 42, 224
 - general case of, 284–293, 308
 - in a plane of symmetry, 270–278, 307
 - Eccentric loading, 223, 270
 - columns under, 649–660, 686
 - design of columns under, 675–683, 686
 - Effective length, of columns, 632, 685
 - Efficient design, for columns, 643
 - Elastic action, 123
 - Elastic core, radius of, 189
 - Elastic curve
 - direct determination from the load distribution, 559–560
 - equation of, 553–558, 563–565, 574–576, 619, A28
 - Elastic deformations, 229–232, 305
 - under axial loading, 130
 - Elastic flexure formula, 230, 305
 - Elastic limit, 63–64, 130
 - Elastic range, 229
 - angle of twist in, 159–163, 211
 - shearing stresses within, 210

- Elastic section modulus, 230, 259, 306
- Elastic strain energy
 - under axial loading, 699–700, 751
 - in bending, 700–701, 751
 - for normal stresses, 698
 - for shearing stresses, 701–703, 751
 - in torsion, 701–702, 751
 - under transverse loading, 703
- Elastic torque
 - formulas for, 149
 - maximum, 187, 213
- Elastic torsion, formulas for, 210
- Elastic unloading, 193, 265
- Elastic versus plastic behavior of a material, 64–65, 130
- Elasticity, modulus of, 54, 62–64, 130
- Elastoplastic materials, 117, 134, 224, 256–257, 307
 - circular shafts made of, 186–189, 212–213
 - members made of, 256–260
- Elementary work, 695
- Elongation
 - maximum, 119
 - percent, 61
- Endurance limit, 66, 130
- Energy methods, 692–758
 - Castigliano's theorem, 734–735, 753
 - computer problems, 757–758
 - deflection under a single load by the work-energy method, 722–732
 - deflections by Castigliano's theorem, 736–739, 753
 - design for impact loads, 718–719
 - elastic strain energy for normal stresses, 698
 - elastic strain energy for shearing stresses, 701–703, 751
 - equivalent static load, 752
 - impact loading, 716–718, 752
 - introduction, 694
 - modulus of resilience, 751
 - modulus of toughness, 750–751
 - review problems, 754–756
 - statically indeterminate structures, 740–749, 753
 - strain energy, 694–696, 750
 - strain-energy density, 696–698, 750
 - strain energy for a general state of stress, 704–715, 752
 - summary, 750–753
 - work and energy under a single load, 719–722, 752–753
 - work and energy under several loads, 732–734
- Engineering strain, 62
- Engineering stress, 61
- Equal-leg angle steel, A24–A25
- Equations
 - of the elastic curve, 553–558, 563–565, 574–576, 619, A28
 - equilibrium, 43
 - of statics, 152
- Equilibrium equations, 43
- Equivalent force-couple system, at shear center, 419
- Equivalent open-ended loadings, 373
- Equivalent static load, 721–722, 752

- Euler, Leonhard, 636
- Euler's formula, 632, 636, 654
 - extension to columns with other end conditions, 638–649
 - for pin-ended columns, 635–638, 684–685
- Experimental materials, 93

F

- Factor of safety, 44, 707
 - selection of appropriate, 31–33
- Failure, of shaft, 185
- Fatigue
 - limit of, 67
 - from repeated loadings, 32, 54, 66–67, 130
- Fiber-reinforced composite materials, 63–64
 - stress-strain relationships for, 103–107, 130, 133
- First moment, 385, A2–A6
 - determination of, A4–A6
- First moment-area theorem, 551, 593, 598–601, 606, 621–622
- Flexural rigidity, 554, 596, 619
- Flexural stress, 230
- Force-couple system, at shear center, equivalent, 419
- Forces
 - determination of, 113, 441
 - unknown, 43
- Formulas
 - elastic flexure, 230, 305
 - elastic torsion, 149, 210
 - Euler's, 632, 635–649, 654
 - interaction, 676–677
 - secant, 632, 649–660, 685–686
- Fracture criteria for brittle materials under plane stress, 439, 469–477, 505
 - maximum-normal-stress criterion, 469–470
 - Mohr's criterion, 470–471
- Free-body diagrams, 4, 17–18, 34–35, 42, 70–71
- Fundamentals of Engineering Examination*, A29–A30

G

- Gages
 - length, 57
 - pressure, 478, 496
 - strain, 440
- Gyration, radius of, A7–A9

H

- Hardening, strain, 64
- Hertz (Hz), 177, 212
- Homogeneous materials, 93
- Hooke, Robert, 62
- Hooke's law, 107, 117, 133, 148, 184, 186
 - generalized, 93–96, 100, 104, 132
 - modulus of elasticity, 62–64, 67, 130
- Hoop stress, 478

Horizontal shear, 385
Horsepower (hp), 212
Hydrostatic pressure, 97
Hz. *See* Hertz

I

IF/THEN/ELSE statements, 355
Impact loading, 694, 716–718, 752
Inertia. *See* Moments of inertia
Influence coefficients, 732
Integration
 constants of, 558
 methods of, 628
Interaction formula, 676–677
Interaction method, design of columns under an eccentric load,
 676–677, 686
Internal torques, 150, 163
Iron. *See* Cast iron
Isotropic materials, 63, 93, 113, 130

J

Joule (J), 695

K

Kinetic energy, 716

L

Lamina, 63
Laminates, 105
Lateral strain, 93, 132
Line of action, of loading, 113
Load and Resistance Factor Design (LRFD), 33, 44, 341–343.
 See also Allowable load and allowable stress
Load distribution, direct determination of the elastic curve
 from, 559–560
Loading diagram, modified, 357
Loadings. *See also* Unloading
 axial, 9–13, 42–43, 52–139, 284–293, 308
 centric, 10, 42, 223, 270, 660–674, 686
 combined, 527–539, 613
 concentrated, 316
 dead, 33
 distributed, 316, 613
 eccentric, 223, 270–278, 284–293, 307–308, 649–660,
 675–683, 686
 general conditions of, 27–30, 44, 541
 impact, 694, 716–718, 752
 line of action of, 113
 multiaxial, 94–96, 132
 open-ended, 373
 redundant reaction, 584, 613
 relation to shear, 329–330

Loadings—*Cont.*

 repeated, 66–67, 130
 statically equivalent, 114
 symmetric, 595–596, 623
 torsional, 519
 transverse, 223, 316, 552–553, 618
 ultimate, 31, 33, 667
 unknown, 79–80
 unsymmetric, 414–426, 429, 605–606, 625–626
 visualizing, 234
Longitudinal normal strain, 228
Longitudinal shear
 on a beam element of arbitrary curved surface, 428
 on a beam element of arbitrary shape, 399–400
Longitudinal stress, 478–479
Lower yield point, 60
LRFD. *See* Load and resistance factor design

M

Macaulay, W.H., 354
Macaulay's brackets, 354
Macroscopic cracks or cavities, detected in a structural
 component, 471
Magnesium alloys, properties of, A14–A15
Margin of safety, 31
Materials. *See also* Anisotropic materials; Brittle materials;
 Composite materials; Ductile materials; Elastoplastic
 materials; Experimental materials; Homogeneous
 materials; Isotropic materials; Orthotropic materials
 bending of members made of several, 242–245, 306
 determining ultimate strength of, 30–31
 elastic versus plastic behavior of, 64–65, 130
Materials used in engineering, A12–A15
 aluminum, A12–A13
 cast iron, A12–A13
 concrete, A14–A15
 copper, A12–A13
 cupronickel, A14–A15
 magnesium alloys, A14–A15
 Monel alloy 400, A14–A15
 plastics, A14–A15
 steel, A12–A13
 timber, A14–A15
 titanium, A14–A15
Matrix, 63, 104
Maximum absolute strain, 228
Maximum absolute stress, 229
Maximum deflection, 552–553, 607–608, 624, 694, 725, A28
Maximum deformation, 716
Maximum-distortion-energy criterion, 439, 468–469, 694
Maximum elastic moment, 224
Maximum elastic torque, 187, 213
Maximum elongation, 119
Maximum-normal-stress criterion, 440, 469–470
Maximum shearing strain, 491, 494

Maximum-shearing-stress criterion, 439, 445, 455–456, 467–469, 505

Maximum stress, 716, 722, 725

Maxwell, James Clerk, 734

Maxwell's reciprocal theorem, 734

Measurements of strain, strain rosette, 494–501, 506

Members

- curved, 294–304, 308
- made of an elastoplastic material, 256–260
- noncircular, 197–200, 214
- with a single plane of symmetry, 260–261
- stability of, 8
- symmetric, 224–225
- thin-walled, 414–426, 429
- two-force, 4–6

Membrane analogy, 199–200

Methods

- of integration, 628
- of problem solution, 16–17, 43
- of statics, review of, 4–6
- of superposition, 551, 580–582, 585–587, 621

Microscopic cracks or cavities, detected in a structural component, 471

Minimum shearing stresses, 150, 152

Mistakes, errors in, 17

Modulus

- bulk, 55, 96–98, 132
- of compression, 97
- elastic section, 230, 259, 306
- of elasticity, 54, 62–64, 130
- plastic section, 259
- of resilience, 694, 697–698, 751
- of rigidity, 55, 100, 105, 133
- of rupture, 185, 212, 256
- of toughness, 694, 697, 750–751

Mohr, Otto, 452, 470

Mohr's circle

- application to the three-dimensional analysis of stress, 464–466
- creating, 454, 457–458, 480, 493
- for plane strain, 440, 506
- for plane stress, 440, 452–462, 489–491, 503, 506

Mohr's criterion, 440, 470–472, 505

Moment-area theorems, 592–595, 610, 618, 621–622

- application to beams with unsymmetric loadings, 605–606, 625–626
- using with statically indeterminate beams, 609–617, 624

Moments of areas, A2–A11

- centroid of a composite area, A4–A6
- centroid of an area, A2–A4
- determination of the first moment, A4–A6
- determination of the moment of inertia of a composite area, A10–A11
- first moment of an area, A2–A4
- parallel-axis theorem, A9–A10
- radius of gyration, A7–A9
- second moment or moment of inertia of an area, A7–A9

Moments of inertia, 235. *See also* Bending moment

- centroidal, 236, 400, 407, 515
- of a composite area, determining, A10–A11
- polar, 165, A7

Monel alloy 400, properties of, A14–A15

Multiaxial loading, 104

- generalized Hooke's law, 94–96, 132

N

National Council of Examiners for Engineering and Surveying, A29

National Design Specification for Wood Construction, 666

Necking, 58–59

Neutral surface, 227–229, 295, 305

Noncircular sections, 200

Nonprismatic beams, 318, 361–369, 373

- beams of constant strength, 373

Normal strains, 487

- under axial loading, 55–57, 129
- longitudinal, 228

Normal stresses, 4, 9–11, 18, 20, 26, 42, 224, 317, 462, 528–530, 532, 694, 723–724, 751. *See also* Maximum-normal-stress criterion

- determination of, 14–15
- elastic strain energy for, 698

Numerical accuracy, 17, 44

O

Oblique parallelepipeds, 98–99

Oblique plane, stresses on, 4, 44

Offset method, for determination of yield strength, 60

Open-ended loadings, equivalent, 373

Orthotropic materials, 55, 105

Overhanging beams, 554

P

Pa. *See* Pascals

Parallel-axis theorem, A9–A10

Parallelepipeds

- oblique, 98–99
- rectangular, 94

Pascals (Pa), 7

Percent elongation, a measure of ductility, 60

Percent reduction in area, a measure of ductility, 60

Permanent deformations, 224

Permanent set, 64, 119, 130

Permanent twist, 190–191, 193

Plane of symmetry, plastic deformations of members with a single, 260–261

Plane strain, 109

Plane stress, 110, 706

- transformation of, 438, 486–488, 506

Plastic deformations, 54–55, 64, 117–123, 130, 134, 224, 255–256, 307, 404–414, 429
 in circular shafts, 144, 184–186, 192, 212
 of members with a single plane of symmetry, 260–261
 modulus of rupture, 212

Plastic hinge, 405

Plastic moment, 224, 264, 307

Plastic section modulus, 259

Plastic torque, 187, 213

Plastic versus elastic behavior of a material, 64–65, 130

Plastics, properties of, A14–A15

Poisson, Siméon Denis, 93

Poisson's ratio, 54–55, 93–94, 101, 132, 233

Polar moments of inertia, 165, A7

Power, 176

Principal stresses, 439, 463, 503
 in a beam, 515–517, 540
 under combined loadings, 527–539
 computer problems, 545–547
 design of transmission shafts, 518–527, 541
 under general loading conditions, 541
 under a given loading, 512–547
 introduction, 514
 maximum shearing stress, 443–451, 503
 review problems, 542–544
 summary, 540–541

Principles and Practice of Engineering, A29

Problem solution, method of, 16–17, 43

Professional Engineer, licensing as, A29

Properties
 of rolled-steel shapes, 520–521, A16–A27
 of selected materials used in engineering, A12–A15

Proportional limit, 62, 130

Pure bending, 220–313
 computer problems, 312–313
 of curved members, 294–304, 308
 deformations in a symmetric member, 226–228
 deformations in a transverse cross section, 233–241, 306
 eccentric axial loading in a plane of symmetry, 270–278, 307
 general case of eccentric axial loading, 284–293, 308
 introduction, 222–224
 members made of an elastoplastic material, 256–260
 of members made of several materials, 242–245, 306
 plastic deformations, 255–256, 260, 307
 residual stresses, 261–269
 review problems, 309–311
 stress concentrations, 246–254, 306
 stresses and deformations in the elastic range, 229–232, 305
 summary, 305–308
 symmetric member in, 224–225
 unsymmetric, 279–283, 308

R

Radius of curvature, 224, 235, 263
 permanent, 265–266

Radius of gyration, A7–A9

Rectangular beams, narrow, distribution of stresses in, 390–399, 428

Rectangular cross section bars, torsion of, 198–199, 214

Rectangular parallelepipeds, 94

Redundant reaction loading, 584, 613

Redundant reactions, 79

Reference tangent, 595, 600–601, 605–606, 611–612, 623

Relative displacement, 69

Repeated loadings, fatigue from, 66–67, 130

Residual stresses, 55, 121–123, 134, 224, 261–269
 in circular shafts, 144, 189–193, 212, 214

Resilience, modulus of, 694, 697–698, 751

Resistance factor, 667. *See also* Load and resistance factor design

Review problems
 analysis and design of beams for bending, 374–377
 axial loading, 135–137
 columns, 687–689
 concept of stress, 45–48
 deflection of beams, 625–626
 energy methods, 754–756
 principal stresses under a given loading, 542–544
 pure bending, 309–311
 shearing stresses in beams and thin-walled members, 427–433
 torsion, 215–217
 transformations of stress and strain, 507–509

Rigid-body rotation, 99

Rigidity
 flexural, 554, 596, 619
 modulus of, 55, 100, 105, 133

Rolled-steel shapes, A16–A27
 American standard channels, A22–A23
 American standard shapes, A20–A21
 angles, A24–A27
 wide-flange shapes, A16–A19

Rotation
 rigid-body, 99
 speed of, 176

Rupture, modulus of, 185, 212, 256

S

Safety factor. *See* Factor of safety; Margin of safety

Saint-Venant, Adhémar Barré de, 114

Saint-Venant's principle, 113–115, 134, 147–148, 234, 284, 391, 517, 528, 552

Secant formula, 632, 649–660, 685–686

Second moment, of areas, A7–A9

Second moment-area theorem, 551, 594, 598–601, 622

Shafts
 axis of, 148
 on failure, 185
 statically indeterminate, 163–167, 211

Shape factor, 259

- Shear
 - double, 13
 - horizontal, 385
 - relation to bending moment, 330–335
 - relation to load, 329–330
 - single, 13, 43
- Shear center, 384, 404, 414–426, 429
 - equivalent force-couple system at, 419
- Shear diagrams, 319–328, 333–335, 342–343, 370–371
- Shear flow, 201, 383, 385, 403, 428
- Shearing strains, 98–101, 133, 487
 - distribution of, 143–144, 147–148
- Shearing stresses, 4, 11–13, 18, 29–30, 43, 317, 392–393, 418, 724. *See also* Maximum-shearing-stress criterion
 - allowable, 156–158, 167
 - average, 18, 43, 386, 428
 - in beams, 386–389, 428
 - in a circular shaft, 148–149
 - components of, 29
 - computer problems, 434–435
 - determination of, 15–16, 386–387, 428
 - within the elastic range, 210
 - elastic strain energy for, 701–703, 751
 - in flanges, 418
 - on the horizontal face of a beam element, 384–386, 427
 - introduction, 382–384
 - longitudinal
 - on a beam element of arbitrary curved surface, 428
 - on a beam element of arbitrary shape, 399–400
 - minimum, 150, 152
 - in a narrow rectangular beam, 390–399, 428
 - plastic deformations, 404–414, 429
 - review problems, 427–433
 - summary, 427–429
 - in thin-walled members, 401–404, 429
 - unsymmetric loading of thin-walled members, 414–426, 429
 - in webs, 418
- Shearing stresses in beams and thin-walled members, 380–435
- Simple structures, analysis and design of, 14–16
- Single shear, 13, 43
- Singularity functions, 318, 551
 - application to computer programming, 355
 - equivalent open-ended loadings, 373
 - step function, 372
 - using to determine shear and bending moment in a beam, 350–361, 372–373
 - using to determine the slope and deflection of a beam, 571–580, 620–621
- Slenderness ratio, 637, 667, 685
- Slip, 64
- Speed of rotation, 176
- Spherical thin-walled pressure vessels, stresses in, 505
- Stability of members, 8
- Stability of structures, in columns, 632–635
- Standard beam (S-beam), 231, 388
- Standard shape steel beams (S shapes), properties of, A20–A21
- Standard shape steel channels (C shapes), properties of, A22–A23
- Statically determinate problems, 317, 370, 554
- Statically equivalent loadings, 114
- Statically indeterminate problems, 54, 78–81, 131, 225, 317, 550–552
 - beams, 561–571, 620
 - distribution of stresses, 10
 - to the first degree, 562, 610, 620–621
 - to the second degree, 562, 610, 620
 - shafts, 143–144, 163–167, 210–211
 - superposition method, 79–81
 - use of moment-area theorems with, 609–617, 624
- Statically indeterminate structures, energy methods for, 740–749, 753
- Statics, 86–87
 - equations of, 152
 - review of methods, 4–6
- Steel. *See also* Rolled-steel shapes; Structural steel
 - properties of, 58, 129, A12–A13
 - stresses in, 63, 248–249
- Step function (STP), 352, 372
- Strain energy, 708, 716, 720, 726
 - under axial loading, 699–700, 751
 - in bending, 700–701, 751
 - and energy methods, 694–696, 750
 - for a general state of stress, 704–715, 752
 - in torsion, 701–702, 751
 - under transverse loading, 703
- Strain-energy density, 694, 696–698, 707
 - energy methods, 696–698, 750
- Strain gages, 440
- Strain hardening, 64
- Strain rosette, 440, 494–501, 506
- Strains. *See also* Stress and strain distribution under axial loading; Stress-strain relationships; True stress and true strain
 - analysis of, 113
 - distribution of, 187
 - engineering, 62
 - lateral, 93, 132
 - normal, under axial loading, 55–57, 129
 - plane, 109
 - thermal, 82, 131
 - three-dimensional analysis of, 491–494
- Strength. *See also* Ultimate strength of a material
 - breaking, 59
 - constant, 319, 362, 373
 - yield, 707
- Stress and strain distribution under axial loading, 52–139
 - deformations under, 67–71, 101–103, 130
 - dilatation, 132
 - elastic versus plastic behavior of a material, 64–65, 130
 - Hooke's law, 62–64, 67, 130
 - introduction, 54–55
 - modulus of rigidity, 133

Stress and strain distribution under axial loading—*Cont.*

- multiaxial loading, 94–96, 132
 - normal strain under, 55–57, 129
 - plastic deformations, 117–121, 134
 - Poisson's ratio, 93–94, 101, 132
 - problems involving temperature changes, 82–87, 131
 - repeated loadings, fatigue, 66–67, 130
 - residual stresses, 121–123, 134
 - review problems, 135–137
 - under Saint-Venant's principle, 113–115, 134
 - shearing strain, 98–101, 133
 - statically indeterminate problems, 78–81, 131
 - summary, 129–134
 - true stress and true strain, 61–62
- Stress concentration factor, 115–116
- Stress concentrations, 55, 134, 224, 246–254, 306
- in circular shafts, 179–180, 212
- Stress-strain relationships, 184–185. *See also* True stress and true strain
- diagrams of, 54, 56–61, 129, 186, 716
 - for fiber-reinforced composite materials, 103–107, 133
 - nonlinear, diagrams of, 185, 189
- Stress trajectories, 517
- Stresses. *See also* Allowable load and allowable stress; Distribution of stresses; Principal stresses; Shearing stresses
- analysis and design, 8
 - application to the analysis and design of simple structures, 14–16
 - average value of, 9, 42
 - bearing, 4, 13, 16, 43
 - under combined loadings, 527–539
 - computing, 17
 - concept of, 2–51
 - critical, 636
 - design considerations, 30–35
 - determination of, 113
 - due to bending, 419
 - due to twisting, 419
 - in the elastic range, 148–153, 210–211
 - engineering, 61
 - flexural, 230
 - under general loading conditions, 44, 541
 - general state of, 462–463, 504, 694
 - hoop, 478
 - introduction, 4
 - longitudinal, 478–479
 - maximum, 716, 722, 725
 - in the members of a structure, 7
 - method of problem solution, 16–17, 43
 - normal, 4, 9–11, 18, 20, 26, 42, 317, 462, 528–530, 532, 694, 723–724, 751
 - numerical accuracy, 17, 44
 - on an oblique plane under axial loading, 26–27, 44
 - plane, 110, 438, 486–488, 506, 706
 - residual, 121–123, 134, 189–193, 214, 261–269

Stresses—*Cont.*

- review of methods of statics, 4–6
 - review problems, 45–48
 - in a shaft, 144–145
 - in steel, 248–249
 - summary, 42–44
 - in thin-walled pressure vessels, 478–485
 - uniaxial, 227
- Stresses and deformations in the elastic range, 229–232, 305
- elastic flexure formula, 305
- Structural steel
- allowable stress design, for columns under a centric load, 662–664
 - load and resistance factor design, for columns under a centric load, 667–669
- Superposition
- application to statically indeterminate beams, 582–592, 621
 - method of, 79–81, 273, 300, 422, 551, 621
 - principle of, 95
- Symmetric loadings, cantilever beams and beams with, 595–596, 623
- Symmetric members, in pure bending of, 224–228, 305
- Symmetry
- axis of, A3
 - center of, 421, A3

T

- Tangential deviation, 594
- Temperature changes, problems involving, 82–87, 131
- Tensile test, 57
- Tension, 227
- Thermal expansion, coefficient of, 82, 131
- Thermal strain, 82, 131
- Thin-walled hollow shafts, 200–203, 214
- Thin-walled pressure vessels, 440, 505
- Three-dimensional analysis of strain, 491–494
- Three-dimensional state of stress, 439
- Timber, properties of, A14–A15
- Titanium, properties of, A14–A15
- Torques, 142. *See also* Elastic torque; Plastic torque
- internal, 150, 163
 - largest permissible, 150
 - maximum permissible, 166
- Torsion, 140–219
- of bars of rectangular cross section, 214
 - computer problems, 218–219
 - introduction, 142–144
 - modulus of rupture in, 185
 - of noncircular members, 197–200, 214
 - plastic deformations in circular shafts, 184–186, 212
 - review problems, 215–217
 - summary, 210–214
- Torsion testing machine, 159
- Torsional loading, 519

Total work, 695

Toughness, modulus of, 694, 697, 750–751

Transformations of stress and strain, 436–511

- application of Mohr's circle to the three-dimensional analysis of stress, 464–466
- computer problems, 510–511
- fracture criteria for brittle materials under plane stress, 469–477, 505
- general state of stress, 462–463, 504
- introduction, 438–440
- maximum shearing stress, 443–451, 503
- measurements of strain, 494–501, 506
- Mohr's circle for plane stress, 452–462, 489–491, 503, 506
- of plane stress, 440–442, 486–488, 502, 506
- principal stresses, 503
- review problems, 507–509
- stresses in thin-walled pressure vessels, 478–485
- summary, 502–506
- three-dimensional analysis of strain, 491–494
- yield criteria for ductile materials under plane stress, 467–469, 504

Transformed sections, drawing, 224

Transmission shafts, 142

- design considerations of, 211
- design of, 143

Transverse cross section, deformations in, 233–241, 306

Transverse loading, 223, 316

- deformations of a beam under, 43, 552–553, 618

Tresca, Henri Edouard, 468

Tresca's hexagon, 468

True stress and true strain, 61–62

Twisting. *See also* Angle of twist; Permanent twist

- stresses due to, 419, 531

Two-force members, 4–6

U

Ultimate loads, 31, 33, 667

Ultimate strength of a material, 4, 59

- determination of, 30–31, 44

Unequal-leg angle steel, A26–A27

Uniaxial stress, 227

Unknown forces, 43

Unknown loads, 79–80

Unloading, 123

- elastic, 193

Unsymmetric bending, 224, 279–283, 308

Unsymmetric loadings

- combined stresses, 419
- distribution of stresses over the section, 418–419
- equivalent force-couple system at shear center, 419
- shear center, 414–426, 429
- shearing stresses in flanges, 418
- shearing stresses in webs, 418
- stresses due to bending, 419
- stresses due to twisting, 419
- of thin-walled members, 414–426

Upper yield point, 60

V

von Mises, Richard, 468

von Mises criterion, 468

W

Watts (W), 212

Wide-flange beam (W-beam), 231, 388

Wide-flange shaped steel (W shapes), properties of, A16–A19

Winkler, E., 294

Wood. *See also* Timber

- design of columns under a centric load, 665–667
- maximum stress in, 248

Work

- elementary, 695
- total, 695

Work and energy

- principle of, 725–726
- under several loads, 732–734
- under a single load, 719–722, 752–753

Working load, 31

Y

Yield criteria for ductile materials under plane stress, 439, 467–469, 504

- maximum-distortion-energy criterion, 468–469
- maximum-shearing-stress criterion, 467–469

Yield points, upper and lower, 60

Yield strength, 58–60, 129, 707

- determination by offset method, 60

Yielding, 32

Young, Thomas, 62

Young's modulus, 62

Answers to Problems

Answers to problems with a number set in straight type are given on this and the following pages. Answers to problems with a number set in italic are not listed.

CHAPTER 1

- 1.1 $d_1 = 22.6 \text{ mm}$; $d_2 = 15.96 \text{ mm}$.
1.2 (a) 35.7 MPa. (b) 42.4 MPa.
1.3 28.2 kips.
1.4 (a) 12.73 ksi. (b) -2.83 ksi.
1.7 (a) 101.6 MPa. (b) -21.7 MPa.
1.8 (a) -640 psi. (b) -320 psi.
1.9 10.64 ksi.
1.10 285 mm^2 .
1.13 -4.97 MPa.
1.14 (a) 17.86 kN. (b) -41.4 MPa.
1.15 5.93 MPa.
1.16 12.33 in.
1.18 60.2 mm.
1.19 63.3 mm.
1.21 10.82 in.
1.22 (a) 3.33 MPa. (b) 525 mm.
1.23 (a) 444 psi. (b) 7.50 in. (c) 2400 psi.
1.26 (a) 25.9 mm. (b) 271 MPa.
1.27 (a) 80.8 MPa. (b) 127.0 MPa. (c) 203 MPa.
1.28 (a) 10.84 ksi. (b) 5.11 ksi.
1.29 $\sigma = 70.0 \text{ psi}$; $\tau = 40.4 \text{ psi}$.
1.30 (a) 1.500 kips. (b) 43.3 psi.
1.31 $\sigma = 489 \text{ kPa}$; $\tau = 489 \text{ kPa}$.
1.32 (a) 13.95 kN. (b) 620 kPa.
1.35 (a) 0 (tension) at $\theta = 90^\circ$;
54.1 MPa (compression) at $\theta = 0^\circ$.
(b) 27.0 MPa at $\theta = 45^\circ$.
1.36 (a) 706 kN. (b) $\theta = 45^\circ$. (c) 18.00 MPa.
(d) 36.0 MPa (compression).
1.37 3.60
1.39 (a) 1.141 in. (b) 1.549 in.
1.40 (a) 3.35. (b) 1.358 in.
1.41 168.1 mm^2 .
1.43 5.75 in.
1.44 1.800.
1.45 10.25 kN.
1.48 2.50.
1.49 (a) 1.550 in. (b) 8.05 in.
1.51 1.683 kN.
1.52 2.06 kN.
1.53 3.02.
1.55 3.72 kN.
1.56 3.97 kN.
1.57 (a) 629 lb. (b) 1.689.
1.58 (a) 362 kg. (b) 1.718.
1.59 14.93 mm.
1.61 (a) 8.92 ksi. (b) 22.4 ksi. (c) 11.21 ksi.
1.63 2.25 kips.
1.65 3.45.
1.67 (a) 5.57 mm. (b) 38.9 MPa. (c) 35.0 MPa.

- 1.68 $\sigma_{\text{all}} d/4 \tau_{\text{all}}$.
1.69 $21.3^\circ \leq \theta \leq 32.3^\circ$.
1.70 (a) 27.5° . (b) 3.31.
1.C2 (c) $16 \text{ mm} \leq d \leq 22 \text{ mm}$. (d) $18 \text{ mm} \leq d \leq 22 \text{ mm}$.
1.C3 (c) $0.70 \text{ in.} \leq d \leq 1.10 \text{ in.}$ (d) $0.85 \text{ in.} \leq d \leq 1.25 \text{ in.}$
1.C4 (b) For $\beta = 38.66^\circ$, $\tan \beta = 0.8$; BD is perpendicular to BC .
(c) $F.S. = 3.58$ for $\alpha = 26.6^\circ$; \mathbf{P} is perpendicular to line AC .
1.C5 (b) Member of Fig. P 1.29, for $\alpha = 60^\circ$:
(1) 70.0 psi; (2) 40.4 psi; (3) 2.14; (4) 5.30; (5) 2.14.
Member of Fig. P 1.31, for $\alpha = 45^\circ$:
(1) 489 kPa; (2) 489 kPa; (3) 2.58; (4) 3.07; (5) 2.58.
1.C6 (d) $P_{\text{all}} = 5.79 \text{ kN}$; stress in links is critical.

CHAPTER 2

- 2.1 (a) 2.45 kN. (b) 50.0 mm.
2.2 (a) 0.381 in. (b) 17.58 ksi.
2.3 (a) 9.09 ksi. (b) 1.760.
2.4 (a) 9.82 kN. (b) 500 MPa.
2.6 (a) 0.546 mm. (b) 36.3 MPa.
2.7 73.7 GPa.
2.9 $d_{\text{min}} = 0.1701 \text{ in.}$; $L_{\text{min}} = 36.7 \text{ in.}$
2.11 9.21 mm.
2.13 1.988 kN.
2.14 1.219 in.
2.15 0.1812 in.
2.18 (a) 9.53 kips. (b) $1.254 \times 10^{-3} \text{ in.}$
2.19 (a) 32.8 kN. (b) 0.0728 mm \downarrow .
2.20 (a) 0.01819 mm \uparrow . (b) 0.0919 mm \downarrow .
2.21 (a) 0.1767 in. (b) 0.1304 in.
2.22 50.4 kN.
2.23 $\delta_{AB} = -2.11 \text{ mm}$; $\delta_{AC} = 2.03 \text{ mm}$.
2.25 $4.71 \times 10^{-3} \text{ in.}$ \downarrow .
2.27 14.74 kN.
2.28 (a) $80.4 \mu\text{m}$ \uparrow . (b) $209 \mu\text{m}$ \downarrow . (c) $390 \mu\text{m}$ \downarrow .
2.29 $Ph/\pi Eab$ \downarrow .
2.30 (a) $\rho g L^2/2E$. (b) $W/2$
2.35 (steel) -15.80 ksi; (concrete) -1.962 ksi.
2.36 (a) -57.1 MPa. (b) -85.7 MPa.
2.37 -0.306 mm.
2.38 (a) (steel) -18.01 ksi; (aluminum) -6.27 ksi.
(b) $-6.21 \times 10^{-3} \text{ in.}$
2.39 177.4 lb.
2.41 (a) 68.2 kN \leftarrow at A; 37.2 kN \leftarrow at E. (b) $46.3 \mu\text{m}$ \rightarrow .
2.42 (a) 45.5 kN \leftarrow at A; 54.5 kN \leftarrow at E. (b) $48.8 \mu\text{m}$ \rightarrow .
2.43 $T_A = P/10$; $T_B = P/5$; $T_C = 3P/10$; $T_D = 2P/5$.
2.45 (a) 9.73 kN. (b) 2.02 mm \leftarrow .
2.46 (a) (BC) 1000 lb; (DE) -400 lb.
(b) $2.21 \times 10^{-3} \text{ in.}$ \rightarrow .
2.47 (steel) -1.448 ksi; (concrete) 54.2 psi.

- 2.49** -8.15 MPa .
2.50 -56.2 MPa .
2.51 142.6 kN .
2.52 (a) -98.3 MPa . (b) -38.3 MPa .
2.53 (a) (AB) -5.25 ksi ; (BC) -11.82 ksi .
 (b) $6.57 \times 10^{-3} \text{ in.} \rightarrow$.
2.56 (a) 21.4°C . (b) 3.68 MPa .
2.57 5.70 kN .
2.58 (a) 201.6°C . (b) 18.0107 in.
2.59 (a) 52.3 kips . (b) $9.91 \times 10^{-3} \text{ in.}$
2.61 (a) $1.324 \times 10^{-3} \text{ in.}$ (b) $-99.3 \times 10^{-6} \text{ in.}$
 (c) $-12.41 \times 10^{-6} \text{ in.}$ (d) $-12.41 \times 10^{-6} \text{ in.}^2$.
2.63 $E = 205 \text{ MPa}$; $G = 70.3 \text{ MPa}$; $\nu = 0.455$.
2.64 94.9 kips .
2.66 1.99551 .
2.67 (a) -63.0 MPa . (b) -13.50 mm^2 . (c) -540 mm^3
2.68 (a) $10.20 \mu\text{m}$. (b) $2.40 \mu\text{m}$. (c) $8.91 \mu\text{m}$.
2.69 (a) $5.13 \times 10^{-3} \text{ in.}$ (b) $-0.570 \times 10^{-3} \text{ in.}$
2.70 (a) 7630 lb. (compression). (b) 4580 lb (compression).
2.75 16.67 MPa .
2.76 $19.00 \times 10^3 \text{ kN/m}$.
2.77 0.0187 in.
2.78 $a = 0.818 \text{ in.}$; $b = 2.42 \text{ in.}$
2.81 $a = 42.9 \text{ mm}$; $b = 160.7 \text{ mm}$.
2.82 75.0 kN ; 40.0 mm .
2.84 (a) $16.55 \times 10^{-6} \text{ in.}^3$. (b) $16.54 \times 10^{-6} \text{ in.}^3$.
2.85 (a) $588 \times 10^{-6} \text{ in.}$ (b) $33.2 \times 10^{-3} \text{ in.}^3$. (c) 0.0294% .
2.86 (a) -0.0746 mm ; -143.91 mm^3 .
 (b) -0.0306 mm ; -521 mm^3 .
2.88 3.00 .
2.91 (a) 0.0303 mm . (b) $\sigma_x = 40.6 \text{ MPa}$; $\sigma_y = \sigma_z = 5.48 \text{ MPa}$.
2.92 (a) $\sigma_x = 44.6 \text{ MPa}$; $\sigma_y = 0$; $\sigma_z = 3.45 \text{ MPa}$. (b) -0.0129 mm .
2.93 (a) 13.31 ksi . (b) 18.72 ksi .
2.94 5.56 kips .
2.95 (a) 11.4 mm . (b) 28.8 kN .
2.96 36.7 mm .
2.97 (a) 92.3 kN ; 0.791 mm . (b) 180.0 kN ; 1.714 mm .
2.98 189.6 MPa .
2.101 176.7 kN ; 3.84 mm .
2.102 176.7 kN ; 3.16 mm .
2.105 2.65 kips ; 0.1117 in.
2.106 3.68 kips ; 0.1552 in.
2.109 (a) 0.292 mm . (b) (AC) 250 MPa ; (CB) -307 MPa .
 (c) 0.0272 mm .
2.110 (a) 990 kN . (b) (AC) 250 MPa ; (CB) -316 MPa .
 (c) 0.0313 mm .
2.111 (a) 112.1 kips . (b) 50 ksi in low strength steel;
 82.9 ksi in high strength steal. (c) 0.00906 in.
2.112 (a) 0.0309 in. (b) 64 ksi . (c) 0.00387 in.
2.113 (a) (AD) 250 MPa ; (BE) 124.3 MPa . (b) $0.622 \text{ mm} \downarrow$.
2.114 (a) (AD) 233 MPa ; (BE) 250 MPa . (b) $1.322 \text{ mm} \downarrow$.
2.115 (a) (AD) -4.70 MPa ; (BE) 19.34 MPa . (b) $0.0967 \text{ mm} \downarrow$.
2.116 (a) -36 ksi . (b) 15.84 ksi .
2.117 (a) (AC) -150 MPa ; (CB) -250 MPa . (b) $0.1069 \text{ mm} \rightarrow$.
2.118 (a) (AC) 56.5 MPa ; (CB) 9.41 MPa . (b) $0.0424 \text{ mm} \rightarrow$.
2.121 (a) 915°F . (b) 1759°F .
2.122 (a) 0.1042 mm . (b) (AC) and (CB) -65.2 MPa .
2.123 (a) 0.00788 mm . (b) (AC) and (CB) -6.06 MPa .
2.124 0.429 in.
2.128 4.67°C .
2.129 30.0 kips .
2.130 (steel) 67.1 MPa ; (concrete) 8.38 MPa .

- 2.131** 137.8°F .
2.133 (a) 262 mm . (b) 21.4 mm .
2.135 (a) $A\sigma_Y/\mu g$. (b) EA/L .
2.C1 Prob. 2.126: (a) $11.90 \times 10^{-3} \text{ in.}$ \downarrow . (b) $5.66 \times 10^{-3} \text{ in.}$ \uparrow .
2.C3 Prob. 2.60: (a) -116.2 MPa . (b) 0.363 mm .
2.C5 $r = 0.25 \text{ in.}$: 3.89 kips
 $r = 0.75 \text{ in.}$: 2.78 kips
2.C6 (a) -0.40083 . (b) -0.10100 . (c) -0.00405

CHAPTER 3

- 3.1** (a) 53.4 MPa . (b) 53.9 MPa .
3.2 (a) $5.17 \text{ kN} \cdot \text{m}$. (b) 87.2 MPa .
3.3 $4.12 \text{ kip} \cdot \text{in.}$
3.5 (a) 70.7 MPa . (b) 35.4 MPa . (c) 6.25% .
3.6 (a) $125.7 \text{ N} \cdot \text{m}$. (b) $181.4 \text{ N} \cdot \text{m}$.
3.8 (a) $19.21 \text{ kip} \cdot \text{in.}$ (b) 2.01 in.
3.10 39.8 mm .
3.11 (a) CD . (b) 85.8 MPa .
3.13 (a) 2.85 ksi . (b) 4.46 ksi . (c) 5.37 ksi .
3.14 (a) 3.19 ksi . (b) 4.75 ksi . (c) 5.58 ksi .
3.15 $9.16 \text{ kip} \cdot \text{in.}$
3.16 (a) 1.503 in. (b) 1.853 in.
3.19 $3.18 \text{ kN} \cdot \text{m}$.
3.20 $3.37 \text{ kN} \cdot \text{m}$.
3.21 (a) 72.5 MPa . (b) 68.7 MPa .
3.22 (a) 59.6 mm . (b) 43.9 mm .
3.24 1.189 in.
3.26 $4.30 \text{ kip} \cdot \text{in.}$
3.27 (a) 55.0 MPa . (b) 45.3 MPa . (c) 47.7 MPa .
3.28 (a) 20.1 mm . (b) 26.9 mm . (c) 36.6 mm .
3.29 (a) $(C_1^2 + C_2^2) \tau_{all}/2\rho g c_2$. (b) $(T/w)_0 [1 + (c_1/c_2)^2]$.
3.30 1.000 ; 1.025 ; 1.120 ; 1.200 ; 1.000 .
3.31 (a) 4.21° . (b) 5.25° .
3.33 0.491 in.
3.34 7.68 ksi .
3.35 (a) 1.384° . (b) 3.22° .
3.37 (a) 14.43° . (b) 46.9° .
3.38 6.02° .
3.39 1.140° .
3.41 3.77° .
3.42 12.22° .
3.43 $(T_A l/GJ) (1/n^4 + 1/n^2 + 1)$.
3.45 62.9 mm .
3.46 42.1 mm .
3.47 (a) 82.1 mm . (b) 109.4 mm .
3.48 22.5 mm .
3.49 1.285 in.
3.50 1.483 in.
3.51 (a) 73.6 MPa . (b) 34.4 MPa . (c) 5.07° .
3.52 4.13° .
3.55 (AB) 9.95 ksi ; (CD) 1.849 ksi .
3.56 (AB) 1.086 ksi ; (CD) 6.98 ksi .
3.59 12.24 MPa .
3.62 0.241 in.
3.63 (a) $T/2\pi tr_1^2$.
3.64 (a) 46.9 MPa . (b) 23.5 MPa .
3.66 6.69 mm .
3.68 2.64 mm .
3.69 40.1 hp .
3.70 (a) 51.7 kW . (b) 6.17° .
3.73 0.3125 in.

- 3.74** (a) 0.799 in. (b) 0.947 in.
3.75 (a) 4.08 ksi. (b) 6.79 ksi.
3.76 (AB) 15.00 mm; (CD) 20.4 mm; (EF) 27.6 mm.
3.77 7.11 kW.
3.78 4.90 Hz.
3.80 $d = 2.82$ in.
3.81 (a) 16.02 Hz. (b) 27.2 Hz.
3.83 33.5 Hz or 2010 rpm.
3.84 (a) 5.36 ksi. (b) 5.02 ksi.
3.86 10.8 mm.
3.87 42.6 Hz.
3.88 63.5 kW.
3.90 (a) 2.61 ksi. (b) 2.01 ksi.
3.91 (a) 203 N · m. (b) 165.8 N · m.
3.92 21.2 N · m.
3.93 (a) 144.7 kip · in. (b) 148.1 kip · in.
3.94 (a) 9.64 kN · m. (b) 9.91 kN · m.
3.95 (a) 18.86 ksi; 1.500 in. (b) 21.0 ksi; 0.916 in.
3.98 (a) 2.47°. (b) 4.34°. **3.99** (a) 6.72°. (b) 18.71°. **3.100** (a) 52.1 kip · in. (b) 80.8 kip · in.
3.101 (a) 977 N · m. (b) 8.61 mm.
3.104 145 MPa; 19.75°. **3.105** (a) 1.126 ϕ_y . (b) 1.587 ϕ_y . (c) 2.15 ϕ_y .
3.106 (a) 5.96 kN · m; 17.94°. (b) 7.31 kN · m; 26.9°. **3.107** (a) 43.0°. (b) 7.61 kN · m.
3.110 671 lb · in.
3.111 (a) 1.826 kip · in. (b) 22.9°. **3.112** 2.32 kN · m.
3.113 2.26 kN · m.
3.114 5.63 ksi.
3.115 14.62°. **3.118** 68.0 MPa at inner surface.
3.119 20.2°. **3.120** (a) $c_0 = 0.75 c$. (b) $0.221 \tau_y c^3$.
3.121 (a) 13.54 kip · in; 3.08°. (b) 17.03 kip · in; 2.26°. **3.122** (a) 11.08 ksi; 2.84°. (b) 8.81 ksi; 1.661°. **3.123** (a) 40.1 MPa; 0.653°. (b) 50.9 MPa; 0.917°. **3.124** (a) 2.25 kN · m; 0.815°. (b) 1.770 kN · m; 0.901°. **3.127** 59.2 MPa.
3.128 5.07 MPa.
3.129 0.944.
3.131 1.356.
3.132 1.198.
3.134 (a) 4.57 kip · in. (b) 4.31 kip · in. (c) 5.77 kip · in.
3.135 (a) 7.52 ksi. (b) 4.61°. **3.136** (a) 70.8 N · m. (b) 8.77°. **3.137** (a) 4.57 ksi. (b) 2.96 ksi. (c) 5.08°. **3.138** (a) 1009 N · m. (b) 9.07°. **3.141** 4.73 MPa at a; 9.46 MPa at b.
3.142 44.2 MPa at a; 27.6 MPa at b.
3.143 16.85 N · m.
3.144 88.1 kip · in or 7.34 kip · ft.
3.146 1.735 in.
3.148 (a) 12.76 MPa. (b) 5.40 kN · m.
3.149 (b) 0.25%; 1.00%; 4.00%. **3.150** (a) $3c/t$. (b) $3c^2/t^2$. **3.151** 9.38 ksi.
3.153 6.37 kip · in.
3.155 (a) 1105 N · m at A; 295 N · m at C. (b) 45.0 MPa. (c) 27.4 MPa.
3.156 127.8 lb · in.

- 3.157** (a) 24.5°. (b) 19.37°. **3.158** 36.1 mm.
3.160 8.47 MPa.
3.162 1.221.
3.C2 Prob. 3.44: 2.21°. **3.C5** (a) -3.282%. (b) -0.853%. (c) -0.138%. (d) -0.00554%.
3.C6 (a) -1.883%. (b) -0.484%. (c) -0.078%. (d) -0.00313%.

CHAPTER 4

- 4.1** (a) -2.38 ksi. (b) -0.650 ksi.
4.2 (a) -61.6 MPa. (b) 91.7 MPa.
4.3 (a) 1.405 kip · in. (b) 3.19 kip · in.
4.4 2.38 kN · m.
4.5 5.28 kN · m.
4.6 4.51 kN · m.
4.9 67.8 MPa; -81.8 MPa.
4.11 15.40 ksi; -10.38 ksi.
4.12 58.8 kN.
4.14 (a) 8.24 kips. (b) 1.332 kips.
4.15 106.1 N · m.
4.17 20.4 kip · in.
4.18 4.11 kip · in.
4.19 177.8 kN · m.
4.21 65.1 ksi.
4.23 (a) 0.602 mm. (b) 0.203 N · m.
4.24 (a) 75.0 MPa; 26.7 m. (b) 125.0 MPa; 9.60 m.
4.25 $8.49 M/a^3$; $12.00 M/Ea^4$. **4.27** (a) $0.889 h_0$. (b) 0.949.
4.28 (a) 1.414. (b) 1.732.
4.29 (a) 334 ft. (b) 0.0464°. **4.30** (a) 1007 in. (b) 3470 in. (c) 0.01320°. **4.31** (a) 139.6 m. (b) 481 m.
4.32 (a) $(\sigma_x)_{\max}(y^2 - c^2)/2\rho c$. **4.33** 1.092 kN · m.
4.34 887 N · m.
4.37 335 kip · in.
4.38 689 kip · in.
4.39 (a) 66.2 MPa. (b) -112.4 MPa.
4.40 (a) -56.9 MPa. (b) 111.9 MPa.
4.42 (a) -2.02 ksi. (b) 14.65 ksi.
4.43 39.8 m.
4.44 43.7 m.
4.46 625 ft.
4.47 (a) 212 MPa. (b) -15.59 MPa.
4.48 (a) 210 MPa. (b) -14.08 MPa.
4.49 11.73 kN · m.
4.50 9.50 kn · m.
4.51 33.9 kip · ft.
4.55 (a) (aluminum) 62.3 MPa; (brass) 62.3 MPa; (steel) 62.3 MPa. (b) 33.7 m.
4.57 (a) -22.5 ksi. (b) 17.78 ksi.
4.59 (a) 6.15 MPa. (b) -8.69 MPa.
4.63 (a) 128 N · m. (b) 142 N · m.
4.64 (a) 219 MPa. (b) 176 MPa.
4.65 (a) 22.8 kip · in. (b) 27.7 kip · in.
4.66 (a) 12.2 ksi. (b) 9.9 ksi.
4.67 (a) 38.4 N · m (b) 52.8 N · m.
4.68 (a) 57.6 N · m (b) 83.2 N · m.
4.69 (a) 0.521 in. (b) 17.50 ft.
4.71 (a) 2.40 kN · m. (b) 3.41 kN · m.
4.72 (a) 1.778 kN · m. (b) 2.60 kN · m.

- 4.75** (a) 3339 kip · in. (b) 4725 kip · in.
4.77 (a) 29.2 kN · m. (b) 1.500.
4.78 (a) 27.5 kN · m. (b) 1.443.
4.79 (a) 4820 kip · in. (b) 1.443.
4.80 (a) 2840 kip · in. (b) 1.611.
4.81 1.866 kN · m.
4.83 911 N · m.
4.85 20.7 kip · in.
4.86 212 kip · in.
4.87 120.0 MPa.
4.88 106.4 MPa.
4.91 (a) 106.7 MPa. (b) $y = -31.2$ mm, 0, 31.2 mm.
 (c) 24.1 m.
4.92 (a) 13.36 ksi. (b) $y = -1.517$ in., 0, 1.517 in. (c) 168.8 ft.
4.94 (a) $0.707 \rho_Y$. (b) $6.09 \rho_Y$.
4.96 7.29 kN · m.
4.99 (a) -212 psi. (b) -637 psi. (c) -1061 psi.
4.100 (a) 4.87 ksi. (b) 5.17 ksi.
4.102 (a) 112.7 MPa. (b) -96.0 MPa.
4.104 (a) (A and B) -8.33 MPa.
 (b) (A) -15.97 MPa; (B) 4.86 MPa.
4.105 623 lb.
4.106 (a) 288 lb. (b) 209 lb.
4.107 (a) -139.3 MPa. (b) -152.5 MPa.
4.108 14.40 kN.
4.109 16.04 mm.
4.111 0.500 d .
4.113 (a) 2.54 kN. (b) 17.01 mm to the right of loads.
4.114 7.86 kips ↓; 9.15 kips ↑.
4.116 (a) 1125 kN. (b) 817 kN.
4.118 2.485 in. < y < 4.56 in.
4.119 (a) 47.6 MPa. (b) -49.4 MPa.
 (c) 9.80 mm below top of section.
4.121 9.00 kN.
4.122 (a) 30.0 mm. (b) 94.5 kN.
4.124 $P = 75.7$ kips ↓; $Q = 87.2$ kips ↓.
4.125 $P = 5.98$ kips ↓; $Q = 49.0$ kips ↓.
4.127 (a) -2.80 MPa. (b) 0.452 MPa. (c) 2.80 MPa.
4.128 (a) -3.37 MPa. (b) -18.60 MPa. (c) 3.37 MPa.
4.129 (a) 1.149 ksi. (b) 0.1479 ksi. (c) -1.149 ksi.
4.130 (a) 0.321 ksi. (b) -0.107 ksi. (c) 0.427 ksi.
4.131 (a) -29.3 MPa. (b) -144.8 MPa. (c) -125.9 MPa.
4.134 (a) 57.8 MPa. (b) -56.8 MPa. (c) 25.9 MPa.
4.135 (a) 9.59°. (b) 77.5 MPa.
4.137 (a) 27.5°. (b) 5.07 ksi.
4.138 (a) 10.03°. (b) 54.2 MPa.
4.139 (a) 11.3°. (b) 15.06 ksi.
4.141 -2.32 ksi.
4.143 113.0 MPa.
4.144 (a) (A) 31.5 MPa; (B) -10.39 MPa.
 (b) 94.0 mm above point A.
4.145 (a) (A) 22.9 MPa; (B) 8.96 MPa.
 (b) 56.0 mm to the right of point B.
4.148 0.1638 in.
4.149 53.9 kips.
4.150 733 N · m.
4.151 1.323 kN · m.
4.152 29.1 kip · in.
4.153 29.1 kip · in.
4.161 (a) 12.19 ksi. (b) 11.15 ksi.
4.162 (A) 10.77 ksi; (B) -3.22 ksi.
4.163 60.9 mm.

- 4.164** -148.6 MPa.
4.167 (a) -154.4 MPa. (b) 75.2 MPa.
4.168 73.2 mm.
4.170 1128 lb.
4.171 (a) -172.4 MPa. (b) 53.2 MPa.
4.172 (a) -131.5 MPa. (b) 34.7 MPa.
4.174 (a) 3.06 ksi. (b) -2.81 ksi. (c) 0.529 ksi.
4.175 (a) -45.2 MPa. (b) 17.40 MPa.
4.176 (a) -43.3 MPa. (b) 14.43 MPa.
4.177 107.8 N · m.
4.178 (a) 6.74 ksi. (b) -3.45 ksi.
4.179 1.584 in.
4.180 (a) -32.5 MPa. (b) 34.2 MPa.
4.183 (a) 69.3 MPa. (b) -58.6 MPa.
4.185 (a) -5.96 ksi. (b) 3.61 ksi.
4.186 (a) -6.71 ksi. (b) 3.24 ksi.
4.192 8.82 ksi; -14.71 ksi.
4.194 4.63 kip · in.
4.195 (a) 46.9 MPa. (b) 18.94 MPa. (c) 55.4 m.
4.197 (a) -82.4 MPa. (b) 36.6 MPa.
4.199 (a) 9.33 ksi. (b) 8.00 ksi.
4.200 (a) $-P/2at$. (b) $-2P/at$. (c) $-P/2at$.
4.202 (a) -500 psi. (b) -822 psi. (c) -667 psi.
 (d) -1280 psi. (e) -1000 psi.
4.203 (a) (A) $-0.5 \sigma_1$; (B) σ_1 ; (C) $-\sigma_1$; (D) $0.5 \sigma_1$. (b) $4.333 \rho_1$.
4.C1 $a = 4$ mm: $\sigma_a = 50.6$ MPa, $\sigma_s = 107.9$ MPa;
 $a = 14$ mm: $\sigma_a = 89.7$ MPa, $\sigma_s = 71.8$ MPa.
 (a) 111.6 MPa. (b) 6.61 mm.
4.C2 $y_Y = 65$ mm, $M = 52.6$ kN · m, $\rho = 43.3$; $y_Y = 45$ mm,
 $M = 55.6$ kN · m, $\rho = 30.0$ m.
4.C3 $\beta = 30^\circ$: $\sigma_A = -7.83$ ksi, $\sigma_B = -5.27$ ksi,
 $\sigma_C = 7.19$ ksi, $\sigma_D = 5.91$ ksi;
 $\beta = 120^\circ$: $\sigma_A = 1.557$ ksi, $\sigma_B = 6.01$ ksi,
 $\sigma_C = -2.67$ ksi, $\sigma_D = -4.89$ ksi.
4.C4 $r_1/h = 0.529$ for 50% increase in σ_{\max} .
4.C5 Prob. 4.10: -102.4 MPa; 73.2 MPa.
4.C6 $y_Y = 0.8$ in.: 76.9 kip · in., 552 in.;
 $y_Y = 0.2$ in.: 95.5 kip · in., 138.1 in.
4.C7 $a = 0.2$ in.: -7.27 ksi, $a = 0.8$ in.: -6.61 ksi.
 For $a = 0.625$ in., $\sigma = -6.51$ ksi.

CHAPTER 5

- 5.1** (b) A to B: $V = Pb/L$; $M = Pb x/L$.
 B to C: $V = -Pa/L$; $M = Pa(L - x)/L$.
5.2 (b) $V = w(x - 2L)/2$; $M = wx(L - x)/2$.
5.3 (b) A to B: $V = -wx$; $M = -wx^2/2$.
 B to C: $V = -wa$; $M = -wa(x - a/2)$.
5.4 (b) $V = -w_0 x^2/2L$; $M = -w_0 x^3/6L$.
5.5 (b) A to B: $V = w(a - x)$; $M = w(ax - x^2/2)$.
 B to C: $V = 0$; $M = wa^2/2$.
 C to D: $V = w(L - x - a)$; $M = w[a(L - x) - (L - x)^2/2]$.
5.6 (b) A to B: $V = w(L - 2a)/2$; $M = wx(L - 2a)/2$.
 B to C: $V = w(L/2 - x)$; $M = w[(L - 2a)x^2 - (x - a)^2]/2$.
 C to D: $V = -w(L - 2a)/2$; $M = w(L - 2a)(L - x)/2$.
5.7 (a) 430 lb. (b) 1200 lb · in.
5.8 (a) 300 N. (b) 67.5 N · m.
5.9 (a) 40.0 kN. (b) 40.0 kN · m
5.11 (a) 120.0 kips. (b) 120.0 kip · ft.
5.12 (a) 85.0 N. (b) 21.25 N · m.
5.14 (a) 900 N. (b) 112.5 N · m.

- 5.15** 7.13 MPa.
5.16 1.013 ksi.
5.18 139.2 MPa.
5.19 9.90 ksi.
5.21 14.17 ksi.
5.22 116.2 MPa.
5.25 10.34 ksi.
5.26 $|V|_{\max} = 6.00 \text{ kN}$; $|M|_{\max} = 4.00 \text{ kN} \cdot \text{m}$;
 $\sigma_{\max} = 14.29 \text{ MPa}$.
5.27 (a) 10.67 kN. (b) 9.52 MPa.
5.28 (a) 3.09 ft. (b) 12.95 ksi.
5.30 (a) 866 mm. (b) 99.2 MPa.
5.31 (a) 819 mm. (b) 89.5 MPa.
5.32 (a) 33.3 mm. (b) 6.66 mm.
5.33 1.021 in.
5.34 See 5.1.
5.35 See 5.2.
5.36 See 5.3.
5.37 See 5.4.
5.38 See 5.5.
5.39 See 5.6.
5.40 See 5.7.
5.41 See 5.8.
5.42 See 5.9.
5.43 See 5.10.
5.46 See 5.15.
5.47 See 5.16.
5.48 See 5.18.
5.49 See 5.19.
5.51 (a) $V = w_0(L^2 - 3x^2)/6L$; $M = w_0(Lx - x^3)/6$.
(b) $0.0642 w_0 L^2$.
5.52 (a) $V = (w_0 L/\pi) \cos(\pi x/L)$; $M = (w_0 L^2/\pi^2) \sin(\pi x/L)$;
(b) $w_0 L^2/\pi^2$.
5.54 $|V|_{\max} = 8.00 \text{ kips}$; $|M|_{\max} = 16.00 \text{ kip} \cdot \text{ft}$; 6.98 ksi.
5.55 $|V|_{\max} = 6.5 \text{ kN}$; $|M|_{\max} = 5.04 \text{ kN} \cdot \text{m}$; 30.3 MPa.
5.57 $|V|_{\max} = 200 \text{ kN}$; $|M|_{\max} = 300 \text{ kN} \cdot \text{m}$; 136.4 MPa.
5.58 $|V|_{\max} = 76 \text{ kN}$; $|M|_{\max} = 67.3 \text{ kN} \cdot \text{m}$; 68.5 MPa.
5.61 $|V|_{\max} = 48 \text{ kN}$; $|M|_{\max} = 12.0 \text{ kN} \cdot \text{m}$; 62.2 MPa.
5.62 $|V|_{\max} = 24.5 \text{ kips}$; $|M|_{\max} = 36.3 \text{ kip} \cdot \text{ft}$; 15.82 ksi.
5.63 $|V|_{\max} = 1150 \text{ N}$; $|M|_{\max} = 221 \text{ N} \cdot \text{m}$; $P = 500 \text{ N}$;
 $Q = 250 \text{ N}$.
5.65 173.2 mm.
5.67 $h > 14.27 \text{ in}$.
5.69 $h > 203 \text{ mm}$.
5.70 $b > 48.0 \text{ mm}$.
5.71 W27 \times 84.
5.72 W27 \times 84.
5.73 W530 \times 66.
5.74 W530 \times 92.
5.76 S510 \times 98.2.
5.77 S15 \times 42.9.
5.79 12.7 mm.
5.80 C9 \times 15.
5.81 11.74 in.
5.82 9 mm.
5.83 W24 \times 68.
5.84 W610 \times 101.
5.87 176.8 kN \cdot m.
5.88 108.8 kN \cdot m.
5.89 (a) 6.49 ft. (b) W16 \times 31.
5.91 (a) S15 \times 42.9. (b) W27 \times 84.
5.92 (a) 1.485 kN/m. (b) 1.935 m.
5.94 W27 \times 84.
5.95 +23.2%.
5.96 383 mm.
5.97 336 mm.
5.98 (a) $V = -w_0 x + w_0 x^2/2a - (w_0/2a)(x - a)^2$; $M = -w_0 x^2/2 + w_0 x^3/6a - (w_0/6a)(x - a)^3$; (b) $-5w_0 a^2/6$.
5.99 (a) $V = -w_0 x + w_0(x - a)^1$;
 $M = -w_0 x^2/2 + (w_0/2)(x - a)^2$.
(b) $-3w_0 a^2/2$.
5.101 (a) $V = -w_0(x - a)^1 - 3w_0 a/4 + (15w_0 a/4)(x - 2a)^0$;
 $M = -(w_0/2)(x - a)^2 - 3w_0 a x/4 + (15w_0 a/4)(x - 2a)^1$.
(b) $-w_0 a^2/2$.
5.102 (a) $V = 1.25P - P(x - a)^0 - P(x - 2a)^0$;
 $M = 1.25Px - P(x - a)^1 - P(x - 2a)^1$.
(b) 0.750Pa.
5.104 (a) $V = -P(x - a)^0$; $M = -P(x - a)^1 - Pa(x - a)^0$.
(b) -Pa.
5.105 (a) $V = -P - P(x - 2L/3)^0$;
 $M = -Px + PL/3 - P(x - 2L/3)^1 - (PL/3)(x - 2L/3)^0$.
(b) -4PL/3.
5.106 (a) $V = -1.5x + 3(x - 0.8)^0 + 3(x - 3.2)^0 \text{ kN}$;
 $M = -0.75x^2 + 3(x - 0.8)^1 + 3(x - 3.2)^1 \text{ kN} \cdot \text{m}$.
(b) 600 N \cdot m.
5.107 (a) $V = 40 - 48(x - 1.5)^0 - 60(x - 3.0)^0 + 60(x - 3.6)^0 \text{ kN}$;
 $M = 40x - 48(x - 1.5)^1 - 60(x - 3.0)^1 + 60(x - 3.6)^1 \text{ kN} \cdot \text{m}$.
(b) 60.0 kN \cdot m.
5.108 (a) $V = 13 - 3x + 3(x - 3)^1 - 8(x - 7)^0 - 3(x - 11)^1 \text{ kips}$;
 $M = 13x - 1.5x^2 + 1.5(x - 3)^2 - 8(x - 7)^1 - 1.5(x - 11)^2 \text{ kip} \cdot \text{ft}$.
(b) 41.5 kip \cdot ft at point D.
5.109 (a) $V = -3 + 9.75(x - 3)^0 - 6(x - 7)^0 - 6(x - 11)^0 \text{ kips}$;
 $M = -3x + 9.75(x - 3)^1 - 6(x - 7)^1 - 6(x - 11)^1 \text{ kip} \cdot \text{ft}$.
(b) 21.0 kip \cdot ft at point E.
5.111 (a) $V = 30 - 24(x - 0.75)^0 - 24(x - 1.5)^0 - 24(x - 2.25)^0 + 66(x - 3)^0 \text{ kN}$;
 $M = 30x - 24(x - 0.75)^1 - 24(x - 1.5)^1 - 24(x - 2.25)^1 + 66(x - 3)^1 \text{ kN} \cdot \text{m}$.
(b) 87.7 MPa.
5.114 (a) 80.0 kip \cdot ft at C. (b) W14 \times 30.
5.115 (a) 121.5 kip \cdot ft at $x = 6.00 \text{ ft}$. (b) W16 \times 40.
5.117 (a) 0.776 kN \cdot m at $x = 1.766 \text{ m}$. (b) 120 mm.
5.119 $|V|_{\max} = 15.30 \text{ kips}$; $|M|_{\max} = 38.0 \text{ kip} \cdot \text{ft}$.
5.120 $|V|_{\max} = 89.0 \text{ kN}$; $|M|_{\max} = 178.0 \text{ kN} \cdot \text{m}$.
5.121 $|V|_{\max} = 35.6 \text{ kN}$; $|M|_{\max} = 25.0 \text{ kN} \cdot \text{m}$.
5.122 (a) $|V|_{\max} = 13.80 \text{ kN}$; $|M|_{\max} = 16.14 \text{ kN} \cdot \text{m}$. (b) 83.8 MPa.
5.123 (a) $|V|_{\max} = 40.0 \text{ kN}$; $|M|_{\max} = 30.0 \text{ kN} \cdot \text{m}$. (b) 40.0 MPa.
5.124 (a) $|V|_{\max} = 3.84 \text{ kips}$; $|M|_{\max} = 3.80 \text{ kip} \cdot \text{ft}$ (b) 0.951 ksi.
5.126 (a) $h = h_0 \sqrt{2x/L}$. (b) 60.0 kN.
5.128 (a) $h = h_0 (x/L)^{1/2}$. (b) 20.0 kips.
5.129 (a) $h = h_0 [(x/L)(1 - x/L)]^{1/2}$. (b) 4.44 kip/in.
5.130 (a) $h = h_0 (x/L)^{3/2}$. (b) 167.7 mm.
5.132 1.800 m.
5.133 1.900 m.
5.134 $l_1 = 6.00 \text{ ft}$; $l_2 = 4.00 \text{ ft}$.
5.137 $d = d_0 (2x/L)^{1/3}$ for $0 \leq x \leq L/2$.
 $d = d_0 [2(L - x)/L]^{1/3}$ for $L/2 \leq x \leq L$.
5.138 (a) $b_0 (1 - x/L)^2$. (b) 160.0 lb/in.
5.139 (a) $b_0 (1 - x/L)$. (b) 20.8 mm.
5.140 (a) 155.2 MPa. (b) 143.3 MPa.
5.141 193.8 kN.
5.143 (a) 11.16 ft. (b) 14.31 in.
5.144 (a) 152.6 MPa. (b) 133.6 MPa.
5.145 (a) 4.49 m. (b) 211 mm.

- 5.146** (a) 25.0 ksi. (b) 18.03 ksi.
5.149 (a) 240 mm. (b) 150.0 MPa.
5.150 (a) 15.00 in. (b) 320 lb/in.
5.151 (a) 30.0 in. (b) 12.80 kips.
5.152 (a) 2000 lb. (b) 19200 lb · ft.
5.153 $|V|_{\max} = 342 \text{ N}$; $|M|_{\max} = 51.6 \text{ N} \cdot \text{m}$; $\sigma = 17.19 \text{ MPa}$.
5.156 73.5 MPa.
5.157 $|V|_{\max} = 30.0 \text{ lb}$; $|M|_{\max} = 24.0 \text{ lb} \cdot \text{ft}$; $|\sigma|_{\max} = 6.95 \text{ ksi}$.
5.158 6.20 in.
5.159 $W250 \times 28.4$.
5.160 7.01 kips.
5.C4 For $x = 13.5 \text{ ft}$: $M_1 = 131.25 \text{ kip} \cdot \text{ft}$;
 $M_2 = 156.25 \text{ kip} \cdot \text{ft}$; $M_C = 150.0 \text{ kip} \cdot \text{ft}$.
5.C6 Prob. 5.112: $V_A = 29.5 \text{ kN}$, $M_{\max} = 28.3 \text{ kN} \cdot \text{m}$,
at 1.938 m from A.

CHAPTER 6

- 6.1** 92.6 lb.
6.2 326 lb.
6.3 738 N.
6.4 747 N.
6.5 193.5 kN.
6.6 217 kN.
6.9 (a) 7.40 ksi (b) 6.70 ksi.
6.10 (a) 920 kPa. (b) 765 kPa.
6.12 (a) 3.17 ksi. (a) 2.40 ksi.
6.13 120.3 kN.
6.15 14.05 in.
6.16 88.9 mm.
6.18 (b) $h = 320 \text{ mm}$; $b = 97.7 \text{ mm}$.
6.19 143.3 kips.
6.21 (a) 31.0 MPa. (b) 23.2 MPa.
6.22 (a) 1.313 ksi. (b) 2.25 ksi.
6.23 32.7 MPa.
6.24 3.00 ksi.
6.26 (a) Line at mid-height. (b) 1.500.
6.28 (a) $h/4$ from neutral axis. (b) 1.125.
6.29 4.28 kN.
6.30 4.63 kN.
6.32 189.6 lb.
6.34 (a) 1.583 ksi. (b) 7.59 ksi.
6.35 (a) 101.6 MPa. (b) 79.6 MPa.
6.36 (a) 41.4 MPa. (b) 41.4 MPa.
6.37 (a) 33.7 MPa. (b) 75.0 MPa. (c) 43.5 MPa.
6.38 (a) 1.167 ksi. (b) 0.513 ksi. (c) 4.03 ksi. (d) 8.40 ksi.
6.40 (a) 18.23 MPa. (b) 14.59 MPa. (c) 46.2 MPa.
6.41 (a) 0. (b) 1.26 ksi. (c) 3.30 ksi. (d) 6.84 ksi. (e) 7.86 ksi.
6.43 53.9 kips.
6.44 20.6 MPa.
6.45 9.05 mm.
6.46 0.371 in.
6.48 (a) 23.2 MPa. (b) 35.2 MPa.
6.49 (a) 10.76 MPa. (b) 0. (c) 11.21 MPa. (d) 22.0 MPa.
(e) 9.35 MPa.
6.51 1.422 in.
6.52 (a) 2.08. (b) 2.10.
6.53 (a) 2.25. (b) 2.12.
6.54 (a) $V \sin \theta / \pi r_m t$.
6.57 (a) 1.323 ksi. (b) 1.329 ksi.
6.59 (a) 6.73 MPa. (b) 1.515 MPa.
6.61 $e = 0.714a$.

- 6.62** $e = 0.345a$.
6.63 (a) $e = 29.4 \text{ mm}$. (b) 0 at A, 39.0 MPa at B in AB;
78.0 MPa at B in BD; 104.1 MPa at C.
6.64 (a) $e = 19.06 \text{ mm}$. (b) 0 at A; 50.5 MPa at B in AB;
25.3 MPa at B in BD; 59.0 MPa at C.
6.67 (a) $e = 10.22 \text{ mm}$. (b) At B, E, G, and J: $\tau = 0$;
At A and H: 41.1 MPa;
Just above D and just below F: 68.5 MPa;
Just to the right of D or F: 13.71 MPa;
Just below D and just above F: 77.7 MPa;
At K: 81.1 MPa.
6.68 (a) $e = 9.12 \text{ mm}$. (b) At B, E, G, and J: $\tau = 0$;
Just to the right of A or H: 50.6 MPa;
Just below A and just above H: 33.8 MPa;
Just above D and just below F: 67.5 MPa;
Just to the right of D or E: 16.88 MPa;
Just below D and just above F: 84.4 MPa;
At K: 88.6 MPa.
6.69 $e = 1.265 \text{ in}$.
6.70 $e = 20.2 \text{ mm}$.
6.71 $e = 6.14 \text{ mm}$.
6.72 $e = 0.482 \text{ in}$.
6.75 $e = 2.37 \text{ in}$.
6.76 $e = 2.21 \text{ in}$.
6.77 0 and 40.0 mm.
6.78 40.0 mm.
6.81 65.9 MPa.
6.82 106.6 MPa.
6.83 (a) 500 lb; 398 lb · in. (b) 2980 psi.
6.84 (a) 500 lb; 398 lb · in. (b) 6090 psi.
6.87 (maximum) P/at .
6.88 (maximum) $1.333 P/at$.
6.89 (a) 155.8 N. (b) 329 kPa.
6.90 12.01 ksi.
6.92 87.3 mm.
6.93 (a) 1.745 ksi. (b) 2.82 ksi.
6.95 (a) 146.1 kN/m. (b) 19.99 MPa.
6.96 (a) 50.9 MPa. (b) 62.4 MPa.
6.98 $e = 3(b^2 - a^2)/(6a + 6b + h)$.
6.99 $e = 0.433 \text{ in}$.
6.C1 (a) $h = 173.2 \text{ mm}$. (b) $h = 379 \text{ mm}$.
6.C2 (a) $L = 37.5 \text{ in}$; $b = 1.250 \text{ in}$.
(b) $L = 70.3 \text{ in}$; $b = 1.172 \text{ in}$.
(c) $L = 59.8 \text{ in}$; $b = 1.396 \text{ in}$.
6.C4 (a) $\tau_{\max} = 2.03 \text{ ksi}$; $\tau_B = 1.800 \text{ ksi}$. (b) 194 psi.
6.C5 Prob. 6.66: (a) 2.67 in. (b) $\tau_B = 0.917 \text{ ksi}$;
 $\tau_D = 3.36 \text{ ksi}$; $\tau_{\max} = 4.28 \text{ ksi}$.

CHAPTER 7

- 7.1** $\sigma = 5.49 \text{ ksi}$; $\tau = 11.83 \text{ ksi}$.
7.2 $\sigma = -0.521 \text{ MPa}$; $\tau = 56.4 \text{ MPa}$.
7.3 $\sigma = 0.1699 \text{ ksi}$; $\tau = 5.10 \text{ ksi}$.
7.4 $\sigma = -49.2 \text{ MPa}$; $\tau = 2.41 \text{ MPa}$.
7.5 (a) -37.0° , 53.0° . (b) -13.60 MPa , -86.4 MPa .
7.6 (a) 18.4° , 108.4° . (b) 55.0 ksi, 5.00 ksi.
7.9 (a) 8.0° , 98.0° . (b) 36.4 MPa. (c) -50.0 MPa .
7.10 (a) -26.6° , 63.4° . (b) 25.0 MPa. (c) 30.0 MPa.
7.11 (a) 14.0° , 104.0° . (b) 17.00 ksi. (c) -4.00 ksi .
7.12 (a) 31.7° , 121.7° . (b) 11.18 ksi. (c) 2.00 ksi.
7.13 (a) $\sigma_{x'} = -2.40 \text{ ksi}$; $\tau_{x'y'} = 0.15 \text{ ksi}$, $\sigma_{y'} = 10.40 \text{ ksi}$.
(b) $\sigma_{x'} = 1.95 \text{ ksi}$; $\tau_{x'y'} = 6.07 \text{ ksi}$, $\sigma_{y'} = 6.05 \text{ ksi}$.

- 7.15** (a) $\sigma_x = 9.02$ ksi; $\tau_{xy} = 3.80$ ksi, $\sigma_y = -13.02$ ksi.
 (b) $\sigma_x = 5.34$ ksi; $\tau_{xy} = -9.06$ ksi, $\sigma_y = -9.34$ ksi.
- 7.17** (a) -0.600 MPa. (b) -3.84 MPa.
- 7.18** (a) 346 psi. (b) -200 psi.
- 7.19** $\sigma = -4.76$ ksi; $\tau = -0.467$ ksi.
- 7.21** (a) 47.9 MPa; 102.7 MPa.
- 7.23** 25.1 ksi, -0.661 ksi; 12.88 ksi.
- 7.24** 5.12 ksi, -1.640 ksi; 3.38 ksi.
- 7.25** 12.18 MPa, -48.7 MPa; 30.5 MPa.
- 7.26** (a) 18.9° , 108.9° ; 18.67 MPa, -158.5 MPa. (b) 88.6 MPa.
- 7.28** 205 MPa.
- 7.30** (a) -2.89 MPa. (b) 12.77 MPa, 1.226 MPa.
- 7.31** (a) -37.0° , 53.0° . (b) -86.4 MPa, -13.6 MPa.
 (a') 8.0° , 98.0° ; 36.4 MPa. (b') -50.0 MPa.
- 7.32** (a) -31.0° , 59.0° . (b) 13.00 ksi, -21.0 ksi.
 (a') 14.0° , 104.0° ; 17.00 ksi. (b') -4.00 ksi.
- 7.33** (a) -26.6° , 63.4° . (b) 25.0 MPa. (c) 30.0 MPa.
- 7.34** (a) 121.7° , 31.7° . (b) 11.18 ksi. (c) 2.00 ksi.
- 7.35** (a) $\sigma_x = -2.40$ ksi; $\tau_{xy} = 0.15$ ksi, $\sigma_y = 10.40$ ksi.
 (b) $\sigma_x = 1.95$ ksi; $\tau_{xy} = 6.07$ ksi, $\sigma_y = 6.05$ ksi.
- 7.37** (a) $\sigma_x = 9.02$ ksi; $\tau_{xy} = 3.80$ ksi, $\sigma_y = -13.02$ ksi.
 (b) $\sigma_x = 5.34$ ksi; $\tau_{xy} = -9.06$ ksi, $\sigma_y = -9.34$ ksi.
- 7.39** (a) -0.600 MPa. (b) -3.84 MPa.
- 7.40** (a) 346 psi. (b) -200 psi.
- 7.41** $\sigma = -4.76$ ksi; $\tau = -0.467$ ksi.
- 7.43** (a) 47.9 MPa. (b) 102.7 MPa.
- 7.45** 25.1 ksi, -0.661 ksi; 12.88 ksi.
- 7.46** 5.12 ksi, -1.640 ksi; 3.38 ksi.
- 7.47** 12.18 MPa, -48.7 MPa; 30.5 MPa.
- 7.48** (a) 18.9° , 108.9° ; -158.5 MPa, 18.67 MPa. (b) 88.6 MPa.
- 7.50** 205 MPa.
- 7.52** (a) -2.89 MPa. (b) 12.77 MPa, 1.23 MPa.
- 7.53** (a) -8.66 MPa. (b) 17.00 MPa, -3.00 MPa.
- 7.55** 24.6° , 114.6° ; 72.9 MPa, 27.1 MPa.
- 7.56** $\theta/2$, $(\theta + \pi)/2$; $\sigma_0 + \sigma_0 \cos \theta$, $\sigma_0 - \sigma_0 \cos \theta$.
- 7.57** -30° , 60° ; $-\sqrt{3} \tau_0$, $\sqrt{3} \tau_0$.
- 7.59** $16.5^\circ \leq \theta \leq 110.1^\circ$.
- 7.60** $-5.1^\circ \leq \theta \leq 132.0^\circ$.
- 7.61** -120.0 MPa $\leq \tau_{xy} \leq 120.0$ MPa.
- 7.62** -141.4 MPa $\leq \tau_{xy} \leq 141.4$ MPa.
- 7.63** (a) 33.7° , 123.7° . (b) 18.00 ksi. (c) 6.50 ksi.
- 7.65** (b) $|\tau_{xy}| = \sqrt{\sigma_x \sigma_y - \sigma_{\max} \sigma_{\min}}$.
- 7.66** (a) 11.00 ksi. (b) 10.00 ksi.
- 7.68** (a) 94.3 MPa. (b) 105.3 MPa.
- 7.69** (a) 100.0 MPa. (b) 110.0 MPa.
- 7.71** (a) 6.50 ksi. (b) 9.00 ksi. (c) 7.00 ksi.
- 7.72** (a) 85.0 MPa. (b) 85.0 MPa. (c) 95.0 MPa.
- 7.73** (a) 97.5 MPa. (b) 85.0 MPa. (c) 120.0 MPa.
- 7.74** 2.00 ksi; 9.33 ksi.
- 7.76** (a) 8.00 ksi. (b) 4.50 ksi.
- 7.77** (a) 40.0 MPa. (b) 72.0 MPa.
- 7.78** -40.0 MPa; 130.0 MPa.
- 7.80** (a) 45.7 MPa. (b) 92.9 MPa.
- 7.81** (a) 1.228. (b) 1.098 (c) Yielding occurs.
- 7.82** (a) 1.083. (b) Yielding occurs. (c) Yielding occurs.
- 7.83** (a) 1.287. (b) 1.018. (c) Yielding occurs.
- 7.84** (a) 1.119. (b) Yielding occurs. (c) Yielding occurs.
- 7.87** 52.9 kips.
- 7.88** 63.0 kips.
- 7.89** Rupture will occur.
- 7.90** Rupture will occur.
- 7.91** No rupture.
- 7.92** Rupture will occur.
- 7.94** ± 8.49 MPa.
- 7.95** $196.9 \text{ N} \cdot \text{M}$.
- 7.96** 50.0 MPa.
- 7.98** $\sigma_{\max} = 72.7$ MPa; $\tau_{\max} = 36.4$ MPa.
- 7.100** 166.5 psi.
- 7.102** (a) 202 psi. (b) 0.0353 in.
- 7.103** (a) 95.7 MPa. (b) 1.699 mm.
- 7.104** $\sigma_{\max} = 89.0$ MPa; $\tau_{\max} = 44.5$ MPa.
- 7.105** 12.55 mm.
- 7.106** $\sigma_{\max} = 136.0$ MPa; $\tau_{\max} = 68.0$ MPa.
- 7.108** $\sigma_{\max} = 78.5$ MPa; $\tau_{\max} = 39.3$ MPa.
- 7.109** 43.3 ft.
- 7.110** $\sigma_{\max} = 16.62$ ksi; $\tau_{\max} = 8.31$ ksi.
- 7.112** (a) 33.2 MPa. (b) 9.55 MPa.
- 7.113** 2.17 MPa.
- 7.114** $-220^\circ \leq \beta \leq 27.0^\circ$ and $63.0^\circ \leq \beta \leq 117.0^\circ$.
- 7.115** (a) 44.2 MPa. (b) 15.39 MPa.
- 7.116** 56.8° .
- 7.118** 474 psi.
- 7.120** $\sigma_{\max} = 45.1$ MPa; τ_{\max} (in-plane) = 9.40 MPa.
- 7.121** $\sigma_{\max} = 45.1$ MPa; τ_{\max} (in-plane) = 7.49 MPa.
- 7.124** (a) 3.15 ksi. (b) 1.993 ksi.
- 7.125** (a) 1.486 ksi. (b) 3.16 ksi.
- 7.126** (a) 5.64 ksi. (b) 282 psi.
- 7.127** (a) 2.28 ksi. (b) 228 psi.
- 7.128** $\epsilon_x = -450 \mu$; $\epsilon_y = 199.8 \mu$; $\gamma_{xy} = 375 \mu$.
- 7.129** $\epsilon_x = 115.0 \mu$; $\epsilon_y = 285 \mu$; $\gamma_{xy} = -5.72 \mu$.
- 7.131** $\epsilon_x = 36.7 \mu$; $\epsilon_y = 283 \mu$; $\gamma_{xy} = 227 \mu$.
- 7.132** $\epsilon_x = -450 \mu$; $\epsilon_y = 199.8 \mu$; $\gamma_{xy} = 375 \mu$.
- 7.133** $\epsilon_x = 115.0 \mu$; $\epsilon_y = 285 \mu$; $\gamma_{xy} = -5.72 \mu$.
- 7.135** $\epsilon_x = 36.7 \mu$; $\epsilon_y = 283 \mu$; $\gamma_{xy} = 227 \mu$.
- 7.136** (a) -33.7° , 56.3° ; -420μ , 100μ , 160μ (b) 520μ . (c) 580μ .
- 7.137** (a) -30.1° , 59.9° ; -702μ , -298μ , 500μ .
 (b) 403μ . (c) 1202μ .
- 7.139** (a) -26.6° , 64.4° ; -150μ , 750μ , -300μ .
 (b) 900μ . (c) 1050μ .
- 7.140** (a) 7.8° , 97.8° ; 56.6μ , 243μ , 0 . (b) 186.8μ . (c) 243μ .
- 7.141** (a) 31.0° , 121.0° ; 513μ , 87.5μ , 0 . (b) 425μ . (c) 513μ .
- 7.143** (a) 37.9° , 127.9° ; -57.5μ , -383μ , 0 . (b) 325μ . (c) 383μ .
- 7.146** (a) -300×10^{-6} in/in. (b) 435×10^{-6} in/in, -315×10^{-6} in/in;
 750×10^{-6} in/in.
- 7.147** (a) 30.0° , 120.0° ; 560×10^{-6} in/in, -140×10^{-6} in/in.
 (b) 700×10^{-6} in/in.
- 7.152** 1.421 MPa.
- 7.153** 1.761 MPa.
- 7.154** -22.5° , 67.5° ; 426μ , -952μ , -224μ .
- 7.155** -29.8 MPa; -70.9 MPa.
- 7.156** $P = 69.6$ kips; $Q = 30.3$ kips.
- 7.157** $P = 34.8$ kips; $Q = 38.4$ kips.
- 7.158** 16.58 kN.
- 7.160** (a) 18.4° . (b) 16.67 ksi.
- 7.161** 0° , 90° ; σ_0 , $-\sigma_0$.
- 7.162** (a) 39.0 MPa. (b) 45.0 MPa. (c) 39.0 MPa.
- 7.164** (a) 1.286. (b) 1.018. (c) Yielding occurs.
- 7.165** $\sigma_{\max} = 68.6$ MPa; $\tau_{\max} = 34.3$ MPa.
- 7.167** 3.43 ksi (compression).
- 7.169** 415×10^{-6} in/in.
- 7.C1** Prob. 7.14: (a) -56.2 MPa, 86.2 MPa, -38.2 MPa.
 (b) -45.2 MPa, 75.2 MPa, 53.8 MPa.
- Prob. 7.16: (a) 24.0 MPa, -104.0 MPa, -1.50 MPa.
 (b) -19.51 MPa, -60.5 MPa, -60.7 MPa.

- 7.C4** Prob. 7.93: Rupture occurs at $\tau_0 = 3.67$ ksi.
7.C6 Prob. 7.138: (a) -21.6° , 68.4° ; 279μ , -599μ , 160.0μ .
 (b) 877μ . (c) 877μ .
7.C7 Prob. 7.142: (a) 11.3° , 101.3° ; 310μ , 50.0μ , 0.
 (b) 260μ . (b) 310μ .
7.C8 Prob. 7.144: $\epsilon_x = 253\mu$; $\epsilon_y = 307$; $\gamma_{xy} = -893$.
 $\epsilon_a = 727\mu$; $\epsilon_b = -167.2$; $\gamma_{\max} = -894$.
 Prob. 7.145: $\epsilon_x = 725\mu$; $\epsilon_y = -75.0$; $\gamma_{xy} = 173.2$.
 $\epsilon_a = 734\mu$; $\epsilon_b = -84.3$; $\gamma_{\max} = 819$.

- 8.64** 0.48 ksi, 44.7 ksi; 22.6 ksi.
8.65 $W10 \times 15$. (b) 23.5 ksi; 4.89 ksi. (c) 23.2 ksi.
8.68 46.5 mm.
8.69 (a) 11.06 ksi; 0. (b) -0.537 ksi; 1.610 ksi. (c) -12.13 ksi; 0.
8.71 $P(2R + 4r/3)/\pi r^3$.
8.72 (a) 3.79 ksi, -8.50 ksi; 33.7° , 123.7° . (b) 6.15 ksi.
8.74 25.2 MPa; -0.87 MPa; 13.06 MPa.
8.76 (a) 7.50 MPa. (b) 11.25 MPa. (c) 56.3° ; 13.52 MPa.
8.C3 Prob. 8.18: 37.3 mm.
8.C5 Prob. 8.45: $\sigma = 6.00$ ksi; $\tau = 0.781$ ksi.

CHAPTER 8

- 8.1** (a) 10.69 ksi. (b) 19.18 ksi. (c) not acceptable.
8.2 (a) 10.69 ksi. (b) 13.08 ksi. (c) acceptable.
8.3 (a) 94.6 MPa. (b) 93.9 MPa. (c) acceptable.
8.4 (a) 91.9 MPa. (b) 95.1 MPa. (c) acceptable.
8.7 (a) $W690 \times 125$. (b) 118.2 MPa, 34.7 MPa. (c) 122.3 MPa.
8.8 (a) $W310 \times 38.7$ (b) 147.5 MPa, 18.18 MPa. (c) 140.2 MPa.
8.9 (a) 134.3 MPa. (b) 132.4 MPa.
8.11 (a) 19.39 ksi. (b) 20.7 ksi.
8.12 (a) 17.90 ksi. (b) 17.08 ksi.
8.14 (a) 126.0 MPa. (b) 115.9 MPa at midspan, 105.1 MPa at B and C.
8.15 873 lb.
8.16 1.578 in.
8.17 1.698 in.
8.19 BC: 21.7 mm; CD: 33.4 mm.
8.22 (a) H: 6880 psi, K: 6760 psi. (b) H: 7420 psi, K: 7010 psi.
8.25 41.3 mm.
8.26 44.8 mm.
8.27 37.0 mm.
8.28 43.9 mm.
8.29 1.822 in.
8.30 1.792 in.
8.31 (a) -11.07 ksi; 0. (b) 2.05 ksi; 2.15 ksi. (c) 15.17 ksi; 0.
8.32 (a) 11.87 ksi; 0. (b) 2.05 ksi, 2.15 ksi. (c) -7.78 ksi; 0.
8.34 (a) -32.5 MPa; 14.06 MPa. (b) -126.2 MPa; 0.
8.35 (a) -37.9 MPa; 14.06 MPa. (b) -131.6 MPa; 0.
8.37 (a) 4.79 ksi; 3.07 ksi. (b) -2.57 ksi; 3.07 ksi.
8.38 -14.98 MPa; 17.29 MPa.
8.39 -3.96 ksi; 0.938 ksi.
8.40 (a) 79.6 MPa; 7.96 MPa. (b) 0; 13.26 MPa.
8.42 (a) 4.3 MPa, -93.4 MPa; 12.1° , 102.1° . (b) 48.9 MPa.
8.43 (a) 30.0 MPa, -30.0 MPa; 30.0 MPa. (b) 7.02 MPa, -96.0 MPa; 51.5 MPa.
8.46 (a) 3.47 ksi; 1.042 ksi. (b) 7.81 ksi; 0.781 ksi. (c) 12.15 ksi; 0.
8.47 (a) 18.39 MPa; 0.391 MPa. (b) 21.3 MPa; 0.293 MPa.
 (c) 24.1 MPa; 0.
8.48 (a) -7.98 MPa; 0.391 MPa. (b) -5.11 MPa; 0.293 MPa.
 (c) -2.25 MPa; 0.
8.49 30.1 MPa, -0.62 MPa; -8.2° , 81.8° ; 15.37 MPa.
8.50 0.12 MPa, -51.4 MPa; 2.8° , 92.8° ; 25.8 MPa.
8.51 1506 psi, -4150 psi; 31.1° , 121.1° ; 2830 psi.
8.53 (a) 86.5 MPa; 0. (b) 57.0 MPa; 9.47 MPa.
8.55 5.59 ksi, -12.24 ksi; 8.91 ksi.
8.56 5.55 ksi, -16.48 ksi; 11.02 ksi.
8.57 12.94 MPa, -1.33 MPa; 7.13 MPa.
8.59 (a) 51.0 kN. (b) 39.4 kN.
8.61 12.2 MPa, -12.2 MPa; 12.2 MPa.
8.62 (a) 12.90 ksi, -0.32 ksi; -8.9° , 81.1° ; 6.61 ksi. (b) 6.43 ksi
 -6.43 ksi; $\pm 45^\circ$; 6.43 ksi.

CHAPTER 9

- 9.1** (a) $y = -(w_0/EIL)(L^3x^2/6 - Lx^4/12 + x^5/120)$.
 (b) $11w_0L^4/120EI \downarrow$. (c) $w_0L^3/8EI \searrow$.
9.2 (a) $y = -(w/24EI)(x^4 - 4L^3x + 3L^4)$. (b) $wL^4/8EI \downarrow$.
 (c) $wL^3/6EI \searrow$.
9.3 (a) $y = -(Px^2/6EI)(3L - x)$. (b) $PL^3/3EI \downarrow$. (c) $PL^2/2EI \searrow$.
9.4 (a) $y = (M_0/2EI)(L - x)^2$. (b) $M_0L^2/2EI \uparrow$. (c) $M_0L/EI \searrow$.
9.6 (a) $y = (w/72EI)(3x^4 - 16ax^3)$. (b) $10wa^4/9EI \downarrow$.
 (c) $4wa^3/3EI \searrow$.
9.8 (a) $y = (w_0/EIL)(L^2x^3/48 - x^5/120 - L^4x/80)$.
 (b) $w_0L^4/256EI \downarrow$. (c) $w_0L^3/120EI \searrow$.
9.9 (a) 2.79×10^{-3} rad \searrow . (b) 1.859 mm \downarrow .
9.10 (a) 3.92×10^{-3} rad \searrow . (b) 0.1806 in. \downarrow .
9.11 (a) $0.06415M_0L^2/EI$ at $x = 0.423L$. (b) 45.3 kN \cdot m.
9.12 (a) $0.00652w_0L^4/EI$ at $x = 0.519L$. (b) 0.229 in. \downarrow .
9.13 0.398 in. \downarrow .
9.16 (a) $(P/EI)(ax^2/2 - aLx/2 + a^3/6)$. (b) 1.976 mm \downarrow .
9.17 (a) $y = w_0(x^6 - 15L^2x^4 + 25L^3x^3 - 11L^5x)/360EIL^2$.
 (b) $11w_0L^3/360EI \searrow$. (c) $0.00916w_0L^4/EI \downarrow$.
9.18 (a) $y = (w_0/EIL^2)(x^6/90 - Lx^5/30 + L^3x^3/18 - L^5x/30)$.
 (b) $w_0L^3/30EI \searrow$. (c) $61w_0L^4/5760EI \downarrow$.
9.19 $3M_0/2L \uparrow$.
9.20 $3wL/8 \uparrow$.
9.23 9.75 kN \uparrow .
9.24 4.00 kips \uparrow .
9.25 $R_B = 9M_0/8L \uparrow$; $M_A = M_0/8$,
 $M_{C-} = -7M_0/16$, $M_{C+} = 9M_0/16$.
9.26 $R_B = 5P/16 \uparrow$; $M_A = -3PL/16$, $M_C = 5PL/32$, $M_B = 0$.
9.27 $R_A = 7wL/128 \uparrow$; $M_C = 0.02734wL^2$, $M_B = -0.07031wL^2$,
 $M = 0.02884wL^2$ at $x = 0.555L$.
9.28 $R_A = 21w_0L/160 \uparrow$, $R_B = 19w_0L/160 \uparrow$; $M_B = -0.0354w_0L^2$,
 $M_C = 0.0240w_0L^2$, $M = 0.0317w_0L^2$ at $x = 0.362L$.
9.29 $R_B = 17wL/64 \uparrow$; $y_C = wL^4/1024EI$.
9.31 $R_B = 5M_0/6L \downarrow$; $y_D = 7M_0L^2/486EI \uparrow$.
9.33 $R_A = w_0L/4 \uparrow$, $M_A = -0.0521w_0L^2$, $M_C = 0.03125w_0L^2$.
9.34 $M_A = PL/8 \uparrow$, $M_B = PL/8 \downarrow$, $M_C = PL/8$.
9.35 (a) $y = (M_0/6EIL)\{x^3 - 3L(x - a)^2 + (3b^2 - L^2)x\}$.
 (b) $M_0(3b^2 - L^2)/6EIL \searrow$. (c) $M_0ab(b - a)/3EIL \uparrow$.
9.36 (a) $y = (P/6EIL)\{bx^3 - L(x - a) - b(L^2 - b^2)x\}$.
 (b) $Pb(L^2 - b^2)/6EIL \searrow$. (c) $Pa^2b^2/3EIL \downarrow$.
9.37 (a) $(P/EI)\{x^3/3 - (x - a)^3/6 - 3ax^2/2\}$.
 (b) $5Pa^2/2EI \searrow$. (c) $7Pa^3/2EI \downarrow$.
9.38 (a) $y = (P/EI)\{-x^3/6 - (x - a)^3/6 + 5a^2x/2 - 7a^3/2\}$.
 (b) $5Pa^2/2EI \searrow$. (c) $7Pa^3/2EI \downarrow$.
9.41 (a) $y = (w/EI)\{ax^3/6 - x^4/24 + (x - a)^4/24 - (x - 3a)^4/24 - 5wa^3x/6\}$. (b) $23wa^4/24EI \downarrow$.
9.42 (a) $y = (w/24EI)\{-x^4 + (x - L/2)^4 - (x - L)^4 + Lx^3 + 3L(x - L)^3 - L^3x/16\}$. (b) $wL^4/768EI \uparrow$.
 (c) $5wL^4/256EI \downarrow$.

- 9.44** (a) $y = w_0 [16x^5 - 32(x - L/2)^5 - 40Lx^4 + 40L^2x^3 - 15L^4x]/960EI$. (b) $3w_0L^4/640EI \downarrow$.
9.45 (a) $2.49 \times 10^{-3} \text{ rad} \curvearrowright$. (b) $1.078 \text{ mm} \downarrow$.
9.47 (a) $5.40 \times 10^{-3} \text{ rad} \curvearrowright$. (b) $3.06 \text{ mm} \downarrow$.
9.48 (a) $14.00 \times 10^{-3} \text{ rad} \curvearrowright$. (b) $0.340 \text{ in.} \downarrow$.
9.49 (a) $9M_0/8L \uparrow$. (b) $M_0L^2/128EI \downarrow$.
9.50 (a) $5P/16 \uparrow$. (b) $7PL^3/168EI \downarrow$.
9.52 (a) $2P/3 \uparrow$. (b) $5PL^3/48EI$.
9.53 (a) $11.54 \text{ kN} \uparrow$. (b) $4.18 \text{ mm} \downarrow$.
9.54 (a) $5.58 \text{ kips} \uparrow$. (b) $0.1065 \text{ in.} \downarrow$.
9.56 (a) $41.25 \text{ kN} \uparrow$. (b) $0.705 \text{ mm} \downarrow$.
9.57 (a) $20P/27 \uparrow$; $4PL/27 \uparrow$. (b) $5PL^3/1296EI \downarrow$.
9.58 (a) $3wL/32 \uparrow$; $5wL^2/192 \uparrow$. (b) $wL^4/768EI \downarrow$.
9.59 $1.401 \text{ mm} \downarrow$ at $x = 0.857 \text{ m}$.
9.60 $0.281 \text{ in.} \downarrow$ at $x = 8.40 \text{ ft}$.
9.61 $3.07 \text{ mm} \downarrow$ at $x = 0.942 \text{ m}$.
9.62 $0.341 \text{ in.} \downarrow$ at $x = 3.34 \text{ ft}$.
9.65 $PL^2/EI \curvearrowright$; $17PL^3/24EI \downarrow$.
9.66 $5PL^2/8EI \curvearrowright$; $7PL^3/16EI \downarrow$.
9.67 $PL^2/24EI \curvearrowright$; $PL^3/48EI \downarrow$.
9.68 $wL^3/48EI \curvearrowright$; $wL^4/384EI \uparrow$.
9.70 $5PL^3/162EI \downarrow$; (b) $PL^2/9EI \curvearrowright$.
9.72 (a) $wL^4/384EI \downarrow$; (b) 0 .
9.73 $6.32 \times 10^{-3} \text{ rad} \curvearrowright$; $5.55 \text{ mm} \downarrow$.
9.75 $7.91 \times 10^{-3} \text{ rad} \curvearrowright$; $0.340 \text{ in.} \downarrow$.
9.76 $6.98 \times 10^{-3} \text{ rad} \curvearrowright$; $0.1571 \text{ in.} \downarrow$.
9.77 (a) $0.601 \times 10^{-3} \text{ rad} \curvearrowright$; (b) $3.67 \text{ mm} \downarrow$.
9.79 $R_A = M_0/2L \uparrow$; $R_B = 5M_0/2L \uparrow$; $R_C = 3M_0/L \downarrow$.
9.81 (a) $41wL/128 \uparrow$. (b) $23wL/128 \uparrow$; $7wL^2/128 \downarrow$.
9.82 (a) $3M_0(L^2 - a^2)/2L^3 \uparrow$. (b) $3M_0(L^2 - a^2)/2L^3 \downarrow$; $M_0(L^2 - 3a^2)/2L^2 \uparrow$.
9.84 $3M_0/2L \downarrow$; $M_0/4 \uparrow$.
9.85 121.5 N/m .
9.86 (a) $5.06 \times 10^{-3} \text{ rad} \curvearrowright$. (b) $0.0477 \text{ in.} \downarrow$.
9.87 $0.210 \text{ in.} \downarrow$.
9.88 (a) $10.54 \text{ mm} \downarrow$. (b) $23.4 \text{ mm} \downarrow$.
9.90 43.9 kN .
9.91 $5.63 \text{ kN} \downarrow$.
9.93 $0.278 \text{ in.} \downarrow$.
9.94 $9.31 \text{ mm} \downarrow$.
9.95 (a) $PL^2/2EI \curvearrowright$. (b) $PL^3/3EI \downarrow$.
9.96 (a) $M_0L/EI \curvearrowright$. (b) $M_0L^2/2EI \downarrow$.
9.97 (a) $w_0L^3/24EI \curvearrowright$. (b) $w_0L^4/30EI \downarrow$.
9.98 (a) $wL^3/6EI \curvearrowright$. (b) $wL^4/8EI \downarrow$.
9.101 (a) $5.84 \times 10^{-3} \text{ rad} \curvearrowright$. (b) $0.300 \text{ in.} \downarrow$.
9.102 (a) $7.15 \times 10^{-3} \text{ rad} \curvearrowright$. (b) $17.67 \text{ mm} \downarrow$.
9.103 (a) $16.56 \times 10^{-3} \text{ rad} \curvearrowright$. (b) $0.379 \text{ in.} \downarrow$.
9.104 (a) $2.55 \times 10^{-3} \text{ rad} \curvearrowright$. (b) $6.25 \text{ mm} \downarrow$.
9.105 (a) $11PL^2/24EI \curvearrowright$. (b) $11PL^3/36EI \downarrow$.
9.108 (a) $3.43 \times 10^{-3} \text{ rad} \curvearrowright$. (b) $6.66 \text{ mm} \downarrow$.
9.109 (a) $PL^2/16EI \curvearrowright$. (b) $PL^2/48EI \downarrow$.
9.110 (a) $5PL^2/32EI \curvearrowright$. (b) $19PL^3/384EI \downarrow$.
9.111 (a) $wa^2(3L - 2a)/12EI \curvearrowright$. (b) $wa^2(3L^2 - 2a^2)/48EI \downarrow$.
9.113 (a) $M_0(L - 2a)/2EI \curvearrowright$. (b) $M_0(L^2 - 4a^2)/8EI \downarrow$.
9.114 (a) $PL^2/32EI \curvearrowright$. (b) $PL^3/128EI \downarrow$.
9.115 (a) $5Pa^2/8EI \curvearrowright$. (b) $3Pa^3/4EI \downarrow$.
9.117 (a) $5.21 \times 10^{-3} \text{ rad} \curvearrowright$. (b) $21.2 \text{ mm} \downarrow$.
9.118 (a) $4.71 \times 10^{-3} \text{ rad} \curvearrowright$. (b) $5.84 \text{ mm} \downarrow$.
9.119 (a) $4.50 \times 10^{-3} \text{ rad} \curvearrowright$. (b) $8.26 \text{ mm} \downarrow$.
9.121 3.84 kN/m .
9.123 $0.211 L$.
9.124 $0.223 L$.
9.125 (a) $5PL^3/768EI \downarrow$. (b) $3PL^2/128EI \curvearrowright$.
9.127 (a) $5w_0L^4/768EI \downarrow$. (b) $7w_0L^3/360EI \curvearrowright$.
9.128 (a) $5wL^4/768EI \downarrow$. (b) $3wL^3/128EI \curvearrowright$.
9.129 (a) $8.74 \times 10^{-3} \text{ rad} \curvearrowright$. (b) $15.10 \text{ mm} \downarrow$.
9.130 (a) $7.48 \times 10^{-3} \text{ rad} \curvearrowright$. (b) $5.35 \text{ mm} \downarrow$.
9.131 (a) $5.31 \times 10^{-3} \text{ rad} \curvearrowright$. (b) $0.204 \text{ in.} \downarrow$.
9.134 (a) $M_0(L + 3a)/3EI \curvearrowright$. (b) $M_0a(2L + 3a)/6EI \downarrow$.
9.135 (a) $2.34 \times 10^{-3} \text{ rad} \curvearrowright$. (b) $0.1763 \text{ in.} \downarrow$.
9.137 (a) $5.33 \times 10^{-3} \text{ rad} \curvearrowright$. (b) $0.01421 \text{ in.} \downarrow$.
9.138 (a) $3.61 \times 10^{-3} \text{ rad} \curvearrowright$. (b) $0.960 \text{ mm} \uparrow$.
9.139 (a) $17PL^3/972EI \downarrow$. (b) $19PL^3/972EI \downarrow$.
9.140 (a) $9wL^3/256EI \curvearrowright$. (b) $7wL^3/256EI \curvearrowright$.
(c) $5wL^4/512EI \downarrow$.
9.142 $0.00652w_0L^4/EI$ at $x = 0.519L$.
9.144 $0.212 \text{ in.} \downarrow$ at $x = 5.15 \text{ ft}$.
9.145 1.841 mm .
9.146 0.1049 in. .
9.148 $5P/16 \uparrow$.
9.149 $7wL/128 \uparrow$.
9.150 $9M_0/8L \uparrow$.
9.151 $R_A = 3P/32 \downarrow$; $R_B = 13P/32 \uparrow$; $R_C = 11P/16 \uparrow$.
9.153 $65.2 \text{ kN} \uparrow$; $M_A = 0$; $M_D = 58.7 \text{ kN} \cdot \text{m}$; $M_B = -82.8 \text{ kN} \cdot \text{m}$.
9.154 $10.18 \text{ kips} \uparrow$; $M_A = -87.9 \text{ kip} \cdot \text{ft}$; $M_D = 46.3 \text{ kip} \cdot \text{ft}$; $M_B = 0$.
9.155 $48EI/7L^3$.
9.156 $144EI/L^3$.
9.157 (a) $y = w_0 (2x^5 - 5Lx^4 + 10L^4x - 7L^5)/120EI$.
(b) $7w_0L^4/120EI \uparrow$. (c) $w_0L^3/12EI \curvearrowright$.
9.158 (a) $0.01604 M_0L^2/EI$ at $x = 0.211L$. (b) 21.5 ft .
9.160 $wL/2 \uparrow$, $wL^2/12 \uparrow$; $M = w[6x(L - x) - L^2]/12$.
9.162 (a) $0.712 \times 10^{-3} \text{ rad} \curvearrowright$. (b) $1.068 \text{ mm} \uparrow$.
9.163 (a) $10.86 \text{ kN} \uparrow$; $1.942 \text{ kN} \cdot \text{m} \uparrow$. (b) $1.144 \text{ kN} \uparrow$; $0.286 \text{ kN} \cdot \text{m} \downarrow$.
9.165 (a) $5.20 \times 10^{-3} \text{ rad} \curvearrowright$. (b) $10.85 \text{ mm} \downarrow$.
9.166 (a) $4.27 \times 10^{-3} \text{ rad} \curvearrowright$. (b) $0.1080 \text{ in.} \uparrow$. (c) $0.206 \text{ in.} \downarrow$.
9.168 (a) $6.87 \text{ mm} \uparrow$. (b) $46.3 \text{ kN} \uparrow$.
9.C1 Prob. 9.74: $5.56 \times 10^{-3} \text{ rad} \curvearrowright$; $2.50 \text{ mm} \downarrow$.
9.C2 $a = 6 \text{ ft}$: (a) $3.14 \times 10^{-3} \text{ rad} \curvearrowright$, $0.292 \text{ in.} \downarrow$;
(b) $0.397 \text{ in.} \downarrow$ at 11.27 ft to the right of A.
9.C3 $x = 1.6 \text{ m}$: (a) $7.90 \times 10^{-3} \text{ rad} \curvearrowright$, $8.16 \text{ mm} \downarrow$;
(b) $6.05 \times 10^{-3} \text{ rad} \curvearrowright$, $5.79 \text{ mm} \downarrow$;
(c) $1.021 \times 10^{-3} \text{ rad} \curvearrowright$, $0.314 \text{ mm} \downarrow$.
9.C5 (a) $a = 3 \text{ ft}$: $1.586 \times 10^{-3} \text{ rad} \curvearrowright$; $0.1369 \text{ in.} \downarrow$;
(b) $a = 1.0 \text{ m}$: $0.293 \times 10^{-3} \text{ rad} \curvearrowright$, $0.479 \text{ mm} \downarrow$.
9.C7 $x = 2.5 \text{ m}$: $5.31 \text{ mm} \downarrow$; $x = 5.0 \text{ m}$: $12.28 \text{ mm} \downarrow$.

CHAPTER 10

- 10.1** kL .
10.2 K/L .
10.3 K/L .
10.4 $2kL/9$.
10.6 $k > 4.91 \text{ kN/m}$.
10.8 $8K/L$.
10.9 (a) 6.65 lb . (b) 21.0 lb .
10.10 305 kN .
10.11 (a) 6.25% . (b) 12.04 kips .
10.13 1.421 .
10.15 164.0 kN .
10.17 69.6 kips .
10.18 335 kips .
10.19 2.44 .
10.21 (1) 319 kg ; (2) 79.8 kg ; (3) 319 kg ; (4) 653 kg .

- 10.22** (a) 2.55. (b) (2):28.3 mm; (3): 14.14 mm; (4):16.72 mm; (5): 20.0 mm.
- 10.23** (a) BC : 4.20 ft; CD : 1.05 ft. (b) 4.21 kips.
- 10.26** 29.5 kips.
- 10.27** 657 mm.
- 10.28** (a) 1/2.00. (b) $d = 28.3$ mm; $b = 14.15$ mm.
- 10.29** (a) 1.658 mm. (b) 78.9 MPa.
- 10.30** (a) 4.32 mm. (b) 44.4 MPa.
- 10.31** (a) 0.410 in. (b) 14.43 ksi.
- 10.33** (a) 0.0399 in. (b) 19.89 ksi.
- 10.35** (a) 13.29 kips. (b) 15.50 ksi.
- 10.36** (a) 370 kN. (b) 104.6 MPa.
- 10.37** (a) 224 kN. (b) 63.3 MPa.
- 10.39** (a) 235 kN. (b) 149.6 MPa.
- 10.40** (a) 151.6 kN. (b) 109.5 MPa.
- 10.41** 58.9°F
- 10.43** (a) 38.6 kips. (b) 0.628.
- 10.45** (a) 189 kN. (b) 229 kN.
- 10.46** (a) 147 kN. (b) 174 kN.
- 10.47** 2.16 m.
- 10.48** 1.302 m.
- 10.49** (a) 13.68 ft. (b) 7.83 ft.
- 10.51** 2.125 in.
- 10.52** 2.625 in.
- 10.53** $W200 \times 26.6$.
- 10.56** 3.09.
- 10.57** (a) 220 kN. (b) 841 kN.
- 10.58** (a) 86.6 kips. (b) 88.1 kips.
- 10.59** (a) 59.6 kips. (b) 31.9 kips.
- 10.60** (a) 1530 kN. (b) 638 kN.
- 10.62** (a) 231 mm. (b) 376 mm. (c) 714 mm.
- 10.64** 35.9 kN.
- 10.65** 76.3 kips.
- 10.68** 144.1 kips.
- 10.69** 39.9 kips.
- 10.70** 107.7 kN.
- 10.71** 1.615 in.
- 10.72** 9 mm.
- 10.74** 123.1 mm.
- 10.75** 6.53 in.
- 10.77** $W250 \times 67$.
- 10.78** $W200 \times 46.1$.
- 10.79** $W14 \times 82$.
- 10.80** 3/8 in.
- 10.82** (a) 30.1 mm. (b) 33.5 mm.
- 10.84** $L89 \times 64 \times 12.7$.
- 10.85** (a) (dead) 433 kN; (live) 321 kN.
(b) (dead) 896 kN; (live) 664 kN.
- 10.86** 56.1 kips.
- 10.87** $W310 \times 74$.
- 10.88** 5/16 in.
- 10.89** 76.7 kN.
- 10.91** (a) 329 kN. (b) 280 kN.
- 10.93** (a) 18.26 kips. (b) 14.20 kips.
- 10.94** (a) 21.1 kips. (b) 18.01 kips.
- 10.95** (a) 0.0987 in. (b) 0.787 in.
- 10.97** (a) 11.89 mm. (b) 6.56 mm.
- 10.98** 7.78 mm.
- 10.99** 45.6 in.
- 10.101** 5.48 m.
- 10.102** 4.81 m.
- 10.105** 12 mm.

- 10.106** 15 mm.
- 10.107** 48.2 mm.
- 10.108** 44.3 mm.
- 10.109** 1/4 in.
- 10.110** 3/16 in.
- 10.113** $W14 \times 145$.
- 10.114** $W14 \times 68$.
- 10.115** $W250 \times 58$.
- 10.116** $W200 \times 59$.
- 10.117** $ka^2/2I$.
- 10.118** 0.384 in.
- 10.120** $\Delta T = \pi^2 b^2 / 12 L^2 \alpha$.
- 10.121** 2.77 kN.
- 10.123** 95.5 kips.
- 10.125** (a) 4.84 mm. (b) 135.7 Mpa.
- 10.126** $W10 \times 54$.
- 10.128** $W8 \times 40$.
- 10.C1** $r = 8$ mm: 9.07 kN. $r = 16$ mm: 70.4 kN.
- 10.C2** $b = 1.0$ in.: 3.85 kips. $b = 1.375$ in.: 6.07 kips.
- 10.C3** $h = 5.0$ m: 9819 kg. $h = 7.0$ m: 13,255 kg.
- 10.C4** $P = 35$ kips: (a) 0.086 in.; (b) 4.69 ksi.
 $P = 55$ kips: (a) 0.146 in.; (b) 7.65 ksi.
- 10.C6** Prob. 10.113: $P_{all} = 282.6$ kips.
Prob. 10.114: $P_{all} = 139.9$ kips.

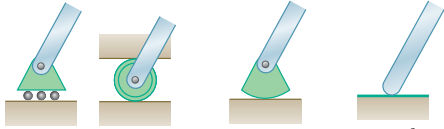
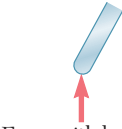
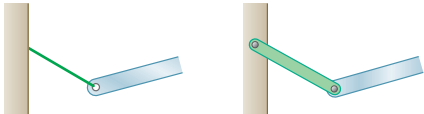

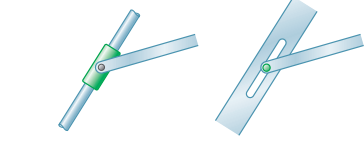
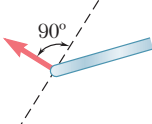

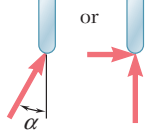
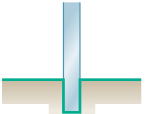
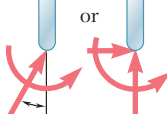
CHAPTER 11

- 11.1** (a) 177.9 kJ/m³. (b) 712 kJ/m³. (c) 160.3 kJ/m³.
- 11.2** (a) 436 in · lb/in³. (b) 64.7 in · lb/in³. (c) 6.40 in · lb/in³.
- 11.4** (a) 21.6 kJ/m³. (b) 336 kJ/m³. (c) 163.0 kJ/m³.
- 11.5** (a) 1296 kJ/m³. (b) 90 MJ/m³.
- 11.6** (a) 58.0 in · lb/in³. (b) 20 in · kip/in³.
- 11.8** (a) 150 KJ/m³. (b) 63 MJ/m³.
- 11.9** (a) 176.2 in · lb (b) AB : 11.72 in · lb/in³; BC : 5.65 in · lb/in³.
- 11.10** (a) 12.18 J. (b) AB : 15.83 KJ/m³; BC 38.6 KJ/m³.
- 11.11** (a) 168. 8 in · lb. (b) CD : 0. 882 in · lb/in³; EF : 5.65 in · lb/in³.
- 11.14** 13.73 mm.
- 11.15** (a) 3.28. (b) 4.25.
- 11.16** 102.7 in · lb.
- 11.18** $1.500 P^2 l / EA$.
- 11.19** $1.398 P^2 l / EA$.
- 11.22** 1.767 kip · in.
- 11.23** 59.8 J.
- 11.24** $w^3 L^5 / 40EI$.
- 11.25** $w^3 L^5 / 240EI$.
- 11.26** $M_0^2 (a^3 + b^3) / 6EIL^2$.
- 11.28** 1048 J.
- 11.29** 670 J.
- 11.30** 388 J.
- 11.32** 15 U/V .
- 11.34** 14.70 J.
- 11.36** (a) 2.33. (b) 2.02.
- 11.38** $-2.65 \text{ MPa} < \sigma_z < 122.65 \text{ MPa}$.
- 11.40** $U = (2M_0^2 L / Ebd^3)(1 + 3Ed^2 / 10GL^2)$
- 11.41** $U = (Q^2 / 4\pi GL) \ln (R_2 / R_1)$.
- 11.42** 9.12 lb.
- 11.43** 25.5 ft/s.
- 11.44** 4.76 kg.
- 11.45** 5.63 kg.
- 11.48** (a) 21.0 kN. (b) 172. 1 MPa. (c) 8.61 mm.
- 11.49** (a) 7.66 kN. (b) 316 MPa. (c) 23.5 mm.

- 11.50** 11.09 ft/s.
11.52 (a) 15.63 mm. (b) 83.8 N · m. (c) 208 MPa.
11.53 (a) 23.6 mm. (b) 64.4 N · m. (c) 157.6 MPa.
11.54 (a) 0.1061 in. (b) 20.2 ksi.
11.56 (b) 7.12.
11.58 $Pa^2(a + L)/3EI \downarrow$.
11.59 $Pa^2b^2/3EI \downarrow$.
11.61 $M_0(a^3 + b^3)/3EIL^2 \curvearrowright$.
11.62 $3Pa^3/4EI \downarrow$.
11.63 $3PL^3/16EI \downarrow$.
11.65 $M_0L/16EI \curvearrowright$.
11.66 32.4 in.
11.68 386 mm.
11.69 2.55°.
11.71 $3.375 PL/EA \downarrow$.
11.73 0.0650 in. \downarrow .
11.74 0.366 in. \downarrow .
11.76 1.111 mm \downarrow .
11.77 (a) and (b) $P^2L^3/6EI + PM_0L^2/2EI + M_0^2L/2EI$.
11.78 (a) and (b) $P^2L^3/48EI + PM_0L^2/8EI + M_0^2L/2EI$.
11.80 (a) and (b) $P^2L^3/48EI$.
11.82 (a) and (b) $5M_0^2L/4EI$.
11.83 $5PL^3/48EI \downarrow$.
11.85 $3PL^2/8EI \curvearrowright$.
11.86 $7wL^3/48EI \curvearrowright$.
11.88 $PL^3/96EI \uparrow$.
11.89 $wL^3/192EI \curvearrowright$.
11.90 $PL^2/48EI \curvearrowright$.
11.91 $7.07 \times 10^{-3} \text{ rad} \curvearrowright$.
11.93 0.317 in. \downarrow .
11.94 3.80 mm \downarrow .
11.95 7.25 mm \downarrow .
11.96 5.12 mm \downarrow .
11.98 $2.07 \times 10^{-3} \text{ rad} \curvearrowright$.
11.99 $PL/2EA \leftarrow$; 3.80 $PL/EA \downarrow$.
11.100 $0 \rightarrow$; 2.80 $PL/EA \uparrow$.
11.103 0.233 in. \downarrow .
11.104 0.1504 in. \rightarrow .
11.105 (a) $2Pl^3/3EI \rightarrow$. (b) $Pl^2/6EI \curvearrowright$.
11.106 (a) $5Pl^3/3EI \rightarrow$. (b) $2PL^2/EI \uparrow$.
11.107 (a) $Pl^3/EI \uparrow$. (b) $3Pl^2/EI \curvearrowright$.
11.109 (a) $PR^3/2EI \rightarrow$. (b) $\pi PR^3/4EI \downarrow$.
11.111 $3M_0/2L \uparrow$; $M = M_0(3x/2 - 1)$.
11.112 $5P/16 \uparrow$; $M_A = -3PL/16$, $M_C = 5PL/32$, $M_B = 0$.
11.113 $41wL/128 \uparrow$; $M_A = 0$; $M = 0.0513wL^2$ at $x = 48L/128$;
 $M_B = -7wL^2/128$.
11.114 $3M_0b(L + a)/2L^3 \uparrow$;
 $M = 3M_0b(L + a)x/2L^3 - M_0(L - a)^0$.
11.117 $P/(1 + 2 \cos^3 \theta)$.
11.118 $3P/4$.
11.119 $7P/8$.
11.120 0.652 P .
11.125 24.7 mm.
11.128 11.57 mm \downarrow .
11.129 3.12°.
11.130 0.0447 in. \downarrow .
11.132 $PL^2/6EI \uparrow$.
11.134 A: $wL/6 \downarrow$; B: $3wL/4 \uparrow$; C: $5wL/12 \uparrow$.
11.C2 (a) $a = 15 \text{ in.}$: $\sigma_D = 17.19 \text{ ksi}$, $\sigma_C = 21.0 \text{ ksi}$;
 $a = 45 \text{ in.}$: $\sigma_D = 36.2 \text{ ksi}$, $\sigma_C = 14.74 \text{ ksi}$.
(b) $a = 18.34 \text{ in.}$, $\sigma = 20.67 \text{ ksi}$.
11.C3 (a) $L = 200 \text{ mm}$: $h = 2.27 \text{ mm}$;
 $L = 800 \text{ mm}$: $h = 1.076 \text{ mm}$.
(b) $L = 440 \text{ mm}$: $h = 3.23 \text{ mm}$.
11.C4 $a = 300 \text{ mm}$: 1.795 mm, 179.46 MPa;
 $a = 600 \text{ mm}$: 2.87 mm, 179.59 MPa.
11.C5 $a = 2 \text{ m}$: (a) 30.0 J; (b) 7.57 mm, 60.8 J.
 $a = 4 \text{ m}$: (a) 21.9 J; (b) 8.87 mm, 83.4 J.
11.C6 $a = 20 \text{ in.}$: (a) 13.26 in.; (b) 99.5 kip · in.;
(c) 803 lb.
 $a = 50 \text{ in.}$: (a) 9.46 in.; (b) 93.7 kip · in.;
(c) 996 lb.

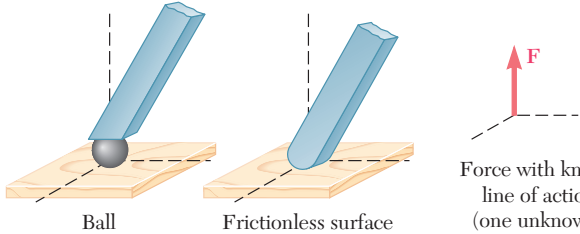
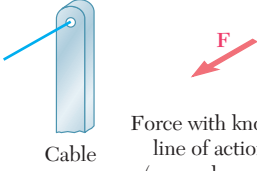
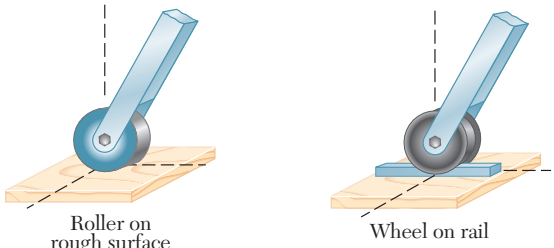
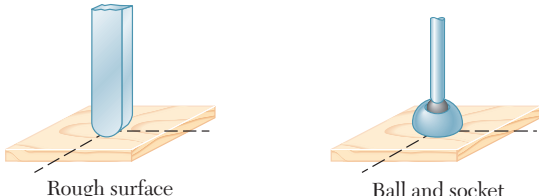
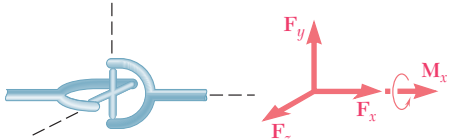

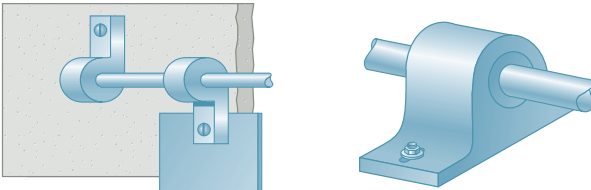
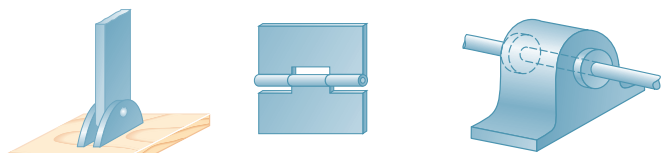
This page intentionally left blank

Reactions at Supports and Connections for a Two-Dimensional Structure

Support or Connection	Reaction	Number of Unknowns
 <p>Rollers Rocker Frictionless surface</p>	 <p>Force with known line of action</p>	1
 <p>Short cable Short link</p>	 <p>Force with known line of action</p>	1
 <p>Collar on frictionless rod Frictionless pin in slot</p>	 <p>Force with known line of action</p>	1
 <p>Frictionless pin or hinge Rough surface</p>	 <p>Force of unknown direction</p>	2
 <p>Fixed support</p>	 <p>Force and couple</p>	3

The first step in the solution of any problem concerning the equilibrium of a rigid body is to construct an appropriate free-body diagram of the body. As part of that process, it is necessary to show on the diagram the reactions through which the ground and other bodies oppose a possible motion of the body. The figures on this and the facing page summarize the possible reactions exerted on two- and three-dimensional bodies.

Reactions at Supports and Connections for a Three-Dimensional Structure

 <p>Ball Frictionless surface</p> <p>Force with known line of action (one unknown)</p>	 <p>Cable</p> <p>Force with known line of action (one unknown)</p>
 <p>Roller on rough surface Wheel on rail</p> <p>Two force components</p>	
 <p>Rough surface Ball and socket</p> <p>Three force components</p>	
 <p>Universal joint</p> <p>Three force components and one couple</p>	 <p>Fixed support</p> <p>Three force components and three couples</p>
 <p>Hinge and bearing supporting radial load only</p> <p>Two force components (and two couples)</p>	
 <p>Pin and bracket Hinge and bearing supporting axial thrust and radial load</p> <p>Three force components (and two couples)</p>	